



HAL
open science

Long term performance of low temperature asphalt pavements containing reclaimed asphalt

Miguel Pérez-Martinez

► **To cite this version:**

Miguel Pérez-Martinez. Long term performance of low temperature asphalt pavements containing reclaimed asphalt. Materials. École centrale de Nantes, 2017. English. NNT : 2017ECDN0009 . tel-02184202

HAL Id: tel-02184202

<https://theses.hal.science/tel-02184202v1>

Submitted on 15 Jul 2019

HAL is a multi-disciplinary open access archive for the deposit and dissemination of scientific research documents, whether they are published or not. The documents may come from teaching and research institutions in France or abroad, or from public or private research centers.

L'archive ouverte pluridisciplinaire **HAL**, est destinée au dépôt et à la diffusion de documents scientifiques de niveau recherche, publiés ou non, émanant des établissements d'enseignement et de recherche français ou étrangers, des laboratoires publics ou privés.

Thèse de Doctorat

Miguel PEREZ MARTINEZ

*Mémoire présenté en vue de l'obtention
du grade de Docteur de l'École Centrale de Nantes
sous le sceau de l'UNIVERSITE BRETAGNE LOIRE*

École doctorale : Sciences pour l'Ingénieur, Géosciences, Architecture

Discipline : Sciences pour l'ingénieur

*Unité de recherche : Institut Français des Sciences et Technologie des Transports
de l'Aménagement et des Réseaux*

Soutenue le 17 mai 2017

Durabilité des enrobés tièdes intégrant des recyclés

JURY

President :	Ahmed LOUKILI , Professeur des Universités, Ecole Centrale de Nantes
Rapporteurs :	Cyrille CHAZALLON , Professeur des Universités, Université de Strasbourg Terhi PELLINEN , Professeure des Universités, Université d'Aalto
Examineurs :	Virginie MOUILLET , Directrice de Recherche, CEREMA Aix-en-Provence Ann VANELSTRAETE , Docteur, Centre de Recherche Routière, Belgique François OLARD , Directeur de Recherche & Innovation, EIFFAGE Infrastructures
Invité :	Paul MARSAC , Ingénieur de Recherche, IFSTTAR Centre de Nantes
Directeur de thèse :	Ferhat HAMMOUM , Directeur de Recherche, IFSTTAR Centre de Nantes
Co-encadrant de thèse :	Thomas GABET , Charge de Recherche, IFSTTAR Centre de Nantes

DURABILITE DES ENROBES TIEDES INTEGRANT DES RECYCLES

Résumé

Les routes constituent le moyen de transport le plus utilisé dans le monde et le développement d'un pays est souvent mesuré en terme de kilométrage total des routes revêtues. Les chaussées sont essentielles à notre réseau social et l'enrobé bitumineux est le matériau le plus utilisé pour leur fabrication. À l'heure actuelle, le réseau routier européen n'est plus en forte croissance et nécessite surtout un entretien. Dans un contexte de développement durable de plus en plus exigeant, la route pourrait donc représenter sa propre source d'approvisionnement en tirant parti du recyclage. Elle doit aussi limiter les quantités d'énergies et de ressources naturelles nécessaires à sa propre maintenance.

La combinaison des techniques d'enrobés tièdes (WMA) et de taux de recyclage élevés d'agrégats d'enrobés (RAP) apparaît comme une solution permettant d'économiser à la fois l'énergie et les ressources naturelles. Mais sa durabilité doit être vérifiée. Un programme expérimental a donc été mis en place pour montrer l'évolution des performances de ces enrobés bitumineux avec le temps, mettant en évidence le vieillissement essentiellement lié à la fraction bitumineuse. A l'échelle du bitume, l'évaluation à long terme est effectuée notamment en appliquant la δ -méthode et en comparant avec les mesures de masses moléculaires par GPC à la fois sur des échantillons modèles à teneur en asphaltènes contrôlée et sur des échantillons de laboratoire. A l'échelle de l'enrobé bitumineux, une étude comparative a été réalisée entre un enrobé à chaud traditionnel et des WMAs incluant 0% ou 50% de RAP soumis à une procédure de vieillissement en laboratoire. Les performances à long terme des mélanges sont comparées au moyen d'essais de module complexe et de fatigue.

Les résultats montrent une relation entre l'évolution de la structure des bitumes par vieillissement et les performances mécaniques. Le vieillissement à court terme au moment de la fabrication est beaucoup moins marqué pour les procédés tièdes. Après vieillissement à long terme, les tendances générales sont similaires pour tous les procédés.

Mots-clés : Durabilité, Enrobé tièdes, Agrégats d'enrobé, Recyclage, Performance mécanique, Moussage de bitume, Vieillissement

Visa du Directeur de Recherche

Acknowledgements

The research presented in this document has been carried out as part of the Marie Curie Initial Training Network (ITN) action, FP7-PEOPLE-2013-ITN. This project has received funding from the European Union's Seventh Framework Programme for research, technological development and demonstration under grant agreement number 607524.

Cette étude a été principalement réalisée au sein de l'équipe Matériaux pour les Infrastructures de Transport à l'IFSTTAR Nantes ainsi qu'au sein de l'équipe d'ingénierie chimique de l'Université de Huelva.

Je tiens vivement à remercier M. Paul Marsac qui m'a choisi pour cette thèse à l'issue du projet SUP&R ITN. Je lui suis profondément reconnaissant pour sa disponibilité permanente, ses encouragements, son aide et sa confiance en ma réussite au cours de ces trois années de thèse.

Je tiens également à remercier sincèrement M. Ferhat Hammoum qui a accepté de diriger cette thèse. Son aide précieuse pour la recherche des matériaux bitumineux et tous ses conseils qui m'ont permis d'évoluer tout au long de cette thèse. Je remercie vivement M. Thomas Gabet qui a également accepté de co-encadrer cette thèse. Son regard sur ce travail a été d'une grande aide tout au long de la thèse.

J'adresse également mes sincères remerciements à M. Emmanuel Chailleux et M. Vincent Gaudefroy pour sa grande disponibilité et toutes les réponses prodiguées à mes questions.

Je souhaite remercier M. Ahmed Loukili d'avoir accepté la Présidence du jury ainsi que M. Cyrille Chazallon et Mme. Terhi Pellinen d'avoir accepté le rôle de rapporteurs. J'ai beaucoup apprécié leurs remarques et questions.

Je remercie Mme. Virgine Mouillet, Mme. Ann Vanelstraete et M. François Olard qui ont accepté de consacrer du temps à la lecture de cette mémoire et d'avoir accepté le rôle d'examineurs. Je vous remercie beaucoup pour le temps consacré et votre disponibilité.

Je suis également très reconnaissant envers les différentes personnes qui ont accepté de prendre du temps pour participer à mes comités de suivi et dont j'ai apprécié les remarques sur mon travail : Pierre Hornych et Simon Pouget.

Je tiens à remercier tout particulièrement les techniciens qui m'ont aidé à la réalisation des nombreux essais et dont la tâche n'a pas été de tout repos : Stéphane, Olivier, Nadège, Gilles, Sébastien, Jérôme, Jean-Philippe, Julien, Anthony et Cédric. Je n'oublie pas non plus le travail fourni par Manuela de Mesquita et Andrea Themeli lors de ses travaux de thèse précédents.

J'exprime également toute ma reconnaissance aux membres de l'équipe MIT et LAMES pour leur soutien qui n'a jamais fait défaut. Je remercie aussi vivement les thésards du laboratoire avec qui j'ai partagé cette expérience, spécialement Laure et Justine.

I would like to express my gratitude to Davide Lo Presti and Gordon Airey for letting me to be part of this project, and to all supervisors, associate partners and fellows for their support and encouragement during these three years. Thanks to Ana and Luca, this project without you would not have been the same.

También quiero dar las gracias al profesor Pedro Partal, por abrirme las puertas del Laboratorio de Fluidos Complejos de la Universidad de Huelva. Por su paciencia, disponibilidad y por permitirme aprender de un campo totalmente desconocido para mí.

Igualmente quiero agradecer a la profesora Mayca Rubio el haberme mostrado y despertado la curiosidad investigadora cuando terminé la carrera, así como la confianza que me has dado durante todos estos años. A Fernando Moreno, no solo por el tiempo pasado en el LabIC sino por todos los años que ya llevamos juntos. A todo el LabIC, siempre formará parte de mi presente y pasado, con especial cariño a Gema, Miguel y Jesús, esta tesis también es tuya.

Gracias a toda mi familia, abuelos, tíos y primos, que aunque dudo mucho que ninguno sea capaz de decir a lo que me dedico, siempre habéis estado ahí apoyándome y animándome. Gracias por vuestras visitas a Nantes en estos tres años, ha sido maravilloso teneros en casa.

A mi familia Hurtado Fernández, Nanni, Pepe, Pablo, Ana y Alex, gracias por hacerme uno más de la familia, y por el apoyo tan grande que me habéis proporcionado y más con la distancia que nos ha separado. Y a los tres sobrinos tan fantásticos que siempre han tenido una sonrisa para su tito el exiliado.

A mis hermanos, Belén y Javi, por la paciencia y cariño que me habéis transmitido durante toda vuestra vida, es lo que tiene que seáis más pequeños. He aprendido mucho de vosotros y me habéis hecho mejor persona. Gracias también a Manu por toda la ayuda que siempre nos das. Y a ti también Bea, gracias especiales por traernos a la pequeña Lucía, que tanta alegría ha traído a la familia.

Gracias a mis padres, Jose Antonio y Nieves. Esto es parte vuestra también, por todo lo que me habéis dado y nunca os podré agradecer lo suficiente. Por vuestro tiempo, por vuestros consejos, paciencia, ánimos y cariños. Por la educación que nos habéis dado, por haberme permitido viajar, conocer mundo y hacerme creer que todo lo que quisiera lo podría conseguir trabajando duro y siendo perseverante, como habéis hecho vosotros siempre.

Elena, llevo un tercio de mi vida contigo, no tengo palabras para agradecerte todo lo que has hecho por mí y todo lo que me hemos pasado. Gracias por darme la oportunidad de disfrutar de la vida a tu lado. Gracias por la paciencia que has tenido durante esta tesis, todo el tiempo que le he dedicado te lo he tenido que quitar a ti. Gracias por darme a Gonzalo, porque es la muestra más grande de lo que somos.

Gracias a todos, thanks to everyone, merci à tous.

Ethics Code



Centrale
Nantes

Along with the right to use sources of information to create or to produce anything, comes the obligation to comply with legal and ethical rules. Copyright compliance and honesty prohibit the passing off of another's work as one's own, whether intentionally or by omission.

The abundance of documents available online, for which content can be appropriated via a simple "copy and paste", gives renewed impetus to the issue of the correct use of bibliographic sources and references.

Thus, all of the following examples, drawn from the library of the Université de Québec à Montréal (UQAM), constitute plagiarism:

- Copying word for word a passage of a book, magazine or Web page without placing it within quotation marks and/or without stating the source;
- Including within a piece of work images, graphs, data etc. from external sources without indicating their source;
- Summarising an author's original idea in one's own words, but omitting the source;
- Translating in part or in whole a text without indicating its source;
- Re-using work produced in another class without prior authorisation from the teacher;
- Using another's work and presenting it as one's own (even with the person's permission).

Not only is plagiarism a lie to oneself, it also constitutes gross misconduct towards others. For this reason and according to a policy to prevent plagiarism, based on information and training, the École Centrale Nantes requires all producers of documentation (students and personnel) to undertake to carefully distinguish at all times between their own work and ideas and those borrowed from others. Sources and authors must be systematically cited.

École Centrale Nantes reserves the right to search for instances of plagiarism, including with the help of electronic tools. The perpetrators may face disciplinary or even criminal sanctions.

I undertake to distinguish explicitly in my academic and/or professional work, that which I borrowed from that which I produced, throughout my activities within and in the name of École Centrale Nantes.

THIS RULES HAVE TO BE FOLLOWED DURING YOUR ENTIRE STAY AT CENTRALE NANTES

SURNAME:

First Name:

At:

date:

Signature preceded by the handwritten words "lu et approuvé" (read and approved):

Table of Contents of the Thesis

Acknowledgements	iii
Ethics Code	v
List of Figures	x
List of Tables	xiv
Chapter 1. Introduction	1
1.1 SUP&R ITN project.....	1
1.1.1 Work packages	2
1.2 Justification of the thesis	3
1.3 Objectives.....	7
1.4 Scope of research.....	8
1.5 Introduction (Français).....	10
Chapter 2. Literature Review	13
2.1 Terminology	13
2.2 Asphalt mixtures.....	13
2.2.1 Materials	14
2.2.2 Properties of asphalt mixtures	16
2.2.3 Viscoelasticity of asphalt mixtures	17
2.2.4 Mixture design.....	22
2.3 Manufacturing procedures	25
2.3.1 Warm mix asphalt procedures	26
2.4 Reclaimed materials.....	32
2.4.1 RAP procedures	32
2.4.2 RAP characteristics.....	34
2.5 Bitumen	36
2.5.1 Origin and manufacture.....	36
2.5.2 Structure and composition.....	37
2.5.3 Bitumen evolution	41
2.6 Ageing detection	43
2.6.1 Ageing indicators and analysis techniques.....	44
2.6.2 Ageing simulation in laboratory	45
Chapter 3. Physico-chemical study of bitumen.....	49
Résumé du chapitre.....	49

3.1	Introduction.....	50
3.2	Materials, methods and experimental program	50
3.2.1	Materials	50
3.2.2	Chemical characterization.....	54
3.2.3	Physical characterization.....	56
3.2.4	Synthesis of the chemical and physical tests	58
3.2.5	Modelling.....	58
3.2.6	δ -method calculus.....	59
3.3	Testing results	61
3.3.1	Asphaltenes and malthenes characterization	61
3.3.2	Validation of the recomposition protocol.....	68
3.3.3	Model bitumens at different m/a ratios	76
3.3.4	Laboratory aged bitumens	84
3.3.5	Relationship between laboratory ageing and model bitumens.....	89
3.4	Conclusions	91
Chapter 4. Ageing evolution of warm mix asphalts combined with reclaimed asphalt pavement .		93
.....		93
Résumé du chapitre.....		93
4.1	Introduction.....	95
4.2	Materials and methods.....	96
4.2.1	Mixtures	96
4.2.2	Materials	97
4.2.3	Ageing procedure.....	100
4.2.4	Laboratory testing	101
4.2.5	Modelling and δ -method representation.....	103
4.3	Analysis of results	104
4.3.1	Influence of manufacturing technique	105
4.3.2	Influence of ageing.....	110
4.3.3	Influence of RAP addition	115
4.3.4	Ageing on mixtures with RAP	120
4.3.5	Evaluation of materials for recycling.....	125
4.4	Conclusions	128
Chapter 5. Correlation between structure and mechanical performance		131
Résumé du chapitre.....		131
5.1	Introduction.....	132

5.2	Model bitumen correlations.....	132
5.2.1	Materials and Methods.....	132
5.2.2	Model parameters vs Bitumen chemistry.....	133
5.2.3	R _{value} and w(co) influence.....	138
5.2.4	SHRP parameters	139
5.3	Correlation between bitumen and asphalt mixture.....	141
5.3.1	Materials and Methods.....	141
5.3.2	Bitumen/Mixture properties relationship.....	141
5.3.3	Huet-Such parameters relation	144
5.3.4	Parameters from Huet-Such versus 2S2P1D	150
5.3.5	SHRP parameters	156
5.4	Conclusions	161
Chapter 6.	Conclusions and perspectives.....	163
6.1	Final conclusions	163
6.2	Recommendations for future research.....	166
6.3	Conclusions finales	167
References	171
ANNEXES	181

List of Figures

Figure 1-1 Principal partners of the SUP&R ITN project	1
Figure 1-2 Evolution of road infrastructure and road maintenance investment in selected countries [2]	4
Figure 1-3 Total production of asphalt mixtures and warm mix asphalts in Europe and USA from 2007 to 2015 [4]	5
Figure 1-4 Total reclaimed asphalt pavement available in Europe and USA [4]	6
Figure 2-1 Conventional asphalt mixture [4]	14
Figure 2-2 Aggregates for asphalt mixture manufacture	15
Figure 2-3 Example of natural and refined bitumen for asphalt mixture manufacture (<i>from google images</i>)	15
Figure 2-4 Material response to a step load (a) Load, (b) Elastic, (c) Viscous, (d) Viscoelastic. Figure taken from Woldekidan Thesis [16]	18
Figure 2-5 Example of master curves of complex modulus (left) and phase angle (right) for a single bitumen	20
Figure 2-6 Summary of the different testing levels	23
Figure 2-7 Level 2 testing devices and mixture slab	24
Figure 2-8 Level 3 and 4 testing devices and fatigue principles [34]	25
Figure 2-9 Managing pavement maintenance and rehabilitation by monitoring riding quality [46]	32
Figure 2-10 Example of nomogram for determining the maximum possible RAP addition [45]	34
Figure 2-11 RAP stockpile ready to be use on mixture manufacture	35
Figure 2-12 Distillation process diagram [62]	37
Figure 2-13 General diagram of fractioning [60]	38
Figure 2-14 Sol and Gel types of bitumens [63]	39
Figure 2-15 SARA fractions, Saturates, Aromatics, Resins and Asphaltenes	41
Figure 2-16 Asphaltenes-Resins transfer [58]	42
Figure 2-17 Asphalt molecules normally present or formed on oxidative ageing, from Petersen (1984) [72]	43
Figure 2-18 Penetration test on bitumen	44
Figure 2-19 Softening point test on bitumen	45
Figure 3-1 Asphaltenes centrifugation and drying, and malthenes recovery	52
Figure 3-2 Asphaltenes and malthenes for bitumen recomposition	52
Figure 3-3 Model bitumens studied by malthenes (M) and asphaltenes (A) content	53
Figure 3-4 Flowchart followed on model bitumens	53
Figure 3-5 Iatroscan MK-6s device used for SARA fractions determination	55
Figure 3-6 Atomic force microscope Multimode™ with a detail of sample position	56
Figure 3-7 PP25 and PP08 geometries used for the testing	57
Figure 3-8 GPC standards for curve calibration	58
Figure 3-9 Bitumen testing protocols	58
Figure 3-10 Huet-Such model, equation and Cole-Cole representation	59
Figure 3-11 Example of curve $cumf(MW)$ and $\delta(AMW)$ [91]	60
Figure 3-12 Analysis of results and discussion schema followed	61
Figure 3-13 ATR-FTIR spectra from malthenes and asphaltenes phases	62

Figure 3-14 TGA diagram from 35/50 and 50/70 asphaltenes fraction	63
Figure 3-15 35/50 Malthenes phase PP25 and PP08 results at 15°C	64
Figure 3-16 35/50 Malthenes phase PP25 and PP08 results at 10°C	65
Figure 3-17 35/50 Malthenes phase PP25 and PP08 results at 0°C	65
Figure 3-18 35/50 100M master curve fitting from DSR measurements at T=0°C ...	66
Figure 3-19 35/50 malthenes fitting model curves	66
Figure 3-20 Master curves at T=0°C of (a) 35/50 and 50/70 Malthenes phase	67
Figure 3-21 δ -method diagrams of 35/50 and 50/70 malthenes fractions	67
Figure 3-22 ATR-FTIR spectrum from 35/50 and 50/70 Neat bitumens	69
Figure 3-23 ATR-FTIR bitumens and solvent spectrum.....	69
Figure 3-24 (a) SARA fractions from neat and recomposed model bitumens, (b) Colloidal indexes of all bitumens.....	71
Figure 3-25 Microstructure of 35/50 Neat and 35/50 85M+15A samples: AFM topography images of 50x50 μm^2 and 20x20 μm^2 after 4 days conditioning	72
Figure 3-26 Master curves at T=0°C of (a) 35/50 Neat and 35/50 85M+15A and (b) 50/70 Neat and 50/70 86M+14A	73
Figure 3-27 δ -method diagrams of 35/50 and 50/70 Neat and model bitumens.....	74
Figure 3-28 GPC plots from 35/50 Neat and 35/50 85M+15A	75
Figure 3-29 ATR-FTIR model bitumens and solvent spectrum.....	76
Figure 3-30 SARA fractions from 35/50 and 50/70 model bitumens.....	78
Figure 3-31 AFM results on 35/50 model bitumens after 4 days at 40°C	79
Figure 3-32 Master curves at T=0°C of (a) 35/50 model bitumens, and (b) 50/70 model bitumens.....	80
Figure 3-33 δ -method diagrams of (a) 35/50 model bitumens, and (b) 50/70 model bitumens	81
Figure 3-34 GPC plots from 35/50 model bitumens.....	82
Figure 3-35 ATR-FTIR spectra from RTFOT and PAV aged bitumens	84
Figure 3-36 SARA fractions from 35/50 and 50/70 aged bitumens	86
Figure 3-37 Master curves at T=0°C of 35/50 bitumens.....	86
Figure 3-38 (a) δ -method diagrams of 35/50 aged bitumens and (b) Cross-over frequencies by asphaltene content.....	87
Figure 3-39 GPC plots from 35/50 aged bitumens	88
Figure 3-40 Polydispersity of 35/50 aged bitumens	88
Figure 3-41 ATR-FTIR spectra from 35/50 80M+20A and PAV bitumens	89
Figure 3-42 Master curves at T=0°C from 35/50 80M+20A and PAV bitumens	90
Figure 3-43 δ -method (a) and GPC (b) curves from 35/50 80M+20A and PAV bitumens	91
Figure 4-1 Mixtures gradations with and without RAP	97
Figure 4-2 Mixtures manufacture procedure for bitumen extraction and mixture testing.....	101
Figure 4-3 Mixtures testing protocols.....	102
Figure 4-4 Bitumen testing protocols.....	103
Figure 4-5 R_{value} and $w(\text{co})$ determination from Black diagram and phase angle diagram.....	103
Figure 4-6 Analysis of results flowchart.....	104
Figure 4-7 Fatigue laws and 95% interval confidence of HMA, WMA and FWMA mixtures	106

Figure 4-8 Penetration and Softening point trend by manufacturing process	107
Figure 4-9 Master curve construction at 0°C for 35/50 Neat bitumen.....	107
Figure 4-10 Recovered bitumen after manufacture master curves at 0°C	108
Figure 4-11 δ -method diagram of recovered bitumens after manufacture	109
Figure 4-12 R_{value} compared in terms of $I_{co}(\%)$ (a) and cross-over frequencies (b)	110
Figure 4-13 Fatigue laws and 95% interval confidence of aged HMA, WMA and FWMA mixtures	112
Figure 4-14 Penetration and Softening point trend after ageing	113
Figure 4-15 Recovered bitumen after ageing master curves at 0°C	114
Figure 4-16 δ -method diagram of recovered bitumens after ageing.....	114
Figure 4-17 R_{value} compared in terms of $I_{co}(\%)$ (a) and cross-over frequencies (b) before and after ageing.....	115
Figure 4-18 Fatigue laws and 95% interval confidence of mixtures with RAP: HMA50, WMA50 and FWMA50	117
Figure 4-19 Penetration and Softening point trend after RAP addition	118
Figure 4-20 Recovered bitumen after 50%RAP mixtures manufacture master curves at 0°C.....	118
Figure 4-21 δ -method diagram of recovered bitumens of RAP mixtures after manufacture	119
Figure 4-22 R_{value} compared in terms of $I_{co}(\%)$ and cross-over frequencies before and after RAP addition	120
Figure 4-23 Fatigue laws and 95% interval confidence of aged HMA50, WMA50 and FWMA50 mixtures after ageing.....	121
Figure 4-24 Penetration and Softening point trend after ageing on RAP mixtures	122
Figure 4-25 Recovered bitumen after ageing on 50%RAP mixtures master curves at 0°C.....	123
Figure 4-26 Fatigue laws and AMWD of HMA, WMA and FWMA technique with 50% of RAP at the end of life situation	124
Figure 4-27 R_{value} compared in terms of $I_{co}(\%)$ and cross-over frequencies before and after ageing on mixtures with RAP	124
Figure 4-28 Penetration and softening point evolution of all mixtures	126
Figure 4-29 Penetration and softening point from available RAP materials	126
Figure 4-30 δ -method diagrams for aged mixtures with 0% and 50% of RAP	127
Figure 4-31 R_{value} analysis of all available aged materials	128
Figure 5-1 Schema of the chapter	132
Figure 5-2 Parameters β and $\tau(s)$ represented in function of saturates	135
Figure 5-3 Parameters β and $\tau(s)$ represented in function of aromatics.....	135
Figure 5-4 Parameters β and $\tau(s)$ represented in function of c7-asphaltene content	136
Figure 5-5 Parameters β and $\tau(s)$ represented in function of i-asphaltenes	136
Figure 5-6 Parameters β and $\tau(s)$ represented in function of the colloidal index ..	137
Figure 5-7 Parameters β and $\tau(s)$ represented in function of the polydispersity ...	137
Figure 5-8 Parameters β and $\tau(s)$ represented in function of the rheological value	138
Figure 5-9 Parameters β and $\tau(s)$ represented in function of the crossover frequency	138

Figure 5-10 Rutting and fatigue parameters evolution with temperature	140
Figure 5-11 Critical temperatures for rutting and fatigue parameters	140
Figure 5-12 Influence of bitumen penetration and softening point on $ E^* $ at 15°C 10 Hz	143
Figure 5-13 Influence of bitumen penetration and softening point on ε_6	143
Figure 5-14 Influence of bitumen index carbonyl on (a) ε_6 and (b) $ E^* $ at 15°C 10 Hz	144
Figure 5-15 Metravib® device and complex modulus testing description	145
Figure 5-16 Relationship between Kinexus® and Metravib® Huet-Such parameters	149
Figure 5-17 2P2S1D model, equation and Cole-Cole representation, from Olard 2003 [22,24]	150
Figure 5-18 2PB complex modulus test results on HMA0 mixture (a) $ E^* $ (MPa), (b) δ (°), (c) WLF shift factors, and (d) Cole-Cole 2S2P1D model fitting	151
Figure 5-19 Shift-Homothety-Shift in time-Shift transformation (SHStS) [134]	151
Figure 5-20 SHStS transformation on HMA asphalt mixtures and recovered bitumens	152
Figure 5-21 Relationship between model mixtures and bitumens parameters	155
Figure 5-22 Relationship between C_1 and C_2 from mixtures and bitumens modelling	156
Figure 5-23 Rutting critical temperatures on mixtures without RAP (a) and with 50% RAP (b)	157
Figure 5-24 Influence of rutting critical temperature on penetration (a) and softening point (b) results	158
Figure 5-25 Fatigue critical temperatures on mixtures without RAP (a) and with 50% RAP (b)	159
Figure 5-26 Influence of carbonyl index on rutting (a) and fatigue (b) critical temperatures	159
Figure 5-27 Influence of RAP addition of the fatigue/rutting parameters relationship	160

List of Tables

Table 2-1 LVE models for bituminous materials [22,23]	21
Table 2-2 Resume of Foaming WMA commercial processes obtained from producers websites	28
Table 2-3 Resume of Organic additives WMA commercial processes obtained from producers websites	30
Table 2-4 Resume of Chemical additives WMA commercial processes obtained from producers websites	31
Table 2-5 From Airey 2003, chronological bitumen ageing methods [76]	46
Table 2-6 From Airey 2003, chronological asphalt mixture ageing methods [76]	47
Table 3-1 Base bitumens of the study	51
Table 3-2 Aged bitumens studied by malthenes and asphaltenes content	54
Table 3-3 Neat bitumens a/m ratio	62
Table 3-4 SARA fractions of malthenes and asphaltenes of 35/50 and 50/70 bitumens.....	63
Table 3-5 Neat and model bitumens a/m ratio	68
Table 3-6 ATR-FTIR analysis of Ico and Iso values	70
Table 3-7 SARA fractions of neat and recomposed bitumens	70
Table 3-8 Molecular weights of 35/50 bitumens.....	75
Table 3-9 ATR-FTIR analysis of Ico and Iso values of 35/50 model bitumens	77
Table 3-10 SARA fractions and colloidal indexes of 35/50 and 50/70 model bitumens.....	78
Table 3-11 Polydispersity of 35/50 model bitumens	83
Table 3-12 Aged bitumens m/a ratio on n-heptane determination	84
Table 3-13 ATR-FTIR analysis of Ico and Iso values of aged bitumens	85
Table 3-14 SARA fractions and colloidal indexes of 35/50 and 50/70 aged bitumens	85
Table 3-15 Polydispersity on 35/50 aged bitumens	88
Table 3-16 ATR-FTIR analysis of Ico and Iso values from 35/50 80M+20A and PAV bitumens...	89
Table 3-17 SARA fractions from model and aged bitumens at the highest asphaltene content.....	90
Table 4-1 Mixtures studied and manufacturing temperature	97
Table 4-2 Base bitumen of the study	98
Table 4-3 Virgin aggregates properties.....	98
Table 4-4 RAP characteristics	99
Table 4-5 RAP bitumen properties [115]	100
Table 4-6 Influence of manufacturing technique on the mechanical performance.	105
Table 4-7 Influence of ageing on the mechanical performance of the different techniques	110
Table 4-8 Influence of RAP addition on the mechanical performance of the different techniques	116
Table 4-9 Influence of ageing on the characteristics of the mixtures with RAP	120
Table 4-10 Characteristics from 0%RAP aged and 50%RAP aged mixtures following EN 13108-8.....	125
Table 5-1 Materials and results selected from Chapter 3	133
Table 5-2 Resume of results for Chapter 3 bitumens	133

Table 5-3 Chapter 3 bitumen parameters	134
Table 5-4 Materials selected from Chapter 3 for further analysis.....	141
Table 5-5 Principal results from asphalt mixtures and extracted bitumens testing	142
Table 5-6 Extracted bitumens parameters from Kinexus® testing.....	146
Table 5-7 Extracted bitumens parameters from Metravib® testing	147
Table 5-8 Asphalt mixtures parameters from complex modulus 2S2P1D modelling	153
Table 5-9 SHRP bitumens tested and compared	157

Chapter 1. Introduction

The research presented in this document has been carried out as part of the European project Sustainable Pavement and Railway Initial Training Network Project (SUP&R ITN)

1.1 SUP&R ITN project

SUP&R ITN project is an EU-funded Marie Curie project that offered a training-through-research programme to 15 selected young researchers across Europe. The SUP&R ITN network comprises industry and research partners who complement each other to bring together the necessary scientific and professional power needed to provide high quality training and cutting edge research in designing sustainable transport infrastructure technologies.



Figure 1-1 Principal partners of the SUP&R ITN project

The university partners are present in four different European countries. The University of Nottingham in England, the University College of Dublin in Ireland, the University of Palermo in Italy and the University of Huelva and University of Granada in Spain.

Then, the industry partners cover the whole stakeholder chain of road pavements and railways from transport infrastructure managers (IRAIL, ADIF, NR), engineering designers (AECOM), research institutions (IFSTTAR), contractors (SACYR, EIFFAGE TP) and manufacturers (REPSOL, NYNAS, AKZO, AI, PI). This consortium is complemented by partners ranging from research and training bodies (TUD, UW, VTTI). Professional European Associations (CEDR, EAPA, ECOPN, EIM), experts in sustainability (GR, CEEQUAL), online training of sustainability (ILL) and communication in transport engineering field (FEHRL).

The project focuses on investigating promising pavements and railway technologies with practical methods, models and tools for estimating their sustainability. The SUP&R ITN programme achieved these results by developing inter-linked research projects aiming at:

- Developing new sustainable technologies and materials for use in road pavements (highways) and railway transport infrastructure (standard railway infrastructure or high speed railways).
- Providing advanced characterisation of recycled and reused materials generated from road and railway infrastructure and/or other production processes for use in road and railway infrastructure.
- Developing detailed material modelling and design approaches for immediate uptake by industrial stakeholders working in the area of transport infrastructure.
- Developing and refining estimation tools so that industry can assess where it currently stands in key sustainability indicators and determine how much it can improve using low-energy and more recycled materials. Such estimation tools will allow industry, road and railway agencies to recognize the sustainability of different construction techniques, materials and methods, as well as the potential cost and resource savings enabling the deployment of more sustainable technologies.

1.1.1 Work packages

The project is divided in three work packages according to the main objectives of the project: The study of sustainable pavement solutions, the study of sustainable railway technologies, and the integration of both in a tool for decision making. This software will allow users to decide the most sustainable solution on their projects.

Work package 1 is focuses on investigating several sustainable technologies for road pavements. The six different projects are listed below. In black the name of the project that has inspired this thesis work.

- Project 1.1 (ESR1) : Pavement design for cold in-situ recycled materials
- Project 1.2 (ESR2) : Design and characterization of bituminous mixes manufactured with biomass
- **Project 1.3 (ESR3) : Long term performance of low-temperature asphalt mixes containing reclaimed asphalt**
- Project 1.4 (ESR4) : Rubberised binder and asphalt mixes for wearing course
- Project 1.5 (ESR5) : Binder design for low-temperature asphalt mixes
- Project 1.6 (ESR6) : Half Warm Mixes Asphalt Recycling Asphalt in urban roads

Then, work package 2, which is focused on studying several sustainable technologies for railway infrastructure, included the following projects:

- Project 2.1 (ESR7) : Optimization of track bed design and maintenance
- Project 2.2 (ESR8) : Characterisation of rubberised asphalt for railways sub-ballasts
- Project 2.3 (ESR9) : Modelling and Design of rubberised asphalt for railways sub-ballast
- Project 2.4 (ESR10) : Settlement monitoring and prediction in railway tracks
- Project 2.5 (ESR11) : Optimisation techniques for geophysical assessment of rail support structures
- Project 2.6 (ESR12) : The use of waste materials in railways

Finally, work package 3 which is focused on the definition of a methodology and the creation of a tool to perform a broad sustainability assessment of the technologies investigated in WP1 and WP2. This tool will be based on environmental Lifecycle Assessment (LCA) that will incorporate cost analysis and social sustainability metrics together with a comprehensive set of economic, social, and environmental indicators. This part of the project also included three tasks, covered by postdoctoral students.

- Project 3.1 (ER1) : Definition of sustainability assessment factors and current state-of-the-art in sustainable practices
- Project 3.2 (ER2) : Sustainability assessment of Railways and SUP&R ITN technologies
- Project 3.3 (ER3) : Life cycle impact assessment of Road and Railway Practices – methodology and tools

Within the basis of the SUP&R ITN project, ESR3 research project has become also a thesis.

1.2 Justification of the thesis

In this new era made of invisible communication networks where we are all connected worldwide, roads still remain as the most widely used mode of transportation in the world. Even more when countries development is often measured in terms of its total paved roads mileage.

Road construction is a major industry in developing countries. Besides, as the infrastructure matures, it will be a major industry in developed countries as well [1]. Pavements are an essential part of our social network and asphalt concrete is the main material used for manufacturing them. Transport in Europe moved a total of 1.3 billion euros, which 46.6%

comprised any kind of pavement uses, giving a total impact of roads of 0.6 billion euros on the overall transport system (Data from European Road Federation, 2011 [2]).

Currently, the European road network is not much growing anymore (5,525 million km of paved roads [2]) and mostly needs maintenance. The budget for road maintenance by the EU is been decreasing since 2008. This trend resumed in Figure 1-2 could endanger the future of the infrastructure system.

In a context of increasing demand of performance and durability of asphalt mixtures, a sustainable, durable and economical conception is required. Indeed, it could be oriented towards a self-sufficient road providing its own raw materials through recycling while limiting the use of energy and other natural resources for its maintenance.

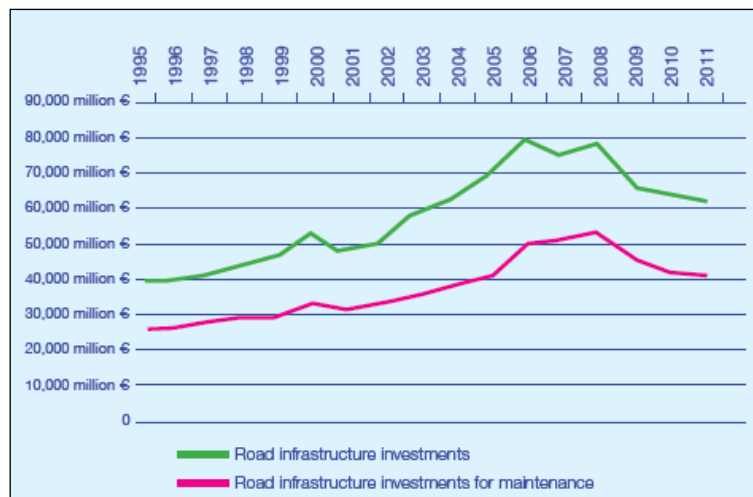


Figure 1-2 Evolution of road infrastructure and road maintenance investment in selected countries [2]

Towards a saving in energy consumption and an emission limitation: warm processes

Conventionally, asphalt mixtures production (HMA) for road construction involves high manufacturing temperatures (~ 160°C) which require a high consumption of energy. These high temperatures also lead to emissions of volatile organic compounds (VOCs) likely to harm the health of workers in a context of greatly reduced social acceptability of occupational risks [3].

Solutions at lower temperatures have been developed by the road industry but, unlike in the United States, these so-called "warm" (WMA) procedures are struggling to establish themselves in Europe. Figure 1-3 illustrates the trend of asphalt mixtures manufacturing (HMA and WMA) from 2007 to 2015 and the production of WMA mixtures in Europe and USA.

In 2015 warm mix processes only represent 2% of the European production of asphalt, while in the USA it has been increasing up to 33% of the total production [4]. This technique must assure

aggregates coating, the stability during production and transportation, and workability during on site lay out, not forgetting enough mechanical performance during service life [5].

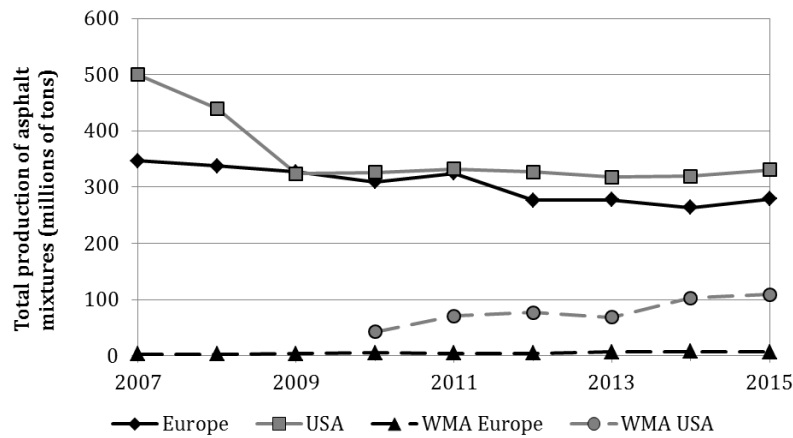


Figure 1-3 Total production of asphalt mixtures and warm mix asphalts in Europe and USA from 2007 to 2015 [4]

As a result, recent pavement industrial developments have been directly linked with temperature reduction in the production process. Warm mix asphalts are manufactured in the temperature range of production of 110°C to 140°C by mainly three different procedures. They are bitumen foaming and the use of chemical or organic additives.

In general, these types of mixtures present several benefits such as reductions on fuel consumption and emissions, as well as an increase of the hauling distances and extended paving period. On the other hand, they present potential problems linked to plastic deformations, water sensitivity and durability [6,7].

Towards the preservation of resources: recycling

European road network could be described as mature in the sense that, after a continuous increase throughout the last century, it no longer requires significant extension. This stabilization is translated into an increasing proportion of road maintenance works to ensure the sustainability of the existing system.

Additionally, by evolving from a production policy to a maintenance approach, road construction has opened up widely for recycling. Indeed, the degradation of a pavement structure does not mean irreversible degradation of the properties of the materials which constitute it. With adapted techniques, these materials after the end of the pavements service life can be recycled in new structures.

In consequence, the ideal situation would include a self-sufficient system. So then, it would produce necessary materials for its maintenance without subtraction from natural resources. In Figure 1-4, the available reclaimed material from 2007 to 2015 in Europe and USA is illustrated.

However, even if under voluntary agreement of road stakeholder's recycling rates have increased significantly in recent years, it is still limited. In Europe, there are on average 50 million tonnes of RAP available per year, but it is mainly re-used throughout conventional procedures, and still at rather low rates of addition [4]. In contrast, in the USA this percentage of addition in the mixtures has been increasing up to integrate 95% of all the available reclaimed asphalt material [4]. In the first place, the substitution approach without input of raw materials could not be generalized because it would imply 100% recycling. Still, performances are not yet technically mastered [8].

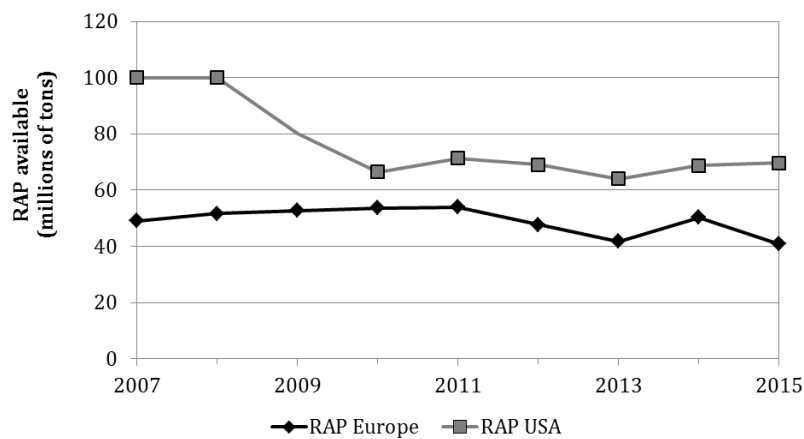


Figure 1-4 Total reclaimed asphalt pavement available in Europe and USA [4]

In the particular case of maintenance works on the French road network, RAP generation is only about 7 Mt annually, whereas the corresponding production of asphalt mixtures is about 31.5 Mt (data from 2015 [4]). Besides, several issues could be remarked. Firstly, French natural aggregates are of extreme quality and at low production costs. In this context, economic incentives to invest in recycling are less powerful than in countries that have a lack of raw materials, such as Iceland or the Netherlands. Secondly, current recycling techniques are generally based on formulation studies designed for new materials. This means that the reclaimed asphalt is roughly characterized and it is considered as disruptive additive material. Then, RAP addition is usually limited in the interest of not modifying the properties of the new mixture. Consequently, the remarkable specific properties of the reclaimed aggregates are not fully engaged and then the rates of addition restricted.

A new track of progress: Recycling and Warm mix asphalts techniques combination

The environmental impact of road construction could still be significantly improved by parallel improvements in recycling techniques and warm mix asphalts procedures. But then again the margin for progress seems much more important if the two developments are combined. It is therefore necessary to redefine and make more reliable the recycling techniques in the specific context of the WMA processes.

Separately, WMA procedures and RAP addition to the mixtures have been widely used. However, innovation related to their combined application is still ambiguous, mainly because of their long term performance. Both techniques present their own benefits. They are considered more environmentally friendly in terms of reduced greenhouse gases emissions, extraction of natural aggregates or disposal in landfill of old pavements [6,7]. On the other hand, concerning durability, rutting or low temperature resistance, their service life could compromise [8–11].

1.3 Objectives

The main objective of this research is to determine the possible application of high rates of reclaimed asphalt pavement under warm mix asphalt technique for providing a sustainable solution to road construction. With the aim of developing this objective in more detail, this thesis has the following secondary operational goals:

- i. The characterization of ageing evolution through the increment of asphaltenes phase concentration on bitumen,
- ii. The study and analysis of mechanical performances in laboratory of a conventional hot mix asphalt in order to serve as reference mixture,
- iii. The addition of 50% of reclaimed asphalt mixture when manufacturing mixtures under foaming warm mix asphalt technique,
- iv. Assessment of ageing or rejuvenation rheological behaviour of bitumen through the δ -method analysis,
- v. Influence of bitumen evolution on Huet-Such model parameters,
- vi. And finally, establishing a possible relationship between bitumen properties and asphalt mixture performances.

1.4 Scope of research

The scope of the thesis consists of a literature review followed by three chapters, each of them focusing on one of the three objectives of the thesis, bitumen, asphalt mixtures and their possible relationship. A final chapter presents the conclusions and perspectives for future research works.

The literature review describes in general terms the asphalt mixtures, their composition and the different existing levels of testing. Warm mix asphalt techniques and reclaimed asphalt pavements are described and presented. Moreover, deeper study is carried out with regard to physico-chemical structure, properties and characteristics of bitumen and its ageing procedures.

The main objectives of the thesis have been divided in three chapters. The first one (Chapter 3), focuses on the study of bitumen. The physico-chemical response of the material is characterized with regards to the evolution of the asphaltene content during ageing. So, in order to understand these effects, laboratory ageing procedures are performed.

Additionally, bitumen mechanical behaviour is usually evaluated by standard empirical tests (penetrability and softening point temperature). These tests are used to classify bitumen according to their consistency. However, they do not provide the intrinsic properties of bitumen. For these reasons, chemical and physical characterisation is carried out. For the chemical evaluation, the Fourier transform infrared analysis, thermogravimetric analysis and thin layer chromatography for SARA fractions determination are performed. Whereas bitumen solubility in n-heptane, gel permeation chromatography, atomic force microscopy and rheological testing are used to evaluate the physical evolution and performance of the materials.

In the second chapter (Chapter 4), mechanical performance evolution of asphalt mixtures is developed. Ageing current knowledge is essentially gained from practical experience on traditional asphalt mixes and typically on HMA. However, as the WMA are relatively new techniques, so little is known about their ageing evolution and end of life state, especially when they are combined with RAP.

Within this framework, the objective of this chapter is to study and compare two WMA techniques when 50% of RAP is added to the mixture. For that reason, an ageing protocol is followed within the lines proposed by the RILEM TC-ATB TG5, consisting of two separate ageing phases. Mixtures long term related performances are compared by means of complex modulus and fatigue testing. Penetration and ring and ball tests are undertaken on the recovered bitumen. Ageing evolution is also characterised by the Fourier Transform Infrared analysis and evaluated through the δ -method analysis.

Finally, the last chapter is focused on comparing the mechanical related performance of the mixtures and its bitumen evolution. The evaluation is developed in terms of SHRP parameters, δ -method parallel analysis of curves and relation between critical design factors.

1.5 Introduction (Français)

Objectifs

L'objectif principal de cette recherche est d'évaluer les possibilités offertes par la combinaison du recyclage d'agrégats d'enrobé à taux élevés et les techniques tièdes de fabrication des enrobés pour fournir une solution durable à la construction routière. De façon plus détaillée, cette thèse a les objectifs opérationnels secondaires suivants:

- i. La caractérisation de l'évolution du vieillissement par le suivi de l'augmentation de la teneur en asphaltènes du bitume,
- ii. L'étude et l'analyse des performances mécaniques en laboratoire d'un enrobé classique à chaud, choisi comme enrobé de référence,
- iii. L'addition de 50% d'agrégats d'enrobé lors de la fabrication d'enrobé pour la technique tiède à la mousse de bitume,
- iv. L'évaluation de l'effet du vieillissement ou de la régénération sur le comportement rhéologique du bitume à travers la δ -méthode,
- v. L'influence de l'évolution du bitume sur les paramètres du modèle Huet - Such,
- vi. Et enfin, établir une éventuelle relation entre les propriétés du bitume et les performances des enrobés bitumineux.

Portée de la recherche

La structure de la thèse comporte une étude bibliographique suivie de trois chapitres, chacun d'eux se concentrant sur l'un des trois objectifs de la thèse, le bitume, les enrobés bitumineux et leur éventuelle relation. Un dernier chapitre présente les conclusions et les perspectives pour les travaux de recherche futurs.

L'état de l'art décrit en termes généraux les enrobés bitumineux, leur composition et les différents niveaux d'essais existants. Les techniques d'enrobage tièdes et l'utilisation des agrégats d'enrobés sont décrits et présentés. En outre, une étude plus détaillée est réalisée en ce qui concerne la structure physico-chimique, les propriétés et les caractéristiques du bitume et ses procédures de vieillissement.

Les principaux objectifs de la thèse ont été divisés en trois chapitres. Le premier (chapitre 3) se concentre sur l'étude du bitume. La réponse physico-chimique du matériau est caractérisée par l'évolution de la teneur en asphaltène pendant le vieillissement. Ainsi, pour comprendre ces effets, des procédures de vieillissement en laboratoire sont appliquées.

Le comportement mécanique du bitume est généralement évalué par des essais empiriques (pénétrabilité et température du point de ramollissement bille anneau). Ces tests sont utilisés pour classer le bitume selon leur consistance. Cependant, ils ne fournissent pas les propriétés intrinsèques du bitume. Pour ces raisons, une caractérisation chimique et physique est effectuée. Pour l'évaluation chimique, l'analyse par infrarouge, l'analyse thermogravimétrique et la chromatographie en couche mince pour la détermination des fractions SARA sont utilisées. Pour évaluer l'évolution physique et la performance des matériaux, on utilise la solubilité du bitume dans le n-heptane, la chromatographie par perméation de gel, la microscopie à force atomique et les tests rhéologiques.

Dans le deuxième chapitre (chapitre 4), l'évolution des performances mécaniques des enrobés est étudiée. Les connaissances actuelles sur le vieillissement des enrobés sont essentiellement tirées de l'expérience acquise sur les enrobés traditionnels et généralement sur les enrobés à chaud. Cependant, comme la procédure tiède est une technique relativement nouvelle, leur évolution avec le vieillissement et leur état de fin de vie est mal connue, surtout lorsqu'ils sont combinés avec les agrégats d'enrobé.

Dans ce cadre, l'objectif de ce chapitre est d'étudier et de comparer deux techniques tièdes lorsque 50% d'agrégats d'enrobé sont ajoutés au mélange. Pour cette raison, un protocole de vieillissement constitué de deux phases de vieillissement séparées est suivi conformément à la procédure proposée par le RILEM TC-ATB TG5. Les performances à long terme des enrobés sont comparées au moyen des essais de module complexe et de fatigue. Des essais de pénétration et de bille-anneau sont aussi effectués sur le bitume récupéré. L'évolution du vieillissement est également caractérisée par l'analyse infrarouge et évaluée par l'analyse de la δ méthode.

Finalement, le dernier chapitre se concentre sur la comparaison des performances mécaniques des enrobés et de l'évolution de leur bitume. L'évaluation est développée en utilisant les critères SHRP et l'analyse comparée des courbes obtenues par la δ méthode. Les relations entre les différents paramètres sont étudiées.

Chapter 2. Literature Review

2.1 Terminology

In British English *bitumen*, in American English *asphalt*, in French *bitume* and in Spanish *betún*, but all of them from the Latin word *bitūmen*. The etymology of the word asphalt comes from the early 14th century. It defined asphalt as *a hard, resinous mineral pitch found originally in Biblical lands*. From the Late Latin *asphaltum*, and from the Greek word *asphaltos* “*asphalt, bitumen*”. Another theory holds it to be from Greek *a-* “not” + *-sphaltos* “able to be thrown down”. Thus taken as verbal adjective of *sphallein* “to throw down”, in reference to a use of the material in construction. Later on, in the mid of the 15th century the word *bitumen* appeared, from Latin *bitumen* “*asphalt*”, probably from Celtic **betu-* “birch, birch resin” (compare Gaulish *betulla* “birch,” used by Pliny for the tree supposedly the source of bitumen).

The Collins Dictionary defines bitumen as *any of various viscous or solid impure mixtures of hydrocarbons that occur naturally in asphalt, tar, mineral waxes, etc, used as a road surfacing and roofing material*. Also, the American Society of Testing Materials (ASTM) defines asphalt as “*a dark brown to black cementitious material in which the predominant constituents are bitumens which occur in nature or are obtained in the petroleum processing*”.

In American English, the refined residue of the distillation process of a selected crude oil is called *asphalt* or *asphalt cement*. In Europe in contrast, *asphalt* has a different meaning, and it usually refers to the asphalt mixture, which combines bitumen with stone aggregates and is used as a paving material. So, outside of the United States, that black product is often called *bitumen*. In this thesis, European terms will be followed, *bitumen* for binder and *asphalt mixture* to the combination of bitumen and aggregates.

2.2 Asphalt mixtures

Road pavements are structures formed by a set of several centimetres thickness of horizontally superposed compacted layers, and composed of different materials [19]. Asphalt pavements are expected to perform adequately and be durable during their service life, without suffering any deterioration that could compromise safety, users comfort or the proper integrity of the road. In order to ensure this, pavements must be designed, constructed, maintained, and managed properly [1].

Commonly, the structure is divided in three layers of asphalt mixtures. From the bottom to the top are base, binder and surface layer. The base layer needs to be strong enough in flexion resistance and bearing capacity, but standard requirements are not the same as for the binder and surface mixtures. The binder layer is very similar to the surface layer, and it usually consists on the same type of mixture but with larger aggregates size. Finally, the layer on the surface of the pavement has to resist the maximum sollicitations and the changing atmospheric conditions (low temperatures, rain, heat, solar radiation...) [1].

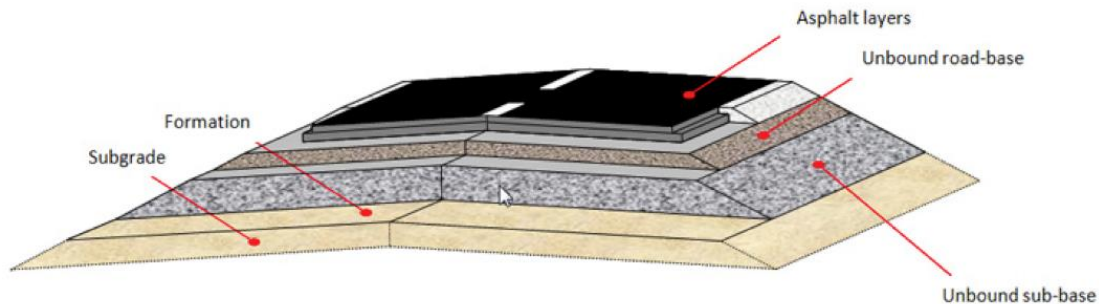


Figure 2-1 Conventional asphalt mixture [4]

Asphalt mixtures are composite materials. They are a combination of aggregates of different sizes (gravel, sand and filler) and binder from hydro-carbonate nature (i.e. bitumen). So that, all the aggregates particles get coated by a continuous and homogeneous thin film, providing the blend an adhesive effect that will keep it together [12].

2.2.1 Materials

Aggregates and filler

Aggregates provide the resistance to the system. They are particles from different nature and with different sizes that usually come from quarries operations. Their performance depends on both their physio-chemical composition and their granulometry distribution. Among the aggregate properties it could be highlighted their porosity, specific gravity, surface texture, shape, hardness and their alkalinity or acidity [13].

On the other hand, filler is in charge of cohesion, and it is defined as the smallest fraction. This means that is the material that passes the 0.063 mm width sieve (EN 13043). Filler can come from a natural source, from the crushing of aggregates or be an added material, which is the usually employed. In general, aggregates and filler represent between 94%-96% of the mixture by weight and 83%-87% by volume [13].



Figure 2-2 Aggregates for asphalt mixture manufacture

Hydrocarbon binder

Hydrocarbon binders are agglomerates of complex hydrocarbon chains with thermoplastic properties [13]. There are different types of hydrocarbon binders, such as asphaltic bitumens, fluxed bitumens or bituminous emulsions. Bitumen usually represents between 4%-6% by weight and 8%-12% by volume in the total mixture. This part will be further described in detail on Section 2.5.



**Figure 2-3 Example of natural and refined bitumen for asphalt mixture manufacture
(from google images)**

Air voids content

Although it is not a direct design input parameter most of the asphalt mixtures are designed to have certain air voids content after layout and compaction. They represent in regular mixtures between 3%-8% of the system by volume, but they can rise up to 20% in porous asphalt mixtures [13].

2.2.2 Properties of asphalt mixtures

Every asphalt mixture has their own intrinsic properties, so it is difficult to design an asphalt mixture that will fulfil all the properties due to the antagonism between some of them. However, the principal properties of an asphalt mixture and pavement could be the followings [13]:

- **Stability.** Capacity of the mixture to resist loads and strains on the tolerable limits. This mechanical resistance is the sum of the one produced by internal aggregates friction and the cohesion provided by the bitumen.
- **Resistance to plastic deformations.** The accumulation of small plastic deformations due to the repetitive loading at low speed and high temperature might happen when the characteristics of the mixture have not been well defined. This may lead to the damage of the pavement. For this purpose special attention should be taken on the filler/bitumen relation as well as on the chosen bitumen and the angularity of the aggregate.
- **Ravelling.** It is the loss of particles due to traffic loading when the resistance of the asphalt mixture is only provided by their internal friction. In order to avoid this anomaly the design of the mixture needs to provide enough cohesion and resistant to the action of water.
- **Skid resistance.** It is determined by the polishing resistance of the aggregates. It is necessary to choose aggregates with high polishing resistance and design a granulometry curve that may provide the adequate surface roughness texture.
- **Impermeability.** In order to avoid the presence of water on the granular layers underneath at least one of the pavement layers must be impermeable.
- **Durability.** Asphalt mixture layers, especially surface layers, need to be resistant to the action of traffic, solar radiation, bitumen ageing, and freeze and thaw cycles or vehicles loss of fuel...
- **Fatigue resistance.** Repetitive loading produce the progressive loss of performance of the material.

The exposure of asphalt mixtures during service to heavy traffic loads and climate effects would cause a deterioration of their properties that may result in the pavements loss of functionality. The different pathologies that road pavements could suffer can be classified in four principal groups as follows [14]:

- **Material displacements:**
 - Bleeding, it is the appearance of bitumen on the pavement surface.
 - Delamination, separation of layers, mainly top wearing course and the layer underneath.

- Material loss:
 - Potholes, bow-shaped holes.
 - Ravelling, loss of bitumen and displacement of aggregates.
 - Aggregates polishing, due to wearing away of the surface of the asphalt mixture.
- Deformations:
 - Corrugations, as a result of lack of stability on the mixture.
 - Rutting, plastic deformations.
- Cracking:
 - Fatigue cracks, due to repeated cycles loading.
 - Block cracking, mainly due to shrinkage of the asphalt mixture.
 - Edge cracks.
 - Longitudinal joint cracks.
 - Reflective cracking.
 - Slippage cracks.
 - Thermal cracks.

2.2.3 Viscoelasticity of asphalt mixtures

Due to the nature of bitumen, the mechanical performance of the asphalt mixture depends not only on the magnitude of the stress applied, but also how this stress is applied (particularly the speed and the temperature of loading). When the asphalt mixture is stressed on compression the friction between particles is opposite to their relative displacement. On the other hand, when the asphalt mixture is submitted to traction stress it is the bitumen which resists [15].

So then, asphalt mixtures could respond from a totally elastic behaviour (at cold temperatures and high loading speed rates, or high frequency) to a more viscous behaviour (at higher temperature and lower loading speed rates). In general, it could be assumed that asphalt mixtures behaviour is a sum of both responses, elastoplastic response for the aggregates and viscous response for the bitumen, evolving to a visco-elasto-plastic behaviour for the system, the asphalt mixture [12,15].

To have elastic response means that when a material with linear elastic characteristics is loaded it responds with in an immediate deformation. Thus, if the load increases linearly, deformation does as well. But once the load is removed, deformation is recovered and the material recovers its original position. Hooke postulated it in 1678 '*ut tension sic vis*', that means, *such as the extension so is the force*.

The proportionality factor that relates stress (loads) and strain (deformations) depends on the origins of the material, temperature, pressure and the type of stress applied. As so, different elastic modulus can be defined and considered constants for some solid materials [16]:

- Young Modulus (E). It establishes the proportional relation between normal stress and longitudinal strain, in simple compression or traction tests. $d\sigma = E \cdot d\varepsilon$
- Shear Modulus (G). It establishes the proportional relation between shear stress and shear strain. $d\tau = G \cdot d\gamma$
- Poisson Coefficient (ν). It establishes the inverse proportional relation between longitudinal strains and transversal strains in simple traction tests. $\varepsilon_t = -\nu \cdot \varepsilon_l$

And the three are related with the formula $G = \frac{E}{2(1+\nu)}$ In the case of only bitumen it is assumed a value of $\nu = 0.5$ as it is considered non-compressible at low temperatures [17].

In contrast, when the deformation increases linearly for a constant load the material is classified as viscous. Thus, the strain on the material remains after load removal. The fundamental equation for this type of materials is the Newton's viscosity law $\tau = \eta \cdot \dot{\gamma}$. In both cases, elastic and viscous, if the material follows Hooke's or Newton's law it can be considered as linear elastic or linear viscous. Otherwise it is called nonlinear [16].

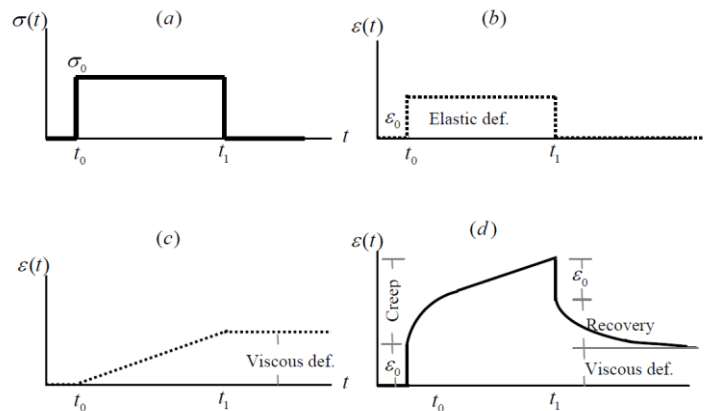


Figure 2-4 Material response to a step load (a) Load, (b) Elastic, (c) Viscous, (d) Viscoelastic. Figure taken from Woldekidan Thesis [16]

Then, viscoelastic materials as asphalt mixtures present characteristics from both behaviours. Firstly an immediate deformation against constants loads, followed by a continuously increasing strain with time. When the load is removed the elastic deformation is recovered while there is a rate of deformation that remains, it is called viscous deformation [16].

Complex modulus representation

Complex modulus ($|E^*|$ or $|G^*|$) of a linear viscoelastic material is the relationship between stress and strain at time dependent sinusoidal loading, i.e. when stress is applied $\sigma \sin(\omega t)$, deformation occurs $\varepsilon \sin(\omega(t-\delta))$ where δ is the phase angle relative to stress.

$$E^* = |E^*| (\cos(\delta) + i \sin(\delta))$$

In general different graphical representations are used to illustrate the variation of the norm of the complex modulus ($|E^*|$ or $|G^*|$) with frequency and temperature. The most common are the isothermal and isochronal curves, the cole-cole diagram and the black space diagram.

Isothermal curves represent the values of the norm of the complex modulus by the corresponding frequency for each temperature tested. On the other hand, isochronal plot illustrates the norm of the complex modulus at a certain temperature for each frequency tested.

The Cole-Cole plan is the representation of the variation of the viscous component of the complex modulus (E'' or G'') by the elastic component (E' or G'). This type of representation allows comparing different bitumens performances at low temperatures/high frequencies. Additionally, the black space diagram represents the norm of the complex modulus ($|E^*|$ or $|G^*|$) by their corresponding phase angle (δ). In this last case, this type of representation shows the different performances at high temperatures or low frequencies.

Time Temperature Superposition Principle

Another way of presenting complex modulus results is by their master curves. These type of curves let determining the complex modulus of the mixture or bitumen at frequencies or temperatures non reachable by experimental testing. In this case it is necessary to use the Time Temperature Superposition Principle (TTSP) [18]. This principle considers that longer periods of loading (or reduced testing frequencies) results in the same effects on the mechanical properties than an increase on the testing temperature.

This principle is based on the idea that the material structure do not evolve within a change of temperature or with the loading time [18]. Thus, considering bitumens as thermorheologically simple materials [19], this principle is applicable to the most of them. Considering the Black space as a singular curve that implies the absence of structural changes during a temperature variation. Then, the same pair of complex modulus and phase angle values could be obtained from different frequency-temperature sets, so that:

$$E^*(T_1, f_1) = E^*(T_2, f_2) = E^*(T_i, f_i)$$

$$E^*(T_i, f_i) = E^*(T_{ref}, \alpha((T_i, f_i)))$$

where T is the testing temperature and T_{ref} is the arbitrary reference temperature. Thus, the function $\alpha(T_i, f_i) = f_i \cdot a_T(T_i)$ represents the translation of the isothermal curve by multiplying the frequencies of each curve by the shift factor (a_T) of each tested temperature.

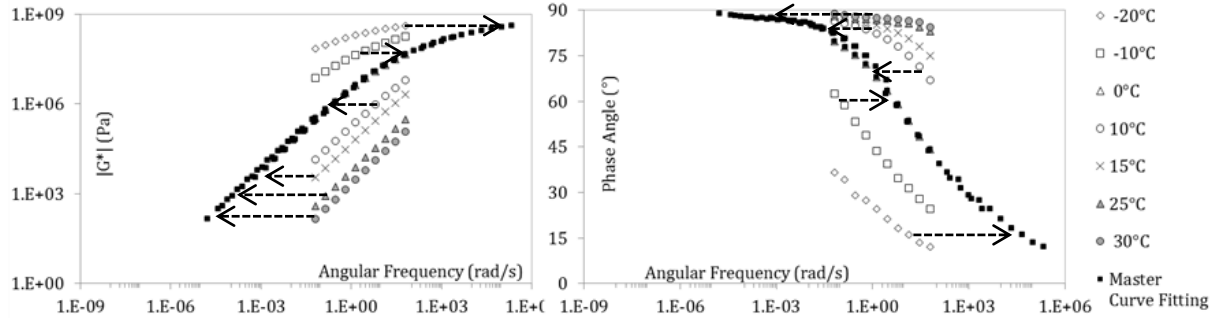


Figure 2-5 Example of master curves of complex modulus (left) and phase angle (right) for a single bitumen

The translational coefficients for each isotherm T to the reference temperature T_{ref} is a function of the logarithm of the shift factor, $\log(a_T)$, so:

$$E^*(\omega, T) = E^*(\omega \cdot a_T(T), T_{ref})$$

with $a_{T_{ref}} = 1$. Several formulas have been proposed for obtaining these logs (a_T). However, two equations are the most commonly used, the Arrhenius law [20] and the William-Landel-Ferry [18]. In this document the WLF equation is chosen for the construction of the master curves. C_1 and C_2 are constants that depend on the material and the reference temperature, T_{ref} .

$$\log a_T = \frac{-C_1(T - T_{ref})}{(T - T_{ref}) + C_2}$$

Based on a series of hypotheses on the mechanical response of the material, in particular Boltzmann's superposition principle and the principle of causality, Chailleux et al. in 2006 [14] have shown that the expressions of modulus and compliance ($1/J''$) are analytic in the lower part of the complex frequency domain.

It has been demonstrated that the real and imaginary parts of a function respecting these conditions, and also without singularities in the real axis, are connected by Kramers-Kronig relationship. Booij and Thoone in 1982 [21] showed that:

$$E''(\omega) \approx \frac{\pi}{2} \left(\frac{dE'(\omega)}{d \ln \omega} \right) \quad E'(\omega) - E'(0) \approx -\frac{\omega \pi}{2} \left(\frac{d[E''(\omega)/\omega]}{d \ln \omega} \right) \quad \delta(\omega) \approx \frac{\pi}{2} \left(\frac{d(\log E_d(\omega))}{d(\log \omega)} \right)$$

Considering now the TTSP, the translation coefficients $a_T(T_i, T_{ref})$ between two isotherms can therefore be calculated as follows:

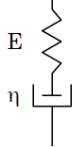
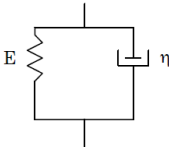
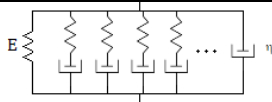
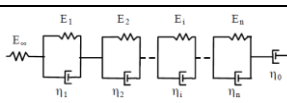
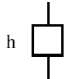
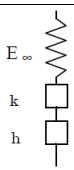
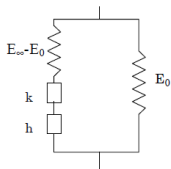
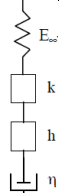
$$\log(a_T(T_i, T_{ref})) \approx \sum_{j=i}^{j_{ref}} \frac{\log|E^*(T_j, \omega)| - \log|E^*(T_{j+1}, \omega)|}{\delta_{moy}^{(T_j, T_{j+1})}(\omega)} \cdot \frac{\pi}{2}$$

Then, it is possible to construct the master curve. Furthermore, it is possible to evaluate the validity of this method by comparing the values obtained for different reference temperatures.

Linear viscoelastic modelling

The purpose of modelling is to provide a mathematical approximation of real material behaviour with the aim of saving the time and cost of performing the test. These types of analytical models are defined by combining springs and dashpots. Springs represent the elastic part of the material, while dashpots represent its Newtonian viscous behaviour.

Table 2-1 LVE models for bituminous materials [22,23]

	Denomination	Description	Schema/Formula
Discrete relaxation spectrum	Maxwell model	One spring and one dashpot in series. Represent the viscoelastic liquid behaviour of the material.	
	Kelvin-Voigt model	One spring and one dashpot in parallel. Represent the viscoelastic solid behaviour of the material.	
	Generalized Maxwell model (Prony series)	Formed by a spring, a group of n Maxwell elements and a dashpot in parallel	
	Generalized Kelvin-Voigt model	Formed by a spring, a group of n Kelvin-Voigt elements and a dashpot in series	
Continuous relaxation spectrum	Parabolic element [24]	Represented by an infinite number of Maxwell elements in parallel or Kelvin-Voigt elements in series. It is an viscous element with a parabolic creep function.	
	Huet model [25]	Initially proposed for bitumens and mixtures. It is an analogical model composed by a combination of a spring and two parabolic elements in series.	
	Huet-Sayegh model [26]	It is an evolution of the previous model proposed for mixtures modelling. Very complete model that can successfully fit mechanical response of most bituminous materials.	
	Huet-Such model [27,28]	Improved the Huet model in order to adequately describe bitumens behaviour at high temperatures and low frequencies.	

Denomination	Description	Schema/Formula
2S2P1D model [22,24]	Very complete model that can successfully fit mechanical response of most bituminous materials.	
Analytical LVE approach	CA model [29] $m_e=1$	$ G^*(f, T) = \frac{G_g}{\left[1 + (f_c / f)^k\right]^{m_e/k}} \text{ [Pa]} \quad \delta = \frac{90m_e}{1 + (f_c / f)^k} [^\circ]$
	CAM model [30]	
	Generalized CAM model [31]	$ G^*(f, T) = G_e + \frac{G_g - G_e}{\left[1 + (f_c / f)^k\right]^{m_e/k}}$

2.2.4 Mixture design

Asphalt mixture design depends on the desired performance. Depending on the application layer of the mixture the desired properties may vary. Base courses are designed in order to distribute loads over the soil foundation and must be resistant to fatigue. Intermediate layers must be compacted, stiff and resistant plastic deformations. And finally, wearing courses which are in direct contact with traffic and environmental agents provides the durability to the system. They need to be resistant to the action of water, to permanent deformations and to have acceptable surface characteristics. But sometimes, the characteristics desired can be contradictory [32].

From the RILEM Report 17 [33], six design methods for road asphalt mixtures can be distinguished:

- i. Formula
- ii. Empirical testing
- iii. Analytical computations
- iv. Volumetric method
- v. Performance related testing
- vi. Fundamental testing

In this thesis, the French design method and the associated testing procedures have been applied. This method is based on the asphalt mixture performance to the greatest extent [32]. The method may be classified as fundamental or empirical depending if the material has a structural function or not. However, the gyratory compactor test is the base test for all asphalt concrete studies, as this test takes into account the volume of the system.

French pavement design is developed in laboratory. It uses materials that should represent the materials of the future construction works. It is based on mechanical performance related limits. The method has four levels of study:

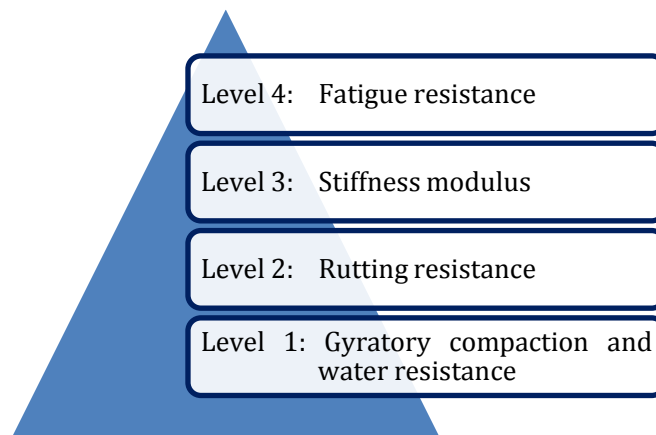


Figure 2-6 Summary of the different testing levels

Test protocols and European standards

A. Gyrotory compactor (EN 12697-31)

Asphalt mixture is introduced, bulked, in the mould and heated to the test temperature, between 130°C and 160°C. A vertical pressure of 0.6 MPa with a deviation angle of $\sim 1^\circ$ is applied on the top of the specimen. At the same time a circular rotation takes place. The increase of compactness, through the decrease of air voids content, is observed against the number of revolutions.

B. Water sensitivity test (EN 12697-12)

Water resistance is at the base of the bituminous mixtures durability. In general, the followed procedure is the indirect tensile strength resistance (ITSR). But within the French scope the regular test carried out is the Duriez direct compression test, described on the Annex B of the standard.

Duriez test consists on the compaction of the asphalt mixture in cylindrical moulds under static pressure. The set of samples is divided in two groups, one conserved in dry conditions and the other immersed under water at 18°C, both during 72h. Then, each specimens group is loaded under simple compression.

In both methods, water resistance ratio is the coefficient of the immersion resistance to dry results.

C. Rutting resistance test (EN 12697-22)

In this case specimens have to be manufacture in function of the device employed, small, large or extra-large. As French procedure is followed the rutting resistance is supplied by the large device. Specimens are of parallelepiped shape (500x180) mm with 100 mm thickness. This slab is submitted to a one-wheel traffic load at 60°C, 1Hz, 5kN and 0.6 MPa of wheel pressure. Results are shown by depth of deformation against number of cycles. Each type of mixture should fulfil the specifications to a certain rut percentage at a given number of cycles.



Figure 2-7 Level 2 testing devices and mixture slab

D. Stiffness modulus test (EN 12697-26)

In order to get input values for the pavement structure design, the complex modulus needs to be measured. The French procedure is included on the European standards on Annex A (two point bending on trapezoidal specimens). The testing conditions are frequency sweep between 1 Hz and 40 Hz, and temperature sweep from -10°C to 40°C.

E. Fatigue test (EN 12697-24)

The resistance to fatigue can be determined by 5 different procedures. French design follows Annex A of the standard, the two point bending on trapezoidal specimens at 25 Hz and 10°C in strain controlled mode. By convention, fatigue life of a specimen is equal to the number of loading cycles needed to decrease the specimen's apparent stiffness modulus by 50%. Three different strain amplitude levels are selected and generally 6 specimens tested for each level. Then fatigue law curves are fitted on the experimental points by linear regression in a log-log diagram of number of cycles by strain level. The parameters that characterize the fatigue performance of a mixture are the strain level ϵ_6 corresponding to 1,000,000 cycles and the slope of the fatigue law (-1/b).

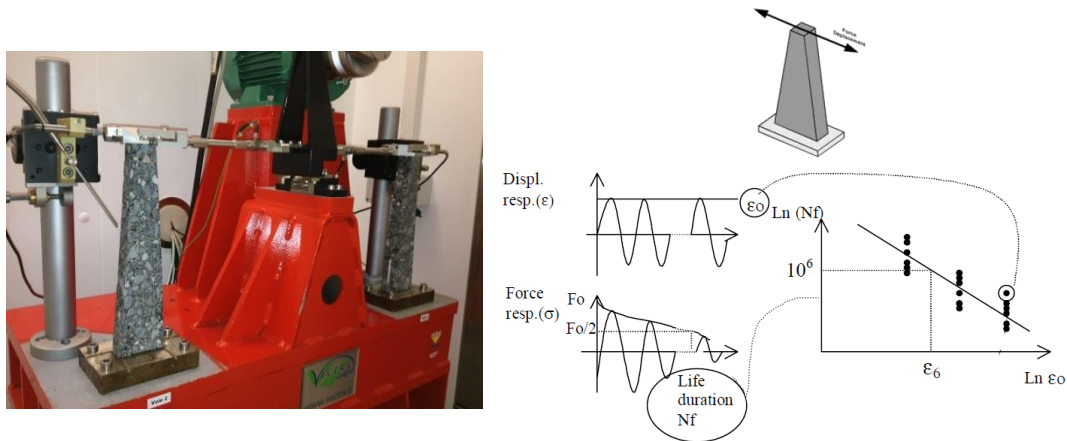


Figure 2-8 Level 3 and 4 testing devices and fatigue principles [34]

All these tests define the 4 levels of testing. Depending on the desired type of mixture, according to the French procedure for pavements design, a certain level of testing may be completed. For example, for base and intermediate courses Level 4 is needed. In contrast, for surface course to Level 2 is required.

2.3 Manufacturing procedures

Over the last century, production and spreading of the asphalt mixtures has evolved from manual works to computerized power plants with equipments highly automated. Along this period, it has been widely accepted that the temperature control is essential. It have to be high enough to ensure aggregates coating, the stability of the matrix during production and transportation, and for the workability on site and performance of the asphalt mixture. And at the same time, it must be below the limit that could cause excessive ageing of the binder [5]. For usual paving grade bitumens the mixing temperature ranges between 200°C to 150°C [32].

In consequence, pavement industry is directly linked to high energy consumption and greenhouse gases emissions [10]. That is why temperature reduction in the production process has been implemented through Warm Mix Asphalt.

Based on the different ranges of manufacturing temperature, asphalt mixtures can be classified as follows [35,36]:

- Hot Mix Asphalts (HMA) is the original and still the most widespread procedure. Their production temperature exceeds 160°C. As discussed above, these high temperatures are necessary to achieve the adequate workability of the mixtures, and the best coating of the aggregates.

- Warm Mix Asphalts (WMA) are in the temperature range of production from 110°C to 140°C. Three different processes can be distinguished, bitumen foaming and the use of chemical or organic additives.
- Half Warm Mix Asphalts (HWMA) are characterized by a production temperature that never exceeds the boiling point of water (100°C). In most of the cases moisturized aggregates are used.
- Cold Mixtures (CM) are the asphalt mixtures produced at ambient temperature (up to 40°C). In order to achieve adequate workability either emulsions or foamed bitumen is employed.

Asphalt mixtures could also be classified by different criterion, such as the air voids content of the mixtures (open graded, dense graded or porous asphalts), the maximum aggregates size (fine or coarse), the aggregate fraction employed (mastic, macadam or concrete) or by the granulometry (continuous, discontinuous or uniform). Also, among all classifications discontinuous micro-surface mixtures, hot rolled asphalts, mastic asphalt or gussasphalt mixtures, stone mastic asphalts or soft asphalts [13] can be find on roads.

2.3.1 Warm mix asphalt procedures

From the study of all the technologies that are currently in use, various classifications can be performed to try to group the various products commercialized. Thus, although the goal of all these technologies is the same (reduce production and extended temperature), initially each product has its particular characteristics.

Several common features can be identified between some of them, and this allow the establishment of a more detailed classification based on their operating principle [7,35–37]:

- Foaming processes: The foaming effect is created by the vaporisation of the water due to its contact with the hot bitumen, increasing the volume and decreasing the apparent viscosity [35]. The process can be:
 - Direct: Injection of water directly to the supply line of bitumen.
 - Indirect: Through materials that absorb and lose water without damaging its crystalline structure, such as synthetic zeolites, or by aggregate moisture.
- Organic additives: Is based on the addition of different types of waxes which cause a decrease in viscosity.
- Chemical additives: These products generally include a combination of emulsifying agents, surfactants and other products to improve workability and compaction of the mixture.

Foaming procedure

It is the first process developed for reducing asphalt mixtures manufacturing temperature. The working principle of such WMA technology is based on the use of small amounts of water. When water gets in contact with the hot bitumen, the high temperatures cause its evaporation and the steam is trapped within the matrix of the bitumen. Thus, a significant amount of steam is generated, which is responsible for temporarily increasing the volume of the bitumen and decreasing its viscosity [7].

This effect gives a remarkable coverage and mix workability improvement. A common feature of the different processes is the limited duration of the foaming effect. The spread and compaction in such mixtures should be carried out soon after their production [37]. Special precautions must be taken in regards to the amount of water added. It means that it must be enough to ensure the foaming effect but not as much as to induce cohesion problems that may occur because of the incorrect evaporation of all the water added [38].

Although the main process is the same for a large number of products, the way in which water is added to the mixture may vary. Thus, it is possible to distinguish between two different types: water-based or direct method and water-containers or indirect method [7,35].

Indirect method

This method is based on the use of the zeolites principle to achieve the foaming process. Due to the honeycomb microstructure of the zeolites, water can be preserved within their micro-pores and released above the boiling point of water when heated [37]. Thus, it is also possible to manufacture synthetic zeolites (Aspha-min® and Advera ®).

These synthetic materials are composed of alkali metal aluminium-silicates, which have been hydrothermally crystallized. The ability to absorb and lose water without damaging its crystal structure is one of the main characteristics of these silicates [39]. The structure is formed by relatively large openings compared to its size, where cations and even molecules or groups of molecules (in this case water) can be stored. The content of water of crystallization is approximately 20%, which is liberated when the temperature increases by the addition of bitumen, causing a micro-foaming effect in the asphalt mixture [40].

Direct method

This group is based on systems that use water in a direct way. Mainly in all the processes the water is injected directly into the flow of hot bitumen, in the most cases through nozzles to create the effect of foaming. This effect is produced when the water evaporates producing a large

volume of steam that slowly disappears [37]. Within this group, a greater distinction can be made based on commercial products.

There is another way to introduce water in the mixture, and it is through the use of aggregates in the wet state. The idea is to make a partial drying so a foaming effect will be produced with the contact of the aggregates with the hot binder. This procedure is known as sequential mixing, where the final water content is about 0.5% at 95°C, thus ensuring sufficient workability and compaction [37,41].

Table 2-2 Resume of Foaming WMA commercial processes obtained from producers websites

Procedure	Product	Description
Foaming Process Indirect Method	Aspha-min®	Supplied by Eurovia Services GmbH. It is a finely powdered synthetic zeolite hydro-thermally crystallized. Added at 0.3% percent by total weight of HMA mix. It can give up 20% of water by mass, which microscopically foams the asphalt to aid coating of the aggregate. (www.eurovia.fr).
	Advera®	Advera is an aluminosilicate or hydrated zeolite powder with about 20% of water. It produces a sustained, time-release foaming of the asphalt binder, to achieve a temperature reduction between 15 and 20°C (www.adverawma.com).
Foaming Process Direct Method	Double Barrel Green	Water is delivered to the system using a positive displacement piston pump capable of accurately metering water into the system. Using feedback controls, pump speed is modulated to maintain the appropriate flow of (www.astecinc.com).
	Ultrafoam GX2™	Gencor has devised a simple, robust and reliable method to inject steam into the foaming process, using only the energy of the pump. As a result, the bitumen and water can be introduced at widely different flow rates and temperatures (gencorgreenmachine.com).
	LT Asphalt	It consists of foamed bitumen hydrophilically additived. The addition of water ranges 0.5%-1 % by bitumen's weight (www.nynas.com).
	WMA Foam	Known as the two-phase method. It is based on a two component binder system, where initially a softer binder is introduced and subsequently one harder foamed within the production cycle. The hard bitumen is foamed by introducing cold water in small amounts so the process can be induced and so, an increase on the ability coverage is generated. This combination of soft bitumen and a stiffer foamed one lowers the viscosity of the global mixture permitting its proper workability (www.shell.com).

Procedure	Product	Description
Foaming Process Direct Method	Low Energy Asphalt (LEA)	Developed by Eiffage TP, the low energy asphalt is a sequential process. First the coarse aggregate and bitumen are heated, then mixed. After the fine aggregates partially dried to create the foam are added, so the expansion of the bitumen is created (www.lea-co.com)
	Low Emission Asphalt	It is an update of LEA. In this case, the process also uses sequential mixing, but now a chemical additive is added to the binder before mixing it with the coarse aggregate, and then the moistured fines, so the foaming effect is induced (www.suit-kote.com).
	EcoFoam II	It is a WMA system for continuous flow and batch plants using the Static Inline Vortex Asphalt Blender (www.asphaltequipment.com).
	Aquablack	The center convergence nozzle design provides more efficient foaming. It reduces the number of nozzles and the maintenance related to each. The high-pressure system enables low water-to-liquid-asphalt ratio during foaming. There are no moving parts in the foaming gun (www.marini-ermont.fayat.com).

Organic additives

This procedure is based on the addition of different types of wax to the mixture. The waxes used in these products are molecules composed of chains of hydrocarbon that melt at temperatures between 80 and 120°C, thus changing the original properties of the binder. The melting point depends largely on the length of the carbon chain (C45 or more) [41]. Between 2% and 4% wax the total mass of the binder is the usual dosage.

Organic additives usually achieve a temperature reduction of between 20 to 30°C, while also improve the deformation resistance [35]. Such processes have been developed since the end of the 1980s, currently distinguishing between three different types. The waxes are Fischer-Tropsch, Fatty acid amides and Montana waxes. Their only difference is the type of wax used to achieve the viscosity reduction. Above the melting point of the waxes a decrease in the viscosity is generally produced [7]. Thus carefully attention is needed on the selection of the type of wax, so that potential problems with the temperatures are avoided. During the cooling period after lay out, the wax additives solidify on microscopic particles uniformly distributed increasing the hardness/stiffness of the binder. That is if the melting point of the wax is lower than the temperatures expected in service asphalt. If not, complications can occur, turning the asphalt in a brittle material at low temperatures [35].

Table 2-3 Resume of Organic additives WMA commercial processes obtained from producers websites

Procedure	Product	Description
Organic Additives	Sasobit	It is a product of Sasol Wax. It is a Fischer-Tropsch wax sold as a powder or granulated (also directly mixed with bitumen ready for use). It is extracted from the process of producing liquid hydrocarbons from synthesis gas. Sasobit is a wax of long aliphatic hydro-carbonated chain, with a melting point ranging from 85°C to 115°C, which allows a temperature reduction between 20-30°C (www.sasolwax.com)
	Asphaltan B	It is a product of Romonta GmbH. Asphaltan B is created especially for rolled asphalt and it consists of a mixture based on montan waxes and high molecular weight hydrocarbon substances. Romonta recommends adding between 2%-4% by weight of bitumen. It can be added in the mixing plant or directly to the bitumen, and also can also contain modified polymers. The melting point is about 100°C. Similar to Sasobit, this wax acts as a flow improver mix, with the associated reduction in production temperatures (www.wachs-und-mehr.de).
	Greenseal BT	It is a product of Green World. Green Seal BT additive is a surfactant for the handling of bitumen, is an energetic reducing agent, which improves the workability of the mix, allowing manufacture hardened asphalt at lower temperatures while maintaining the mechanical properties of these hot. Greenseal BT is made from vegetable resins and esters, solvent less source of petroleum or carbo-chemical vegetable oils. Contains no volatile organic matter and is free of polycyclic aromatic hydrocarbons (ceacor.lu/gw)
	3E LT	It is a product of Colas. 3E mixes achieves a reduction temperature of manufactured and application between 40°C to 45°C. These manufacturing temperatures allows a 15-25% reduction in greenhouse gas emissions, savings in energy consumption, and less fumes during application (www.colas.com)

Chemical additives

The last type of WMA technologies to be considered is the chemical additives. These products do not depend on any foaming process or reduction of viscosity to reduce the mixing and compaction temperatures [35,39]. Instead, they typically include a combination of emulsifying agents, surfactants, polymers and other products to improve the coating, the workability and the compaction of the mixture. They are as well adhesion promoters. The amount of added additive and the temperature reduction achieved by these technologies depend on the specific product used. The additives are usually mixed with the binder before it is introduced into the mixing drum. Its use has spread mainly in the USA, but also in European countries like France and Norway [37].

Table 2-4 Resume of Chemical additives WMA commercial processes obtained from producers websites

Procedure	Product	Description
Chemical Additives	Evotherm	Evotherm is product of Eurovia. It consists on a chemical package designed to promote adhesion, coverage, compaction and workability of asphalt mixtures at lower temperatures. Base components of the chemical compounds are the surfactants, which act as emulsifiers. Approximately 50% of the chemical package is derived from renewable resources. Evotherm allows a reduction of between 50°C to 75°C, both in the production and spread, compared with the HMA (www.eurovia.fr).
	Cecabase RT	It is a product of Arkema group. CECABASE is a surfactant based on compounds of at least 50% of renewable raw material, that when mixed with the bitumen, the temperature spread can be reduced by up to 50°C, without any adverse effect on the performance of pavement. It is therefore a process that uses less energy (reducing consumption between 20% and 50%) and that ultimately is therefore less harmful to the environment. The incorporation of the additive is between 2 and 4 kg per ton of asphalt mix, reducing the temperature to 120°C, while that retains the same properties as conventional mixtures (www.arkema.fr).
	Rediset WMA	It is a product of Azkonobel. The system was designed in order to solve the problems with the water in WMA, the reduced stiffness and the existing uncertainty in the properties at low temperatures. Rediset WMA consists of a chemical additive in solid tablet form is added to the binder before or during the mixing process. The amine product technology provides it with adhesion promoting properties and antioxidant effects, whereas the physical form of the product causes some reduction in viscosity at temperatures of the mixture, increasing the rigidity at service temperatures (www.akzonobel.com).
	Iterlow T	It is a liquid product, added in quantities of 0.3%-1% that allows a reduction between 90°C-120°C. Iterlow T, acts on the bitumen's surface tension. It limits the gas emissions that cause the greenhouse effect and reduces fuel consumption. The mechanical characteristics of the obtained mixes are identical to the ones produced at normal temperatures (www.coldlay.co.uk).

2.4 Reclaimed materials

The concept of recycling goes far back in time, both ways the use and reuse of materials has been around since the early days of human history. To recycle consists on subjecting a used material to a process, so that it can be used again (Oxford English dictionary). The purpose of this process is turning waste into new available products, reducing raw materials consumption, energy usage and greenhouse gasses emissions.

All the economic and environmental considerations have encourage the recycling of paper, paperboard, glass, steel, plastic and many other materials, where asphalts materials are included. The term RAP (Reclaimed Asphalt Pavement) appeared in 1915 [42], but it was not until the oil embargo in the mid-1970's when the first sustained efforts were developed. The main cause was the increase of asphalt price as well as the lack of quality aggregates near some utilization points [43]. Nowadays, the restricted environmental laws in conjunction with the economic incentives applied make the manufacture of asphalt mixtures integrating RAP a prominent technique. Moreover, by recycling, the bitumen contained is reutilized reducing virgin asphalt contribution and helps to decrease the quantity of waste produced resolving the disposal problems of road construction engineering [44].

2.4.1 RAP procedures

There are several problems on the road that can be solved through milling and recycling. When the road achieves the time of resurfacing or when it has ended its service life, recycling appears as a suitable solution [45].

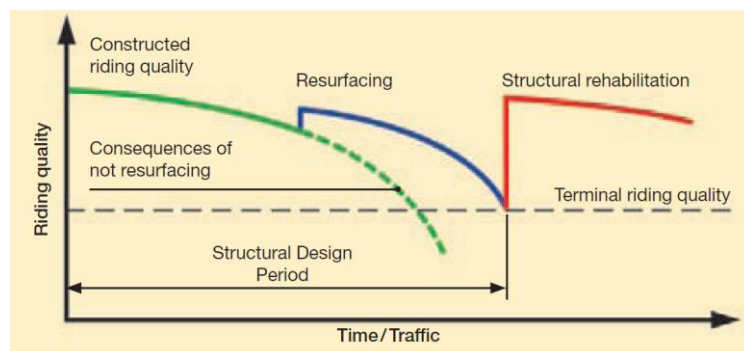


Figure 2-9 Managing pavement maintenance and rehabilitation by monitoring riding quality [46]

The effects of adding RAP to asphalt mixtures have been studied by several authors during the years, concluding that any road is a candidate for recycling. Also, any asphalt layer is susceptible of RAP incorporation [47] if the best practices are followed. According to different researchers the percentage of addition can vary from 0% to 100% or full recycling, depending on the type of road, the quality of the RAP material and the manufacture process [45,48]. Special attention is

needed for the performance of mixtures containing RAP against rutting, water and fatigue resistance. While permanent deformations and stiffness modulus are typically improved, issues are raised as regards to the fatigue life and low temperature properties [49–51].

Reclaimed asphalt pavement is generally obtained through two processes, milling and ripping [45]. When milling in layers, the reclaimed material can be stored and processed separately. When ripping, the slabs obtained needs to be crushed until the size desired. In this case, special attention may be needed to characterize the different fractions. The recycling techniques can be classified into different categories, according to the working temperature and the location where it is performed [47,52]. Thus the following types of recycled processes can be distinguished:

- In plant recycling:
 - Hot recycling
 - RAP heated by the aggregates
 - RAP heated with the aggregates
 - RAP heated in a separate device
 - Cold recycling
 - With emulsion
- In situ recycling:
 - Hot recycling (Reshape, remix and remix compact)
 - Cold recycling with emulsion

Reclaimed asphalt pavement is a material where certain characteristics have to be noted as EN 13108-8 standard requires. Before milling it is important to verify that the layers do not contain hazardous materials like PAHs (Polycyclic Aromatic Hydrocarbons) or asbestos can be avoided. This determines the suitability for being recycled.

The challenge of recycling is to create a homogeneous material from different sources. For this purpose the material can be classified to be treated and stocked separately. To facilitate the mix design for high RAP content it can also be separated in different fractions [53].

As a rule of thumb, for a given property the asphalt mixture, the additional scatter due to the added RAP depends on the scatter of this property in the RAP multiplied by the RAP content in the mix [54]. As the obtained mix must generally comply given homogeneity requirements, RAP with highly scattered properties implies low RAP content. For this reason, limit values for recycling or maximum content of RAP is allowed [54]. To avoid moisture accumulation, the recommendation is to cover the stockpile so the rain might not penetrate, as well as leave a sloped surface underneath so water can drain naturally [53].

If best practices are taken, RAP stockpiles should have lower variability on gradation. The tests that may be done to get data from the RAP are according to West (2010) [53] and the European Standard EN 13108-8, the asphalt binder content (and properties, softening point, if using high percentages of incorporation), the granulometry (<0.063 mm; between 0.063 and 2 mm; > 2mm), bulk density and consensus properties of the aggregate of the processes material. In the case of layer specifications, as happens with surface layers, polishing or mineralogical composition of the RAP aggregate may be needed.

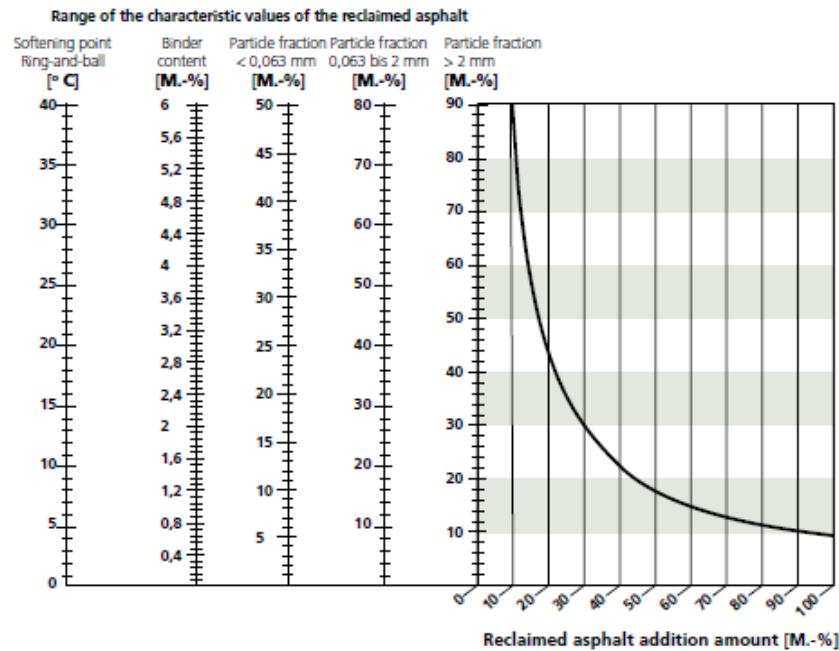


Figure 2-10 Example of nomogram for determining the maximum possible RAP addition [45]

Following the German Asphalt Pavement Association [45] indications on the report Recycling of Asphalt, the addition of RAP can be determined depending on the range of the corresponding characterization results. The amount of added material depends on the type of layer. In the nomogram presented in Figure 2-10, the maximum possible material addition can be calculated with reference to its characteristics. The ranges of each parameter are entered in the nomogram at each corresponding ordinate, where the most restricting determines the maximum percentage of RAP to be added.

2.4.2 RAP characteristics

The fact of incorporating RAP material into asphalt mixtures should be considered as addition of a constituent element. That is why, their service characteristics, physical and rheological changes should be taken into account for a correct design of the resulting mix. In any case, the performance requirements for the mixture with RAP are the same as for conventional hot mix asphalts [44].

In general, the following characteristics are asked in the European countries (EN 13108-8):

- Type of bitumen
- Bitumen content and properties (Penetration and softening point)
- Content of foreign materials
- Type of aggregates, granularity and maximum diameter D
- Maximum size of reclaimed particles (U)
- Homogeneity

In order to estimate the properties of the mixed bitumens the formulas from the EN 13108-1 standard are widely used:

$$a \log \text{PEN}_1 + b \log \text{PEN}_2 = (a+b) \log \text{PEN}_{mix}$$

$$\text{SP}_{mix} = a \text{SP}_1 + b \text{SP}_2 \quad a + b = 1$$

It should be noted that in these equations, a complete blending of the binders is assumed.

RAP bitumen

Several authors have investigated the different stages of ageing that suffer the bitumen when being manufactured and during service life [44,47,55,56]. There are two phases of ageing inducing an increase of the asphalt viscosity. Knowing the level of damage and ageing of the binder, soft binders, softening agents and rejuvenators can be chosen to reactivate the old binder.



Figure 2-11 RAP stockpile ready to be use on mixture manufacture

Use of rejuvenators

The rheological properties of the bitumen contained in RAP could be restored, and for this purpose rejuvenating agents or softer asphalts are used. There is a need of lowering binder viscosity by softening agents, as well as restoring physical and chemical properties of the aged binder [43,55,57,58].

The importance of the physical and chemical bonding arrives when talking about mixture performance. An asphalt section constructed by the New York DoT suffered ravelling due to the fact that the virgin bitumen only covered the aged one, but did not interact chemically with it [43] (double coating effect).

2.5 Bitumen

Among all the exposed pathologies that could cause the failure of the pavement, a common element is the performance of bitumen. So as the mechanical performance of the mixture is highly dependent upon the properties of the bitumen, it has to fulfil certain mechanical and rheological requirements to ensure the integrity of the pavement [59].

Bitumen is a crucial component of the asphalt mixtures, it is used to build roads that connect our cities, our countries and hold our city streets together. Bitumen is a very valuable material with countless applications, it is not only flexible as well as durable, it is also 100% recyclable [60]. It is a popular belief, even among engineers that asphalt can be made from the heavy end of any crude oil. But unfortunately this belief is far from being correct because the asphalt product must have a series of properties in order to meet the specifications for the different grades [61].

2.5.1 Origin and manufacture

In general, bitumen is viscous material at relatively high temperatures and solid or semisolid at room temperature. It can occur in nature as such or obtained as residue by refining petroleum [62], though they vary enormously in their composition and their properties [63].

Natural bitumen

Naturally occurring asphalts could be divided in three groups, lake asphalts, rock asphalts and gilsonite [63]. Lake asphalts contain actual bitumen but also a proportion of mineral matter i.e. southern part of Trinidad, Kentucky, Alberta, Albania or the Dutch East Indies. The rock asphalts provided the foundations of the modern asphalt industry; it consists of natural rocks impregnated with bitumen, i.e. Piryment-Volant or Avejan (France), Val de Travers (Switzerland), Syracuse (Sicily) or Hanover (Germany). Finally, the gilsonite, also known as “asphaltites” is a bitumen characterized by a high softening point, i.e. Utah (USA) or Albania [1,63].

Refined bitumen

On the other hand, crude oil refining is the principal source of bitumen for road engineering. It is primarily obtained by vacuum distillation of carefully selected crude oils or blends of crude oils. Among the crude oils or blends that are available not all of them are suitable for producing bitumen as the quality standards require. In general heavy crude oils (specific gravity > 0.9) are used, but these types of crude oils tend to present higher sulphur contents (>1 %m) [64]. The manufacture procedure followed to produce bitumen is called fractional distillation. During this process, the different hydrocarbon chains are separated according to their different boiling

points. Distillation is carried out in tall steel towers (fractionating or distillation columns), divided inside at intervals by horizontal steel trays punctured to allow the steam to rise up.

The crude oil is initially distilled under atmospheric pressure and normally involves heating between 345°C-450°C to separate the lighter fractions as overhead products and the bitumen left as a residuum. In order to obtain the desired bitumen consistency as well as to recover all the high boiling fractions for other purposes it is necessary to complete the process. So a second fractionating tower is added, operating under low pressure (10-100 mmHg) and high temperature (350-425°C) [17,64]. Depending upon the specification grade requirements, the vacuum residuum can be used either directly, further processed, or used as a component of blended bitumen. The non-distillable materials as residuum on the vacuum distillation are described by bitumen and residues (petroleum) vacuum [64,65].

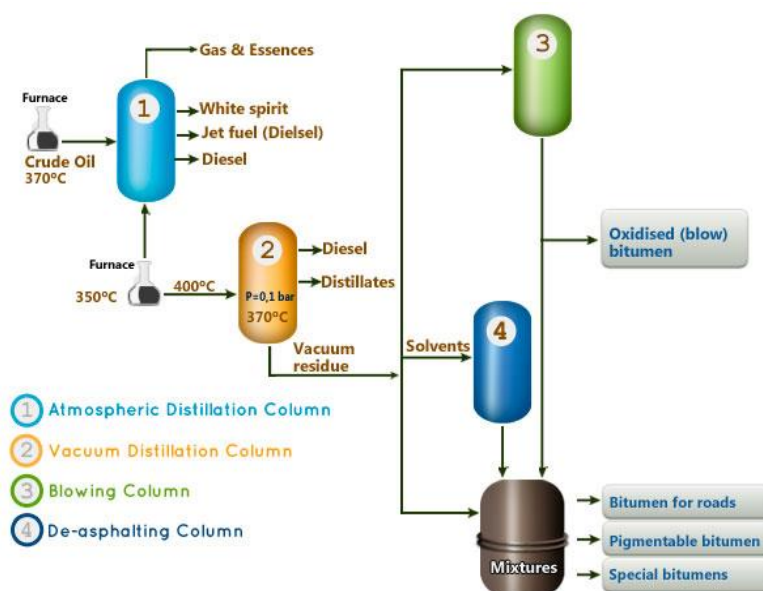


Figure 2-12 Distillation process diagram [65]

These materials can be rectified by a mild degree of air-blowing to make minor adjustments to the physical properties. Also, the vacuum residue can be modified by solvents deasphalting. It uses different solvents in order to separate asphaltene-type fractions, and the hard bitumen remaining can be blended to produce specification grade bitumens [64].

2.5.2 Structure and composition

Generally, asphaltic bitumens elementary composition reveals that the chemical elements present in the highest amounts are hydrocarbons (C 82% - 88% and H 8% - 11%). Then, most of the bitumens also contain small amounts of sulphur (S 0% - 6%), oxygen (O 0% - 1.5%), nitrogen (N 0% - 1%) and traces of different metals as calcium, iron, magnesium, nickel or vanadium [17,63].

In terms of elementary analysis, the carbon to hydrogen ratio is an important parameter of hydrocarbons. It indicates to what degree the hydrocarbons deviate from paraffinic structures of the general formula C_nH_{2n+2} . The two elements next in importance are nitrogen and sulphur [63], influencing the chemical make-up and the behaviour of the asphaltic bitumen. The degree of chemical stability or inertness is determined by the chemical arrangements of the elements in the various molecules and on the ratio of reactive to non-reactive components. Therefore, it is generally accepted to subdivide asphaltic bitumens into asphaltenes and malthenes, and a relatively loose subdivision of the malthenes into resins and oils [63].

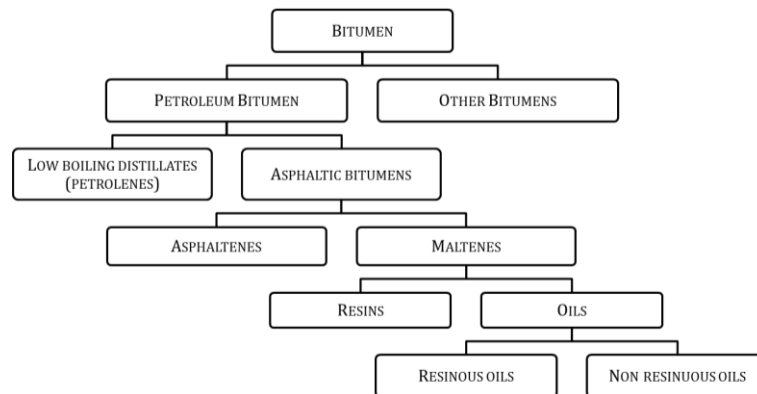


Figure 2-13 General diagram of fractioning [63]

Physical characterization

Regarding chemical structures, bitumens differ from one another not only physically, but also as to molecular weight, boiling points, and other characteristics [62]. Physically it depends on the concentration, particle size and nature of the dispersed phase, and the nature of the dispersion medium [59]. They are colloidal dispersions of asphaltenes (high molecular weight hydrocarbons) in malthenes (dispersion medium, including resins, aromatics and saturates). Each of these groups may be separated from the other.

Two types of colloid structures are distinguished, the sol and gel bitumens. The division line between them is diffused, calling the materials falling there sol-gel bitumens [62]. Figure 2-16 illustrates the typical sol and gel structures.

- Gel bitumens display a large micelle together with high content of asphaltenes and moderate to low peptization of the latter due to low and often insufficient resin content. Gel bitumens maintained in fluid condition show no instability or sedimentation, as do some highly cracked bitumen, which are seriously deficient in resins. At ambient temperature their structure is only slowly destroyed by solvents or by an increase in temperature [62].

- Sol bitumen. The sol term is used because such materials are in reality true solutions rather than dispersions of high molecular weight materials in malthenes. These types of bitumens show Newtonian behaviour at high temperatures. These sol bitumens could be divided in three groups, A, B and C [62]. Group A contains only oils and resins; there is no sign of micelles. Group B has low and medium asphaltene content; it is similar to A but containing asphaltenes in low percentage. Finally, group C bitumens contain pronounced micelle count with a high percentage of asphaltenes (25%-40%). They are quite similar to group B and often called sol-gel types.

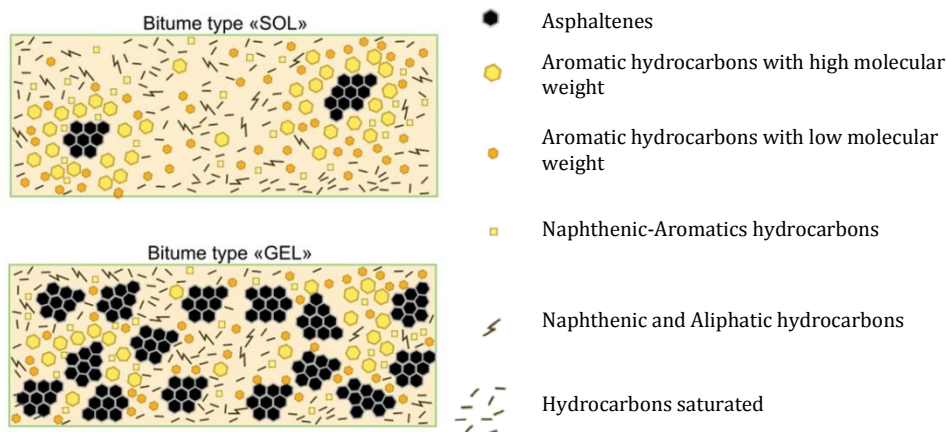


Figure 2-14 Sol and Gel types of bitumens [66]

Nearly all bitumens contain asphaltenes, besides the resins and oils, at different quantities. But what physically distinguishes bitumens is the presence or absence of micelles [62]. Then, bitumen physical properties not only determine the suitability for a given application, but also define the conditions under which the product must be handled and placed in the structure [64].

The behaviour and properties of bitumens are dependent on their constitution [62]. From the manufacturing process petroleum light components are removed leaving behind relatively high molecular weight and low volatility compounds [64]. Then, bitumens are engineering designed products and therefore the product specifications focus on defining physical properties, rather than being based upon chemical composition.

Chemical characterization

Bitumen is the resulting product from engineering distillation. Generally it is a solid or semi-solid material at ambience temperature. It softens as the temperature increases behaving as Newtonian fluids when it is elevated, and hardens as the temperature decreases behaving as brittle material when it is too low [62,63].

Citing Hoiberg's book [63], it can be considered that bitumens are viscous materials with relatively high-boiling points. This could be justified by the chemical reactions involved in the natural formation of bitumens. Polymerization, condensation, and oxidation reactions combined with evaporation, filtration, and blending operations form bitumens. Then, geologically, it could be said that older deposits usually contain higher molecular weight products, indicating further polymerization and condensation of the material. In both natural and manufactured bitumens it can be observed that the older is the material the harder it becomes, obtaining higher melting points and less solubility in low-boiling hydrocarbons [62,63].

However, chemically speaking, bitumens are a mix of heterogeneous chemical compounds. But yet all bitumens have certain common characteristics and properties which indicate that the components of all bitumens, independently of their origin, must be similar in many significant properties [63]. In order to establish the nomenclature used in this document, the following definitions are suggested:

- Asphaltenes. Their structure varies considerably with the origin of the asphalt. This is the heaviest fraction and can be obtained by precipitation methods. Usually n-pentane, n-hexane or n-heptane are commonly used as solvents, resulting on the c5, c6 or c7 asphaltenes. They are dark brown to jet black friable solids that show no definite melting point [62,63,67].

They are normally characterized as highly polar due to the presence of nitrogen, oxygen and sulphur. Asphaltenes have different molecular weight ranging from 500 to 10,000 g/mol [68]. The values of molecular weight may vary in relation to the polar strength of the solvents used and the temperature of determination [69]. So it is no surprise to find in the literature a very wide range of molecular weight values for asphaltenes. They usually represent 5% to 20% of the total bitumen [70,71].

- Malthenes. Resins, aromatics and saturates compose the malthenes. Opposite to the asphaltene fraction, the malthenes are soluble in the solvents that make asphaltenes precipitate, i.e. n-heptane.
 - Resins. The term resin refers to the material eluted from various solid adsorbents, but it does not include the oils (aromatics and saturates). They are a transition from oils to asphaltenes [72]. Resins are dark coloured material, heavy, semisolid or solid, and very adhesive [17,62]. This group shows molecular weights ranging from 300 to 2,000 g/mol [72]. And as happens with the asphaltenes on the literature it can be find a very wide range of molecular weight values.

Resin fractions contain considerable unsaturated hydrocarbon constituents, but still their molecular weight fractions are lower than those of asphaltenes. They are present by 13% to 25% in the total bitumen [17]. Their composition depends on the kind of precipitating solvent employed.

- Aromatics are non-polar hydrocarbon chains in which the unsaturated ring systems dominate. They have a high dissolving ability for other high molecular weight hydrocarbons, and represent the major proportion of the dispersion medium for the peptised asphaltenes. Aromatics are dark brown colour and represent from 40% to 65% of the total bitumen. They have an average molecular weight of 800 g/mol but it can appear on a range between 300 and 2,000 g/mol [72].
- Saturates. They are non-polar viscous oils which are straw or white in colour. Their average molecular weight is the smallest (600 g/mol) [72], but similar to that of aromatics (300 to 2,000 g/mol). The components are essentially linear aliphatic hydrocarbons, ramified and naphthenic elements [66]. They constitute between 5% and 20% on the SARA fractions in general [73].

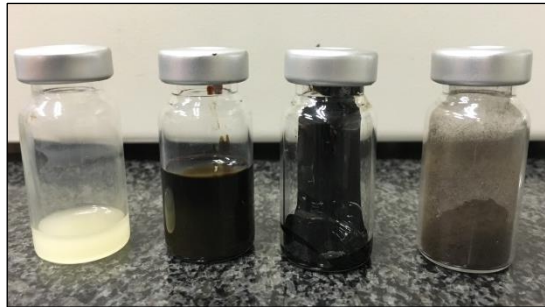


Figure 2-15 SARA fractions, Saturates, Aromatics, Resins and Asphaltenes

Moreover, since the real molecular weight cannot be determined, the concept of average molecular weight, introduced by polymer chemistry, is used. On Greenfeld's research [74], it is remarked that although the average molecular weight of asphaltenes decreases during ageing, the total amount of asphaltenes molecules in the bitumen increases. Thus, the asphaltenes created by ageing has substantially lower molecular weight than those originally present.

2.5.3 Bitumen evolution

Bitumen characterization is very important in order to determine the effect of temperature and stress on the engineering properties. There are mainly two principal applications or steps where the choice of the right bitumen is essential, the mix design and the construction process [1]. Through the asphalt mixture design, the bitumen must be of such a grade that it can produce a mix able to resist the traffic and environment effects during its service life. But previously, it has

to resist the construction process, including transport from refinery, storage in plant, pumping and mixing during manufacture. Then it needs to be hauled to the construction site, laid down and compacted at the specific temperatures. Therefore, the influence of the different techniques could condition the selection of the bitumen.

According to the colloidal model, the asphalt oxidizing mechanisms could be explained as a change of the asphaltenes to resins and resins to oils by hydrogenation [61]. But resins can also be oxidized to asphaltenes and oil to resins.

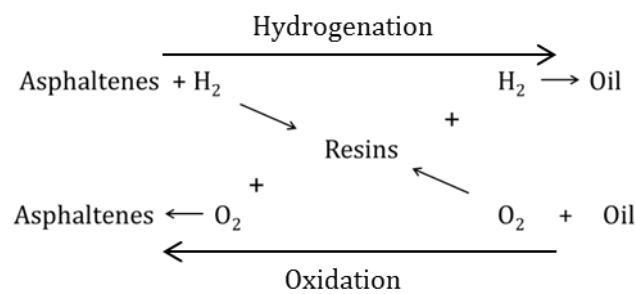


Figure 2-16 Asphaltenes-Resins transfer [61]

For example, during the refining process, the air blown generates a polymerization that leads to a decrease of penetration, an increase of softening point. This induces a reduction of ductility as the bitumen hardens due to the increase of asphaltene content [61]. The steps that conduct this polymerization could be resumed as the addition of oxygen to form unstable compounds from which water is eliminated, leaving unsaturated compounds that polymerize. Then the further addition of oxygen leads the formation of carboxyl derivatives from which carbon dioxide is eliminated and followed again by polymerization. Finally, the formation and elimination of volatile oxidation products other than water and carbon dioxide are again followed by polymerization [61]. Those structural changes are dependent of the oxygen exposure. Thus, ageing is faster when the bitumen is in thin films rather than in bulk quantities as happens in service materials [62].

During mixture manufacture where high temperatures are employed, a loss of volatile oils compounds may occur to some level. However, this loss is considered minor during service because the material is working at ambient temperatures [61].

The phenomenon of ageing implies deep chemical changes within the bitumen. Thus, bitumen durability covers both rheological and physicochemical, or colloidal changes that lead to the failure of the pavement [62]. Additionally, temperature susceptibility is key for the performance of the bitumen, whose oxidation changes the relationship penetration - softening point [64].

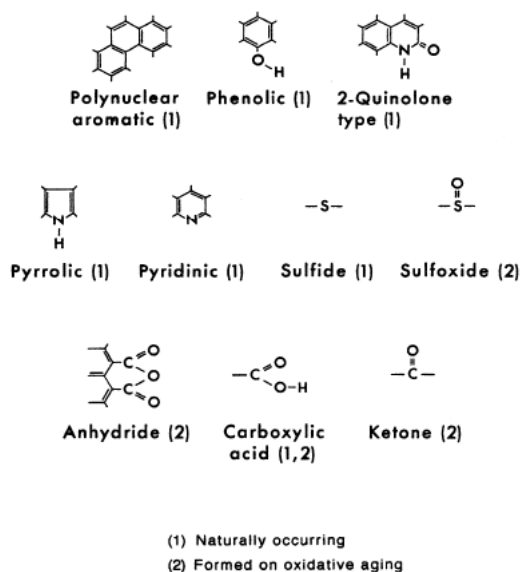


Figure 2-17 Asphalt molecules normally present or formed on oxidative ageing, from Petersen (1984) [75]

Bitumen hardening could be reversible or irreversible, depending if the changes are physical or chemical. Reversible hardening does not alter the composition of bitumen, and the adhesive properties of the material remain practically unaltered. In this case the original penetration of the bitumen could be restored by heating, stirring or other forms of physical actions, as long as the loss of penetration is not so accused that it could lead to the pavements break up [62].

On the other hand, irreversible hardening implies rheological changes due to oxidation. As a result, the loss of bitumen-aggregate adhesion induces stripping of the mixture in presence of water and heterogeneity [62]. As the resin content decreases, the asphaltenes in the dispersion medium are less stable.

2.6 Ageing detection

Bitumen ageing can be divided in two principal phases, a short term ageing and a long term ageing. The first one is basically associated with oxidation and the loss of volatile compounds during the asphalt mixture manufacture. Then, the long term is due to the progressive oxidation in the field as part of the exposure of the mixture to environmental agents. During all this period, there are also other factors that may contribute to ageing, such as steric hardening (molecular structuring over time) and actinic light (mainly ultraviolet radiation) [76].

However, the list of factors is not the same for all researchers. Vallerga and co-workers [77] listed six factors in 1957, then Traxler in 1963 [78] added three more up to nine, while Petersen in 1984 [75] reduced them to three and Mallick and El-Korchi in 2013 [1] gave a list of fifteen

factors. Although the identified list of factors can vary, oxidation in the darkness, volatilization, steric or physical factor and the exudation of oils are considered to be the most important ones [1]. All these factors produce common effects. The stiffness increase leads to higher bearing capacity and permanent deformation resistance. However, the loss of flexibility could result in cracking and total failure of the system [76,79].

2.6.1 Ageing indicators and analysis techniques

In Europe, ageing characterization is made traditionally by monitoring the response of the bitumen to specific testing configurations and conditions. But it is necessary to distinguish between tests related to ageing on bitumens or ageing on asphalt mixtures. Penetration test and softening point test are the classical semi-empirical tests (they do not measure mechanical properties) performed with the aim of measuring the hardening experienced by bitumen.

Penetration test

The penetration test follows the European Standard EN 1426 and it consists in evaluating the consistency of the bitumens expressed in terms of depth 1/10 mm. It is performed by a standard needle that penetrates vertically on the asphalt sample at specified conditions of temperature (25°C), load (100 g) and time (5 seconds). Figure 2-18 illustrates the procedure and device of testing. The purpose of this test is to classify the bitumens in different grades depending on the penetration value range.

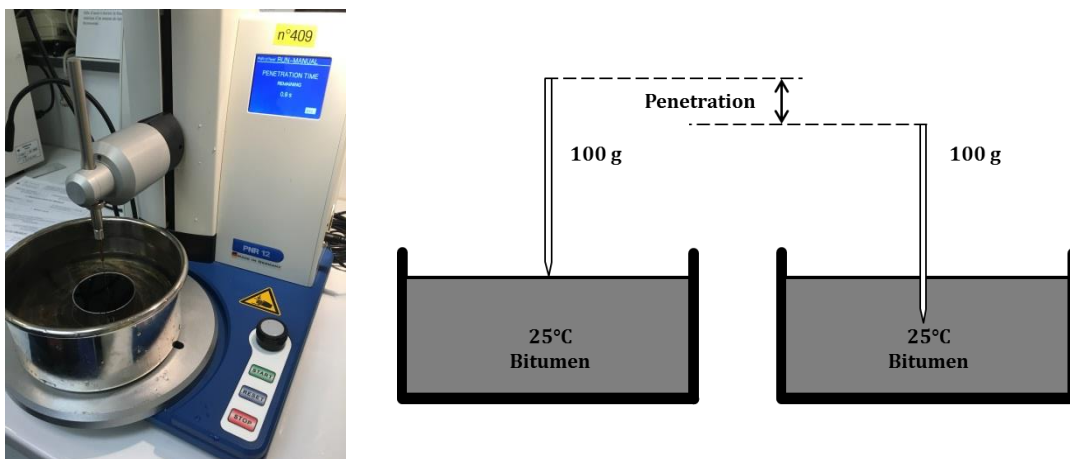


Figure 2-18 Penetration test on bitumen

Softening point test

The EN 1427 is the European Standard that regulates the softening point test (T_{RB}), colloquially known as “ring and ball test”, that determines the temperature at which the bitumen starts to flow. A sample of bitumen is casted in a metallic ring and it is loaded with a standard steel ball until it reaches a specific deformation. The test is performed under a controlled increase rate of temperature of 5°C/minute. Figure 2-19 shows the procedure and device of testing.

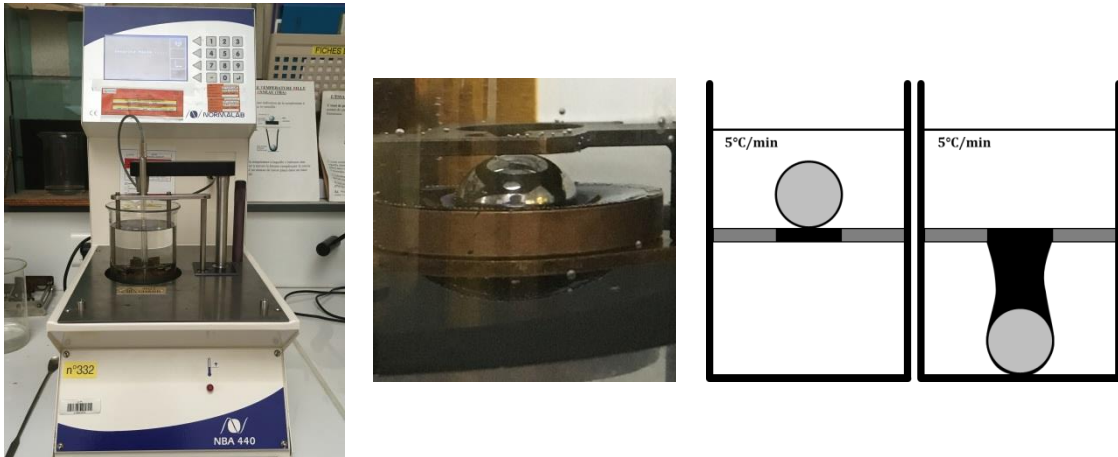


Figure 2-19 Softening point test on bitumen

Hardening

Penetration index (PI) defines the susceptibility of the bitumen to temperature changes, hardening [64]. It generally ranges from -1 to +1 and as higher is the value of PI, the lower is the susceptibility.

$$PI = \frac{20 - 500 A}{1 + 50 A} \qquad A = \frac{\log P \text{ at } T_1 - \log P \text{ at } T_2}{T_1 - T_2}$$

Where A represents the temperature susceptibility of the material, and can be measured with the penetration at two different temperatures.

Fourier Transform Infrared Analysis

The Fourier Transform Infrared (FTIR) analysis consists of exciting the material with infrared light. A quantification of the different types of molecular bonds through characteristic absorption bands in the transmitted infrared light spectrum is carried out. Carbonyl groups (esters, ketones etc.) and sulfoxides are among the major functional groups formed during oxidative ageing [80] and it was demonstrated that their formation changes the physical properties of the binder in a predictable way [81]. They are characterised by C=O and S=O double bonds. The test can be performed both on transmission or reflection (ATR) mode. Once the signal is obtained, Ico and ISo values can be calculated following different procedures [82].

2.6.2 Ageing simulation in laboratory

In order to evaluate the effect of ageing on short and long term conditions, the ageing of the bituminous materials, bitumen itself and asphalt mixture, can be simulated in laboratory.

Ageing tests for bitumens

The correlation between laboratory ageing and field performance has been a battle for more than eighty years already [76]. The most common laboratory procedures are the standardised

test RTFOT (EN 12607-1) and PAV (EN 14769) for simulating the short term and long term ageing respectively. Airey, 2003 [76] summarizes all the available tests for ageing simulation on bitumen.

Table 2-5 From Airey 2003, chronological bitumen ageing methods [76]

Test method	Temperature (°C)	Duration	Sample size (g)	Film thickness	Extra features
Thin film oven test (TFOT) ASTM D1754, EN 12607-2	163	5 h	50	3.2 mm	-
Shell microfilm test	107	2 h	-	5 µm	-
Rolling thin film oven test (RTFOT) AASHTO T240, ASTM D2872, EN12607-1	163	75 min	35	1.25 mm	Air flow—4000ml/min
Modified Shell microfilm test (Traxler, 1961; Halstead and Zenewitz, 1961)	107	2 h	-	15 µm	-
Modified Shell microfilm test (Hveem et al., 1963)	99	24 h	-	20 µm	-
Rolling microfilm oven test (RMFOT)	99	24 h	0.5	20 µm	Benzene solvent
Modified RMFOT	99	48 h	0.5	20 µm	1.04 mm Ø opening
Iowa durability test (IDT)	65	1,000 h	TFOT residue - 50	3.2 mm	2.07 MPa - pure oxygen
Tilt-oven durability test (TODT)	113	168 h	35	1.25 mm	-
Alternative TODT	115	100 h	35	1.25 mm	-
Modified thin film oven test (MTFOT)	163	24 h	-	100 µm	-
Pressure oxidation bomb (POB)	65	96 h	ERTFOT residue	30 µm	2.07 MPa - pure oxygen
Extended rolling thin film oven test (ERTFOT)	163	8 h	35	1.25 mm	Air flow—4000ml/min
Thin film accelerated ageing test (TFAAT)	130/113	24/72 h	4	160 µm	3 mm Ø opening
Accelerated ageing test device/ Rotating cylinder ageing test (RCAT)	70-110	144 h	500	2 mm	4 - 5 l/h - pure oxygen
Pressure ageing vessel (PAV)	90-110	20 h	RTFOT or TFOT residue - 50	3.2 mm	2.07 MPa - air
Modified rolling thin film oven test (RTFOTM)	163	75 min	35	1.25 mm	Steel rods
High pressure ageing test (HiPAT)	85	65 h	RTFOT residue - 50	3.2 mm	2.07 MPa - air
Nitrogen rolling thin film oven test (NRTFOT)	163	75 min	35	1.25 mm	N ₂ flow—4000ml/min
Rotating Flask Test (RFT)— DIN 52016, EN12607-3	165	150 min	100	-	Flask rotation - 20 rpm

Ageing tests for asphalt mixtures

In the case of asphalt mixtures, the idea of these ageing procedures is to assess the effect on key material properties as stiffness, viscosity or strength. Ageing methods for asphalt mixtures can be divided in extended heating procedures (EH), oxidation tests (O), ultraviolet treatment (UV) and steric hardening (SH). Table 2-6 summarizes all the available tests for ageing simulation on asphalt mixtures [76].

Table 2-6 From Airey 2003, chronological asphalt mixture ageing methods [76]

Test method	Temperature (°C)	Duration	Sample	Extra features
Ottawa sand mixtures (Pauls and Welborn, 1952)	163	Various periods	50 x 50 mm ² cylinders	EH
Huveem et al. (1963)	60	1,000 h	50 x 50 mm ² cylinders	Air stream of 41°C (UV)
Huveem et al. (1963)	60	24 h	305mm long semi-cylindrical specimens	Cohesiograph test (SH)
Traxler (1963)	-	-	-	UV-SH (Several methods)
Plancher et al. (1976)	150	5 h	25 x 40 mm ² Ø	EH
Kumar and Goetz (1977)	60	1,2, 4, 6, 10 days	Compacted specimens	Air at 0.5 mm of water (O)
Ottawa sand mixtures (Kemp and Prodoehl, 1981)	60	1,200 h	-	EH
Kemp and Prodoehl, (1981)	35	18 h	-	1,000 MW/cm ² Amgtrôm actinic radiation (UV)
Hugo and Kennedy (1985)	100	4 or 7 days	-	80% relative humidity (EH)
Hugo and Kennedy (1985)	-	54 h	-	Actinic light (UV)
Hugo and Kennedy (1985)	-	14 days	-	Atlas weathometer
Oregon mixtures	60	0, 1, 2, 3, 5 days	Compacted specimens	0.7 MPa – air (O)
Production ageing (Von Quintas, 1988)	135	8, 16, 24, 36 h	Loose material	EH
Long-term ageing (Von Quintas, 1988)	60	2 days	Compacted specimens	EH
	107	3 days	Compacted specimens	EH
Long-term ageing (Von Quintas, 1988)	60	5 to 10 days	Compacted specimens	0.7 MPa – air (O)
	135	2 h	Loose material	EH
Bitutest protocol	85	5 days	Compacted specimens	EH
	135	4 h	Loose material	EH
SHRP short-term oven ageing (STOA)	135	4 h	Loose material	EH

Test method	Temperature (°C)	Duration	Sample	Extra features
SHRP long-term oven ageing (LTOA)	85	5 days	Compacted specimens	EH
SHRP low pressure oxidation (LPO)	60 or 85	5 days	Compacted specimens	Oxygen - 1.9 l/min (O)
PAV mixtures	100	72 h	Compacted specimens	2.07 MPa – air (O)
Khalid and Walsh (2000)	60	Up to 25 days	Compacted specimens	Air - 3 l/min (O)
RILEM Protocol (Short term ageing and Long term ageing)	135	4 h	Loose material	EH
	85	9 days	Compacted specimens	EH

Chapter 3. Physico-chemical study of bitumen

Résumé du chapitre

Comme cela a été décrit dans la littérature (Chapitre 2), la composition élémentaire du bitume est la suivante : le carbone, l'hydrogène, puis le soufre, l'oxygène, l'azote et des traces de différents métaux comme le calcium, le fer, le magnésium, le nickel ou le vanadium. Le degré de stabilité chimique du bitume est déterminé par les caractéristiques chimiques des différentes molécules et le rapport des composants réactifs et non réactifs. Par conséquent, il est généralement admis de subdiviser les bitumes en asphaltènes et maltènes, puis les maltènes en résines, aromatiques et saturés, par affinité polaire. Ces fractions correspondent au modèle colloïdal (dispersions d'asphaltènes dans les maltènes), qui explique bien les propriétés physiques et mécaniques du bitume.

Dans ce chapitre, l'objectif est de déterminer l'influence de la fraction d'asphaltènes sur la réponse physico-chimique du mélange. Les bitumes utilisés sont présentés. Le protocole de séparation des phases d'asphaltènes et de maltènes pour une recombinaison ultérieure est également montré. Ensuite, des bitumes contenant différentes proportions d'asphaltènes sont recomposés et étudiés. De plus, dans le but de comprendre les effets du vieillissement sur les espèces chimiques et sur l'organisation physico-chimique du bitume, des procédures de vieillissement en laboratoire sont appliquées aux échantillons à des fins de comparaison.

Le comportement mécanique des bitumes est habituellement évalué par des tests empiriques de consistance (pénétrabilité et température de ramollissement). Néanmoins, ces tests ne fournissent ni les propriétés rhéologiques des bitumes, ni ses caractéristiques chimiques, ni ses performances mécaniques. Pour ces raisons, une caractérisation chimique et physique est réalisée. Pour chaque bitume, on effectue une analyse infrarouge par transformée de Fourier, une analyse thermogravimétrique, une chromatographie en couche mince (fractions SARA), une solubilité du bitume dans le n-heptane, une chromatographie par perméation de gel, une microscopie à force atomique et les tests rhéologiques.

Enfin, à partir des tests rhéologiques et de l'application de la δ -méthode, on étudie la corrélation entre le vieillissement du bitume et le taux d'asphaltènes. La capacité de la δ -méthode pour suivre le vieillissement du bitume est ainsi évaluée.

3.1 Introduction

As it has been described in the literature, the elementary composition of bitumen is carbon and hydrogen, then sulphur, oxygen, nitrogen and traces of different metals as calcium, iron, magnesium, nickel or vanadium [17,63]. Bitumen degree of chemical stability is determined by the chemical arrangements of the elements in the various molecules and on the ratio of reactive to non-reactive components. Therefore, it is generally accepted to subdivide asphaltic bitumens into asphaltenes and malthenes, and then malthenes into resins, aromatics and saturates in polar affinity [63]. These fractions fit in the colloidal model (dispersions of asphaltenes in malthenes), that is still the model that best explains the physical and mechanical properties of bitumen. It is therefore the model considered in this work.

In this chapter, the objective is to determine the influence of asphaltenes fraction onto the physico-chemical response of the material. The bitumens used for the study are presented at the beginning. The protocol for separating asphaltenes and malthenes phases for later recomposition is also shown. Then, bitumens containing different asphaltenes ratios are recomposed and studied. Moreover, in order to understand the effects of ageing on the chemical species and on the physico-chemical organization of the bitumen, laboratory ageing procedures are performed on some samples for comparison.

Bitumens mechanical behaviour is usually evaluated by standard empirical tests of consistency (penetrability and softening point temperature). However, such tests do not provide intrinsic properties of bitumens. For these reasons, chemical and physical characterisation is carried out. For the chemical evaluation, the Fourier transform infrared analysis, thermogravimetric analysis and thin layer chromatography for SARA fractions determination are performed. Whereas bitumen solubility in n-heptane, gel permeation chromatography, atomic force microscopy and rheological testing are used to evaluate the physical evolution and performance of the materials.

Additionally, from rheological testing and through the application of the δ -method, bitumen ageing and asphaltenes ratio are tried to be correlated. In fact, the ability of the δ -method to track bitumen ageing is assessed.

3.2 Materials, methods and experimental program

3.2.1 Materials

Neat bitumens

The physico-chemical study is conducted on two neat bitumens, conventional 35/50 and 50/70. The proximity in the gradation will also allow discussing the differences that exist between two grades of bitumens. Bitumen main characteristics defined by EN 1426 and EN 1427 standards

are summarized in Table 3-1. Additionally, following the EN 12592 standard, asphaltene content is determined by n-heptane precipitation, denominating this type of asphaltenes as c7-asphaltenes.

Table 3-1 Base bitumens of the study

Bitumen	Penetration (1/10 mm)	Softening Point (°C)	c7-Asph (%)
35/50	40 ± 3	52.6 ± 2.5	14.7 ± 0.5
50/70	58 ± 3	49.0 ± 2.5	14.3 ± 0.5

Model bitumens

Protocol for bitumen separation and reconstitution

With the aim of manufacturing model bitumens with defined asphaltenes content, a protocol for fractions separation and further recombination is followed. The protocol can be divided in its two principal phases, asphaltenes-malthenes separation and asphaltenes-malthenes reconstitution. The first step consists of separating bitumen in its two principal fractions, asphaltenes (n-heptane insoluble phase) and malthenes (n-heptane soluble phase). The second phase of the process is the reconstitution of constituents, both soluble on dichloromethane.

Asphaltenes-malthenes separation

This first step consists of solubilizing the malthenes phase of the bitumen on n-heptane for precipitating the asphaltenes (c7) fraction. A dispersion around 15 g of bitumen is separated in ~450 ml of solvent (ratio is 30 ml per gram of bitumen) and assembled in a 500 ml Erlenmeyer flask. Through stirring, the solution is heated up to 110°C in a heater plate until boiling and left then at 90°C during 60 min, so that a good dispersion of phases is assured. After cooling during 15 min still stirring, the flask is kept in the darkness for 120 min in order to favour a proper sedimentation of asphaltenes particles.

Subsequently, the dispersion is placed in sample holders of 20 ml and centrifuged at 3,000 rpm during 5 min for asphaltenes separation. This process is repeated several times until cleaning the asphaltenes and recovering the n-heptane transparent from centrifugation. The separated asphaltenes are left at mild temperature for drying. Meanwhile, the malthenes liquid phase is ready for solvent removal. The extraction is done with a rotatory evaporator in two steps. Firstly the flask is kept at 75°C, 4-7 mbar during approximately 90 min, and again for 30 min at 7 mbar and 98°C to assure the n-heptane evaporation. Figure 3-1 shows different parts and results of the process.



Figure 3-1 Asphaltenes centrifugation and drying, and malthenes recovery

Asphaltenes-malthenes recombination

The second phase of the process is the reconstitution of constituents, but at certain rates of combination. The first step of this phase is to weight the malthenes obtained after two processes of separation (around 26-27 g) in order to choose a concentration of asphaltenes. So the malthenes-asphaltenes (m/a) ratio is well defined.

Figure 3-2 illustrates the still separated phases, in an Erlenmeyer flask, before dichloromethane is poured inside the flask (25 ml per gram of bitumen). Then, the solution is stirred on a heating plate during 30 min at 70°C to assure the mixing and dissolution of both components. Afterwards, the flask is placed in the rotatory evaporator for solvent removal. The conditions followed are the same as for the separation step (75°C, 4-7 mbar, 90 min, and then for 30 min at 7 mbar and 98°C).



Figure 3-2 Asphaltenes and malthenes for bitumen recombination

Finally, model bitumens with defined m/a ratio are ready to pass control tests in order to check solvent presence. Then, once the validation is done, bitumens are ready to be stored and tested. Figure 3-3 shows the 10 bitumens of this study by their malthenes and asphaltene content. Denomination code will follow the sequence “Bitumen” + “Percentage” + “Fraction”. So 35/50 85M+15A bitumen is the model bitumen from 35/50 with 85% malthenes and 15% asphaltene.

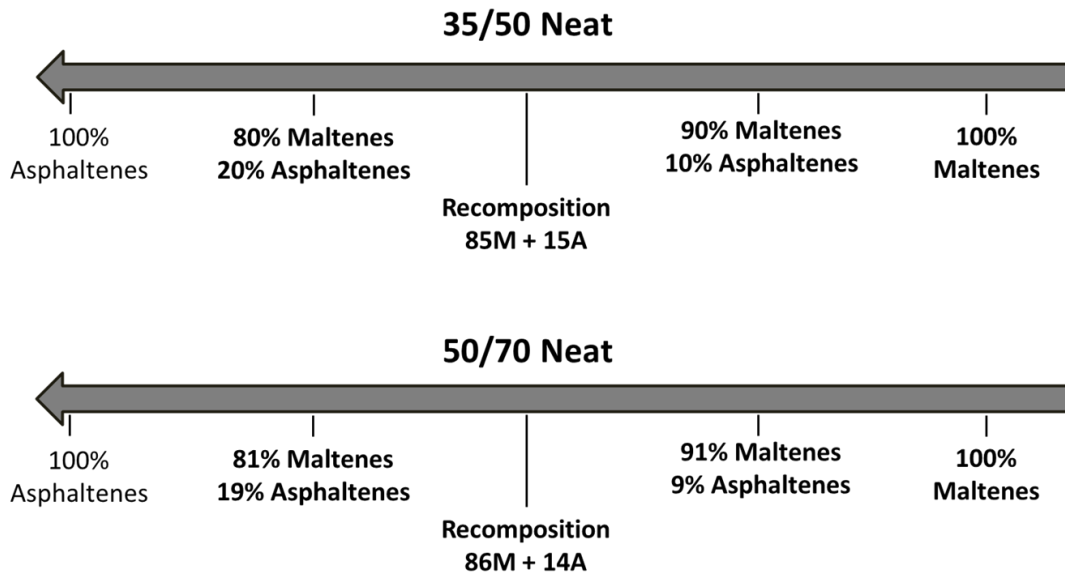


Figure 3-3 Model bitumens studied by malthenes (M) and asphaltenes (A) content

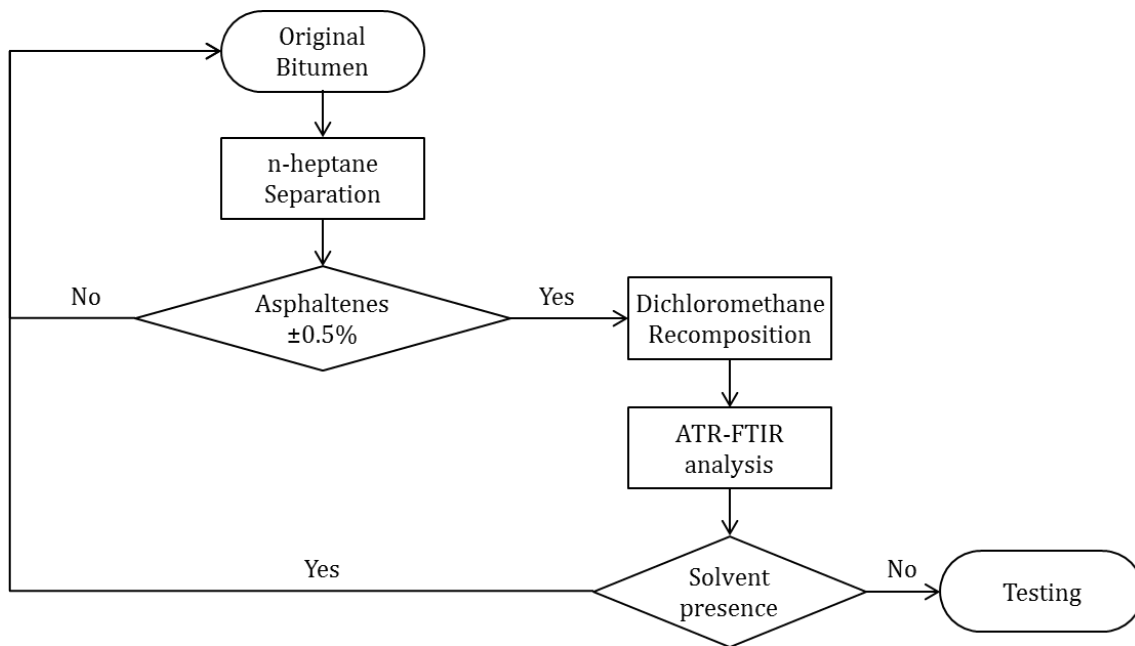


Figure 3-4 Flowchart followed on model bitumens

Ageing procedure

Furthermore, with the aim of studying the properties and performance of the bitumen over time, both rolling thin film oven test (RTFOT) and pressure ageing vessel (PAV) test are carried out. These two methods are intended to represent in laboratory the ageing experienced during manufacture, transport, laying, compaction and service life.

With both procedures short term and long term ageing are simulated. The short term ageing is performed through the RTFOT procedure (EN 12607-1). The ageing is conducted in eight glass bitumen containers with 35 g of bitumen each. Then, the flasks are introduced into a ventilated oven with a rolling carriage at 163°C for 75 min with an air flow of 4 l/min. In addition, the standard PAV procedure (EN 14769) is conducted to simulate the long term ageing in-service caused by time exposure. In this case 50 g samples are placed after RTFOT in pans and aged on a vessel pressure of 2.10 MPa for 20 h at 100°C. Table 3-2 summarizes the principal characteristics in terms of malthenes-asphaltenes relation of the 35/50 aged bitumens from n-heptane precipitation (EN 12592).

Table 3-2 Aged bitumens studied by malthenes and asphaltenes content

Bitumen denomination	% Malthenes	% c7-Asphaltenes
35/50 RTFOT	82.2 ± 0.5	17.8 ± 0.5
35/50 PAV	78.6 ± 0.5	21.4 ± 0.5
50/70 RTFOT	84.1 ± 0.5	15.9 ± 0.5
50/70 PAV	79.4 ± 0.5	20.6 ± 0.5

3.2.2 Chemical characterization

ATR FTIR analysis

The Attenuated Total Reflectance Fourier Transform Infrared (ATR-FTIR) spectroscopy analysis is performed with the purpose of verifying the evaporation of the solvent when manufacturing the model bitumens. Additionally, it is also used to monitor ageing on the laboratory aged bitumens (RTFOT and PAV).

Carbonyl groups (Ico) and sulphoxide groups (Iso) are characterized from the raw ATR-FTIR spectra according to the RILEM method [82]. The spectrum (5 spectra per sample) is collected in the wavenumber range of 4,000-400 cm⁻¹. Limits are fixed for the carbonyl area (peak centred on 1,700 cm⁻¹), sulphoxide area (~1,030 cm⁻¹) and the reference area for the methyl and ethylene groups (CH₂ ~1,380 cm⁻¹ and CH₃ ~1,430 cm⁻¹). Only those areas above the baseline between limits are taken into account. The limits on the spectra for carbonyl compounds are fixed in this study between 1,642 and 1,723 cm⁻¹, the sulphoxide area fixed between 980 and 1,082 cm⁻¹, while the reference area is fixed between 1,350 and 1,525 cm⁻¹.

Thermogravimetric analysis

Thermogravimetric analysis (TGA) is a method of thermal analysis. With the TGA Q50 device, physical and chemical changes on material are measured as a function of increasing temperature

or time, with constant heating rate or with constant temperature and/or constant mass loss respectively. TGA measurements are made in temperature ramp (10°C/min in nitrogen atmosphere, between 30°C and 600°C), in samples of 5-10 mg, measuring a constant mass loss rate to show specific reaction kinetics in the asphaltenes fraction.

Thin layer chromatography with flame ionization detector

Thin Layer Chromatography coupled with a Flame Ionization Detector (TLC-FID) performed with an Iatroscan MK-6s device is used to determine SARA fractions (Saturates, Aromatics, Resins and Asphaltenes). From this type of analysis the asphaltenes will not be c7-asphaltenes as the solvent used for separation is not n-heptane. Following Le Guern [83] notation, this type of asphaltenes will be called i-asphaltenes.

For the samples preparation, 0.05 g of bitumen is diluted in 5 ml of toluene solution of HPLC purity. A microliter syringe is used for loading 1 µl of sample, resulting on one spot of 1 – 1.5 mm size on the 10 different silica bars (Chromarod-SIII) employed on each test. Rods are then sequentially developed using hexane (~ 100% of the bar length), toluene (~ 50%), and solution of dichloromethane:methanol (95:5 v:v, ~ 25%) before the analysis.

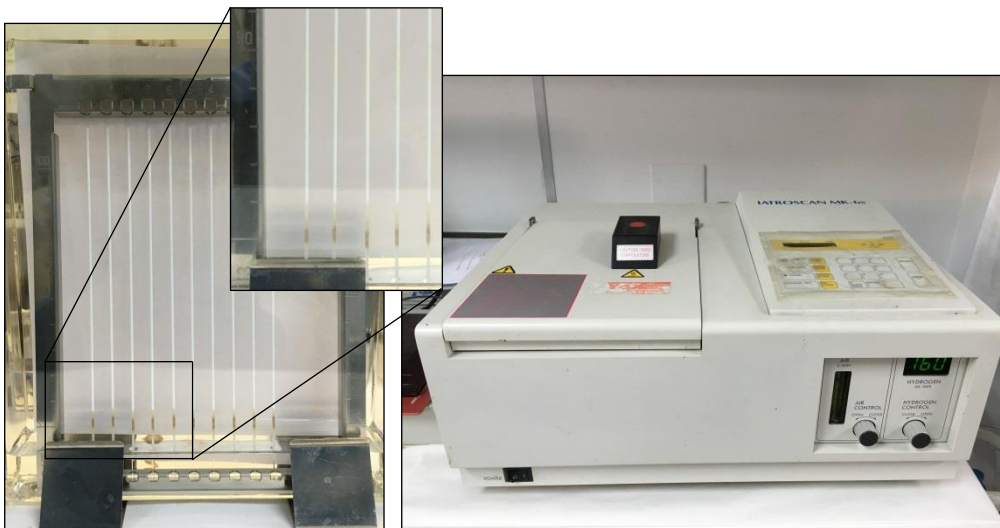


Figure 3-5 Iatroscan MK-6s device used for SARA fractions determination

Results from the TLC-FID Iatroscan test are used to determine the different SARA fractions content of each sample. Moreover, it serves to determine the colloidal index (I_c) [84] of the samples when doing the relation between them. The colloidal instability index is based on the colloidal model [85,86] to explain the difference between sol and gel bitumens. I_c typically ranges from 0.5 to 2.7 for road bitumens and is presented as follows [87]:

$$I_c = \frac{i - \text{Asphaltenes} + \text{Saturates}}{\text{Aromatics} + \text{Resins}}$$

3.2.3 Physical characterization

Atomic force microscopy (AFM)

Atomic force microscope Multimode™ connected to a Nanoscope IV scanning probe microscope controller (Digital Instruments, VeecoMetrology Group Inc., Santa Barbara, USA) placed over a vibration isolator is used for images acquisition. This technique is used to measure phase and topography in order to characterize the microstructural features of the surface of the bitumen samples. It reflects possible colloidal and intermolecular interactions in the binder as well as its chemical composition.

Bitumen films are prepared by applying gout of sample onto a 12 mm steel disk. The samples are prepared by heat-casting, a method that causes a negligible effect on the material morphology if compared to solvent-casting [88]. The disk is then heated on a heater plate at 110°C for a short period of time while turning it for assuring its spread on a thin film, this process is repeated several times. The film is afterwards cooled at room temperature and covered to prevent dust pollution, and annealed for 96 hours before testing. This annealing is performed to allow the ordering of the asphaltenes responsible for steric hardening [89]. For each bitumen disk, topographic and phase-lag AFM images of 50 x 50 μm^2 and 20 x 20 μm^2 are acquired in piezoelectric tapping mode at 40°C.

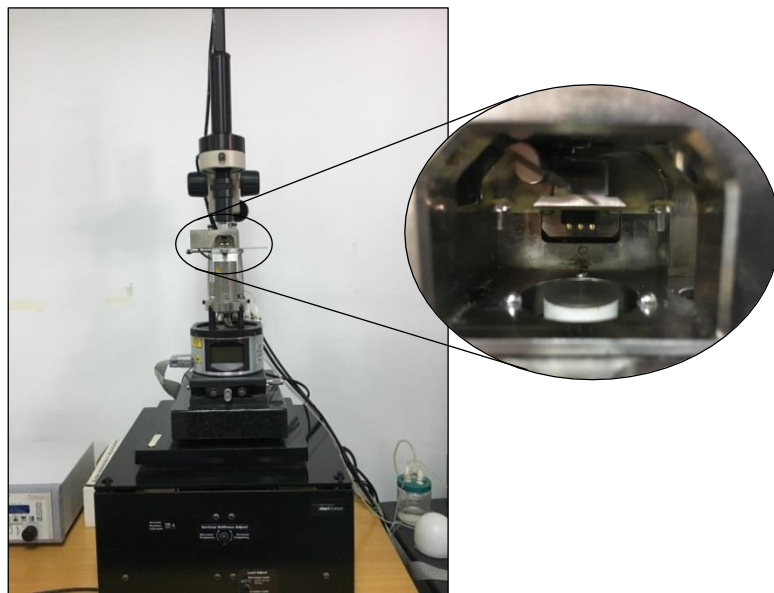


Figure 3-6 Atomic force microscope Multimode™ with a detail of sample position

Complex shear modulus test

The determination of the complex shear modulus (norm and phase angle) is performed using the dynamic shear rheometer Anton Paar MCR 501 + Peltier System to assess the rheological properties of the bitumens. The primary purpose is the construction of the master curves that

allow observing the rheological changes in the bitumen over time. The complex shear modulus (G^*) is obtained by combining the measurements performed on geometries of parallel plates of 25 mm (PP25) and 8 mm (PP08) from 10 to 0.01 Hz as frequency range and at different temperatures, -20, -10, 0, 15, 25 and 30°C for the PP08 and 15, 25, 30, 45 and 60°C for the PP25. In all cases, two tests of each sample are carried out at stress control mode, but to be sure that the samples remain in the linear domain, a stress sweep is performed at each testing temperature for each sample.

In addition, with the aim of controlling the contraction effects that the samples may suffer at low temperatures, special attention is taken for the PP08 test. Bitumen as many other materials is contracted when the temperature decrease. In order to control that there is no loss of contact between the device and the sample, a cooling rate of 1°C/min is established, imposing at the same time a normal force of zero on the sample. This last condition maintains the contact as the sample is contracting. However, during the test it is removed so there is no normal force applied on the sample.

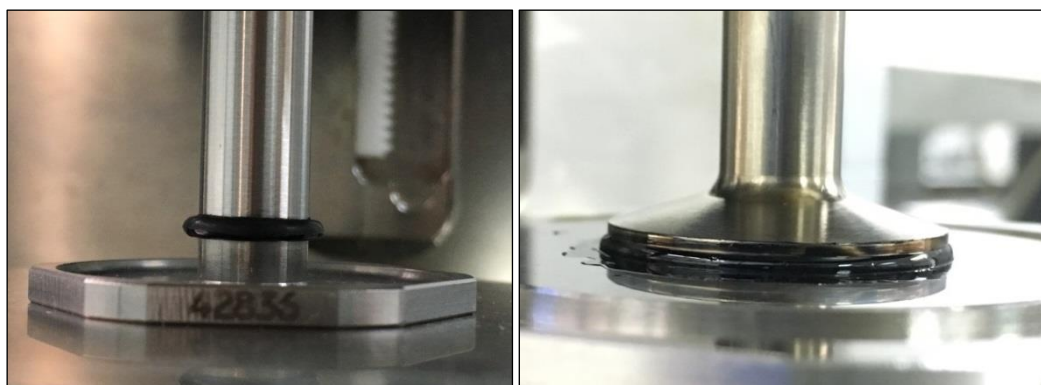


Figure 3-7 PP25 and PP08 geometries used for the testing

Gel permeation chromatography test

Neat, model and aged bitumens are analysed using gel permeation chromatography test. GPC separates and measures their molecular size distribution and the changes produced by the different asphaltenes content. Waters 2414 Refractive Index Detector equipment is used for chromatographic analysis with a Styragel® HR3 column (500 to 30,000 g/mol range) for separating the constituents dissolved in tetrahydrofuran (THF).

In order to assign a molecular weight to the different peaks measured on the bitumens tested, a calibration curve based on monodisperse polymeric standards of similar molecular architecture and nature is carried out. The calibration curve is obtained by plotting the molecular weights provided by the supplier (Sigma-Aldrich) versus the retention times determined. Figure 3-8,

shows the standards used to calibrate the apparatus curves. The molecular weights are then calculated by integration of the peaks from 500 to 30,000 g/mol.

GPC measurements are carried out on 0.1 wt.% solutions in THF. Each bitumen sample is dissolved in THF and filtered through a 0.45 µm syringe filter prior to the injection. Each test lasts for 18 minutes, and is repeated three times. The average value is taken as material molecular weight distribution.



Figure 3-8 GPC standards for curve calibration

3.2.4 Synthesis of the chemical and physical tests

A total of 14 bitumen samples are tested according to the 6 different tests chosen. All the tests are summarized in Figure 3-9.

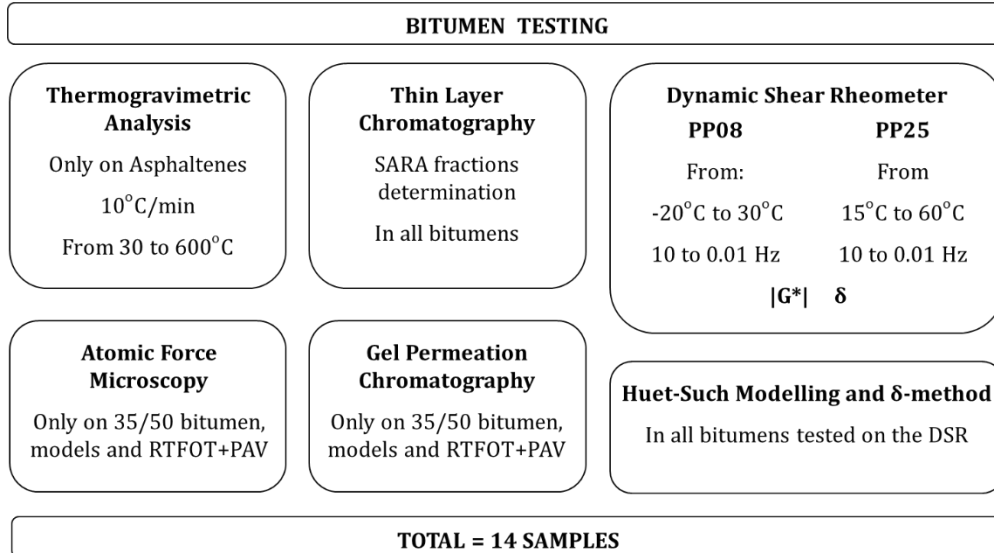


Figure 3-9 Bitumen testing protocols

3.2.5 Modelling

In order to get a comprehensive overview of the trends for the complex shear modulus a rheological model is fitted on the experimental points. Viscoelastic modelling is applied to overcome the processing problems induced by the large amount of data (for each bitumen sample there are approximately 80 values for the norm $|G^*|$ and the phase angle δ). This step

concentrates the information of the frequency and temperature sweeps in a limited number of model parameters describing the properties of the bitumen in the whole time-temperature domain.

Several studies carried out in different countries demonstrated that the Huet-Such model is one of the best suited rheological models for bitumens. This model is a combination of one spring, two parabolic creep elements and one dashpot all placed in series with a coefficient that regulates the balance between the two parabolic elements, illustrated in Figure 3-10. The 6 model parameters were determined by fitting the experimental complex modulus data $|G^*|$ and δ measured at different frequencies and temperatures. The τ parameter is determined for a reference temperature $T_{ref} = 0^\circ\text{C}$.

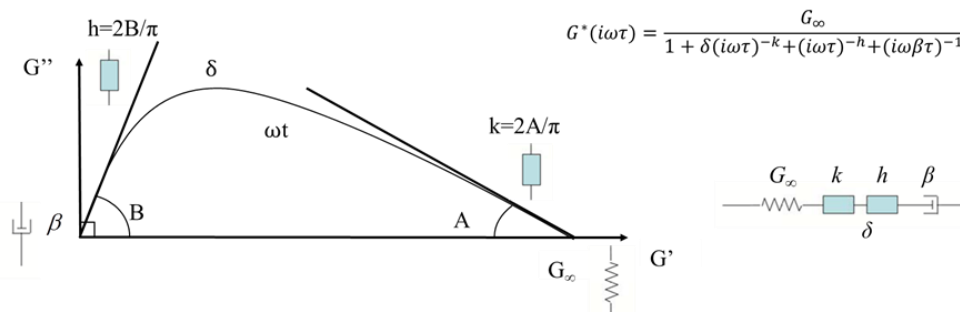


Figure 3-10 Huet-Such model, equation and Cole-Cole representation

3.2.6 δ -method calculus

It has been generally assumed that Molecular Weight Distribution (MWD) of bitumen and its rheological properties can be related [71,90–93]. Themeli’s work in 2015 [94], suggests that the phase angle (δ) of the complex modulus for a given frequency is proportional to the fraction of relaxed molecules at this frequency. It considers the material as a combination of monodispersed molecular weight (MW) species, so therefore, a relationship between the oscillation frequency and the MW of the material can be established [95].

From vapour pressure osmometry measurements, Zanzotto established a relationship between the crossover frequencies ($\omega(\text{co})$, i.e. storage modulus equal to loss modulus) at a temperature $T=0^\circ\text{C}$ and the MW [93], defined by the formula:

$$\log(\text{MW}) = 2.880 - 0.06768 \cdot \log(\omega) \quad (1)$$

When this equation is applied to the frequency axis of the phase angle master curve, it can be plotted as a function of the MW. Considering the hypothesis that the cumulative molecular weight distribution, cumf, is proportional to the phase angle master curve, the formula that relates both can be obtained. Figure 3-11 shows an example of this relation.

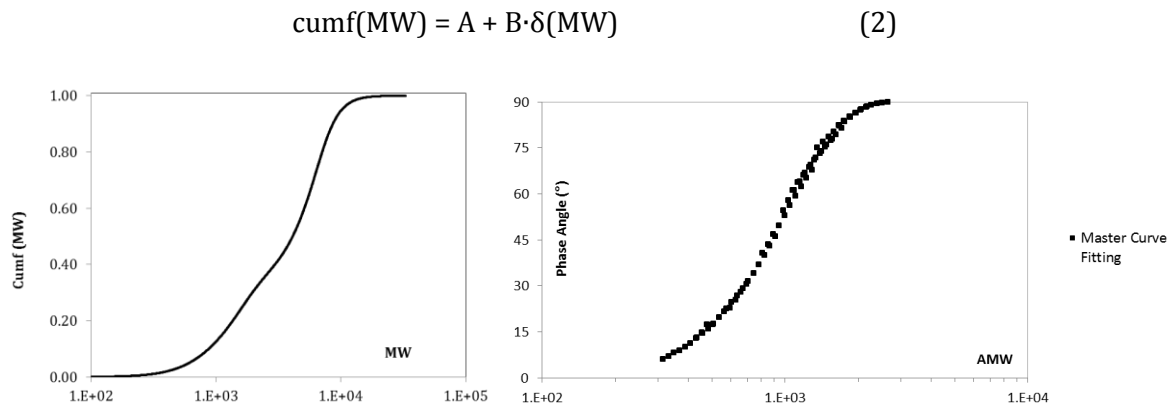


Figure 3-11 Example of curve $\text{cumf}(MW)$ and $\delta(AMW)$ [94]

Where f is a differential distribution, A and B are the proportionality constants which are calculated from the boundary conditions:

$$\begin{aligned} \text{for } MW \rightarrow 0 & \quad \delta(MW)=0^\circ \quad \text{cumf}(MW)=0 \\ \text{for } MW \rightarrow \infty & \quad \delta(MW)=90^\circ \quad \text{cumf}(MW)=1 \end{aligned}$$

As a result of the calculus, $A = 0$ and $B = 1/(90^\circ)$.

It should be noted that, according to these assumptions, the cross-over frequency, $\delta(MW)=45^\circ$ corresponds to the median of the AMWD probability distribution, $\text{cumf}(MW)=0.5$.

If this last formula (2) is differentiated, the differential molecular weight distribution (DMWD) can be calculated [95]. The differentiation can be obtained numerically according to the equation:

$$f(MW) = \frac{dcumf(MW)}{d \log MW} \cong \frac{\Delta cumf(MW)}{\Delta \log MW} \quad (3)$$

This differentiation requires a continuous curve, so the data from DSR measurements must be fitted with a continuous model. The Huet-Such model parameters fitted as describe in §2.4 are used for this purpose.

The numerical differentiation was carried out applying a numerical differential step of $1/3,000$ to the $\log(MW)$ in order to achieve the convergence. The MWD is termed “apparent” because the proportionality to the phase angle, proved for polymers, is assumed for bitumen in this study. This assumption is still to be confirmed. The word “apparent” is also used because the δ -method appears to capture the effect of groups of molecules (like clusters of asphaltenes) and not only individual molecules.

3.3 Testing results

In this section all results are presented, analysed and discussed. The structure is divided in five points as Figure 3-12 summarizes. In the first place both malthenes and asphaltenes phases from both neat bitumens are characterized. Secondly, the protocol of bitumen fractions separation and reconstitution is validated. This decision is taken in order to avoid solvents waste in the case that recomposition of bitumens is inaccurate. Then all results for the model bitumens are exposed, followed by the results concerning the bitumens aged in laboratory conditions. Finally, a relationship between laboratory ageing bitumens and model bitumens is assessed.

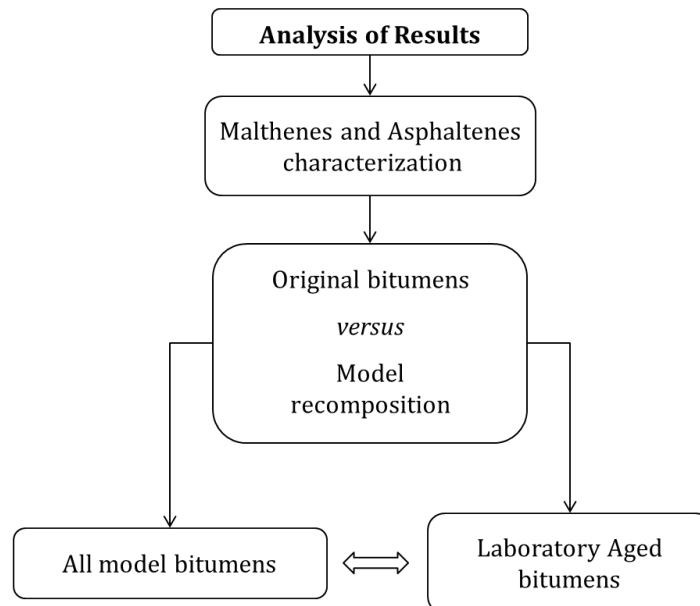


Figure 3-12 Analysis of results and discussion schema followed

3.3.1 Asphaltenes and malthenes characterization

As it is described in Materials and Methods Model bitumens section, both neat bitumens are separated in their two principal phases, asphaltenes and malthenes. With this purpose, this first section analyses the characteristics of both malthenes and asphaltenes from both neat bitumens.

Table 3-3 summarizes the ratio of malthenes and asphaltenes of each neat bitumen. 35/50 Neat bitumen has an asphaltene content of 14.7% and 50/70 Neat bitumen has an asphaltene content of 14.3%.

Table 3-3 Neat bitumens a/m ratio

Bitumen	% Malthenes	% c7 - Asphaltenes
35/50 Neat	86.6 ± 0.5	14.7 ± 0.5
50/70 Neat	85.4 ± 0.5	14.3 ± 0.5

ATR-FTIR results

ATR-FTIR is used to differentiate the quality of the bitumen fractions separation protocol. With this type of analysis the presence of solvent (n-Heptane) is traced. Figure 3-13 shows ATR-FTIR spectra from 35/50 and 50/70 Neat malthenes and asphaltenes phases. Additionally, the spectrum from n-heptane solvent is added for reference in the case of it is present in the system.

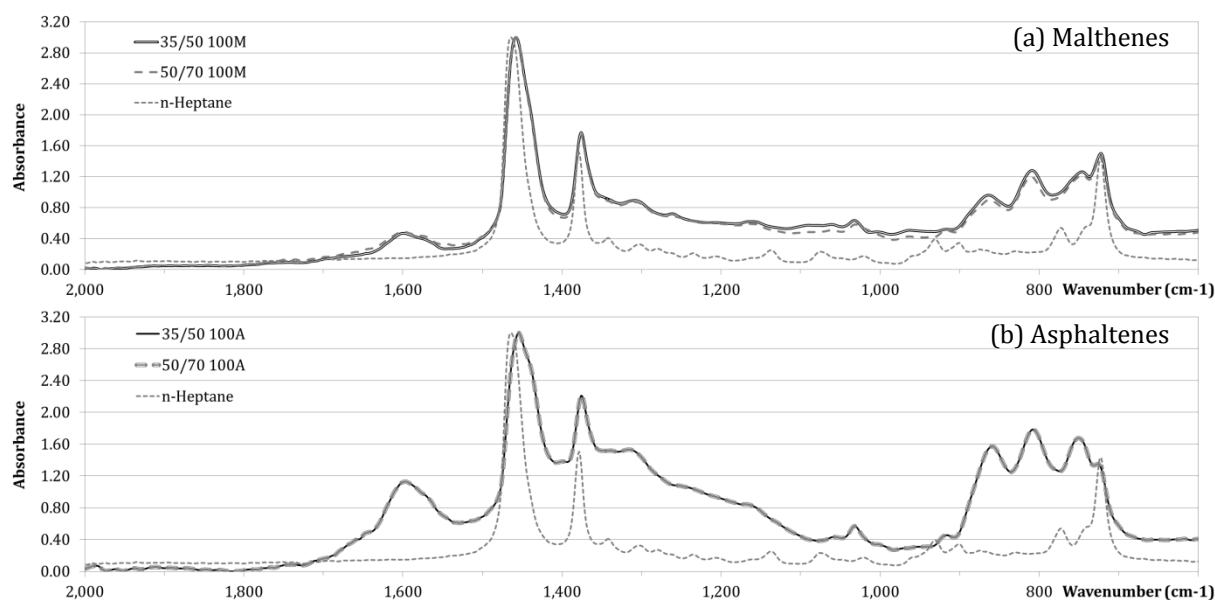


Figure 3-13 ATR-FTIR spectra from malthenes and asphaltenes phases

Both parts, (a) and (b), from Figure 3-13 show the spectra of malthenes and asphaltenes respectively. Malthenes and asphaltenes spectra are equal for both bitumens. Solvent seems to have disappeared from the samples.

TGA results

Thermogravimetric analysis is only performed on the c7-asphaltenes phases. Results presented in Figure 3-14 show the loss of sample weight in % (straight line) and its derivative as respect to temperature (dashed line) for the two tests (A-1 and A-2) per sample.

It can be observed that there is no specific kinetics reaction of asphaltenes below 300°C, which is far from conventional mixtures manufacturing temperature (160°C). However, weight loss of

0.8% at 98°C (boiling point of n-Heptane) would suggest that the solvent is not 100% removed after separation. Actually, TGA tests have been used to detect that asphaltenes from both bitumens have the same response to thermal analysis. Asphaltene residue in both tests is 60% on average of carbon black or dust.

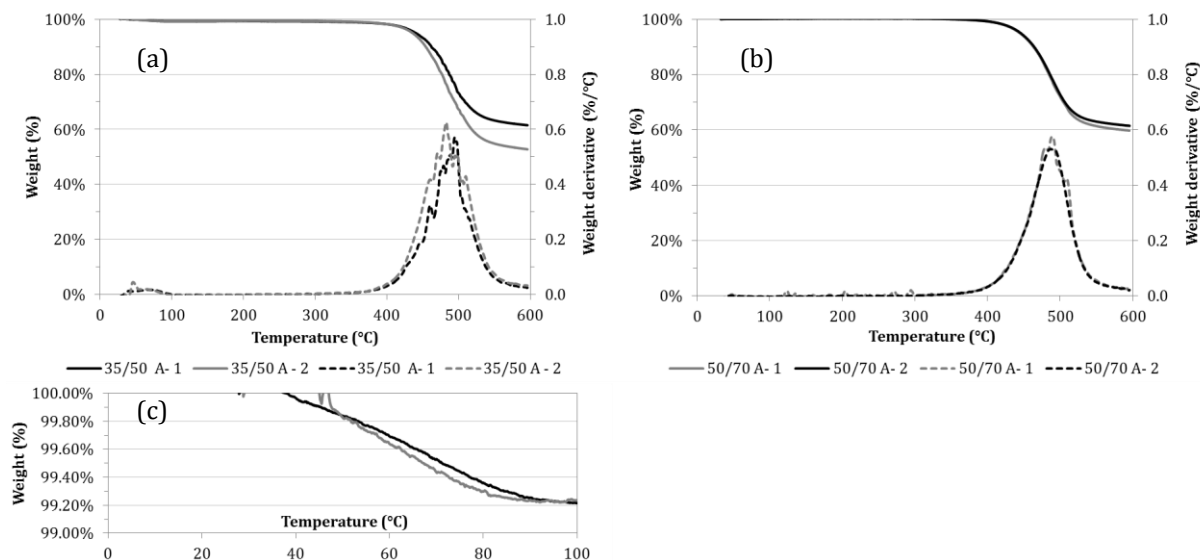


Figure 3-14 TGA diagram from 35/50 and 50/70 asphaltene fraction

SARA fractions

Bitumen chemical composition can be commonly described by its content of saturates, aromatics, resins and asphaltenes, or SARA fractions [70,75]. As it is described in the methodology §3.2.2, this analysis is done with a thin layer chromatograph, Iatroscan MK-6s. Results from fractions separation, 100M (100% malthenes) and 100A (100% asphaltenes), are summarized in Table 3-4.

Table 3-4 SARA fractions of malthenes and asphaltenes of 35/50 and 50/70 bitumens

Bitumen / Parameter	Saturates (%)	Aromatics (%)	Resins (%)	i-Asph (%)	Ic
35/50 100M	3.04 ± 0.43	73.43 ± 4.31	17.44 ± 3.14	6.09 ± 1.09	0.10
50/70 100M	1.95 ± 0.12	86.43 ± 1.35	8.41 ± 1.20	3.21 ± 0.31	0.05
35/50 100A	0.10 ± 0.17	1.91 ± 0.33	7.10 ± 2.73	90.89 ± 2.67	10.11
50/70 100A	0.04 ± 0.04	1.65 ± 0.71	5.86 ± 0.45	92.44 ± 0.82	12.32

In general, they show very similar SARA content for each fraction. On the one hand, both malthenes fractions present a high content of aromatics, going up to 86% in the case of 50/70 100M. Moreover, due to solvent employed, malthenes phase presents certain presence of asphaltenes (i-asphaltenes). In terms of Ic, values are very low which recalls the softness of the material (Ic < 0.22 leads to a softer material [72]).

On the other hand, asphaltenes phases present traces of saturates and aromatics. But again, the presence of resins in this case, it is due to the solvent (toluene) employed for fractions separation. The value of I_c is not really important here because such as values are not found on road bitumens, as they are more like a solid rather than a viscoelastic material.

DSR results: Overlapping temperature results

Regarding rheological testing, as it is mentioned on the methodology, the results of both DSR geometries PP25 and PP08 at the overlapping temperatures are compared. This is needed to prove that the material has the same rheological response with both geometries, and in order to achieve a smooth and complete Black diagram [96]. In the following figures, Figure 3-15, 16 and 17 rheological results for G' (Pa), G'' (Pa), δ ($^\circ$) and $\tan(\delta)$ are compared at the overlapping temperatures 15 $^\circ$ C, 10 $^\circ$ C and 0 $^\circ$ C for the 35/50 malthenes phase. This analysis is carried out for all bitumens (results can be found in Annex 1).

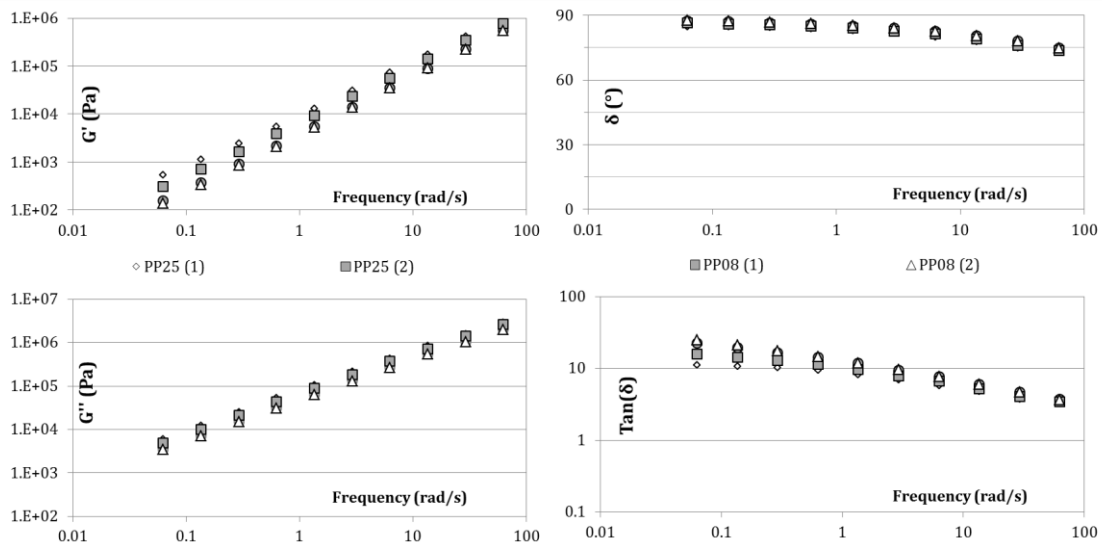


Figure 3-15 35/50 Malthenes phase PP25 and PP08 results at 15 $^\circ$ C

Figure 3-15 shows the results of two tests (PP08-PP25) at 15 $^\circ$ C. At low frequencies there is a difference in measurements. However, in the case of 10 $^\circ$ C curves in Figure 3-16 is less pronounced. The chosen values were from PP08 in all cases as they seem more consistent.

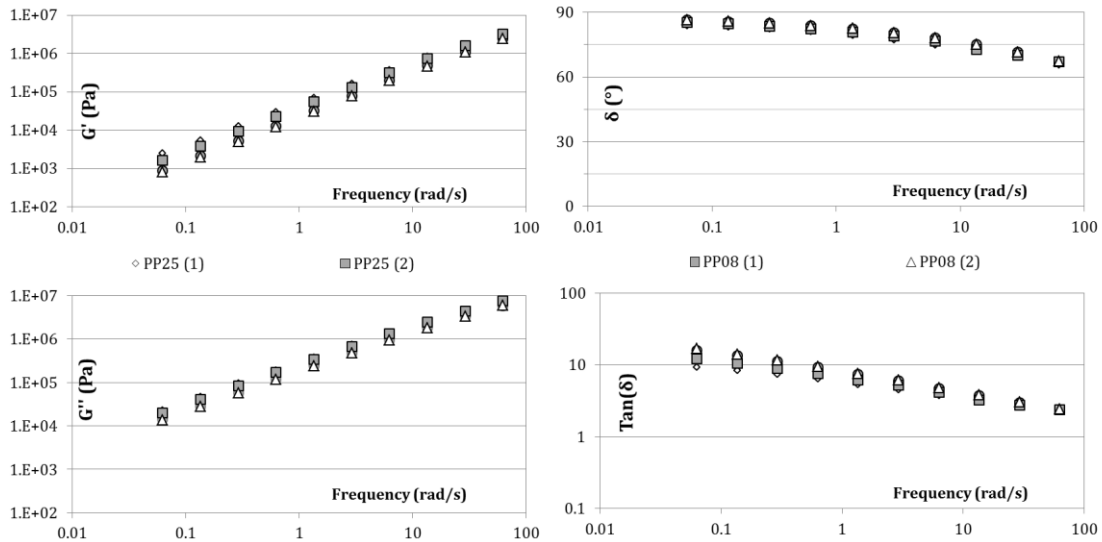


Figure 3-16 35/50 Malthenes phase PP25 and PP08 results at 10°C

On the other hand, in Figure 3-17 the differences between PP25 and PP08 geometries are at high frequencies. In order to avoid compliance of the apparatus with PP25 geometry, results from PP08 are taken into account for the calculus of the master curve.

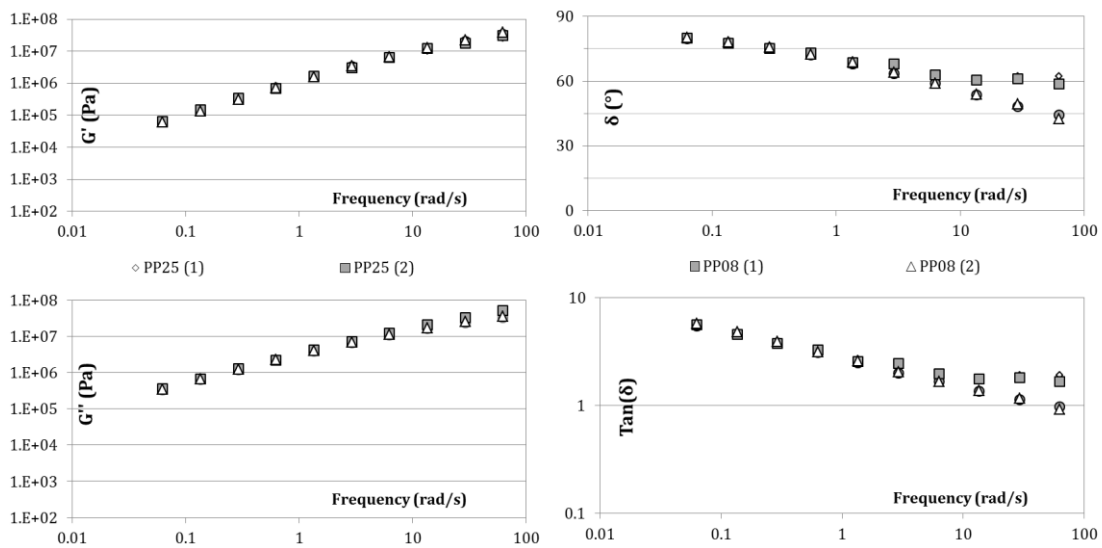


Figure 3-17 35/50 Malthenes phase PP25 and PP08 results at 0°C

DSR master curves

DSR results from 35/50 and 50/70 bitumens are respectively plotted in Annex 2. As an example, Figure 3-18 illustrates the results of the malthenes phase from the 35/50 bitumen and the master curve at $T=0^{\circ}\text{C}$ as an example. It shows the values of the norm of the complex modulus $|G^*|$ (Pa) and phase angle δ ($^{\circ}$) as a function of the frequency (rad/s). In addition, the translation

coefficients for each temperature are calculated by the William-Landel-Ferry adjustment [14]. WLF translation fits well and minimizes the errors in the calculus of shift factors.

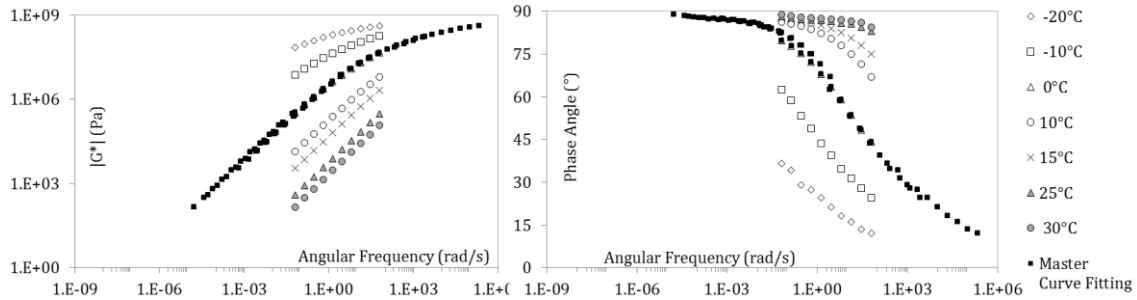


Figure 3-18 35/50 100M master curve fitting from DSR measurements at T=0°C

Huet-Such modelling

Huet-Such model fitting is carried out by an error minimisation procedure that is applied at the same time on the norm and the phase angle results. The software Viscoanalyse is used for identifying the parameters of the model. The adjusted parameters (G_{∞} , δ , k , h , β and τ) of each bitumen are summarized in Annex 3.

Figure 3-19 shows as an example the fitting of the model to the 35/50 malthenes Cole-Cole diagram (a), Black diagram (b) and master curve (c-d).

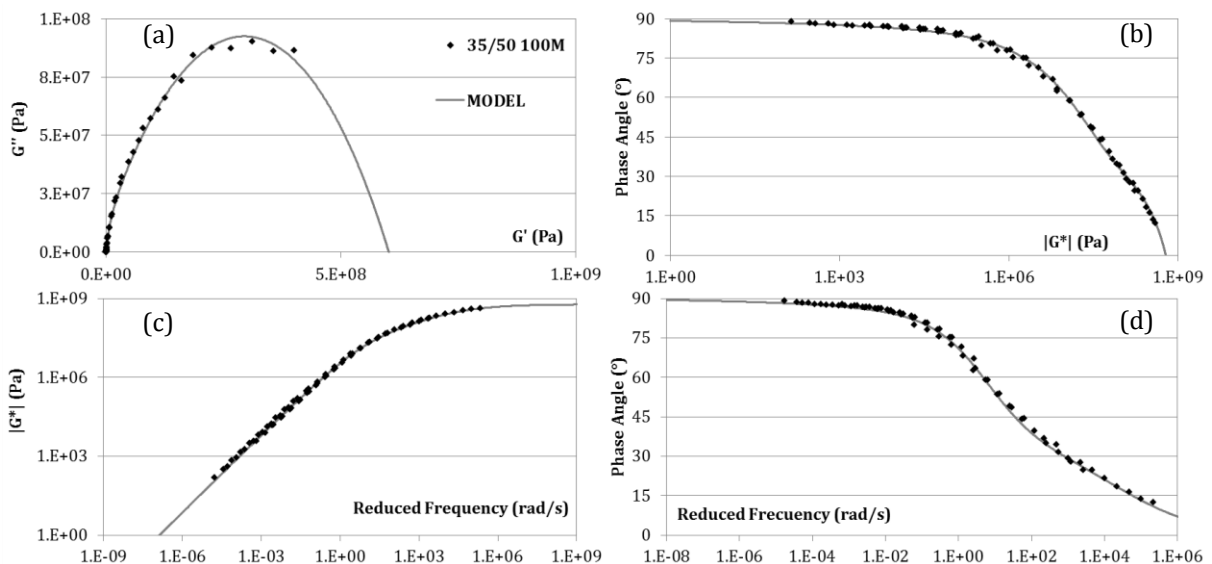


Figure 3-19 35/50 malthenes fitting model curves

As a result of applying this calculus to both malthenes samples, the master curves and fitting model curves are presented in Figure 3-20. Apparently there is no difference in rheological behaviour in between both malthenes phases. Experimentally, it could be said that they are identical.

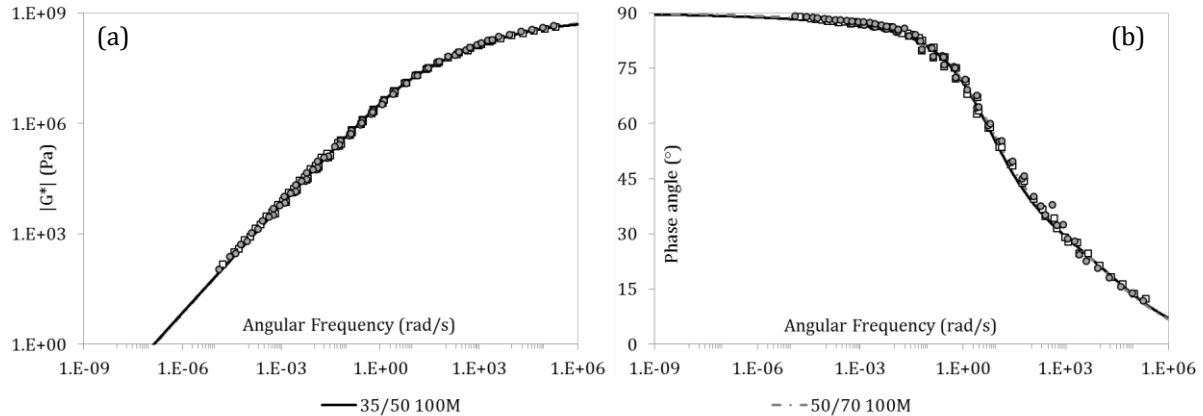


Figure 3-20 Master curves at $T=0^{\circ}\text{C}$ of (a) 35/50 and 50/70 Malthenes phase

δ -method analysis

Regarding to δ -method representation, the so-called AMWD is illustrated in Figure 3-21. According to the assumption made in section §3.2.6 the curves are plotted in the range of 100 and 10,000 g/mol in logarithmic scale. The ordinate axis corresponds to the probability density $f(\text{AMW})$. The cross-over frequency point $\omega(\text{co})$ (i.e. storage modulus equal to loss modulus, $G' = G''$) is also plotted in the graphs for each bitumen. In fact, the cross-over frequency corresponds to the median of the AMWD probability distribution

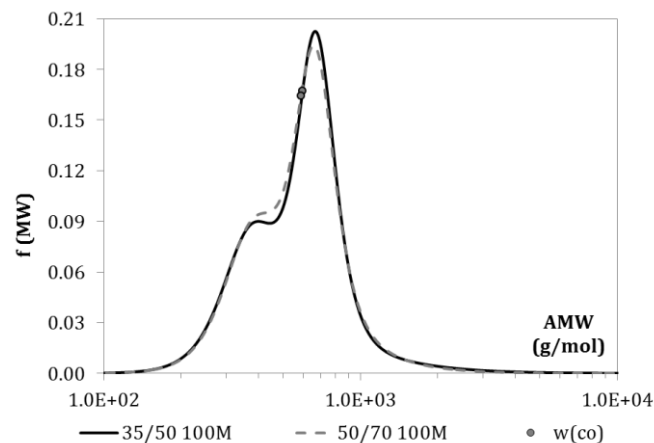


Figure 3-21 δ -method diagrams of 35/50 and 50/70 malthenes fractions

After testing the asphaltenes on the TGA and remark their superposed response, the idea is to test the malthenes phase. Rheological behaviours for malthenes fractions are identical. In the case of the δ -method, where the model curve is derived from the black diagram, it is then normal to find equivalent distributions.

Conclusion

Bitumen main phases, asphaltenes and malthenes, are very similar for the two different neat bitumens. However, even if they are composed of the same components, they don't show the same consistency, neither the same rheological behaviour. This could indicate that the asphaltenes/malthenes ratios would play an important role.

3.3.2 Validation of the recomposition protocol

After characterizing both malthenes and asphaltenes phases from the neat bitumen, in this section neat and model bitumen are compared in order to validate the process of recomposition.

Table 3-5 Neat and model bitumens a/m ratio

Bitumen	Malthenes (%)	c7 - Asphaltenes (%)
35/50 Neat	85.3 ± 0.5	14.7 ± 0.5
35/50 85M+15A	85.0	15.0
50/70 Neat	85.7 ± 0.5	14.3 ± 0.5
50/70 86M+14A	86.0	14.0

Table 3-5 summarizes the ratio of malthenes and asphaltenes of each bitumen. 35/50 Neat bitumen is recomposed with 15% of c7-asphaltenes content. On the other hand, 50/70 Neat recomposition is rounded down to 14% of c7-asphaltenes in order to differentiate both recomposed bitumens.

ATR-FTIR results

ATR-FTIR is used to differentiate the quality of the bitumen model manufacturing protocol. Additionally, it is employed as ageing detector through Ico and Iso characterization. With this type of analysis the presence of solvents (Dichloromethane) is traced. Ico and Iso values are calculated to check the influence of the process on these indicators. Figure 3-22 shows ATR-FTIR spectra from 35/50 and 50/70 Neat bitumens, plotting the absorbance versus the wavelength number on cm^{-1} .

First results show no difference in terms of neat spectra. This is not surprising due to the fact that this type of analysis is not adapted to distinguish bitumens grades [97]. The chemical composition of both bitumens is the same at the FTIR scale.

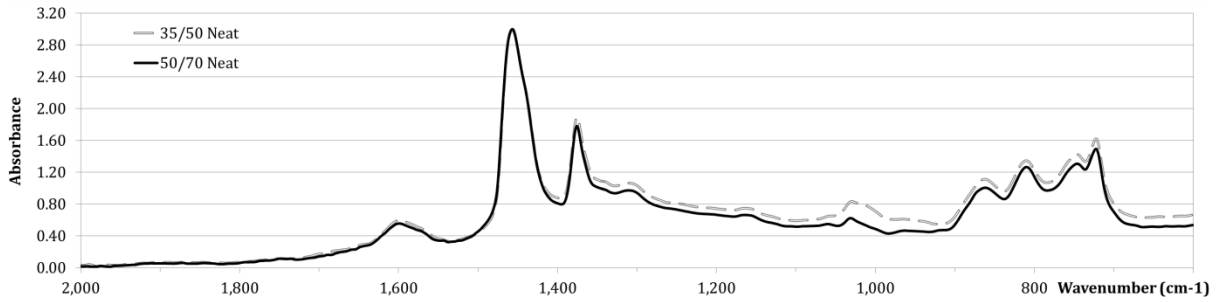


Figure 3-22 ATR-FTIR spectrum from 35/50 and 50/70 Neat bitumens

Secondly, in Figure 3-23 (a), 35/50 Neat bitumen and two reconstituted bitumens are shown. One of the reconstituted bitumens is considered as wrong after its comparison with the neat bitumen. This is in terms of FTIR spectrum, especially at 1600, 1500 and around 800 cm^{-1} . It is believed that in the first separation/recomposition procedure an error happened during the process that is reflected with a very different spectrum.

Furthermore, in Figure 3-23 (b) the 50/70 model is not as accurate but considered acceptable. It seems that there are traces of dichloromethane on the recomposed 50/70 86M+14A. These two bitumens are the first ones to be reconstituted, and helped improving the process for next steps.

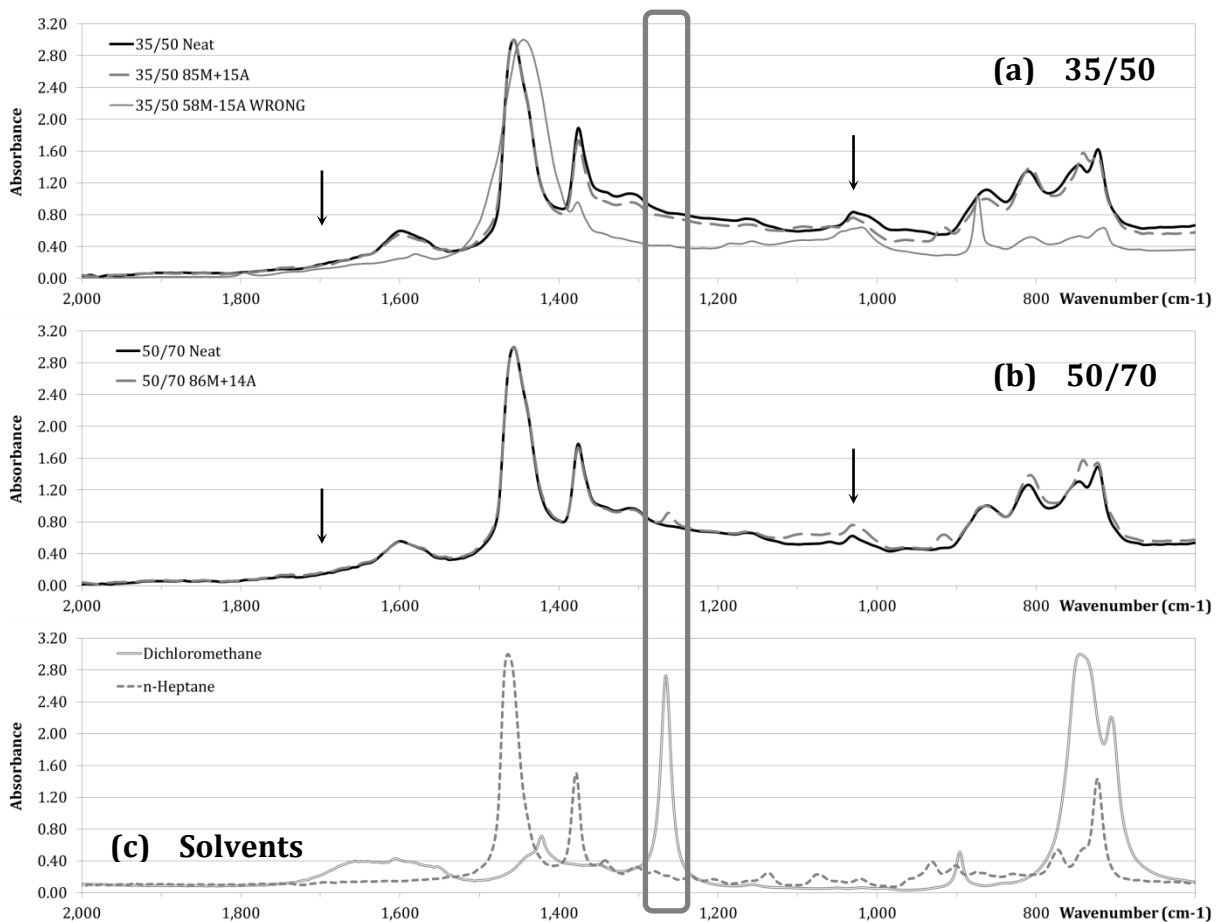


Figure 3-23 ATR-FTIR bitumens and solvent spectrum

Regarding to Ico and Iso results, in Figure 3-23 the arrows point at the carbonyl ($1,700\text{ cm}^{-1}$) and sulphoxide ($1,030\text{ cm}^{-1}$) peaks. Table 3-6 summarizes Ico and Iso values for all bitumens. Both neat bitumens do not exhibit carbonyl groups but they do show sulphoxide groups already. In addition, it seems that sulphoxide groups are more sensitive to the process of reconstitution, due to the higher values exhibited by the recomposed bitumens. This could be due to the polarity of asphaltenes. When added to malthenes phase, they have a tendency to connect better with sulphoxide groups [83].

Table 3-6 ATR-FTIR analysis of Ico and Iso values

Bitumen / Parameter	Ico (%)	Iso (%)
35/50 Neat	0.00	5.71
35/50 85M+15A	0.27	9.46
50/70 Neat	0.00	4.86
50/70 86M+14A	0.00	7.84

SARA fractions

In this section, SARA fractions are measured in order to see the presence of each fraction in the total system. Results from fractions separation are summarized in Table 3-7 differentiating between i-asphaltenes and c7-asphaltenes.

Table 3-7 SARA fractions of neat and recomposed bitumens

Bitumen / Parameter	Saturates (%)	Aromatics (%)	Resins (%)	i-Asph (%)	c7 Asph (%)	Ic
35/50 Neat	2.99 ± 0.68	66.03 ± 5.02	12.84 ± 2.02	18.14 ± 4.15	14.7	0.27
35/50 85M+15A	3.66 ± 0.67	66.76 ± 5.22	13.57 ± 2.38	16.02 ± 3.04	15.0	0.25
50/70 Neat	2.08 ± 0.11	65.07 ± 1.98	12.36 ± 1.04	20.49 ± 1.40	14.3	0.29
50/70 86M+14A	2.12 ± 0.41	68.27 ± 4.77	10.26 ± 1.25	19.36 ± 4.35	14.0	0.27

They show very similar content for each fraction. It should be remarked the high content of aromatics in all bitumens. i-Asphaltenes and c7-asphaltenes do not have the same presence on the bitumens. This is due to the solvent employed for their separation. Some researchers [98] have defined this difference as “polar resins” that are trapped in the i-asphaltenes. In terms of SARA fractions, bitumen reconstitution respects the balances between fractions.

Moreover, in the last column of Table 3-7, the colloidal indexes are calculated. The colloidal index typically ranges from 0.5 to 2.7 for current road bitumens. A marked gel (non-Newtonian behaviour) character is observed for $Ic > 1.2$ and a typical sol (Newtonian) behaviour is found for

$I_c < 0.7$ [71,87]. Overall, all bitumens seem to present sol behaviour. Model bitumens present a slightly inferior value of I_c , but still it is very similar to the corresponding neat bitumen.

In Figure 3-24 (a) SARA fractions are illustrated by percentage with their respective error bars, while in Figure 3-24 (b) the colloidal indexes calculated for all systems are shown.

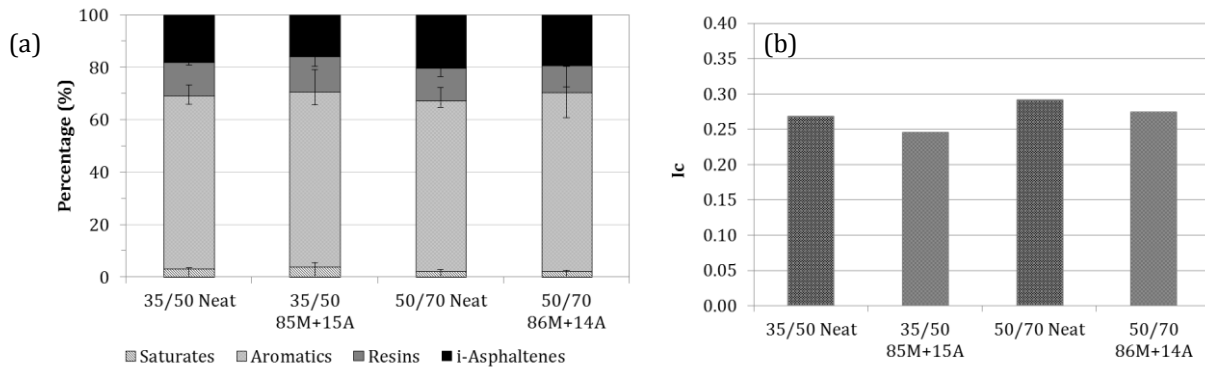


Figure 3-24 (a) SARA fractions from neat and recomposed model bitumens, (b) Colloidal indexes of all bitumens

AFM results

Microstructure morphology of 35/50 Neat and model bitumens is presented as topography in Figure 3-25. Both bitumens are reachable as a microstructural overview by $50 \times 50 \mu\text{m}^2$ that displays the characteristics of the materials.

Qualitative observation of 35/50 Neat bitumen (Figure 3-25 a and c) shows similar results with other researchers [83,99,100] about the apparition of bee structure. Commonly linked to the presence of asphaltene in the bitumen, recent researches have cleared up that its presence is strongly related to the cooling rate of the sample and the presence of waxes on the bitumen [100]. Three distinct phases can be identified [101] on both bitumens. They are the Catana or Bee phase, the Periphase that recovers the first one and the Perpetua phase [89,99,102,103], all highlighted in (c) and (d) with a resolution of $20 \times 20 \mu\text{m}^2$.

On the other hand, 35/50 85M+15A bitumen images (b) and (d) reveal the development of small structures at the bitumen/air interfaces exhibiting rippled surface (some bees) as it is found by other researchers when recomposing the asphaltene-malthenes phases [99]. They may not be as clear as 35/50 Neat bitumen images, but their distribution within the image does.

According to these observations, after bitumen separation and recombination, bitumen microstructure is very similar.

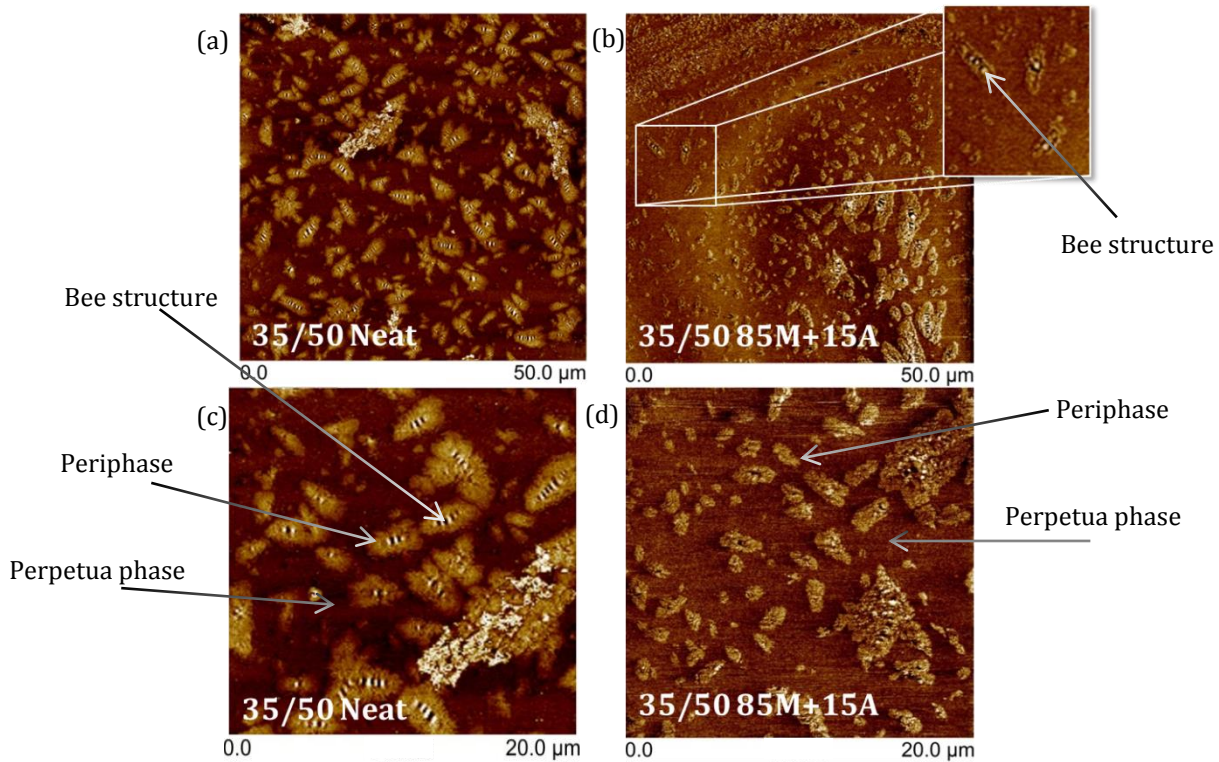


Figure 3-25 Microstructure of 35/50 Neat and 35/50 85M+15A samples: AFM topography images of 50x50 μm^2 and 20x20 μm^2 after 4 days conditioning

Rheological performance

All tests are performed under the same conditions, as it is described in Materials and methods section § Complex shear modulus test. Overlapping temperatures are 30°C, 25°C and 15°C for PP25 and PP08. Then, the most suitable temperature is chosen for assuring a smooth Black diagram [76].

All coupling results are presented in Annex 1. As a summary, it can be said that in general, at 30°C there is a difference at low frequencies in the phase angle δ and $\tan(\delta)$ response for the PP08 geometry. It is considered that PP08 is a too small geometry to study the material response at this temperature. In contrast, the response of the material for the PP25 geometry at 15°C is not accurate. The measuring system gets to compliance of the device due to the needed torque in order to stress the material at the required level at high frequencies, as $\delta(^{\circ})$ and $\tan(\delta)$ show.

Huet-Such modelling

Once the master curves of all bitumens are constructed, following the same procedure described in the previous section, the modelling can be applied. Figure 3-26 (a) illustrates the master curves at 0°C for both 35/50 Neat and its recomposed bitumen, and then Figure 3-26 (b) the results for the 50/70 Neat and model bitumen.

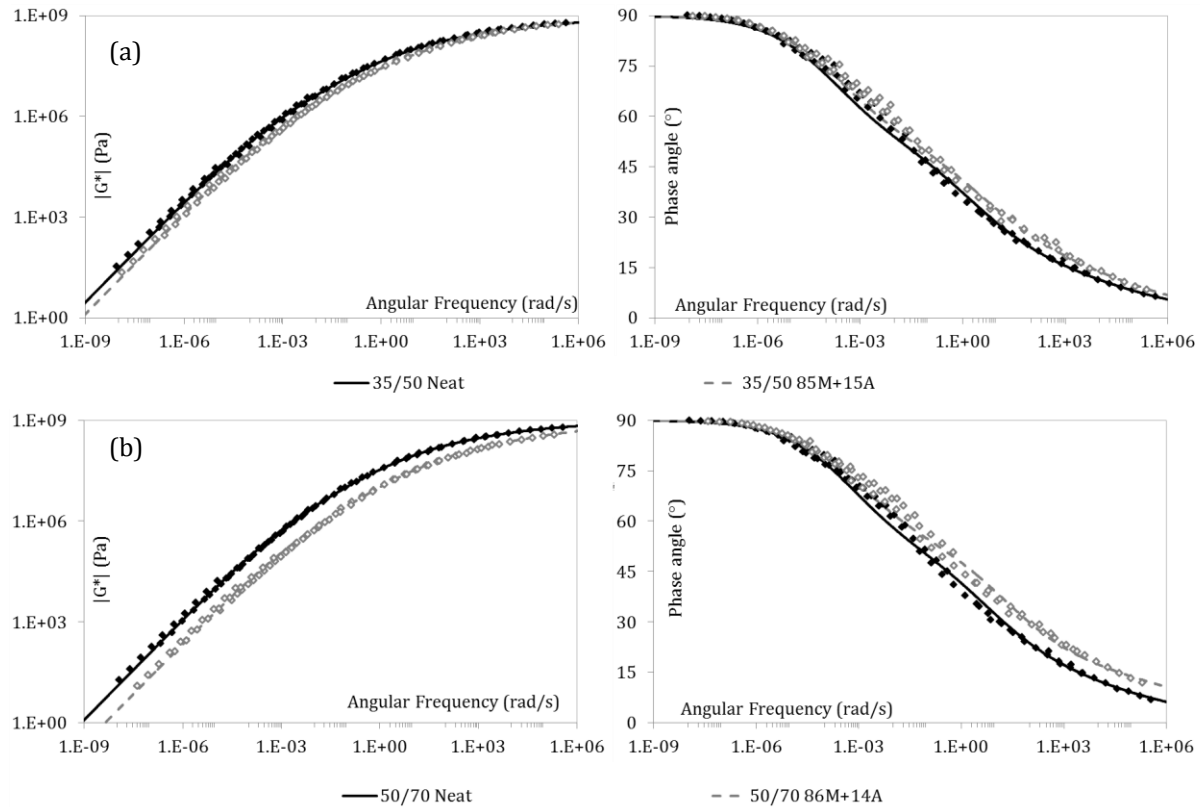


Figure 3-26 Master curves at $T=0^\circ\text{C}$ of (a) 35/50 Neat and 35/50 85M+15A and (b) 50/70 Neat and 50/70 86M+14A

In Figure 3-26 (a) a slight difference between 35/50 and 35/50 85M+15A can be found at high frequencies. Even having higher *c7*-asphaltene content, the model bitumen seems to have softer rheological response. In the case of 50/70 bitumens presented in Figure 3-26 (b) the softer response of the model bitumen can be directly justified by the difference in the asphaltene content. These results are in accordance with the higher I_c values found for both neat bitumen (See Table 3-7 above).

 δ -method analysis results

The δ -method analysis is focused on the changes on the apparent molecular weight distribution. The AMWD is illustrated in Figure 3-27 in the range between 100 and 10,000 g/mol in logarithmic scale with the ordinate axis corresponding to the probability density $f(\text{AMW})$, including cross-over frequency points $\omega(\text{co})$.

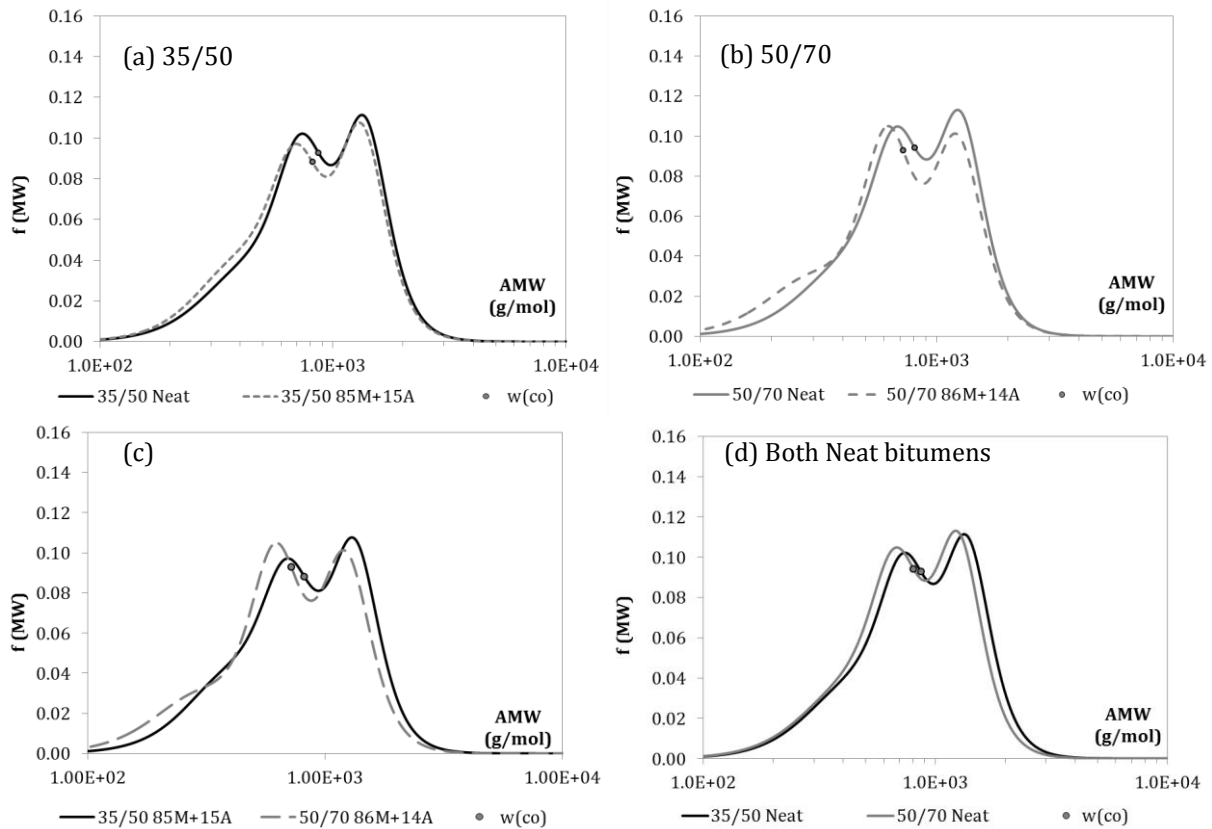


Figure 3-27 δ -method diagrams of 35/50 and 50/70 Neat and model bitumens

δ -method analysis applied on the four bitumens show the similarities on the curves. Both 35/50 bitumens in Figure 3-27 (a) have the same shape. Even cross-over frequencies are close to each other. In the case of 50/70 bitumens in Figure 3-27 (b) the curves are not as similar as the others, but still the model bitumen represent the shape of the neat one.

Looking at Figure 3-27 (c), recomposed bitumens from 35/50 and 50/70 with only 1% difference in asphaltene content show a similar curve. In Figure 3-27 (d), it can be observed the similarity on the curve distribution for both neat bitumens. All characteristics (penetration, softening point, asphaltene content and rheological behaviour) showed that 35/50 bitumen is harder than 50/70. The δ -method does as well but the difference is not very important. In the same way, the value of the cross over frequency is slightly different with a trend to move to higher AMW.

GPC results

The GPC results from 35/50 bitumens are used to have an indication of the variation in molecular size from a more conventional test. When a bitumen sample is dissolved in a solvent (THF), the different molecules separate. Then if the solution is applied to the top of the porous column, the smaller molecules are distributed through a larger volume of gel than is available to

the large molecules. Consequently, the large molecules move faster through the column and in this way out, the detector can measure the intensity of the signal for the different components.

Figure 3-28 (a) represents molecules retention time versus the normalized signal from the device. The first molecules that appear at shorter retention times are the large molecules and then the smaller ones. In the case of Figure 3-28 (b) the ordinate axis corresponds to the translated molecular weight after the application of the calibration curve.

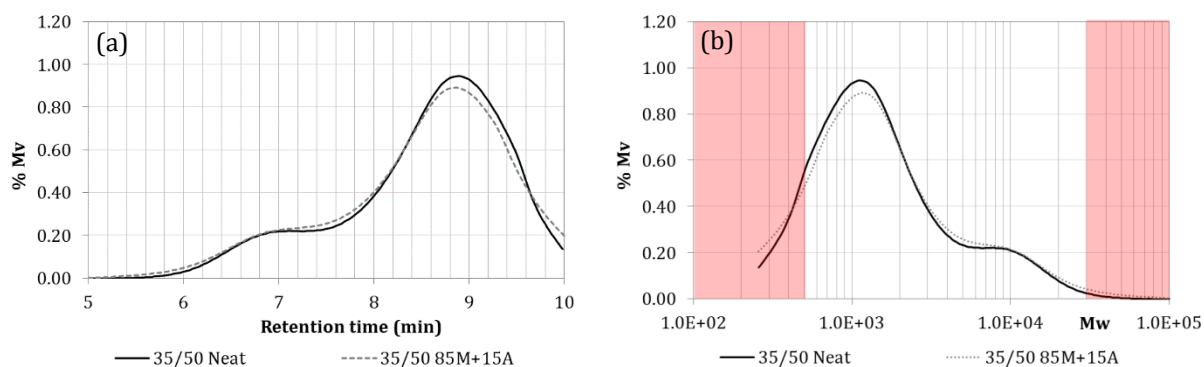


Figure 3-28 GPC plots from 35/50 Neat and 35/50 85M+15A

From both figures it can be noted again the similarity between curves. Higher molecules seem to appear at highest concentrations at 7 min of retention time, corresponding to 10,000 g/mol of average molecular weight. Besides, at 8.8 min the peak of the smaller molecules is obtained, corresponding to 1,000 g/mol of molecular weight. The red bands in the borders correspond to extrapolation calculus, as the column only covers between 500 and 30,000 g/mol.

Moreover, Table 3-8 summarizes the results of the molecular weights of 35/50 Neat and model bitumen, where M_n is the number-average molecular weight (g/mol), M_w is the weight-average molecular weight (g/mol), M_p is the peak molecular weight (g/mol), M_z is the z-average molecular weight (g/mol) and $PDI = M_w/M_n$ is the polydispersity index, relative to the spread in MW. PDI is usually used as a measure of the broadness of the distribution. $PDI=1$ indicates a monodisperse distribution, $PDI = 1.1$ to 2.0 shows an intermediate polydisperse distribution type. $PDI > 2$ indicates a broad distribution, while narrow distribution shows a PDI between 1.02-1.10.

Table 3-8 Molecular weights of 35/50 bitumens

	M_n (g/mol)	M_w (g/mol)	M_p (g/mol)	M_z (g/mol)	M_{z+1} (g/mol)	PDI
35/50 Neat	664	949	876	1,275	1,571	1.43
35/50 85M+15A	857	1,162	1,061	1,509	1,853	1.36

As to the MW obtained from the GPC spectra, model bitumen seems to have higher MW than the Neat bitumen.

Conclusions

Bitumen recomposition is possible in laboratory using dissolution and recomposition processes described in this thesis. The responses obtained by recomposed model bitumens are quasi equivalent in general to the neat bitumens. There is a big difference between manufacturing procedures, refining versus laboratory recomposition. However, bitumen response is not so different. This step validates the process of separation and recomposition for further analysis.

3.3.3 Model bitumens at different m/a ratios

Once the separation-recomposition protocol is validated for the reference bitumens the rest of the model bitumens could be manufactured. In the following subsections the line of analysis is going to be the same as before.

ATR-FTIR results

Figure 3-29 represents in (a) the spectra of the 35/50 model bitumens, in (b) the spectra of the 50/70 model bitumens and in (c) the spectra from the solvents employed during the separation and recomposition. With the arrows pointing at the carbonyl and sulfoxide peaks

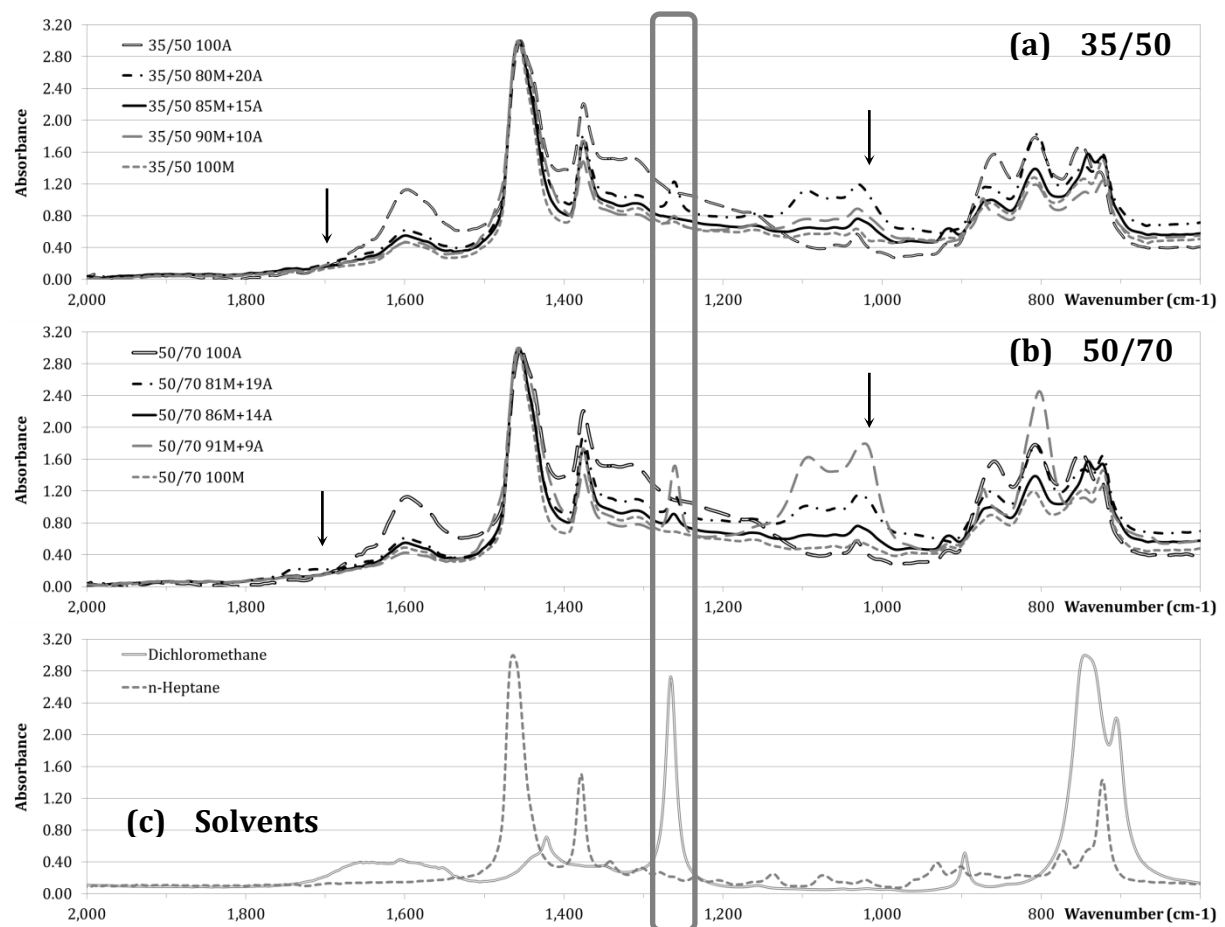


Figure 3-29 ATR-FTIR model bitumens and solvent spectrum

In general, it can be highlighted that the dichloromethane solvent extraction protocol is not 100% assured in all cases. It seems that there are still traces in the model bitumens for both types and at different ratios. Moreover, the variation of asphaltenes content has led to variations in the ATR-FTIR spectra. For example 50/70 91M+9A model bitumen presents higher absorbance between 1,100 and 1,000 cm^{-1} , which is not usually common in bitumens spectra. The changes of other molecular structures (e.g. benzene, methylene and methyl) can also reflect the chemical modification of bitumen [104], as the increment on the C=C bonds for the asphaltene phase in both bitumens.

Table 3-9 ATR-FTIR analysis of Ico and Iso values of 35/50 model bitumens

Bitumen / Parameter	Ico (%)	Iso (%)
35/50 90M+10A	0.75	9.74
35/50 85M+15A	0.27	9.46
35/50 80M+20A	0.09	12.60
50/70 91M+9A	0.00	29.54
50/70 86M+14A	0.00	7.84
50/70 81M+19A	0.00	12.92

Regarding Ico and Iso values, the influence of manufacturing process in possible ageing of the samples is summarized in Table 3-9. There is no real correlation between the m/a ratio and the evolution of aging indexes. Carbonyls groups are commonly employed for tracing ageing evolution. However, in this case the material is not naturally aged, so the measure of Ico can be influenced by the increase of C=C bonds at 1600 cm^{-1} . On the other hand, sulfoxide groups are one of the most polar parts of the bitumen, so then the asphaltenes play an important role on the increase of this value [83].

SARA fractions

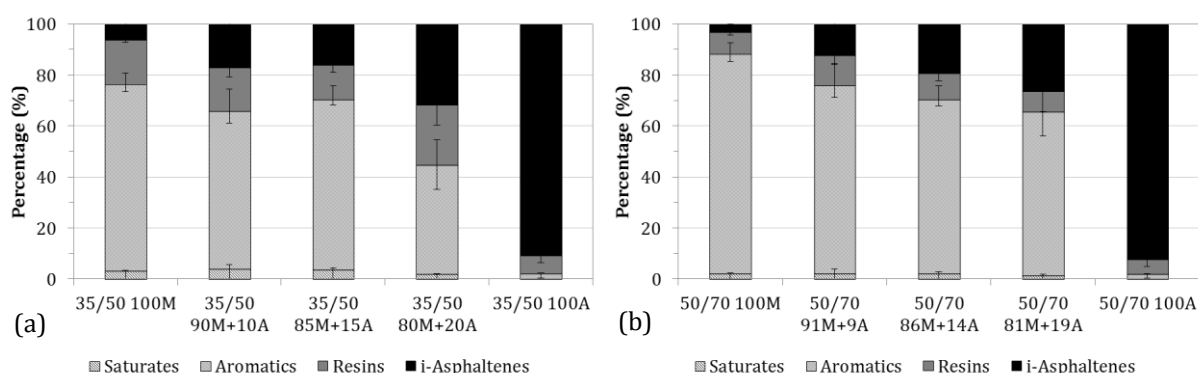
The different family fractions are measured in order to see how they vary according the different c7-asphaltene content. Table 3-7 summarizes the SARA fraction results. It differentiates i-asphaltenes and c7-asphaltenes for all model bitumens. Figure 3-30 represents graphically those results.

Iatroscan separation results are organized by c7-asphaltenes content. Generally, the i-asphaltenes (i-Asph) content follow the same track.

Table 3-10 SARA fractions and colloidal indexes of 35/50 and 50/70 model bitumens

Bitumen / Parameter	Saturates (%)	Aromatics (%)	Resins (%)	i-Asph (%)	c7 Asph (%)	Ic	
35/50	100M	3.04 ± 0.43	73.43 ± 4.31	17.44 ± 3.14	6.09 ± 1.09	0	0.10
	90M+10A	3.90 ± 1.79	61.87 ± 8.63	17.16 ± 4.75	17.07 ± 3.72	10	0.27
	85M+15A	3.66 ± 0.67	66.76 ± 5.22	13.57 ± 2.38	16.02 ± 3.04	15	0.25
	80M+20A	1.74 ± 0.39	43.05 ± 9.85	23.61 ± 9.59	31.60 ± 8.09	20	0.50
	100A	0.10 ± 0.17	1.91 ± 0.33	7.10 ± 2.73	90.89 ± 2.67	100	10.11
50/70	100M	1.95 ± 0.12	86.43 ± 1.35	8.41 ± 1.20	3.21 ± 0.31	0	0.05
	91M+9A	1.95 ± 0.71	73.92 ± 4.81	11.79 ± 1.43	12.34 ± 2.69	9	0.17
	86M+14A	2.12 ± 0.41	68.27 ± 4.77	10.26 ± 1.25	19.36 ± 4.35	14	0.27
	81M+19A	1.38 ± 0.11	64.19 ± 3.55	8.17 ± 1.46	26.26 ± 3.83	19	0.38
	100A	0.04 ± 0.04	1.65 ± 0.71	5.86 ± 0.45	92.44 ± 0.82	100	12.32

It can be observed that the increment of asphaltenes on the blend is inversely proportional to the aromatics. The equilibrium between fractions will play a role on the colloidal index stability. Asphaltenes and saturates are the highest and lowest fractions in polarity, and the solubility of the first ones in the colloidal system is enriched by the presence of aromatics and resins, intermediate polarity fractions [105]. Then, as happens with the 100% asphaltene fraction, the highest the Ic the more unstable is the system. For an almost constant rate of saturates in all model bitumens, the increase on the asphaltenes content has a direct impact on the Ic, increasing its value, so hardening the resulting bitumen.

**Figure 3-30 SARA fractions from 35/50 and 50/70 model bitumens**

AFM results

Atomic force microscopy on model bitumens is presented in Figure 3-31. Microstructure morphology of 35/50 model bitumens corresponds to (a-b) 20% asphaltenes, (c-d) 15% asphaltenes, (e-f) 10% asphaltenes and (g-h) 100% malthenes. All images are topographic providing microstructural overview by 50x50 μm^2 on top and 20x20 μm^2 on the bottom images.

In general, in all model bitumens independently of their asphaltenes content the catana or bee-like structure can be distinguished, even if the size is not always constant. Qualitative observation of 20% asphaltenes (Figure 3-31 (a-b)) bitumen shows more crowded population of catana phase and bigger dimensions. Then when decreasing to 15% asphaltenes content (Figure 3-31 (c-d)) the perception of the ripple structure is not obvious but it is present.

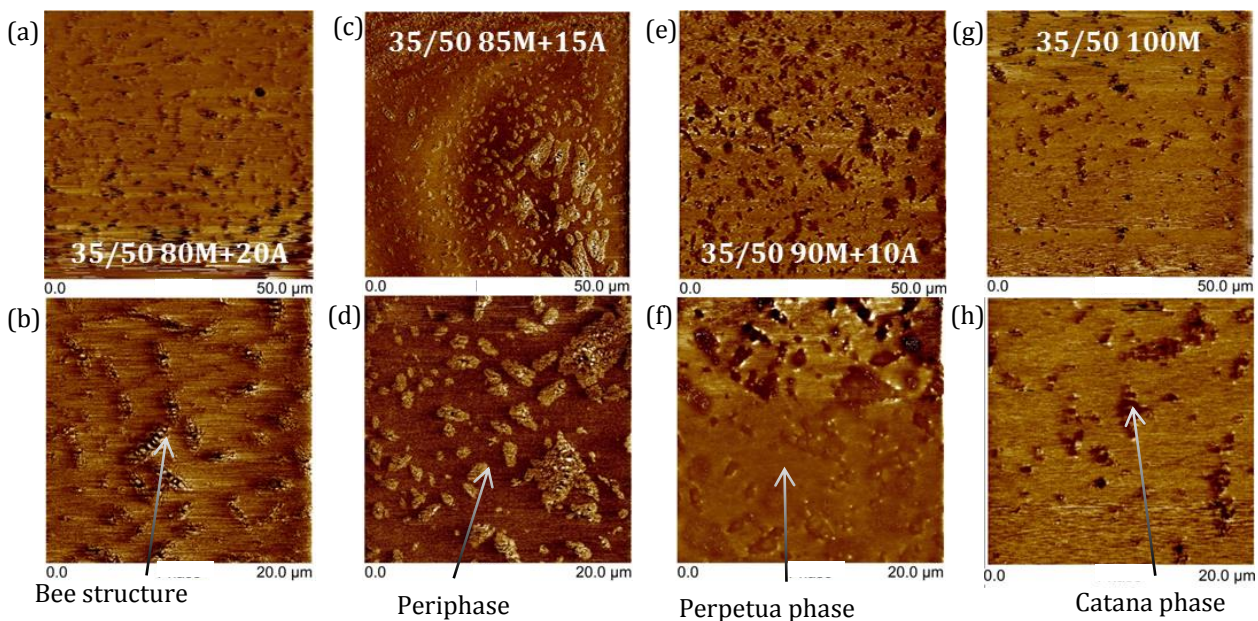


Figure 3-31 AFM results on 35/50 model bitumens after 4 days at 40°C

When the asphaltene content is only 10% (Figure 3-31 (e-f)), the differentiation of all three phases becomes challenging.

Finally, malthenes fraction in Figure 3-31 (g-h) presents again in a clearer way the wrinkling structure. This results goes in concordance with Mercé's [100] findings. They pointed out that asphaltenes are not strictly mandatory for the "bee" like formation, although they play a very important role in the kinetics of its generation.

Rebelo et al. 2014 [106] attributed the lack of bee structure to the absence of wax in their samples, while Mercé et al. 2015 [100] and Masson et al. 2007 [107] also studied the influence of

the cooling rate of the sample. In this case, cooling ratio was not controlled. After samples preparation at 110°C they were left freely to cool to room temperature ($\sim 25^\circ\text{C}$), leading the asphaltenes to participate as “cold spots” [100].

All these measurements show only bitumen surface characteristics. They seem very powerful but they require very strict protocol for sample preparation and thermal conditioning.. Any change on the methodology may change the surface visualization and conclusions about bitumen characteristics.

Rheological performance and Huet-Such modelling

DSR testing is performed for the model bitumen under the same conditions, as it is described in Materials and methods section §3.2.3 Complex shear modulus test. After doing the coupling between geometries and dealing with the same problems of compliance as in the previous subsection, rheological master curves are built at $T = 0^\circ\text{C}$.

Then, once the master curves are constructed, Huet-Such modelling is applied. All results from bitumen modelling, including parameters values for the fitting are included and resumed in Annex 3. Figure 3-32 (a) illustrates the master curves at 0°C for all 35/50 model bitumen and Figure 3-32 (b) the results for the 50/70 model bitumen.

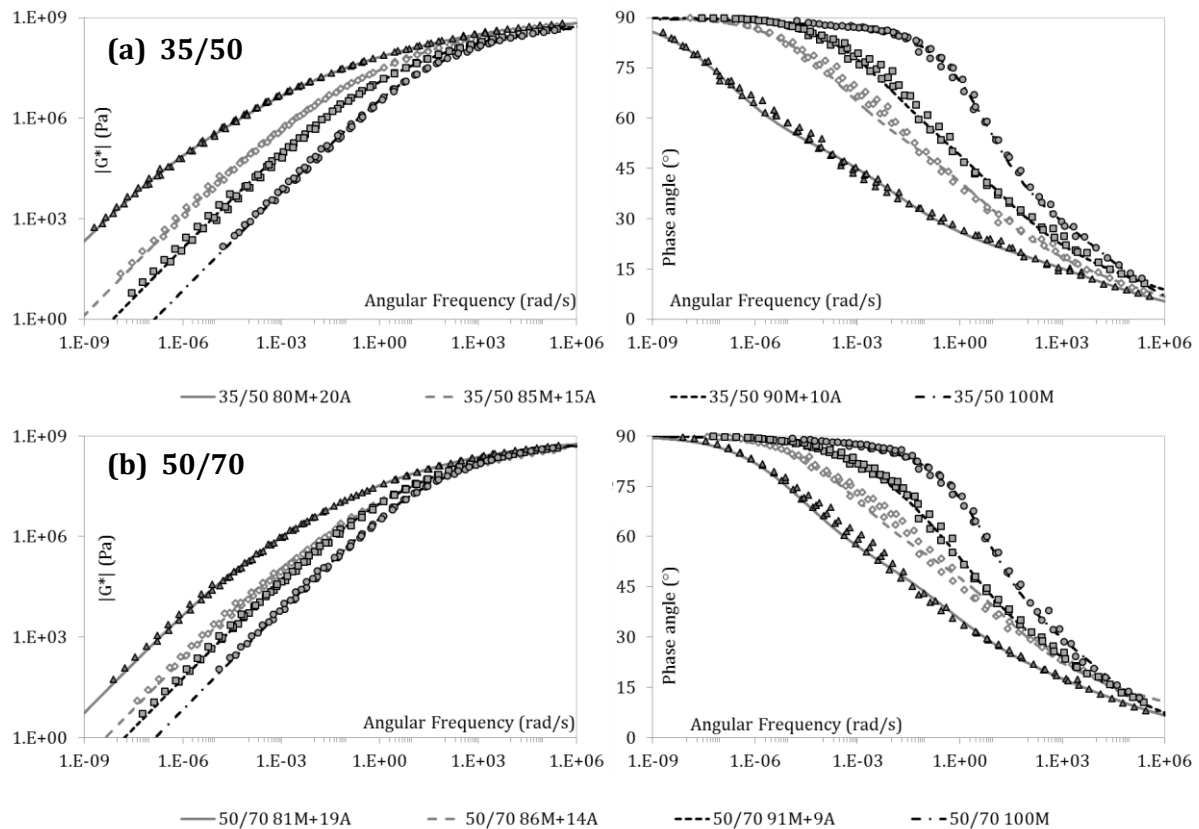


Figure 3-32 Master curves at $T=0^\circ\text{C}$ of (a) 35/50 model bitumens, and (b) 50/70 model bitumens

Rheological behaviour shows in both types of bitumens a clear difference by their asphaltene content. In this sense it could be assured that the increase of asphaltene content induces an evolution similar to the hardening experienced by the bitumens with ageing.

δ -method analysis results

After applying the δ -method calculations, Figure 3-33 presents the AMWD in the range between 100 and 10,000 g/mol with the ordinate axis corresponding to the probability density $f(\text{AMW})$, including cross-over frequency points $\omega(\text{co})$.

As the asphaltene content increases, a shift of the curve to the right (towards higher AMW) is observed. Also, the shape of the curves evolves from mono-modal, to bimodal or tri-modal distribution. As well, the cross-over frequency points moves towards higher AMWs and lower $f(\text{MW})$.

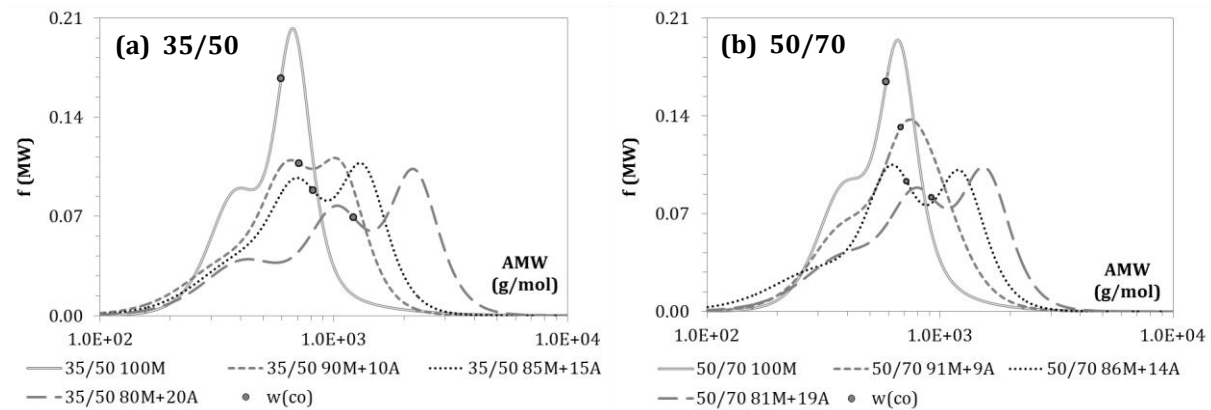


Figure 3-33 δ -method diagrams of (a) 35/50 model bitumens, and (b) 50/70 model bitumens

In Figure 3-33 (a), the δ -method curves obtained for the 35/50 model bitumens are shown. The highest peak corresponds to the malthenes fraction of the bitumen. This is a fraction without c7-asphaltenes so it can serve as reference of how everything changes when the c7-asphaltenes fraction is added. The increment of 10% of c7-asphaltenes has a drastic effect on the rheological behaviour: the bitumen becomes “harder”. The change from an almost mono-modal distribution to bi-modal distribution is clear as the increase of the cross-over frequency.

Then, another 5% of asphaltenes is added to have the 35/50 85M+15A model bitumen. This bitumen is the one that represents the neat bitumen curve, the middle point of the study. Again the shift is towards higher AMW, cross-over frequency keeps increasing and the bi-modal distribution is more accused, bitumen is becoming harder. Finally, the highest asphaltene content of 20% that turns the curve to tri-modal distribution. Differences between all model bitumens are led by the addition of asphaltenes to the malthenes phase.

The analysis is equivalent for the 50/70 model bitumens illustrated in Figure 3-33 (b). Furthermore, in Annex 3 all model bitumens represented by the δ -method are shown in the same graphic. And the trend is followed in line by asphaltene content. The curves from 35/50 and 50/70 model bitumens get one after the other as asphaltene content increase.

GPC results

The GPC results from 35/50 model bitumens are used to have an indication of the variation in molecular size. Regarding the trends obtained from δ -method analysis, the decision of applying GPC on one type of model bitumen is done. What is expected from this test is to see the increase of concentration of high molecular weight due to the increase of asphaltene content on the system.

Figure 3-34 (a) represents molecules retention time versus the normalized signal obtained. However, in Figure 3-34 (b) the ordinate axis corresponds to the translated molecular weight after the application of the calibration curve from 500 to 30,000 g/mol as it is the range of the column.

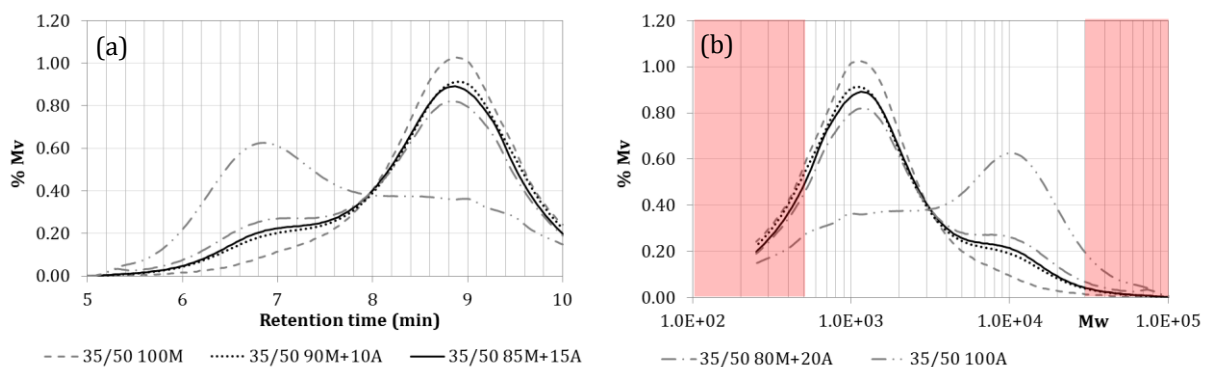


Figure 3-34 GPC plots from 35/50 model bitumens

As it is observed in previous analysis, in Figure 3-34 (a) the presence of the asphaltene phase is notice at 6.8 min. At this retention time 35/50 100A shows the highest peak, and then it decreases as the asphaltene content decrease. Still, in the case of malthenes phase, there are molecules at those retention times.

The second big family of molecules is centred at 8.9 min and in could simply be called malthenes family. The peak of the 35/50 100M (only malthenes) is the one supporting this denomination. Again, the decrease in malthenes content follows the inverse trend of the asphaltenes.

When talking about molecular weights instead of retention times, as Figure 3-34 (b) illustrates. The two “big families” are centred at 1,000 g/mol (malthenes) and 10,000g/mol (asphaltenes).

Typically chromatograms are partitioned in slices and divided in parts (large, medium or small molecules) [108,109]. From these divisions, in Table 3-11 are summarized the results of the molecular weights of 35/50 model bitumens. Where M_n is the number-average molecular weight (g/mol), M_w is the weight-average molecular weight (g/mol), M_p is the peak molecular weight (g/mol), M_z is the z-average molecular weight (g/mol) and $PDI = M_w/M_n$ is the polydispersity index, relative spread in MW. PDI is usually used as a measure of the broadness of the distribution. $PDI=1$ indicates a monodisperse distribution, $PDI = 1.1$ to 2.0 shows an intermediate polydisperse distribution type, $PDI>2$ broad distribution, while narrow shows a PDI between 1.02-1.10.

Table 3-11 Polydispersity of 35/50 model bitumens

	M_n (g/mol)	M_w (g/mol)	M_p (g/mol)	M_z (g/mol)	M_{z+1} (g/mol)	PDI
35/50 100M	753	1,012	932	1,275	1,509	1.34
35/50 90M+10A	785	1,111	994	1,478	1,829	1.42
35/50 85M+15A	795	1,120	1,052	1,493	1,856	1.41
35/50 80M+20A	811	1,150	1,042	1,542	1,929	1.42
35/50 100A	9,472	11,959	10,715	15,096	18,607	1.26

Weight of average molecular weight (M_w) is around 1,100 g/mol. M_n and M_w increase with the addition of asphaltenes. The general trend for all parameters is the increase of value as the rate of asphaltene content increases. On the other hand, it does not mean that polydispersity follows the same tendency. Actually, PDI remains around 1.42 for the three model bitumen showing an intermediate distribution of molecules.

Conclusion

Model bitumens have represented the changes that produce the asphaltenes on the bitumen. They provide the stiffness to the material by interconnecting fractions within its colloidal distribution. Based on other studies, on AFM it is seen that the sign of bee-like structures is not obvious and directly linked to the asphaltene content. However, rheologically speaking, the increment of asphaltenes gives a straight forward increase of bitumen stiffness. This influence is also observed on the δ -method curves and on the GPC molecular weight measurements.

3.3.4 Laboratory aged bitumens

With the aim of relating ageing with the ratio of m/a on the bitumen, in this section Neat bitumens are submitted to laboratory ageing procedures, RTFOT and PAV. Table 3-12 summarizes the ratio of malthenes and asphaltenes of each aged bitumen.

Table 3-12 Aged bitumens m/a ratio on n-heptane determination

Bitumen / Parameter	Malthenes (%)	c7-Asphaltenes (%)
35/50 Neat	85.3	14.7
35/50 RTFOT	82.2	17.8
35/50 PAV	78.6	21.4
50/70 Neat	85.7	14.3
50/70 RTFOT	84.1	15.9
50/70 PAV	79.4	20.6

Ageing on 35/50 Neat bitumen increases the asphaltene content 3.1% after RTFOT, and 3.5% more after PAV. Besides, 50/70 Neat bitumen has an asphaltene content augmentation of 1.6% and 4.7% respectively.

ATR-FTIR analysis

In this case bitumens are not submitted to any separation in n-heptane or recomposition in dichloromethane, so ATR-FTIR analysis will just look for the Ico and Iso variations with ageing. Figure 3-35 (a) and (b) represents the spectra from 35/50 and 50/70 bitumens respectively.

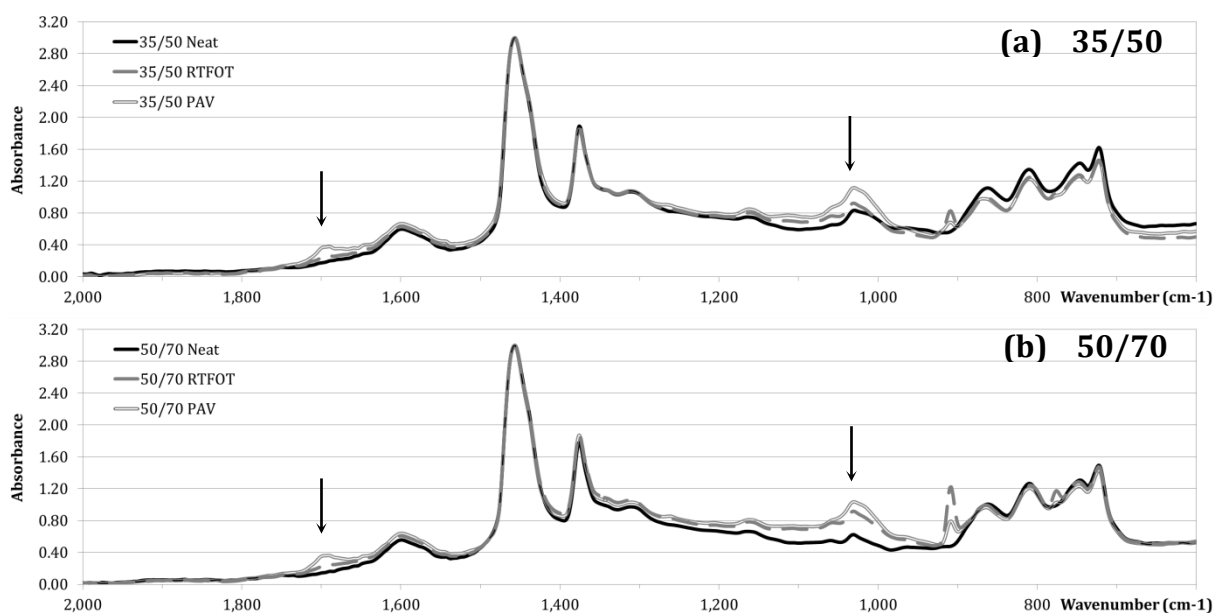


Figure 3-35 ATR-FTIR spectra from RTFOT and PAV aged bitumens

The only parts of the spectra that changes are pointed with arrows. Those areas determine the variation in terms of Ico and Iso. These results follows the general ageing trend (Neat < RTFOT < PAV) for both indicators. Table 3-13 summarized the values of Ico and Iso of all bitumens.

Table 3-13 ATR-FTIR analysis of Ico and Iso values of aged bitumens

Bitumen / Parameter	Ico (%)	Iso (%)
35/50 Neat	0.00	5.71
35/50 RTFOT	0.88	13.28
35/50 PAV	3.22	20.10
50/70 Neat	0.00	4.86
50/70 RTFOT	0.65	12.46
50/70 PAV	3.94	16.86

Sulphoxide index, Iso, increases rapidly their values. Growth ratio is much higher than Ico that varies from 0% for Neat bitumen, to 3.94% in the case of 50/70 PAV. These parameters by themselves do not indicate the level of ageing of the material. They always need to be presented as an evolution.

SARA fractions

In order to add more information and to know more about the internal changes on the bitumens with ageing, the different family fractions are measured. Table 3-14 summarizes the SARA fraction results, differentiating between i-asphaltenes and c7-asphaltenes for all aged bitumens.

Table 3-14 SARA fractions and colloidal indexes of 35/50 and 50/70 aged bitumens

Bitumen / Parameter	Saturates (%)	Aromatics (%)	Resins (%)	i-Asph (%)	c7 Asph (%)	Ic
35/50 Neat	2.99 ± 0.68	66.03 ± 5.02	12.84 ± 2.02	18.14 ± 4.15	14.7	0.27
35/50 RTFOT	1.94 ± 0.60	60.84 ± 6.04	11.46 ± 3.24	25.77 ± 3.67	17.8	0.38
35/50 PAV	1.29 ± 0.45	45.12 ± 12.12	16.69 ± 5.42	36.91 ± 9.78	21.4	0.62
50/70 Neat	2.08 ± 0.11	65.07 ± 1.98	12.36 ± 1.04	20.49 ± 1.40	14.3	0.29
50/70 RTFOT	6.85 ± 2.53	53.44 ± 5.20	17.68 ± 2.50	22.03 ± 3.36	15.9	0.41
50/70 PAV	2.96 ± 0.68	50.03 ± 10.30	12.66 ± 2.91	34.35 ± 8.05	20.6	0.60

The evolution of fraction families is very similar for both 35/50 and 50/70 bitumens. Aromatics decrease with ageing. In contrast i-asphaltenes increase. There is no obvious general trend for

saturates and resins. Moreover, colloidal indexes also increase with ageing, representing a hardening of the material (still all show typical sol behaviour, $I_c < 0.7$ [71,87]). This I_c increase is mainly led by the asphaltenes and the reduction on the aromatic fraction. Figure 3-36 represents graphically the variation of fractions with ageing.

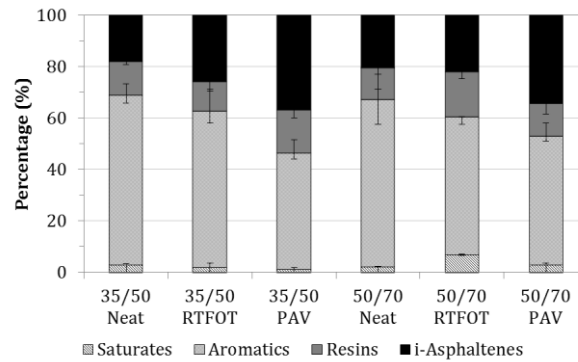


Figure 3-36 SARA fractions from 35/50 and 50/70 aged bitumens

Rheological performance and Huet-Such modelling

DSR testing is performed on 35/50 aged bitumen assuming it is representative of the evolution for both bitumens. As already developed, after coupling between geometries and dealing with the same problems of compliance at high/low frequencies for the two geometries, rheological master curves are built at $T = 0^{\circ}\text{C}$.

At that point, Huet-Such modelling is applied. All results from bitumen modelling, including parameters values for the fitting are included and resumed in Annex 2. Figure 3-37 (a) shows the master curves at 0°C for all 35/50 Neat, RTFOT and PAV bitumens. Ageing plays an important role on bitumen hardening as rheological master curves show. There is strong difference after RTFOT and PAV. This could be linked to the variation of aromatic and asphaltene content.

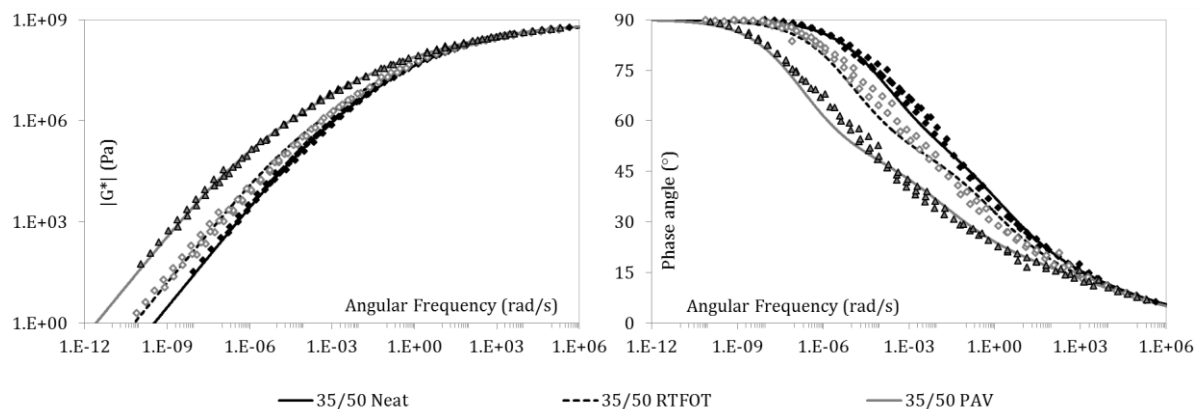


Figure 3-37 Master curves at $T=0^{\circ}\text{C}$ of 35/50 bitumens

δ -method analysis results

Subsequently the δ -method calculations are applied, Figure 3-38 shows the AMWD in the range between 100 and 10,000 g/mol with the ordinate axis corresponding to the probability density $f(\text{AMW})$, including cross-over frequency points $\omega(\text{co})$ of the aged bitumens.

As it has been presented, ageing (or asphaltenes content increase) induces growth of the higher molecular weights. On the δ -method curves, it is illustrated as a displacement of the curve to the right, with a possible evolution of the shape of the curve from mono-modal, to bimodal or tri-modal distribution. However, Figure 3-38 (b) shows that the fitting process for the angle is not as accurate as for the $|G^*|$. This leads to overestimate peaks in the distribution. As well, the cross-over frequency points moves towards higher AMWs and lower $f(\text{MW})$.

The differences between curves reflects evolutions of particles inside bitumen, aromatics evolve to resins and then to polar resins and asphaltenes. These results are in accordance with the literature. It is described that with ageing, part of the oily fraction (mainly resins) seems to be absorbed by the asphaltenes and dispersed in the light matrix [71,83]. Molecules are reorganized into new colloidal system and could produce some clustering as well.

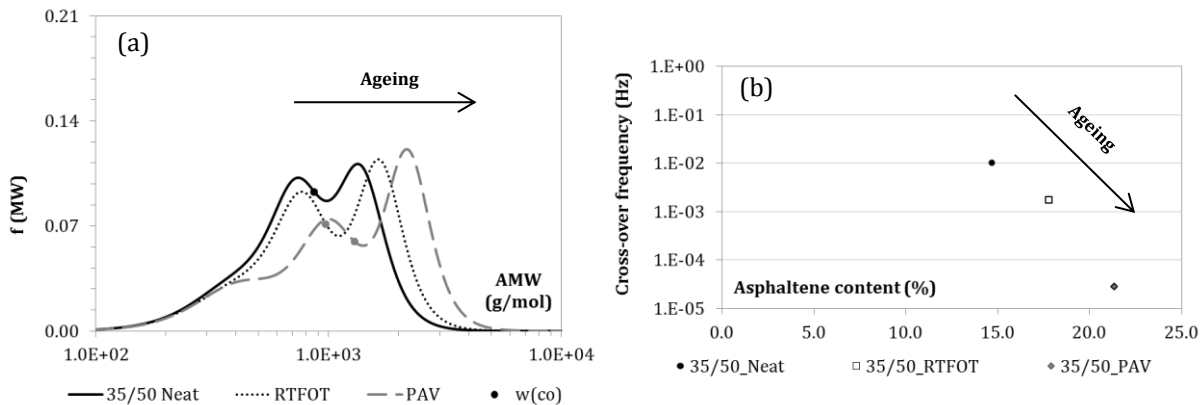


Figure 3-38 (a) δ -method diagrams of 35/50 aged bitumens and (b) Cross-over frequencies by asphaltene content

Figure 3-38 (a) shows how the 35/50 Neat curve develops a deeper valley and increase of the second peak to get to 35/50 RTFOT bitumen. Then, it moves to the right and increase even more the second peak, concentrating the biggest part of the material over 1,000 g/mol of AMW. Regarding to cross-over frequencies in Figure 3-38 (b), they tend to decrease when the asphaltene content increase.

GPC results

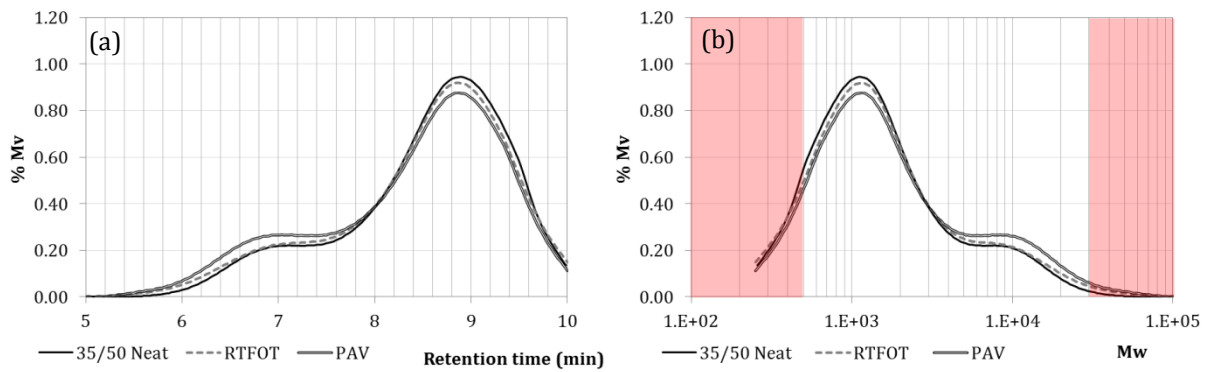


Figure 3-39 GPC plots from 35/50 aged bitumens

Concerning GPC measurement on artificial aged bitumens, Figure 3-39 shows the spectra by retention time and molecular weight. There is an increment on the peak at 7 min (10,000 g/mol) and a reduction of concentration on the other one. Results experience by artificial ageing are in accordance with Lee et al. 2008 [108] findings. The increase in the molecular size of the binder is in accordance with the displacement of the AMWD curve to the right part of the representation (Figure 3-39 (b)).

Looking at the values of number average molecular weight (M_n), weight average molecular weight (M_w), they increase with ageing. Table 3-15 resumes the results of GPC average molecular weights.

Table 3-15 Polydispersity on 35/50 aged bitumens

	M_n (g/mol)	M_w (g/mol)	M_p (g/mol)	M_z (g/mol)	M_{z+1} (g/mol)	PDI
35/50 Neat	664	949	876	1,275	1,571	1.43
35/50 RTFOT	753	1,056	969	1,404	1,740	1.40
35/50 PAV	810	1,087	1,002	1,392	1,682	1.34

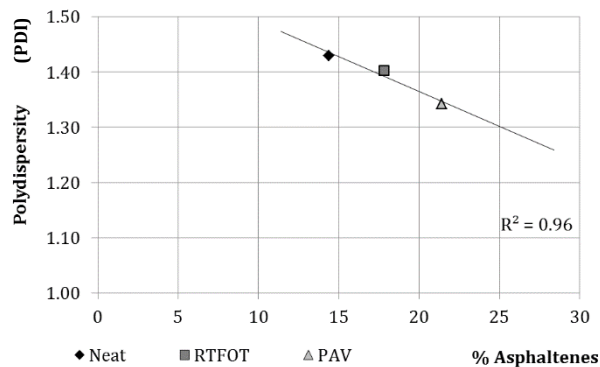


Figure 3-40 Polydispersity of 35/50 aged bitumens

On the other hand, if polydispersity (PDI) is represented versus the asphaltene content of each bitumen (Figure 3-40), the trend followed is equivalent to the one obtained for the cross-over frequencies of the δ -method.

Conclusions

After chemical and physical characterization of 35/50 Neat, RTFOT and PAV bitumens, the central point of the study is the asphaltenes fraction. Bitumen principal families, saturates, aromatic, resins and asphaltenes modify their presence on the material with ageing, raising up or decreasing their content. But among them, the asphaltenes phase plays the most important role by increasing the stiffness of the material.

3.3.5 Relationship between laboratory ageing and model bitumens

In this section, model bitumen with high c7-asphaltenes content (35/50 80M+20A) and ageing bitumen (35/50 PAV) are compared.

ATR-FTIR spectra shows in Figure 3-41 the difference between bitumens on the pointed peaks, Ico ($1,700\text{ cm}^{-1}$) and Iso ($1,030\text{ cm}^{-1}$) respectively. Compared with the Neat bitumen (Ico 0.00% and Iso 5.71%) the 20A model bitumen does not show much variation in terms of Ico (0.09%). However, in relation to Iso (12.60%) separation and recombination procedure have make it grows. On the other hand, after PAV bitumen experiences an increase of both indicators due to the chemical evolutions (Ico 3.22% and Iso 20.10%).

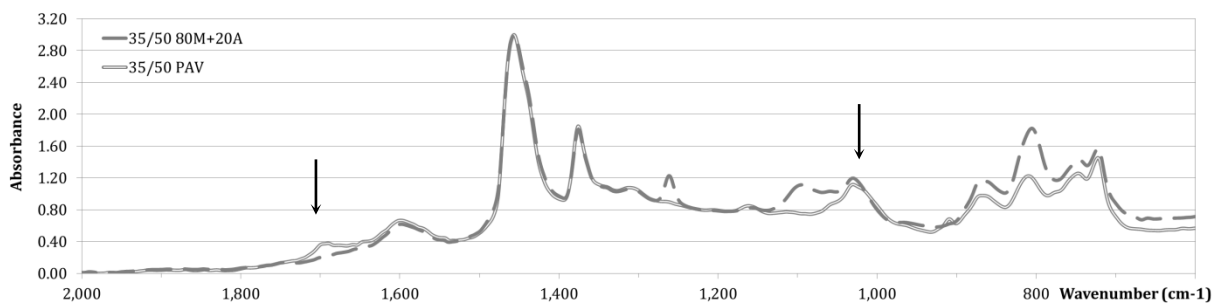


Figure 3-41 ATR-FTIR spectra from 35/50 80M+20A and PAV bitumens

Table 3-16 ATR-FTIR analysis of Ico and Iso values from 35/50 80M+20A and PAV bitumens

Bitumen / Parameter	Ico (%)	Iso (%)
35/50 Neat	0.00	5.71
35/50 80M+20A	0.09	12.60
35/50 PAV	3.22	20.10

On Table 3-17 the main bitumens fractions are resumed. Both bitumens present in general similar chemical composition. Still, c7-asphaltene content is 1.4% more in the case of PAV bitumen.

Table 3-17 SARA fractions from model and aged bitumens at the highest asphaltene content

Bitumen / Parameter	Saturates (%)	Aromatics (%)	Resins (%)	i-Asph (%)	c7 Asph (%)	Ic
35/50 80M+20A	1.74 ± 0.39	43.05 ± 9.85	23.61 ± 9.59	31.60 ± 8.09	20.0	0.50
35/50 PAV	1.29 ± 0.45	45.12 ± 12.12	16.69 ± 5.42	36.91 ± 9.78	21.4	0.62

Regarding to rheological, the response master curves at $T=0^{\circ}\text{C}$ of both bitumens are shown in Figure 3-42. It should be remarked that the curves are very similar for the 2 bitumen. Nevertheless, a stiffer response can be differentiated from PAV bitumen at low frequencies in part (a) of the figure.

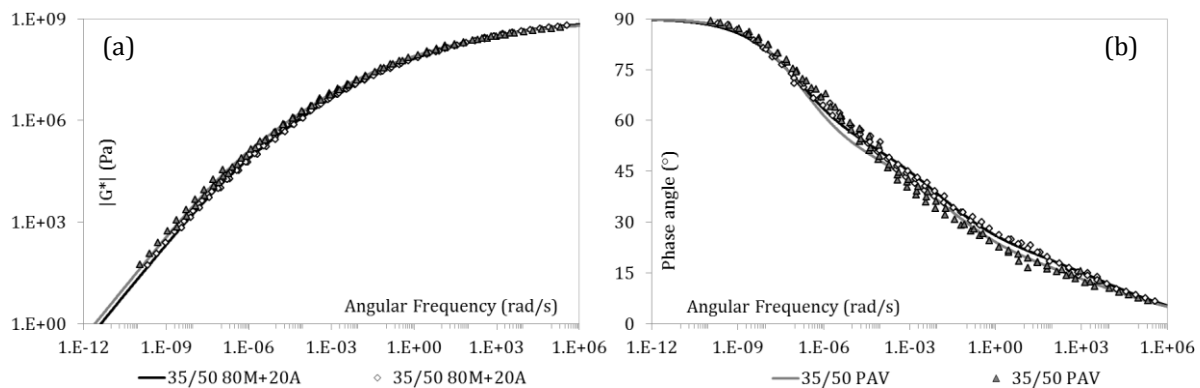


Figure 3-42 Master curves at $T=0^{\circ}\text{C}$ from 35/50 80M+20A and PAV bitumens

Physical distribution of bitumen molecules is presented in Figure 3-43 with the δ -method representation in part (a) and the GPC results in part (b) of the figure. Independently of the origin of asphaltenes, added as in the model bitumen, or evolved from internal chemical transformation for the aged bitumen, both curves show the same shape. δ -method curves in Figure 3-43 (a) illustrate the tri-modal response of the material. On the other hand, GPC results in Figure 3-43 (b) present a two peak curve for both bitumens.

The differences seen between the two methods could be related to the type of sample preparation. δ -method curves come from rheological measurements and modelling derivation. In contrast, GPC curves depend on the measuring method and testing conditions [110] that come from the dilution and molecular separation of the bitumen. GPC do not take into account the interaction between molecular species.

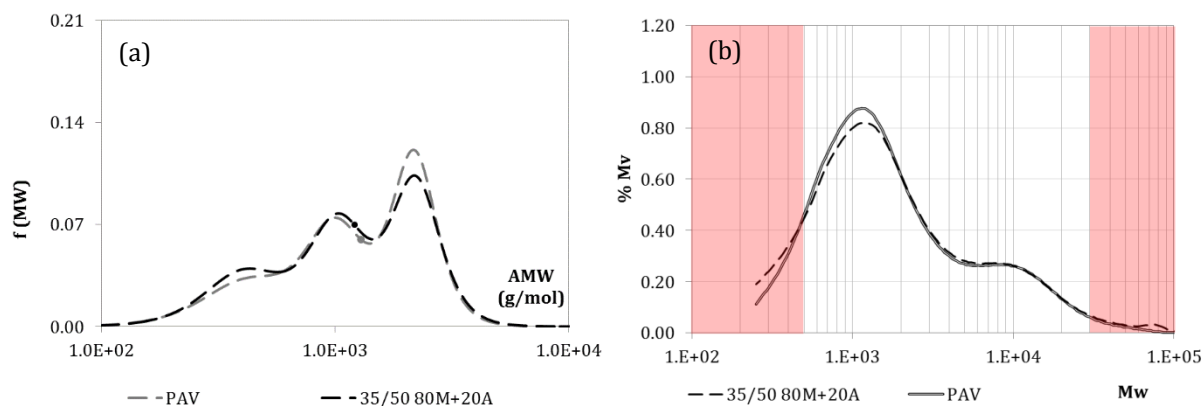


Figure 3-43 δ -method (a) and GPC (b) curves from 35/50 80M+20A and PAV bitumens

What can be highlighted from this comparison is that aged bitumen and bitumen with high asphaltenes content can have the same mechanical response with a different origin of the asphaltenes part.

3.4 Conclusions

In this chapter, a study of the influence of the asphaltene content is carried out both in neat, model and laboratory aged bitumens. The objective is to evaluate the influence of this fraction on the physical and chemical characteristics of bitumen and to understand the effects of aging on chemical species and their organization. From the results obtained during the investigation the following conclusions can be drawn:

- i. In terms of ATR-FTIR analysis, sulfoxide groups seem to be more affected by the addition of asphaltenes fractions than carbonyl groups, indicating the affinity of polar fractions towards these components.
- ii. By Iatroscan chromatography for SARA fractions determining, it can be observed that asphaltenes increase with ageing. It has also been exposed that during aging the increase in asphaltenes content is due to the association of aromatics to resins (and polar resins) and then to asphaltenes. In addition, the oxidation of aromatics or resins to polar resins or asphaltenes is also possible during aging.
- iii. By AFM observation, asphaltenes micelles appeared in all bitumens tested. Then in the malthenes fraction bee-like structure is present, so the presence of asphaltenes is not mandatory for their apparition as other researchers have stated already.
- iv. Rheological behaviour is linked to the asphaltenes content of the bitumen.

- v. δ -method analysis has proven as a powerful tool for ageing determination. Curves shifting when asphaltenes content increase is clear. This shift is directly represented by the decrease of the Cross-over frequency. This value could be taken as an indicator of ageing.
- vi. By GPC testing, ageing and model bitumens have followed the same trends. Colloidal indexes have increased with asphaltenes ratio, as the number and weight average molecular weight.

Chapter 4. Ageing evolution of warm mix asphalts combined with reclaimed asphalt pavement

Résumé du chapitre

La réduction de la température de fabrication des enrobés bitumineux et la réutilisation des agrégats d'enrobé, habituellement classés comme déchets solides, présentent de nombreux avantages par rapport à l'enrobé à chaud traditionnel. Ce couplage durable d'un point de vue environnemental doit montrer qu'il est durable d'un point de vue de ses performances techniques. Chaque technique possède ses avantages et inconvénients. D'un point de vue technique, des problèmes potentiels de tenue à l'eau, d'orniérage ou de résistance à basse température pourraient apparaître prématurément. D'un autre côté, il existe de nombreux avantages environnementaux associés à l'utilisation de ces techniques, comme la réduction de la consommation de carburant et des émissions de gaz à effet de serre, l'extraction réduite de granulats naturels et l'élimination des stocks d'agrégats d'enrobés.

Les enrobés tièdes sont fabriqués dans la gamme de température 110°C-140°C. Trois processus différents permettent cette réduction de la température: la mousse de bitume, les additifs chimiques et les additifs organiques. Ces technologies réduisent la consommation d'énergie, améliorent la maniabilité, et opèrent comme agents de compactage. Ces améliorations sur le compactage et les densités réalisées in situ tendent à réduire la perméabilité et le vieillissement du bitume, ce qui se traduit généralement par une meilleure performance des mélanges en termes de résistance aux fissures et de sensibilité à l'eau.

En ce qui concerne l'agrégat d'enrobé, ce matériau peut répondre aux exigences d'une solution de chaussée durable. Il peut présenter des économies de coûts, en réduisant de 23% l'impact environnemental lors de sa fabrication. Les agrégats d'enrobé sont généralement plus rigides en raison du bitume vieilli. Ceci peut induire une fragilité de l'enrobé à basse température en fonction de la proportion contenue dans le nouveau mélange.

Plusieurs auteurs ont étudié les différentes étapes du vieillissement des liants bitumineux pendant la fabrication de l'enrobé et au long de sa vie. Deux phases peuvent ainsi être distinguées: le vieillissement à court terme et le vieillissement à long terme. Le vieillissement à court terme se produit plus exactement pendant la fabrication et la construction de la chaussée, et entraîne une augmentation importante de la viscosité du bitume; le vieillissement à long terme est progressif et est induit par différents mécanismes. Les origines de ces vieillissements sont multiples: l'oxydation, l'évaporation de composants plus légers, la thixotropie et la synérèse, la polymérisation par réaction chimique de composants moléculaires ou encore la

séparation des composants par l'absorption de constituants huileux par certains types d'agrégats...

Les connaissances actuelles sur le vieillissement sont essentiellement tirées de l'expérience pratique sur les enrobés traditionnels. L'objectif de ce chapitre est d'étudier et de comparer la technique tiède mousse aux autres techniques tièdes, en utilisant jusqu'à 50% d'agrégats d'enrobé dans le mélange. Pour ce qui traite du comportement à long termes des enrobés, un protocole de vieillissement est appliqué aux échantillons avant caractérisation mécanique. Ce vieillissement s'inspire de la méthode proposée par la RILEM TC-ATB TG5. Il comporte deux phases de vieillissement séparées. Les performances mécaniques à long terme sont comparées au moyen des essais de module complexe et de fatigue. Des essais de pénétration et de point de ramollissement sont effectués sur les bitumes récupérés. L'évolution du vieillissement est également caractérisée par une analyse infrarouge.

Finalement, l'effet de vieillissement est évalué par l'analyse de la δ -méthode décrite dans le chapitre précédent. Le potentiel de la δ -méthode comme outil d'étude du recyclage est évalué.

4.1 Introduction

The reduction of the manufacturing temperature of asphalt mixtures and the re-use of materials from old pavements, usually classified as solid waste disposals, present numerous advantages compared with traditional HMA. The use of WMA and RAP separately are not new concepts, however innovation related to their combined application and performance is still ambiguous in terms of durability. Both techniques present their own benefits and drawbacks [6,7], as to durability issues, rutting or low temperature resistance that could be compromised during their service life. There are many environmental advantages associated with using these techniques, including reduction in fuel consumption and greenhouse gas emissions, reduced extraction of natural aggregates and disposal of old asphalt [6,9–11].

As it has been described in Chapter 2, warm mix asphalts are produced in the range of temperature of 140°C and 110°C. And three different processes that enable this temperature reduction can be distinguished. They are the foaming of bitumen, the use of chemical additive and the use of organic additives.

Those same processes that reduce energy consumption and improve workability in WMA technologies also allow them to act as compaction agents [37,111]. These improvements on compaction and densities achieved in situ tend to reduce permeability and bitumen ageing, which generally results in better performance of the blends in terms of crack resistance and moisture sensitivity [37].

Regarding RAP, this material can fulfil the requirements for a sustainable pavement solution. It can present material cost savings while reducing the environmental impact of the asphalt manufacturing stage by 23% [112]. RAP is usually considered a stiffer material due to the aged bitumen, which can promote unexpected failures [113] depending on the percentage content in the new mixture.

Several authors have investigated the different stages of ageing of the asphalt binder during the mix manufacture and the pavement service life [44,47,55,56]. Two phases can be distinguished: short term ageing and long term ageing. Short term ageing takes places during manufacturing and construction of the road, and leads to an increase in bitumen viscosity. Meanwhile, long term ageing depends on the time of service and is related to progressive ageing by various mechanisms. Both types of ageing are associated with numerous phenomena, such us oxidation, evaporation of lighter components, thixotropy and syneresis, polymerization through chemical reaction of molecular components or components separation through the absorption of oily constituents by some type of aggregates [44,56].

The current knowledge on ageing is essentially gained from practical experience on traditional asphalt mixes and typically on HMA. However, the road industry has embraced recycling and developed new techniques, particularly with WMA in order to limit its environmental impacts.

Within this framework, the objective of this chapter is to study and compare the foamed asphalt technique for WMA production when 50% of RAP is added to the mixture. For that reason, an ageing protocol is followed within the lines proposed by the RILEM TC-ATB TG5, consisting of two separate ageing phases. Mixtures long term related performances are compared by means of complex modulus and fatigue testing. Penetration and softening point tests are undertaken on the recovered bitumens. Ageing evolution is also characterised by the Fourier Transform Infrared analysis.

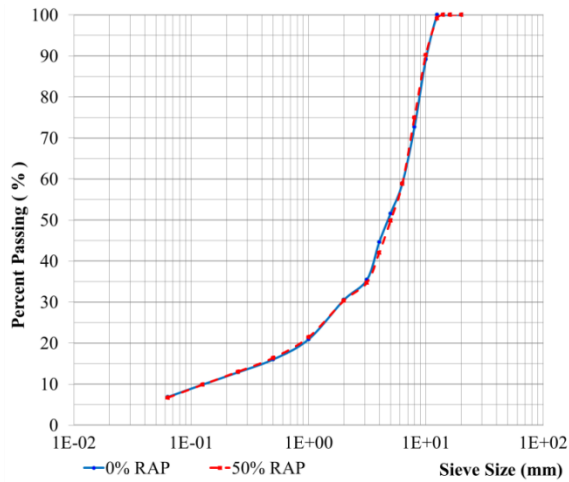
Finally, the ageing effect is evaluated through the δ -method analysis described in the previous chapter. The potential of the δ -method as a tool for recycling studies is assessed.

4.2 Materials and methods

4.2.1 Mixtures

With the aim of comparing different manufacturing techniques, three types of mixtures are chosen for the study. One hot mix asphalt of reference and two warm mix asphalts, one with a surfactant product and the other under the foaming process. The reference hot mix asphalt and the warm mix asphalt with surfactant were initially designed by Manuela de Mesquita Lopes in her thesis [114] and are now used in this work as comparison.

The reference mixture is an AC10, typically used as both a thick surface/structural layer. Figure 4-1 illustrates the grading curves and design of the mixtures. In all cases, a constant bitumen content of 5.4% [115] is selected. A MLPC BBMAX 80 is used as mixer. The working sequence lasts for 75 seconds, with 15 seconds for the aggregates and fines mixing (and RAP when used) plus 60 seconds after the addition of the bitumen. RAP is preheated for 2h at 110°C before manufacture, whereas virgin aggregates are heated at different temperatures depending on the type of mixture as shown in Table 4-1.



		0% RAP	50% RAP
Aggregates	6/10	44.0	20.0
	2/6	22.5	16.0
	0/2	33.0	14.0
	Filler	0.5	-
RAP	8/12	-	25.0
	4/8	-	10.0
	2/4	-	8.0
	0/2	-	7.0
Total		100.0	100.0

Figure 4-1 Mixtures gradations with and without RAP

Table 4-1 Mixtures studied and manufacturing temperature

Mixture	Bitumen Denomination	%RAP	Aggregates (°C)	RAP (°C)	Manufacture (°C)	Ageing Procedure
Hot Mix Asphalt	HMA0	0	160	-	160	-
	HMA0a					✓
	HMA50	50	210	110	160	-
	HMA50a					✓
Warm Mix Asphalt	WMA0	0	130	-	130	-
	WMA0a					✓
	WMA50	50	150	110	130	-
	WMA50a					✓
Foamed Warm Mix Asphalt	FWMA0	0	130	-	130	-
	FWMA0a					✓
	FWMA50	50	150	110	130	-
	FWMA50a					✓

Bitumen always at 160°C

4.2.2 Materials

Bitumen

The neat bitumen chosen for the manufacture of all mixtures is conventional 35/50 bitumen with a penetration index of 37 [1/10 mm] (EN 1426) and a softening point temperature of 53.8°C (EN 1427). This bitumen is the same type of bitumen from RAP.

For the first WMA, the WMA with surfactant, the base bitumen was chemically modified by adding a surfactant product (CECABASE RT®) in laboratory [114]. For the second WMA, using the foam technique, the foaming effect was produced by injecting 1.5% of water under pressure into the hot bitumen pipe during its introduction into the mixer. This type of mixture was manufacture at EIFFAGE Travaux Public facilities in Corbas, Lyon, as part of the Marie Curie project partnership [116–118].

Table 4-2 Base bitumen of the study

Denomination	Bitumen	Additive Nature	Addition Process	Mixture Manufacture Temperature (°C)
Hot Mix Asphalt	35/50	None	-	160
Warm Mix Asphalt	35/50 + 0.5 % Additive	Surfactant	On bitumen	130
Foamed Warm Mix Asphalt	35/50	1.5% water	Direct Foaming	130

Virgin aggregates

Gneiss rock, the original aggregate from RAP, is the virgin aggregate used for both coarse and fine fractions (0/2, 2/6 and 6/10 mm) in order to retain continuity between grading curves.

Table 4-3 resumes virgin aggregates properties.

Table 4-3 Virgin aggregates properties

Test / Aggregate Type	Coarse Aggregate		Fine Aggregates		Filler
	6/10 Gneiss	2/6 Gneiss	0/2 Gneiss	Gneiss	
Grain size (EN 933-1) / (EN 933-10) Sieves (mm)					
14	100.0	100.0	100.0	100.0	
12.5	98.0	100.0	100.0	100.0	
10	79.2	100.0	100.0	100.0	
8	44.6	99.9	100.0	100.0	
6.3	17.7	95.7	100.0	100.0	
5	11.2	76.0	100.0	100.0	
4	5.0	51.4	100.0	100.0	
3.15	3.3	30.0	90.0	100.0	
2	1.6	12.4	87.1	100.0	
1	1.2	5.2	61.2	100.0	
0.500	1.1	3.5	46.0	100.0	
0.250	1.1	3.0	35.8	99.8	
0.125	1.0	2.4	26.4	96.0	
0.063	0.9	1.9	17.3	82.1	
Density (EN 1097-6) (kg/dm ³)	2.64	2.64	2.64	2.64	

Reclaimed asphalt pavement

Reclaimed asphalt pavement comes from the milling operation of an asphalt concrete located on the fatigue carousel track at IFSTTAR [119]. The original bitumen in the RAP is also conventional 35/50. RAP is characterized to guarantee good homogeneity. In order to achieve a continuous gradation for the correct design of the new mixtures, the material is split by sieving in four granular fractions (0/2, 2/4, 4/8 and 8/12 mm) [115]. The penetration grade (EN 1426) and softening point (EN 1427) measured on the bitumen extracted from RAP are 18 [1/10 mm] and 63°C respectively. Table 4-4 lists RAP properties and Table 4-5 the characteristics from the bitumen extracted.

Table 4-4 RAP characteristics

Test / Aggregate Type	RAP Recovered		RAP Fractions			RAP Recomposition
	0/12	0/2	2/4	4/8	5/12	0/12
Grain size (EN 933-1) / (EN 933-10) Sieves (mm)						
16	100	100.0	100.0	100.0	99.4	100.0
14	98.7	100.0	100.0	100.0	97.2	100.0
12.5	93.2	100.0	100.0	100.0	88.9	96.5
10	80.3	100.0	100.0	100.0	64.2	89.2
8	68.5	100.0	99.4	99.0	39.5	78.5
6.3	58.7	100.0	98.7	81.1	27.0	70.7
5	52.0	100.0	96.3	52.4	23.2	-
4	46.7	100.0	87.5	34.8	20.9	56.0
3.15	40.0	100.0	71.7	29.3	19.5	-
2	35.7	99.9	39.6	24.3	16.8	42.3
1	26.3	74.2	27.0	19.3	13.3	32
0.500	22.0	55.7	22.3	16.0	11.2	25.3
0.250	17.2	43.4	18.9	13.5	9.5	20.3
0.125	13.7	31.8	15.4	11.0	7.8	15.6
0.063	10.0	21.7	11.8	8.6	6.1	11.1
Impurity content (EN 12697-42)	F1 Category					
Density (EN 1097-6) (kg/dm³)	2.46					

Table 4-5 RAP bitumen properties [115]

	Bitumen from RAP	RAP fraction				Bitumen from RAP Recomposition
		0/2	2/4	4/8	8/12	
Bitumen Content (%) (EN 12697-3)	4.8	8.5	6.2	4.5	3.2	5.45
Penetration Grade (1/10 mm) <i>confidence interval of +/- 3 1/10mm</i>	18	19	19	15	17	P₁₅
Softening Point (°C) <i>confidence interval of +/- 2.5°C</i>	63.0	61.8	62.8	64.4	64.6	S₇₀
Asphaltene content <i>confidence interval of +/- 2.5%</i>	20.2	17.8	19.0	20.0	19.4	-
Carbonyl Index - Ico (%) <i>confidence interval of +/- SD%</i>	8.60	9.60	9.60	9.10	9.50	-

4.2.3 Ageing procedure

The purpose of this ageing step is to characterise in laboratory the ageing experienced by the mixtures during road construction and its service life. This procedure is applied to 6 of the 12 mixtures manufactured. The ageing protocol carried out is based on the one proposed by the RILEM Technical Committee ATB TG5 [120]. It consists of two phases of oxidative thermal ageing on asphalt mixtures, a short term ageing simulating the manufacturing and construction phase of the road and a long term ageing that reproduces the end of life of the pavement. The short term ageing is performed after manufacturing on the loose mix, and involves its heating at 135°C during 4h before compaction. Then, the long term ageing holds the mixtures for 9 days at 85°C in a ventilated oven. This step was performed on compacted samples.

Figure 4-2 illustrates the manufacturing procedure followed.

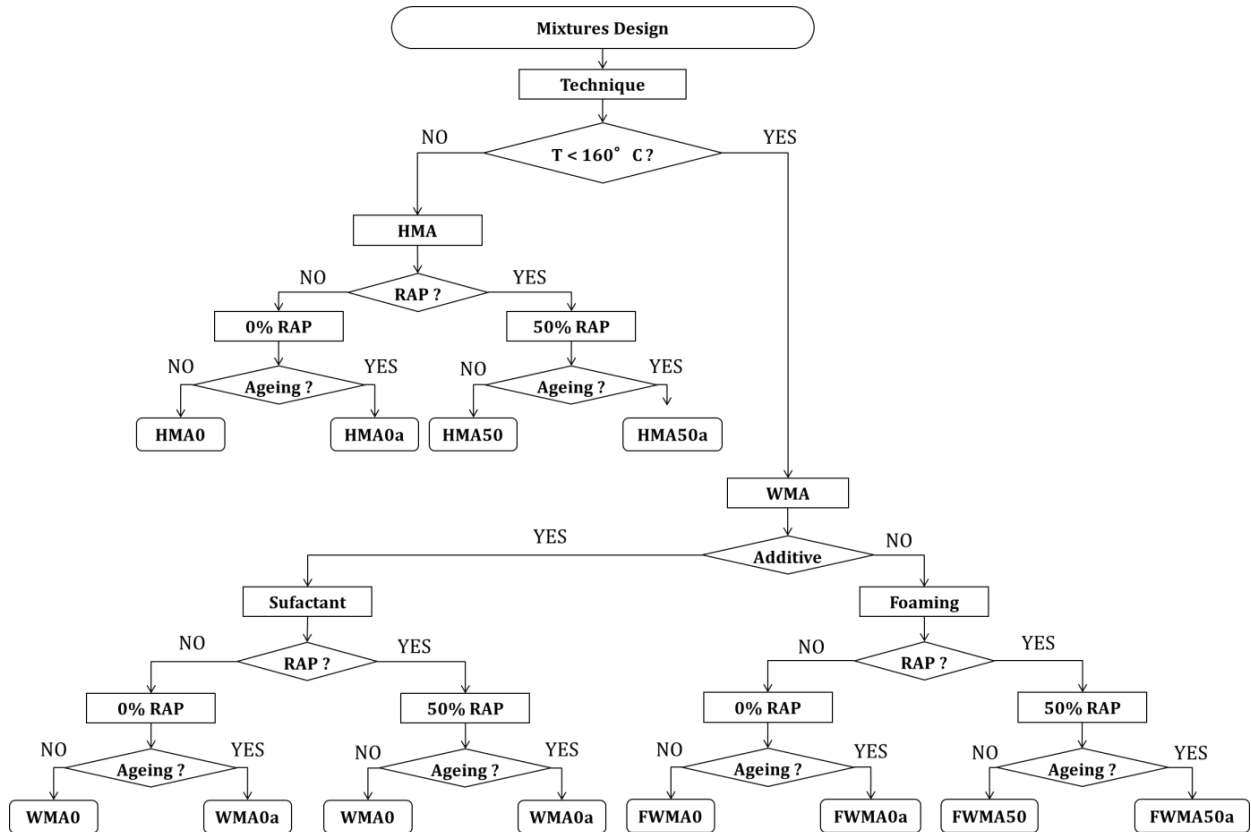


Figure 4-2 Mixtures manufacture procedure for bitumen extraction and mixture testing

4.2.4 Laboratory testing

Tests on mixtures

Complex modulus

To study the rheological and stiffness evolution of the mixtures, the complex modulus is measured according to EN 12697-26, Annex A (two point bending on trapezoidal specimens) between 1 Hz and 40 Hz, and from -10°C to 40°C. In all cases, four samples are tested for each mixture.

Fatigue resistance

The resistance to fatigue is determined according to EN 12697-24, Annex A (2PB on trapezoidal specimens) at 25 Hz and 10°C in strain controlled mode. The fatigue law curves are fitted on the experimental points by linear regression in a log-log diagram of number of cycles by strain level. In order to compare the value of ϵ_6 under the same air voids content (C), the formula $\Delta\epsilon_6 (\mu\text{def}) = 3.3 \cdot \Delta C(\%)$ [121] is used to correct the results. This formula allows the value of ϵ_6 at 4.5% of voids to be evaluated and compared.

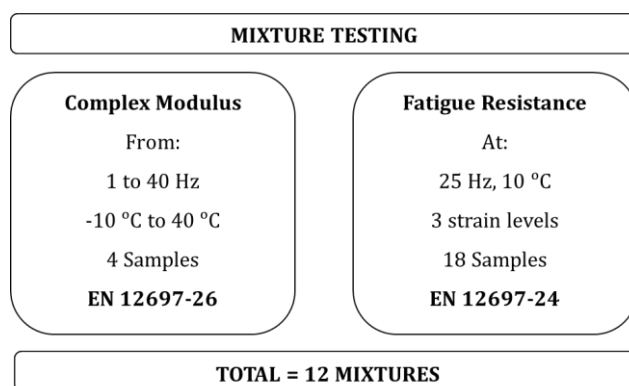


Figure 4-3 Mixtures testing protocols

Tests on bitumen

After the 12 mixtures are manufactured and the ageing protocols applied, bitumen are extracted and recovered using the rotary evaporator for bitumen recovery following the EN 12697-3 standard. The aged bitumen from the RAP (35/50 RAP) is also recovered under the same procedure. Additionally, with the original (35/50 Neat) and the foamed bitumen (35/50 Foam), a total of 15 bitumen samples are tested.

Standard consistency tests

The standard consistency of the bitumen is characterized by the penetration depth (1/10 mm) (EN 1426) and the temperature of the softening point (°C) (EN 1427).

ATR - FTIR analysis

ATR-FTIR analysis is performed with the purpose of monitoring the ageing of the binders. Carbonyl index, I_{co}, is calculated from the raw FTIR spectra according to the RILEM method [82]. The limits on the spectra for carbonyl compounds are between 1.660 and 1.753 cm⁻¹ while the reference area is between 1.350 and 1.525 cm⁻¹.

Complex shear modulus test

The determination of the complex shear modulus and phase angle is performed using the dynamic shear rheometer Kinexus® device to assess the rheological properties of the bitumen. The complex shear modulus (G*) is obtained by combining the measurements performed on geometries of parallel plates of 25 mm and 8 mm from 20°C to 60°C and -20°C to 20°C respectively, and at a frequency range from 1 to 25 Hz.

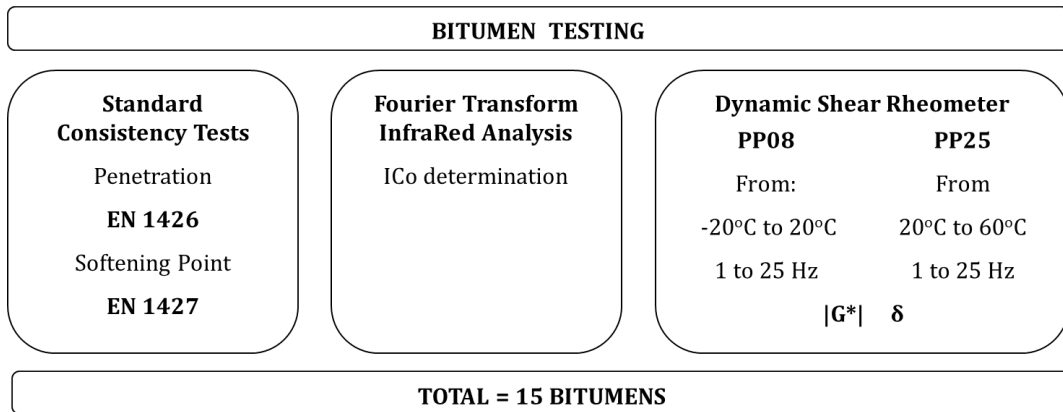


Figure 4-4 Bitumen testing protocols

4.2.5 Modelling and δ-method representation

In this chapter, bitumen rheology is modelled following the procedure described in Chapter 3. The modelling has followed the same principles, but with different device sources. Chapter 3 bitumen results are from Anton Paar MCR 501 DSR and in this chapter results are from Kinexus® device.

Moreover, from the different modelled master curves, the changes in rheology are also discussed via the determination of the rheological value (R_{value}) [29,122]. The R_{value} is the logarithmic distance between the value of the complex modulus $|G^*_{\infty}|$ from the model and at the crossover frequency ($G'=G''$, phase angle 45°). This index will allow assessing the ageing evolution of the materials.

$$Rvalue = \log \frac{|G^*_{\infty}|}{|G^*_{45^\circ}|}$$

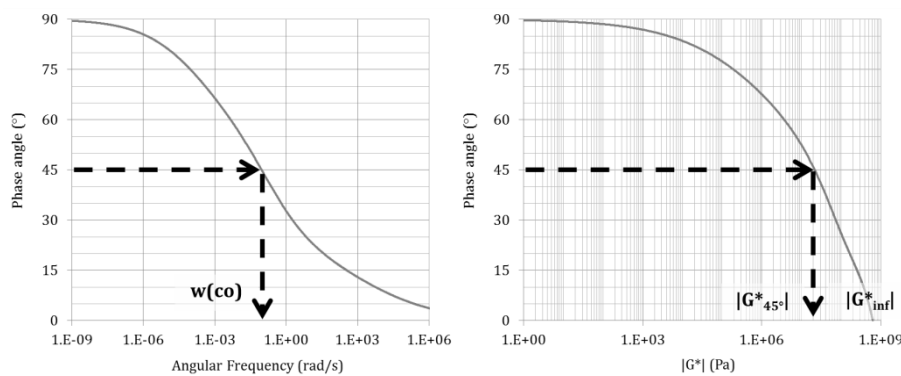


Figure 4-5 R_{value} and $w(\omega)$ determination from Black diagram and phase angle diagram

Cross-over frequencies $\omega(\omega)$ at 0°C and R -values of bitumen are determined in order to assess the ageing effect of the different analyses. Bitumen crossover frequencies are measured as in the literature [29,122]. On the other hand, the glassy modulus value, usually taken as 1,000 MPa in shear loading, is taken from the parameters of the model $|G^*_{inf}|$.

In general, cross-over frequencies decrease with ageing while R-values tend to increase. According to several authors [122,123], crossover frequency versus R-value could be used to visually evaluate binders' ageing as well as rejuvenation when RAP is used.

4.3 Analysis of results

In this section all results are presented as Figure 4-6 illustrates. The results analysis is divided in five points. In the first place, an analysis of the manufacturing technique is carried out. Secondly, the way these mixtures age is discussed. It is important to see how the different techniques evolve with time.

In addition, the influence of RAP addition and how it changes the response of the system is part of the third point, continuing with the evaluation of aged RAP mixtures. Finally, the last subsection tries to give a global perspective of the state of the materials for a first recycling step in the case of aged mixtures and second recycling phase for the mixtures with RAP. This last part should be taken into account for assessing the sustainability of each process.

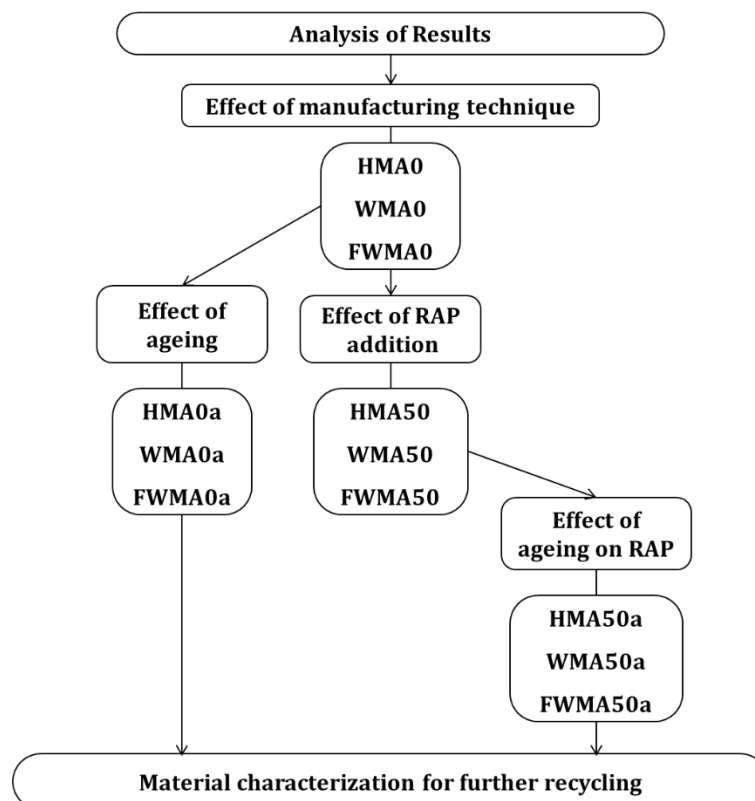


Figure 4-6 Analysis of results flowchart

4.3.1 Influence of manufacturing technique

This first analysis compares conventional HMA, WMA and FWMA processes in terms of stiffness and fatigue resistance. In addition, extracted bitumen responses to the manufacturing process are studied. The tests carried out are the standard indicators, penetration and softening point, and the characterization through rheology and the δ -method representation. This type of analysis is going to be repeated in all subsections.

Table 4-6 Influence of manufacturing technique on the mechanical performance

Technique	Mixtures				Bitumen			
	$ E^* $ 15°C, 10Hz (MPa)	Phase Angle (°)	ϵ_{6c} (μdef)	Slope (-1/b)	Pen (1/10 mm)	Soft Point (°C)	Ico (%)	R _{value}
HMA0	12,497	15.0	115	5.99	22	55.0	1.80	1.58
WMA0	12,498	14.6	100	5.69	26	57.4	1.46	1.58
FWMA0	10,921	16.1	98	4.82	32	55.6	0.48	1.45
35/50 Neat					37	53.8	0.00	1.46
35/50 Foam					34	53.6	0.00	1.46

The results obtained for the dynamic complex modulus and the fatigue resistance, including the values of ϵ_6 (strain level leading to 1,000,000 cycles) obtained and corrected to the target air voids of 4.5%, are presented in Table 4-6. Additionally, the values of penetration, softening point, carbonyl index and rheological index from the original, Foam and recovered bitumen are indicated.

Complex modulus

The values obtained for the dynamic complex modulus at 15°C and 10 Hz are all above the standard required for this type of mixtures ($|E^*| > 7,000$ MPa; EN13108-1). The stiffness modulus is similar for HMA0 and WMA0 and slightly lower for the FWMA process.

Fatigue

Fatigue laws of each procedure and the 95% confidence interval hyperboles are illustrated in Figure 4-7. FWMA and WMA are similar (ϵ_{6c} respectively 98 and 100 μdef). In all cases, they could be considered on the limit of the standard ($\epsilon_6 > 100$ μdef).

Regarding to the slopes of fatigue law for the three mixtures, they can be considered equivalent. Thus, the 15% more performance in terms of ϵ_6 compared to warm procedures for the HMA0 can be assimilated to a translation of the fatigue law. This effect may be due to the ageing experienced by the bitumen during HMA manufacturing.

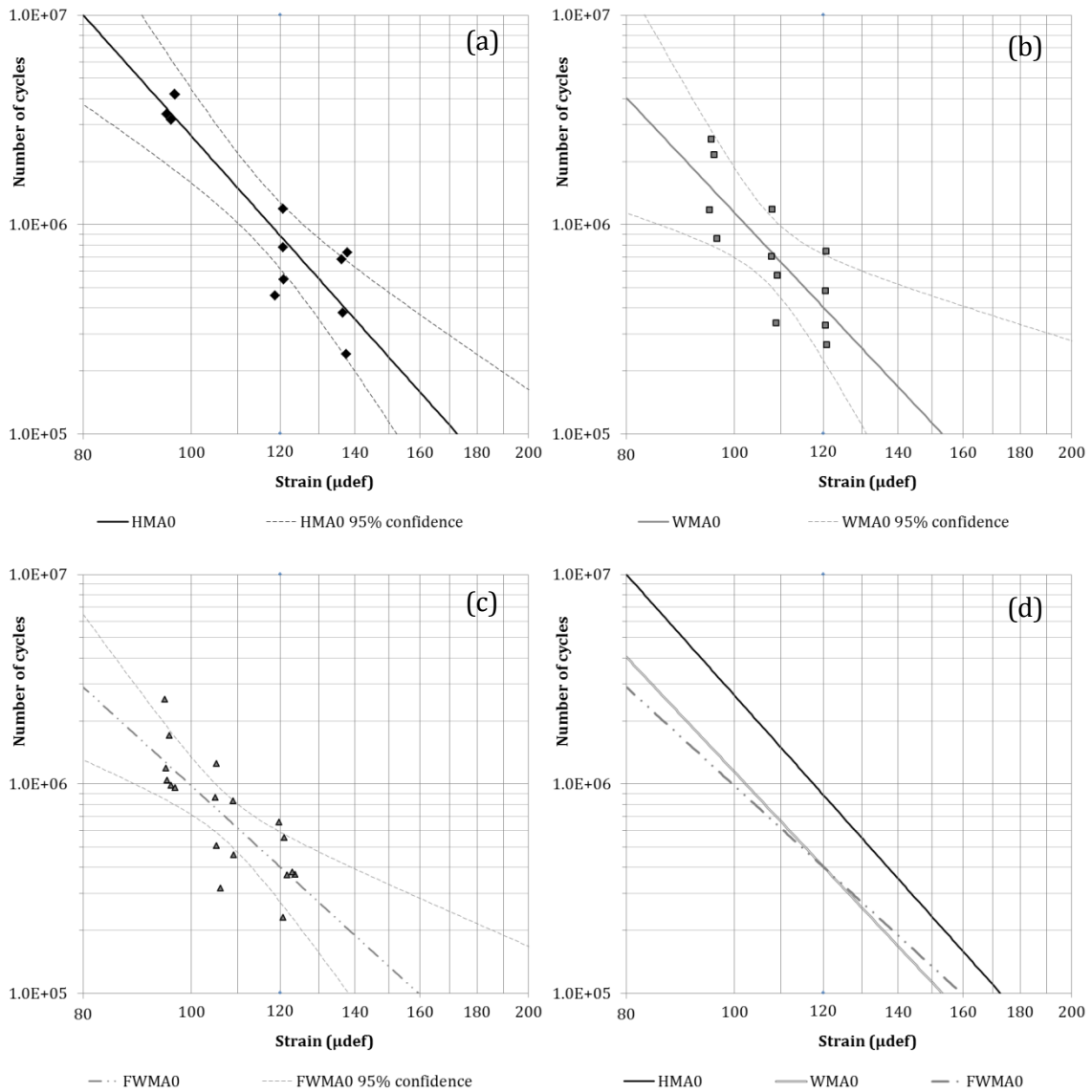


Figure 4-7 Fatigue laws and 95% interval confidence of HMA, WMA and FWMA mixtures

Penetration and softening point

Penetration and softening point values of original and foamed bitumen are represented in Figure 4-8 with the results obtained for the recovered bitumens after manufacture. The conventional high temperature manufacturing process, 160°C, induces a drastic decrease of the bitumen penetration value, by 40% for HMA0 (37 to 22). If this value of 22 is compared to the techniques produced at 130°C, the effect on penetration is a hardening of 30% (WMA0) and just 13% on the case of FWMA0. The value of the softening point measured for the HMA0 is inconsistent with the rest of the data. If this value is not taken into account the trends for the softening are in accordance with the trends observed for the penetration.

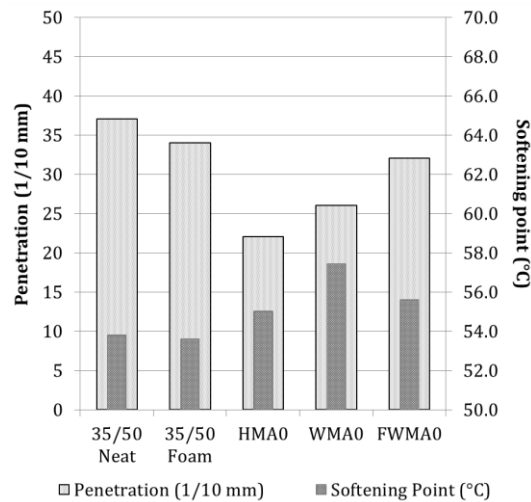


Figure 4-8 Penetration and Softening point trend by manufacturing process

Foaming process may preserve the bitumen but it somehow still needs to achieve certain levels of transformation in order to perform under the specifications. So then, harder bitumen (type 10/20 or 15/25) might be recommended for mixtures manufacture through the foaming process.

Dynamic shear rheometer

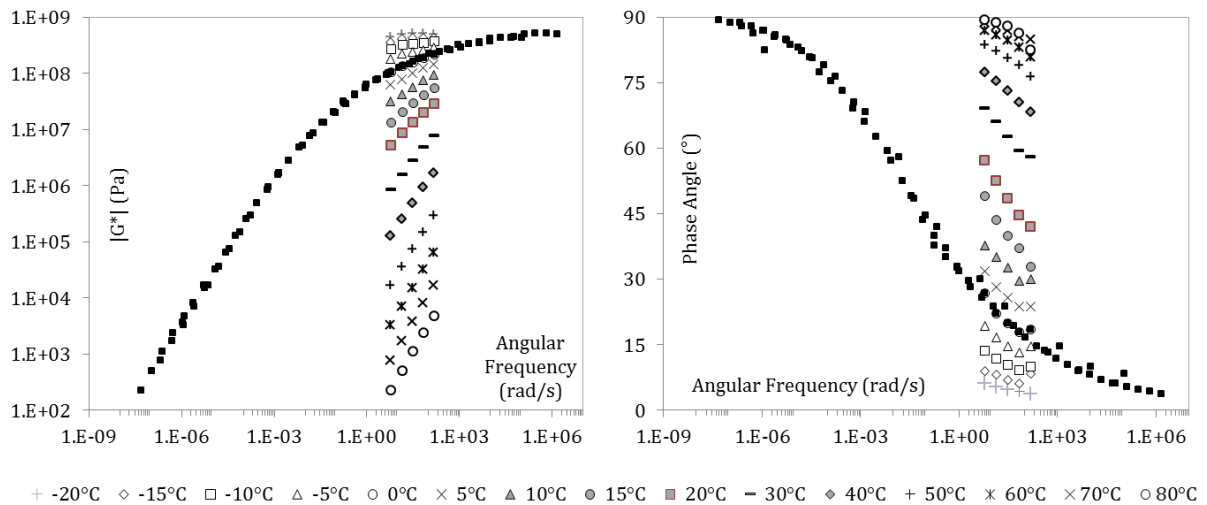


Figure 4-9 Master curve construction at 0°C for 35/50 Neat bitumen

As it has been developed in Chapter 3, the raw data obtained from DSR testing on the Kinexus® device is presented in terms of master curves and model fitting curves at $T=0^{\circ}\text{C}$. As an example, 35/50 Neat bitumen is shown in Figure 4-9.

The values of the norm of the complex modulus $|G^*|$ (Pa) and phase angle $\delta(^{\circ})$ are shown as a function of frequency (rad/s). Additionally, the translation coefficients according to the temperature (a_T) are calculated by the William-Landel-Ferry adjustment [14] along with the experimental points and the Huet-Such modelling in the Cole-Cole and Black space.

For the different extracted bitumens from the HMA0, WMA0 and FWMA0 mixtures, $|G^*|$ and phase angle master curves at 0°C are presented in Figure 4-10. It illustrates the evolution of the rheological behaviour of 35/50 Neat bitumen for the different manufacturing procedures.

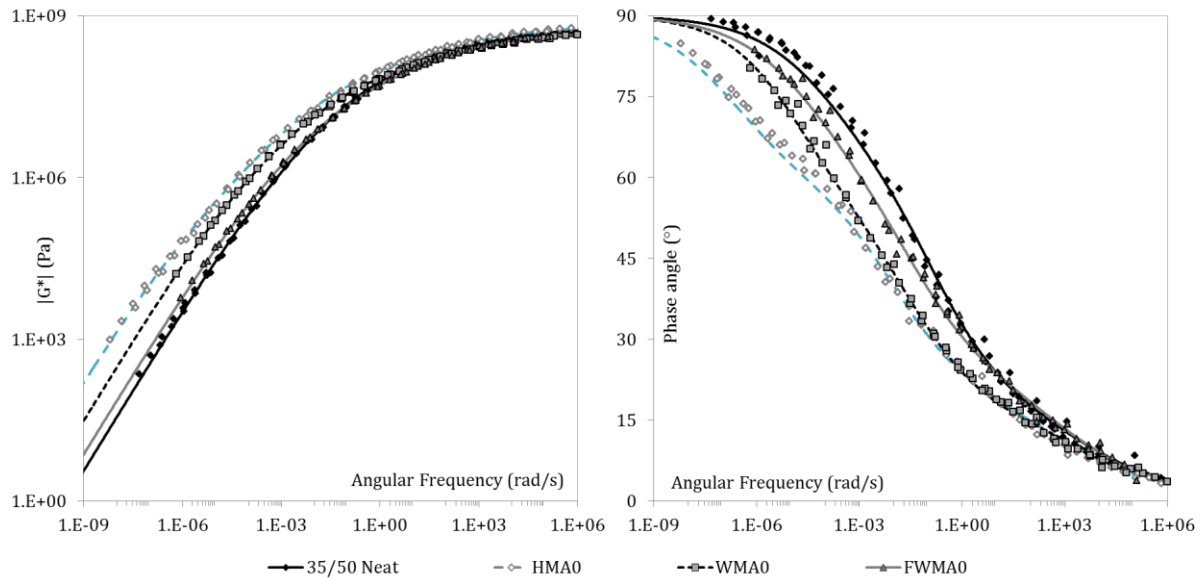


Figure 4-10 Recovered bitumen after manufacture master curves at 0°C

Bitumen master curves show the hardening experienced by the bitumen after manufacture. The trend is the same as for the penetration values. The procedure that apparently modifies less the 35/50 Neat bitumen, i.e. induces less ageing, is the foaming process. Reducing 30°C the manufacturing temperature shows a clear difference in both diagrams.

δ -method analysis

Furthermore, when regarding to δ -method representation, the so named AMWD is again illustrated and presented in Figure 4-11 with the ordinate axis corresponding to the probability density $f(\text{AMW})$. The cross-over frequency point $\omega(\omega_c)$ (i.e. storage modulus equal to loss modulus, $G' = G''$) is also plotted in the graphs for each bitumen.

Looking at Figure 4-11 (a) the four bitumens can be observed. Ageing is presented as a displacement of the curves to the right. Also as a decrease of the cross-over frequency value ($\omega(\omega_c)$).

The curve for the base bitumen 35/50 Neat shows an almost mono-modal distribution. Then, the distribution for FMWA0 bitumen, that has a very similar shape, shows the trend towards lower probability. In the case of WMA0 and HMA0 bitumens, the curves turn to bimodal look with HMA curve displaced to the right. All curves show a principal peak around 900 g/mol.

At that point, hardening of bitumens could be ordered as Neat, FWMA, WMA and HMA. Regarding $w(\text{co})$, the classification would be the same. Cross over frequencies tend to decrease with ageing or hardening (i.e. to appear at higher AMW).

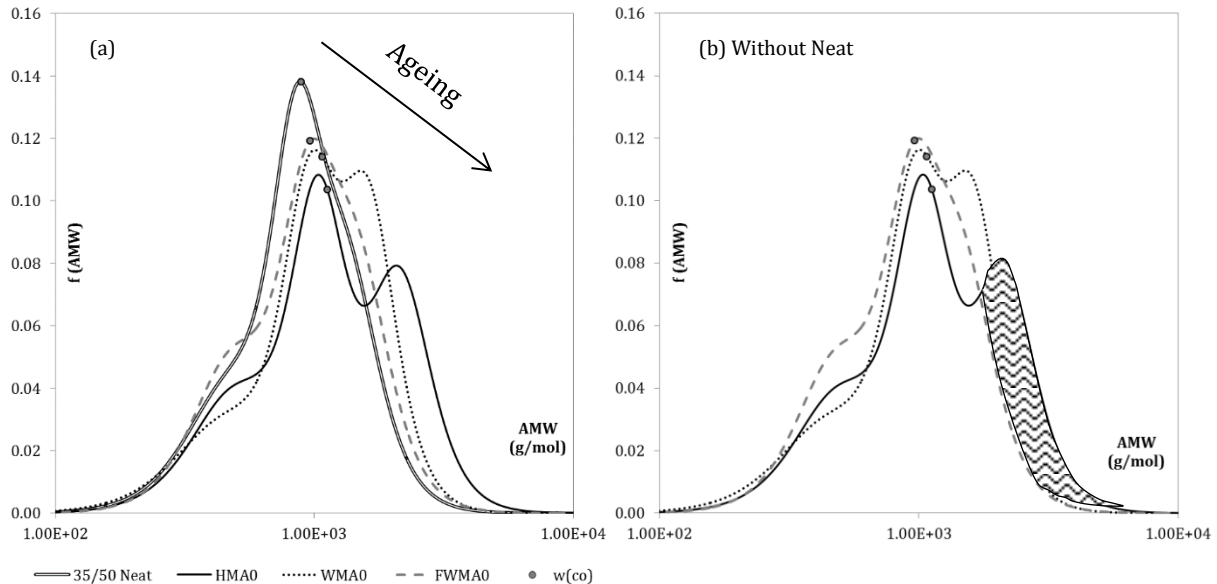


Figure 4-11 δ -method diagram of recovered bitumens after manufacture

In the right part, Figure 4-11 (b) it can be observed shadowed the increment of ageing between the foaming and the conventional procedure. These results are in accordance with the literature, where it is described that, with ageing, part of the oily fraction (mainly resins) seems to be absorbed by the asphaltenes and dispersed in the light matrix [71,83].

R_{value} - I_{co} - crossover frequency correlations

In addition, recovered bitumens are evaluated as well by comparing cross-over frequencies and carbonyl results with the R_{value} [122]. Figure 4-12 shows both associations. Firstly, ageing is traced by an increment of I_{co} . Finally, the R_{value} , which is the logarithmic difference between $|G^*_{45^\circ}|$ and $|G^*_{\infty}|$, provides a measure of stiffness in an equi-elastic state and at a given temperature ($T = 0^\circ\text{C}$). So for the same elasticity level, it can be said that the greater the R_{value} the stiffer is the bitumen.

In Figure 4-12 (a) and (b), 35/50 Neat bitumen with $R_{\text{value}} = 1.46$ is the reference value. It corresponds to zero I_{co} and to the highest $w(\text{co})$. Consequently, the ageing effect by the manufacture process is expressed as a shift to higher R_{values} , higher I_{co} and lower $w(\text{co})$.

In this sense, it can be said that high temperature manufacture procedures results in more elastic and stiffer bitumens than warm procedures.

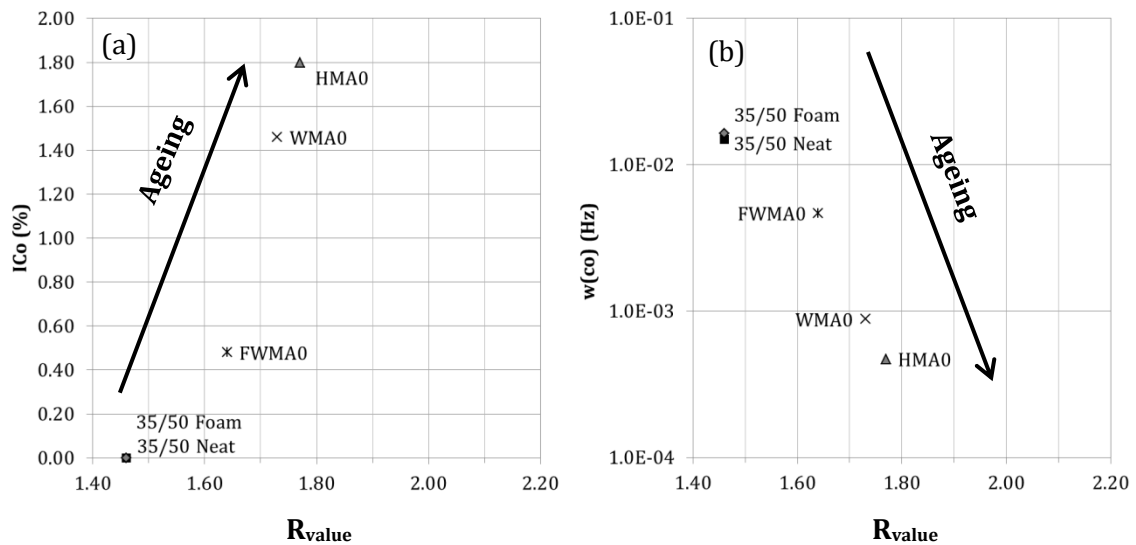


Figure 4-12 R_{value} compared in terms of $I_{co}(\%)$ (a) and cross-over frequencies (b)

4.3.2 Influence of ageing

Table 4-7 summarizes the results obtained for the dynamic complex modulus and the fatigue resistances, for all procedures after ageing. As well, the values of penetration, softening point, carbonyl index and rheological value from the original, RAP, Foam and recovered bitumen are indicated. RAP bitumen is being added to the analysis with the aim of comparing the ageing experience in laboratory with bitumen aged on service.

Table 4-7 Influence of ageing on the mechanical performance of the different techniques

Technique after ageing	Mixtures				Bitumen				R_{value}
	$ E^* $ 15°C, 10Hz (MPa)	Phase Angle (°)	ϵ_{6c} (μ def)	Slope (-1/b)	Pen (1/10 mm)	Soft Point (°C)	I_{co} (%)		
<i>HMA0</i>	12,497	15.0	115	5.99	22	55.0	1.80	1.58	
HMA0a	14,156	10.8	123	8.35	15	65.8	4.96	1.81	
<i>WMA0</i>	12,498	14.6	100	5.69	26	57.4	1.46	1.58	
WMA0a	15,492	10.7	123	7.68	17	65.2	5.40	1.98	
<i>FWMA0</i>	10,921	16.1	98	4.82	32	55.6	0.48	1.45	
FWMA0a	14,448	12.2	113	7.64	18	63.8	5.40	1.73	
35/50 Neat	-	-	-	-	37	53.8	0.00	1.46	
35/50 RAP	-	-	-	-	18	63.0	8.60	1.80	
35/50 Foam	-	-	-	-	34	53.6	0.00	1.46	

Complex modulus

All mixtures are stiffer after applying the ageing protocol. The highest growth has been for the foaming technique (32%), which is consistent with the decrease of bitumen penetration from 34 to 18.

Fatigue

In the case of fatigue behaviour, from Table 4-7, the increment shown by the ε_6 parameter after ageing is linked to an increment of the slope ($-1/b$) of the fatigue law. Thus, on the foaming process that increase of fatigue life could be explained by the increment of stiffness and reduction of penetration on the bitumen.

In Figure 4-13 the fatigue law for the different aged asphalt mixtures is presented. In general, when ageing takes place the fatigue slope increases. This means that the fatigue resistance of the material is more sensitive to the strain level.

In part (b) of the figure, WMA0a mixture show high level of dispersion. This is represented by the hyperboles of the 95% confidence intervals. With these high levels of dispersion it is difficult to conclude on any real effect of the ageing stage in this case. For example, the hypothesis of 0 slope (no influence of the strain level on the fatigue life) is not rejected for WMA0a results. At the moment, it is not clear whether these high dispersions should be attributed to flaws in the test procedure, test execution or if it reflects the intrinsic properties of the mixtures.

On the other hand, in Figure 4-13 (a) and (c), HMA0a and FWMA0a mixtures do not experience such dispersion. Additionally, in figure (d) the three fatigue laws are plotted. All fatigue laws are quasi-parallel i.e. with similar slopes after ageing.

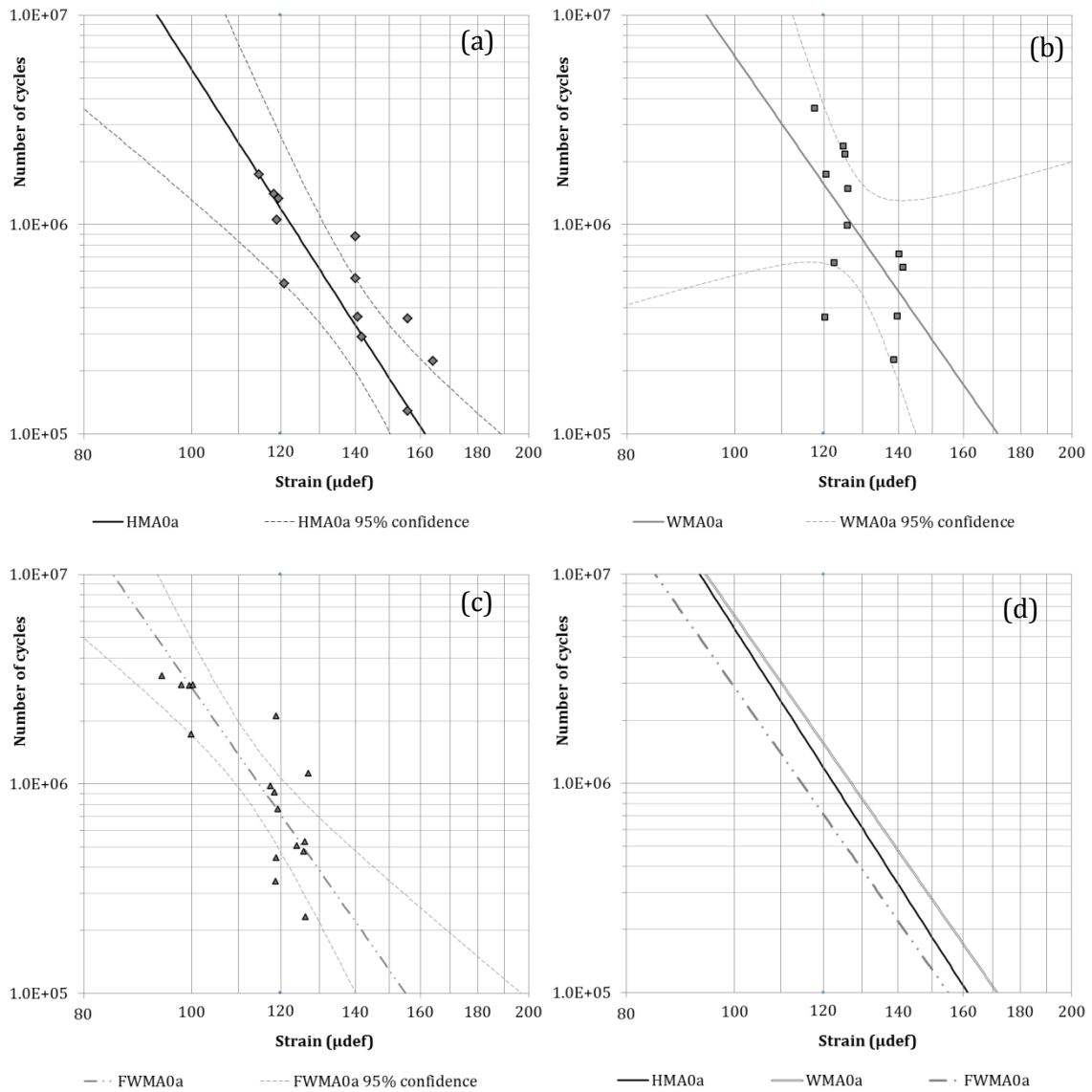


Figure 4-13 Fatigue laws and 95% interval confidence of aged HMA, WMA and FWMA mixtures

Ageing, Ico, penetration and softening point discussion

From Table 4-7, penetration, softening point and Ico values seem to achieve respectively an imaginary minimum (~15 1/10 mm) and maximum (~66°C and ~5.50%). These values show how important is to include in the analysis the evolution of results with ageing as the starting point was different.

The foaming procedure does not age bitumen at the same ratio as WMA or as HMA does. Besides, it seems that the lesser the ageing experienced by the bitumen during manufacture, the higher will be the ratio of ageing (Ico) during service life.

In Figure 4-14 penetration and softening point are shown before and after ageing. Comparing laboratory ageing procedure and natural ageing from RAP, it seems that the first one is more aggressive.

However, if results are compared by Ico evolution (Table 4-7), it can be appreciated that without being at the same ageing stage the same values of penetration and softening point can be obtained. As an example, FWMA0a and RAP bitumen have the same values of penetration and softening point, but they are in a different ageing stage in term of Ico (5.40 % and 8.60 % respectively).

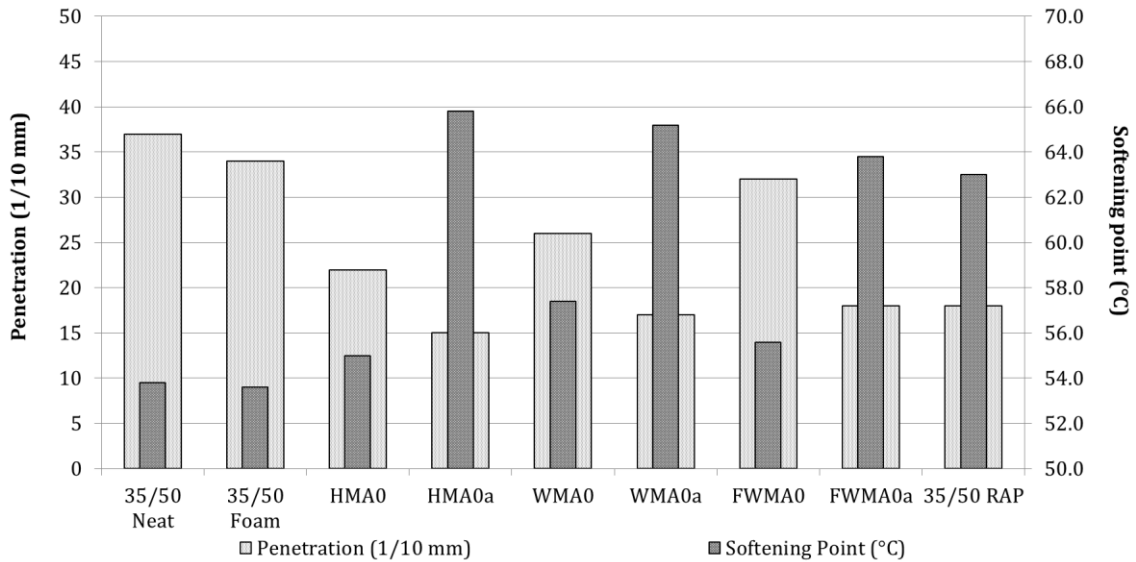


Figure 4-14 Penetration and Softening point trend after ageing

DSR results

Considering now the rheological performance of the extracted bitumen, they tend to have the same response. This observation is illustrated in Figure 4-15, where the master curves of the different aged bitumen are plotted with the 35/50 Neat bitumen. Although the response at medium/low frequencies is different depending on the procedure, the difference at high frequencies is not so clear at this scale. In this sense, the δ -method analysis may help to evaluate these differences.

From the measurements shown in Figure 4-15, it can be noted that the adjustment for the phase angle master curve may seem weak. However, the process of modelling calculus takes into account the cole-cole and the black plan, and both master curves. Indeed, these measurements highlight the quality needed for the test in order to be well modelled.

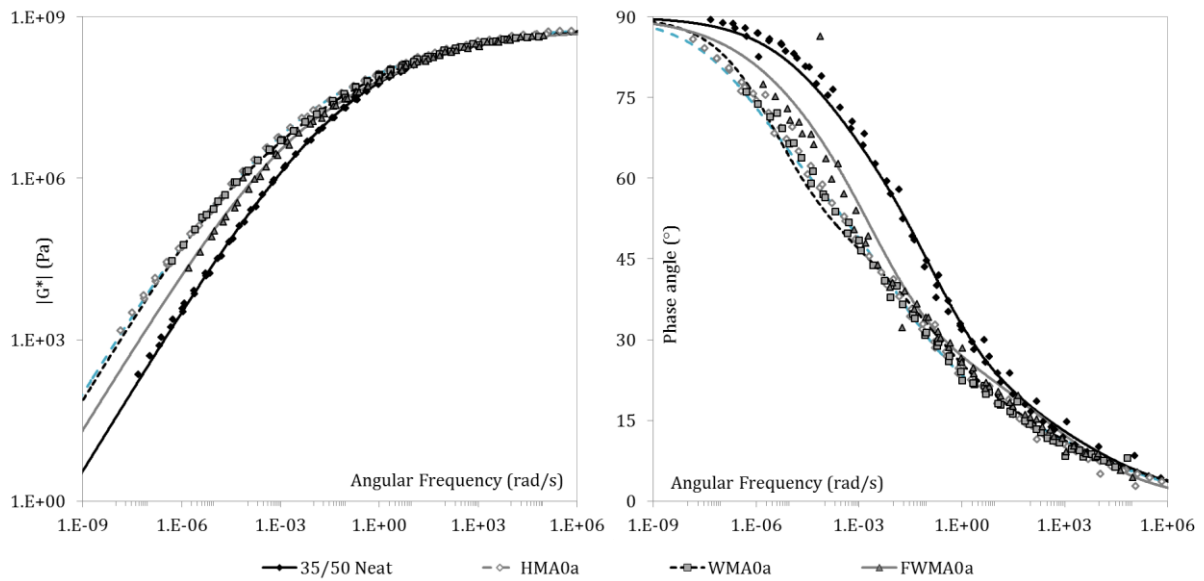


Figure 4-15 Recovered bitumen after ageing master curves at 0°C

δ-method analysis

Figure 4-16 represents the δ -method curves for the neat bitumen and the bitumen extracted after ageing. In part (a) of the figure the aged bitumens are compared with the 35/50 Neat bitumen. They show all an evolution with ageing. After ageing they are all centred around 1,100 g/mol and present a clearer bimodal distribution, showing in the case of HMA0a bitumen the beginning of a third peak at the beginning of the curve.

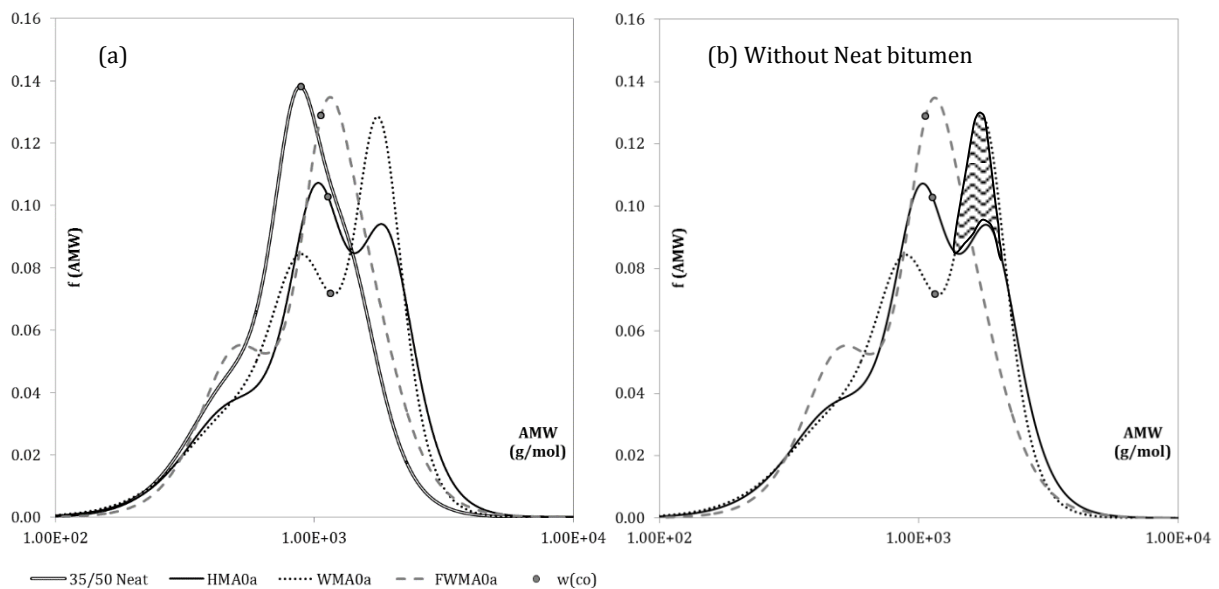


Figure 4-16 δ -method diagram of recovered bitumens after ageing

Then in part (b), it is highlighted the difference of ageing between the WMA process and the other procedures. This higher concentration (maybe due to asphaltenes increase) could explain

the brittleness and scattering of performances. The greater stiffness of WMA0a may be explained as well by the presence of higher concentration of asphaltenes in the bitumen.

It is clear that this analysis would not be possible only considering the values of I_{co} or the standard indicators of penetration and softening point.

R_{value} - I_{co} - crossover frequency correlations

In Figure 4-17, I_{co} by R_{value} (a) and cross-over frequencies by R_{value} (b) are illustrated. In the first place, I_{co} normally increases after ageing more than after manufacture. For the analysis, I_{co} and R_{value} should increase always with ageing.

However, the evolution of cross-over frequencies and R_{value} seems to follow a more consistent relationship. The path towards higher R_{values} and lower cross-over frequencies of each pair of data is clearer than for the I_{co} evolution.

Once more, the R_{value} for WMA0a is the highest of all aged mixtures with a very low cross-over frequency. This difference in elasticity with the other aged materials would explain the fragility of the mixtures when tested to fatigue.

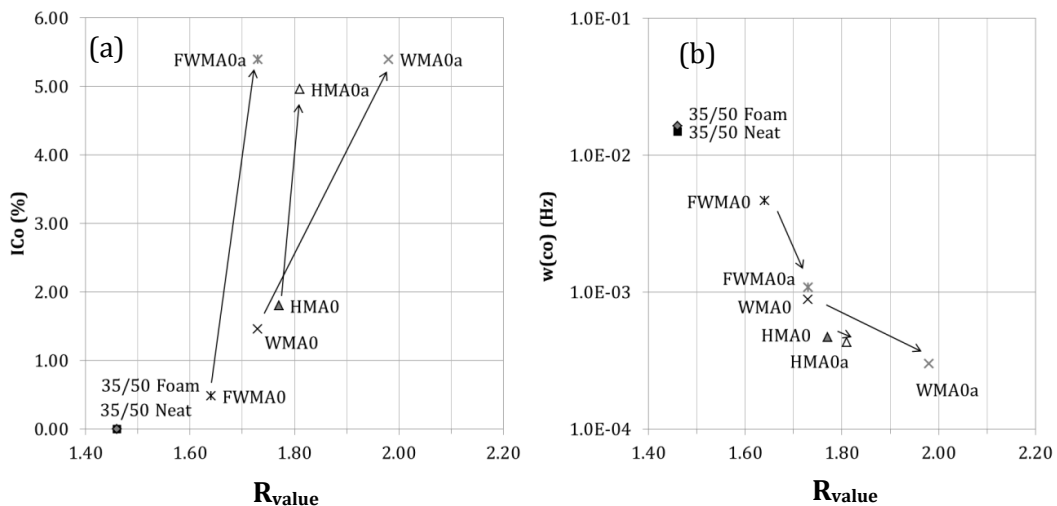


Figure 4-17 R_{value} compared in terms of I_{co} (%) (a) and cross-over frequencies (b) before and after ageing

4.3.3 Influence of RAP addition

The specificity of mixtures with RAP is the presence of already aged bitumen in the mixture. Table 4-8 summarizes the principal results found for the mixtures without RAP (0) and with RAP (50).

Table 4-8 Influence of RAP addition on the mechanical performance of the different techniques

Technique with 50% RAP	Mixtures				Bitumen			
	$ E^* $ 15°C, 10Hz (MPa)	Phase Angle (°)	Corrected ϵ_6 (μdef)	Slope (-1/b)	Pen (1/10 mm)	Soft Point (°C)	Ico (%)	R_{value}
<i>HMA0</i>	12,497	15.0	115	5.99	22	55.0	1.80	1.58
HMA50	14,590	12.2	127	7.08	19	62.8	4.08	1.71
<i>WMA0</i>	12,498	14.6	100	5.69	26	57.4	1.46	1.58
WMA50	13,721	12.7	119	5.55	19	61.6	3.74	1.74
<i>FWMA0</i>	10,921	16.1	98	4.82	32	55.6	0.48	1.45
FWMA50	13,122	14.0	106	5.12	24	60.4	5.47	1.68
35/50 Neat	-	-	-	-	37	53.8	0.00	1.46
35/50 RAP	-	-	-	-	18	63.0	8.60	1.80
35/50 Foam	-	-	-	-	34	53.6	0.00	1.46

Complex modulus

The effect of RAP addition to the mixture is developed in the literature [6,8,53,124]. Our results mostly follow in general the same path. Regarding in detail, dynamic complex modulus has increased in 2,000 MPa for HMA50 and FWMA50, but for the WMA procedure, the difference with the original mixture without RAP is not clear within this test.

Fatigue

The fatigue performance of all materials in terms of ϵ_6 increases with RAP, performing in all cases above the 100 μdef specified on the standards for these types of mixtures (EN 13108-1). This could be a result of the increment of stiffness experienced by the addition of 50% of RAP [6,8,53,124].

Besides, slopes of fatigue laws do not vary much with RAP addition. In fact they experience a translation to higher resistances whatever the strain solicitation level is. In Figure 4-18 the fatigue laws for all procedures with 50% of RAP are illustrated (a-b-c) and the comparison with HMA0 (d) mixture as well.

In the case of WMA50 (b), the dispersion found on the results let some doubt on the performances of the material tested. Once again, it is not clear whether these high dispersions should be attributed to flaws in the test procedure, test execution or if it reflects the intrinsic properties of the mixtures.

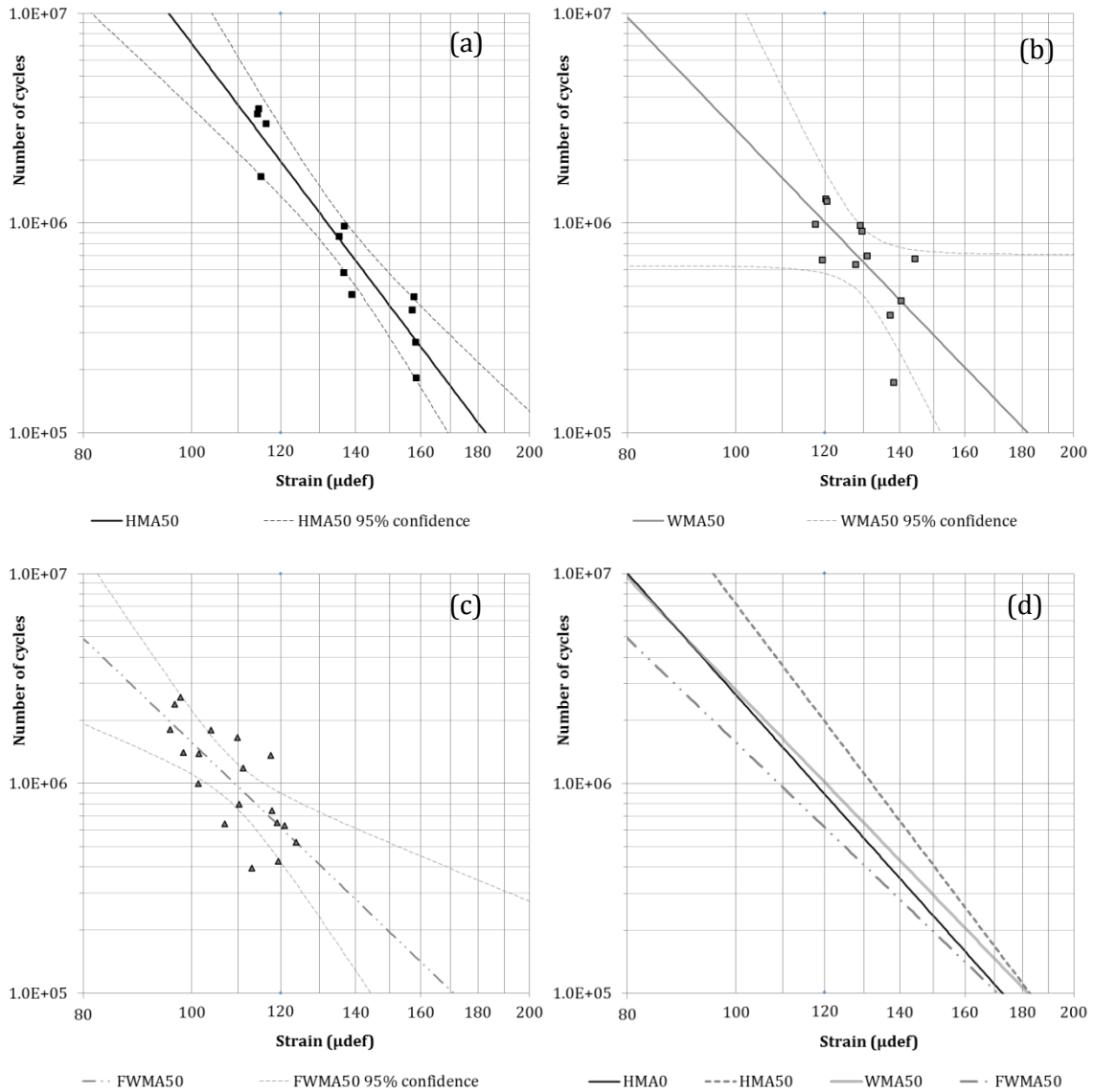


Figure 4-18 Fatigue laws and 95% interval confidence of mixtures with RAP: HMA50, WMA50 and FWMA50

Technical and environmental performances analysis

If the three techniques are compared, the conventional procedure for mixtures manufacture HMA shows higher results than warm techniques, despite all perform above minimum required on the standards. However, warm materials with 50% of RAP, are produced 30°C lower. This could be considered as more efficient materials from an environmental point of view.

Ageing, Ico, penetration and softening point discussion

Additionally, in Figure 4-19 penetration and softening point results are shown. As expected, the addition of RAP makes the bitumen stiffer, due to the presence of the already aged bitumen.

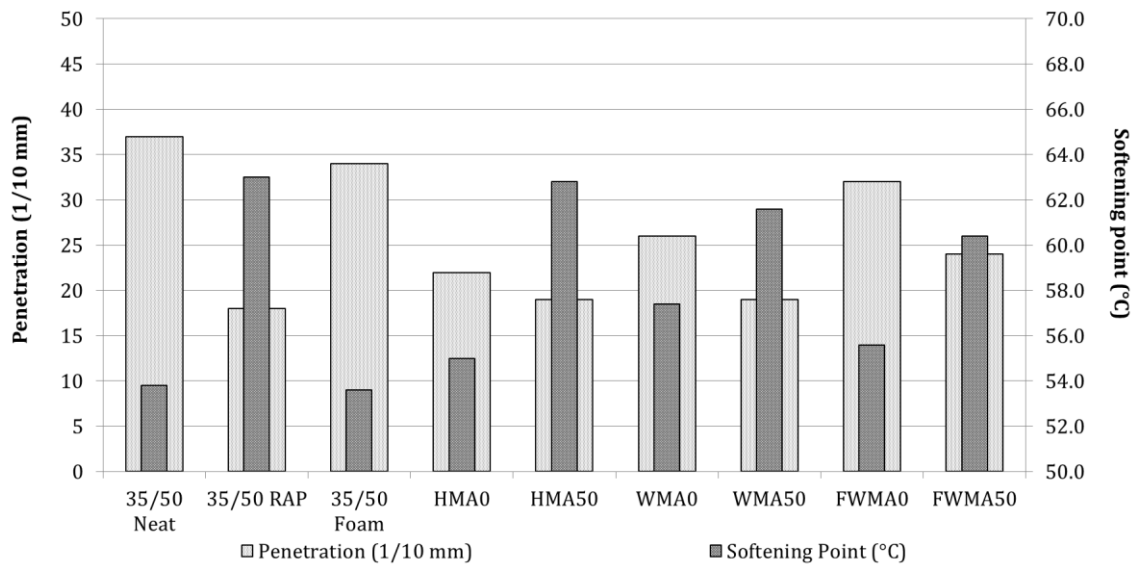


Figure 4-19 Penetration and Softening point trend after RAP addition

DSR results

Figure 4-20 illustrates the master curves obtained from rheological testing of all bitumens. The rheological evolution of bitumen blending during manufacture follows the trend observed for the standard indicators. The “softer” bitumen would be the one from the foaming process even having a greater Ico index, while the “harder” would be the conventional HMA procedure.

Master curves are very close, but still HMA50 is harder than WMA bitumen. The softest of the three bitumens is the FWMA50.

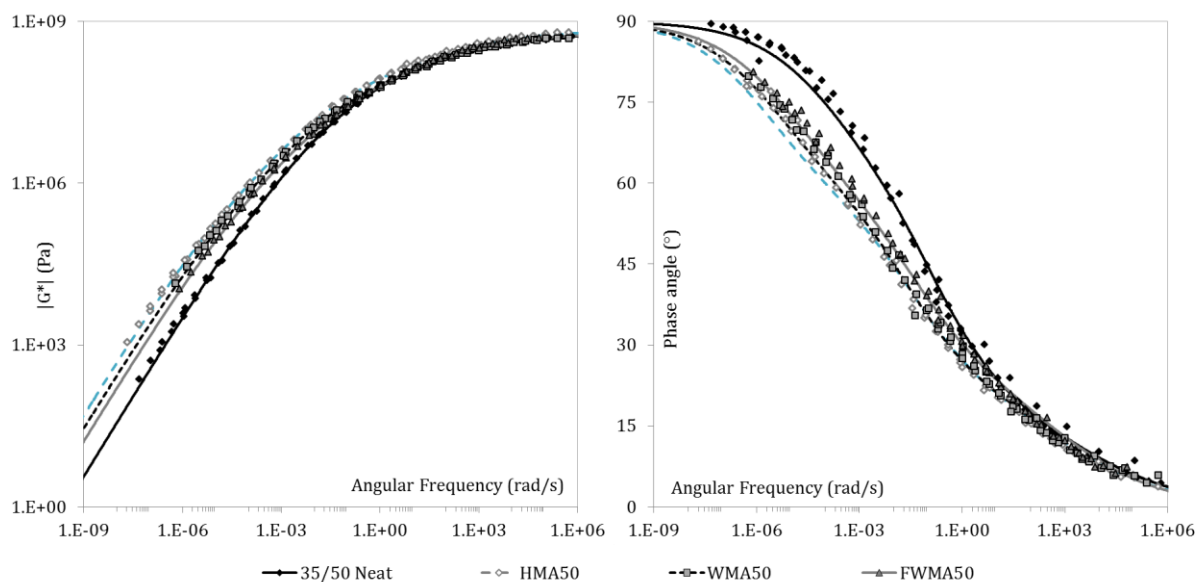


Figure 4-20 Recovered bitumen after 50%RAP mixtures manufacture master curves at 0°C

δ -method analysis

For an accurate development of the analysis, the data obtained at low temperatures with the dynamic shear rheometer is very important. From derivation of the model curves, the δ -method analysis is presented. In Figure 4-21 each bitumen curve is shown with respect to 35/50 Neat bitumen (a). Also, in part (b) of the figure, the comparison is done with respect to 35/50 RAP bitumen.

On the part (a) of the figure, the trend followed by the δ -curves is the same as for the master curves (FWMA50<WMA50<HMA50). At high frequencies the response of the material is better distinguished through the δ -method.

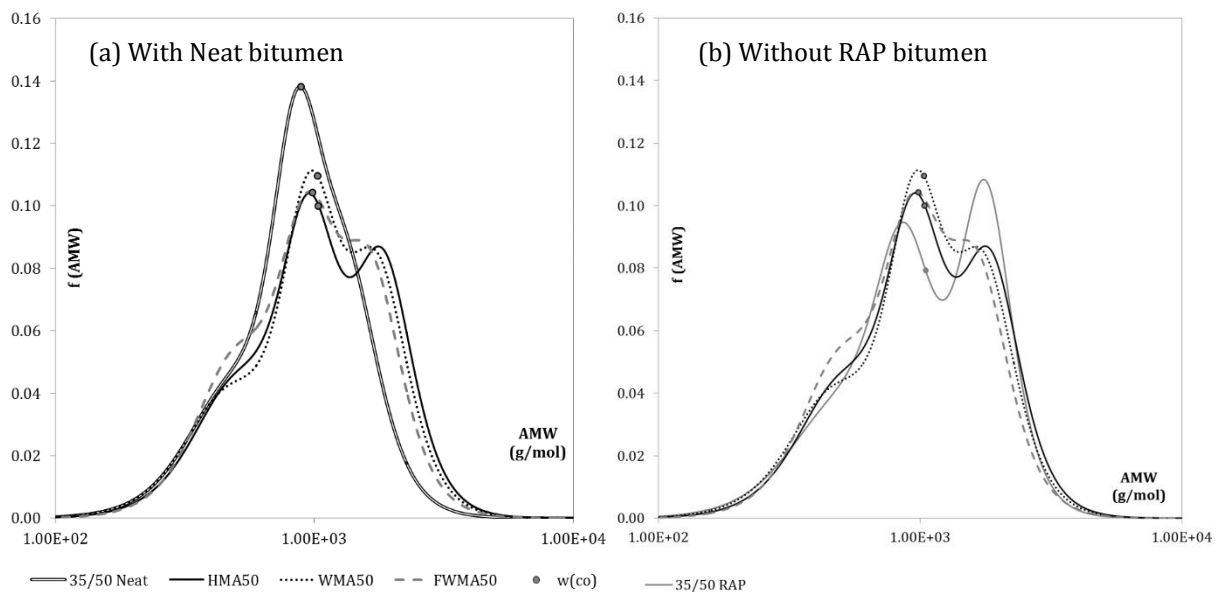


Figure 4-21 δ -method diagram of recovered bitumens of RAP mixtures after manufacture

On the right part (b) of the figure 4-21, the 35/50 RAP bitumen is shown, in clear grey full line. It presents a bimodal distribution, but when mixed with virgin bitumens for all procedures and techniques the second peak becomes smaller.

In general, if ageing analysis were done just in terms of Ico results, it might seem confusing. Ico value for FWMA50 is the highest (5.47%), however considering penetration or stiffness, this bitumen could be considered the softest. This proves that soft is not equivalent to “young”. This is the true potential of the δ -method, the evaluation of bitumens from rheological measurements.

R_{value} - I_{co} - crossover frequency correlations

Regarding to the viscoelastic response of the material expressed in terms of R_{value} and compared by I_{co} and cross-over frequencies, in Figure 4-22 (a) an increase of I_{co} can be observed when RAP is used, without any clear change in the R_{value}.

Then, in Figure 4-22 (b), the addition of RAP leads the R_{value} to increase or decrease, as well as the cross over frequencies. Then, no clear correlation can be established between R_{value} and I_{co} or R_{value} and w(co).

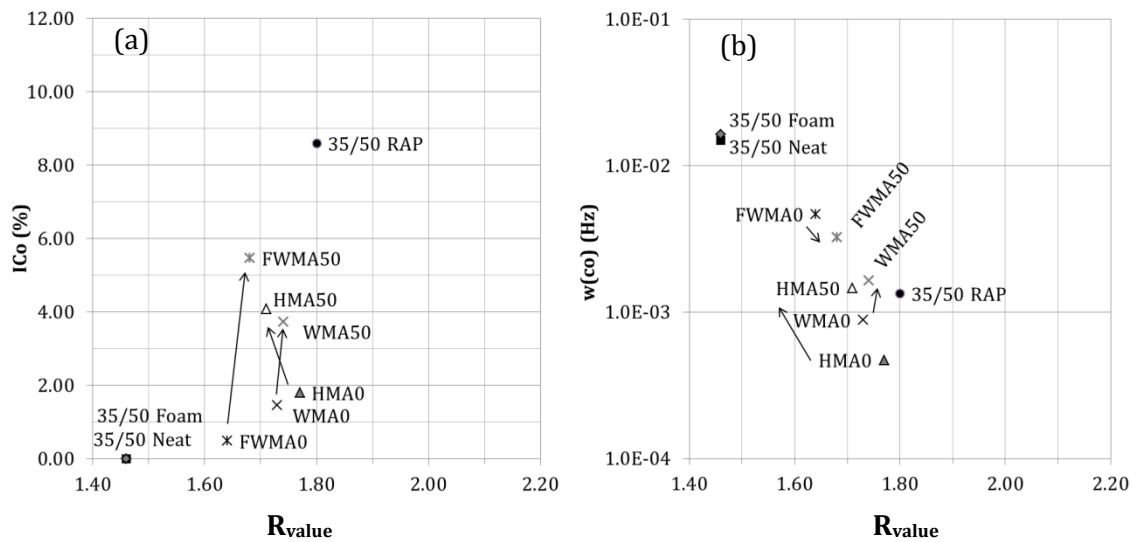


Figure 4-22 R_{value} compared in terms of I_{co}(%) and cross-over frequencies before and after RAP addition

4.3.4 Ageing on mixtures with RAP

Table 4-9 Influence of ageing on the characteristics of the mixtures with RAP

Technique with 50% RAP	Mixtures				Bitumen			
	E* 15°C, 10Hz (MPa)	Phase Angle (°)	ε _{6c} (μdef)	Slope (-1/b)	Pen (1/10 mm)	Soft Point (°C)	I _{co} (%)	R _{value}
HMA50	14,590	12.2	127	7.08	19	62.8	4.08	1.71
HMA50a	15,847	11.3	122	6.99	15	66.0	8.27	1.84
WMA50	13,721	12.7	119	5.55	19	61.6	3.74	1.74
WMA50a	16,035	11.0	108	16.70	14	66.8	8.39	1.98
FWMA50	13,122	14.0	106	5.12	24	60.4	5.47	1.68
FWMA50a	15,460	11.5	115	5.49	17	66.0	10.35	1.99
35/50 Neat	-	-	-	-	37	53.8	0.00	1.46
35/50 RAP	-	-	-	-	18	63.0	8.60	1.80
35/50 Foam	-	-	-	-	34	53.6	0.00	1.46

Table 4-9 is a synthesis of the results, in terms of complex modulus, fatigue resistances, penetration depth, softening point temperature, carbonyl index and R_{value} for the mixtures with 50% of RAP, submitted to the RILEM ageing protocol. As well, 35/50 Neat bitumen, RAP bitumen and Foam bitumen are also presented.

Complex modulus

From Table 4-9 it can be observed that warm mix asphalts, WMA and FWMA with 50% of RAP have suffered the highest increment of complex modulus ($\sim 2,300$ MPa).

Fatigue

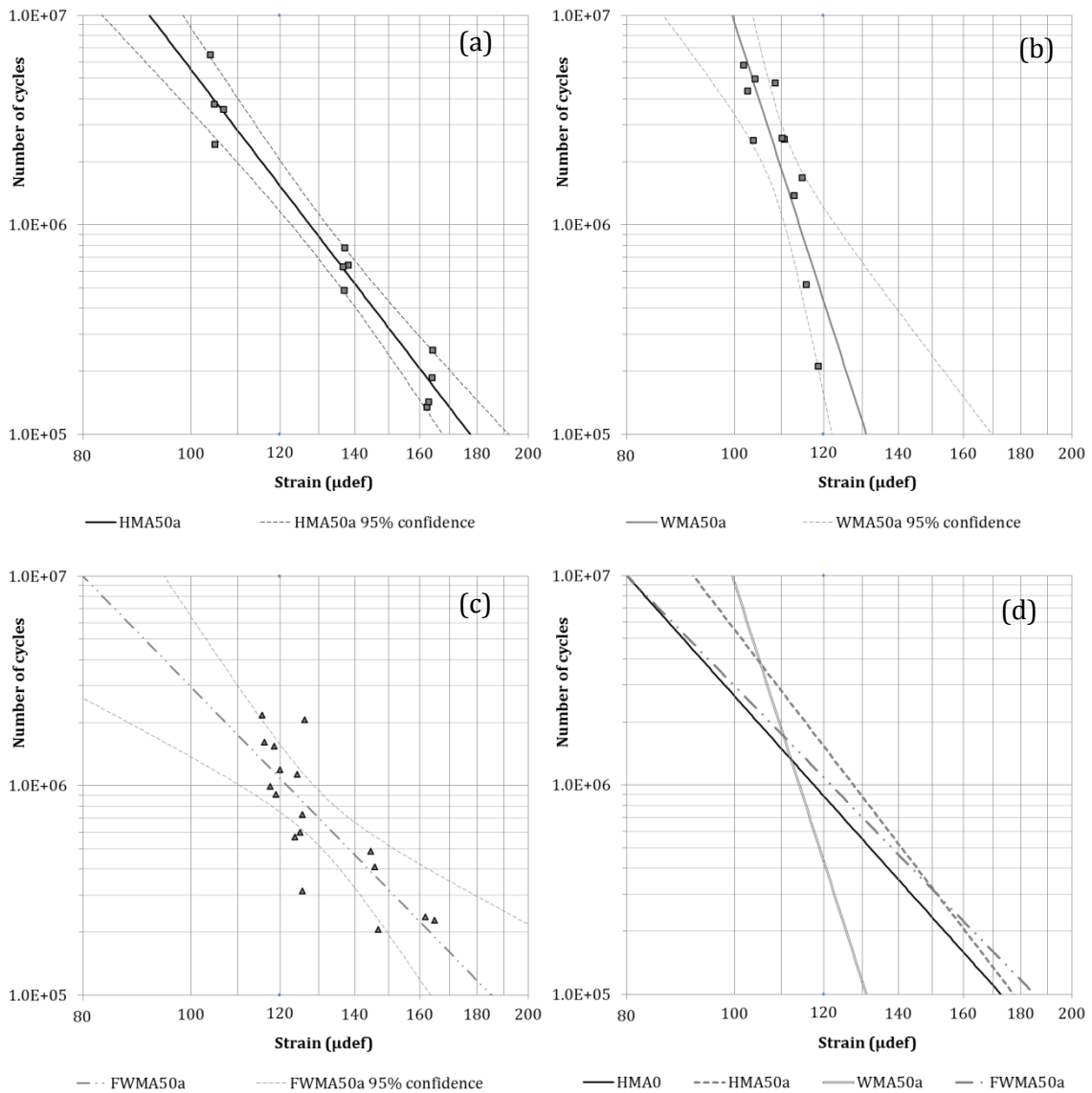


Figure 4-23 Fatigue laws and 95% interval confidence of aged HMA50, WMA50 and FWMA50 mixtures after ageing

Regarding to fatigue performance, Figure 4-23 illustrates all fatigue laws and also the comparison between them. From Table 4-9, it can be observed that HMA50a mixture suffers a translation to lower performance, as the slope remains almost constant. In Figure 4-23 (b) it can be observed that WMA50a mixture dramatically increases its slope (from 5.55 to 16.70) becoming very sensitive to strain changes. Thus, the combination of surfactant process and RAP seems particularly affected by ageing.

Meanwhile, FWMA50a mixture (Figure 4-34 (c)) keeps responding better than the non-aged stage with an increment of 9 μ def of ϵ_6 for the same slope. It seems like the ageing experienced by the foamed bitumen supplies the needed changes on the bitumen for a better global performance.

Ageing, Ico, penetration and softening point discussion

From penetration and softening point results, resumed in Figure 4-24. Ageing evolution follows the line of previous results. In this case maximum penetration is 15, and the maximum softening point is achieved at 66.8°C. In contrast, Ico results show a very different ageing state for the FWMA50a mixture (10.35%) compared to the other procedures (~8.30%). This confirms the trend already observed for FWMA0a.

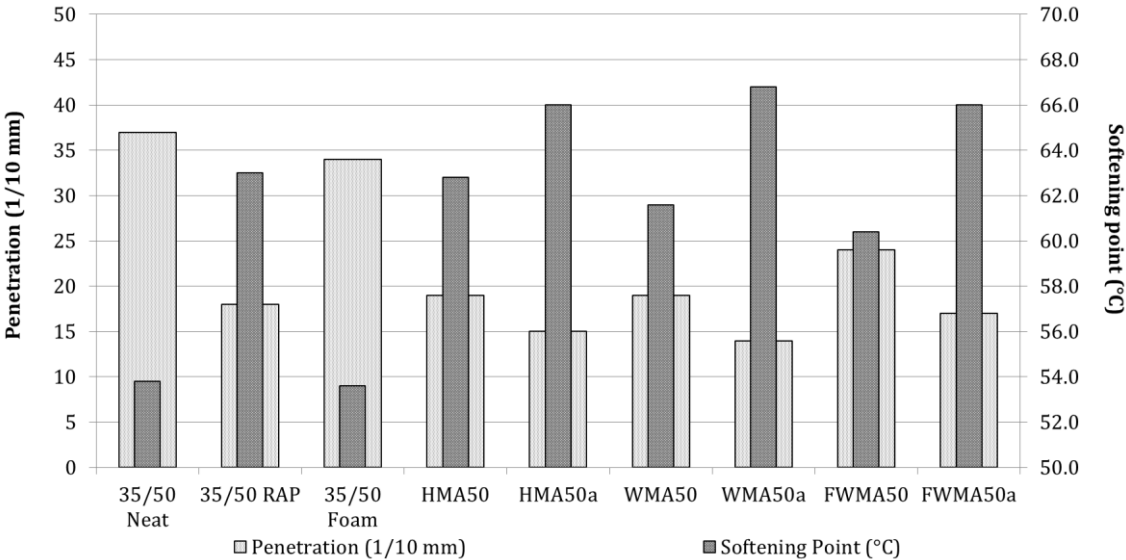


Figure 4-24 Penetration and Softening point trend after ageing on RAP mixtures

DSR results

When looking at the rheological master curves plotted in Figure 4-25 there is little room for analysis as the three curves are almost similar. The big change is again between these bitumens and the original 35/50 Neat bitumen.

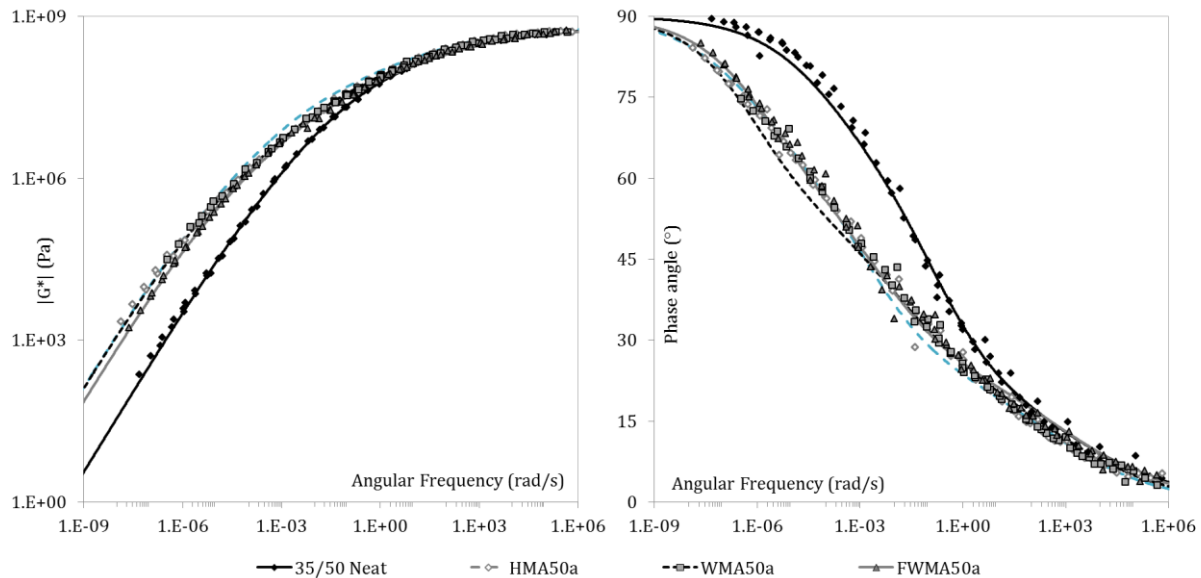


Figure 4-25 Recovered bitumen after ageing on 50%RAP mixtures master curves at 0°C

δ -method analysis

In this case of rheological data superposition, the δ -method could play good role for data treatment. Figure 4-26 represent the model derived of the curves. On the left part (a) the curves for HMA50a, WMA50a and FWMA50a are shown compared to 35/50 Neat bitumen.

From the last analysis (50% RAP not aged), the changes induced by ageing are different in each case (Curves shown in Annex 5). Through this analysis, ageing of materials could be classified as HMA50a < FWMA50a < WMA50a.

In Figure 4-26 (b), it is highlighted the difference between WMA50a and HMA50a. They have very similar values of penetration (14 and 15), softening point (66.8 and 66°C), Ico (8.39 and 8.27%). However, the difference shown by the δ -method could explain why stiffness and fatigue performance are different.

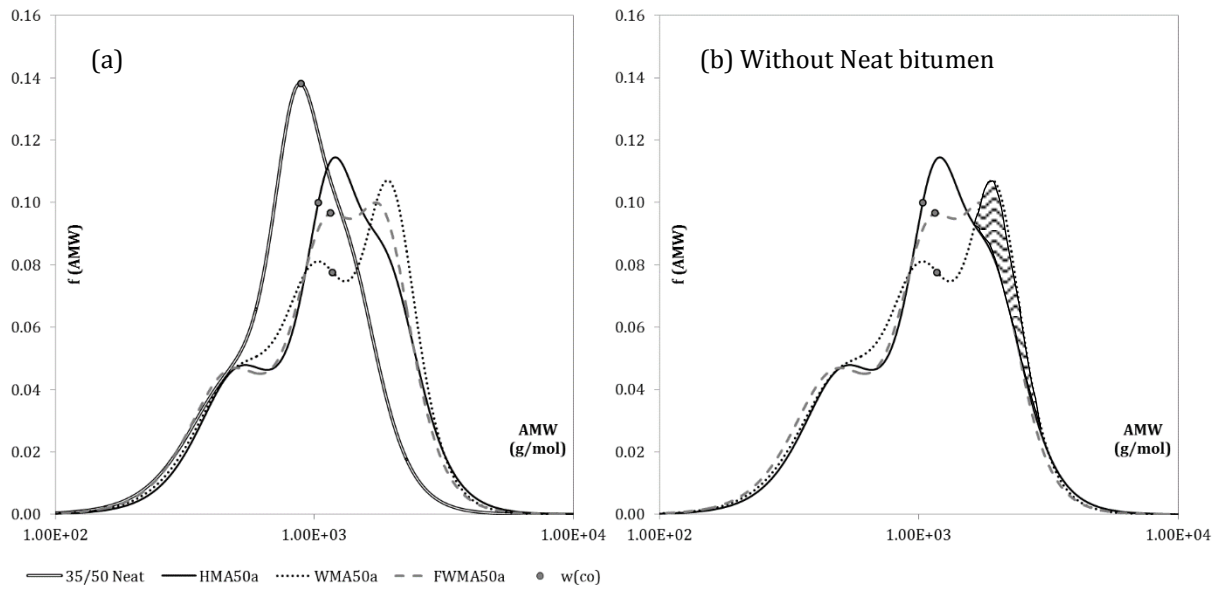


Figure 4-26 Fatigue laws and AMWD of HMA, WMA and FWMA technique with 50% of RAP at the end of life situation

R_{value} - I_{co} - crossover frequency correlations

Regarding now to R_{value} evolutions presented in Figure 4-27, the trend follows the standard path (increase of R_{value} , I_{co} and decrease of $w(co)$).

In general, R_{value} results seem to show a more elastic response of warm bitumens compared to the conventional procedure with 50% of RAP. The difference in this case is that the glassy modulus is 100 times bigger than the complex modulus at 45° ($R_{value} = \log(|G^*_{45^\circ}|/|G^*_{\infty}|)$).

From Figure 4-27 (a) it is observed the big increase suffered by I_{co} . Then, in part (b) this could be translated as a big decrease of $w(co)$ with respect to the R_{values} .

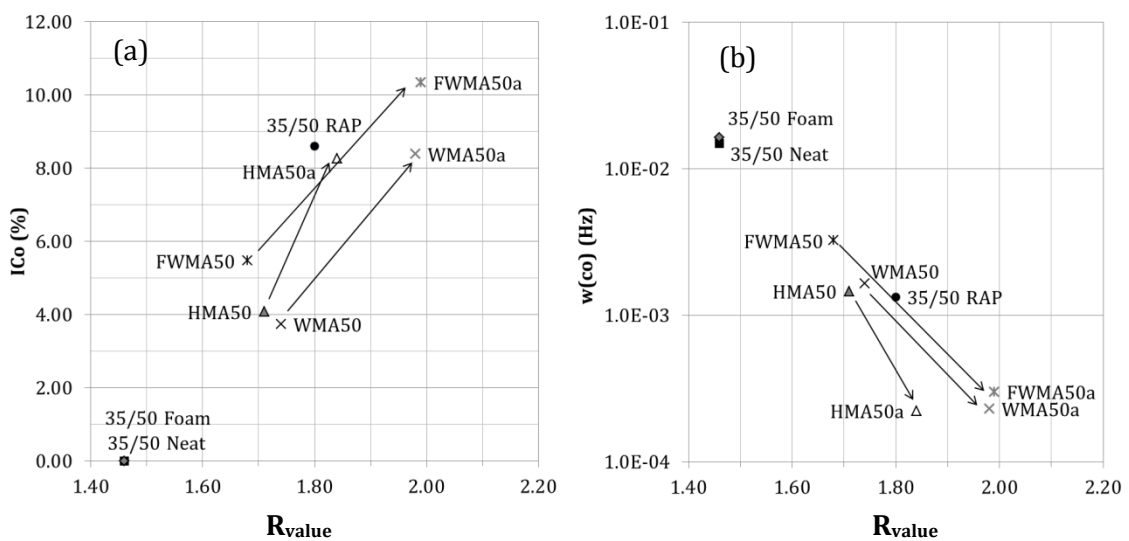


Figure 4-27 R_{value} compared in terms of I_{co} (%) and cross-over frequencies before and after ageing on mixtures with RAP

4.3.5 Evaluation of materials for recycling

The aim of recycling should not only be to assure certain characteristics and performances of the mixtures, but also to determine the sustainability of these new mixtures for further reuse. There are many questions to answer. Such as: how long can a bitumen be reuse without using rejuvenating agents or if standard indicators as penetration and softening point give the require information.

In this section, an evaluation of our studied materials for further recycling is assessed.

From EN 13108-8 standard, the principal characteristics of previously tested materials are summarized in Table 4-10.

Table 4-10 Characteristics from 0%RAP aged and 50%RAP aged mixtures following EN 13108-8

Source	Impurities content	Type of bitumen	Additive	Aggregates	D_{max} (mm)	Pen (1/10 mm)	Soft Point (°C)	RAP from:
A	F1	35/50	No	Gneiss	12	P ₁₅	S ₇₀	HMA0a
B	F1	35/50	Surfactant	Gneiss	12	P ₁₅	S ₇₀	WMA0a
C	F1	35/50	No	Gneiss	12	P ₁₅	S ₇₀	FWMA0a
D	F1	35/50	No	Gneiss	12	P ₁₅	S ₇₀	HMA50a
E	F1	35/50	Surfactant	Gneiss	12	P ₁₅	S ₇₀	WMA50a
F	F1	35/50	No	Gneiss	12	P ₁₅	S ₇₀	FWMA50a

According to the standard, all materials are the same, except for the surfactant WMA material which contains of course surfactant. Thus, it is known by us that the manufacturing procedure is a warm procedure. If not, it could be thought that the surfactant is used for other reasons as it could be the improvement of mixture workability. Moreover, in the list of materials (A, B, C, D, E, F and G) there is no specification about the presence of already aged material. The information required be the standard is incomplete. In fact, if it only gives general information, or there is unknown data, RAP addition will still be misused due to the lack of information of the material.

In Table 4-10, the last column includes the letter denomination of the materials tested in previous sections as the standard specifies. Each material has suffered both a short and a long term ageing. The influence of the manufacture procedure is key for determining how is going to age and evolve the material.

Ageing evolution

In Figure 4-28 the evolution of penetration and softening point of all mixtures is illustrated, comparing results before and after ageing. It can be seen that foaming procedures ages less the bitumen at the beginning of its service life, but at the end of life it is at the same level than HMA mixtures. Then, the effect of ageing is bigger for these warm techniques.

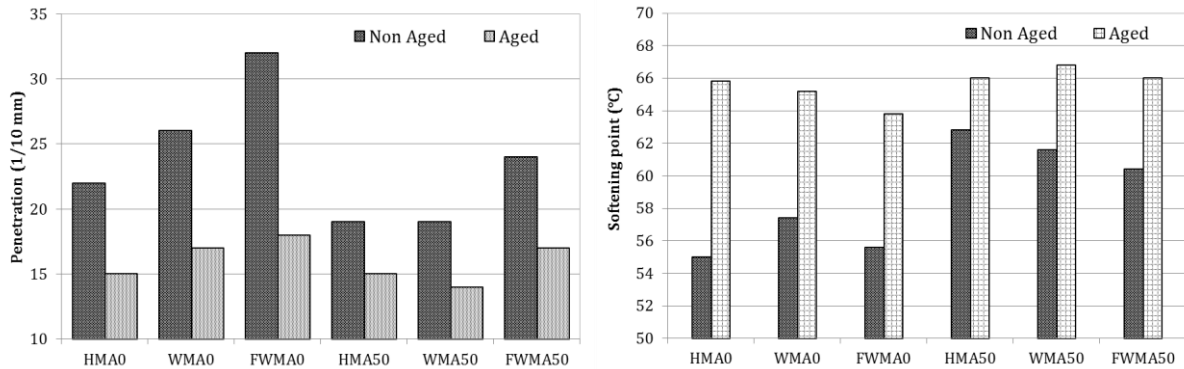


Figure 4-28 Penetration and softening point evolution of all mixtures

EN 13108-8 characterization

The information provided by the standard for RAP, penetration P_{15} and softening point S_{70} , covers all the available materials shown in Figure 4-29. Standard indicators give the possibility of easily characterize materials, but not the evolution and history followed, which also seems important. Information about the last state of a material is not enough. Not considering the evolution of the material, and the path followed to that last state may lead to overrate the quality or underestimate its possibilities.

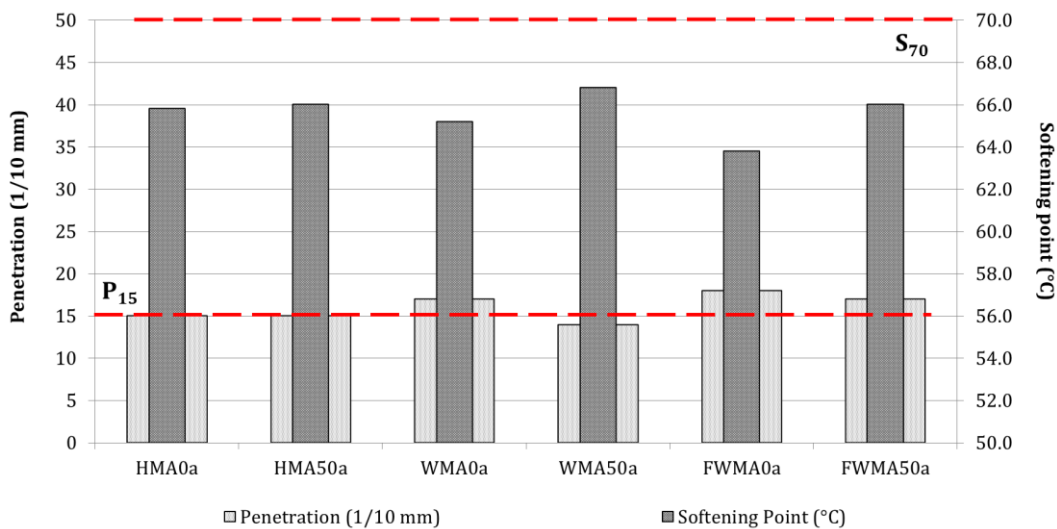


Figure 4-29 Penetration and softening point from available RAP materials

δ-method analysis

The δ -method diagrams increase the information of the material. Figure 4-30 illustrates the δ -method curves of the previous recovered aged bitumen.

Figure 4-30 (a) shows δ -curves from materials equivalent to a first ageing level, before a first recycling situation. Figure 4-30 (b) shows δ -curves from bitumen containing RAP, representing a second level of recycling situation. The comparison shows a displacement of the curves to the right (materials more aged).

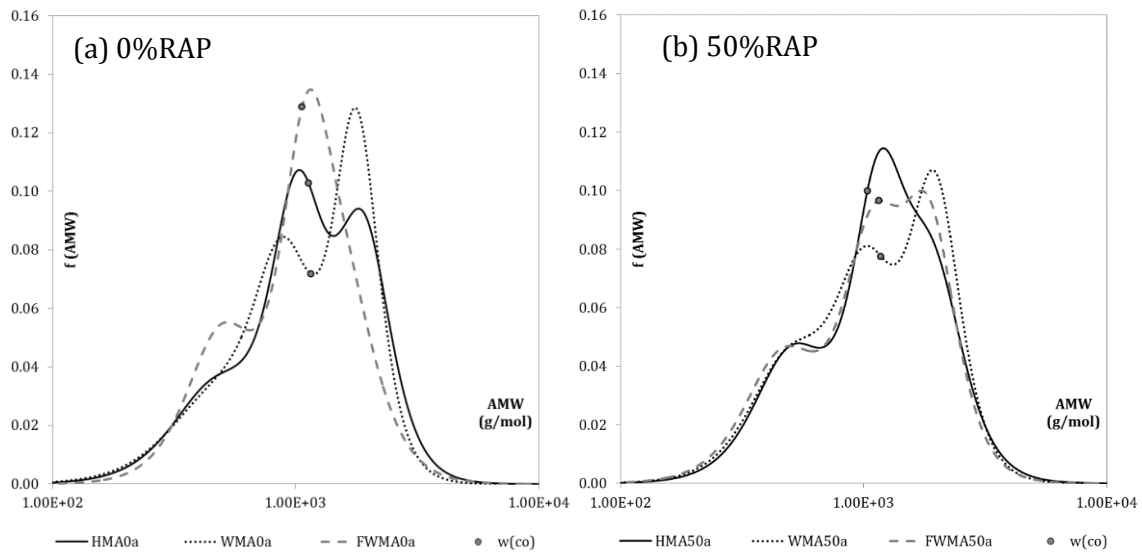


Figure 4-30 δ -method diagrams for aged mixtures with 0% and 50% of RAP

From δ -method diagrams it could be extracted that RAP is not the same in both cases. Depending if it has RAP already added or not, then it should be a characteristic to consider. Thus, the manufacture procedure makes the bitumen evolve in a different way. Recall: δ -curves evolution from mono-modal distribution to bi-modal or tri-modal as in Chapter 3 PAV bitumen is important (see also Annex 3 results).

R_{value} , I_{co} and $w(co)$ analysis

In terms of R_{value} , Figure 4-31 shows the evolution of this parameter versus I_{co} (a) and cross-over frequencies (b) for all recyclable materials. The analysis should be global because WMA0a and WMA50a could be considered as equal, but regarding R_{value} , I_{co} or $w(co)$ they are not. One is more aged than the other. The idea of these two graphics is that for further recycling it is important to perform a global analysis of the material and to have all available information to choose the best way of using it.

In part (a) the difference on I_{co} results are important between mixtures without RAP and with 50% of RAP. Then, in part (b) these RAP mixtures may seem closer as the scale is in log.

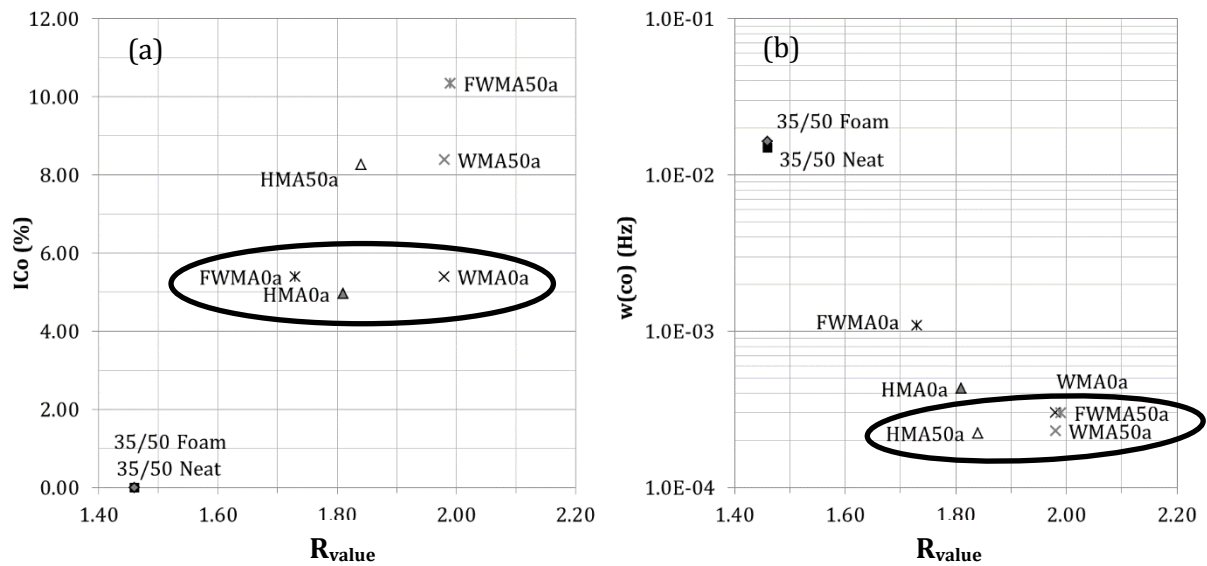


Figure 4-31 R_{value} analysis of all available aged materials

4.4 Conclusions

In this chapter, a comparison between three techniques, conventional HMA, surfactant WMA and foaming WMA is carried out. These procedures can also include the addition of 50% of RAP, in order to evaluate the influence of the use of reclaimed materials at high rates. Additionally, ageing of the mixtures is simulated using a laboratory procedure adapted from the RILEM TG5 protocol. The results obtained during the investigation led to the following conclusions:

In terms of stiffness:

- i. Temperature reduction for the manufacture of foamed warm mix asphalts may lead to a lack of stiffness after the process. This decrease, compared to the other mixtures, may be related to the reduced ageing experienced by the bitumen during the production process.

In terms of fatigue:

- ii. Concerning the fatigue related performance all procedures reach the standards limits. It is very interesting that reducing by 30°C the production of the mixture, with all the advantages associated, the performance of the mixture is over the minimum standards.
- iii. The addition of RAP increases in general the immediate performance of the mixtures, both for conventional and warm mixtures.

- iv. However, when RAP is added or after long term ageing, the fatigue slope increases and consequently, the fatigue resistance of the material tends to be more sensitive to the strain level.

In terms of bitumen performances:

- v. Regarding bitumen performance, the foaming process ages the bitumen to a lower degree during manufacture compare to the conventional procedure. When long term ageing is applied, the levels become comparable in both cases. Similarly, the hardening experienced when RAP is added is less pronounced due to the already aged bitumen present in the RAP.
- vi. The application of the δ -method reveals contrasting ageing effects for the different processes, as well as the influence of RAP addition. The general pattern observed on the curves is a decrease of the lower molecular weight fractions and an increase of the high molecular weight fractions due to ageing for the samples with or without RAP.
- vii. Compared to the FWMA technique, the HMA production process induces a significant displacement of the distribution towards higher AMW. After ageing or RAP addition the distributions tend to be similarly shifted for the all processes.
- viii. Combined with standard bitumen testing, the δ -method appears to be a powerful tool for the quantification of structural evolutions of bitumen, providing a clear visualization of the structural modifications induced. These results are likely to confirm that a structural interpretation of RAP addition and ageing evolution is possible with the δ -method.
- ix. The δ -method can also show some rejuvenation aspects, like the presence of low AMW in bitumen aged, not seen with other tests. These results can be helpful when a decision must be taken for recycling again the material.

Chapter 5. Correlation between structure and mechanical performance

Résumé du chapitre

Ce chapitre présente les résultats relatifs à l'influence du vieillissement, du taux d'agrégats d'enrobé et de la technique de fabrication sur la relation entre les enrobés et le bitume. Dans le but de contribuer à l'étude de cette relation, des corrélations ont été établies pour les fractions SARA, la teneur en asphaltènes c7, les paramètres SHRP, le R_{value} pour les bitumes, et la fatigue et les résultats des modules complexes dans les enrobés.

- Les matériaux considérés sont déjà décrits aux chapitres 3 et 4.
- Bien que tous les paramètres du modèle Huet-Such aient été étudiés et comparés avec les différentes caractéristiques du matériau, seule la viscosité β et le multiplicateur de fréquence τ (s) à 0°C sont représentés dans le chapitre. En fait, ces deux paramètres montrent la meilleure corrélation en termes de fractions SARA, de teneur en asphaltènes c7, d'indice colloïdal et de polydispersité des bitumes.
- La relation entre les paramètres du modèle de Huet-Such calculés à partir des mesures réalisées avec le rhéomètre Metravib® et à partir des mesures réalisées avec le rhéomètre Kinexus® est étudiée. Ensuite, une comparaison est faite entre les paramètres du modèle de Huet-Such des bitumes et les paramètres de la modélisation 2S2P1D des enrobés.
- Les critères SHRP d'orniérage et de fatigue sont comparés avec les paramètres standards Européens. Le paramètre SHRP d'orniérage $(G^*/\sin\delta)_{RTFOT} > 2200$ Pa est calculé sur les bitumes vieillis après RTFOT. Le paramètre de fatigue $(G^* \sin\delta)_{PAV} < 5$ MPa est mesuré sur les échantillons vieillis après PAV.

5.1 Introduction

This chapter presents findings relative to the influence of ageing, RAP content and manufacturing technique on the relationship between asphalt mixtures and bitumen. With the aim of further contributing to the study of this relationship, correlations have been established for SARA fractions, c7-asphaltenes content, SHRP parameters, R_{value} and fatigue and complex modulus results.

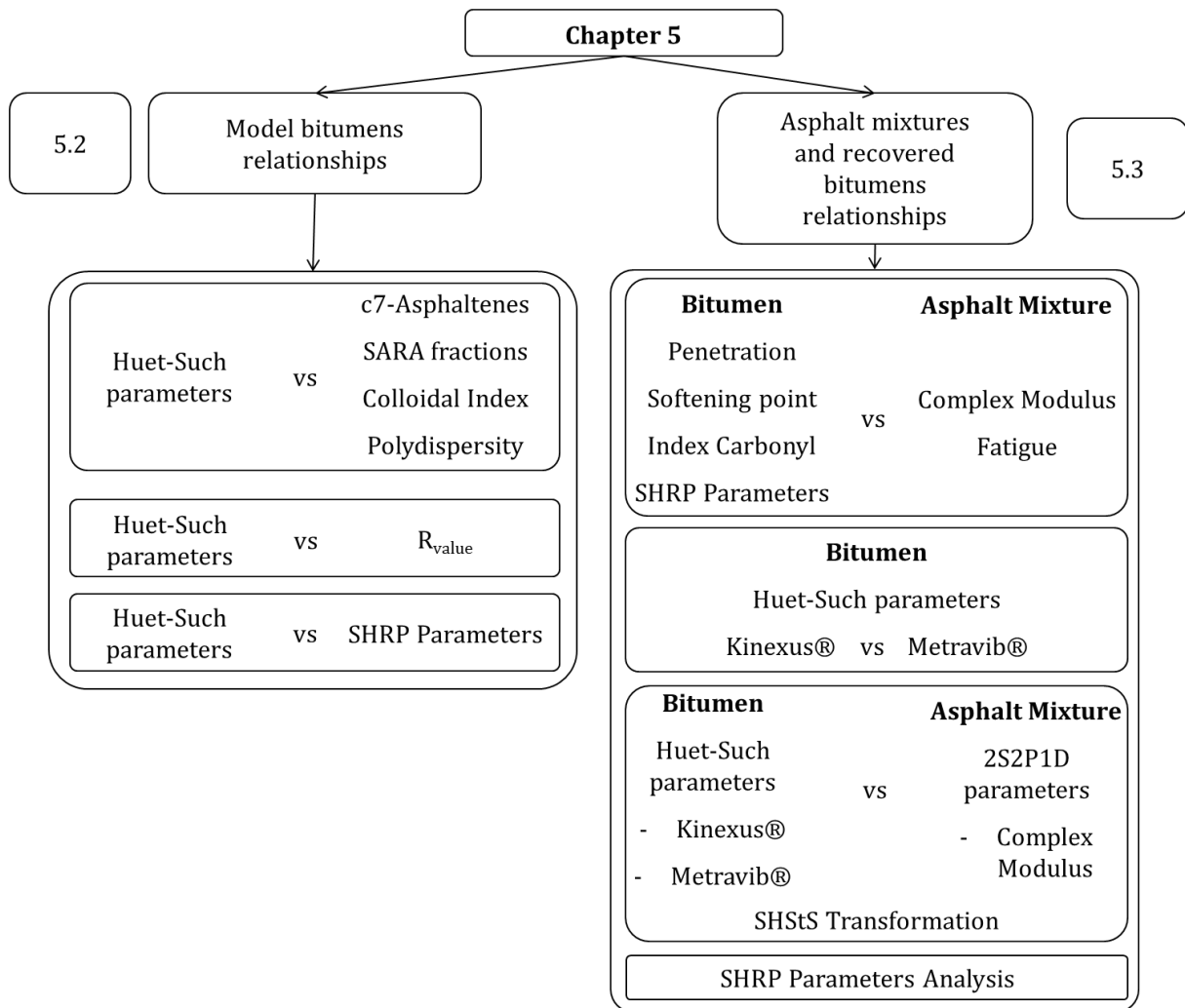


Figure 5-1 Schema of the chapter

5.2 Model bitumen correlations

5.2.1 Materials and Methods

The materials considered for analysis in this section are already described in Chapter 3. Table 5-1 summarizes bitumens and test results chosen for comparisons from Chapter 3.

Table 5-1 Materials and results selected from Chapter 3

Denomination	Data from
35/50	c7-Asphaltenes
35/50 RTFOT	TLC-FID (SARA fractions)
35/50 PAV	
35/50 100M	$I_c = \frac{i - \text{Asphaltenes} + \text{Saturates}}{\text{Aromatics} + \text{Resins}}$
35/50 90M+10A	GPC (Polydispersity)
35/50 85M+15A	
35/50 80M+20A	Huet-Such model parameters

5.2.2 Model parameters vs Bitumen chemistry

Table 5-2 summarizes the principal characteristics of Chapter 3 bitumens. On the different columns it can be found the content in % of asphaltenes c7, saturates, aromatics, resins and i-asphaltenes. Additionally, the colloidal index, polydispersity, rheological value and crossover frequency are presented.

Table 5-2 Resume of results for Chapter 3 bitumens

	Bitumen	c7-Asph (%)	Sat (%)	Arom (%)	Res (%)	i-Asph (%)	Ic	PDI	R _{value}	w(co) (Hz)
35/50 aged	Neat	14.70	2.99	66.03	12.84	18.14	0.27	1.43	1.81	2.14E-02
	RTFOT	17.80	1.94	60.84	11.46	25.77	0.38	1.40	2.06	4.03E-03
	PAV	21.40	1.29	45.12	16.69	36.91	0.62	1.34	2.45	5.85E-05
35/50 model	85M+15A	15.00	3.66	66.76	13.57	16.02	0.24	1.41	1.66	5.23E-02
	90M+10A	10.00	3.90	61.87	17.16	17.07	0.27	1.42	1.55	4.20E-01
	80M+20A	20.00	1.74	43.05	23.61	31.60	0.50	1.42	2.42	1.52E-04
	100M	0.00	3.04	73.43	17.44	6.09	0.10	1.34	1.12	5.63E+00

Parameters from Huet-Such modelling

On Chapter 3, 35/50 neat and model bitumens are submitted to DSR testing. Bitumen samples are tested from -20°C to 60°C at frequency range from 10 Hz to 0.01 Hz. Master curves for the norm of the complex modulus and phase angle are built at T = 0°C, where TTSP is verified.

Through Huet-Such modelling, experimental data from the frequency and temperature sweeps are concentrated in the 6 model parameters (G_{∞} , δ , k , h , β and τ), describing the properties of the bitumen in the whole time-temperature domain. All bitumen master curves, shift factors a_T , Black space, Cole-Cole plan and Huet-Such model curves are reported in Annexes 2 and 3.

Table 5-3 summarizes all parameters obtained from the modelling of bitumen rheological results from Chapter 3 testing. In the denomination of the samples, as a recall M means malthenes and A asphaltenes, and the number attached to them the percentage of the fraction.

Table 5-3 Chapter 3 bitumen parameters

	Bitumen	G_{∞} (MPa)	δ	k	h	β	τ (s)	C_1	C_2
35/50 aged	Neat	835.55	3.47	0.23	0.59	186.19	1.90E-02	22.52	137.35
	RTFOT	788.30	3.59	0.22	0.57	557.42	3.62E-02	25.59	168.00
	PAV	813.48	5.88	0.23	0.56	1576.50	3.05E-01	32.89	206.87
35/50 model	85M+15A	879.43	3.75	0.24	0.60	222.56	6.74E-03	23.59	151.48
	90M+10A	870.76	3.80	0.24	0.61	102.53	1.53E-03	20.47	133.32
	80M+20A	875.79	7.35	0.25	0.60	1033.60	2.65E-01	26.92	162.99
	100M	601.61	0.01	0.84	0.37	402.05	3.22E-05	18.18	122.74

Although all Huet-Such model parameters have been studied and compared with the different characteristics of the material, in this section only the viscosity β and the frequency multiplier τ (s) at 0°C are shown. In fact, these two parameters show better correlation in terms of the SARA fractions, c7-asphaltene content, the colloidal index and the bitumen polydispersity.

In Annex 7 all model parameters correlations are reported.

Saturates vs. model parameters

In Figure 5-2 (a) viscosity β and (b) τ (s) at 0°C are plotted in function of saturates content from Iatroscan. In general, saturates content evolve less than the asphaltenes, however good correlations are found.

There is good correlation for all systems, aged and model samples. On part (a) of the figure it can be observed that β increases as saturates content decreases. On part (b), τ shows good

correlation for all 35/50 bitumens (aged and model). As β , $\tau(s)$ is inversely proportional to saturates content.

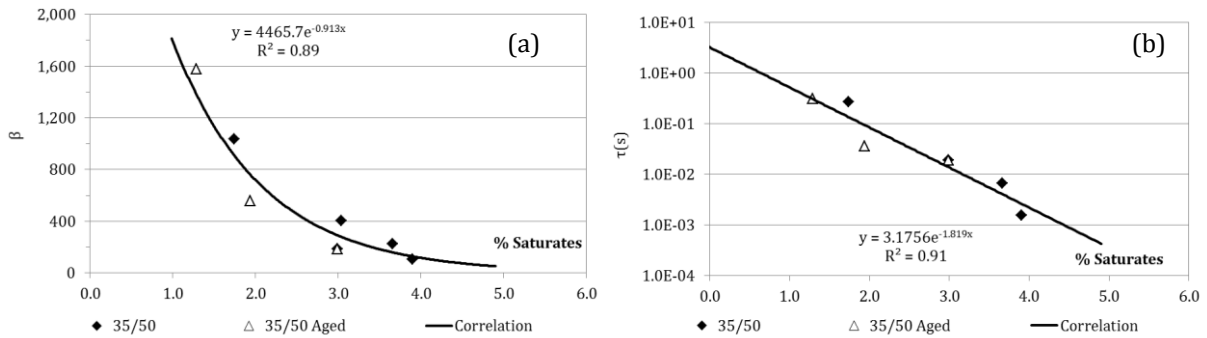


Figure 5-2 Parameters β and $\tau(s)$ represented in function of saturates

Aromatics vs. model parameters

In the cases of aromatics, in Figure 5-3 (a) viscosity β and (b) $\tau(s)$ are illustrated. This fraction is present on bitumens in a higher content, but it does not seem to correlate as good. Once more, as saturates do, the decrease in the aromatics content increase the viscosity of the system at high temperatures (a). In part (b), better correlation would be found for the laboratory aged bitumens. However, weaker relationship is found including all samples.

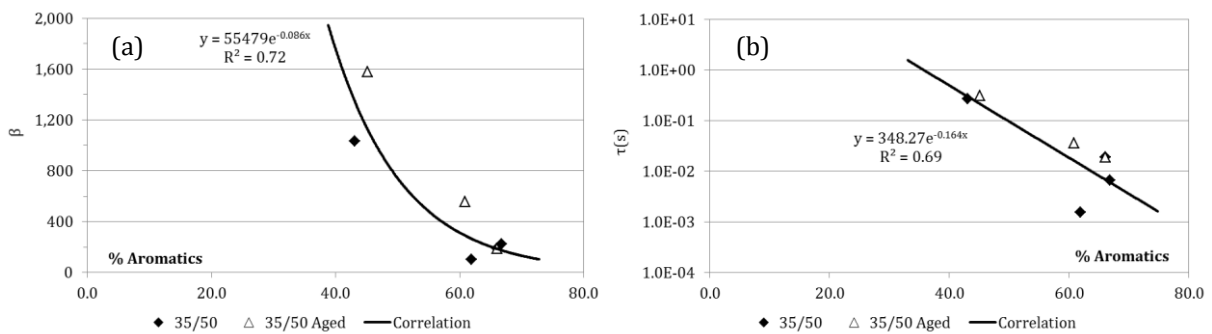


Figure 5-3 Parameters β and $\tau(s)$ represented in function of aromatics

Resins vs. model parameters

Resins content from IatrosScan does not seem to follow any good correlation with the Huet-Such model parameters. Annex 7 includes all figures that drove to this conclusion.

Asphaltenes vs. model parameters

In Figure 5-4 (a) β and (b) the frequency multiplier $\tau(s)$ at 0°C are plotted in function of c7-asphaltene content. In part (a) of the figure, the best correlation is found for an exponential fitting, with $R^2 = 96\%$ for the viscosity parameter.

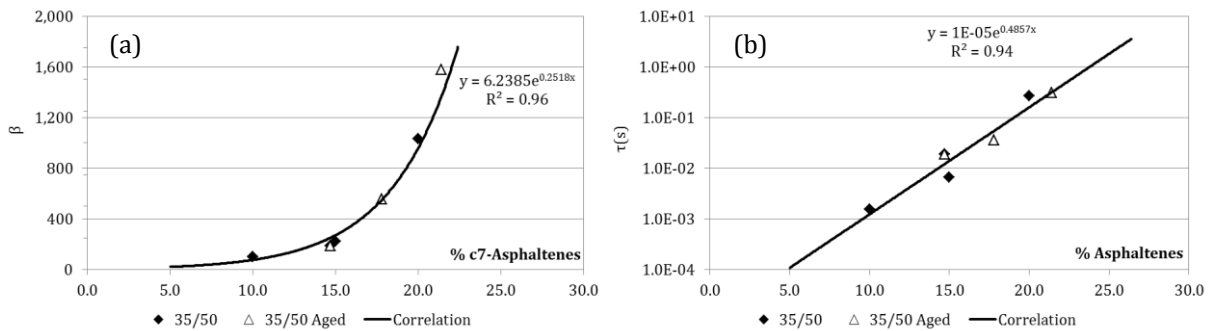


Figure 5-4 Parameters β and $\tau(s)$ represented in function of c7-asphaltene content

Moreover, 35/50 aged and model samples experience an increase of $\tau(s)$ with ageing (higher asphaltenes content $R^2 \sim 94\%$).

In Figure 5-5 (a) viscosity β and (b) $\tau(s)$ are plotted in function the asphaltene content from Iatroscan (i-asphaltenes). The trend follows the same line as c7-asphaltenes, but with lower correlation values (mainly for $\tau(s)$ with 84%)

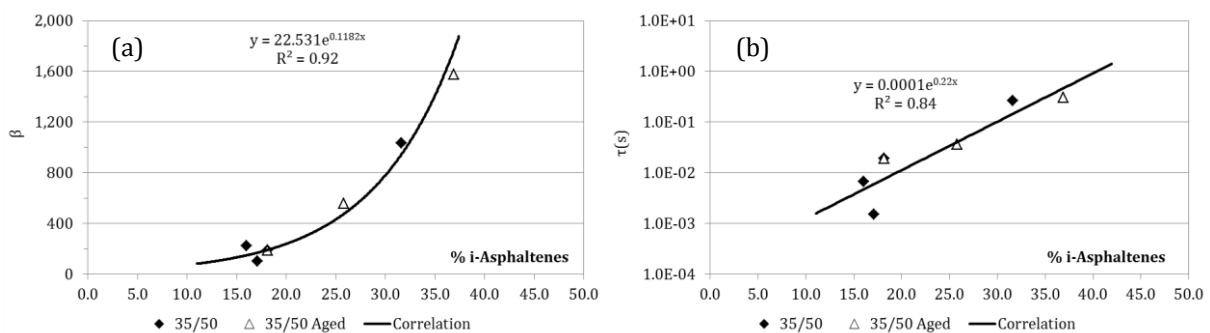


Figure 5-5 Parameters β and $\tau(s)$ represented in function of i-asphaltenes

Ageing leads to an increase in the asphaltenes content (c7 and i). As the bitumen samples age, they viscosity increases.

Colloidal Index

In Figure 5-6 (a) viscosity β and (b) $\tau(s)$ are plotted in function of the colloidal index ($Ic = \text{saturates} + \text{asphaltenes} / \text{aromatics} + \text{resins}$). As it was stated on Chapter 3, the increase of the

colloidal index is a manner of showing the ageing of the system. This is traduced with as increase of the viscosity of the samples at high temperatures or low frequencies, graph (a).

In contrast, in graph (b), weaker relationship is found between $\tau(s)$ and the colloidal index. Laboratory aged bitumens seems to show better the increase of this parameter as the material ages.

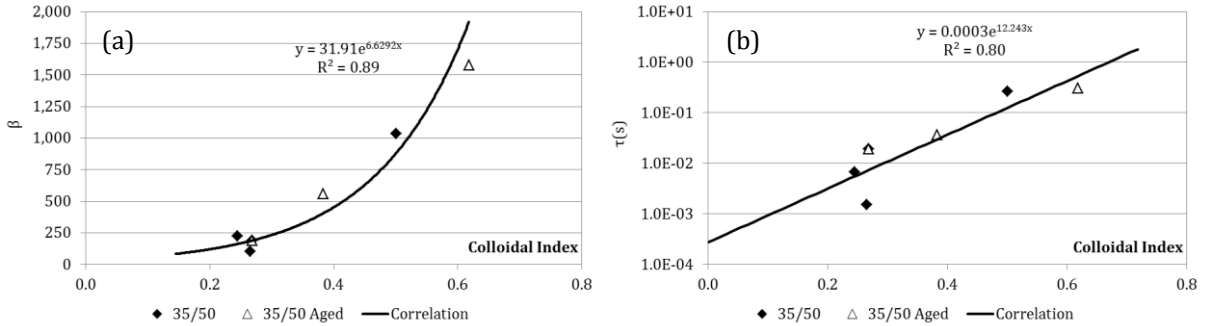


Figure 5-6 Parameters β and $\tau(s)$ represented in function of the colloidal index

Polydispersity vs model parameter

In Figure 5-7 (a) viscosity β and (b) $\tau(s)$ are plotted in function of polydispersity. Polydispersity is calculated by dividing the weight average molecular weight (Mw) by the number average of molecular weight (Mn). Correlation is done only for aged materials (dashed line) in laboratory due to the absence of relation with the model bitumens.

Contrary to what the colloidal index shows, polydispersity reflects ageing with a decrease of its value. It means that the weight average MW and the number average MW get closer, narrowing the GPC distribution. Both figures (a) and (b) follow the same line of previous descriptions. β and $\tau(s)$ increase as the PDI decreases.

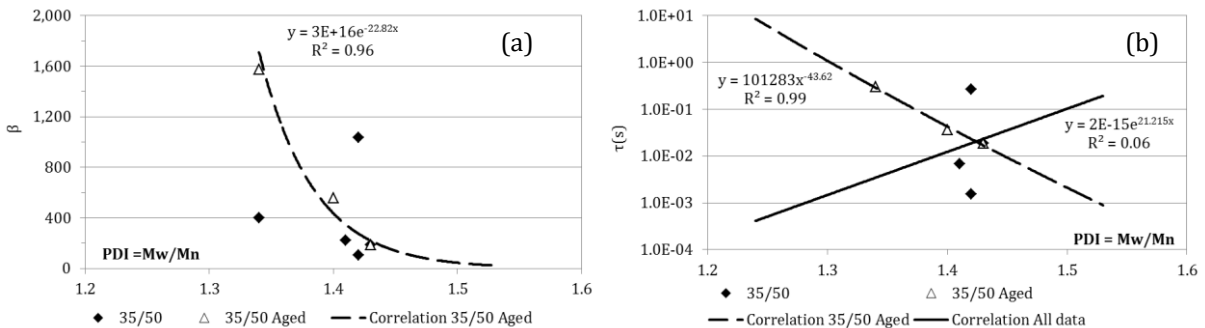


Figure 5-7 Parameters β and $\tau(s)$ represented in function of the polydispersity

5.2.3 R_{value} and w(co) influence

Moreover, on model bitumens, the changes in rheology are also discussed via the cross over frequency and the determination of the rheological value (R_{value}) [29,122] from the different previous modelled master curves. This adimensional index allows assessing the ageing evolution of the materials. The R_{value} is the distance, in the log space, between the glassy modulus |G*_∞| and the crossover frequency modulus (G'=G'', phase angle 45°). Ageing leads to widen the curve, so the distance between G*_{45°} and G*_∞ increases, and so the R_{value}. It is calculated with the following formula:

$$R_{value} = \log \frac{|G^*_{\infty}|}{|G^*_{45^\circ}|}$$

In Figure 5-8 (a) viscosity β and (b) τ(s) are plotted in function of the rheological values (R_{value}) of the systems. Both parameters increase their value, β exponentially and τ(s) potentially with the increase of Rvalue.

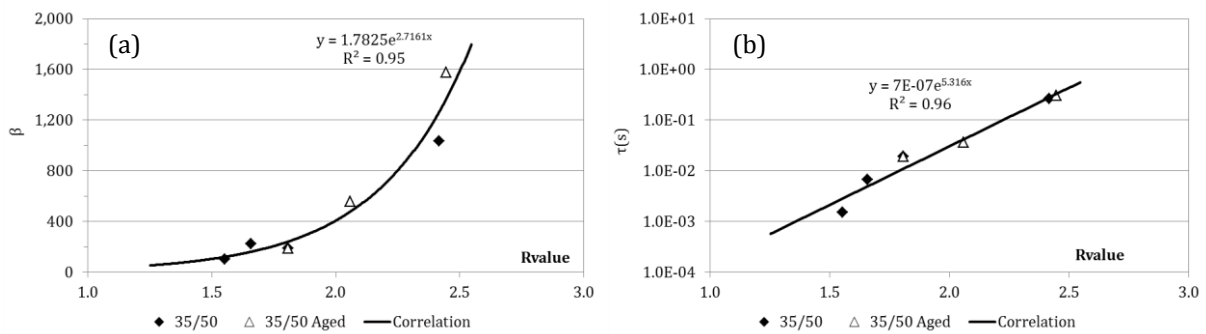


Figure 5-8 Parameters β and τ(s) represented in function of the rheological value

In Figure 5-9 (a) viscosity β and (b) τ(s) are plotted in function of the crossover frequencies. As happens with the R_{value}, crossover frequencies show good correlation with these parameters.

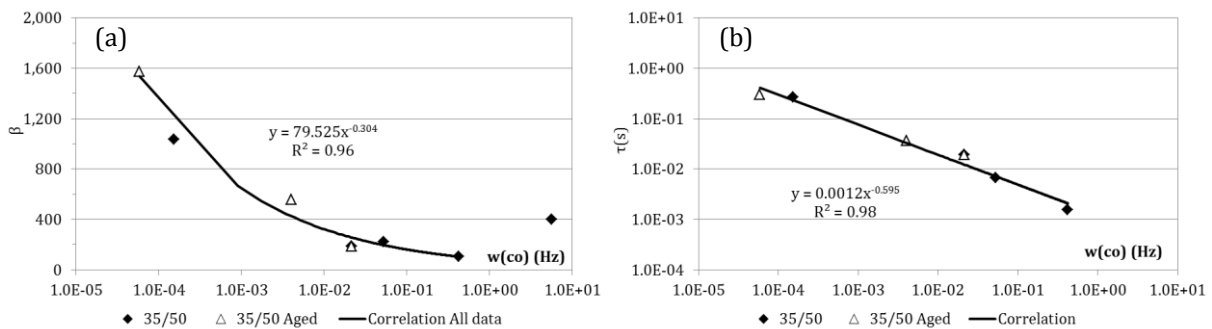


Figure 5-9 Parameters β and τ(s) represented in function of the crossover frequency

5.2.4 SHRP parameters

SHRP specifications for bitumens

Through the project A-002A [125], the Asphalt Research Program of the Strategic Highway Research Program (SHRP) has developed several bitumen tests that measure its physical properties. Rutting and fatigue parameters from complex modulus tests are the ones with the most interest for our analysis.

Rutting parameter ($G^*/\sin\delta$)

Even though global properties of asphalt mixtures govern rutting, bitumen properties cannot be neglected on this phenomenon. This is more relevant in the case of RAP addition and ageing as they increase stiffness and promote rutting resistance. In general, rutting takes place at high temperatures, so the properties related to it should be measured for the same conditions. So then, RTFOT aged bitumen are used for testing [126].

With this purpose, SHRP established a non-recoverable deformation at high temperatures as bitumen rutting parameter. Dynamic sinusoidal testing at 10 rad/s (1.59 Hz) simulates truck speeds of 80 km/h. Rutting criterion is taken as the loss compliance ($1/J''$), which is numerically equivalent to the complex modulus divided by the sinus of the phase angle ($G^*/\sin\delta$) [125]. Consequently, the SHRP specification stated that at the maximum pavement design temperature, this rutting parameter should fulfil the following requirements [125,126]:

$$(G^*/\sin\delta)_{\text{unaged bitumen}} > 1.0 \text{ kPa} \quad (G^*/\sin\delta)_{\text{RTFOT aged bitumen}} > 2.2 \text{ kPa}$$

However, this relationship has not always been verified in France with the LPC rutting tester. In contrast, it was found that $(G^*\sin\delta) > 3.8 \text{ kPa}$ leads to lower rutting rates [32].

Fatigue parameter ($G^*\sin\delta$)

Fatigue is related to the end of life of the pavement when the bitumen has experienced long term ageing (PAV bitumen). This parameter is related to the dissipated energy per load cycle at the same frequency than rutting, 10 rad/s. Fatigue parameter is calculated for the intermediate pavement design temperature by multiplying the complex modulus by the sin of the phase angle $G^*\sin\delta$ [127], and the requirements are as follows:

$$(G^*\sin\delta)_{\text{PAV}} < 5.0 \text{ MPa}$$

Critical temperature

The critical temperature (T_c) is obtained by interpolation for the rutting and fatigue parameter when:

$$G^*/\sin\delta = 2.2 \text{ kPa} \quad \text{and} \quad G^*\sin\delta = 5 \text{ MPa}$$

On Figure 5-10 the evolution of the parameters by temperature increment is illustrated on 35/50 laboratory aged bitumen. The area where fatigue or rutting parameter does not fulfil the requirements is defined in red. It can be observed how rutting resistance decreases with temperature. The concept of critical temperature can be observed in both figures.

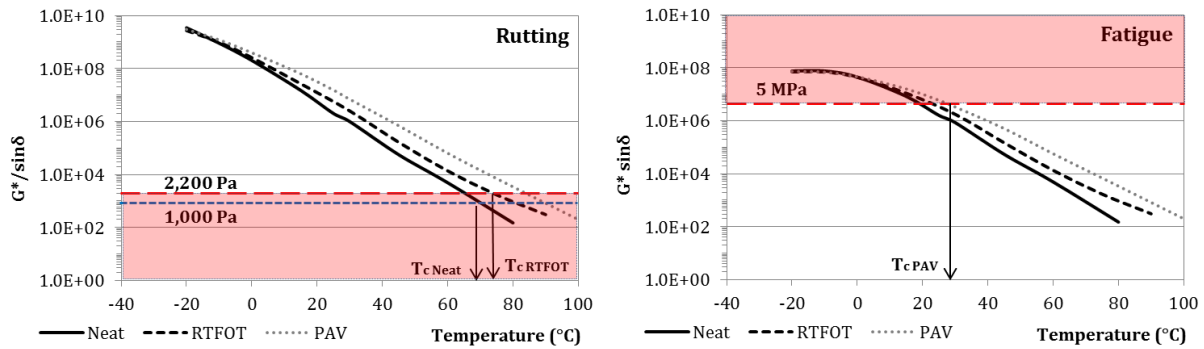


Figure 5-10 Rutting and fatigue parameters evolution with temperature

For the neat bitumen, $G^*/\sin\delta_{\text{unaged bitumen}} > 1,000 \text{ Pa}$ (blue pointed line) and $(G^*/\sin\delta)_{\text{RTFOT aged bitumen}} > 2,200 \text{ Pa}$ (red dashed line) limits are figured. On the other hand, fatigue critical temperature would be determined by PAV results. SHRP criterion is that $G^*\sin\delta < 5 \text{ MPa}$ at the average pavement temperature.

Then, Figure 5-11 illustrates the evolution of critical temperatures with the asphaltenes content for all studied bitumens. These temperatures have been calculated for the limit SHRP criteria. It can be observed that asphaltenes content decrease leads to a decrease of the critical temperatures for both parameters.

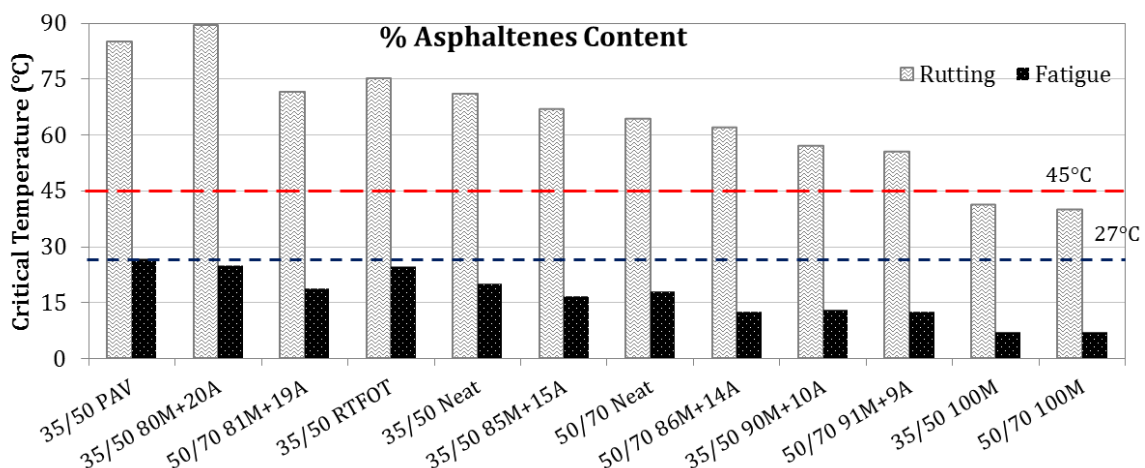


Figure 5-11 Critical temperatures for rutting and fatigue parameters

As an example, if 45°C is considered as test temperature (T_t), it can be observed that all materials would fulfil the rutting requirements but 35/50 100 M and 50/70 100M (malthenes

fraction). Bitumens with asphaltene content at least equal to 9% would have less chances to experience rutting. However, if test temperature is higher than the critical ($T_t > T_c$), rutting would be a problem to consider. In the case of fatigue requirements, the limit would be established by long term ageing testing (35/50 PAV) with a result of 27°C as minimum service temperature of the pavement to suffer fatigue cracking.

5.3 Correlation between bitumen and asphalt mixture

5.3.1 Materials and Methods

The materials considered for analysis in this section are already described in Chapter 4.

Table 5-4 summarizes the materials selected and the tests taken into account.

Table 5-4 Materials selected from Chapter 3 for further analysis

Denomination b for bitumen	Denomination m for mixture	Data from
HMA0 _b	HMA0 _m	Bitumens Penetration, softening point and Ico Complex Modulus $ E^*_{\text{bitumen}} $ (Kinexus® and Metravib®)
HMA0a _b	HMA0a _m	
HMA50 _b	HMA50 _m	
HMA50a _b	HMA50a _m	
WMA0 _b	WMA0 _m	
WMA0a _b	WMA0a _m	
WMA50 _b	WMA50 _m	Huet-Such modelling parameters
WMA50a _b	WMA50a _m	Mixtures 2PB Fatigue (ϵ_6) 2PB Complex Modulus $ E^*_{\text{mixture}} $
FWMA0 _b	FWMA0 _m	
FWMA0a _b	FWMA0a _m	
FWMA50 _b	FWMA50 _m	
FWMA50a _b	FWMA50a _m	

5.3.2 Bitumen/Mixture properties relationship

This part of the Chapter is conducted with all data available from mixtures and their extracted bitumens. The comparisons is done considering, when possible, the three techniques together HMA, WMA and WMA. Table 5-5 summarizes the principal results obtained for asphalt mixtures and extracted bitumens.

*Asphalt mixtures and recovered bitumens principal results***Table 5-5 Principal results from asphalt mixtures and extracted bitumens testing**

Parameter	E*	Phase Angle (°)	ϵ_{6c} (μdef)	Slope (-1/b)	Pen (1/10 mm)	Soft Point (°C)	ICo (%)	R value	w(co) (Hz)	T _c Rutting (°C)	T _c Fatigue (°C)	G* Sin (δ)	G*/Sin (δ)
	15°C, 10Hz (MPa)											30°C, 10rad/s	30°C, 10rad/s
35/50 Neat	-	-	-	-	37	53.8	0	1.46	1.49E-02	72.1	21.2	1.10E+06	1.28E+06
35/50 RAP	-	-	-	-	18	63.0	8.6	1.80	1.34E-03	85.2	26.8	9.40E+05	1.07E+06
35/50 Foam	-	-	-	-	34	53.6	0	1.46	1.63E-02	67.8	19.2	2.55E+06	3.97E+06
HMA0	12,497	15.0	115	5.99	22	55.0	1.8	1.77	4.71E-04	77.6	27.7	3.40E+06	5.39E+06
HMA0a	14,156	10.8	123	8.35	15	65.8	4.96	1.81	4.31E-04	80.7	28.0	3.64E+06	6.16E+06
HMA50	14,590	12.2	127	7.08	19	62.8	4.08	1.71	1.46E-03	78.1	26.8	2.62E+06	3.99E+06
HMA50a	15,847	11.3	122	6.99	15	66.0	8.27	1.84	2.24E-04	83.5	27.3	3.34E+06	5.75E+06
WMA0	12,445	14.6	100	5.69	26	57.4	1.46	1.73	8.81E-04	77.8	26.1	2.64E+06	4.01E+06
WMA0a	15,343	10.7	123	7.68	17	65.2	5.4	1.98	3.01E-04	83.0	26.6	3.09E+06	5.40E+06
WMA50	13,688	12.7	119	5.55	19	61.6	3.74	1.74	1.65E-03	77.3	26.1	2.49E+06	3.67E+06
WMA50a	15,851	11.0	108	16.70	14	66.8	8.39	1.98	2.30E-04	84.1	27.7	3.41E+06	5.96E+06
FWMA0	10,921	16.1	98	4.82	32	55.6	0.48	1.64	4.67E-03	68.0	20.7	1.33E+06	1.71E+06
FWMA0a	14,448	12.2	113	7.64	18	63.8	5.4	1.73	1.09E-03	80.7	26.2	2.85E+06	4.97E+06
FWMA50	13,122	14.0	106	5.12	24	60.4	5.47	1.68	3.27E-03	73.4	24.1	1.92E+06	2.66E+06
FWMA50a	15,460	11.5	115	5.49	17	66.0	10.35	1.99	3.01E-04	81.0	24.2	2.79E+06	4.90E+06

Influence of bitumen penetration and softening point on complex modulus

Figure 5-12 presents the evolution of complex modulus on the mixtures by penetration and softening point of bitumens. As expected, in both cases the increase of hardening is represented by an increase of the complex modulus at 15°C 10 Hz. Thus, a good correlation is found in (a) with a potential law, and in (b) with a linear law.

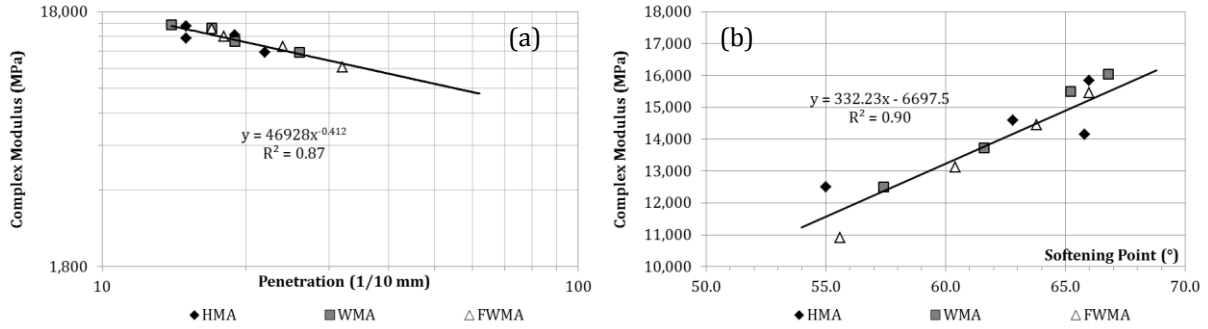


Figure 5-12 Influence of bitumen penetration and softening point on |E*| at 15°C 10 Hz

Influence of bitumen penetration and softening point on fatigue life

Figure 5-13 shows the evolution of the parameter ϵ_6 on the mixtures by penetration (a) and softening point (b) of bitumens. In general the correlation is weak. No correlation at all is found between bitumen and mixtures for the WMA procedure, while the HMA technique is proven weak. However, for the FWMA procedure (triangles with white background) the correlation is perfect. This correlation is shown by a dashed grey line.

It is observed in Chapter 4 analysis that the foaming process shows reduced initial ageing but greater gradient after mixing. Then, the observed trend is an increase of the fatigue life, in terms of ϵ_6 (micro deformation for 10^6 cycles), with the hardening of the bitumen.

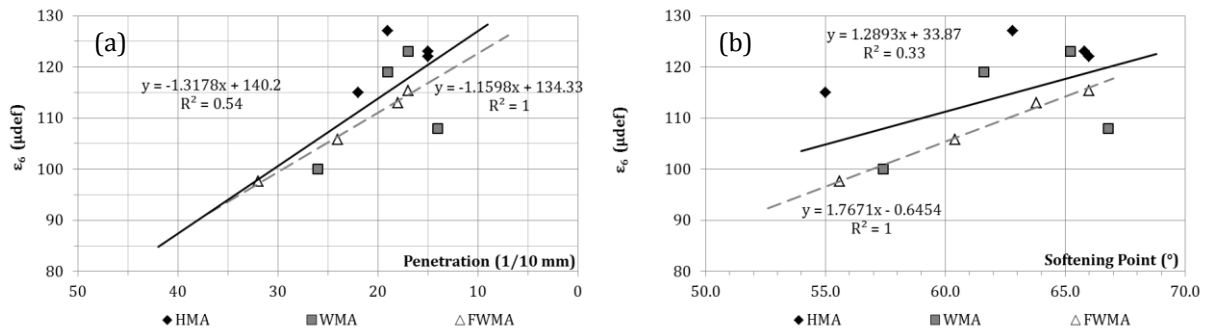


Figure 5-13 Influence of bitumen penetration and softening point on ϵ_6

Influence of index carbonyl on fatigue life and complex modulus

On Figure 5-14 results of ε_6 and $|E^*|$ 15°C 10 Hz are plotted against the carbonyl index of their respective bitumen. The parameter ε_6 (Figure a) shows no or weak correlation at all for the WMA and HMA procedures. Once more, it becomes more dependent for the FWMA procedure. This leads to the same analysis as in Chapter 4, where FWMA mixtures ages so little during manufacture that they need to achieve certain grade of ageing for a good performance.

In the cases of part (b), the correlation for the norm of the complex modulus is obtained with a logarithmic function of the carbonyl index. It is in this graphic all procedures show good independent correlation with I_{co} .

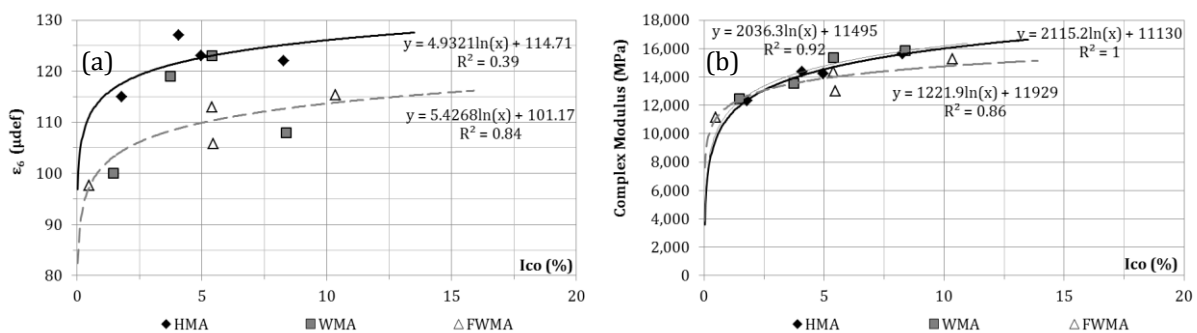


Figure 5-14 Influence of bitumen index carbonyl on (a) ε_6 and (b) $|E^*|$ at 15°C 10 Hz

5.3.3 Huet-Such parameters relation

Complex modulus on bitumen samples with Kinexus®

On Chapter 4, bitumens extracted from asphalt mixture manufacture and original bitumens are submitted to dynamic shear rheometer testing on a Kinexus® device for obtaining their rheological behaviour. Then, throughout Huet-Such modelling, the information of the frequency and temperature sweeps is concentrated in the 6 model parameters (G_∞ , δ , k , h , β and τ), describing the properties of the bitumen in the whole time-temperature domain. The parameters are determined for a reference temperature $T_{ref} = 0^\circ\text{C}$.

Complex modulus on bitumen samples with Metravib®

Metravib® device allows obtaining complex modulus of bitumens through tension-compression testing. Cylindrical samples of 20 mm long and 10 mm diameter of bitumen are submitted to sinusoidal displacements in strain control mode. Tests are carried out from 1 to 80 Hz in the range of temperatures from -20°C to 20°C . Figure 5-2 shows the device and a representation of the testing geometries.

On the same device, the complex shear modulus (G^*) is obtained by annular shearing on the same frequency range and from 20°C to 60°C. The geometry has an inner diameter of 8 mm, and outer diameter of 10 mm and height of 20 mm. The conversion from $|G^*|$ to $|E^*|$ is made assuming a Poisson's ratio of 0.5 [17].

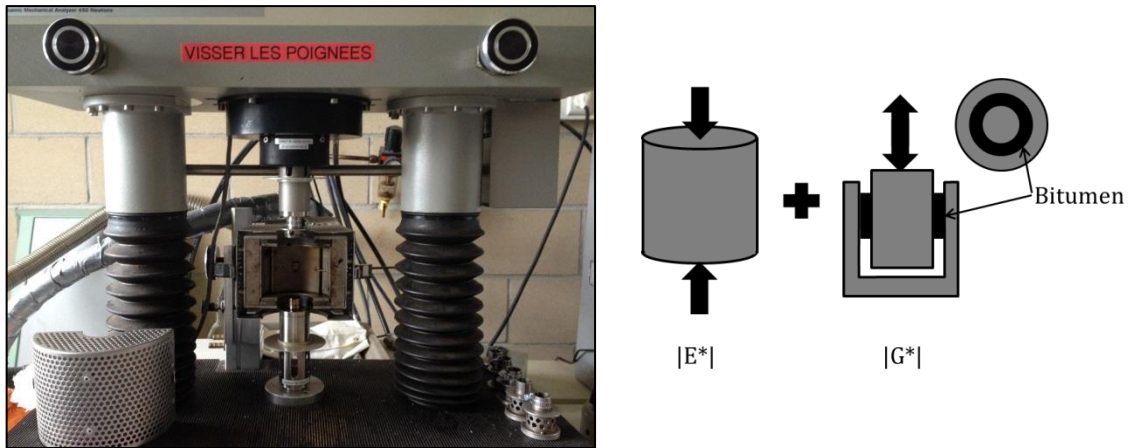


Figure 5-15 Metravib® device and complex modulus testing description

Table 5-6 summarizes all model parameters obtained for extracted bitumen tested with Kinexus® device.

Table 5-7 summarizes all model parameters obtained for extracted bitumen tested with Metravib® testing device. For the combination of traction-compression testing at low temperatures and annular testing at high temperatures it is considered a Poisson's coefficient of $\nu = 0.5$ [17], so $|G^*| = |E^*| / 3$.

Recall of denomination: HMA (conventional procedure), WMA (surfactant included in the bitumen) and FWMA (foamed bitumen) are the three manufacture procedures. Then 50 or 0 is the percentage of RAP added into the mix. And finally "a" which notes if the mixtures has been submitted to ageing.

In Annex 5 and 6 bitumens master curves at $T=0^\circ\text{C}$, shift factors a_T , Black space, Cole-Cole plan and Huet-Such model curves are reported.

Table 5-6 Extracted bitumens parameters from Kinexus® testing

Bitumen	G_{∞} (MPa)	δ	k	h	β	τ (s)	C_1	C_2
35/50 Neat	630.49	4.13	0.26	0.66	37.88	1.54E-01	20.75	124.59
35/50 Foam	568.66	3.63	0.24	0.63	46.18	1.07E-01	20.90	123.74
35/50 RAP	706.85	3.75	0.23	0.59	368.07	1.75E-01	23.37	143.46
HMA0	660.18	5.54	0.25	0.65	212.60	1.25E+00	26.08	151.61
HMA0a	646.73	5.34	0.24	0.62	172.83	9.35E-01	23.68	139.02
HMA50	691.68	4.70	0.26	0.64	162.72	4.59E-01	23.44	140.83
HMA50a	636.38	6.98	0.28	0.66	79.15	2.90E+00	23.59	137.38
WMA0	542.58	4.82	0.22	0.61	112.58	5.13E-01	21.21	122.33
WMA0a	620.03	3.71	0.22	0.56	526.09	2.33E-01	26.74	166.50
WMA50	606.81	5.39	0.26	0.64	119.03	4.08E-01	27.43	174.71
WMA50a	598.39	5.01	0.27	0.60	349.63	6.51E-01	31.55	200.97
FWMA0	523.11	5.11	0.28	0.66	49.68	2.87E-01	20.89	123.09
FWMA0a	522.10	7.08	0.30	0.69	30.43	1.37E+00	20.02	122.39
FWMA50	611.04	4.82	0.28	0.65	92.44	2.99E-01	24.97	157.34
FWMA50a	600.22	6.82	0.27	0.63	158.23	8.15E-01	21.39	122.94
Mean	611.02	5.12	0.26	0.63	167.84	7.00E-01	23.73	143.39
Standard Dev	55.35	1.13	0.02	0.03	143.22	7.20E-01	3.18	23.31

Table 5-7 Extracted bitumens parameters from Metravib® testing

Bitumen	G_{∞} (MPa)	δ	k	h	β	τ (s)	C_1	C_2
35/50 Neat	669.28	5.75	0.26	0.71	31.07	1.92E+00	23.12	120.87
35/50 Foam	617.79	6.26	0.32	0.74	11.70	5.60E-01	18.94	107.97
35/50 RAP	748.41	6.20	0.29	0.66	91.82	1.00E+00	19.97	115.17
HMA0	690.57	7.92	0.28	0.69	46.22	3.31E+00	22.46	128.31
HMA0a	672.13	6.35	0.26	0.63	126.76	2.01E+00	23.52	133.13
HMA50	745.18	6.74	0.28	0.67	65.97	1.26E+00	21.45	125.40
HMA50a	650.15	4.37	0.24	0.59	637.31	3.94E-01	27.03	169.13
WMA0	709.80	7.62	0.27	0.67	34.55	3.14E+00	18.08	91.49
WMA0a	766.41	13.74	0.30	0.76	19.18	1.87E+00	19.96	131.21
WMA50	725.83	5.58	0.27	0.65	78.95	6.87E-01	21.69	126.17
WMA50a	751.62	7.11	0.27	0.65	105.32	1.88E+00	21.71	125.21
FWMA0	672.91	6.58	0.30	0.70	32.05	4.42E-01	21.86	135.07
FWMA0a	769.89	4.64	0.25	0.58	361.18	3.62E-01	25.52	150.81
FWMA50	704.27	6.44	0.30	0.69	50.26	6.83E-01	20.50	120.89
FWMA50a	671.07	7.95	0.28	0.68	86.54	1.65E+00	21.91	129.98
Mean	704.35	6.88	0.28	0.67	118.59	1.41E+00	21.85	127.39
Standard Dev	45.88	2.16	0.02	0.05	166.41	9.50E-01	2.34	17.56

In Figure 5-16 the relationship between parameters is developed. In the ordinate axis it is shown the parameter from Huet Such modelling. Then, in the abscise axis the parameter from 2S2P1D modelling results on the asphalt mixtures.

G_{∞} parameter

The glassy modulus G_{∞} represents the value of G^* at infinite frequency. This parameter remains seems to be higher for the Metravib® modelling. It seems as traction-compression testing obtains higher values of complex modulus than shear testing. There is a difference between means around 100 MPa.

δ parameter

The δ parameter represents the balance between the two parabolic elements k and h at medium temperatures or frequencies. In both models this parameter tends to be similar.

k parameter

The k parameter, first parabolic element, is proportional to the slope of the model in the Cole-Cole plan at low temperature and/or high frequency (proportional to the ratio $\Delta E''/\Delta E'$). This parameter is higher in the case of Metravib® modelling. However, the means are not very different (0.26 for Kinexus® and 0.28 for Metravib®).

h parameter

The h parameter of the second parabolic element is proportional to the slope of the model in the Cole-Cole plan at high temperature and/or low frequency (proportional to the ratio $\Delta E''/\Delta E'$). This parameter seems to be linked to β , as they tend to find the equilibrium between them. In the Figure-16 the samples that are farther from the unity are highlighted.

β parameter

The dashpot parameter β represents the viscosity of the model at very high temperatures or very low frequencies. β is found smaller for Kinexus. As it is said for h parameter, samples farther from the unity are highlighted. All come from aged bitumens. And they have an inverse tendency, when h increases, β decreases to give equilibrium to the model.

τ parameter

Finally, the frequency multiplier τ at 0°C seems to increase between devices. In general, the disposition of this parameter is to change with ageing phases, being the main parameter on affecting the value of $|G^*|$.

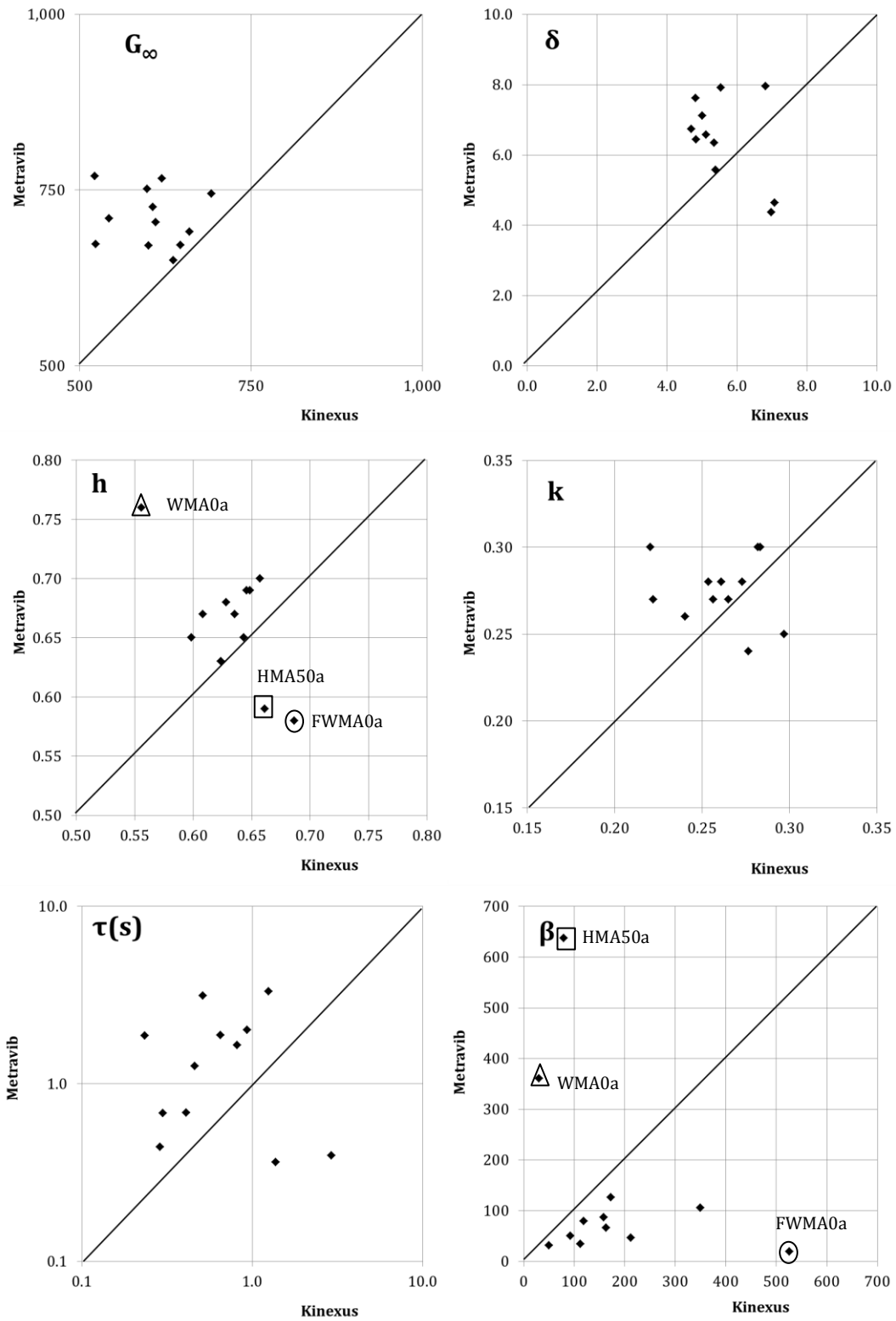


Figure 5-16 Relationship between Kinexus® and Metravib® Huet-Such parameters

No obvious correlation is found between the parameters determined from the two sets of data. The parameters determination seems very sensitive to the test device and test conditions. Additionally, differences can also be attributed to modelling and fitting process as compensation are noted between h and b parameters.

5.3.4 Parameters from Huet-Such versus 2S2P1D

2S2P1D model

According to literature review, 2S2P1D model is the best suited rheological model for asphalt mixture. This model is a combination of two springs, two parabolic creep elements and one dashpot with a coefficient that regulates the balance between the two parabolic elements. Figure 5-17 illustrates the model Cole-Cole representation and its formula.

The 7 model parameters are determined by fitting the experimental complex modulus data $|E^*|$ and δ (phase angle) measured at different frequencies and temperatures. The τ parameter is determined for a reference temperature $T_{ref} = 0^\circ\text{C}$. The software Viscoanalyse is used for fitting the parameters.

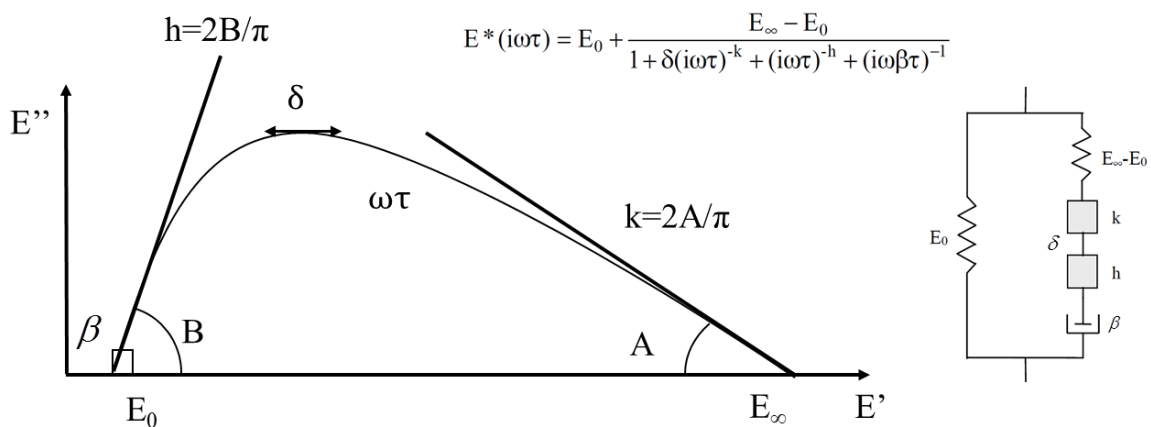


Figure 5-17 2P2S1D model, equation and Cole-Cole representation, from Olard 2003 [22,24]

In Chapter 4, complex modulus testing on asphalt mixtures samples with two points bending configuration allowed obtaining their rheological performance. Then, through 2S2P1D modelling, the information of the frequency and temperature sweeps is concentrated in the 7 model parameters (E_0 , E_∞ , δ , k , h , β and τ), describing the properties of the mixture in the whole time-temperature domain. The parameters are determined for a reference temperature $T_{ref} = 0^\circ\text{C}$.

As an example of the obtained data, isothermal curves of the norm of complex modulus and phase angle of HMA0 mixture, with their respective master curve are shown in Figure 5-18. Experimental data from all mixtures, WLF fitting, shift factors a_T , Black and Cole-Cole curves, and 2S2P1D model curves are reported in Annex 6.

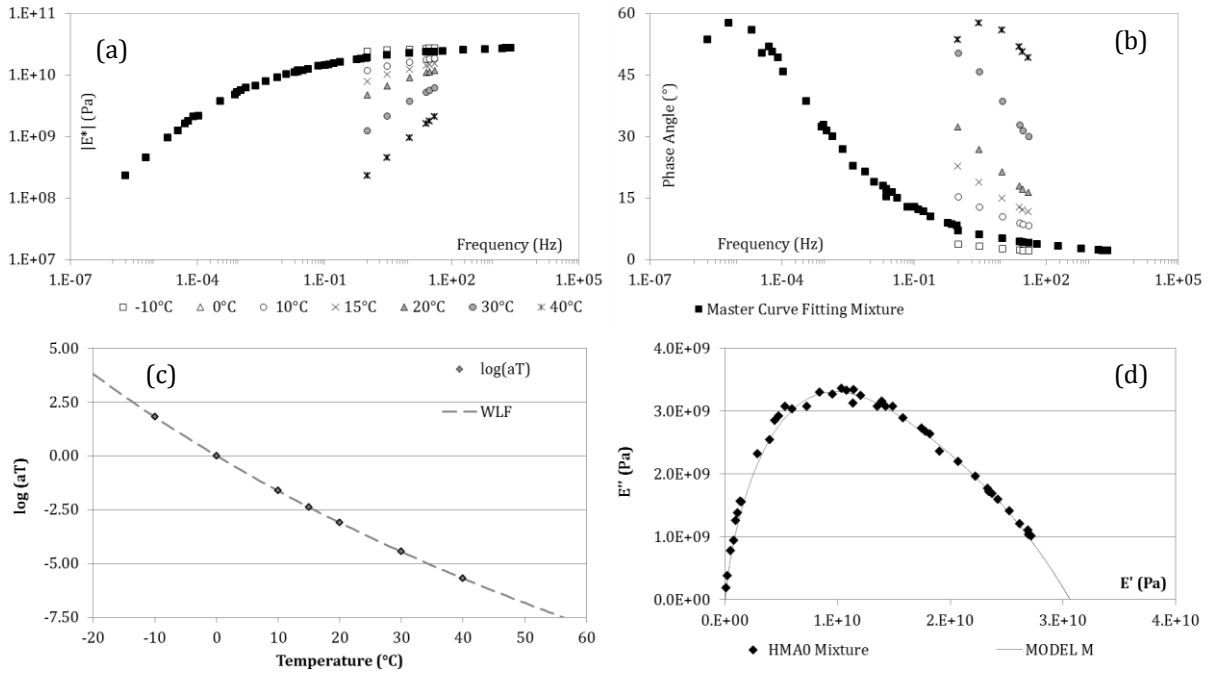


Figure 5-18 2PB complex modulus test results on HMA0 mixture (a) $|E^*|$ (MPa), (b) δ (°), (c) WLF shift factors, and (d) Cole-Cole 2S2P1D model fitting

SHStS transformation

Based on mechanical testing different approaches can be followed in order to establish a relationship between bitumen and mixture properties [24,31,128–135]. In this chapter, bitumen and mixture performances correlation is developed through the Shift-Homothety-Shift in time-Shift transformation (SHStS) [24,135]. This transformation is illustrated in Figure 5-18 as a Cole-Cole diagram.

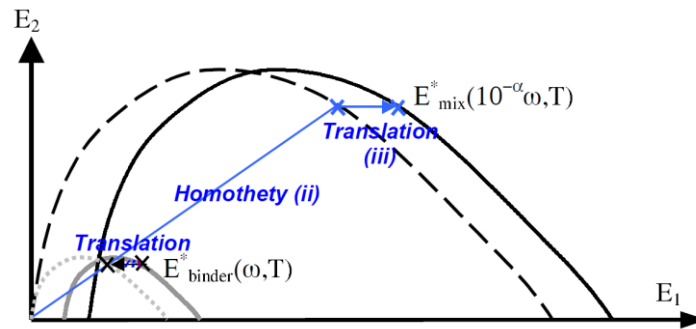


Figure 5-19 Shift-Homothety-Shift in time-Shift transformation (SHStS) [135]

This transformation is based on a rheological approach, allowing the prediction of mixtures complex modulus from linear viscoelastic behaviour of the bitumen. Thus, it takes into account the aggregate gradation of the mixture. In order to compare bitumen and mixture complex modulus, it is convenient to normalize them.

$$E_{norm}^* = \frac{E^* - E_0}{E_\infty - E_0}$$

E_{∞} and E_0 are the maximum (glassy modulus) and the minimum values of the complex modulus are obtained from the Huet-Such (for the bitumens) and 2S2P1D (for the mixtures) shown on previous Tables. Mixtures and recovered bitumens rheological performance, through the Cole-Cole plan (E' , E''), can be compared.

Figure 5-20 represent the normalized Cole-Cole curves obtained for the (a) HMA0, (b) HMA0a, (c) HMA50 and (d) HMA50a mixtures and their respective bitumens. It serves as an example of the trend followed by the other procedures. Complex modulus measurements on bitumens were performed both on Metravib® and Kinexus® devices. As it is hard to define which apparatus is the most appropriate to characterize the rheological behaviour of bitumen, it was decided to present both results. 2PB complex modulus values are obtained for the respective asphalt mixtures. All individual results and transformations are reported in Annex 9.

In general, transformation curves show a difference (a) and slightly difference (b-c-d) between bitumens and mixtures. Thus, this difference reflects the asphalt mixture results of complex modulus as more viscous than the bitumen. At medium-high temperatures, the increase of E'' is greater for all mixtures than for the bitumen results.

As a result, experimental calculations of mixtures complex modulus from bitumens measurements would not be very accurate. These differences may not be extensible to all type of mixtures. However, caution should be taken due to the presence of RAP, the warm mix procedures or the different ageing states considered

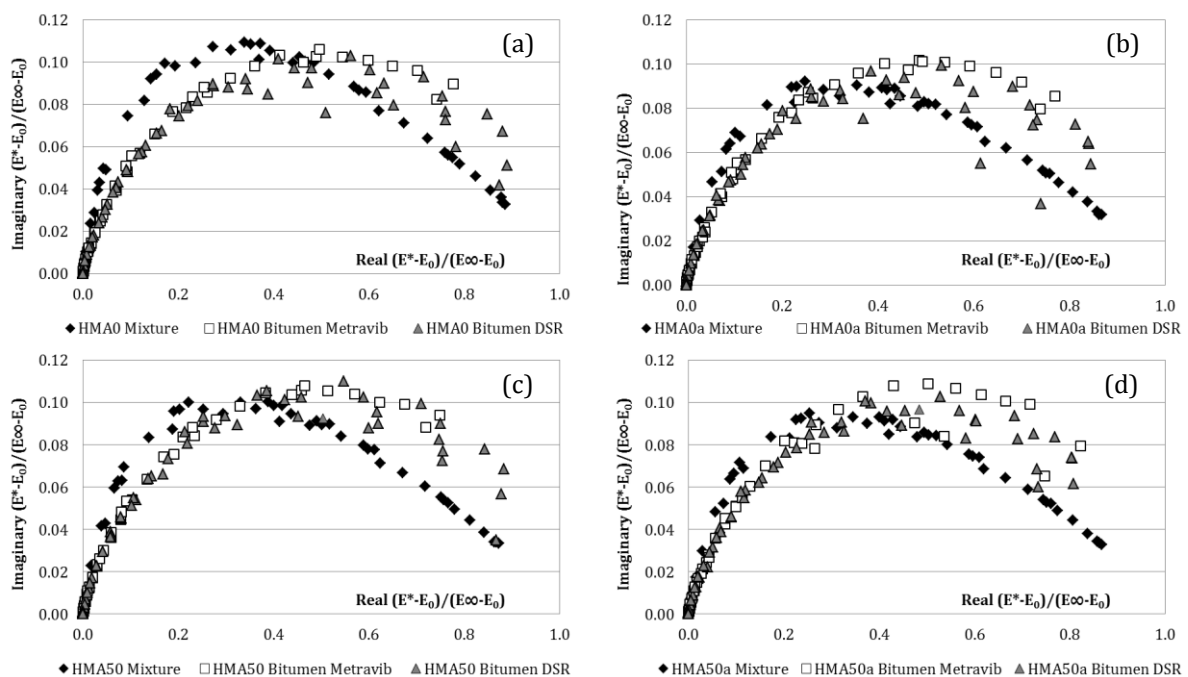


Figure 5-20 SHStS transformation on HMA asphalt mixtures and recovered bitumens

Relationship between Huet-Such and 2S2P1D parameters

Table 5-8 summarizes all parameters obtained from the 2S2P1D modelling of asphalt mixtures dynamic complex modulus results from Chapter 4 and the coefficients C_1 and C_2 when constructing the master curves.

Table 5-8 Asphalt mixtures parameters from complex modulus 2S2P1D modelling

Bitumen	E_0 (MPa)	E_∞ (MPa)	δ	k	h	β	τ (s)	C_1	C_2
HMA0	67.73	30,626	1.68	0.19	0.56	26.40	3.01E+01	34.30	200.90
HMA0a	40.28	31,010	2.02	0.17	0.54	64.08	1.79E+02	34.53	196.87
HMA50	74.34	32,584	1.79	0.18	0.54	36.23	6.43E+01	33.89	202.76
HMA50a	77.77	34,874	2.00	0.18	0.54	47.58	1.22E+02	32.56	192.54
WMA0	67.31	29,653	1.52	0.18	0.55	26.31	2.97E+01	33.25	193.39
WMA0a	74.72	33,740	1.99	0.17	0.54	47.06	1.84E+02	35.26	200.53
WMA50	77.59	31,154	1.84	0.18	0.56	26.91	5.51E+01	33.10	200.60
WMA50a	56.05	34,903	2.03	0.18	0.55	53.52	1.43E+02	30.72	179.00
FWMA0	43.16	27,155	1.80	0.21	0.61	25.57	2.32E+01	35.15	213.36
FWMA0a	85.82	33,111	1.86	0.18	0.53	41.07	8.97E+01	31.61	177.95
FWMA50	60.36	30,823	1.96	0.20	0.59	24.94	4.34E+01	32.43	196.21
FWMA50a	84.65	34,087	1.98	0.18	0.55	41.77	1.09E+02	30.28	176.96
Mean	67.48	31,977	1.87	0.18	0.55	38.45	8.94E+01	33.09	194.26
Standard Dev	14.93	2,327	0.16	0.01	0.02	12.93	5.78E+01	1.64	11.17

In Figure 5-21 the relationship between parameters is developed. In the ordinate axis it is shown the parameter from Huet Such modelling (Metravib® and Kinexus®). Then, in the abscise axis the parameter from 2S2P1D modelling results on the asphalt mixtures.

From the 7 parameters of 2S2P1D modelling, only 5 can be compared with Huet Such parameters, they are δ , k , h , β and τ (s). Those are the parameters presented in both models. E_0 and E_∞ are not taken into account (Results can be seen in Annex 7) due to the absence of elastic modulus on bitumen ($E_0=0$) and the big difference on the glassy modulus. Moreover, α parameter that relates mixture and bitumen frequency multiplier is studied.

$$\tau_{\text{mixture}} = 10^\alpha \tau_{\text{bitumen}} \qquad \alpha = \log (\tau_{\text{mixture}} / \tau_{\text{bitumen}})$$

δ parameter

Figure 5-21 shows that in the case of the bitumen, this parameter has a wide range of variation, while on the mixture it seems to remain constant around 2.00 for the mixture.

k parameter

As it can be observed, an almost constant average value of ≈ 0.18 is obtained for all mixtures, but for the bitumens it changes from 0.20 to 0.30.

h parameter

The tendency for h is to increase, but not in the same ratio for mixtures and bitumens.

β parameter

The standardized tendency observed is to substantially increase in the case of bitumens compared to the low values experienced by the mixtures results.

τ parameter

From a mechanical point of view, the relation between bitumen and mixture should be equivalent to multiplying the angular frequency by a factor of 10. However, the factor found is closer to 100.

α parameter

This parameter relates bitumen and mix design though the formula $\alpha = \log (\tau_{\text{mixture}} / \tau_{\text{bitumen}})$ at any temperature. It has been calculated for the ordinate axis on Kinexus results, and on the abscise axis on Metravib results. In our study, α is the only parameter that stays close to the identity curve.

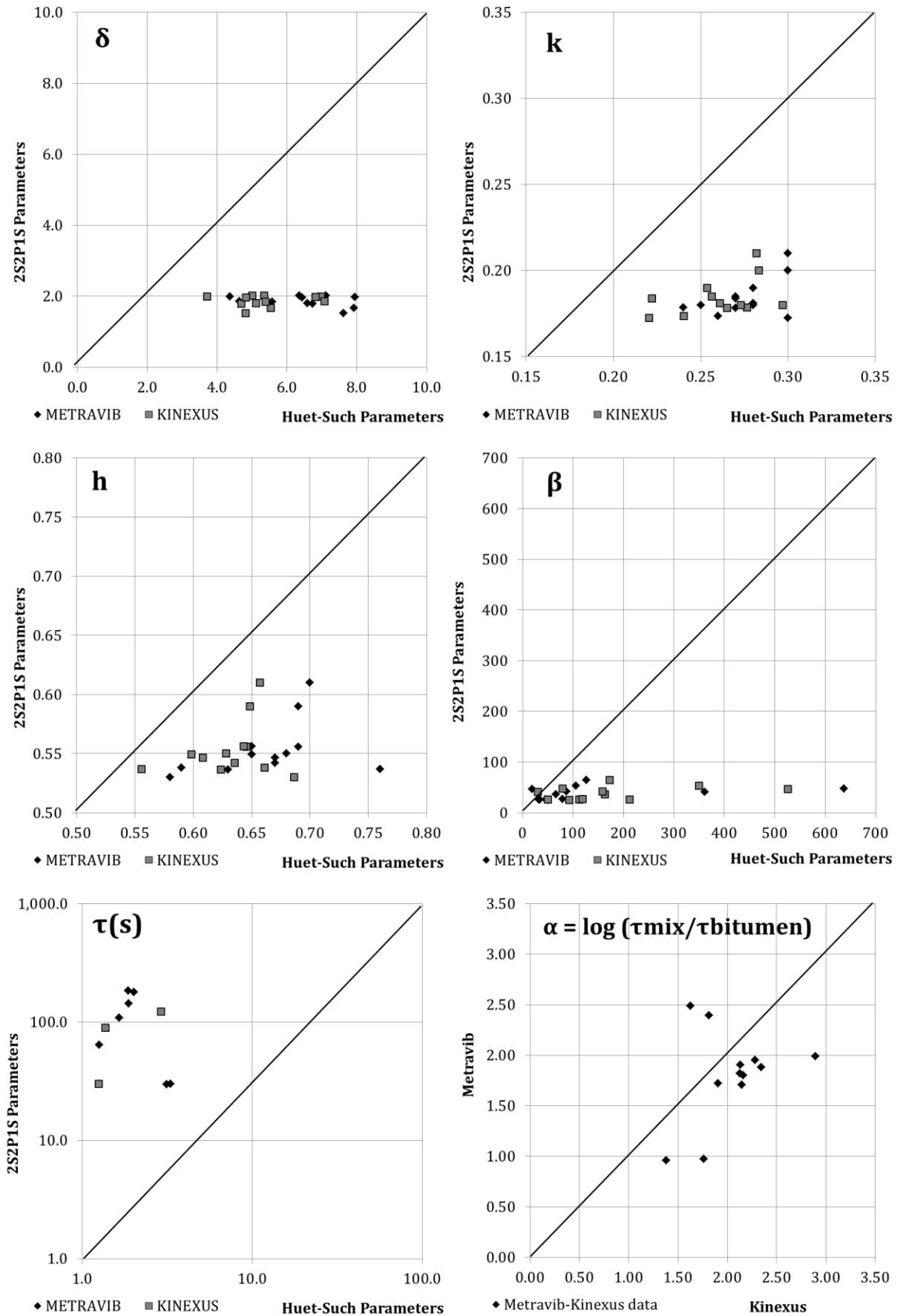


Figure 5-21 Relationship between model mixtures and bitumens parameters

On Figure 5-22 the relationship between C_1 and C_2 parameters for the construction of the master curves is illustrated. In the ordinate axis C_1 and C_2 from Kinexus® and Metravib® is plotted. Then, on the abscise axis the respective C_1 and C_2 from 2S2P1D modelling on mixture is shown.

Also when both components are close to each other, they are not the same. It can be observed how C_1 and C_2 parameters fluctuate more for the bitumens than for the mixtures.

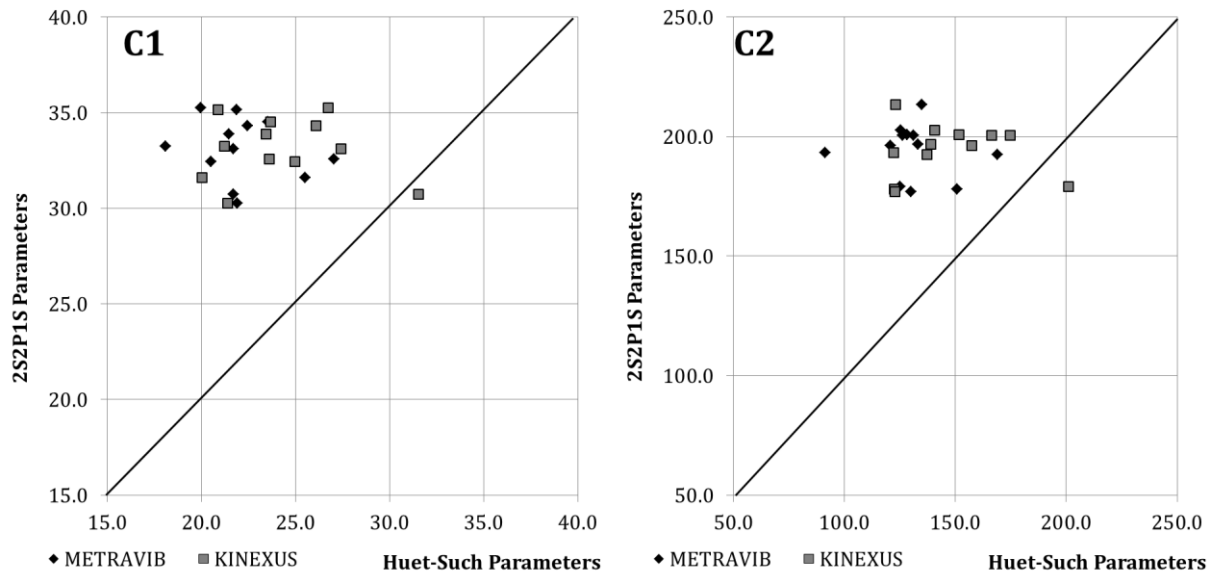


Figure 5-22 Relationship between C_1 and C_2 from mixtures and bitumens modelling

5.3.5 SHRP parameters

As explained in Section 5.2.4 the SHRP rutting and fatigue parameters are considered for comparison with European Standard testing parameters. SHRP rutting parameter is measured on aged bitumens, so then on RTFOT aged samples $(G^*/\sin\delta)_{\text{RTFOT aged bitumen}} > 2,200$ Pa. However, neat bitumens also need to fulfil the requirement of $(G^*/\sin\delta)_{\text{unaged bitumen}} > 1,000$ Pa [14]. In addition, fatigue parameter is measured on PAV samples and the criterion is that $(G^*\sin\delta)_{\text{PAV}} < 5.0$ MPa.

On Table 5-9 each bitumen extracted from mixture manufacture that has been tested is summarized with its corresponding ageing state, Neat, RTFOT or PAV.

Table 5-9 SHRP bitumens tested and compared

Bitumen	State	Bitumen	State	Bitumen	State
35/50 Neat	NEAT	35/50 Neat	NEAT	35/50 Foam	NEAT
HMA0	RTFOT	WMA0	RTFOT	FWMA0	RTFOT
HMA0a	PAV	WMA0a	PAV	FWMA0a	PAV
HMA50	RTFOT	WMA50	RTFOT	FWMA50	RTFOT
HMA50a	PAV	WMA50a	PAV	FWMA50a	PAV

Rutting criterion

On Figure 5-23 maximum temperatures before rutting for all type of mixtures manufactured are shown. In part (a) of the figure are represented the three mixtures without RAP, and in part (b) the mixtures with 50% RAP.

An increase in the parameter $G^*/\sin\delta$ would indicate an improvement in rutting resistance of the asphalt mixtures under operational conditions of heavy traffic loadings and at high service temperatures. So then, a higher factor of $G^*/\sin\delta$ is required from rutting resistance point of view. In line with SHRP report A-409 [136], the implication is that for temperatures above these threshold values, bitumen may contribute to rutting.

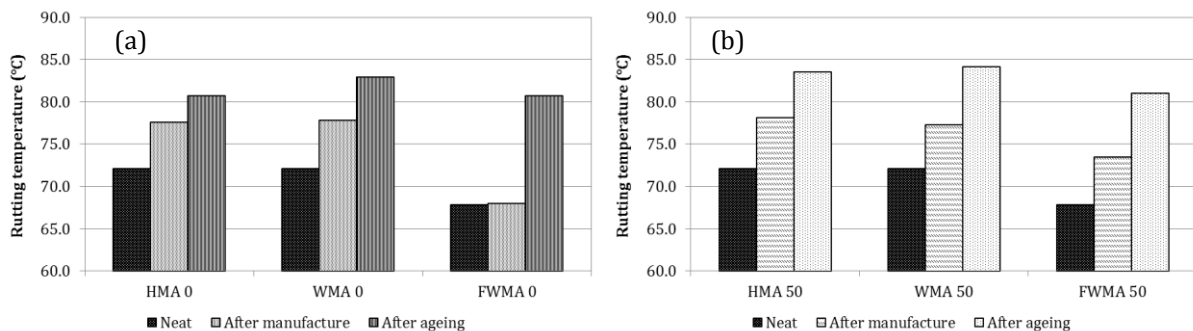


Figure 5-23 Rutting critical temperatures on mixtures without RAP (a) and with 50% RAP (b)

Mixtures without RAP, Figure 5-23 (a), show that HMA0 and WMA0 mixtures have similar threshold temperature (T_c) around 78°C. On the other hand, this edge temperature is 10°C lower for the foaming procedure. FWMA0 needs to suffer long term ageing to get to the same level of the other procedures.

However, incorporating RAP to the mixture (Figure 5-23 (b)) increases $G^*/\sin\delta$, and in fact the critical temperature. The effect is to stiff the material and subsequently allow the asphalt pavement to resist permanent deformations at generally high pavement temperatures.

Influence of rutting criterion on penetration and softening point results

In general, permanent deformations resistance mainly depends on aggregate properties and mix design. But still, bitumen characteristics cannot be neglected as it has an influence around 30% [136]. In Figure 5-24, penetration (a) and softening point (b) results from each manufacture technique are represented in function of the critical temperature.

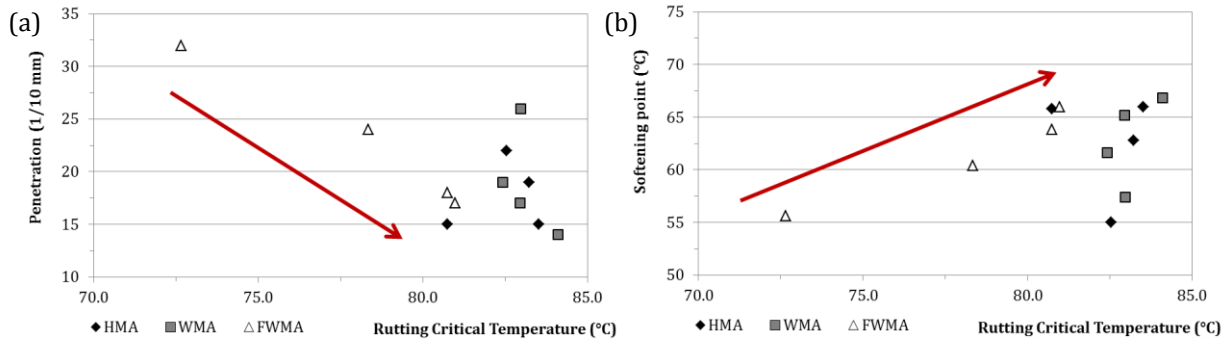


Figure 5-24 Influence of rutting critical temperature on penetration (a) and softening point (b) results

Bitumen stiffness and resistance to rutting is presented as a penetration reduction (increase of softening point) and an increase of T_c . It can be observed that both penetration and softening point seems to saturate for T_c between 82 and 85°C. Global correlation is not obvious for all procedures. FWMA technique seems to be still evolving.

With the red arrow bitumen stiffness increase with penetration and softening point is pointed out for the FWMA process. In the case of rutting critical temperature the increase of material stiffness is shown normally by an increase of temperature. Even if there is no direct correlation, there is a trend in both graphics that relates all results.

Influence of fatigue criterion on penetration and softening point results

Fatigue parameter, $G^*\sin\delta$ indicates material stiffness at intermediate temperatures as a result of long-term aging [137]. On Figure 5-25, critical temperatures for $G^*\sin\delta = 5$ MPa is shown for all mixtures. In this case, the critical temperature of each material is presented in the last column of each set of samples (aged material after PAV). All the materials have equivalent behaviour with a critical temperature at around 25°C for all of the, it can probably be expected that FWMA asphalt mixes would resist a little bit better due to slightly lower T_c , with or without RAP.

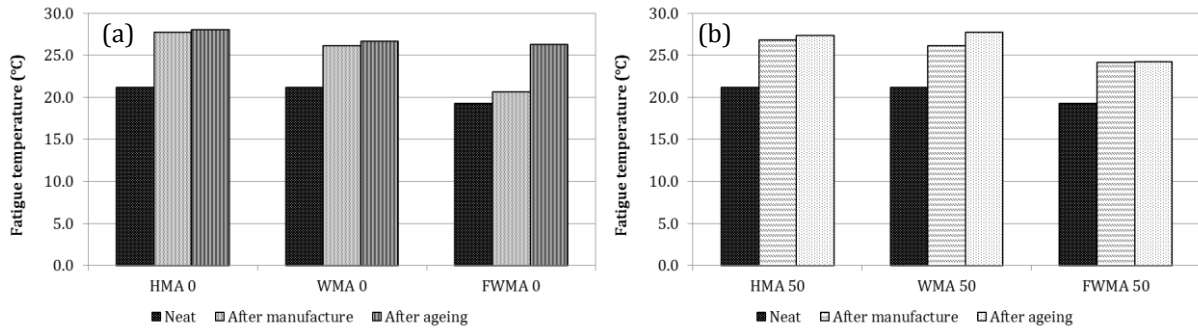


Figure 5-25 Fatigue critical temperatures on mixtures without RAP (a) and with 50% RAP (b)

Influence of index carbonyl on fatigue and rutting critical temperatures

As carbonyl index is taken in general as a parameter showing ageing evolution on asphalt mixtures, in this subsection it is compared to the critical temperatures for rutting (a) and fatigue (b) in Figure 5-26. Both graphics show that once achieved certain level of Ico (~2%) the variation of rutting and fatigue SHRP parameters correlation with Ico is not evident.

In contrast, for the FWMA procedure that saturation is not clearly achieved. The less ageing experienced by this process at the beginning seems to widen the ageing window for Ico.

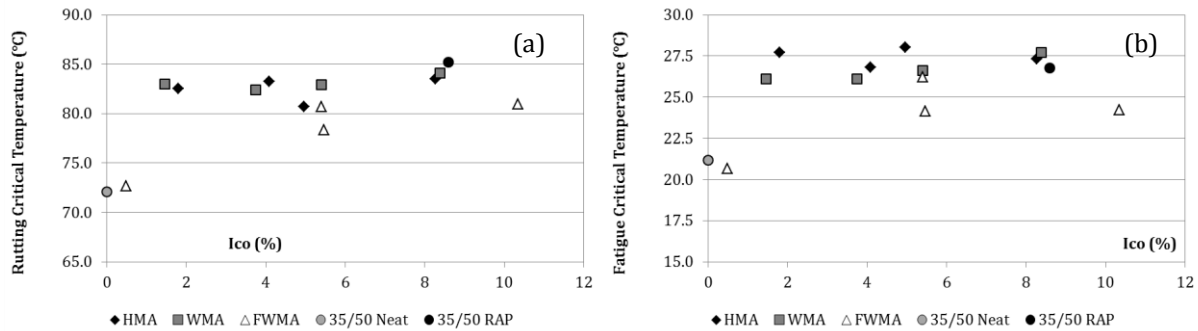


Figure 5-26 Influence of carbonyl index on rutting (a) and fatigue (b) critical temperatures

Influence of RAP addition on SHRP parameters

What is presented in Figure 5-27 is the temperature swept of these parameters for each pair of asphalt mixture without and with RAP. On the top (a) conventional mixtures HMA are shown, then in the middle (b) the surfactant procedure WMA and finally on the bottom the foaming process FWMA. In all cases, in the abscise axis fatigue parameter is represented and in the ordinate axis rutting parameter. In red are the limit requirements and pointed with the arrows the T_c of each type of mixture.

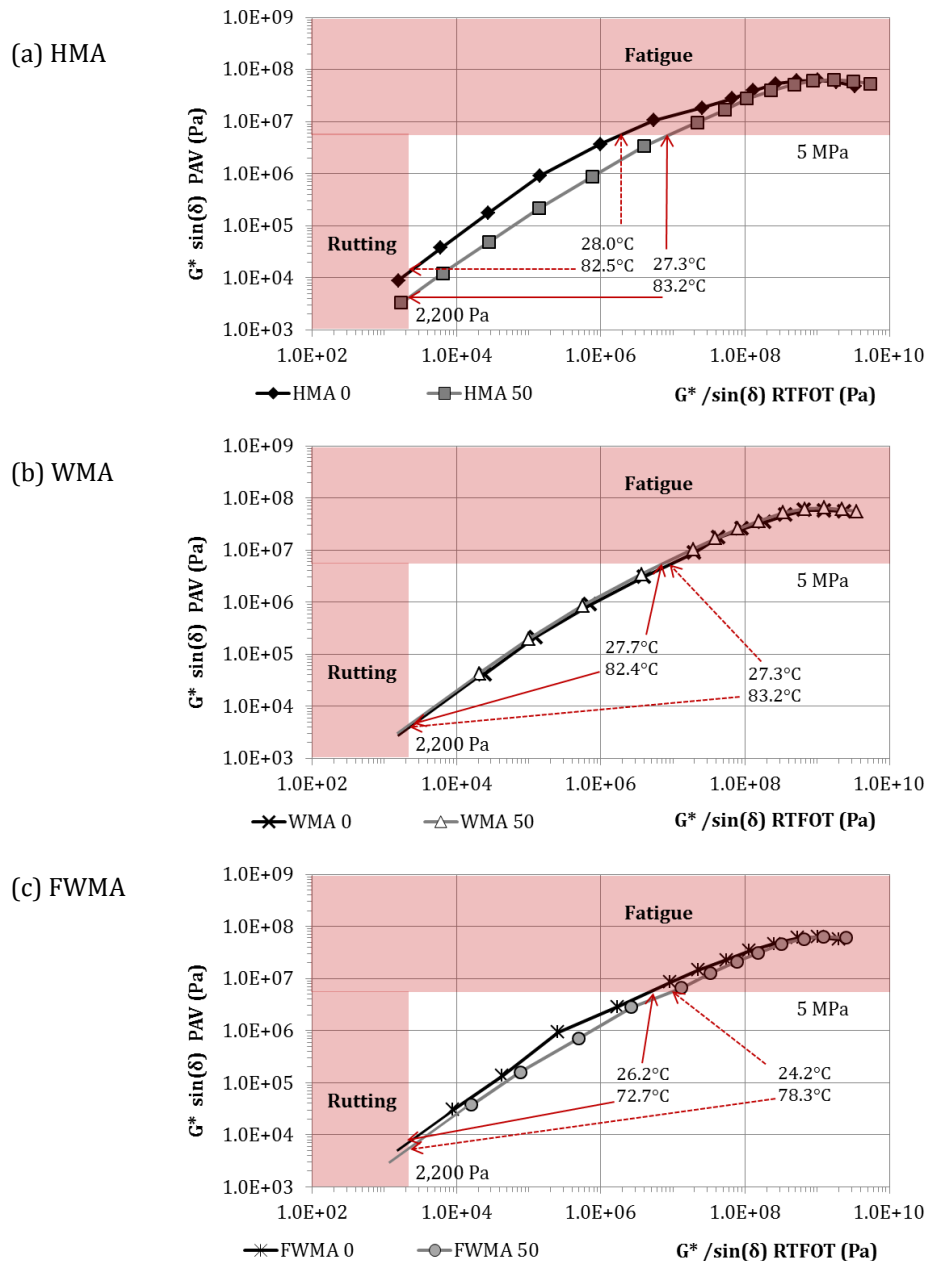


Figure 5-27 Influence of RAP addition of the fatigue/rutting parameters relationship

In general, RAP addition to the mixture could be seen as an increase of rutting critical temperature and a decrease of fatigue critical temperature. In the case of HMA mixtures, the addition of 50% of RAP widens the “window” of pavement service temperatures. In contrast, this increment is not so clear for WMA procedure, even if the tendency follows the same path; both curves are very close, with a difference in T_c lower than 1°C.

For the foaming FWMA procedure, the addition of RAP increases substantially (~6°C) the rutting critical temperature allowing higher service pavement temperature. Then, a reduction of 2°C is experienced for the fatigue by adding 50% of RAP. Again, asphalt mixtures performances must be studied in detail with more pertinent testing; however, these simple parameters show the line to follow to take into account the service temperatures.

5.4 Conclusions

In this chapter, a study of the influence of bitumen characteristics on asphalt mixture performance is developed. In addition, the effect of the asphaltene content on neat, model and laboratory aged bitumen modelling parameters is investigated. From the results obtained in previous chapters some correlations of results are obtained in certain cases.

The following conclusions can be drawn:

Model and laboratory aged bitumens

- i. Asphaltenes content plays an important role on bitumens structure. The variation of the asphaltene fraction, induced by model bitumen or by ageing procedures, shows fairly good correlation with β and τ parameters of the Huet-Such modelling.
- ii. In contrast, no obvious correlation is observed between the glassy modulus G_{∞} or the parabolic element h and the asphaltene content.
- iii. For the rutting and fatigue SHRP parameters, asphaltenes content plays an important role on bitumen stiffness. So then, critical service temperatures would increase (rutting) or decrease (fatigue) as the asphaltene content increases.

Mixtures and bitumens relationship

- iv. The parameters obtained after Huet-Such and 2S2P1D modelling on bitumens and mixtures respectively do not show clear correlation, for both Metravib® and Kinexus results. This effect may be due to the presence of RAP, the effect of the manufacture procedure or the ageing experienced by the mixtures.
- v. In terms of complex modulus, good correlation is found for bitumens between penetration, softening point and stiffness. The increase of stiffness in the asphalt mixture is presented as a reduction of penetration and an increase of softening point.
- vi. On the other hand, fatigue parameter ϵ_6 does not follow any correlation. However, for the foaming procedure FWMA, an increase of softening point (and decrease of penetration) is directly linked to better fatigue resistance. These findings should be taken with caution, due to the fact that fatigue slopes are not considered.

- vii. SHRP rutting and fatigue critical service temperatures do not show clear correlation with penetration and softening point results. Nevertheless, in terms of recycling, RAP addition widens the temperature range for the resulting mixtures independently of the manufacture procedure.

These conclusions highlight the difficulty to establish correlations between all the tests performed on bitumen and mixtures, empirical or rheological. It shows the complexity of bituminous mixtures, their evolution in time and the difficulty to model such material for further predictions.

Chapter 6. Conclusions and perspectives

6.1 Final conclusions

The general objective of this thesis is to study the durability of low temperature asphalt mixture containing reclaimed asphalt pavement. For this purpose, bitumen structure is studied in order to set the basis of the changes produced by asphalt mixtures ageing. In particular, the influence of the asphaltenes content on bitumens properties is studied. Model bitumens with different asphaltenes content are built by separation and recombination of asphaltenes and maltenes fractions. These model bitumens are characterized both physically and chemically.

With the aim of studying the mechanical performance of warm mix asphalt mixtures and their evolution during ageing, an experimental plan is set. Twelve asphalt mixtures are characterized through different tests performed both on asphalt mixtures and recovered bitumens. The chosen manufacture techniques are conventional hot mix asphalt, warm mix asphalt with surfactant addition and foamed bitumen. Then, 50% of reclaimed asphalt is added to the mixtures. Finally, laboratory ageing procedure in loose and compacted samples is applied in order to assess the response of the materials after simulated long term ageing.

Consequently, the main conclusions drawn from all studied can be summarized as follows:

Influence of asphaltene content during ageing

- I. In terms of ATR-FTIR analysis, sulphoxide groups seem to be more affected by the addition of asphaltenes fractions than carbonyl groups, indicating the affinity of polar fractions towards these components.
- II. By Iatroscan chromatography for SARA fractions determining, it is observed an increase of asphaltenes with ageing. It is also exposed that during ageing the increase of asphaltenes content is due to the evolution of aromatics to resins (and polar resins) and then to asphaltenes. In addition, the oxidation of aromatics or resins to polar resins or asphaltenes is also possible during ageing.
- III. By AFM observation, asphaltenes micelles appeared in all bitumens tested. Then in the maltenes fraction bee-like structure is observed, so the presence of asphaltenes does not seem necessary for their apparition as other researchers have stated.
- IV. Rheological behaviour of bitumen is mainly characterized by its stiffness. Then, it is strongly controlled by the asphaltenes content of the bitumen. Small changes in the ratio asphaltenes/maltenes have a direct impact on the material.

- V. δ -method analysis is proven as a powerful tool for ageing determination. Curve shifting is clearly observed when asphaltene content increases. Cross-over frequencies, corresponding to the median of the AMWD probability distribution, could be taken as an indicator of ageing.
- VI. By GPC testing, aged and model bitumen follow the same line of asphaltene content consideration. Colloidal indexes increase with asphaltene ratio, as the number and weight average molecular weight.
- VII. Asphaltene content plays an important role on bitumen structure. The variation of the asphaltene fraction, induced by model bitumen or by ageing procedures, leads to a fairly good correlation with β and τ parameters of the Huet-Such modelling.
- VIII. For the rutting and fatigue SHRP parameters, asphaltene content plays an important role on bitumen stiffness. So then, critical service temperatures would increase (rutting) or decrease (fatigue) as the asphaltene content increases, widening the range of use.
- IX.

Influence of manufacturing procedure

- X. Temperature reduction for the manufacture of foamed warm mix asphalts may lead to a lack of stiffness after the process. This decrease, compared to the other mixtures, is related to the reduced ageing experienced by the bitumen during the production process.
- XI. Concerning fatigue related performance; all procedures reach the standards limits. It is very interesting that reducing by 30°C the production of the mixture, with all the advantages associated, the performance of the mixture is on the standards.
- XII. In terms of complex modulus, good correlation has been found for penetration and softening point for all tested mixtures. The reduction of penetration and an increase of softening point of the bitumen are indicators of an increase of stiffness of the mix.
- XIII. On the other hand, fatigue parameter ϵ_6 does not follow any clear evolution with manufacturing temperature. However, for the foaming procedure FWMA, an increase of softening point (and decrease of penetration) is directly linked to better fatigue resistance. These findings should be taken with caution, due to the fact that fatigue slopes are not considered.

Influence of reclaimed asphalt pavement addition

- XIV. In general, the addition of RAP increases the performance of the mixtures, both for conventional and warm mixtures. However, when RAP is added or ageing occurs, the fatigue slope increases and consequently, the fatigue resistance of the material tends to be more sensitive to the strain level.
- XV. Regarding bitumen performance, the foaming process ages the bitumen to a lower degree during manufacture compare to the conventional procedure. When long term ageing is applied, the levels become comparable in both cases. Similarly, the hardening experienced when RAP is added is less pronounced due to the already aged bitumen present in the RAP.
- XVI. For the SHRP criteria, rutting and fatigue critical service temperatures for pavements do not show clear relation with empirical penetration and softening point results. Nevertheless, in terms of recycling, RAP addition widens the temperature range of application independently of the manufacture procedure.

 δ -method for ageing detection

- XVII. The application of the δ -method reveals contrasting ageing effects for the different processes, as well as the influence of RAP addition. The general pattern observed on the curves is a decrease of the lower molecular weight fractions and an increase of the high molecular weight fractions due to ageing for the samples with or without RAP. Compared to the FWMA technique, the HMA production process induces a significant displacement of the distribution towards higher AMW. After ageing or RAP addition the distributions tend to be similarly shifted for the all processes.
- XVIII. Combined with standard bitumen testing, the δ -method appears to be a suitable tool for the quantification of structural evolutions of bitumen, providing good visualization of the modifications induced. These results could be considered as a first step towards possible prediction of materials response. Structural interpretation of RAP addition and ageing evolution would be possible with the δ -method.

6.2 Recommendations for future research

The potential of applying reclaimed asphalt pavements on warm mix asphalt manufacturing procedures has been widely discussed throughout this thesis. During the different stages of this thesis new research lines have come up with the aim of improving all procedures employed. The work presented here opens up new perspectives and practical possibilities which are listed below:

- I. The proposed method for rheological testing at low temperatures on PP08 geometry is promising. However, the comparison of these measurements with a smaller geometry as it is PP04 could allow improving rheological results at very low temperatures.
- II. This study would go in line with the effect of reliability of measurements for the δ -method calculus. Data source for modelling should cover all temperature spectrums from elastic response of the material to Newtonian behaviour.
- III. The facts of having studied the influence of the asphaltene content on two close grade bitumen opens the possibility of widen the range of grades. It would be very interesting to see these effects on soft bitumen.
- IV. Deeper study of fatigue response of warm mix asphalts is recommended. Fatigue life comparison through different types of testing, as four point bending or indirect traction, could be interesting in order to choose the most accurate system to measure fatigue life.
- V. Further investigation should be carried out on the relationship between bitumen and asphalt mixture. It has been generally focused on complex modulus prediction, but somehow it should also be orientated to the study of fatigue life.

6.3 Conclusions finales

L'objectif général de cette thèse est d'étudier la durabilité des enrobés tièdes intégrant des recyclés. À cette fin, la structure du bitume est étudiée afin de définir l'origine des changements produits par le vieillissement des enrobés bitumineux. En particulier, l'influence de la teneur en asphaltènes sur les propriétés des bitumes est étudiée. Des bitumes modèles à teneurs en asphaltènes différentes sont fabriqués à partir de la séparation et la recombinaison de fractions d'asphaltènes et de malthènes. Ces bitumes modèles sont caractérisés physiquement et chimiquement.

Dans le but d'étudier la performance mécanique des enrobés tièdes et leur évolution au cours du vieillissement, un plan expérimental est défini. Douze enrobés sont caractérisés par différents essais, effectués à la fois sur des enrobés et leurs bitumes récupérés. Les techniques de fabrication choisies sont à chaud, tiède avec surfactant et tiède à la mousse du bitume. Ensuite, 50% d'agrégats d'enrobés sont ajoutés aux mélanges. Finalement, la procédure de vieillissement en laboratoire sur des échantillons foisonnés et compactés est appliquée afin d'évaluer la réponse des matériaux après un vieillissement simulé à long terme.

Les principales conclusions des études conduites peuvent être résumées comme suit:

Influence de la teneur en asphaltènes sur le vieillissement:

- I. En ce qui concerne l'analyse ATR-FTIR, les groupes sulfoxyde semblent être plus affectés par l'addition de fractions d'asphaltènes que les groupes carbonyle, ce qui indique l'affinité des fractions polaires vis-à-vis de ces composants.
- II. La détermination des fractions SARAP par chromatographie Iatroscan nous permet d'observer une augmentation des asphaltènes avec le vieillissement. Il est également montré qu'au cours du vieillissement, l'augmentation de la teneur en asphaltènes est due à l'évolution des composés aromatiques en résines (et aux résines polaires) puis en asphaltènes. De plus, l'oxydation des composés aromatiques ou des résines en résines polaires ou en asphaltènes est également possible pendant le vieillissement.
- III. Par l'observation de l'AFM, des micelles d'asphaltènes apparaissent dans tous les bitumes testés. Dans la structure malthénique, on observe une structure en abeille. Ainsi, la présence d'asphaltènes ne semble pas une condition nécessaire pour leur apparition contrairement à ce qui a été proposé par d'autres chercheurs.
- IV. Le comportement rhéologique du bitume se caractérise principalement par sa rigidité. En conséquence, il est fortement contrôlé par la teneur en asphaltènes du bitume. De

petits changements dans le rapport asphaltènes / malthènes ont un impact direct sur le matériel.

- V. L'analyse par la δ -méthode s'avère être un outil puissant pour la détermination du vieillissement. Une translation des courbes de distribution est clairement observée lorsque la teneur en asphaltènes augmente. Les fréquences de cross-over, correspondant à la médiane de la distribution de probabilité de l'AMWD, pourraient être considérées comme un indicateur du vieillissement.
- VI. Selon les tests de GPC, les types de bitumes vieillis et modèles suivent la même tendance en matière de teneur en asphaltènes. Les indices colloïdaux augmentent avec le taux d'asphaltènes, comme les masses moléculaires moyennes en poids et en nombre.
- VII. La teneur en asphaltènes joue un rôle important dans la structure des bitumes. La variation de cette fraction, contrôlée dans un bitume modèle ou induite par le vieillissement, présente une corrélation assez bonne avec celles des paramètres β et τ du modèle de Huet-Such.
- VIII. Pour les critères SHRP d'orniérage et fatigue, la teneur en asphaltènes joue un rôle important sur la rigidité du bitume. Ainsi, les températures critiques de service augmentent (orniérage) ou diminuent (fatigue) lorsque la teneur en asphaltène augmente, ce qui élargit la plage d'utilisation.

Influence de la procédure de fabrication

- IX. La réduction de la température de fabrication des enrobés à la mousse de bitume peut entraîner une plus faible rigidité après la fabrication. Cette diminution, par rapport aux autres types d'enrobés, est liée au vieillissement réduit par le bitume pendant la fabrication.
- X. Concernant la réponse à la fatigue, toutes les procédures donnent des résultats conformes aux exigences normatives. Il est très intéressant de constater qu'avec une diminution de 30°C de la température de fabrication d'enrobés, et tous les avantages associés, les performances mécaniques restent conformes aux normes.
- XI. En termes de module complexe, une bonne corrélation a été trouvée avec la pénétration et le point de ramollissement bille anneau de tous les bitumes testés. Une réduction de la pénétration et une augmentation du point de ramollissement du bitume sont des indicateurs d'une augmentation de la rigidité du mélange.
- XII. D'autre part, le paramètre de fatigue ε_6 ne suit aucune évolution claire avec la température de fabrication. Cependant, pour la procédure de moussage FWMA, une

augmentation du point de ramollissement (et une diminution de la pénétration) est directement liée à une meilleure résistance à la fatigue. Ces résultats doivent être pris avec précaution, car les pentes des droites de fatigue ne sont pas prises en considération.

Influence de l'ajout de chaussée d'asphalte récupérée

- XIII. En général, l'addition d'agrégats d'enrobés (AE) augmente la performance des enrobés bitumineux, à la fois pour les enrobés à chaud et les tièdes. Néanmoins, lorsque les AE sont ajoutés ou après vieillissement, la pente de la fatigue augmente. Par conséquent la résistance à la fatigue du matériau tend à être plus sensible au niveau de déformation.
- XIV. En ce qui concerne la performance du bitume, le processus de moussage vieillit moins le bitume pendant la fabrication en comparaison avec la procédure à chaud. Lorsque le vieillissement à long terme est appliqué, les niveaux deviennent comparables dans les deux cas. De même, le durcissement expérimenté lorsque les AE sont ajoutés est moins prononcé car du bitume déjà vieilli est présent dans les AE.
- XV. Pour les critères SHRP, les températures critiques du service d'orniérage et de fatigue pour les chaussées ne montrent pas de relation claire avec les résultats empiriques de pénétration et point de ramollissement. Néanmoins, en termes de recyclage, l'addition d'AE élargit la gamme de température d'application indépendamment de la procédure de fabrication.

δ -méthode de détection du vieillissement

- XVI. L'application de la δ -méthode révèle des effets de vieillissement contrastés pour les différents processus, ainsi que l'influence de l'addition d'AE. Le schéma général observé sur les courbes est une diminution des fractions de faible masse moléculaire apparente et une augmentation des fractions de masse moléculaire apparente élevée en raison du vieillissement des échantillons avec ou sans AE. Par rapport à la technique tiède moussée, le processus de production à chaud induit un déplacement important de la distribution vers une masse moléculaire apparente plus élevée. Après le vieillissement ou l'addition d'AE, les distributions ont la tendance à être déplacées de manière similaire pour tous les processus.
- XVII. Combinée aux essais standards sur bitume, la δ méthode semble être un outil approprié pour la quantification des évolutions structurelles du bitume permettant une bonne visualisation des modifications induites. Ces résultats pourraient être considérés comme une première étape vers une prédiction possible de la réponse des matériaux. L'interprétation structurelle de l'addition d'AE et de l'évolution du vieillissement serait ainsi possible avec la δ méthode.

References

- [1] Mallick RB, El-Korchi T. Pavement Engineering: Principles and Practice. Second Edi. Taylor & Francis Group; 2013.
- [2] ERF. European Road Federation. [Http://www.irfnet.eu/index.php](http://www.irfnet.eu/index.php) 2016.
- [3] Pérez-Martínez M, Moreno-Navarro F, Martín-Marín J, Ríos-Losada C, Rubio-Gámez MC. Analysis of cleaner technologies based on waxes and surfactant additives in road construction. *J Clean Prod* 2014;65:374–9. doi:10.1016/j.jclepro.2013.09.012.
- [4] EAPA. European Asphalt Pavement Association 2017.
- [5] Newcomb D. An introduction to warm-mix asphalt. Retrieved Febr 2007:7.
- [6] Hill B. Performance evaluation of warm mix asphalt mixtures incorporating reclaimed asphalt pavement. University of Illinois at Urbana-Champaign, 2011.
- [7] Zaumanis M. Warm Mix Asphalt Investigation. Riga Technical University, 2010.
- [8] Copeland A. Reclaimed Asphalt Pavement in Asphalt Mixtures: State of the Practice. 2011.
- [9] Hamzah MO, Jamshidi A, Shahadan Z. Evaluation of the potential of Sasobit® to reduce required heat energy and CO2 emission in the asphalt industry. *J Clean Prod* 2010;18:1859–65. doi:10.1016/j.jclepro.2010.08.002.
- [10] Rubio M del C, Moreno F, Martínez-Echevarría MJ, Martínez G, Vázquez JM. Comparative analysis of emissions from the manufacture and use of hot and half-warm mix asphalt. *J Clean Prod* 2013;41:1–6. doi:10.1016/j.jclepro.2012.09.036.
- [11] Rubio-Gámez MC, Menedez A, Moreno-Navarro F, Belmonte A, Ramirez A. Mechanical properties of hot bituminous mixes manufactured with recycled aggregate of Silestone(R) waste. *Mater Constr* 2011;61:49–60. doi:10.3989/mc.2011.52709.
- [12] Kraemer C, Pardillo JM, Rocci S, Romana M, Sanchez V, del Val MA. *Ingeniería de Carreteras Vol. II*. McGraw Hill; 2004.
- [13] Bardesi A. *Introducción a las mezclas bituminosas (Spanish)*. Barcelona: Curso de Mezclas Bituminosas: dosificación, fabricación, puesta en obra y control de calidad. Intevia; 2010.
- [14] Chailleux E, Ramond G, Such C, de La Roche C. A mathematical-based master-curve construction method applied to complex modulus of bituminous materials. *Road Mater Pavement Des* 2006;7:75–92. doi:10.1080/14680629.2006.9690059.
- [15] Moreno-Navarro F. Design of a laboratory test method for the analysis of asphalt mix response to fatigue cracking. University of Granada, 2013.
- [16] Woldekidan MF. Response modelling of bitumen, bituminous mastic and mortar. TU Delft, 2011.
- [17] Read J, Whiteoak D. *The Shell Bitumen Industrial Handbook*. 5th ed. Thomas Telford Publishing; 2003.
- [18] Williams D, Landel R, Ferry J. The temperature dependence of relaxation mechanisms in amorphous polymers and other glass form liquids. *J Am Chem Soc* 1955;77:3701–7.

- [19] Corté J-F, Di Benedetto H. Matériaux routiers bitumineux 1: Description et propriétés des constituants. Hermes-Lavoisier; 2005.
- [20] Arrhenius S. On the reaction velocity of the inversion of cane sugar by acids. *Zeitschrift Für Phys Chemie* 1889;4:226–48.
- [21] Booji HC, Thoone GPJM. Generalization of Kramers-Kronig transforms and some approximations of relations between viscoelastic quantities. *Rheol Acta* 1982;21:15–24.
- [22] Olard F. Comportement thermomécanique des enrobés bitumineux à basses températures: Relations entre les propriétés du liant et de l'enrobé [Thermomechanical behavior of bituminous mixtures at low temperatures: Relations between binder and mixture properties]. INSA Lyon, 2003.
- [23] Mangiafico S. Linear viscoelastic properties and fatigue of bituminous mixtures produced with Reclaimed Asphalt Pavement and corresponding binder blends. Ecole Nationale des Travaux Publics de l'Etat, 2014.
- [24] Olard F, Di Benedetto H. General "2S2P1D" Model and Relation Between the Linear Viscoelastic Behaviours of Bituminous Binders and Mixes. *Road Mater Pavement Des* 2003;4:185–224. doi:10.1080/14680629.2003.9689946.
- [25] Huet C. Etude par une méthode d'impédance du comportement viscoélastique des matériaux hydrocarbures. Faculté des Sciences de Paris, 1963.
- [26] Sayegh G. Variation des modules de quelques bitumes purs et enrobés bitumineux. Université de Paris, 1965.
- [27] Such C. Etude de la structure du bitume – analyse du comportement visqueux. Rapport interne CHG01189. 1982.
- [28] Such C. Analyse du comportement visqueux des bitumes. *Bulletin de liaison des laboratoires des ponts et chaussées* 127. 1983.
- [29] Christensen DW, Anderson DA. Interpretation of Dynamic Mechanical Test Data for Paving Grade Asphalt. *J Assoc Asph Paving Technol* 1992;61:67–116.
- [30] Marasteanu MO. Inter-conversions of the linear viscoelastic functions used for the rheological characterization of asphalt binders. Pennsylvania State University, 1999.
- [31] Zeng M, Bahia HU, Zhai H, Anderson MR, Turner P. Rheological modeling of modified asphalt binders and mixtures. *J Assoc Asph Paving Technol* 2001;70:403–41.
- [32] Delorme J-L, de La Roche C, Wendling L. Manuel LPC d'aide à la formulation des enrobés. Première. Paris: 2007.
- [33] RILEM. Bituminous Binders and Mixes: State of the art and interlaboratory tests on mechanical behaviour and mix design. E & FN Spon; 1998.
- [34] Soenen H, Roche C de La, Redelius P. Fatigue Behaviour of Bituminous Materials: From Binders to Mixes. *Road Mater Pavement Des* 2011.
- [35] EAPA. The use of warm mix asphalt. Eur Asph Paving Assoc 2014. www.eapa.org (accessed November 12, 2014).
- [36] Vaitkus A, Čygas D, Laurinavičius A, Perveneckas Z. Analysis and evaluation of possibilities for the

- use of warm mix asphalt in Lithuania. *Balt J Road Bridg Eng* 2009;4:80–6. doi:10.3846/1822-427X.2009.4.80-86.
- [37] D'Angelo J, Harm E, Bartoszek J, Baumgardner G, Corrigan M, Cowsert J, et al. *Warm-Mix asphalt : European Practice*. Alexandria, Virginia: 2008.
- [38] Jenkins KJ. *Mix design considerations for cold and half-warm bituminous mixes with emphasis on foamed bitumen*. University of Stellenbosch, 2000.
- [39] Chowdhury A, Button J. *A review of warm mix asphalt*. Report 473700-00080-1. Texas Transportation Institute. Texas A&M University System. vol. 7. 2008.
- [40] Hurley GC, Prowell BD. *NCAT Report 05-06 - Evaluation of Sasobit for Use in Warm Mix Asphalt*. 2005.
- [41] Bueche N. *Warm asphalt bituminous mixtures with regards to energy , emissions and performance* 2009.
- [42] Taylor NH. *Life expectancy of recycled asphalt paving*. In: Wood LE, editor. *Recycl. Bitum. pavement, ASTM STP 662*, American Society for Testing and Materials; 1978, p. 3–15.
- [43] Sondag MS, Bruce A, Chadbourn A, Drescher A. *Investigation Of Recycled Asphalt Pavement (RAP) Mixtures*. 2002.
- [44] Al-Qadi IL, Elseifi M, Carpenter SH. *Reclaimed asphalt pavement - A literature review*. Urbana, Illinois: 2007. doi:http://hdl.handle.net/2142/46007.
- [45] GAPA G. *Recycling of asphalt. New set of rules and standards shows the way forward*. Bonn, Germany: 2011.
- [46] Wirtgen GmbH. *Cold recycling. Wirtgen cold recycling technology*. 1st ed. Wirtgen GmbH; 2012.
- [47] Karlsson R, Isacsson U. *Material-Related Aspects of Asphalt Recycling—State-of-the-Art*. *J Mater Civ Eng* 2006;18:81–92. doi:10.1061/(ASCE)0899-1561(2006)18:1(81).
- [48] Makowska M, Pellinen TK. *Development of specifications and guidelines for hot in-place recycling in Finland*. 8th RILEM Int. Symp. Test. Charact. Sustain. Innov. Bitum. Mater., Ancona, Italy: 2015, p. 851–62.
- [49] Tam KK, Joseph P, Lynch DF. *Five-year experience of low-temperature performance of recycled hot mix*. *Transp Res Rec* 1992;1362:56–65.
- [50] Oliver JWH. *The Influence of the Binder in RAP on Recycled Asphalt Properties*. *Road Mater Pavement Des* 2001;2:311–25. doi:10.1080/14680629.2001.9689906.
- [51] Judycki J. *Fatigue of asphalt mixes*. University of Oulu, Finland, 1991.
- [52] Decker D. *State-of-the-practice for use of recycled asphalt pavement (RAP) in hot-mix asphalt*. 1998.
- [53] West RC. *Reclaimed Asphalt Pavement Management : Best Practices*. 2010.
- [54] Ipavec A, Marsac P, Mollenhauer K. *Synthesis of the european national requirements and practices for recycling in HMA and WMA (DIRECT_MAT PROJECT)*. 5th Eurasphalt Eurobitume Congr., 2012, p. 8.

- [55] Roberts FL, Kandhal PS, Brown ER, Lee D-Y, Kennedy TW. Hot Mix Asphalt Materials, Mixture Design and Construction. Second Edi. Lanham, MD: Napa Education Foundation; 1991.
- [56] Thyriou FC. Asphalt Oxidation, Asphaltenes and Asphalts. vol. 40B. New York, USA: Elsevier; 2000. doi:10.1016/S0376-7361(09)70287-0.
- [57] Blomberg T, Makowska M, Pellinen T. Laboratory Simulation of Bitumen Aging and Rejuvenation to Mimic Multiple Cycles of Reuse. *Transp Res Procedia* 2016;14:694–703. doi:10.1016/j.trpro.2016.05.335.
- [58] Makowska M, Pellinen TK. The “false positive” on antiaging properties of asphalt fines investigated by RTFO laboratory aging of mastics. *Funct. Pavement Des. Proc. 4th Chinese-European Work. Funct. Pavement Des., Delft, The Netherlands*: 2016.
- [59] Airey GD. Bitumen properties and test methods. *ICE Man. Constr. Mater.*, UK: Institution of Civil Engineers; 2009. doi:10.1680/mocm.35973.0263.
- [60] Eurobitume. <http://www.eurobitume.eu> 2016.
- [61] Jones DSJ, Pujadó PR. Handbook of petroleum processing. Springer; 2006.
- [62] Barth EJ. Asphalt: Science and Technology. First. Gordon and Breach; 1962.
- [63] Hoiberg AJ. Bituminous Materials: Asphalts, Tars and Pitches. First. Interscience, John Wiley Sons; 1965.
- [64] Asphalt Institute, Eurobitume. The Bitumen Industry - A Global Perspective: Production, chemistry, use, specification and occupational exposure (IS-230). 3rd ed. Lexington, KY: 2015.
- [65] bitumina.co.uk. Bitumen Production 2016. <http://www.bitumina.co.uk/bitumen-production.html> (accessed August 26, 2016).
- [66] Hammoum F, Chailleux E. La structure chimique des bitumes pétroliers. *Actual Chim* 2014; 385:63–4.
- [67] Redelius P. Asphaltenes in Bitumen, What They Are and What They Are Not. *Road Mater Pavement Des* 2009;10:25–43. doi:10.1080/14680629.2009.9690234.
- [68] Mullins OC, Sabbah H, Eyssautier J, Pomerantz AE, Barré L, Andrews AB, et al. Advances in asphaltene science and the Yen-Mullins model. *Energy Fuels* 2012;26:3986–4003. doi:dx.doi.org/10.1021/ef300185p.
- [69] Yen TF, Chilingar G V. Asphaltenes and asphalts. 1. Elsevier Science; 1994.
- [70] Corbett LW. Composition of Asphalt Based on Generic Fractionation Using Solvent Deasphalting, Elution-Adsorption Chromatography and Densimetric Characterization. *Anal Chem* 1969;41:576–9.
- [71] Lesueur D. The colloidal structure of bitumen: consequences on the rheology and on the mechanisms of bitumen modification. *Adv Colloid Interface Sci* 2009;145:42–82. doi:10.1016/j.cis.2008.08.011.
- [72] Paliukaitė M, Vaitkus A, Zofka A. Evaluation of bitumen fractional composition depending on the crude oil type and production technology. 9th Int. Conf. Environ. Eng., Vilnius: 2014, p. 7.
- [73] Such C, Francken L, Lesage J. Les matériaux de chaussées traités aux liants hydrocarbonés. Les

- liants Hydrocarb., Hermes Science; 2002.
- [74] Greenfeld SH. Chemical changes occurring during the weathering of two coating-grade asphalts. *J Res Natl Bur Stand* (1934) 1960;64C.
- [75] Petersen JC. Chemical Composition of Asphalt As Related To Asphalt Durability: State of the Art. *Transp Res Rec* 1984;999:13–30.
- [76] Airey GD. State of the Art Report on Ageing Test Methods for Bituminous Pavement Materials. *Int J Pavement Eng* 2003;4:165–76. doi:10.1080/1029843042000198568.
- [77] Vallerga BA, Monismith CL, Granthem K. A study of some factors influencing the weathering of paving asphalts. *Assoc Asph Paving Technol Proc* 1957;26:126–50.
- [78] Traxler RN. Durability of asphalt cements. *Assoc Asph Paving Technol Proc* 1963;32:44–58.
- [79] Vallerga BA. Pavement deficiencies related to asphalt durability. *Assoc Asph Paving Technol Proc* 1981;50:481–91.
- [80] Petersen JC. A Review of the Fundamentals of Asphalt Oxidation: Chemical, Physicochemical, Physical Property, and Durability Relationships. Washington, D.C.: Transportation Research Board; 2009. doi:10.17226/23002.
- [81] Liu M, Lunsford K, Davison R. The kinetics of carbonyl formation in asphalt. *AIChE J* 1996;42:1069–76. doi:10.1002/aic.690420417.
- [82] Marsac P, Piérard N, Porot L, Van den bergh W, Grenfell J, Mouillet V, et al. Potential and limits of FTIR methods for reclaimed asphalt characterisation. *Mater Struct* 2014;47:1–14. doi:doi:10.1617/s11527-014-0248-0.
- [83] Le Guern M, Chailleux E, Farcas F, Dreessen S, Mabilie I. Physico-chemical analysis of five hard bitumens: Identification of chemical species and molecular organization before and after artificial aging. *Fuel* 2010;89:3330–9. doi:10.1016/j.fuel.2010.04.035.
- [84] Krishnan JM, Rajagopal KR. On the mechanical behavior of asphalt. *Mech Mater* 2005:1085–100.
- [85] Nellensteyn FJ. The constitution of asphalt. *J Inst Pet Technol* 1924;10:311–25.
- [86] Pfeiffer JP, Saal RNJ. Asphaltic Bitumen as Colloid System. *J Phys Chem* 1940;44:139–49. doi:10.1021/j150398a001.
- [87] Gaestel C, Smadja R, Lamminan KA. Contribution à la connaissance des propriétés des bitumes routiers. *Rev Générale Des Routes Aérodrômes* 1971;466:85–92.
- [88] Martin-Alfonso MJ, Partal P, Navarro FJ, Garcia-Morales M, Bordado JCM, Diogo AC. Effect of processing temperature on the bitumen/MDI-PEG reactivity. *Fuel Process Technol* 2009;90:525–30. doi:10.1016/j.fuproc.2009.01.007.
- [89] Masson JF, Leblond V, Margeson J. Bitumen morphologies by phase-detection atomic force microscopy. *J Microsc* 2006;221:17–29. doi:10.1111/j.1365-2818.2006.01540.x.
- [90] Tuminello WH, Cudré-Mauroux N. Determining molecular weight distributions from viscosity versus shear rate flow curves. *Polym Eng Sci* 1991;31:1496–507. doi:10.1002/pen.760312009.
- [91] Wu S. Characterization of polymer molecular weight distribution by transient viscoelasticity: Polytetrafluoroethylenes. *Polym Eng Sci* 1988;28:538–43. doi:10.1002/pen.760280809.

- [92] Tuminello WH. Molecular weight and molecular weight distribution from dynamic measurements of polymer melts. *Polym Eng Sci* 1986;26:1339–1347. doi:10.1002/pen.760261909.
- [93] Zanzotto L, Stastna J, Ho S. Molecular weight distribution of regular asphalts from dynamic material functions. *Mater Struct* 1999;32:224–9. doi:10.1007/BF02481519.
- [94] Themeli A. Etude du potentiel d'emploi des bitumes naturels dans la production des liants bitumineux durs et des enrobés à module élevé. University of Strasbourg, 2015.
- [95] Themeli A, Chailleux E, Farcas F, Chazallon C, Migault B. Molecular weight distribution of asphaltic paving binders from phase-angle measurements. *Road Mater Pavement Des* 2015;16:228–44. doi:10.1080/14680629.2015.1029667.
- [96] Airey GD. Use of Black Diagrams to Identify Inconsistencies in Rheological Data. *Road Mater Pavement Des* 2002;3:403–24. doi:10.1080/14680629.2002.9689933.
- [97] Pieri N. Etude du vieillissement simulé et in situ des bitumes routiers par IRTF et fluorescence UV en excitation-émission synchrones : détermination des relations structures chimiques - propriétés rhéologiques par analyse en composantes principales. Université d'Aix-Marseille, 1994.
- [98] Planche J-P, Dreessen S, Le Guern M, Chailleux E, Farcas F. Identification of chemical species and molecular organization of bitumens. *Petersen Asph. Res. Conf.*, Laramie, WY, USA: 2010.
- [99] Hofko B, Eberhardsteiner L, Füssl J, Grothe H, Handle F, Hospodka M, et al. Impact of maltene and asphaltene fraction on mechanical behavior and microstructure of bitumen. *Mater Struct* 2015. doi:10.1617/s11527-015-0541-6.
- [100] Merce M, Saadaoui H, Dole F, Buisson L, Bentaleb A, Ruggi D, et al. Importance of thermal gradient in the bitumen bees genesis. *J Mater Sci* 2015;50:6586–600. doi:10.1007/s10853-015-9202-y.
- [101] Soenen H, Besamusca J, Fischer HR, Poulikakos LD, Planche J-P, Das PK, et al. Laboratory investigation of bitumen based on round robin DSC and AFM tests. *Mater Struct* 2014;47:1205–20. doi:10.1617/s11527-013-0123-4.
- [102] Jäger A, Lackner R, Eisenmenger-Sittner C, Blab R. Identification of four material phases in bitumen by atomic force microscopy. *Road Mater Pavement Des* 2004;5:9–24. doi:10.1080/14680629.2004.9689985.
- [103] Das PK, Baaj H, Tighe S, Kringos N. Atomic force microscopy to investigate asphalt binders: a state-of-the-art review. *Road Mater Pavement Des* 2016;17:693–718. doi:10.1080/14680629.2015.1114012.
- [104] Feng ZG, Wang SJ, Bian HJ, Guo QL, Li XJ. FTIR and rheology analysis of aging on different ultraviolet absorber modified bitumens. *Constr Build Mater* 2016;115:48–53. doi:10.1016/j.conbuildmat.2016.04.040.
- [105] Oliver JWH. Changes in the Chemical Composition of Australian Bitumens. *Road Mater Pavement Des* 2009;10:569–86. doi:10.1080/14680629.2009.9690214.
- [106] Rebelo LM, De Sousa JS, Abreu AS, Baroni MPMA, Alencar AE V, Soares SA, et al. Aging of asphaltic binders investigated with atomic force microscopy. *Fuel* 2014;117:15–25. doi:10.1016/j.fuel.2013.09.018.
- [107] Masson JF, Leblond V, Margeson J, Bundalo-Perc S. Low-temperature bitumen stiffness and viscous paraffinic nano- and micro-domains by cryogenic AFM and PDM. *J Microsc* 2007;227:191–202.

- doi:10.1111/j.1365-2818.2007.01796.x.
- [108] Lee S-J, Amirkhani SN, Shatanawi K, Kim KW. Short-term aging characterization of asphalt binders using gel permeation chromatography and selected Superpave binder tests. *Constr Build Mater* 2008;22:2220–7. doi:10.1016/j.conbuildmat.2007.08.005.
- [109] Jennings PW, Pribanic PW, Campbell W, Dawson K, Shane S, Taylor R. High pressure liquid chromatography as a method of measuring asphalt composition. FHWA, U.S. Department of Transportation; 1980.
- [110] Lesueur D. La rhéologie des bitumes: Principes et modification. *Rhéologie* 2002;2:1–30.
- [111] Kristjansdottir O. Warm Mix Asphalt for Cold Weather Paving. Washington University, 2006.
- [112] Chiu C-T, Hsu T-H, Yang W-F. Life cycle assessment on using recycled materials for rehabilitating asphalt pavements. *Resour Conserv Recycl* 2008;52:545–56. doi:10.1016/j.resconrec.2007.07.001.
- [113] Xiao F, Amirkhani SN, Juang CH. Rutting Resistance of Rubberized Asphalt Concrete Pavements Containing Reclaimed Asphalt Pavement Mixtures. *J Mater Civ Eng* 2007;19:475–83. doi:10.1061/(ASCE)0899-1561(2007)19:6(475).
- [114] de Mesquita Lopes Gennesseaux M. Avaliação da durabilidade de misturas asfálticas a quente e mornas contendo material asfáltico fresado. Biblioteca Digital de Teses e Dissertações da Universidade de São Paulo, 2015.
- [115] Lopes M, Gabet T, Bernucci L, Mouillet V. Durability of hot and warm asphalt mixtures containing high rates of reclaimed asphalt at laboratory scale. *Mater Struct* 2015;48:3937–48. doi:10.1617/s11527-014-0454-9.
- [116] Perez-Martinez M, Marsac P, Gabet T, Pouget S, Hammoum F. Ageing evolution of foamed warm mix asphalt combined with reclaimed asphalt pavement. *Mater Constr* 2017;67:14. doi:10.3989/mc.2017.04716.
- [117] Perez Martinez M, Marsac P, Lopes M, Gabet T, Pouget S, Hammoum F. Durability analysis of different warm mix asphalt containing reclaimed asphalt pavement. XXVth World Road Congr., Seoul: 2015, p. 1–15.
- [118] Perez-Martinez M, Marsac P, Gabet T, Hammoum F, de Mesquita Lopes M, Pouget S. Effects of Ageing on Warm Mix Asphalts with High Rates of Reclaimed Asphalt Pavement. 8th RILEM Int. Conf. Mech. Crack. Debonding Pavements, 2016, p. 113–8. doi:10.1007/978-94-024-0867-6_16.
- [119] LCPC. Fatigue carousel at IFSTTAR, Nantes. Nantes, France: 2007.
- [120] De La Roche C, Van de Ven MFC, Planche J-P, Van den bergh W, Grenfell J, Gabet T, et al. Hot Recycling of Bituminous Mixtures. In: Partl MN, Bahia HU, Canestrari F, de La Roche C, Di Benedetto H, Piber H, et al., editors. *Adv. Interlab. Test. Eval. Bitum. Mater. - State-of-the-Art*, Springer; 2013, p. 361–429. doi:10.1007/978-94-007-5104-0_7.
- [121] Moutier F. Etude statistique de l'effet de la composition des enrobés bitumineux sur leur comportement en fatigue et leur module complexe. *Bull Liaison Du Lab Des Ponts Chaussées* 1991:71–9.
- [122] Rowe GM, Barry J, Crawford K. Evaluation of a 100 % rap recycling project in Fort Wayne, Indiana. In: Canestrari F, Partl MN, editors. *RILEM Bookseries*, vol. 11, Springer; 2016, p. 941–51. doi:10.1007/978-94-017-7342-3_75.

- [123] Jimenez del Barco Carrion A. Design and characterisation of reclaimed asphalt mixtures with biobinder. University of Nottingham, 2017.
- [124] Kodippily S, Holleran G, Holleran I, Henning T, Wilson D. Performance of Recycled Asphalt Pavement Mixes - Comparing New Zealand Experience to American Experience. Transp. Res. Board 93rd Annu. Meet., 2014, p. 14.
- [125] Anderson DA, Kennedy TW. Development of SHRP binder specification. J Assoc Asph Paving Technol 1993;62:481-507.
- [126] Petersen JC, Robertson RE, Branthaver JF, Harnsberger PM, Duvall JJ, Kim SS, et al. Binder Characterization and Evaluation. Volume 1. No SHRP-A-367. Washington DC: 1994.
- [127] Ferry JD. Viscoelastic properties of polymers. New York, USA: John Wiley and Sons; 1971.
- [128] Heukelom W, J.G. K. Road design and dynamic loading. Proceeding Assoc Asph Pavement Technol 1964;33:92-125.
- [129] Ugé P, Guest G, Garvois A. Nouvelle méthode de calcul du module complexe des mélanges bitumineux. Bull Liaison Du Lab Des Ponts Chaussées 1977;Special V:199-213.
- [130] Franken L, Vanelstraete A. Relation between mix stiffness and binder complex modulus. Rheol. Bitum. Bind. Eur. Work. Brussels, 5-7 April, 1995.
- [131] Francken L, Vanelstraete A. Complex moduli of bituminous binders and mixes: interpretation and evaluation. Eurasphalt Eurobitume Congr., 1996.
- [132] Witczak MW, Fonseca OA. Revised predictive model for dynamic (complex) modulus of asphalt mixtures. Transp Res Rec J Transp Res Board 1996;1540:15-23. doi:10.3141/1540-03.
- [133] Christensen DW, Pellinen T, Bonaquist RF. Hirsch Model for Estimating the Modulus of Asphalt Concrete. Assoc Asph Paving Technol 2003;72:97-121.
- [134] Bari J, Witczak MW, You Z, Solamian M, Huang B, Mohseni A, et al. Development of a new revised version of the Witczak E Predictive Model for hot mix asphalt mixtures. Asph Paving Technol Assoc Asph Paving Technol Tech Sess 2006;75:381-424.
- [135] Di Benedetto H, Olard F, Sauzéat C, Delaporte B. Linear viscoelastic behaviour of bituminous materials: From binders to mixes. Road Mater Pavement Des 2004;5:163-202. doi:10.1080/14680629.2004.9689992.
- [136] Leahy RB, Harrigan ET, Von Quintus H. Validation of relationships between specification properties and performance. Report SHRP-A-409. Washington D.C.: 1994.
- [137] Asphalt Institute . Performance graded asphalt binder specification and testing. Superpave Series No 1; 2003.

Standards

- [138] EN 13108-1:2007 Bituminous mixtures - Material specifications - Part 1: Asphalt Concrete
- [139] EN 13108-8:2006 Bituminous mixtures - Material specifications - Part 8: Reclaimed asphalt
- [140] EN 13043:2003 Aggregates for bituminous mixtures and surface treatments for roads, airfields and other trafficked areas

-
- [141] EN 12697-12:2009 Bituminous mixtures - Test methods for hot mix asphalt - Part 12: Determination of the water sensitivity of bituminous specimens
 - [142] EN 12697-22:2008 Bituminous mixtures - Test methods for hot mix asphalt - Part 22: Wheel tracking
 - [143] EN 12697-24:2012 Bituminous mixtures - Test methods for hot mix asphalt - Part 24: Resistance to fatigue
 - [144] EN 12697-26:2012 Bituminous mixtures - Test methods for hot mix asphalt - Part 26: Stiffness
 - [145] EN 12697-31:2008 Bituminous mixtures - Test methods for hot mix asphalt - Part 31: Specimen preparation by gyratory compactor
 - [146] EN 1426:2007 Bitumen and bituminous binders - Determination of needle penetration
 - [147] EN 1427:2007 Bitumen and bituminous binders - Determination of the softening point - Ring and Ball method
 - [148] EN 12607-1:2015 Bitumen and bituminous binders - Determination of the resistance to hardening under influence of heat and air - Part 1: RTFOT method
 - [149] EN 14769:2012 Bitumen and bituminous binders - Accelerated long-term ageing conditioning by a Pressure Ageing Vessel (PAV)
 - [150] EN 12591:2009 Bitumen and bituminous binders. Specifications for paving grade bitumens.
 - [151] EN 13108:2007 Bituminous mixtures. Material specifications. Part 1: Asphalt concrete.

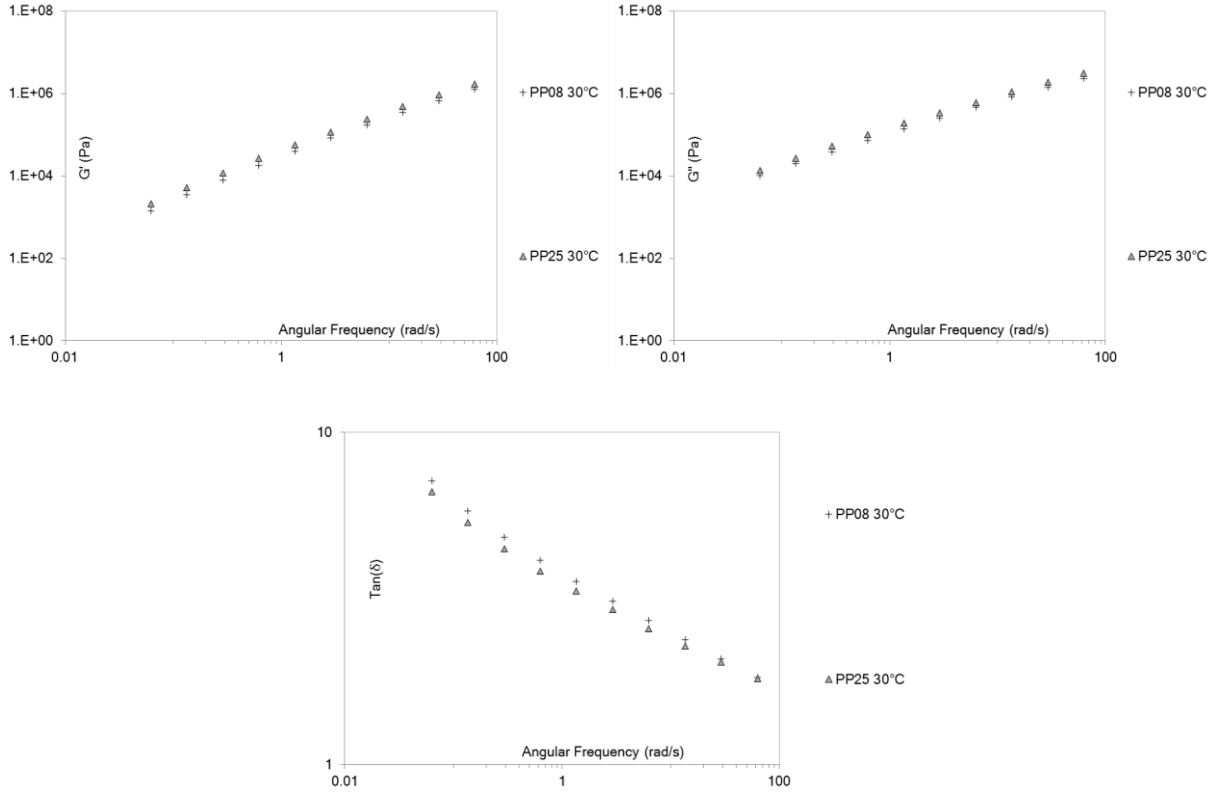
ANNEXES

- Annex 1 – OVERLAPPING TEMPERATURES FOR MODEL AND AGED BITUMENS
- Annex 2 – MASTER CURVES, WLF ADJUSTMENT, BLACK DIAGRAMS AND COLE-COLE PLAN OF MODEL AND AGED BITUMENS
- Annex 3 – HUET-SUCH MODELLING PARAMETERS AND δ -METHOD CURVES OF MODEL AND AGED BITUMENS
- Annex 4 – MASTER CURVES, WLF ADJUSTMENT, BLACK DIAGRAMS AND COLE-COLE PLAN OF RECOVERED BITUMENS FROM ASPHALT MIXTURES MANUFACTURE
- Annex 5 – HUET-SUCH MODELLING PARAMETERS AND δ -METHOD CURVES FROM KINEXUS® DEVICE -RECOVERED BITUMENS FROM ASPHALT MIXTURES
- Annex 6- 2S2P1D MODELLING PARAMETERS AND MASTER CURVES OF ASPHALT MIXTURES
- Annex 7 – HUET-SUCH MODELLING PARAMETERS BY C7-ASPHALTENES, SARA FRACTIONS, COLLOIDAL INDEX, POLYDISPERSITY RVALUE AND W(co)
- Annex 8 – SHRP RUTTING AND FATIGUE PARAMETERS CURVES WITH TEMPERATURE
- Annex 9 - SHSTH TRANSFORMATION BETWEEN ASPHALT MIXTURES RESULTS AND RECOVERED BITUMEN RESULTS

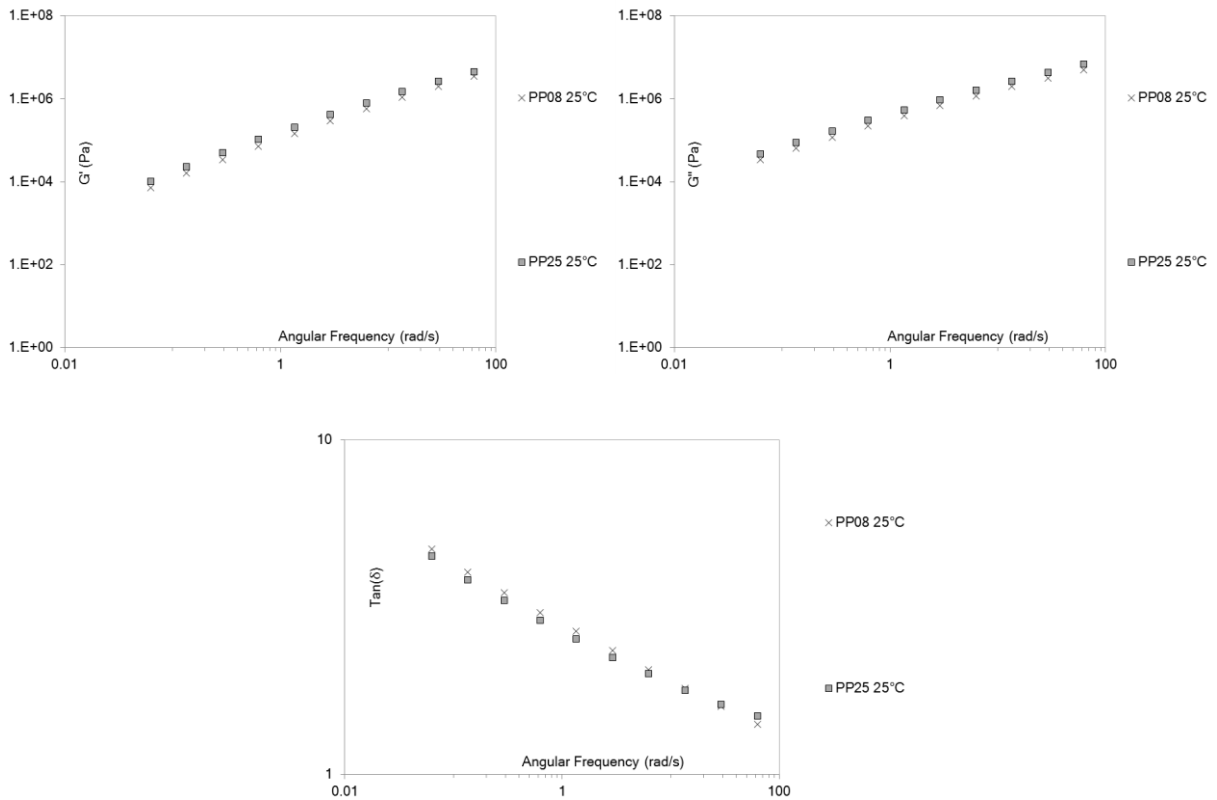
Annex 1

OVERLAPPING TEMPERATURES FOR MODEL AND AGED BITUMENS

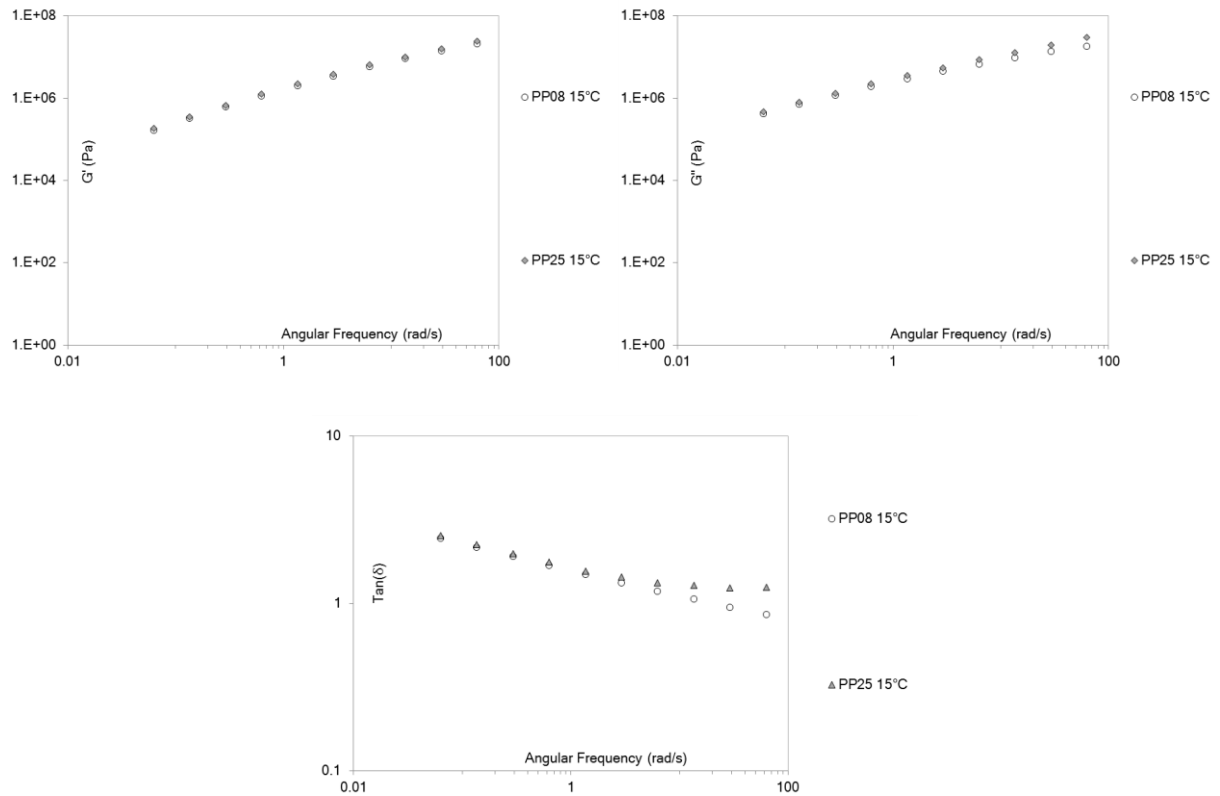
35/50 NEAT BITUMEN



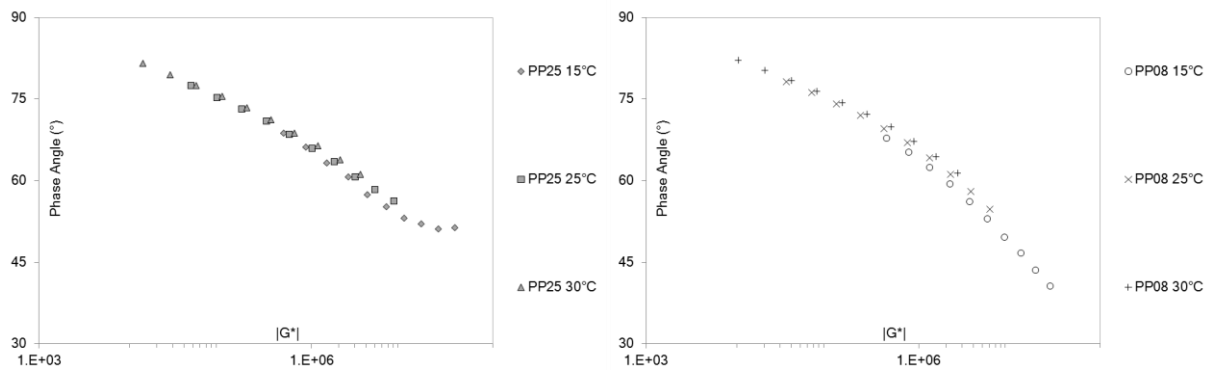
Overlapping of G' (Pa), G'' (Pa) and $\tan(\delta)$ at $T = 30^\circ\text{C}$



Overlapping of G' (Pa), G'' (Pa) and $\tan(\delta)$ at $T = 25^\circ\text{C}$

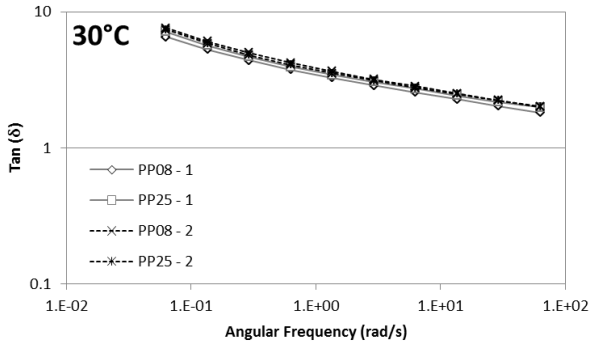
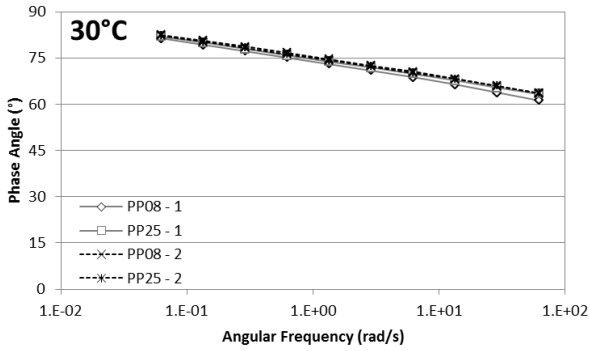
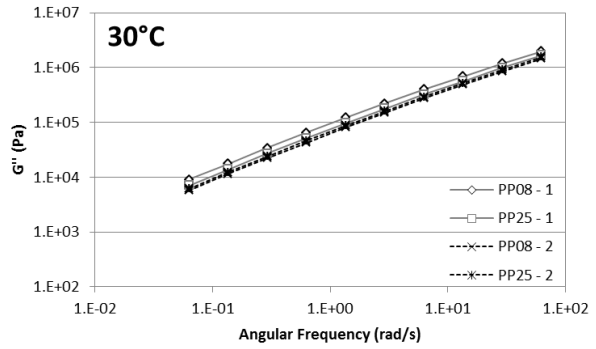
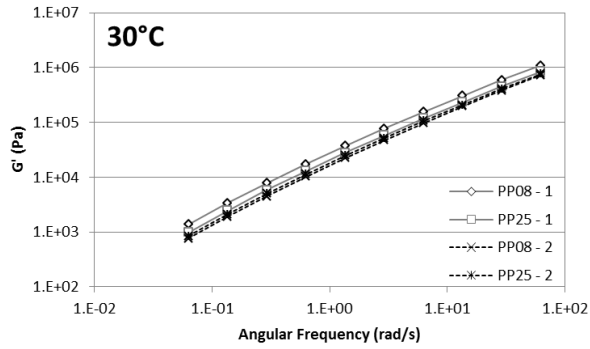


Overlapping of G' (Pa), G'' (Pa) and $\tan(\delta)$ at $T = 15^\circ\text{C}$

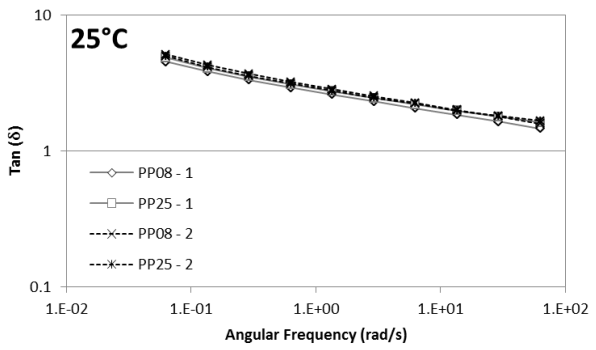
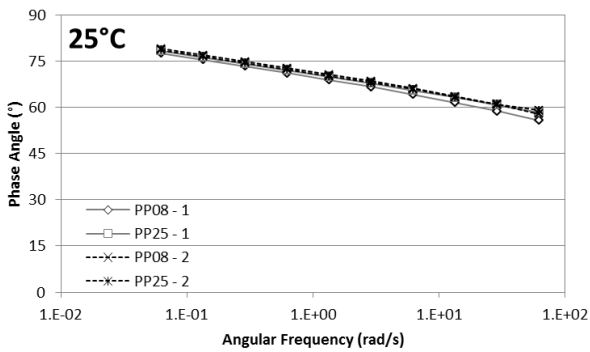
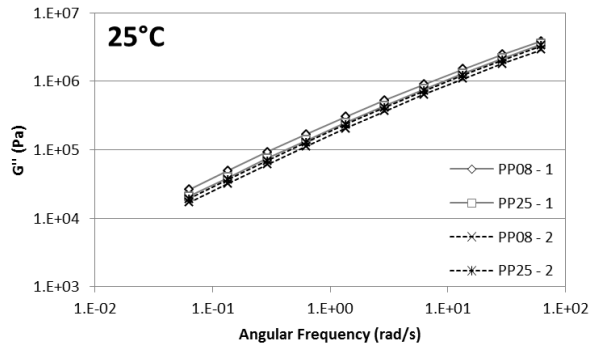
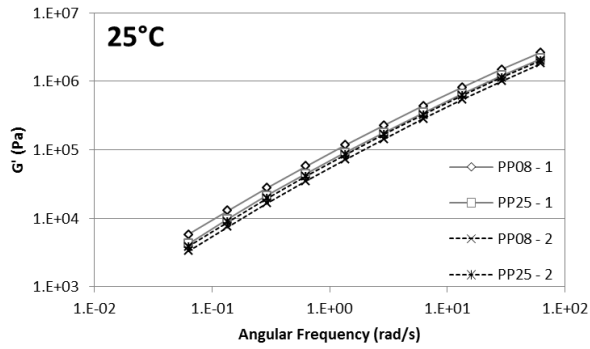


Overlapping of $\delta(^\circ)$ for PP25 and PP08 results

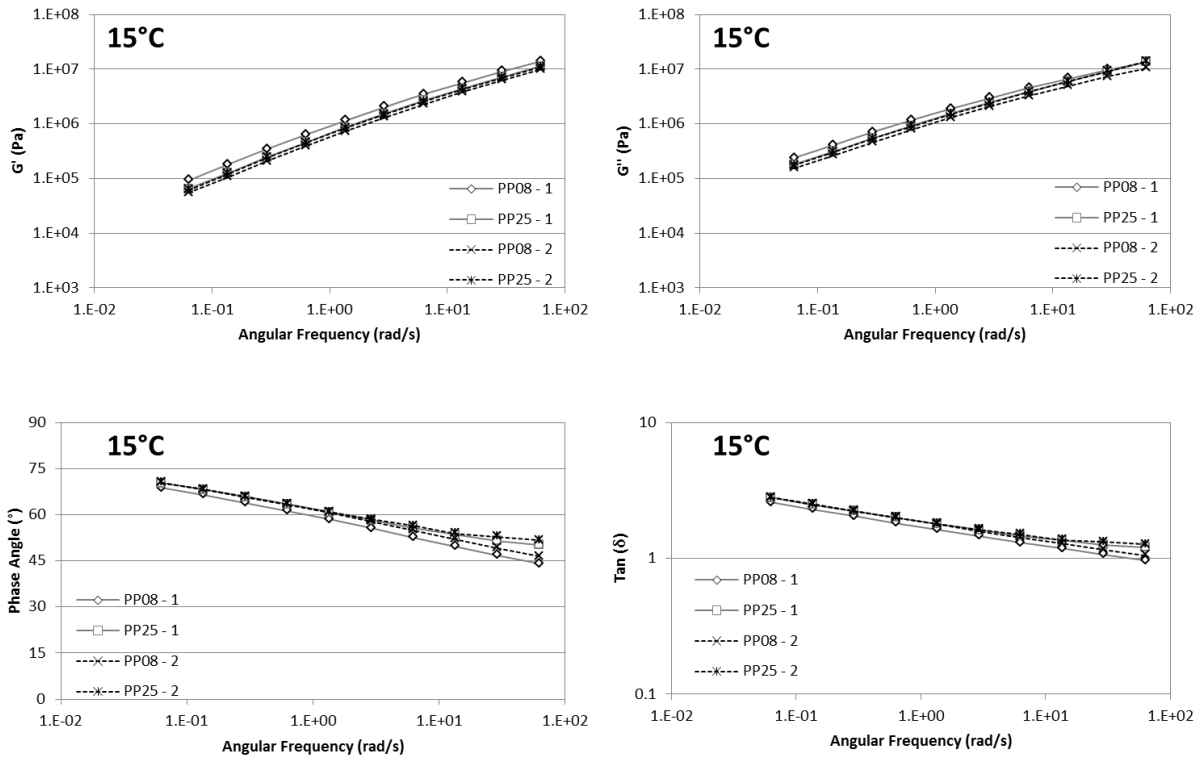
35/50 85M+15A



Overlapping of G' (Pa), G'' (Pa), δ (°) and $\text{Tan}(\delta)$ at $T = 30^\circ\text{C}$

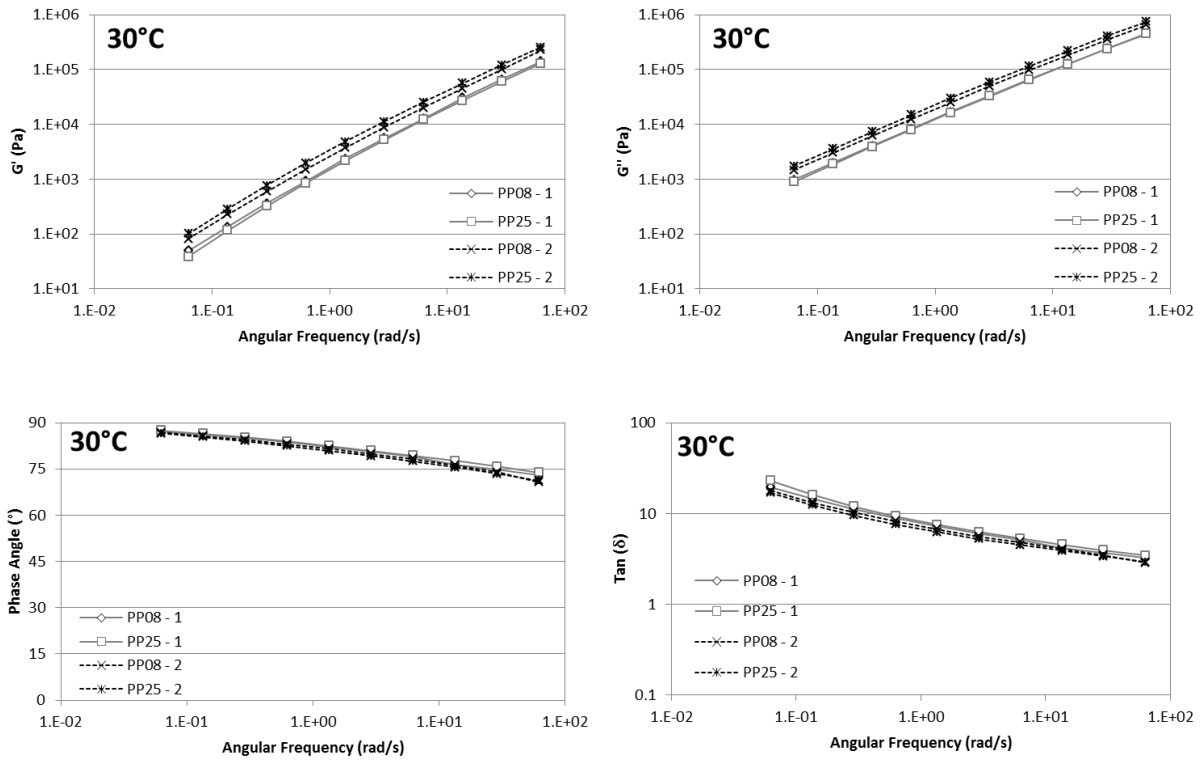


Overlapping of G' (Pa), G'' (Pa), δ (°) and $\text{Tan}(\delta)$ at $T = 25^\circ\text{C}$

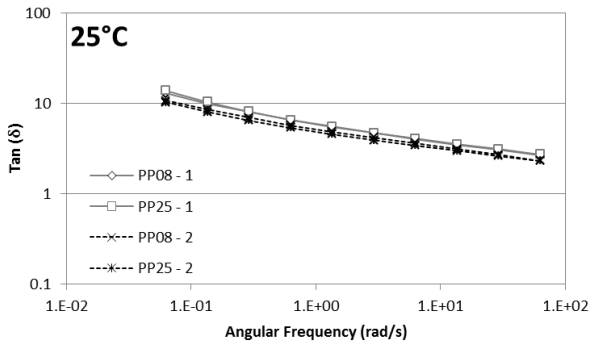
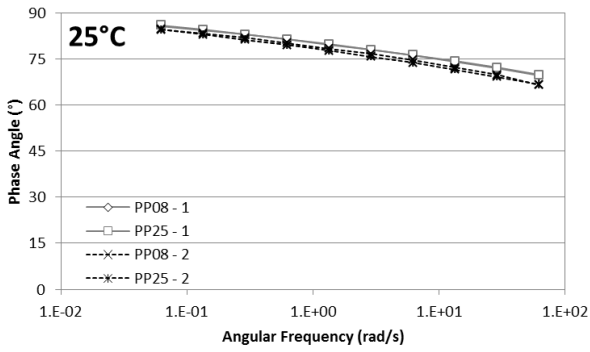
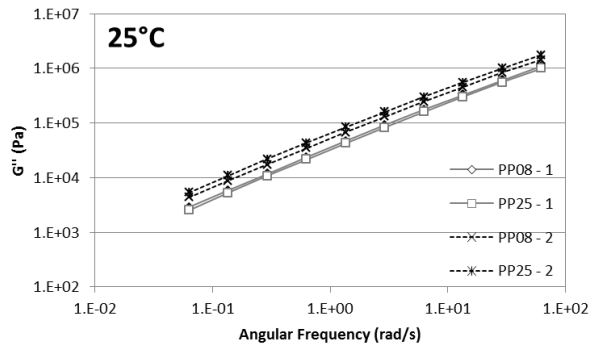
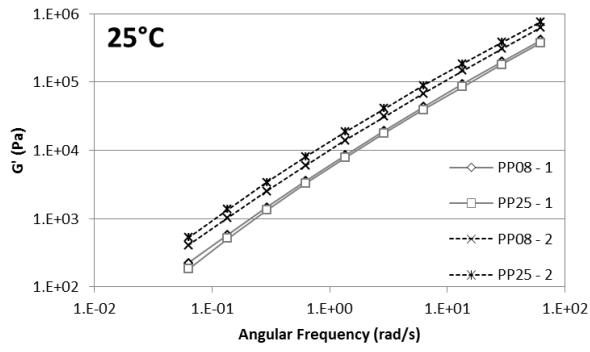


Overlapping of G' (Pa), G'' (Pa), δ (°) and $\tan(\delta)$ at $T = 15^\circ\text{C}$

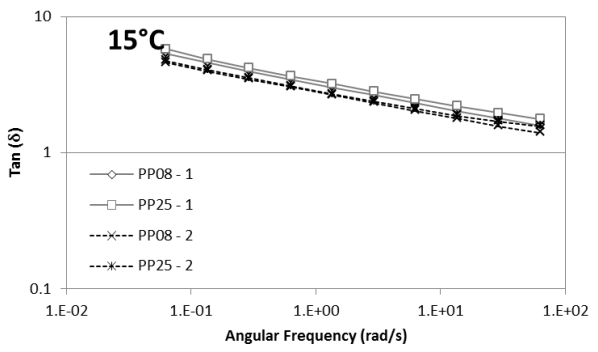
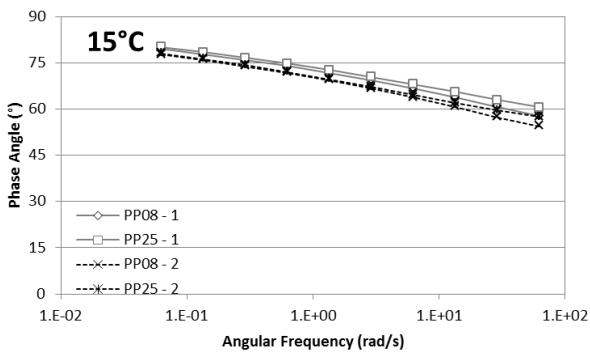
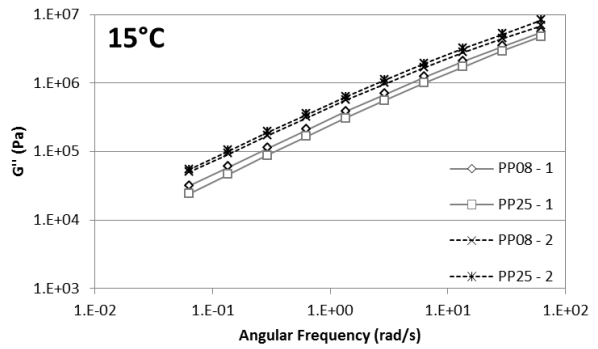
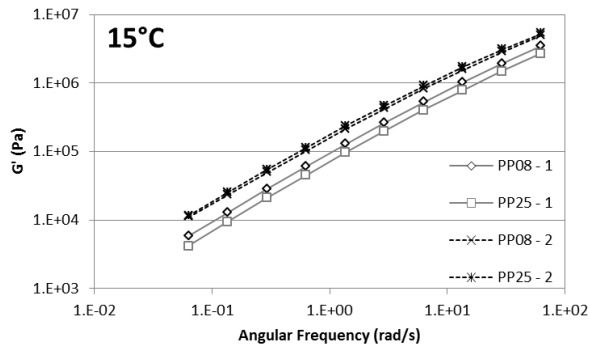
35/50 90M+10A



Overlapping of G' (Pa), G'' (Pa), δ (°) and $\tan(\delta)$ at $T = 30^\circ\text{C}$

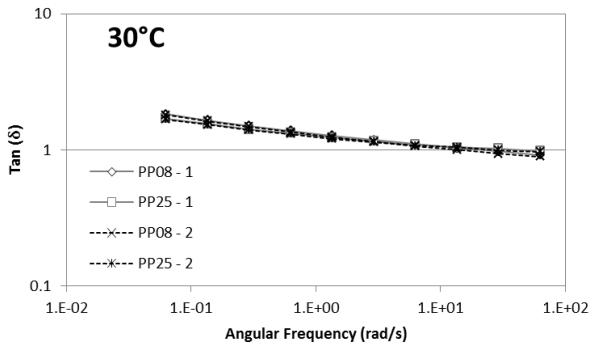
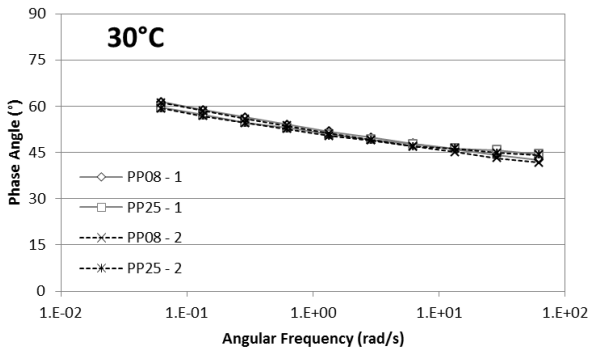
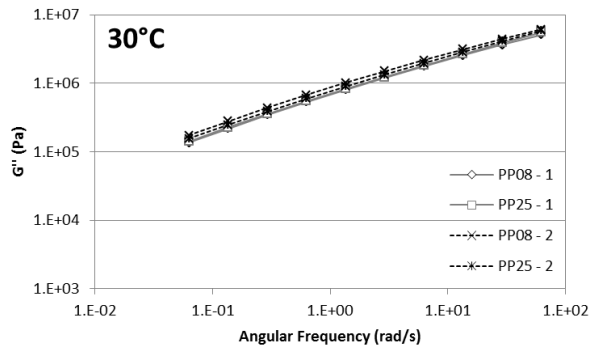
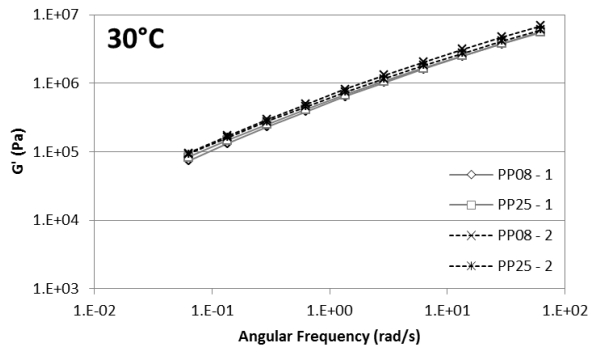


Overlapping of G' (Pa), G'' (Pa), δ (°) and $\text{Tan}(\delta)$ at $T = 25^\circ\text{C}$

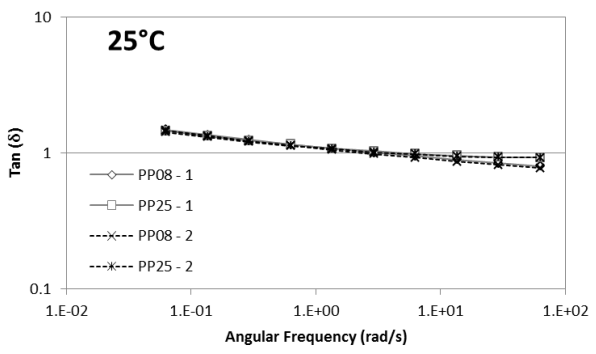
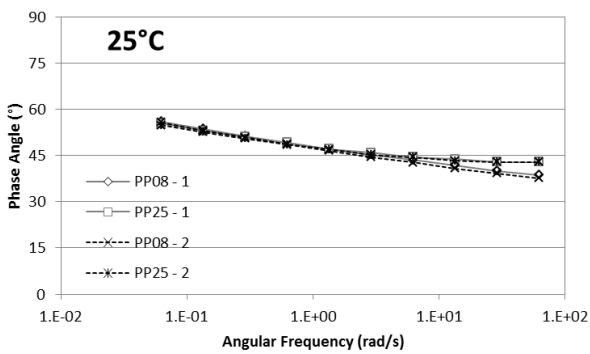
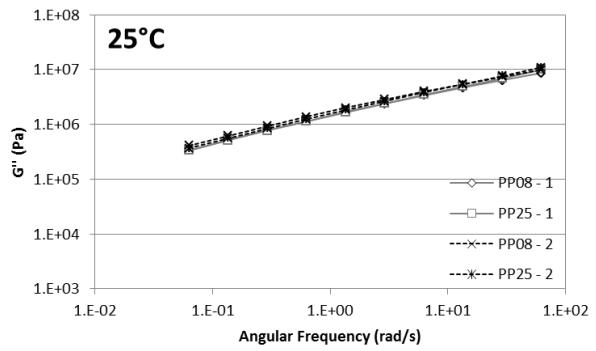
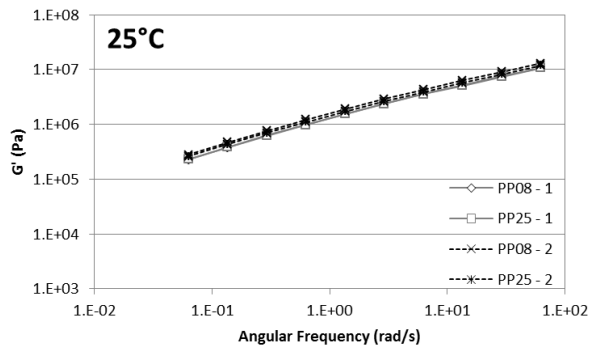


Overlapping of G' (Pa), G'' (Pa), δ (°) and $\text{Tan}(\delta)$ at $T = 15^\circ\text{C}$

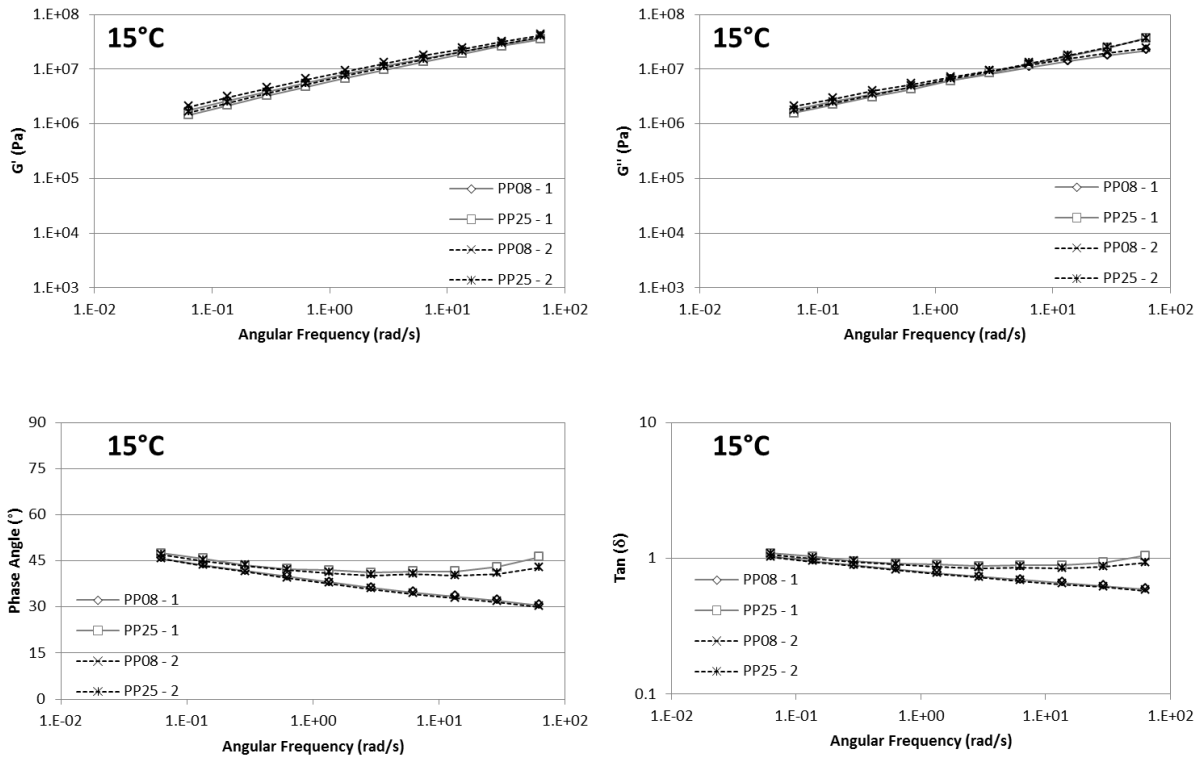
35/50 80M+20A



Overlapping of G' (Pa), G'' (Pa), δ (°) and $\text{Tan}(\delta)$ at $T = 30^\circ\text{C}$

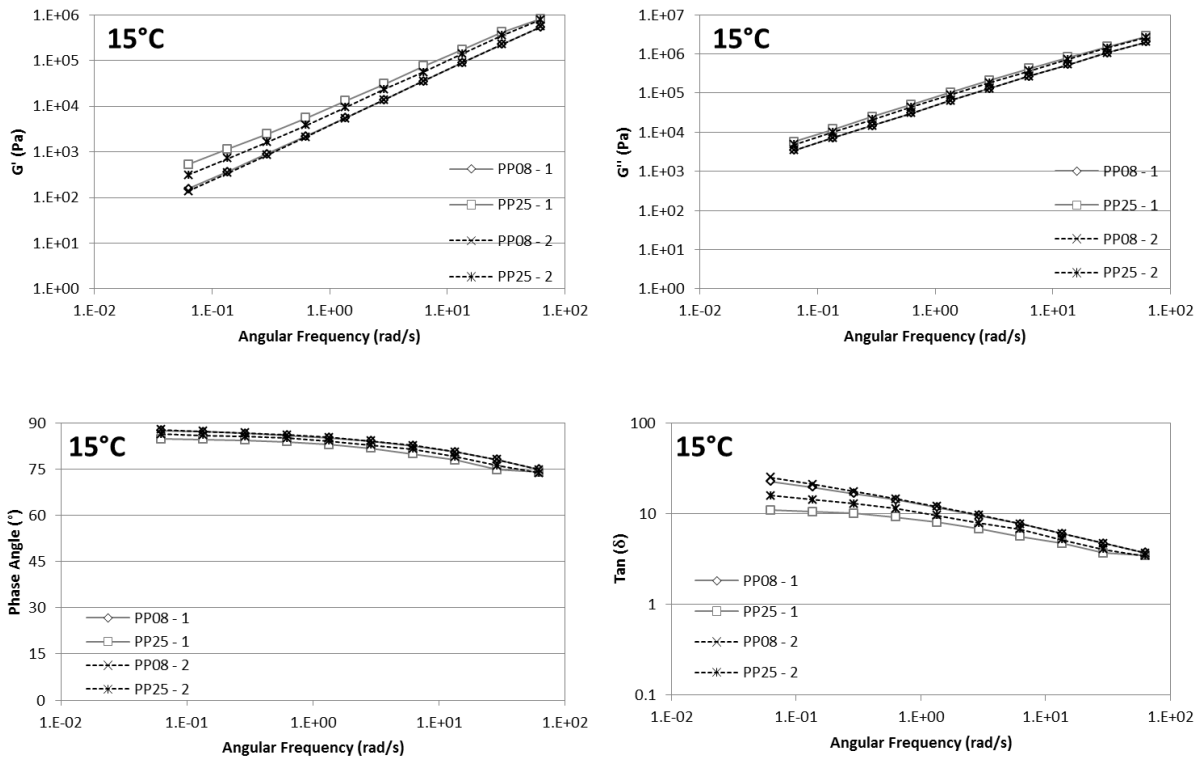


Overlapping of G' (Pa), G'' (Pa), δ (°) and $\text{Tan}(\delta)$ at $T = 25^\circ\text{C}$

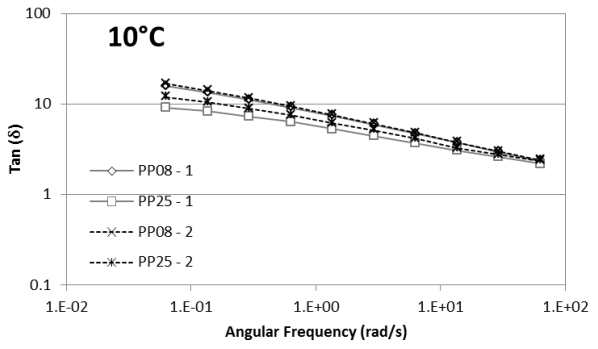
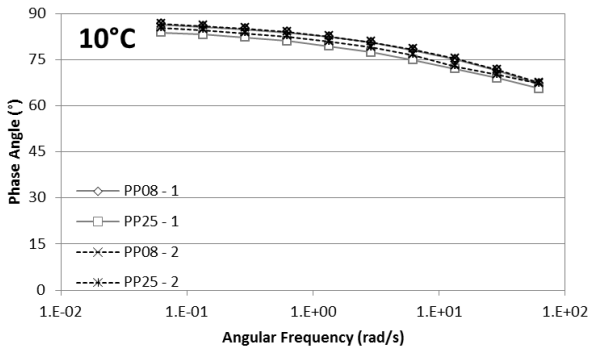
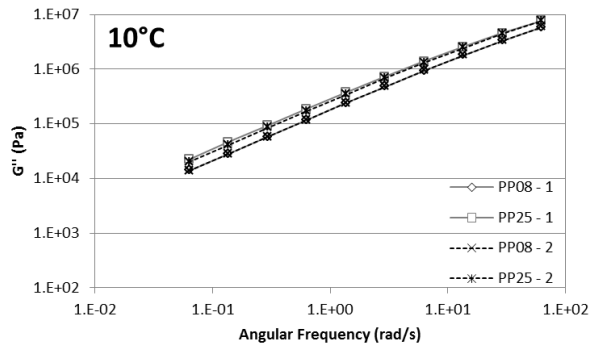
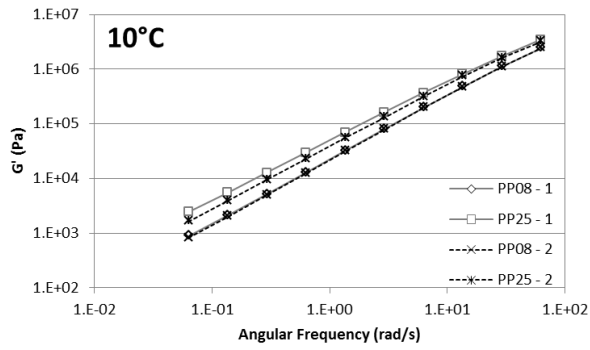


Overlapping of G' (Pa), G'' (Pa), δ (°) and $\tan(\delta)$ at $T = 15^\circ\text{C}$

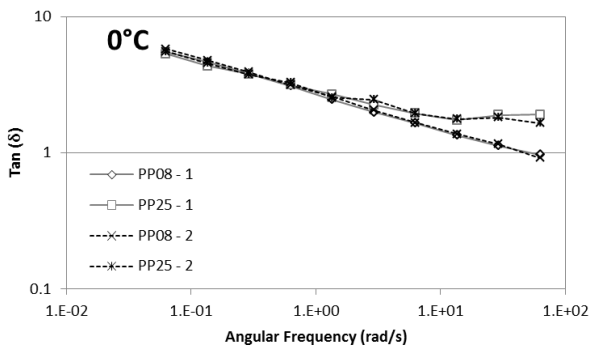
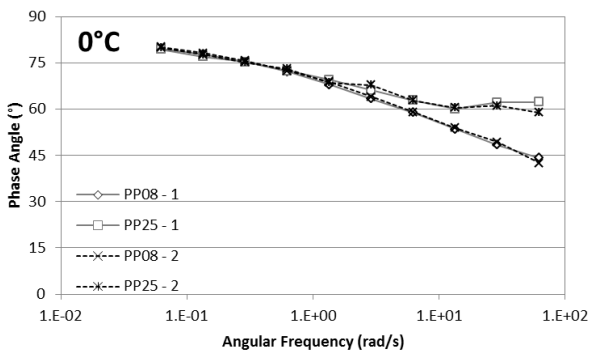
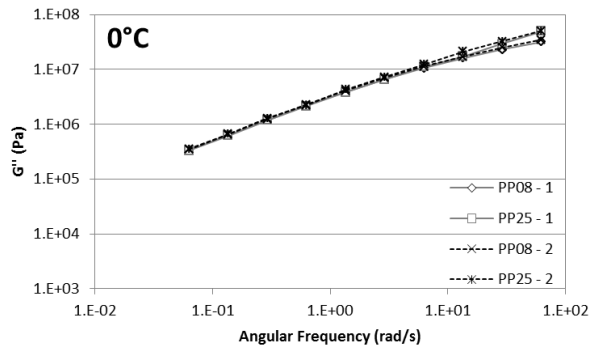
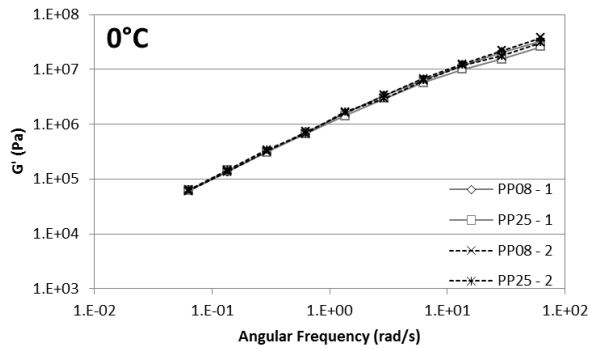
35/50 100M



Overlapping of G' (Pa), G'' (Pa), δ (°) and $\tan(\delta)$ at $T = 15^\circ\text{C}$

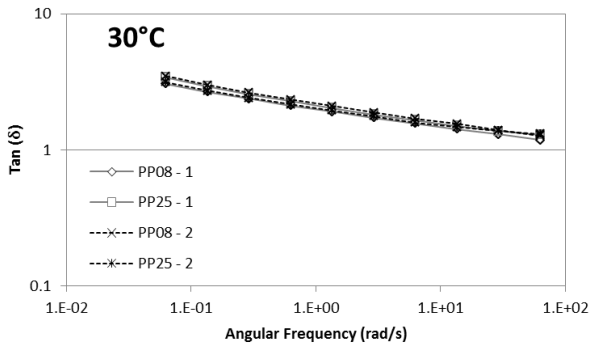
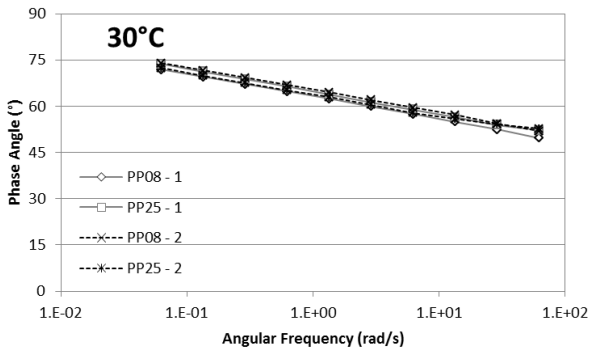
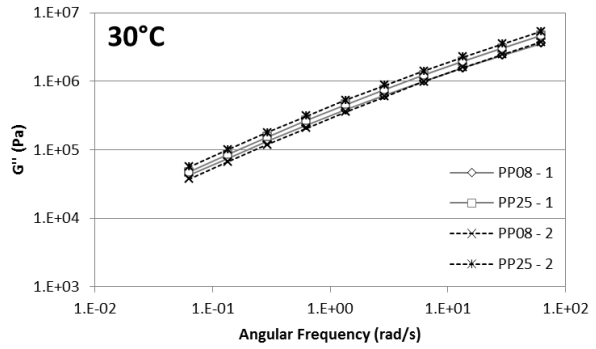
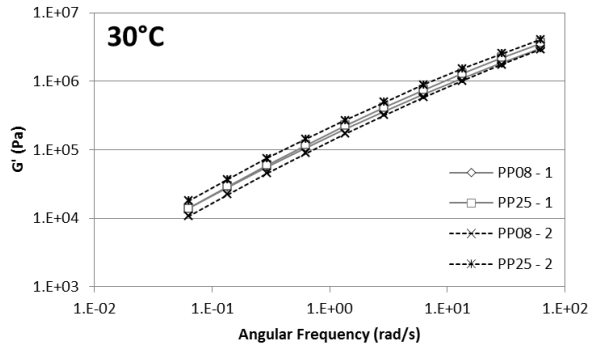


Overlapping of G' (Pa), G'' (Pa), δ (°) and $\text{Tan}(\delta)$ at $T = 10^\circ\text{C}$

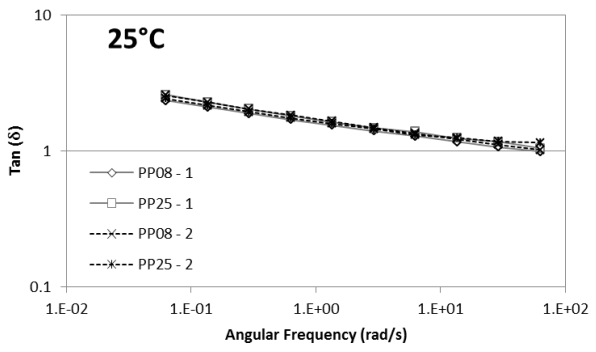
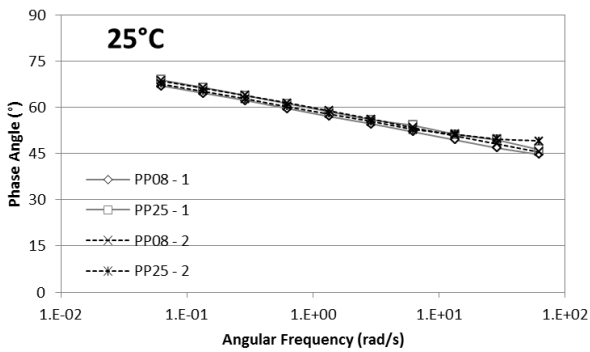
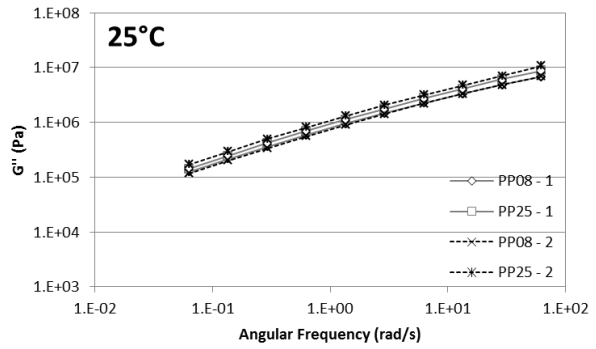
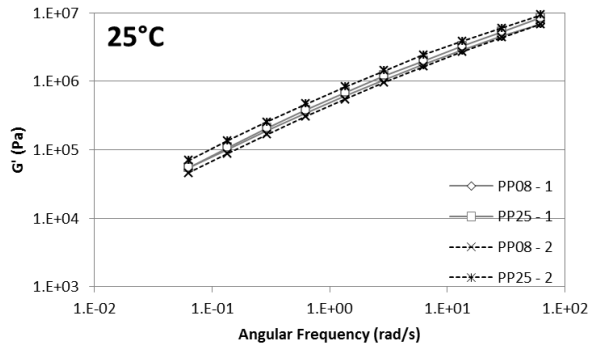


Overlapping of G' (Pa), G'' (Pa), δ (°) and $\text{Tan}(\delta)$ at $T = 0^\circ\text{C}$

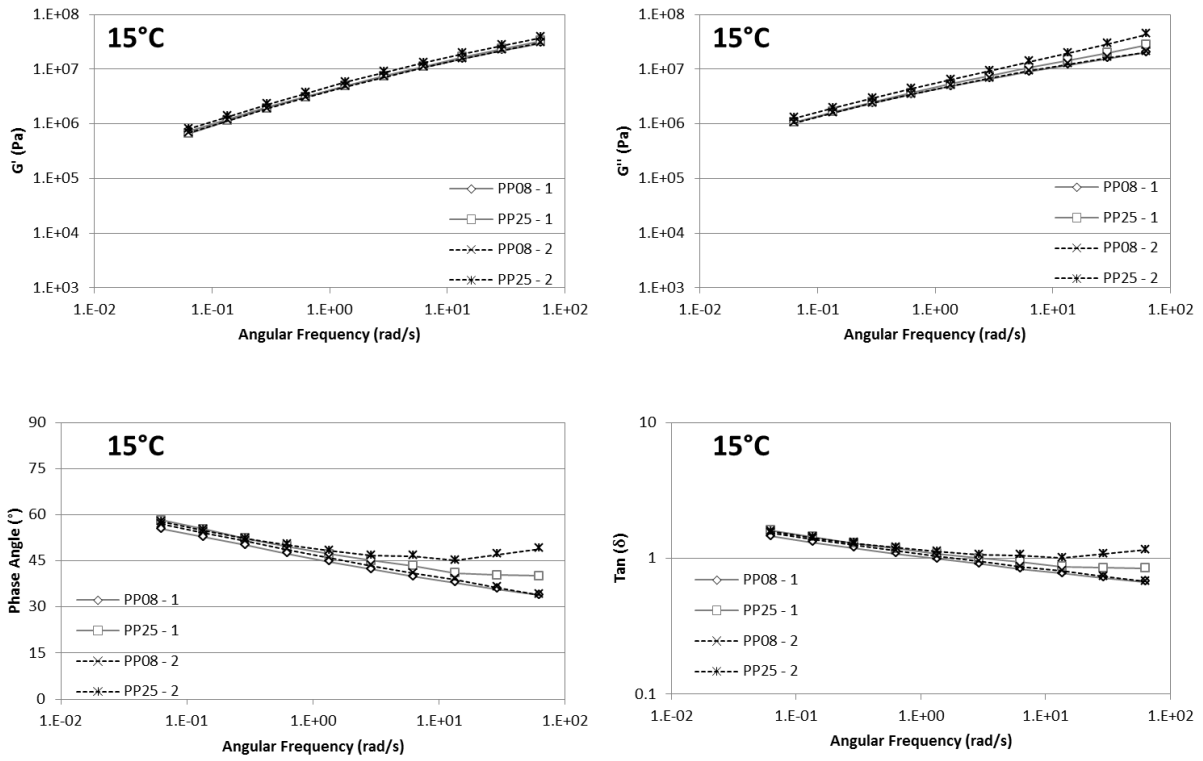
35/50 RTFOT



Overlapping of G' (Pa), G'' (Pa), δ (°) and $\text{Tan}(\delta)$ at $T = 30^\circ\text{C}$

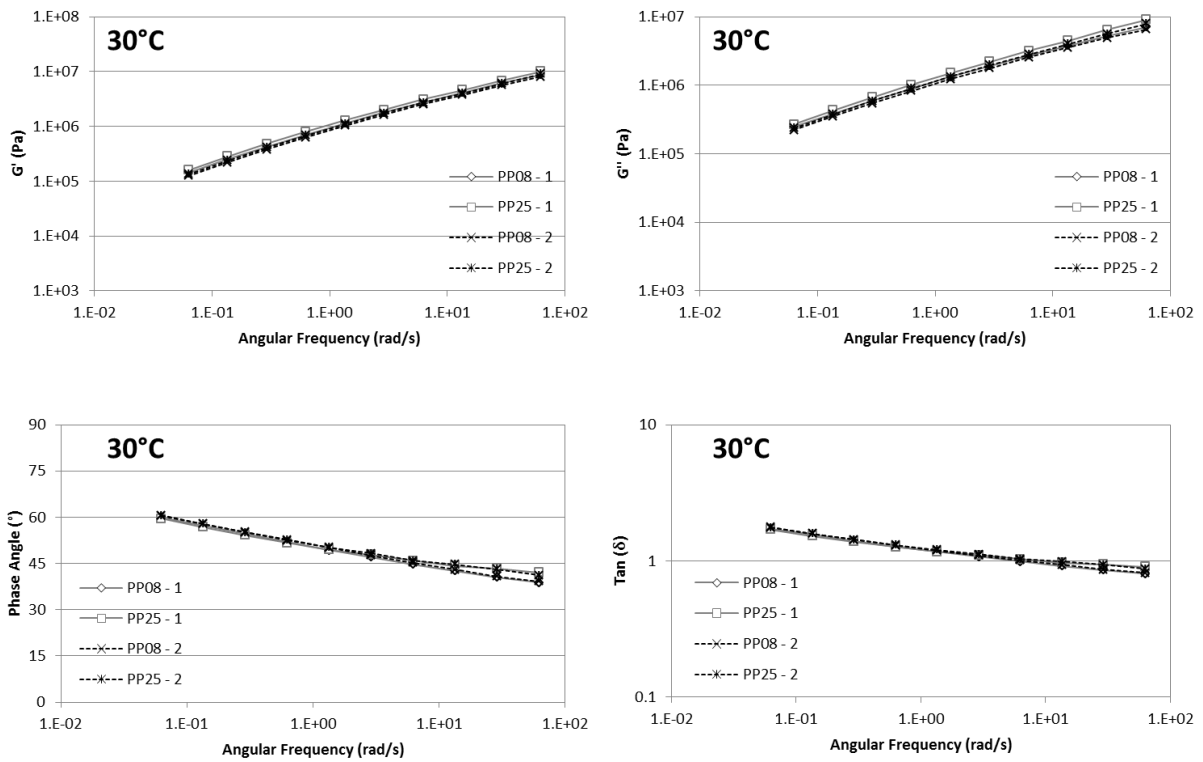


Overlapping of G' (Pa), G'' (Pa), δ (°) and $\text{Tan}(\delta)$ at $T = 25^\circ\text{C}$

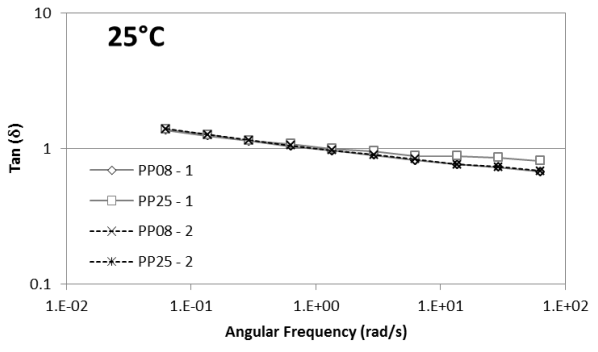
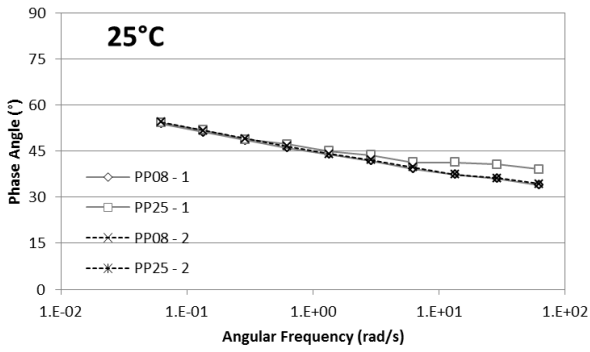
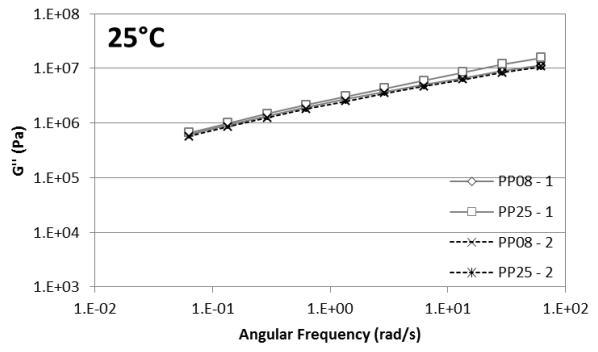
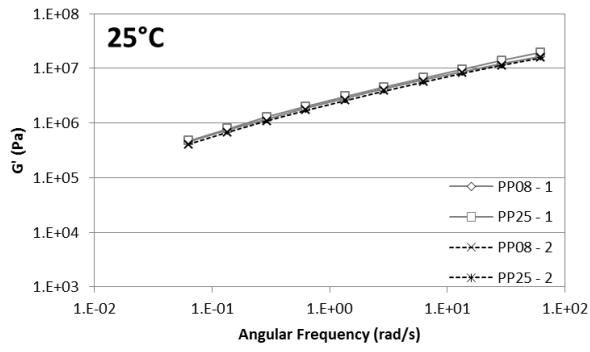


Overlapping of G' (Pa), G'' (Pa), δ (°) and $\tan(\delta)$ at $T = 15^\circ\text{C}$

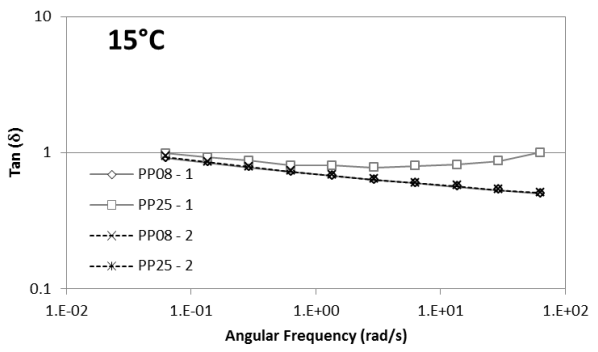
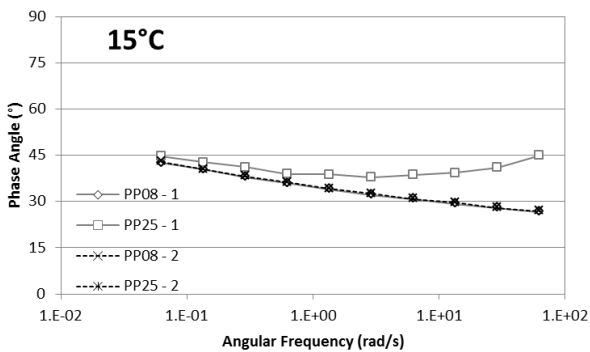
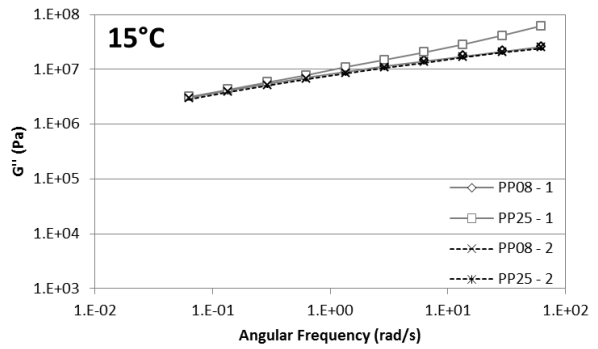
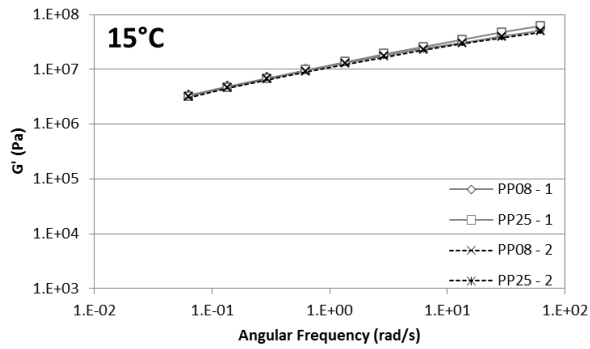
35/50 PAV



Overlapping of G' (Pa), G'' (Pa), δ (°) and $\tan(\delta)$ at $T = 30^\circ\text{C}$

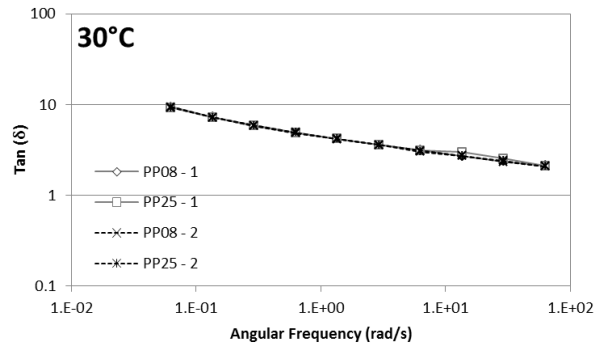
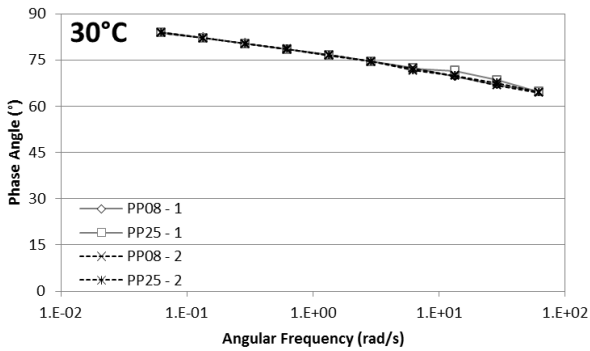
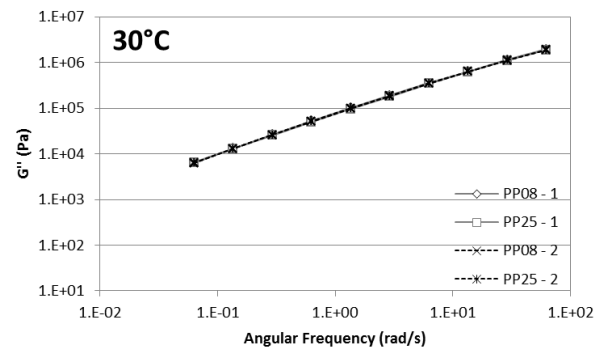
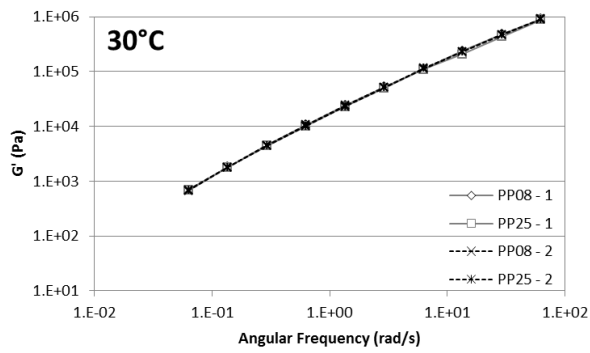


Overlapping of G' (Pa), G'' (Pa), δ (°) and $\text{Tan}(\delta)$ at $T = 25^\circ\text{C}$

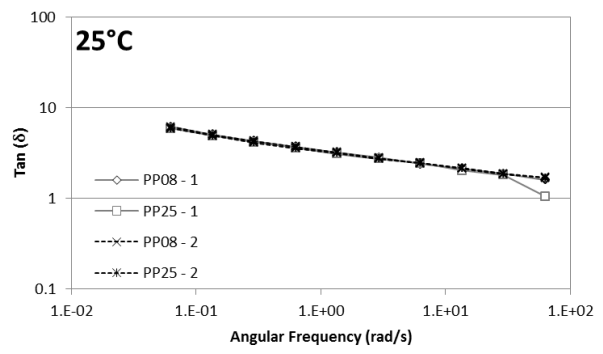
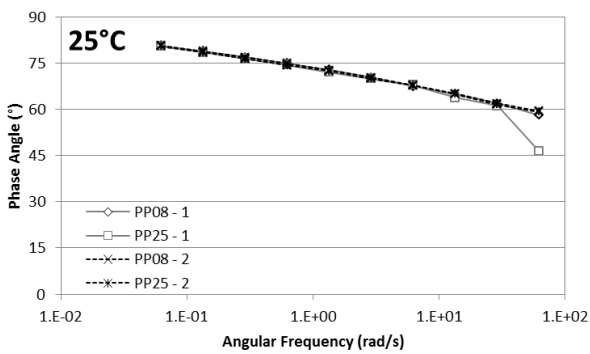
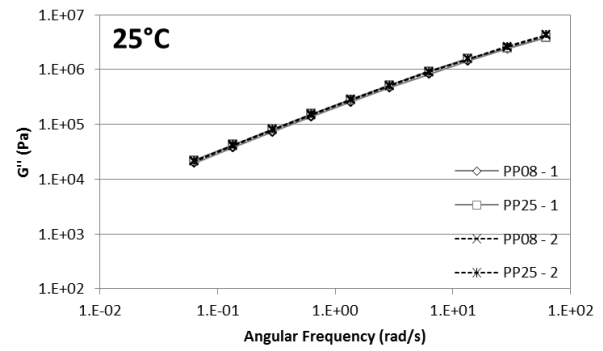
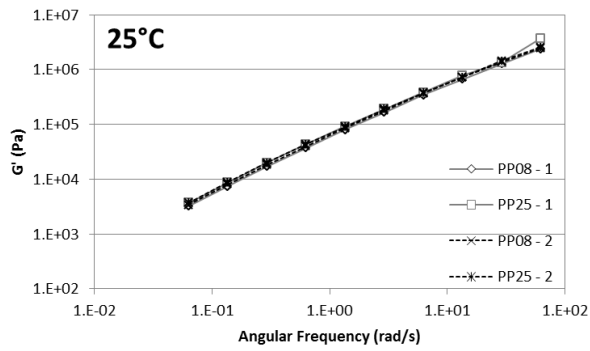


Overlapping of G' (Pa), G'' (Pa), δ (°) and $\text{Tan}(\delta)$ at $T = 15^\circ\text{C}$

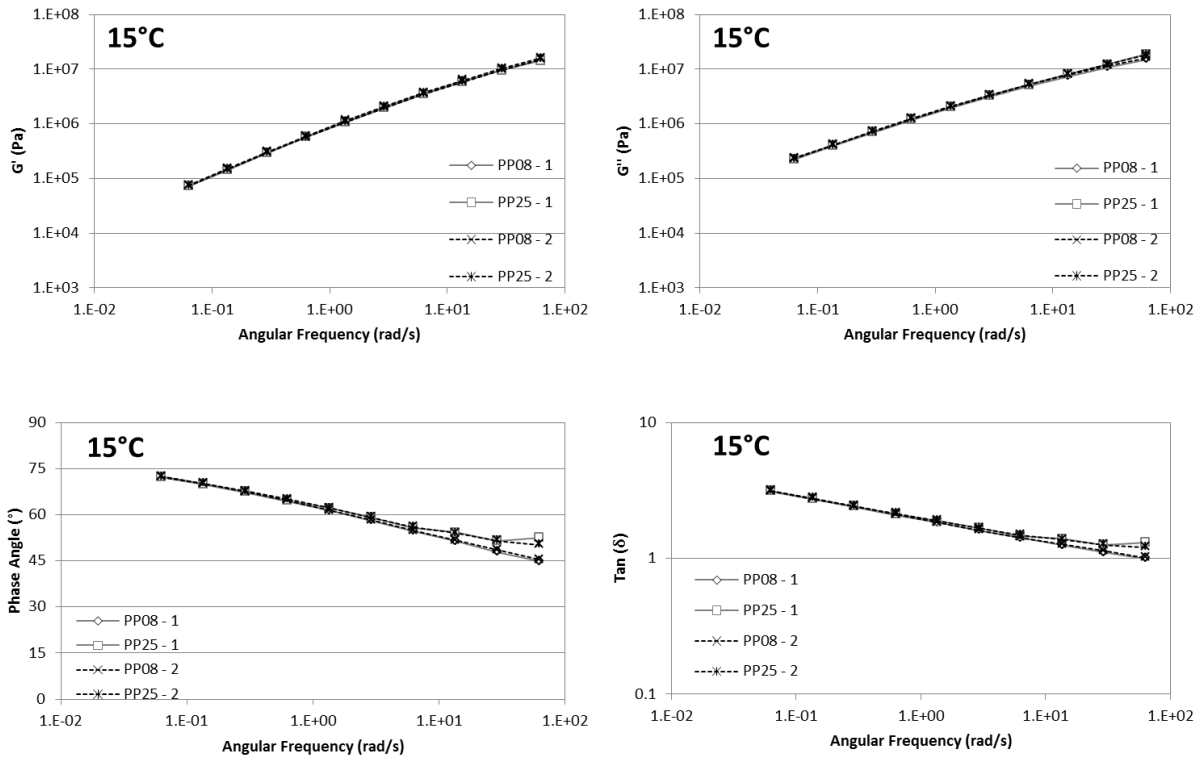
50/70 NEAT BITUMEN



Overlapping of G' (Pa), G'' (Pa), δ (°) and $\text{Tan}(\delta)$ at $T = 30^\circ\text{C}$

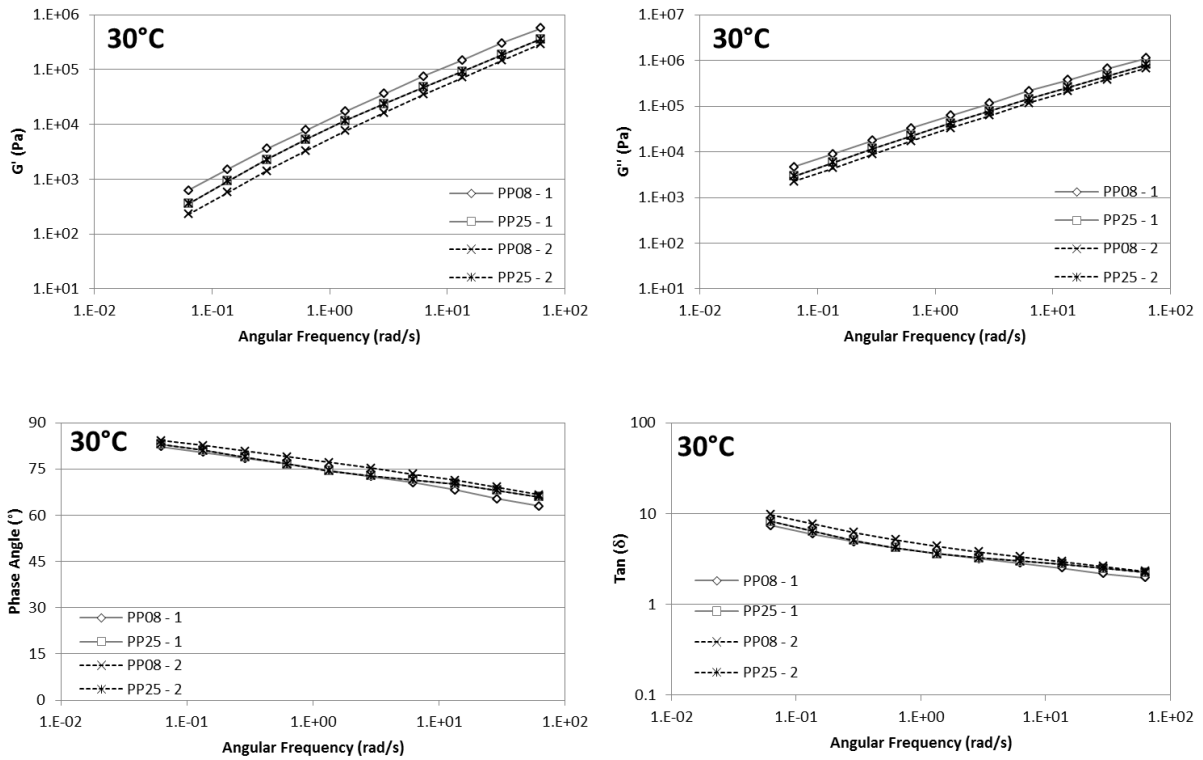


Overlapping of G' (Pa), G'' (Pa), δ (°) and $\text{Tan}(\delta)$ at $T = 25^\circ\text{C}$

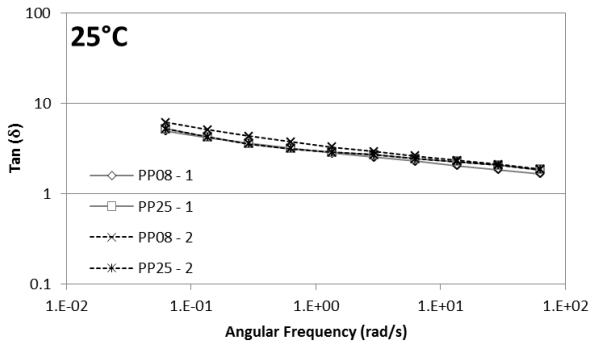
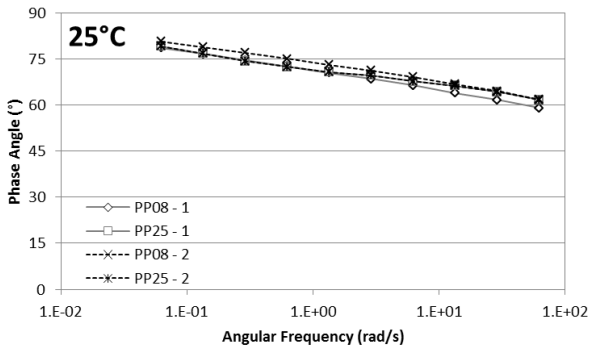
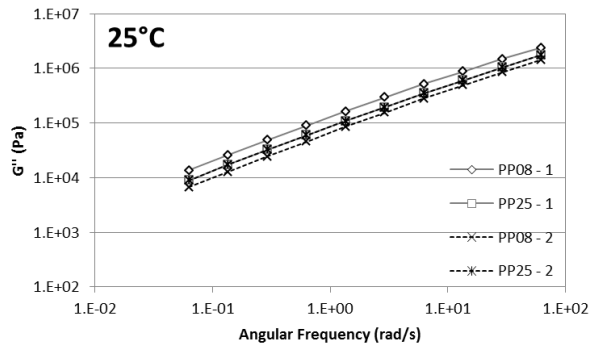
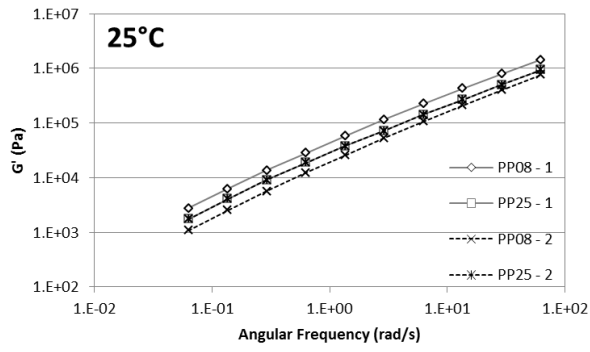


Overlapping of G' (Pa), G'' (Pa), δ ($^\circ$) and $\tan(\delta)$ at $T = 15^\circ\text{C}$

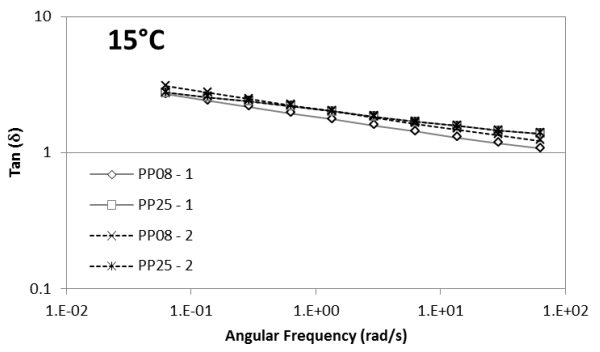
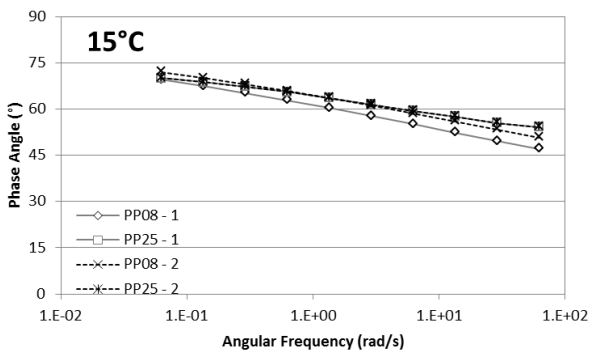
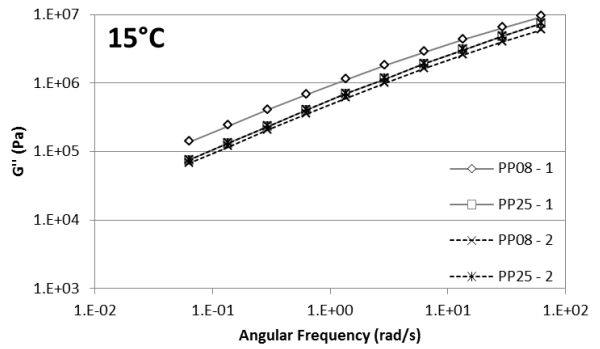
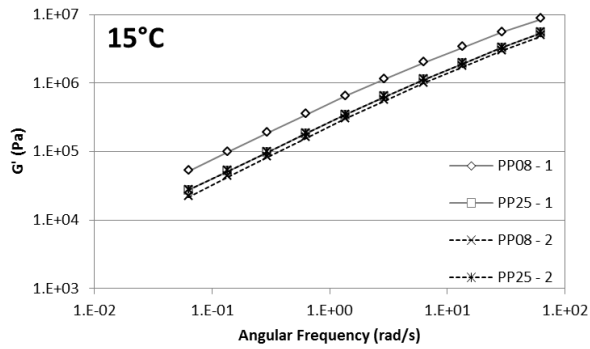
50/70 86M+14A



Overlapping of G' (Pa), G'' (Pa), δ ($^\circ$) and $\tan(\delta)$ at $T = 30^\circ\text{C}$

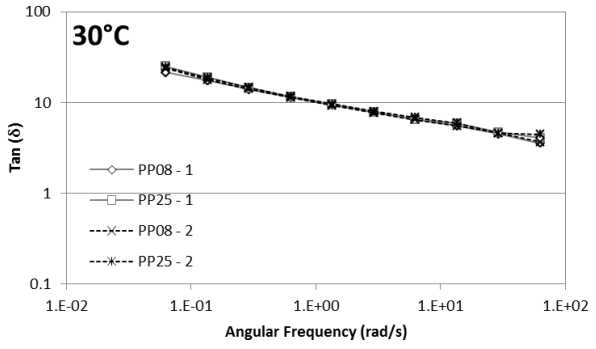
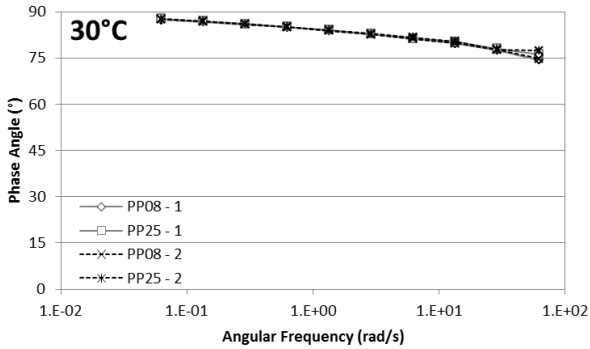
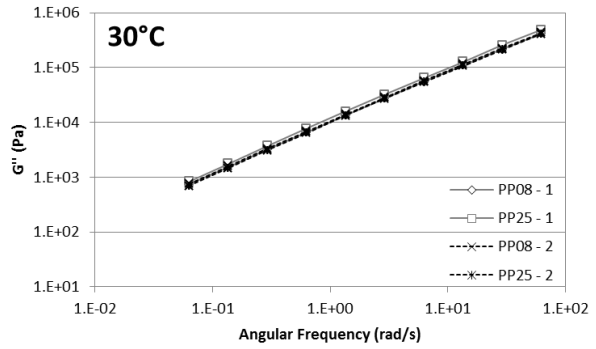
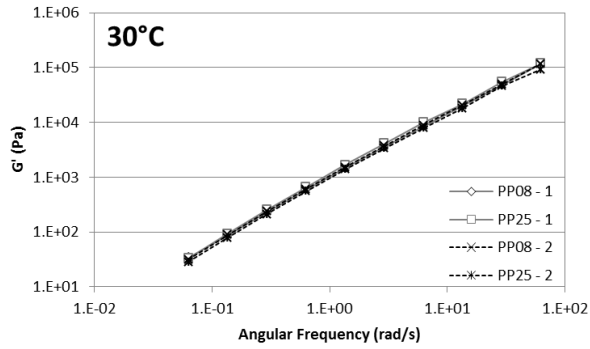


Overlapping of G' (Pa), G'' (Pa), δ (°) and $\text{Tan}(\delta)$ at $T = 25^\circ\text{C}$

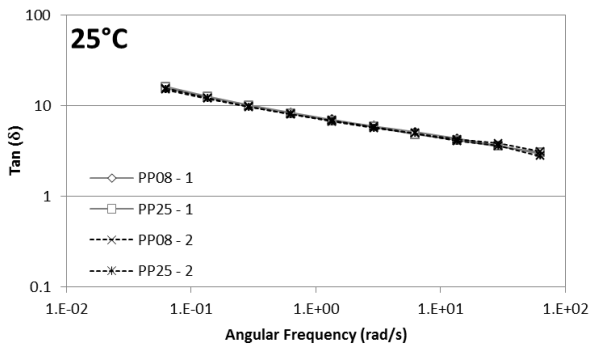
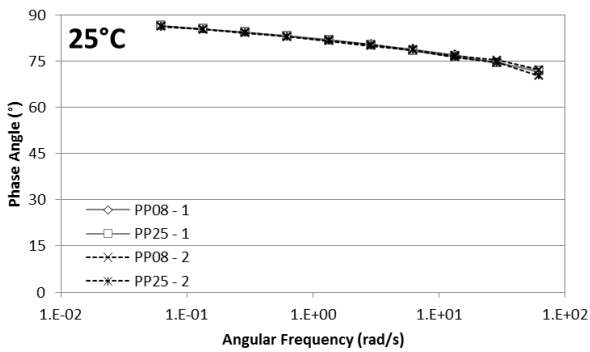
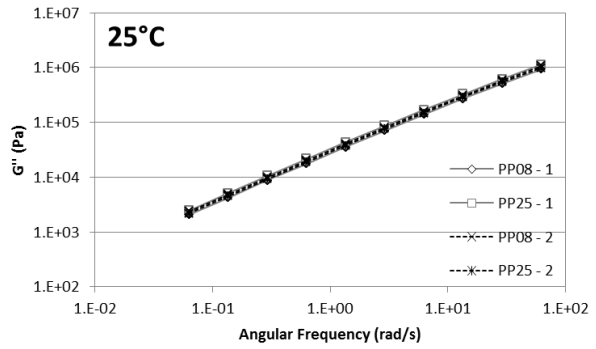
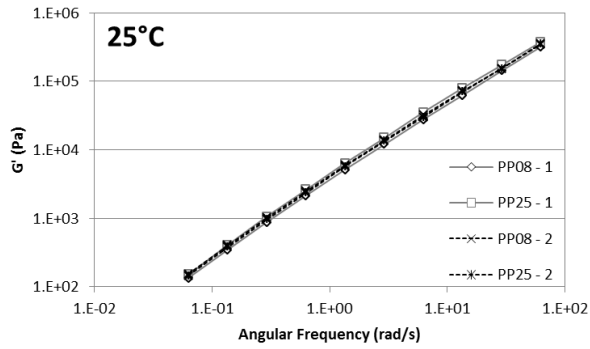


Overlapping of G' (Pa), G'' (Pa), δ (°) and $\text{Tan}(\delta)$ at $T = 15^\circ\text{C}$

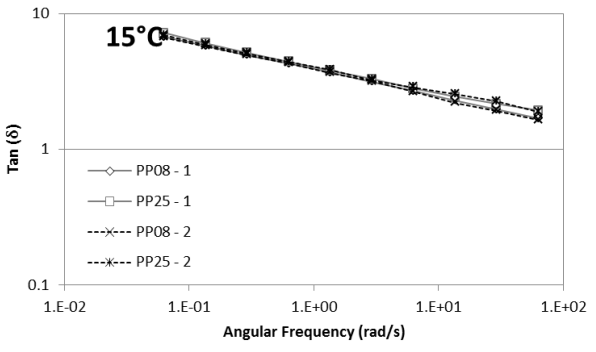
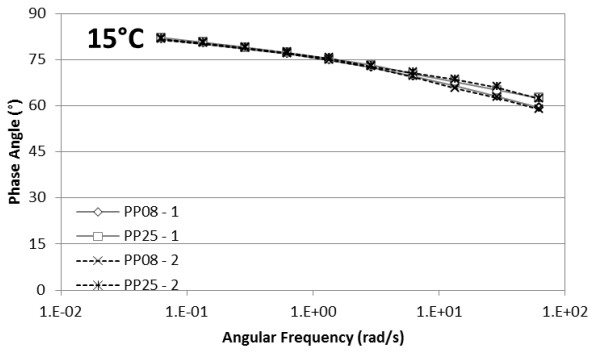
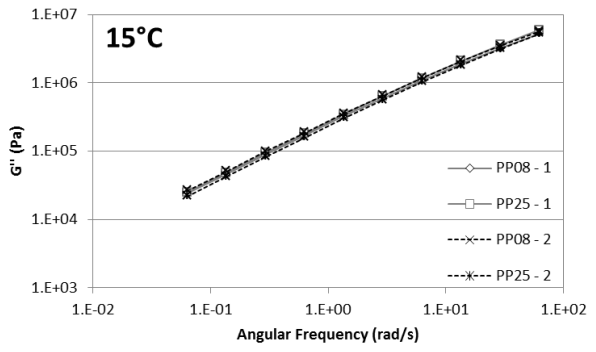
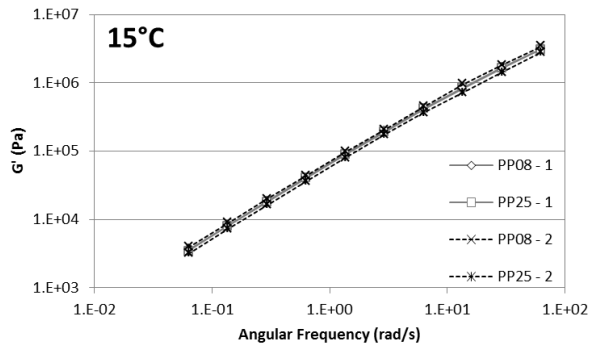
50/70 91M+9A



Overlapping of G' (Pa), G'' (Pa), δ (°) and $\text{Tan}(\delta)$ at $T = 30^\circ\text{C}$

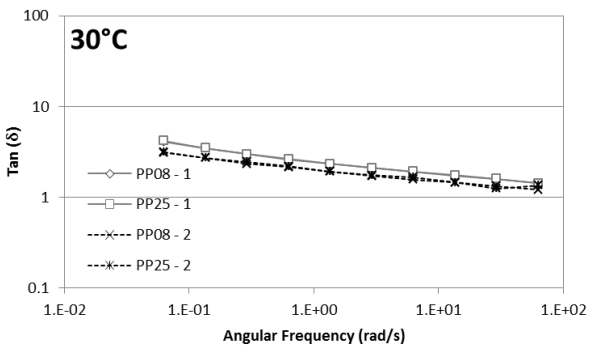
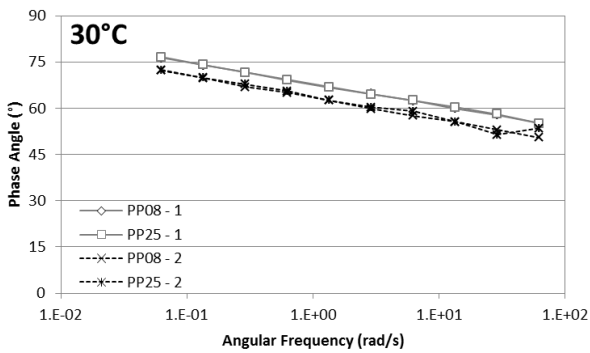
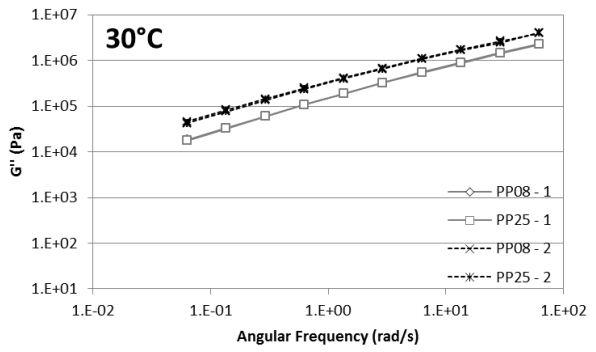
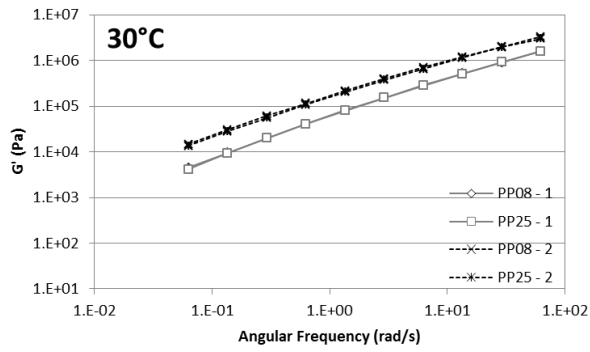


Overlapping of G' (Pa), G'' (Pa), δ (°) and $\text{Tan}(\delta)$ at $T = 25^\circ\text{C}$

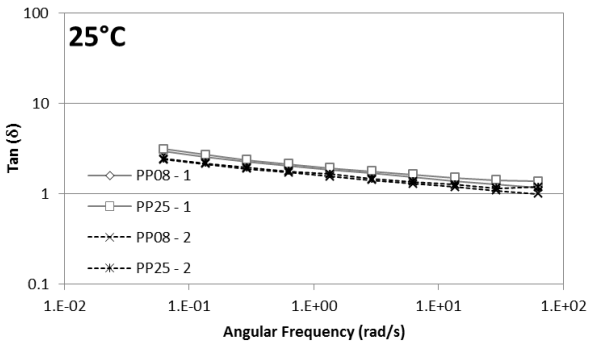
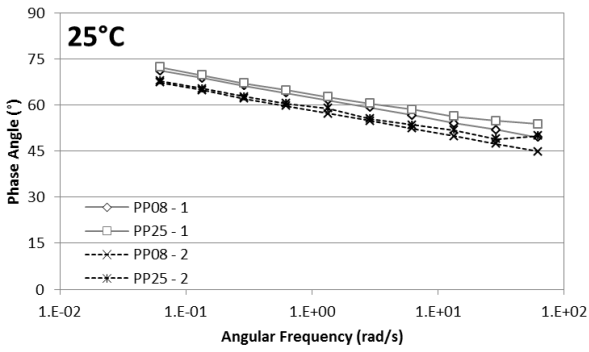
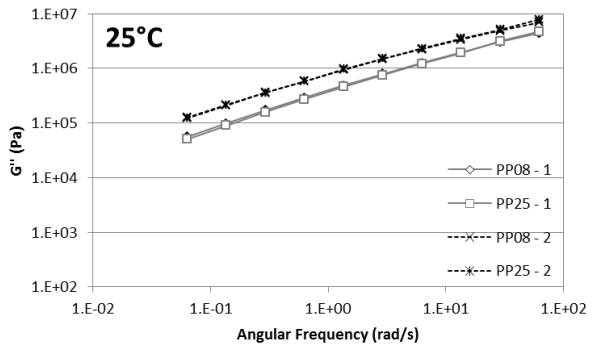
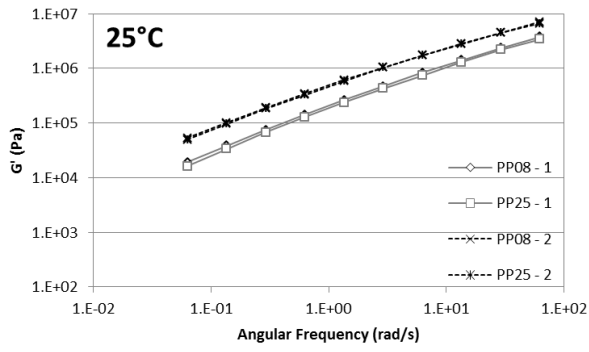


Overlapping of G' (Pa), G'' (Pa), δ (°) and $\text{Tan}(\delta)$ at $T = 15^\circ\text{C}$

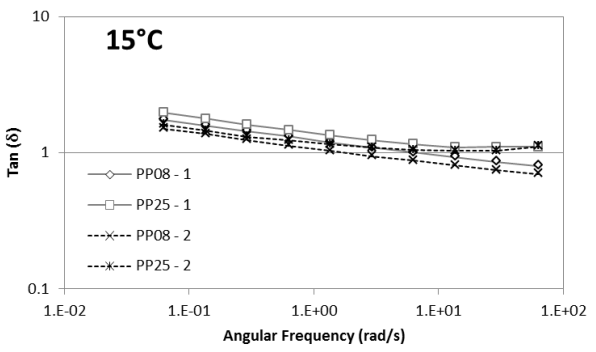
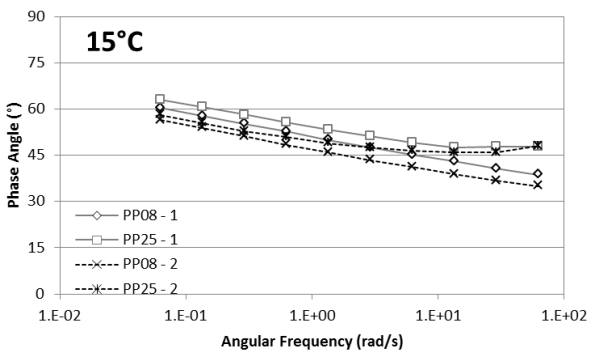
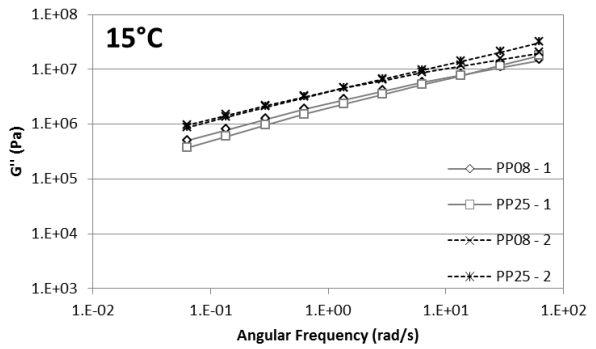
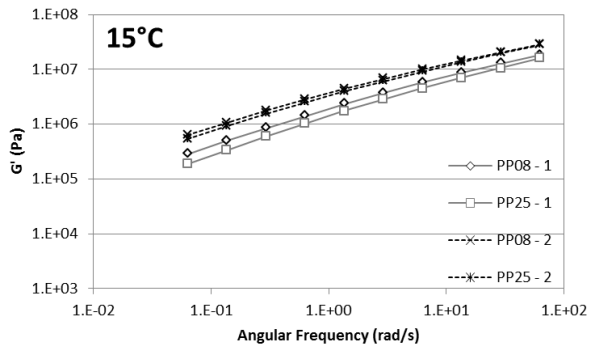
50/70 81M+19A



Overlapping of G' (Pa), G'' (Pa), δ (°) and $\text{Tan}(\delta)$ at $T = 30^\circ\text{C}$

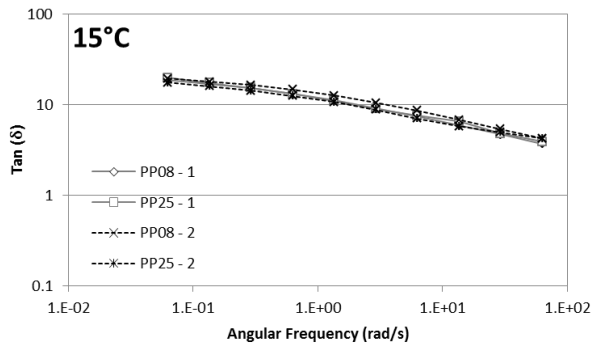
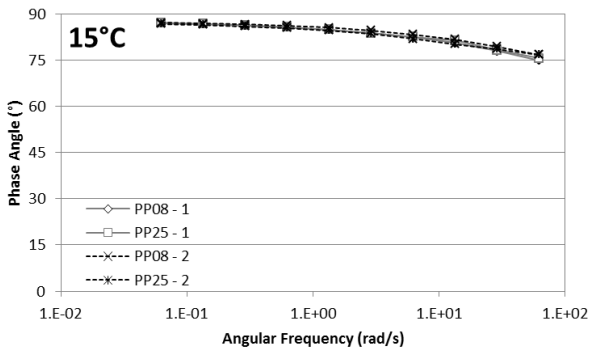
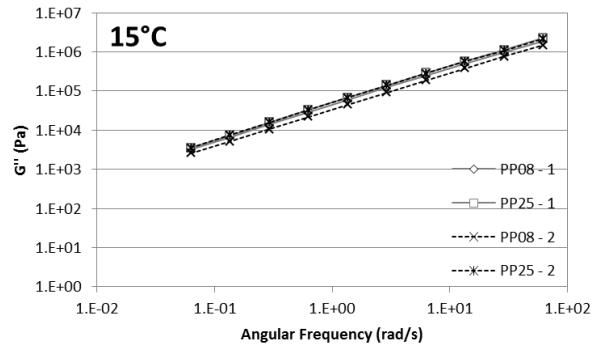
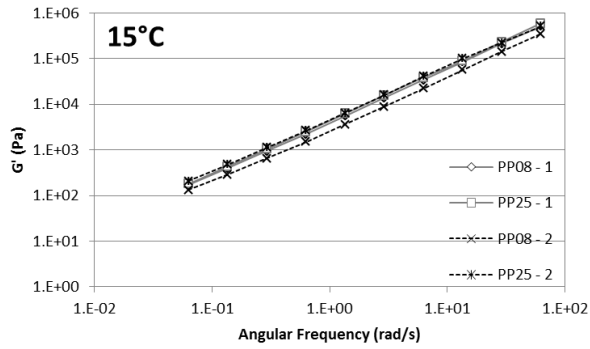


Overlapping of G' (Pa), G'' (Pa), δ (°) and $\text{Tan}(\delta)$ at $T = 25^\circ\text{C}$

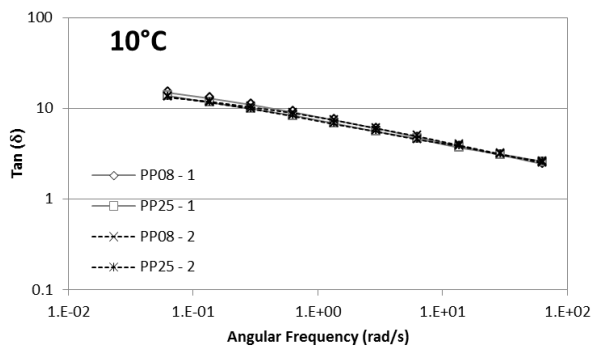
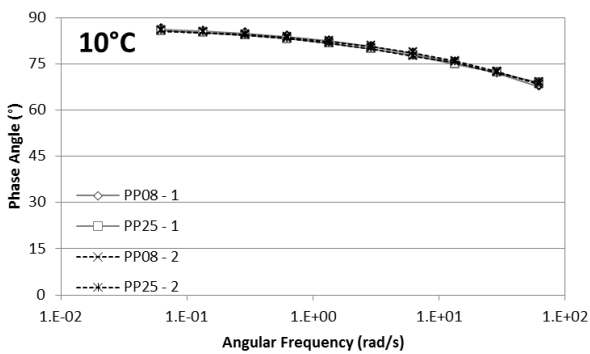
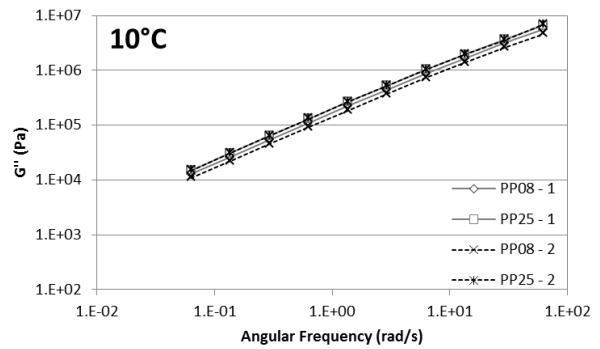
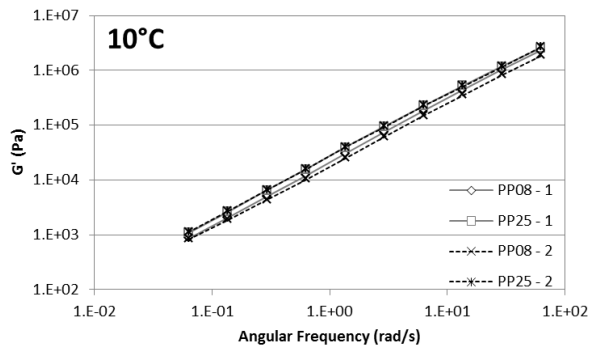


Overlapping of G' (Pa), G'' (Pa), δ (°) and $\text{Tan}(\delta)$ at $T = 15^\circ\text{C}$

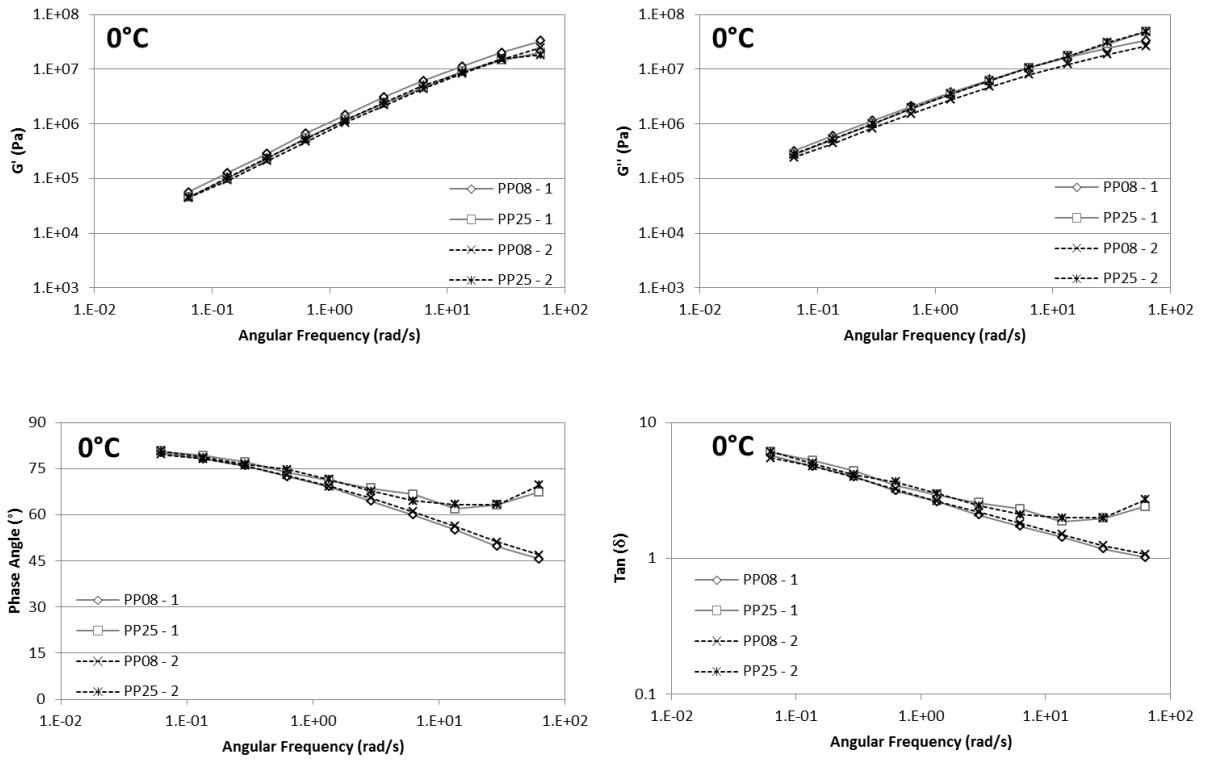
50/70 100M



Overlapping of G' (Pa), G'' (Pa), δ (°) and $\text{Tan}(\delta)$ at $T = 15^\circ\text{C}$



Overlapping of G' (Pa), G'' (Pa), δ (°) and $\text{Tan}(\delta)$ at $T = 10^\circ\text{C}$

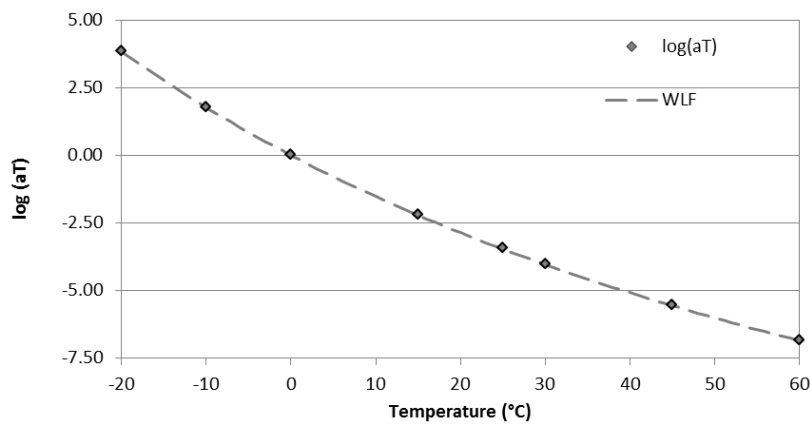
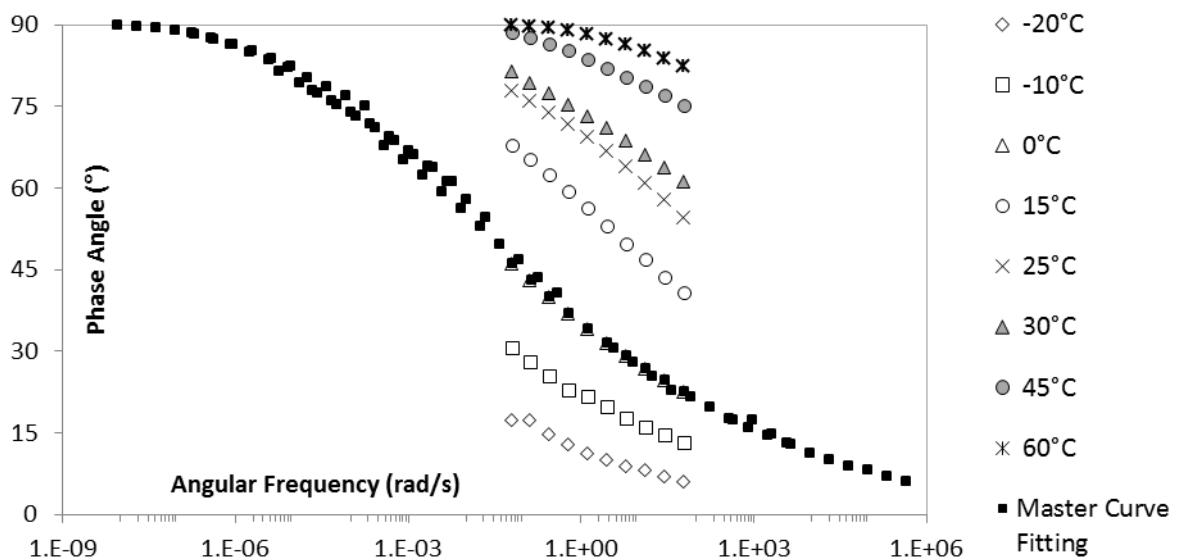
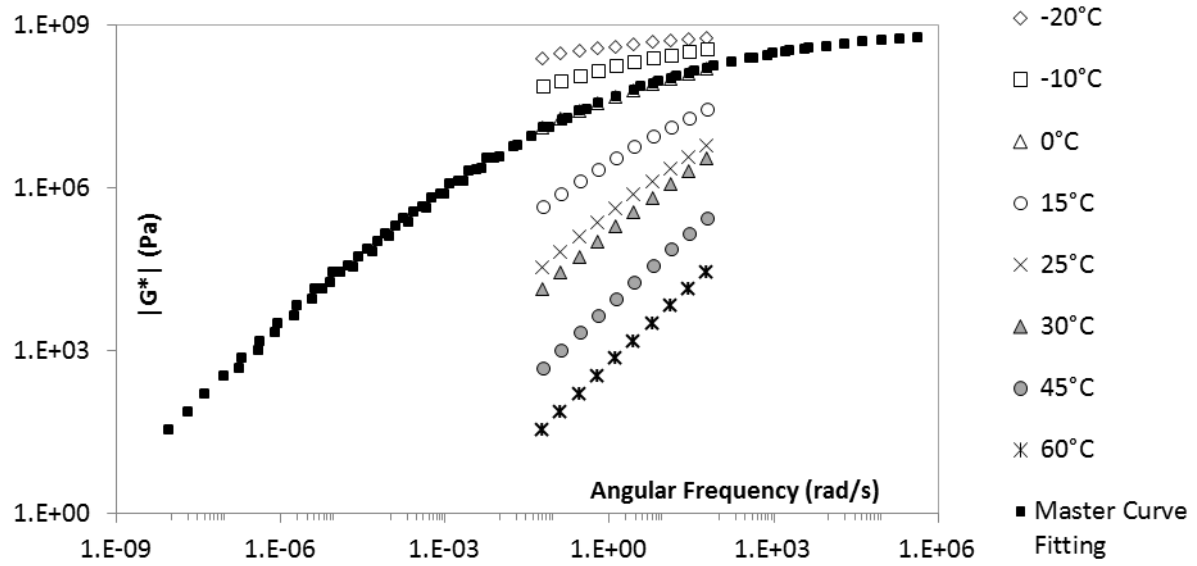


Overlapping of G' (Pa), G'' (Pa), $\delta(^{\circ})$ and $\text{Tan}(\delta)$ at $T = 0^{\circ}\text{C}$

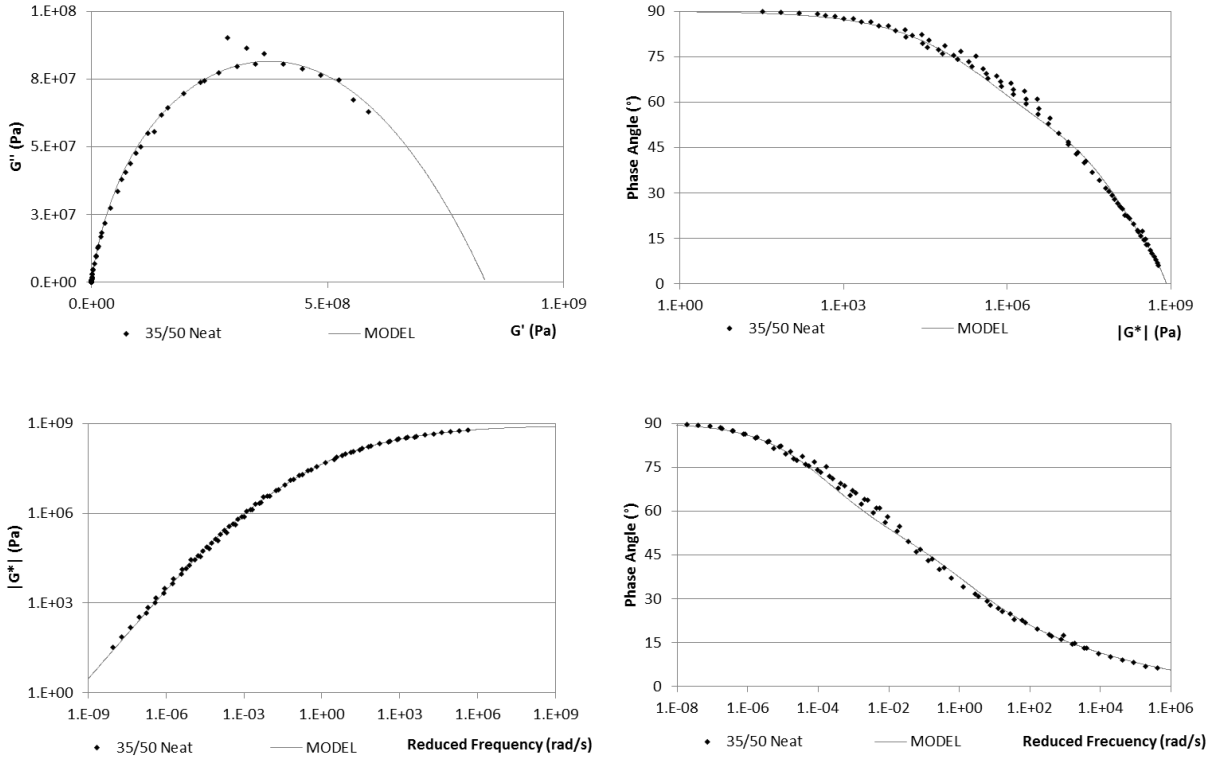
Annex 2

MASTER CURVES, WLF ADJUSTMENT, BLACK DIAGRAMS AND COLE-
COLE PLAN OF MODEL AND AGED BITUMENS

35/50 NEAT BITUMEN

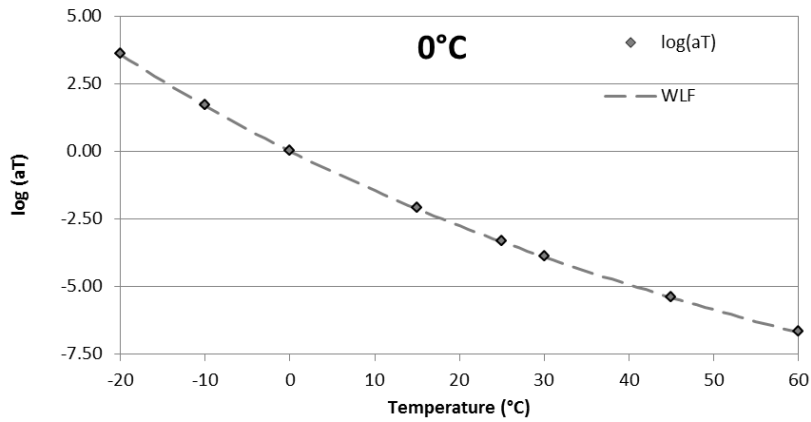
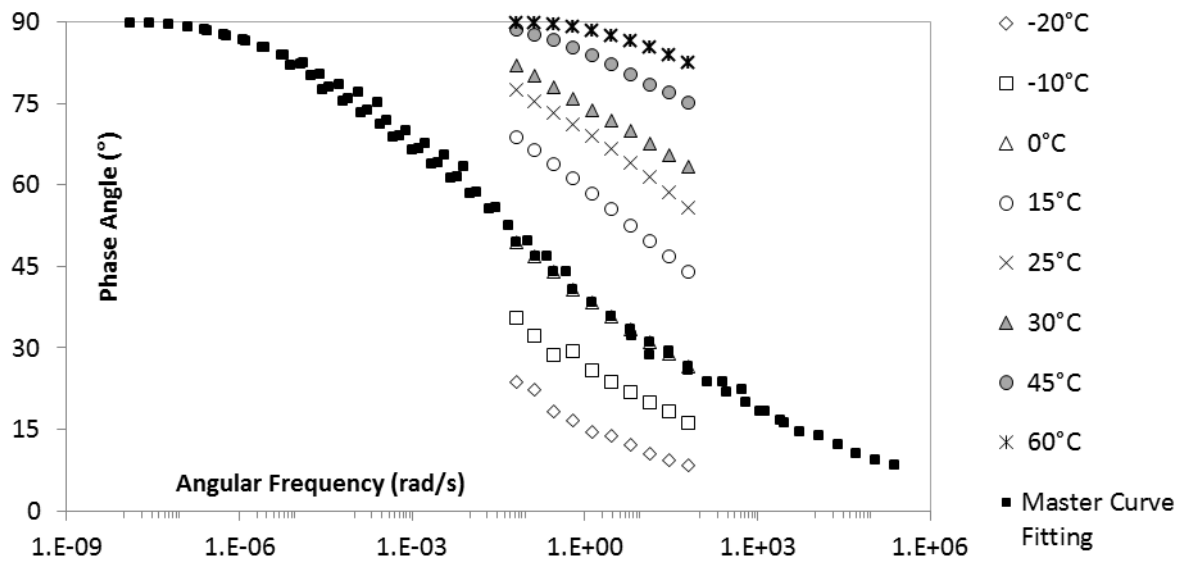
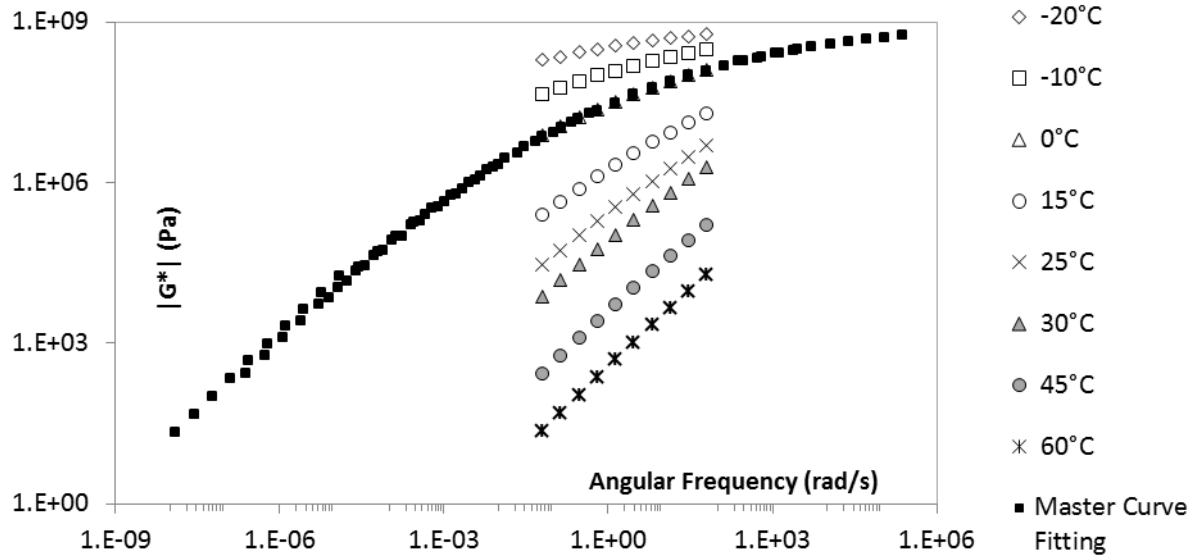


Rheological data measurements and WLF adjustment

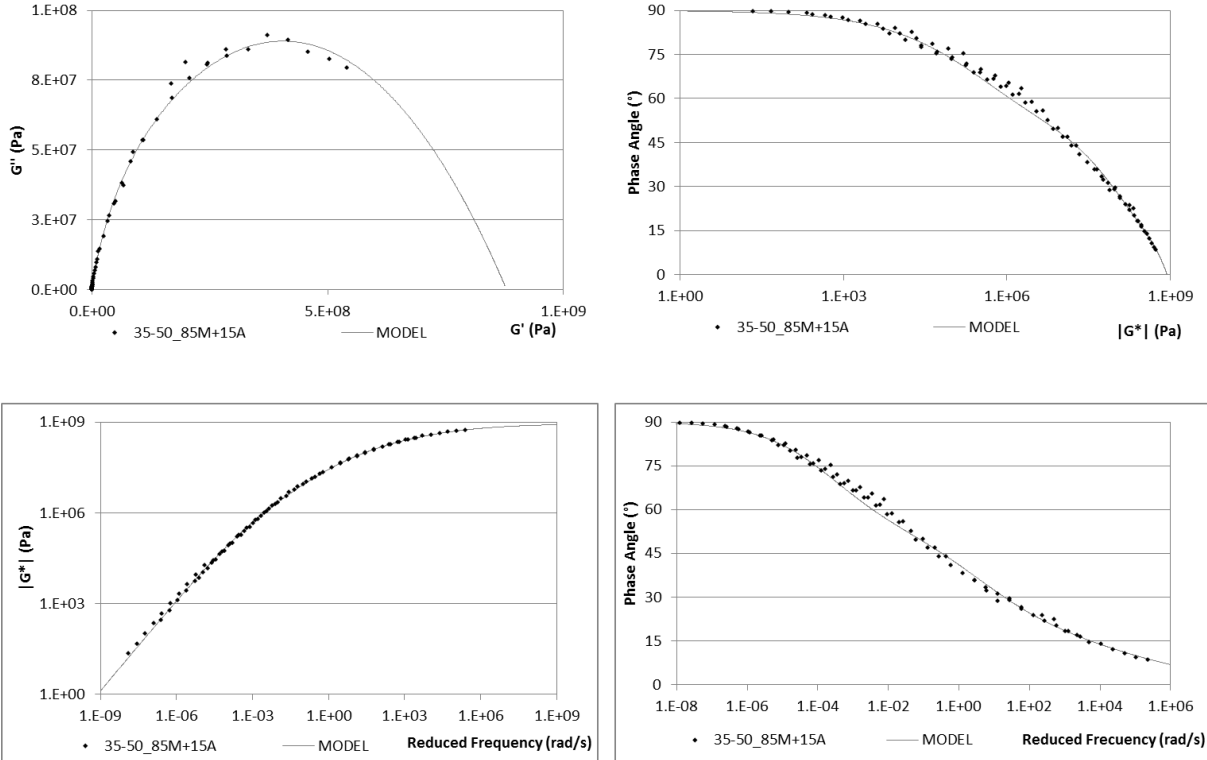


Cole-Cole plan, Black diagram and $|G^*|$ and δ master curves

35/50 85M+15A

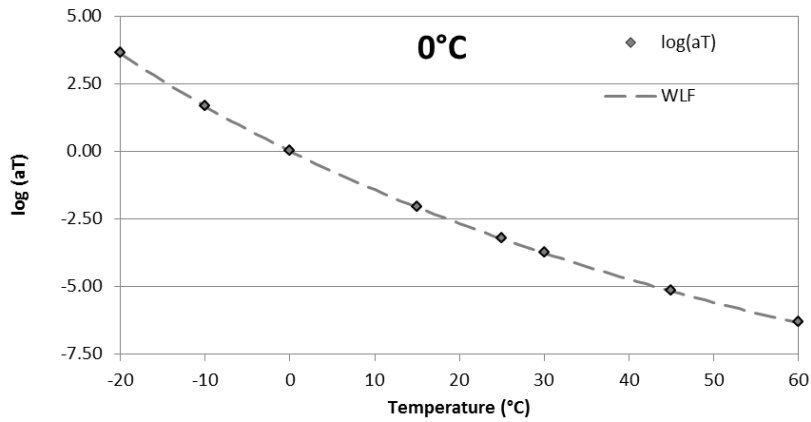
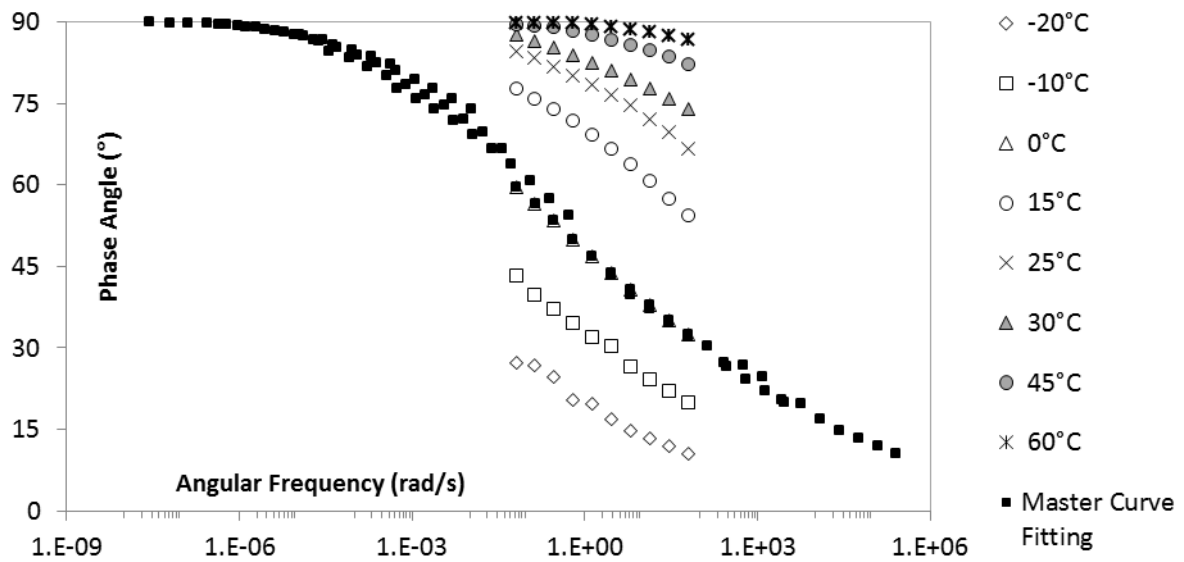
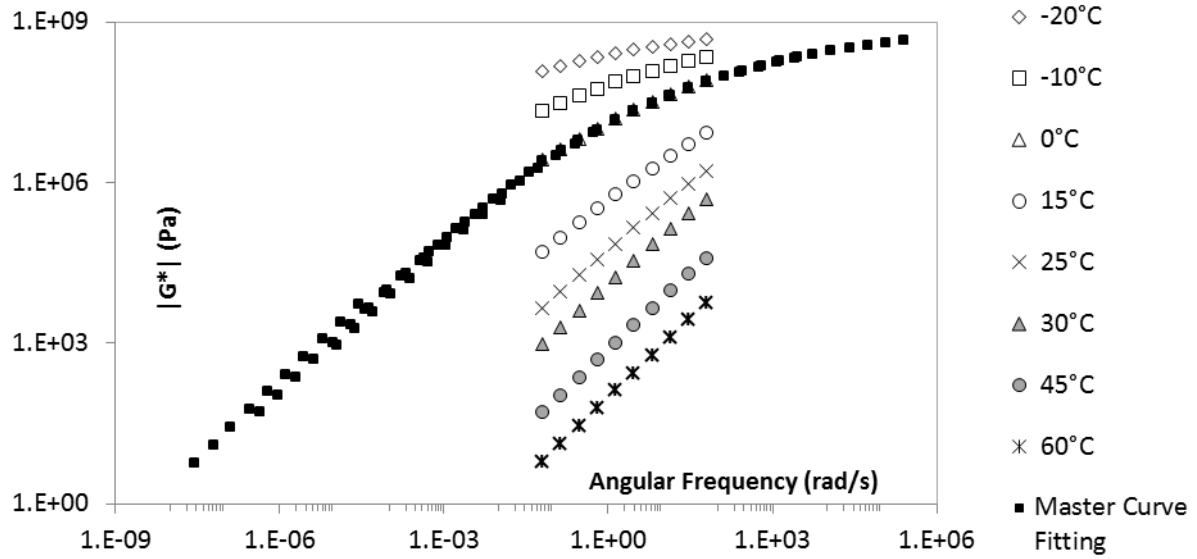


Rheological data measurements and WLF adjustment

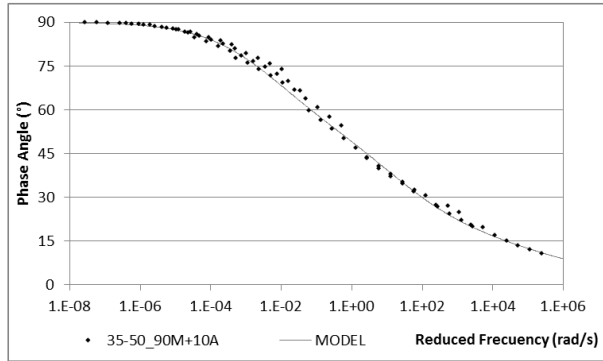
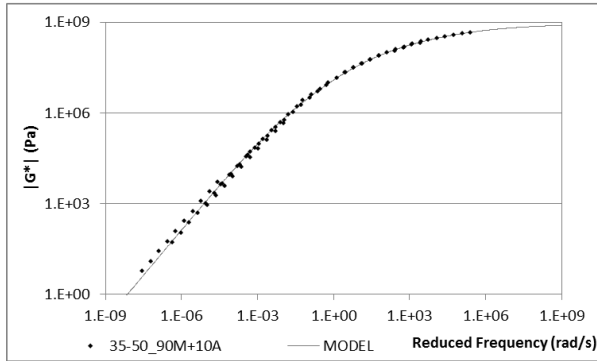
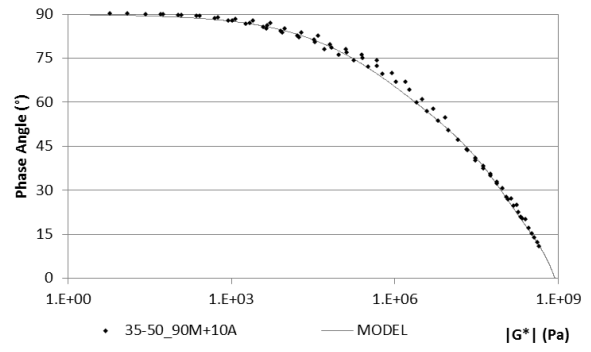
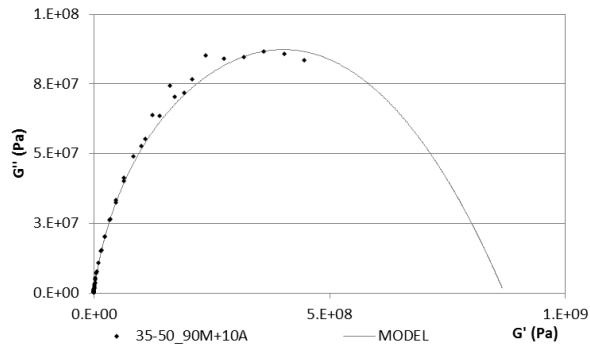


Cole-Cole plan, Black diagram and $|G^*|$ and δ master curves

35/50 90M+10A

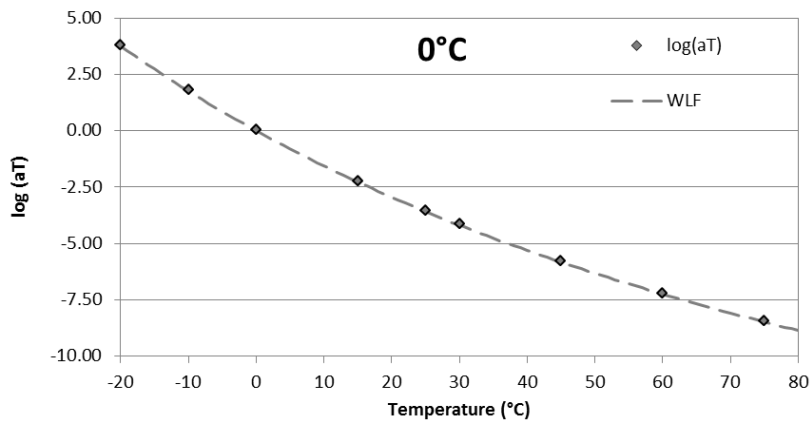
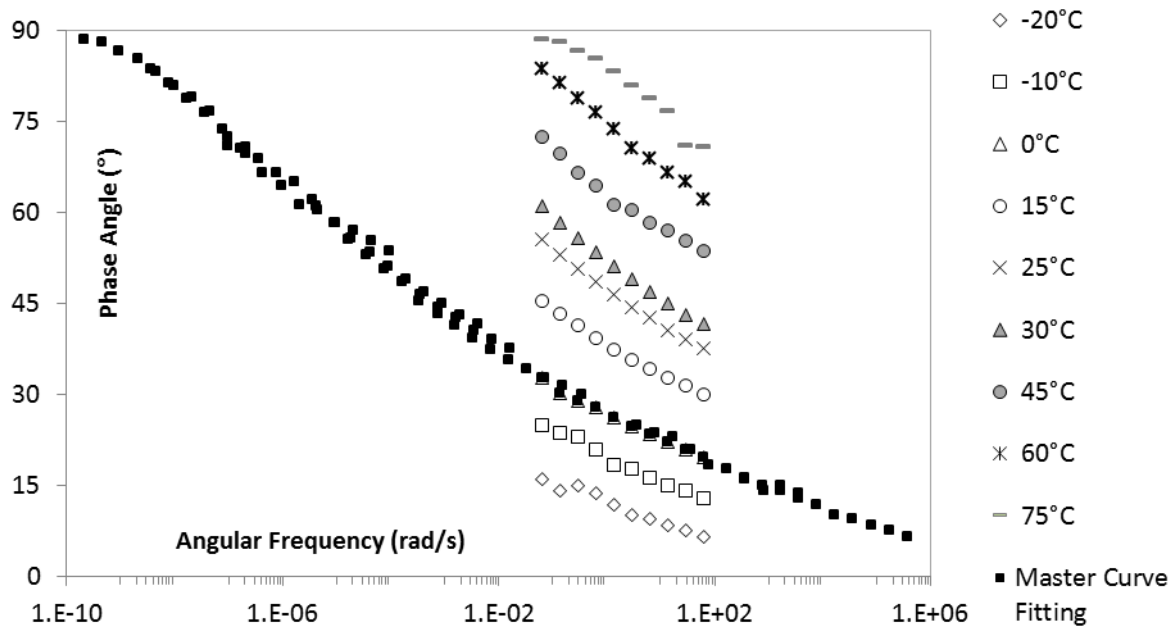
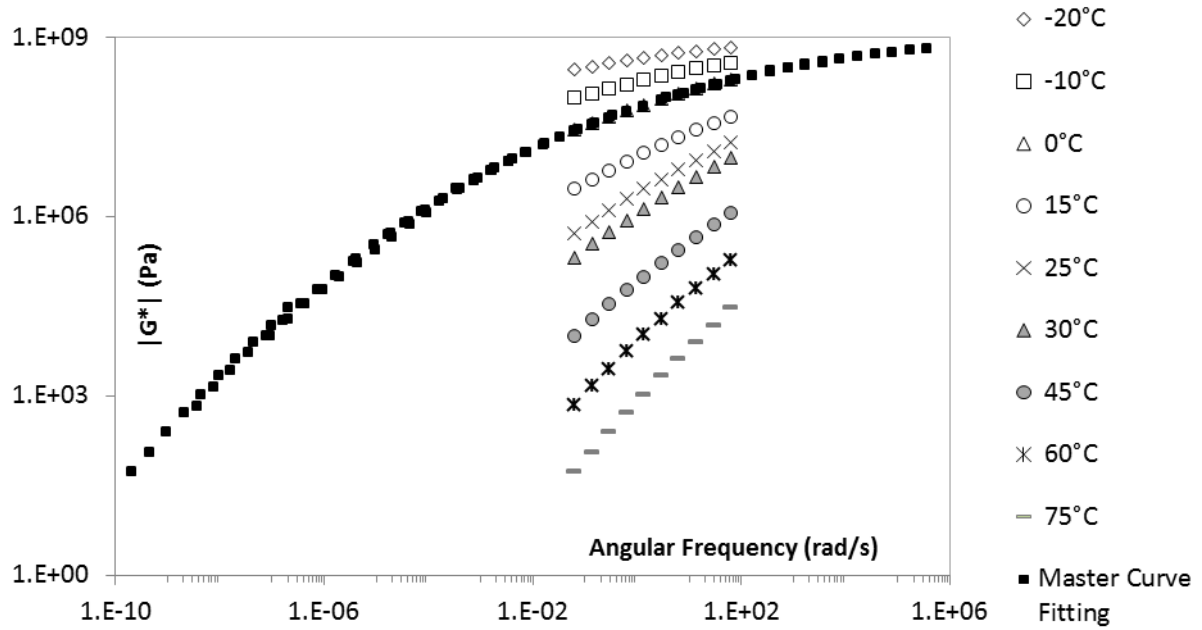


Rheological data measurements and WLF adjustment

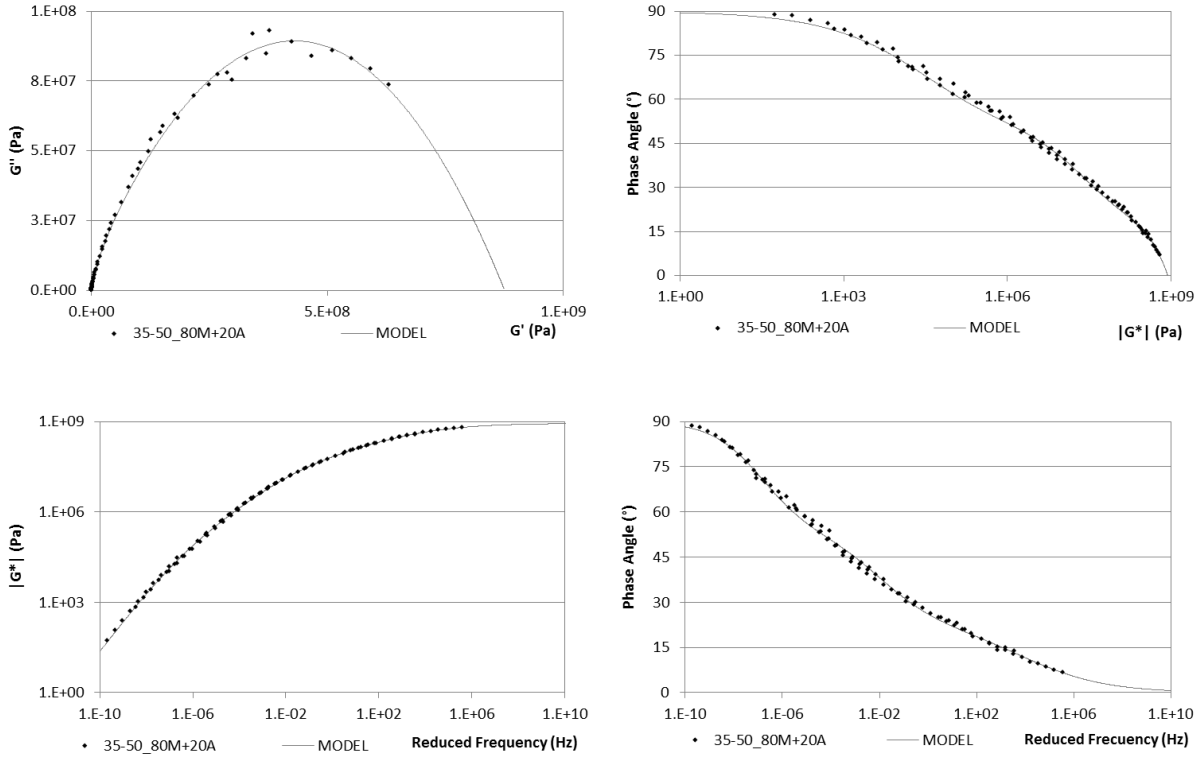


Cole-Cole plan, Black diagram and $|G^*|$ and δ master curves

35/50 80M+20A

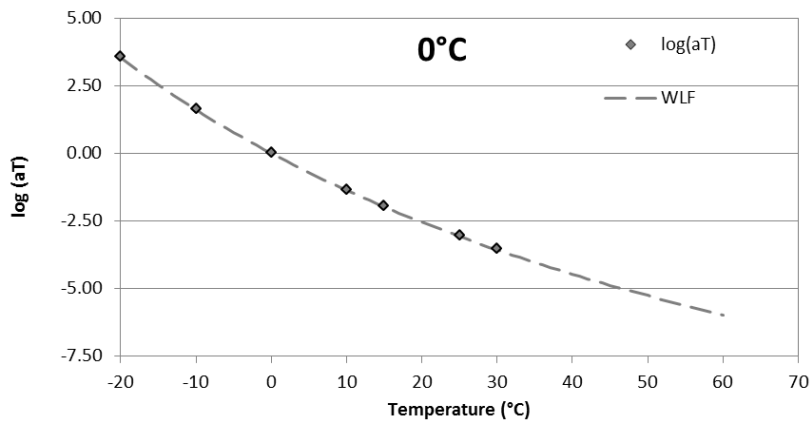
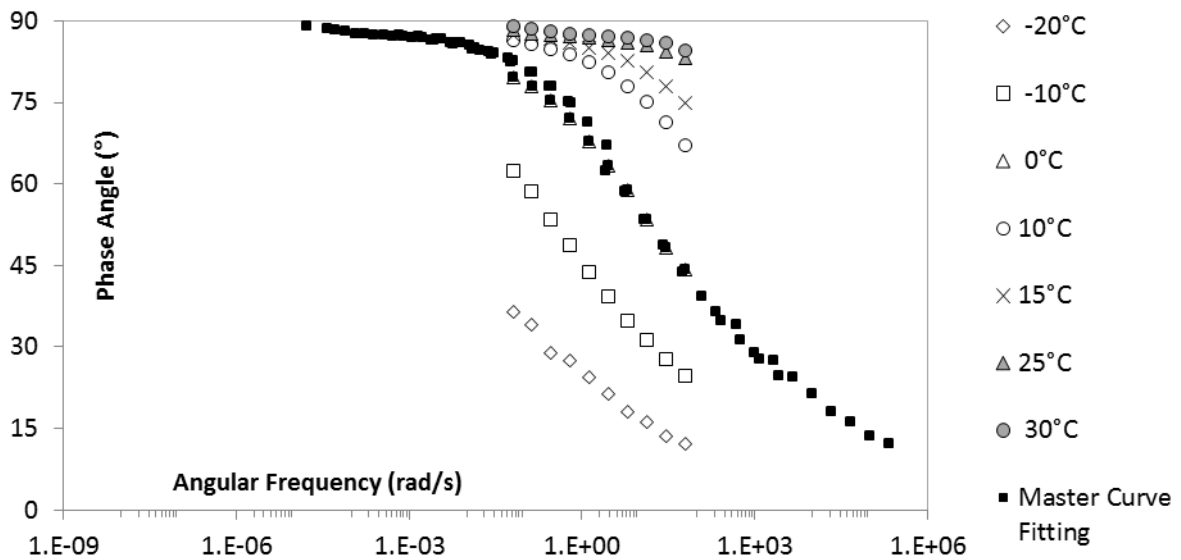
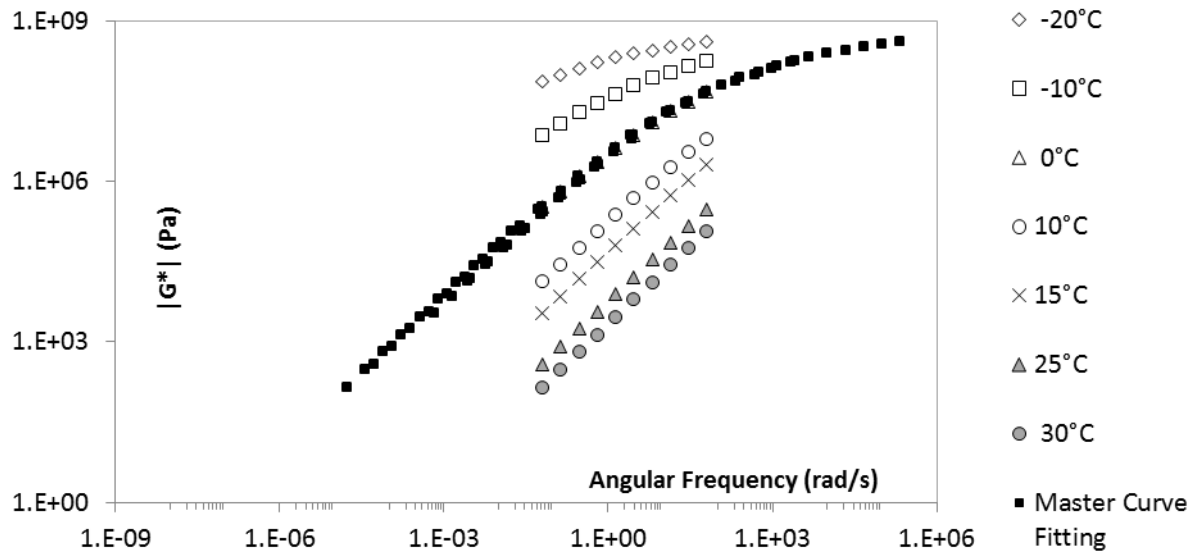


Rheological data measurements and WLF adjustment

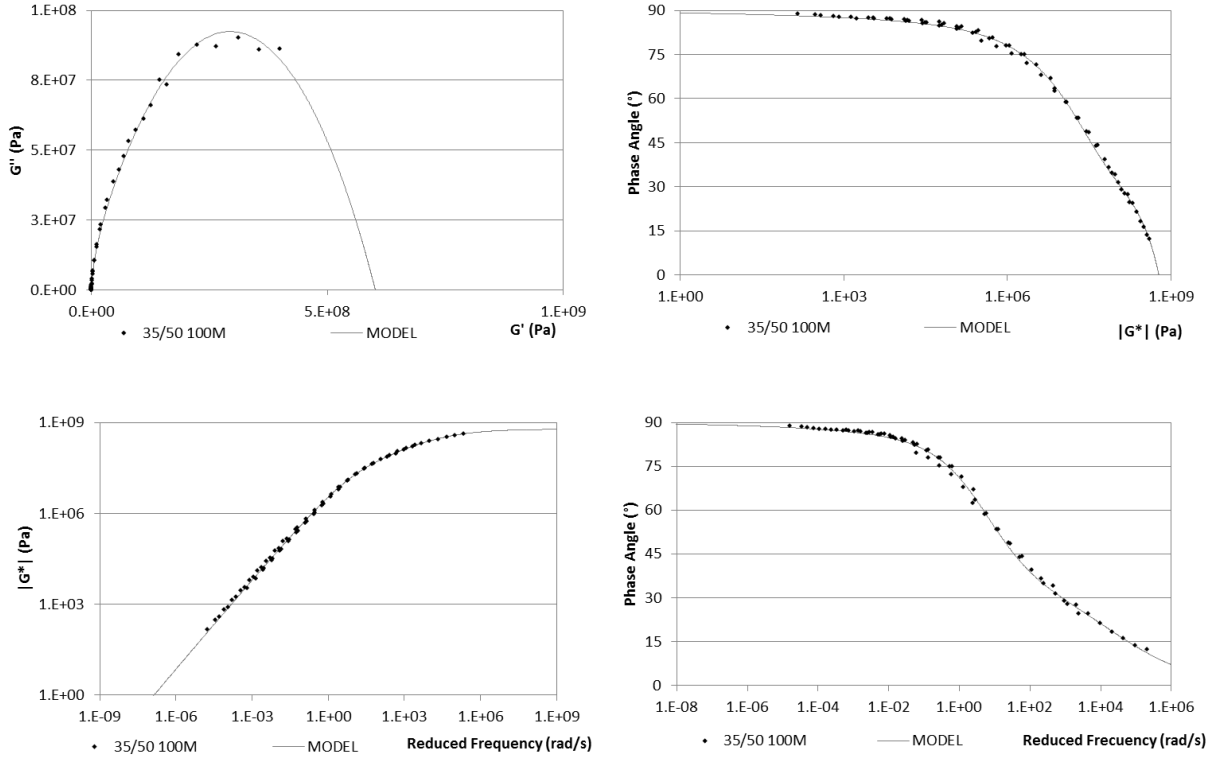


Cole-Cole plan, Black diagram and $|G^*|$ and δ master curves

35/50 100M

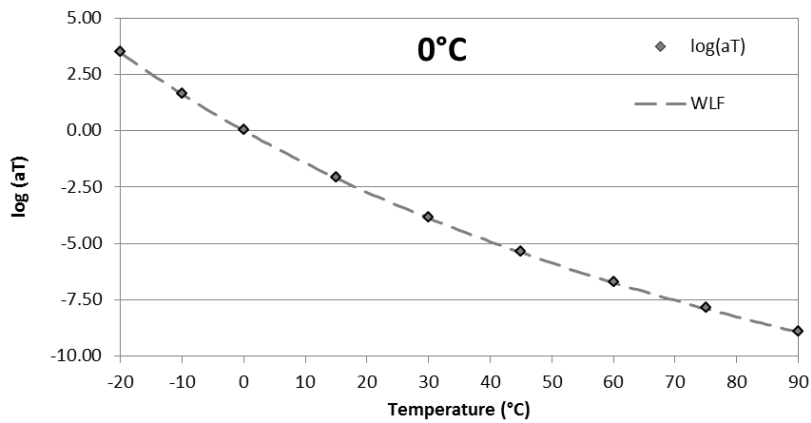
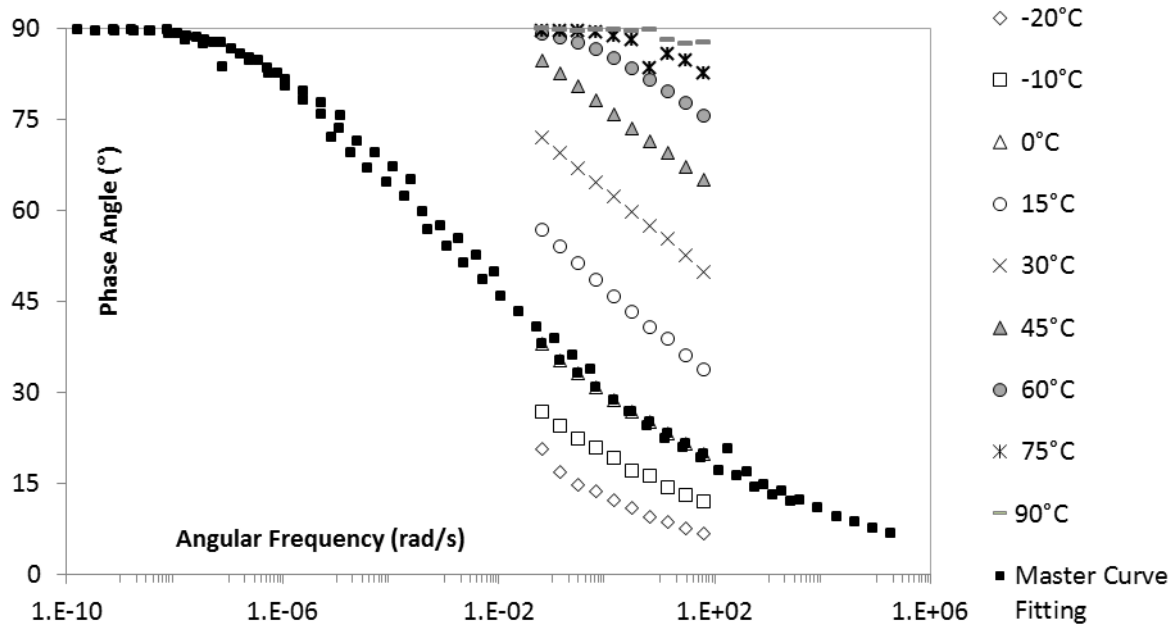
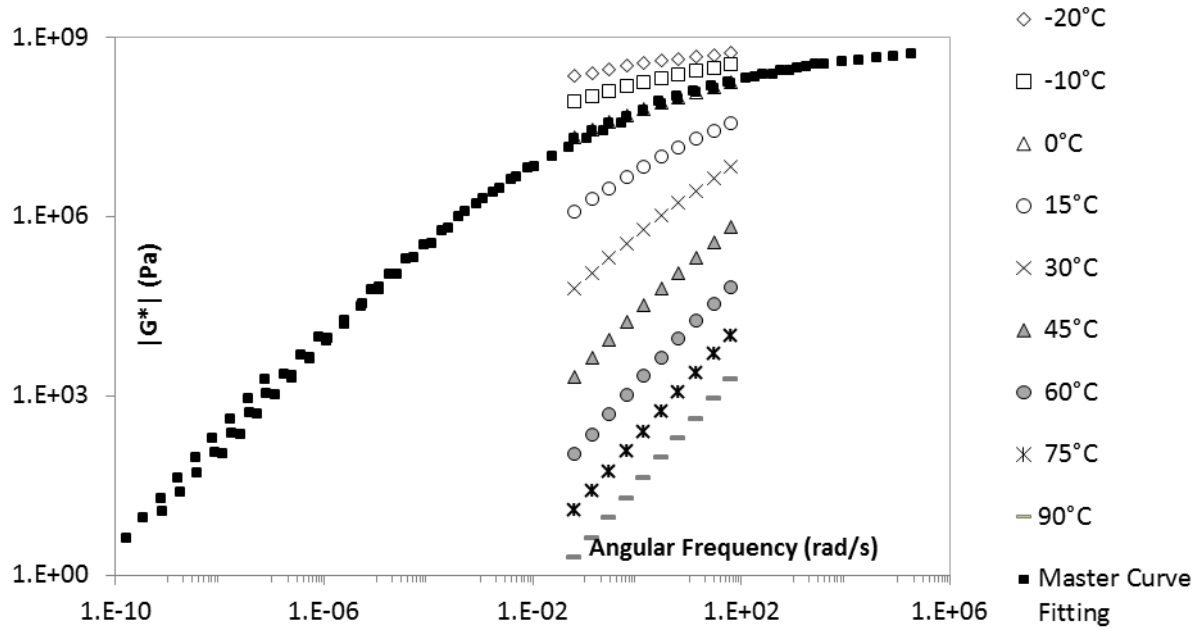


Rheological data measurements and WLF adjustment

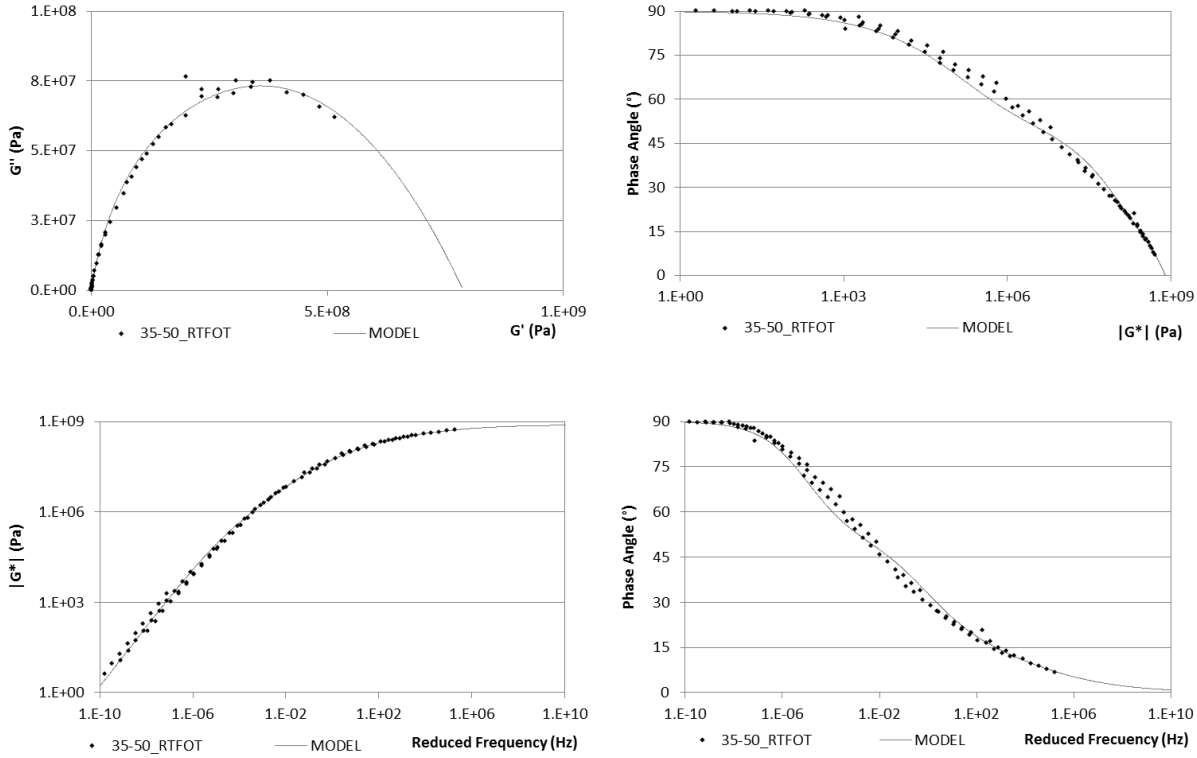


Cole-Cole plan, Black diagram and $|G^*|$ and δ master curves

35/50 RTFOT

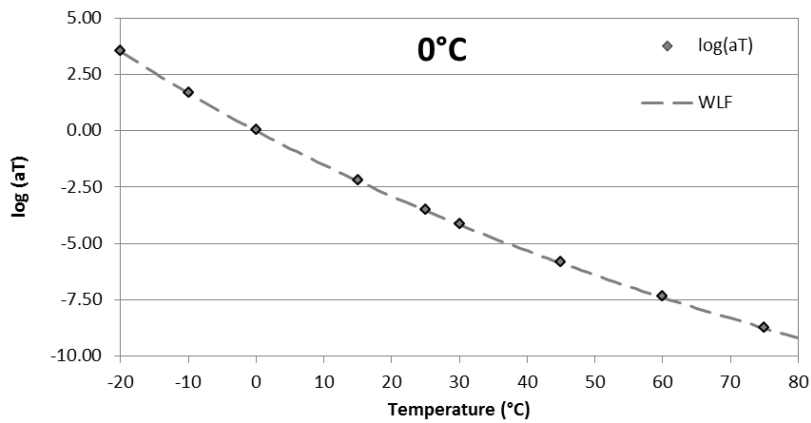
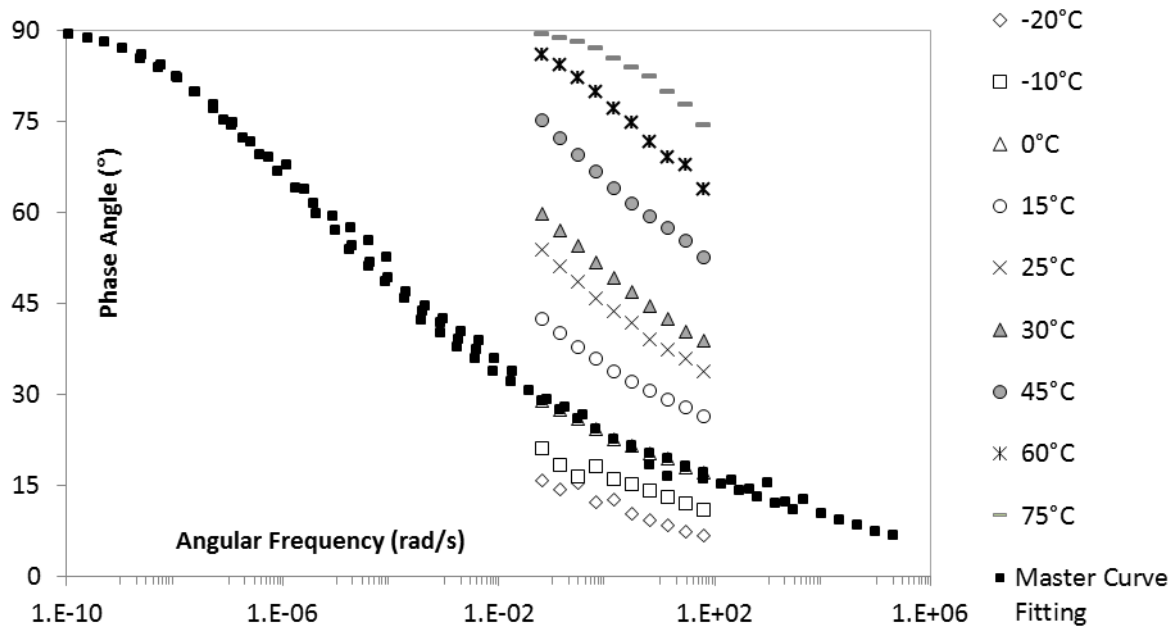
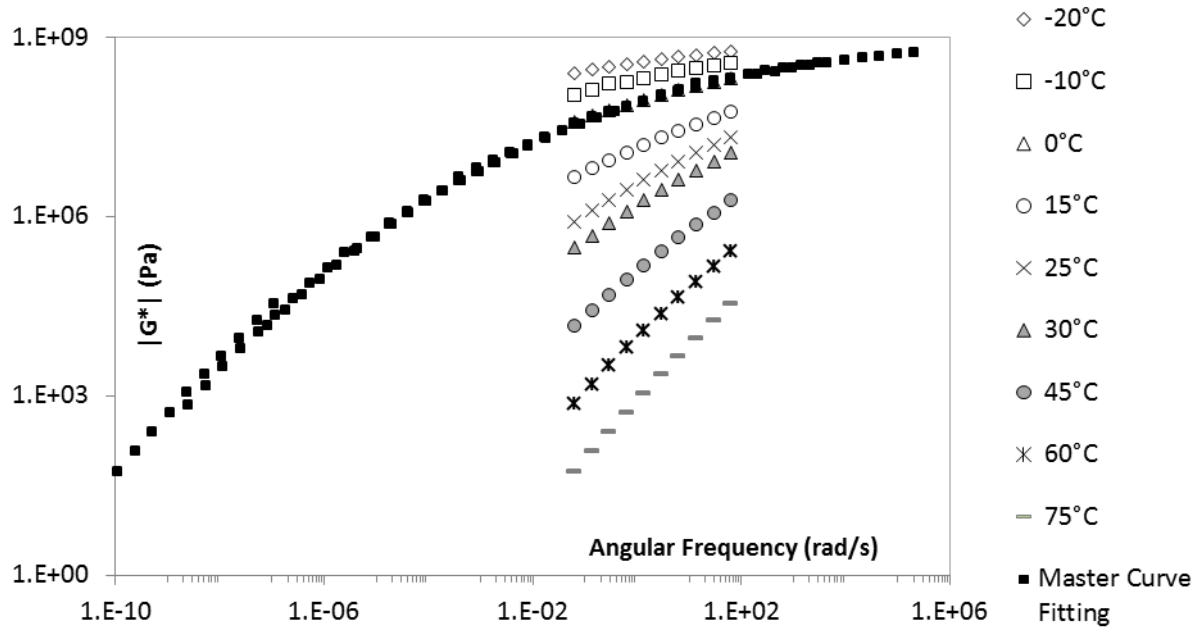


Rheological data measurements and WLF adjustment

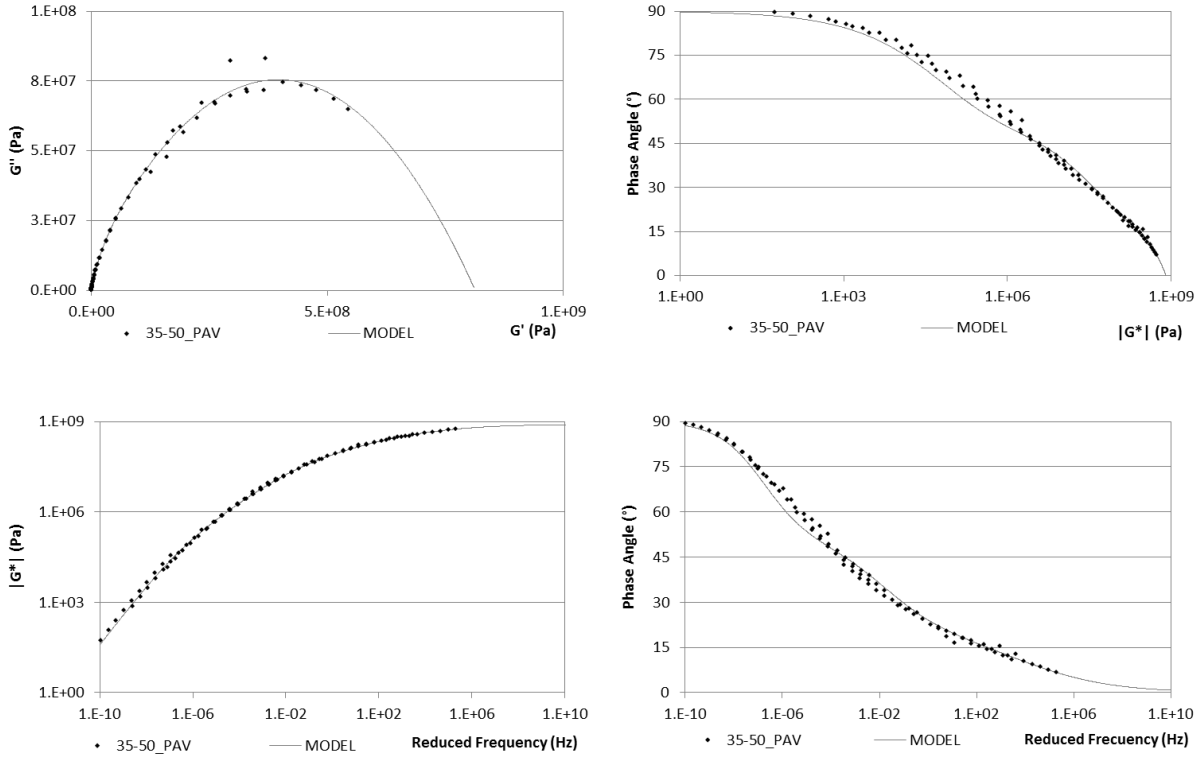


Cole-Cole plan, Black diagram and $|G^*|$ and δ master curves

35/50 PAV

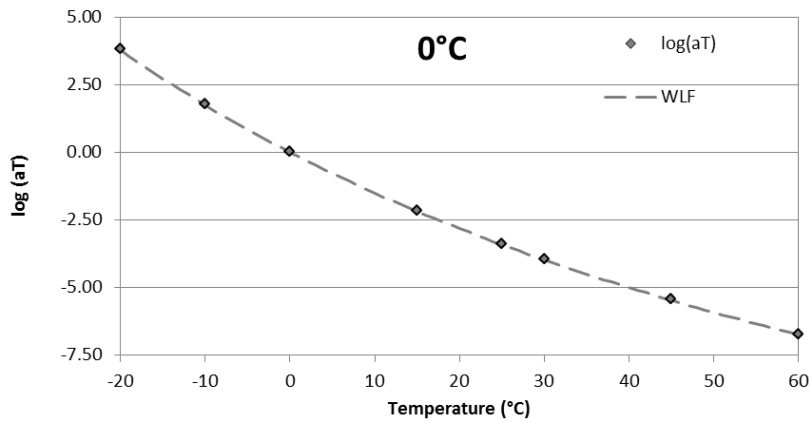
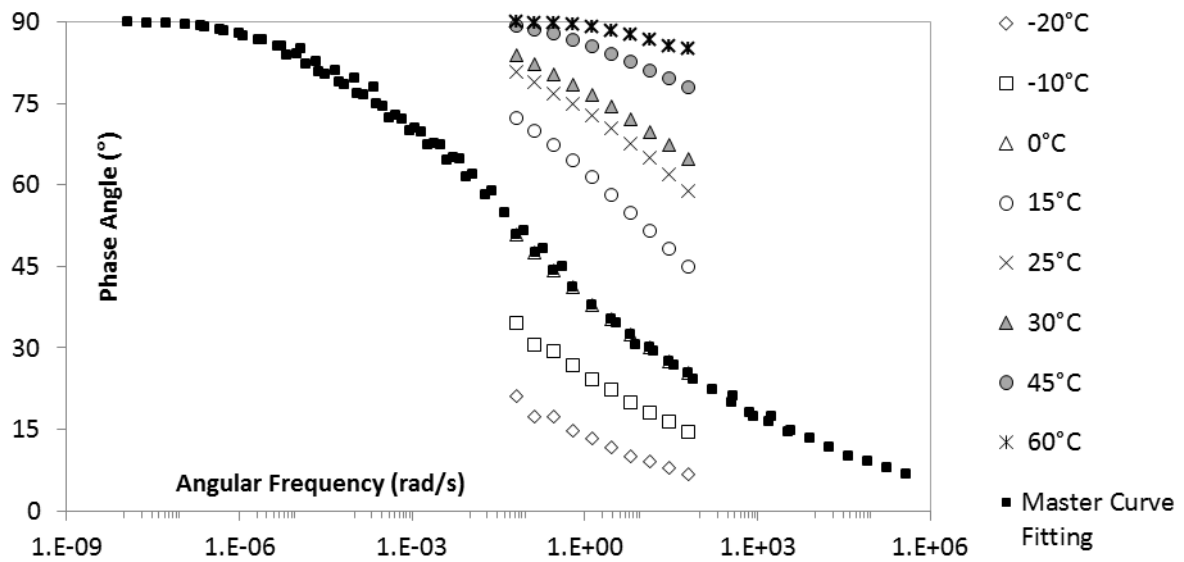
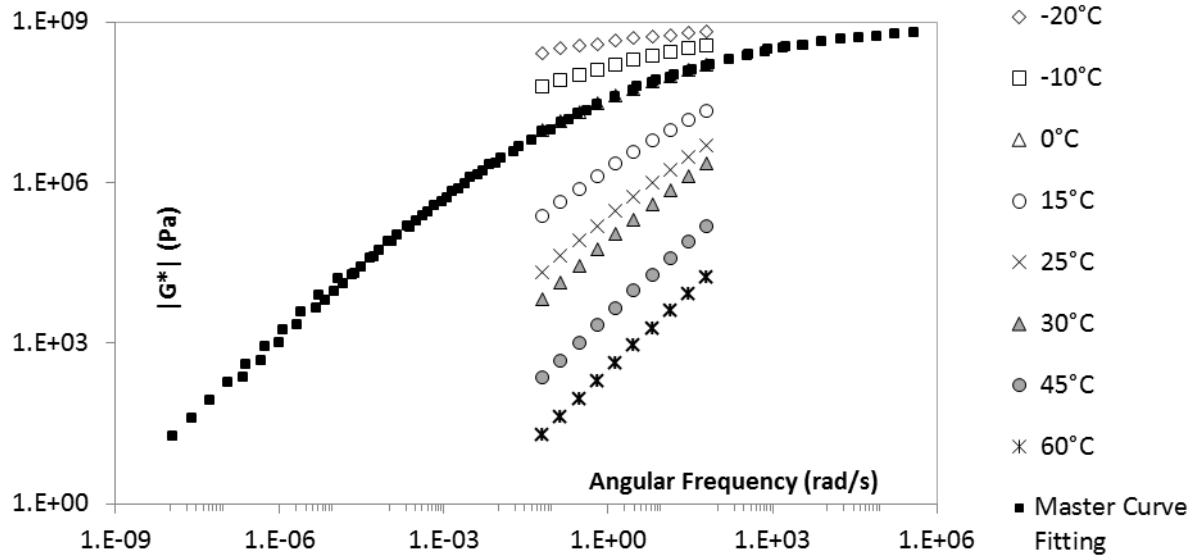


Rheological data measurements and WLF adjustment

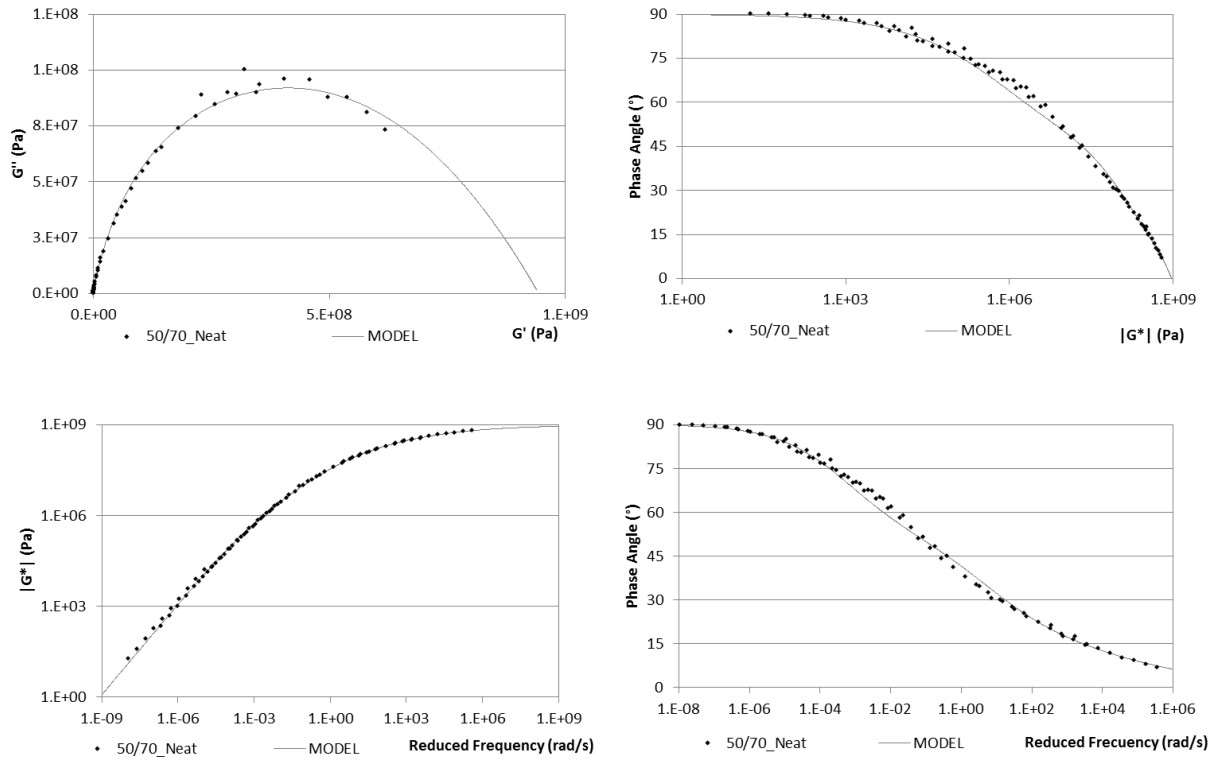


Cole-Cole plan, Black diagram and $|G^*|$ and δ master curves

50/70 NEAT BITUMEN

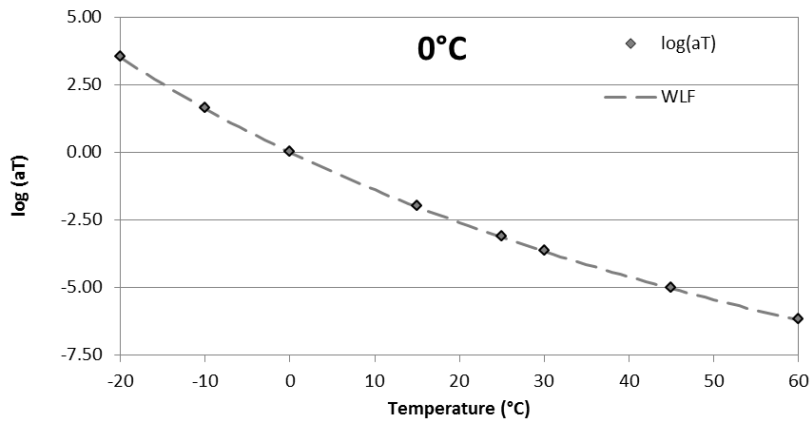
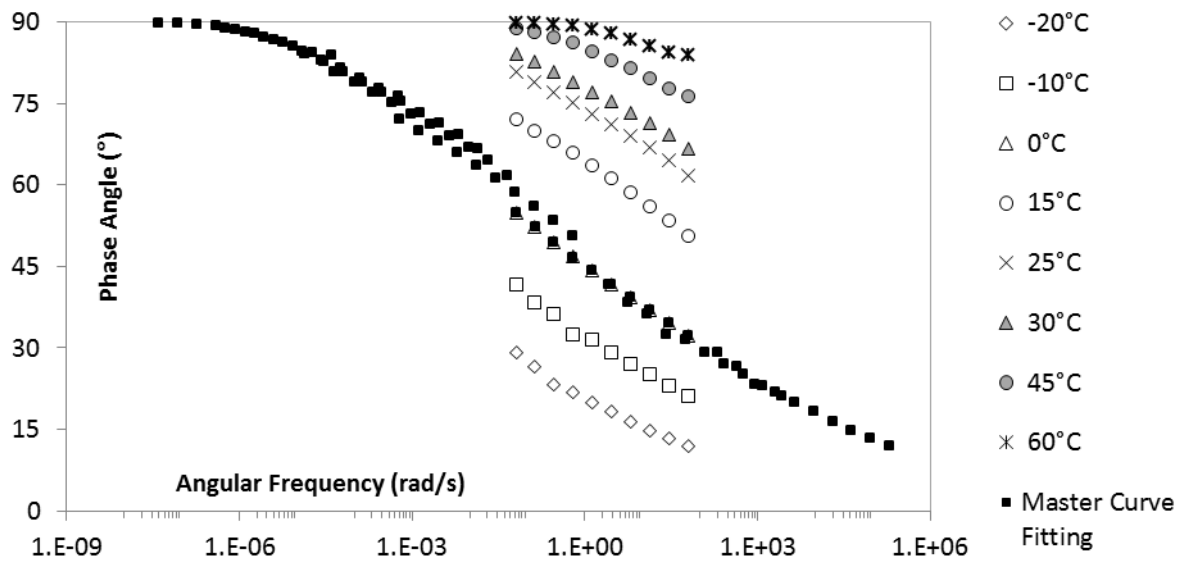
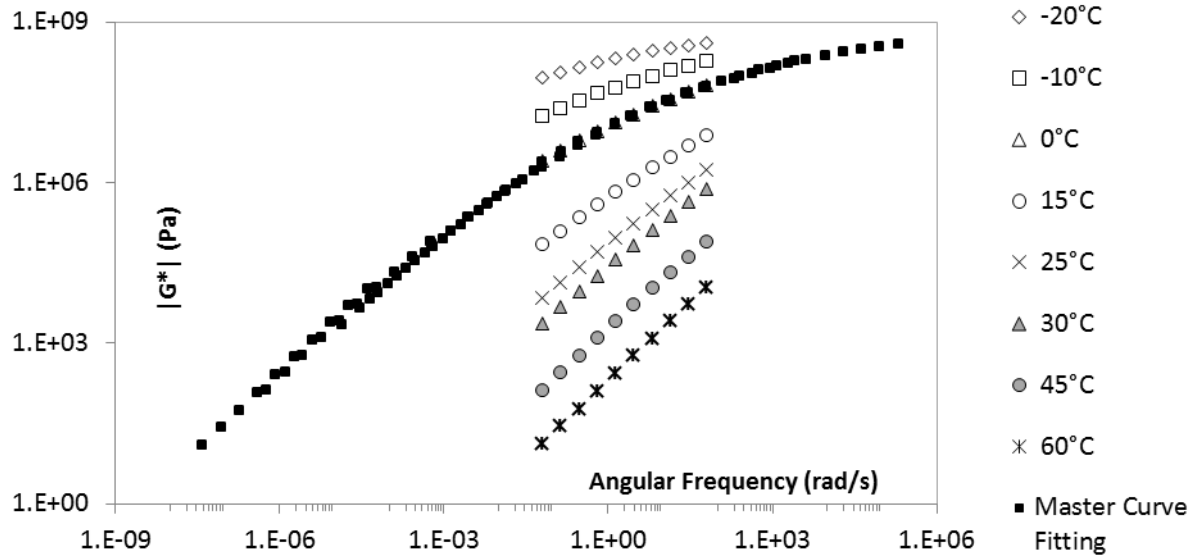


Rheological data measurements and WLF adjustment

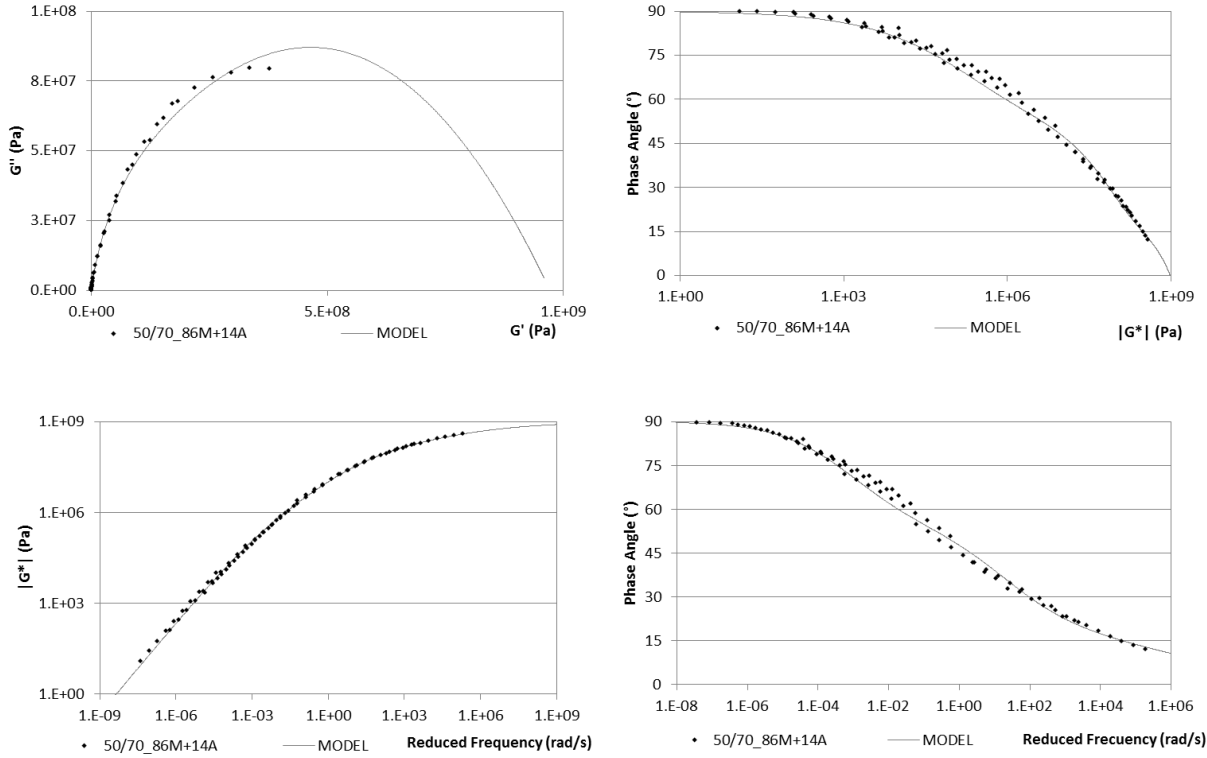


Cole-Cole plan, Black diagram and $|G^*|$ and δ master curves

50/70 86M+14A

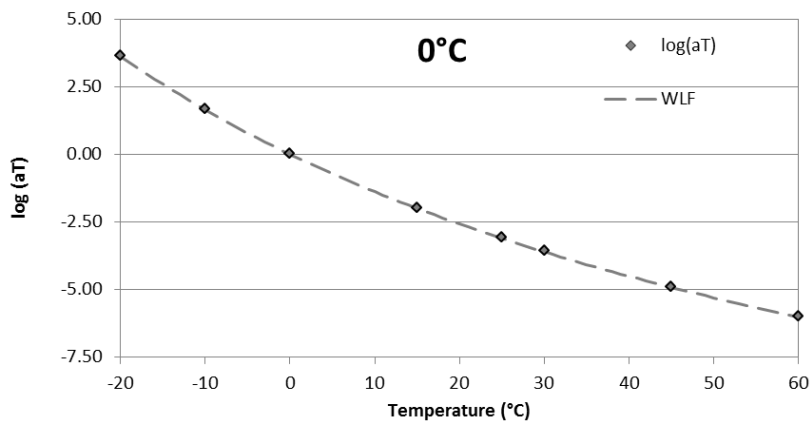
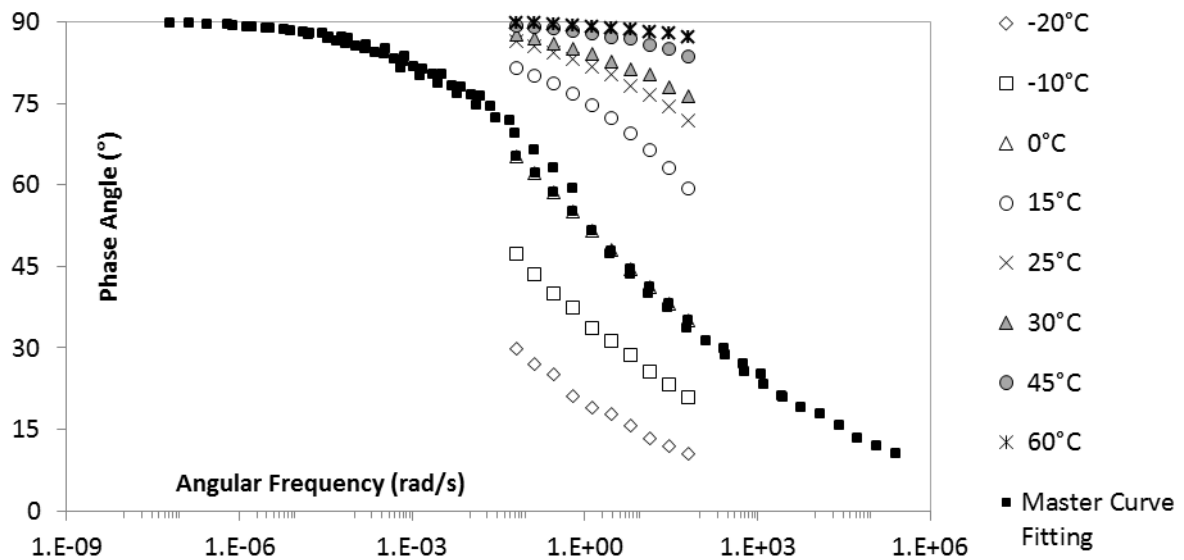
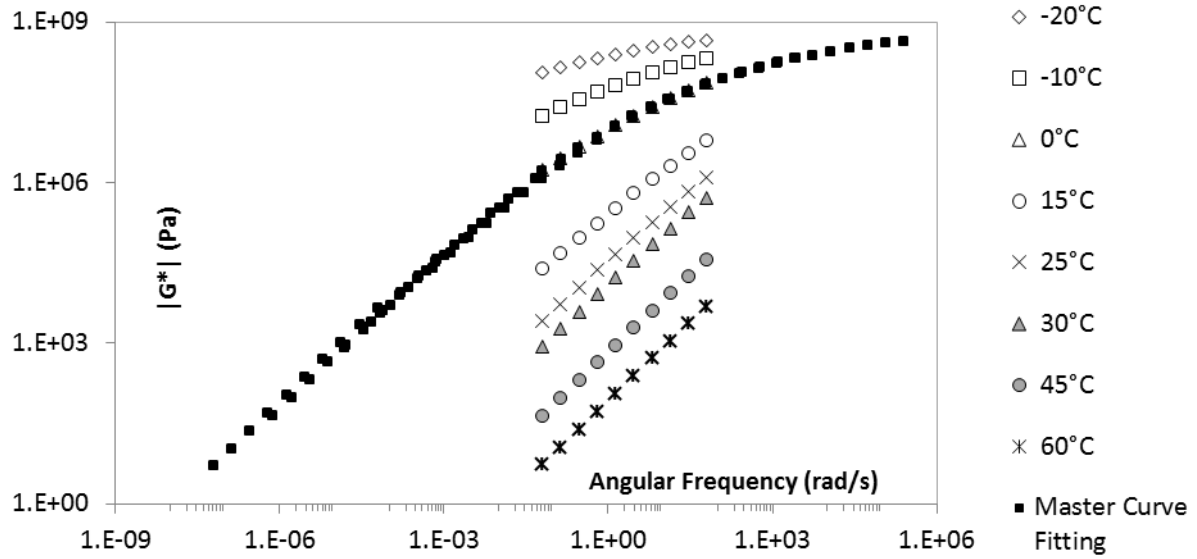


Rheological data measurements and WLF adjustment

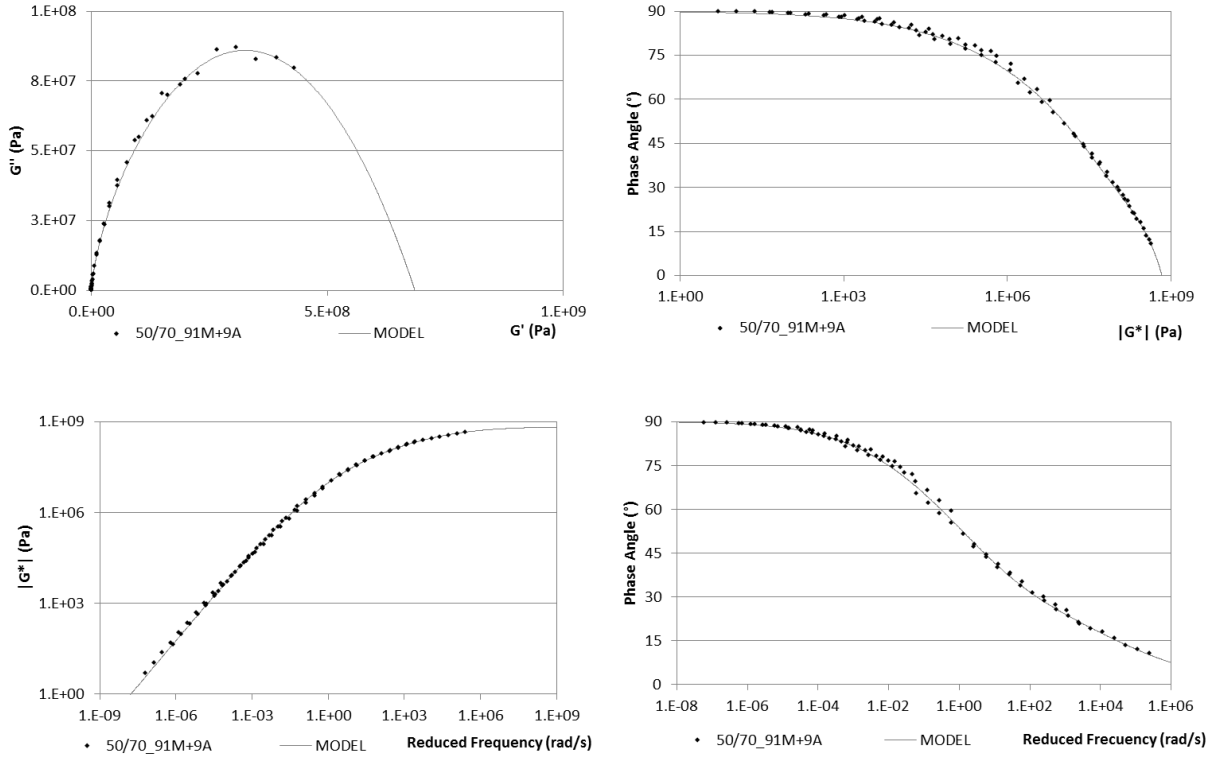


Cole-Cole plan, Black diagram and $|G^*|$ and δ master curves

50/70 91M+9A

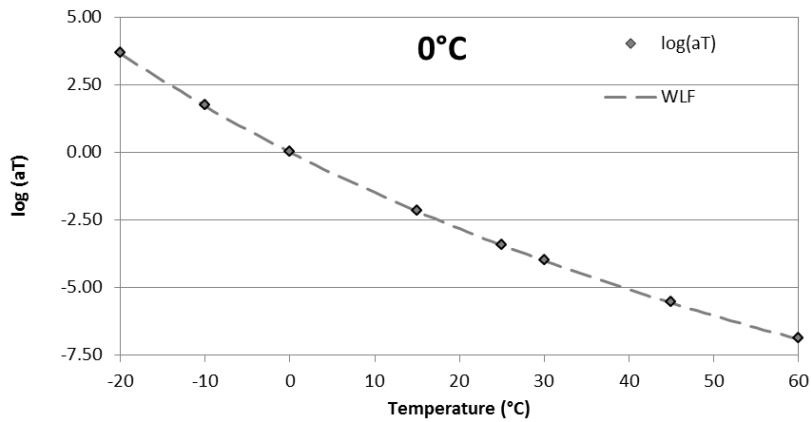
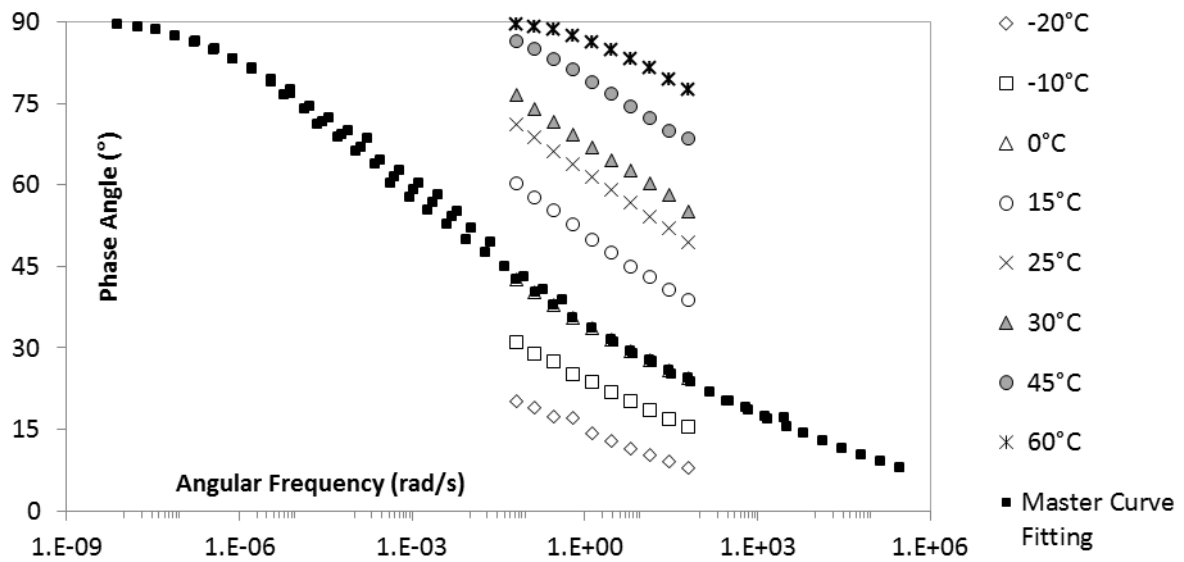
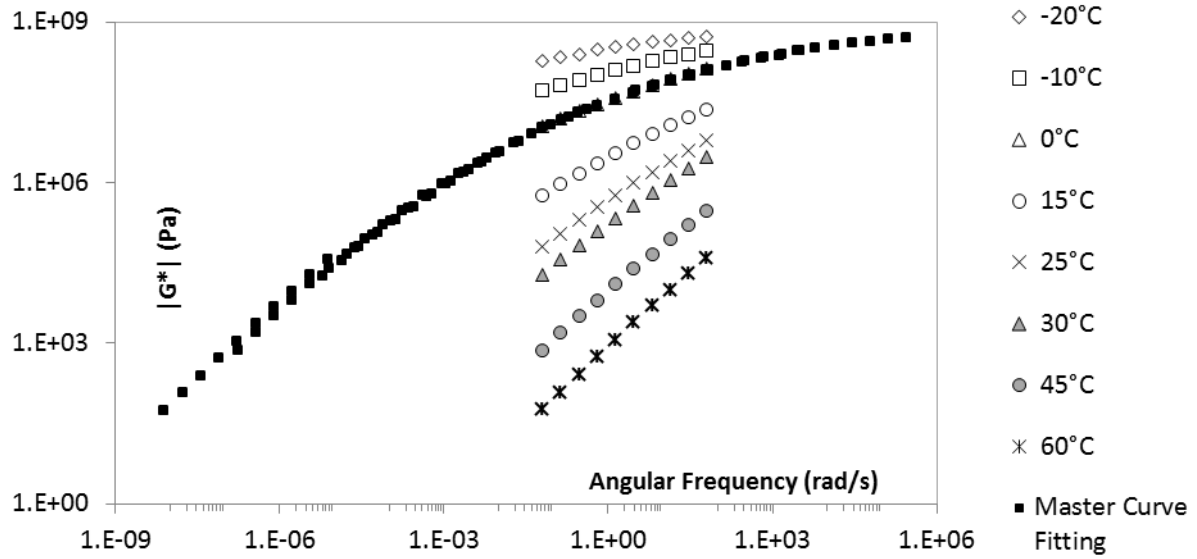


Rheological data measurements and WLF adjustment

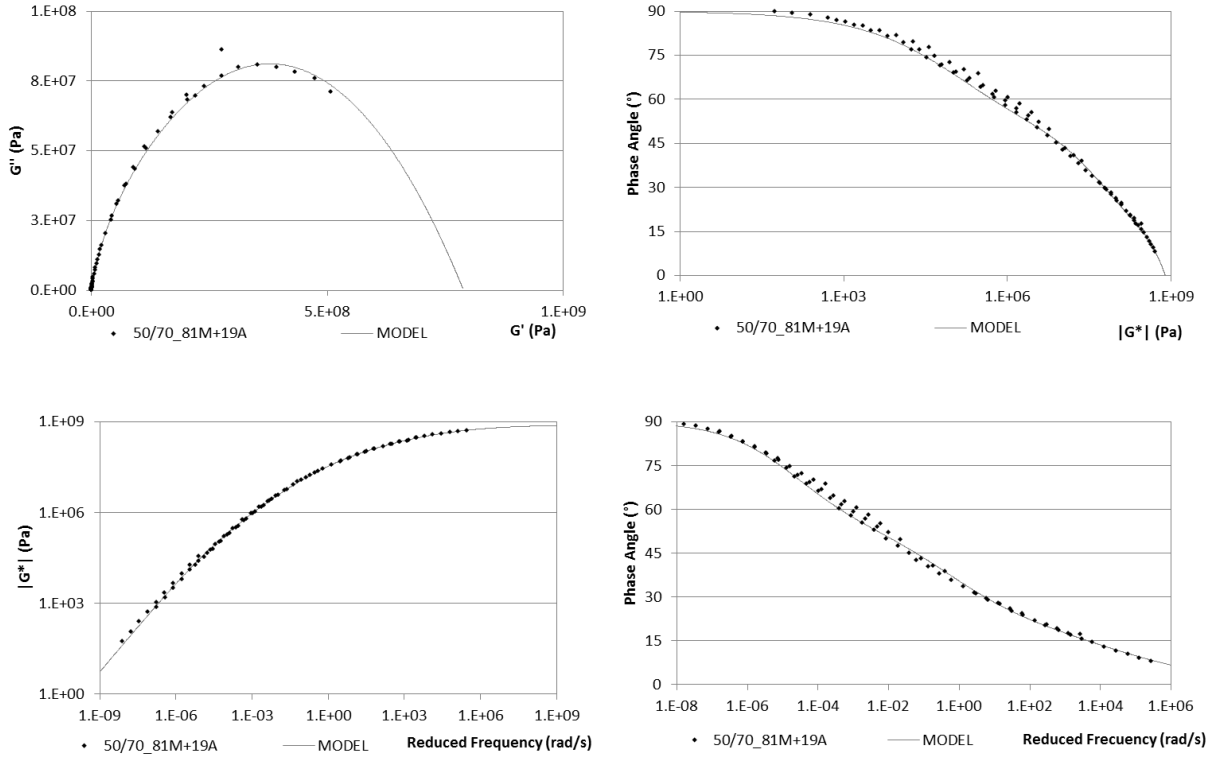


Cole-Cole plan, Black diagram and $|G^*|$ and δ master curves

50/70 81M+19A

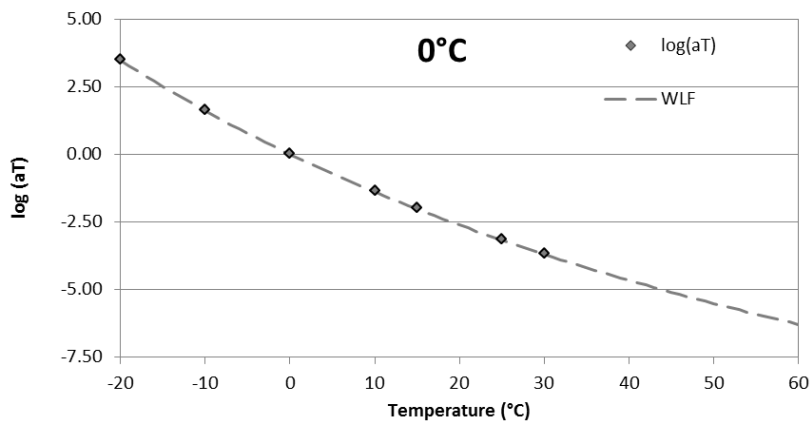
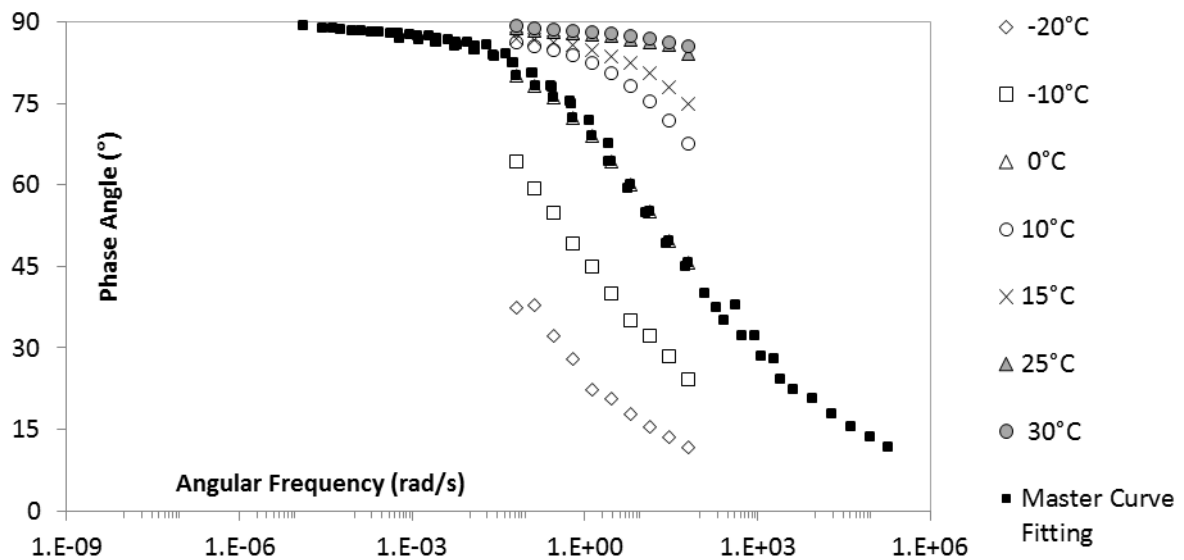
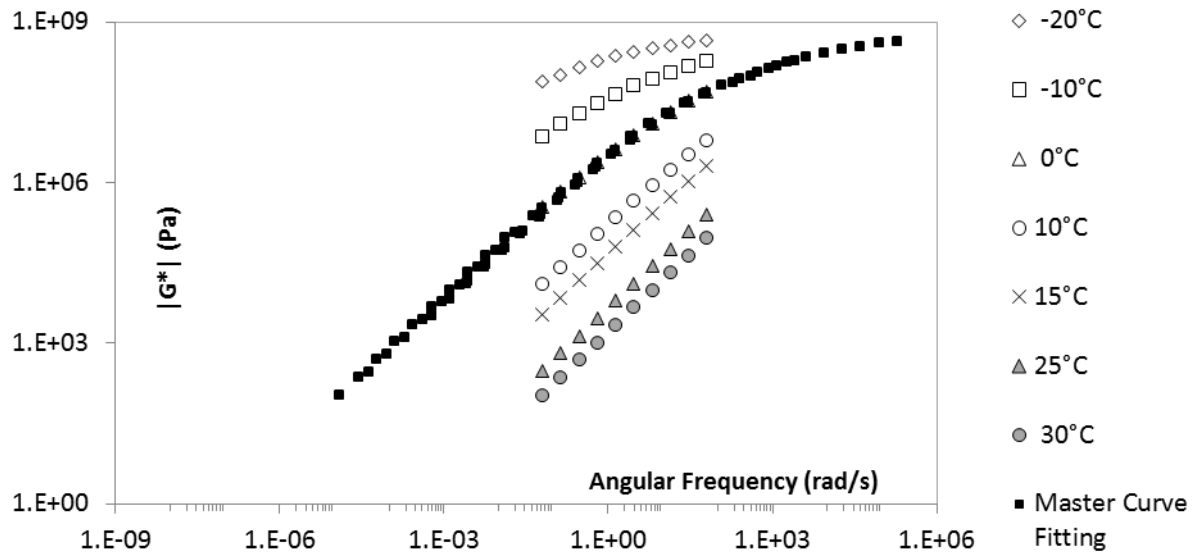


Rheological data measurements and WLF adjustment

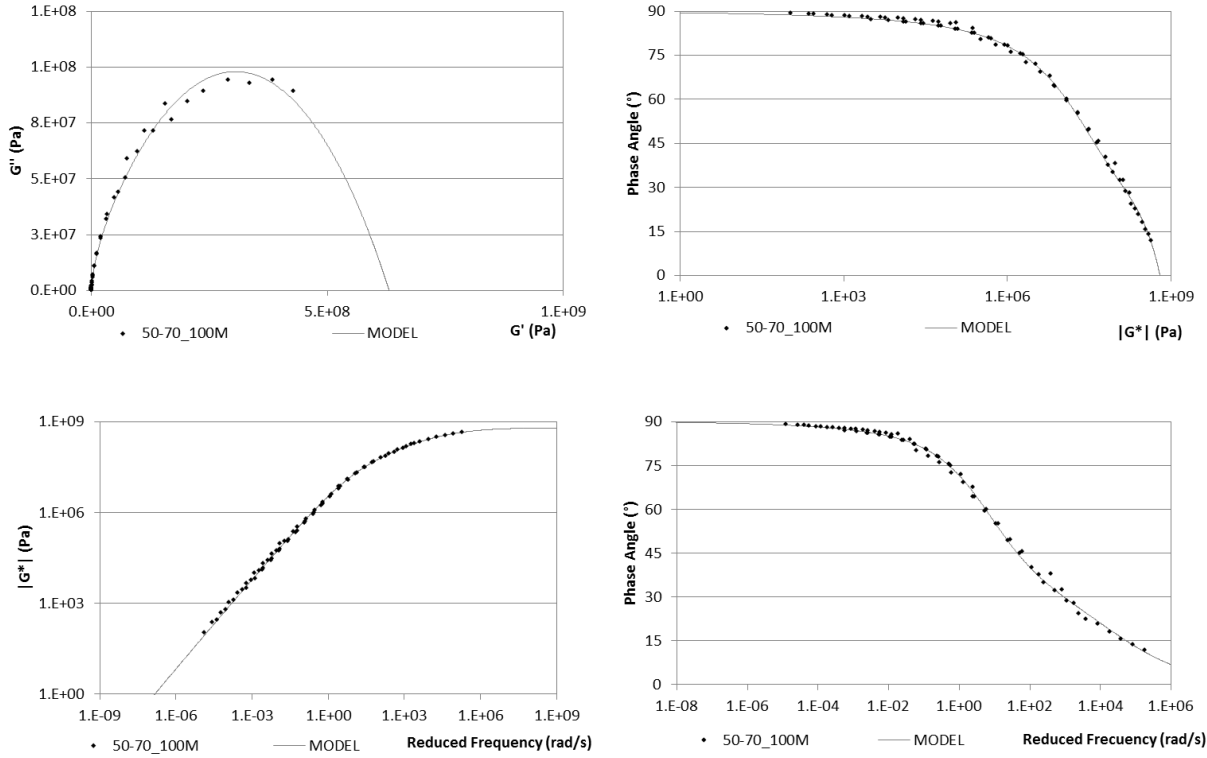


Cole-Cole plan, Black diagram and $|G^*|$ and δ master curves

50/70 100M



Rheological data measurements and WLF adjustment



Cole-Cole plan, Black diagram and $|G^*|$ and δ master curves

Annex 3

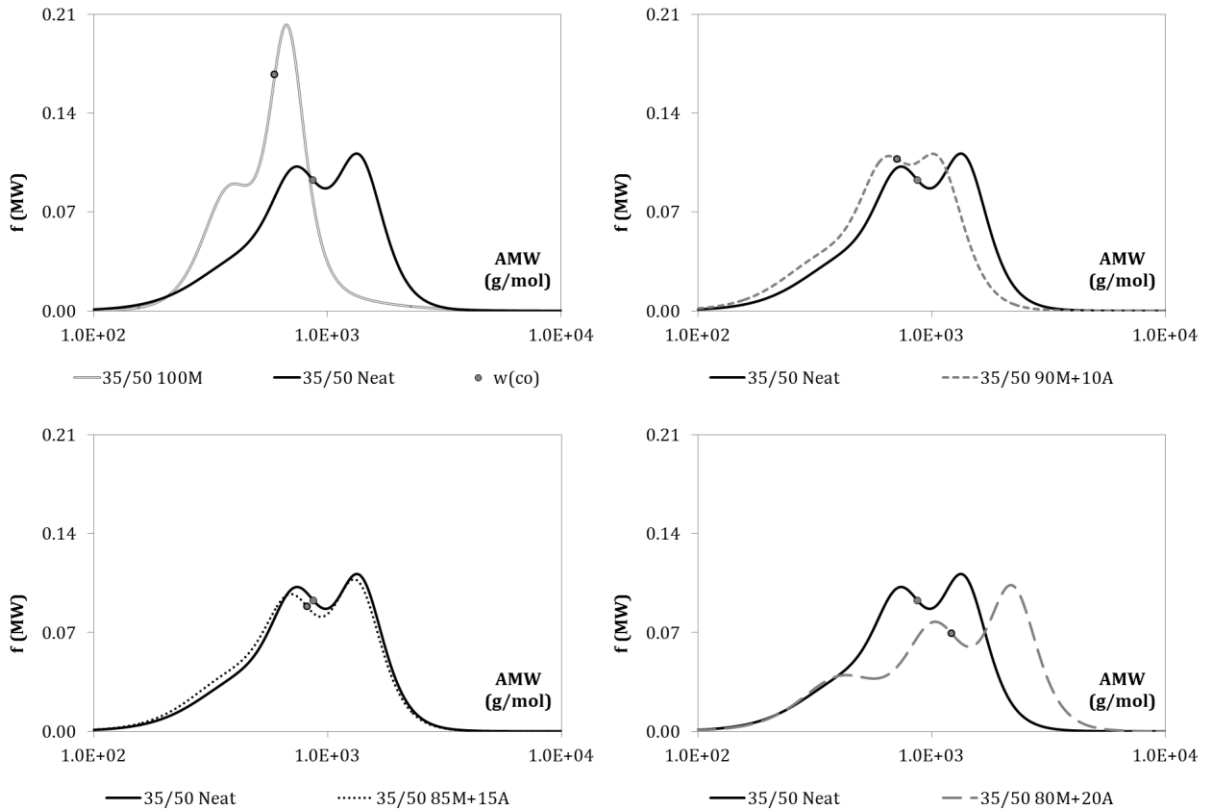
HUET-SUCH MODELLING PARAMETERS AND δ -METHOD CURVES OF
MODEL AND AGED BITUMENS

HUET-SUCH MODELLING PARAMETERS

Reference temperature for master curve $T=0^{\circ}\text{C}$

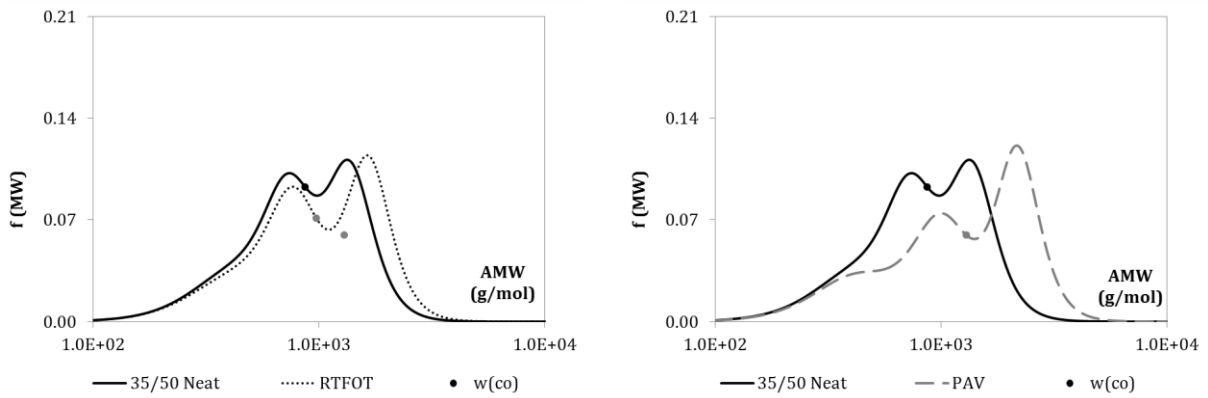
	Bitumen	G_{∞} (MPa)	δ	k	h	β	τ (s)	C_1	C_2
35/50 aged	Neat	835.55	3.47	0.23	0.59	186.19	1.90E-02	22.52	137.35
	RTFOT	788.30	3.59	0.22	0.57	557.42	3.62E-02	25.59	168.00
	PAV	813.48	5.88	0.23	0.56	1576.50	3.05E-01	32.89	206.87
35/50 model	85M+15A	879.43	3.75	0.24	0.60	222.56	6.74E-03	23.59	151.48
	90M+10A	870.76	3.80	0.24	0.61	102.53	1.53E-03	20.47	133.32
	80M+20A	875.79	7.35	0.25	0.60	1033.60	2.65E-01	26.92	162.99
	100M	601.61	0.01	0.84	0.37	402.05	3.22E-05	18.18	122.74
50/70 model	Neat	943.70	3.18	0.23	0.59	170.73	7.43E-03	22.16	137.27
	86M+14A	971.68	4.68	0.22	0.60	282.74	8.27E-04	20.19	135.36
	91M+9A	685.62	4.49	0.30	0.67	22.52	3.88E-03	17.99	119.63
	81M+19A	788.87	4.93	0.25	0.60	346.79	2.02E-02	24.80	155.48
	100M	630.97	6.41	0.37	0.80	2.07	5.43E-03	21.07	141.12

35/50 MODEL BITUMENS



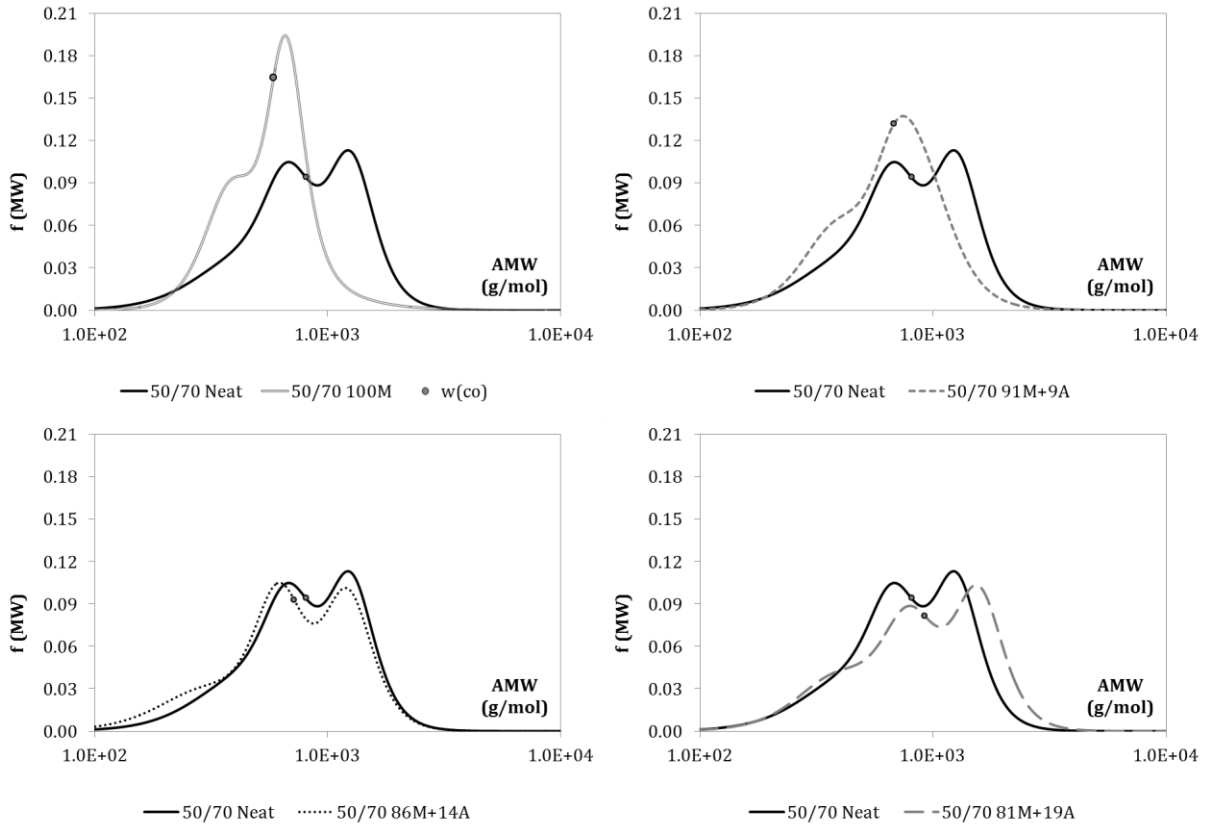
δ -method representation curve

35/50 LABORATORY AGED BITUMENS

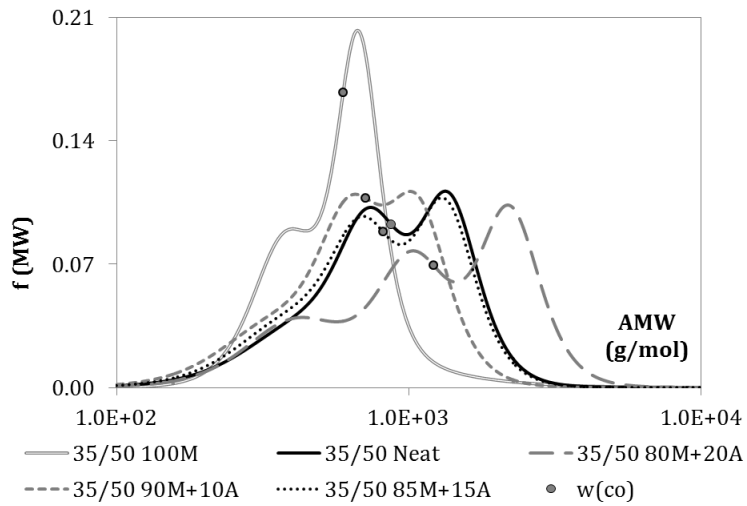


δ -method representation curve

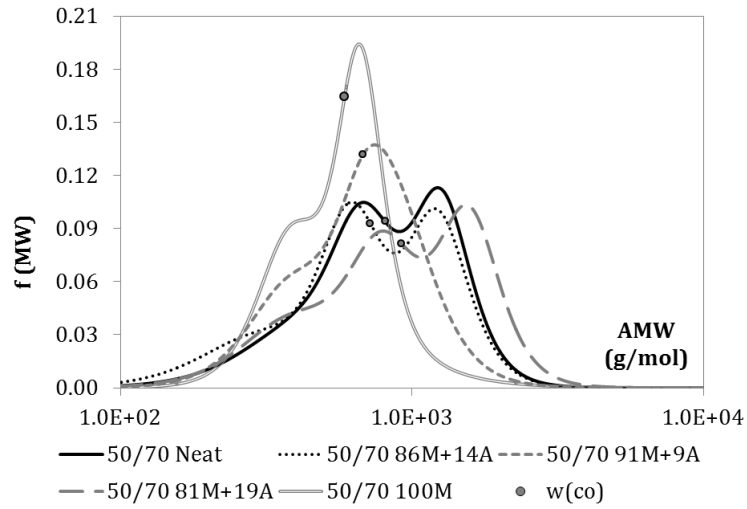
50/70 MODEL BITUMENS



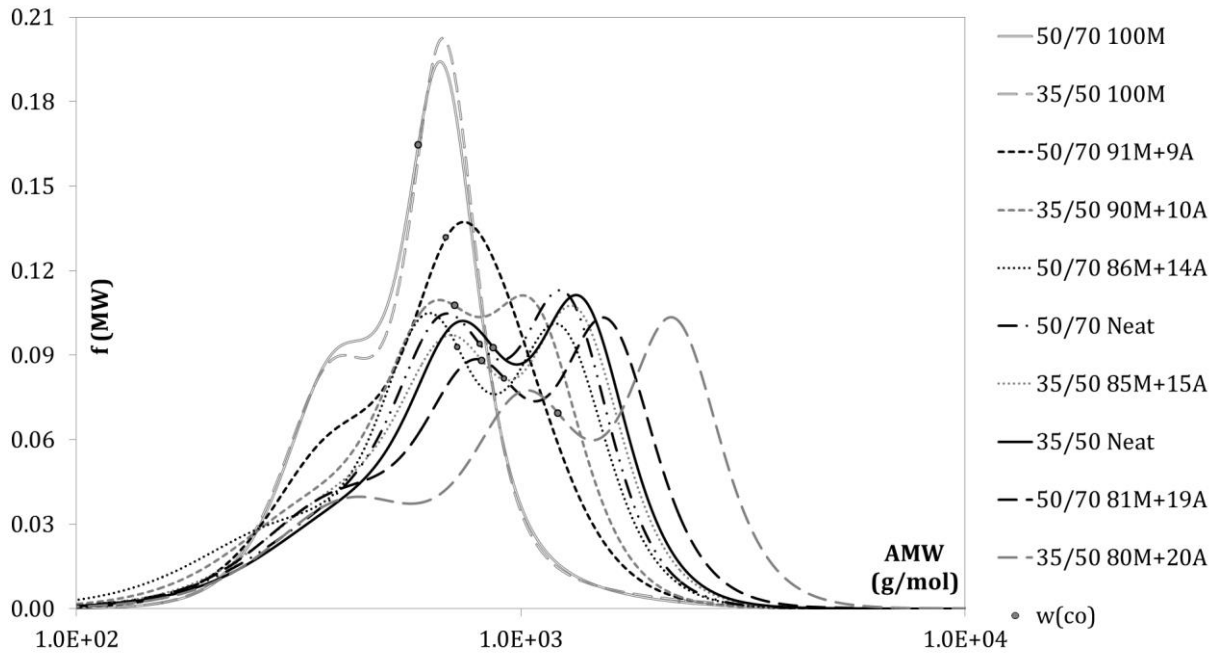
δ -method representation curve



δ -method representation 35/50 model bitumens



δ -method representation 50/70 model bitumens

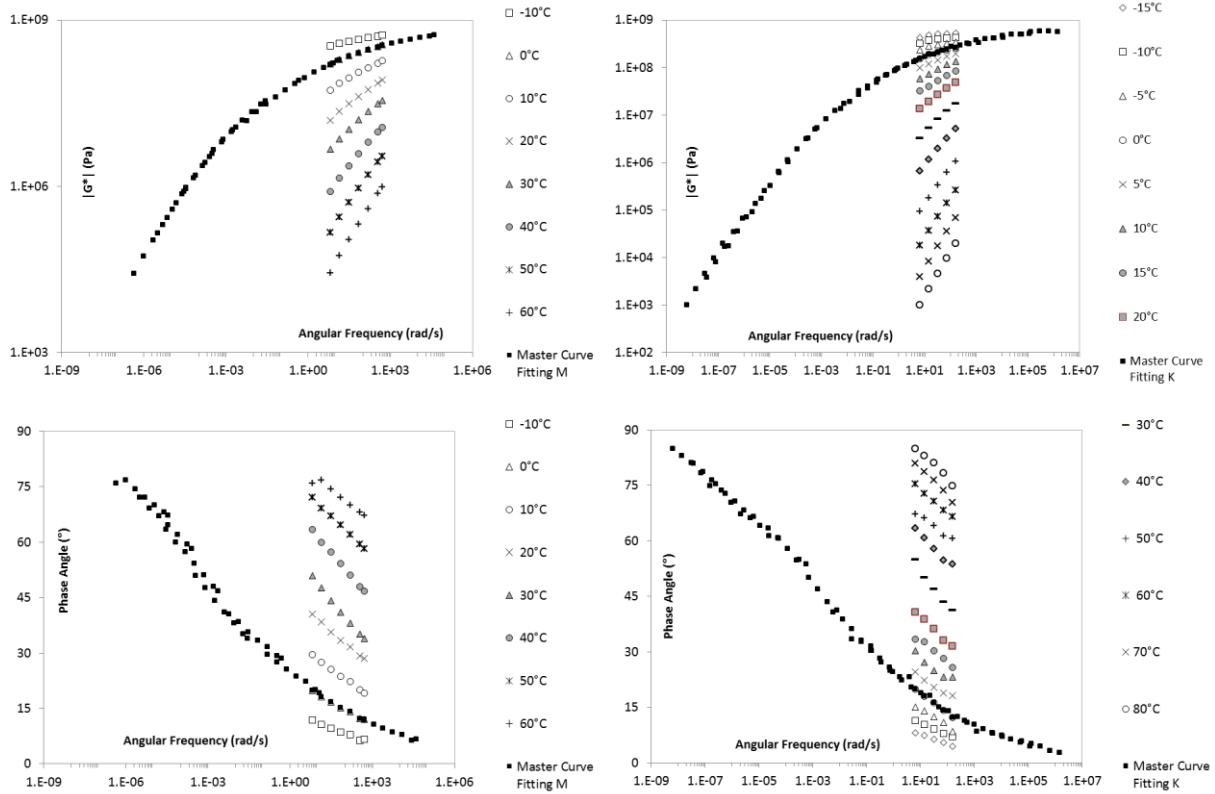


δ -method representation ALL model bitumens

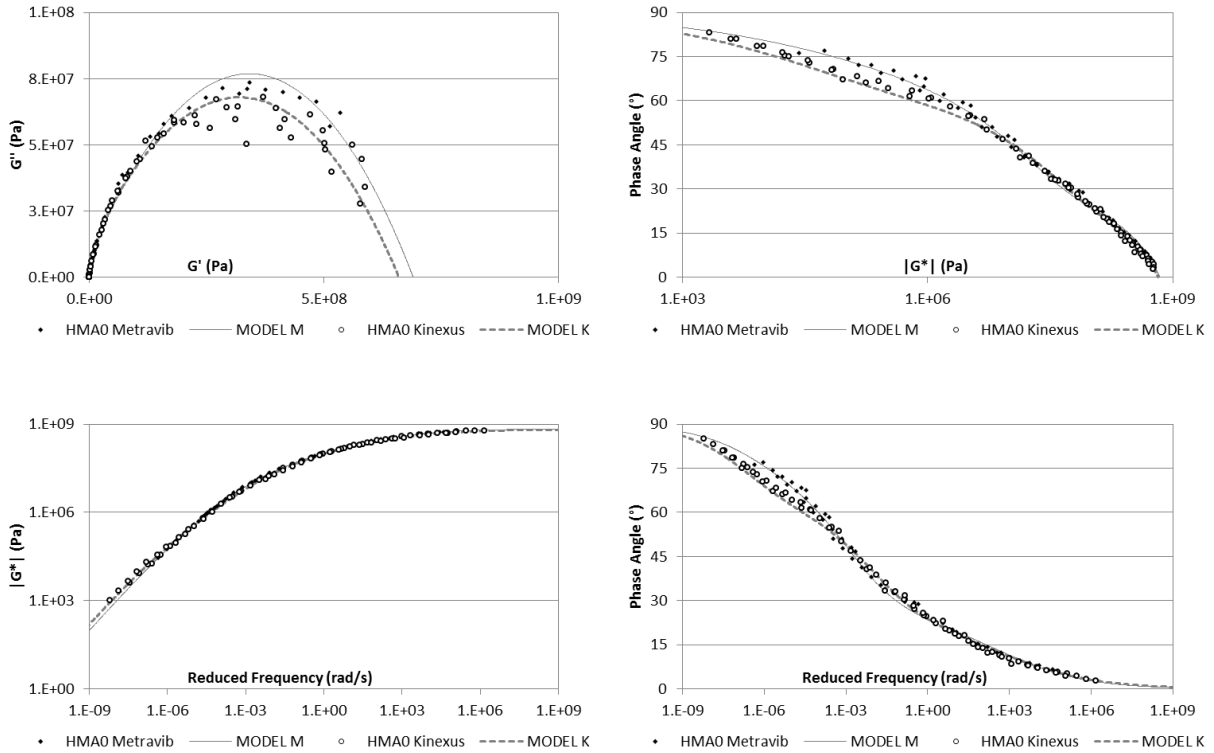
Annex 4

MASTER CURVES, WLF ADJUSTMENT, BLACK DIAGRAMS
AND COLE-COLE PLAN OF RECOVERED BITUMENS
FORM ASPHALT MIXTURES MANUFACTURE

HMA0

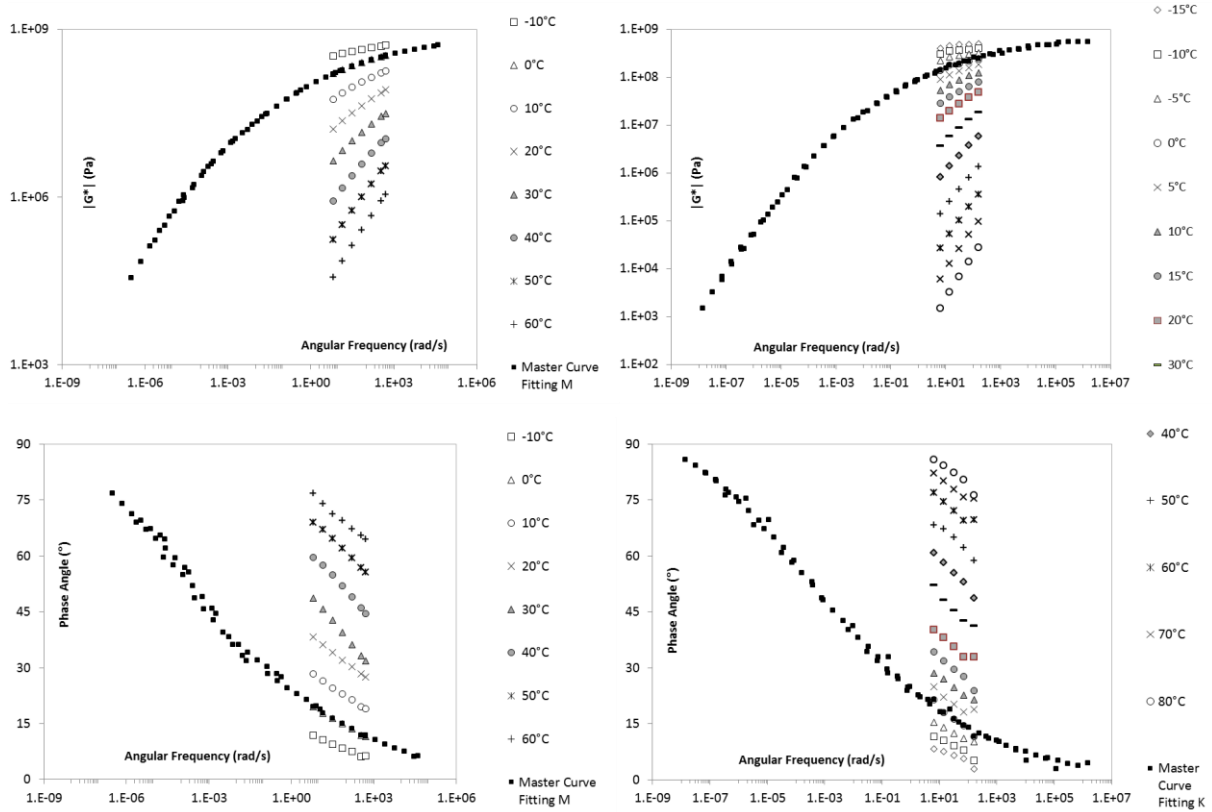


Rheological data measurements from Metravig® (left) and Kinexus® (right)

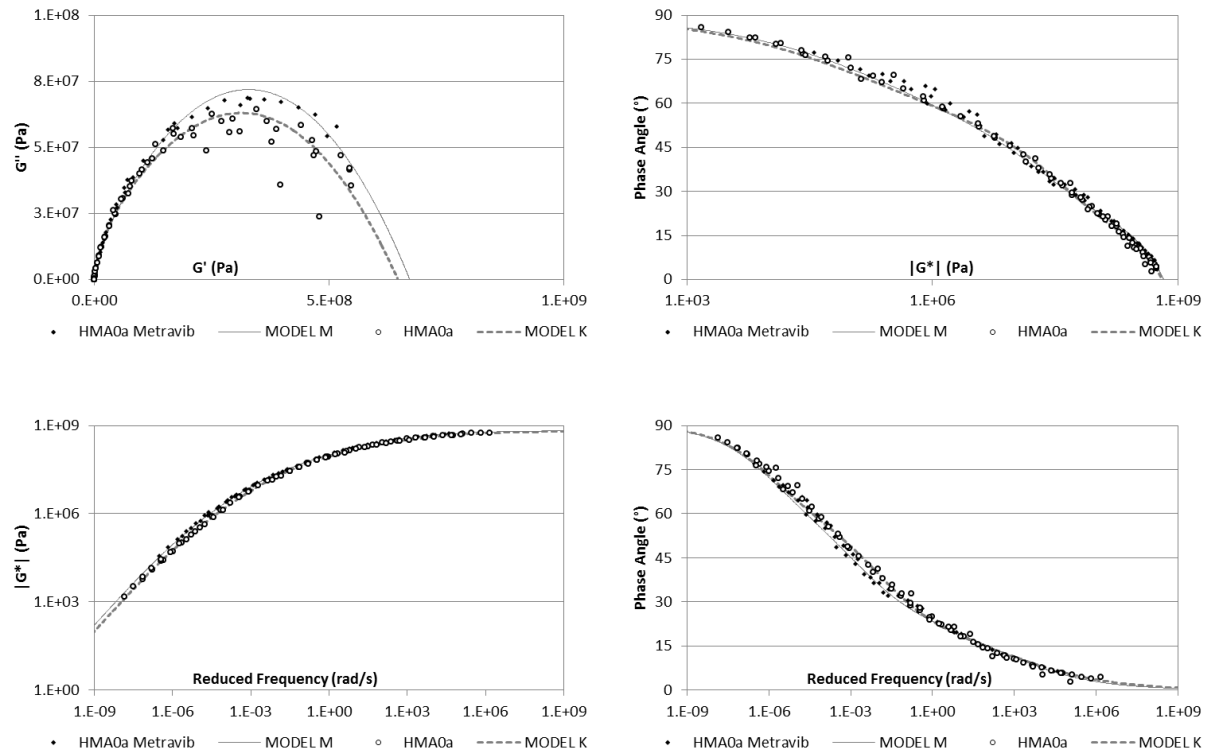


Cole-Cole plan, Black diagram and $|G^*|$ and δ master curves

HMA0a

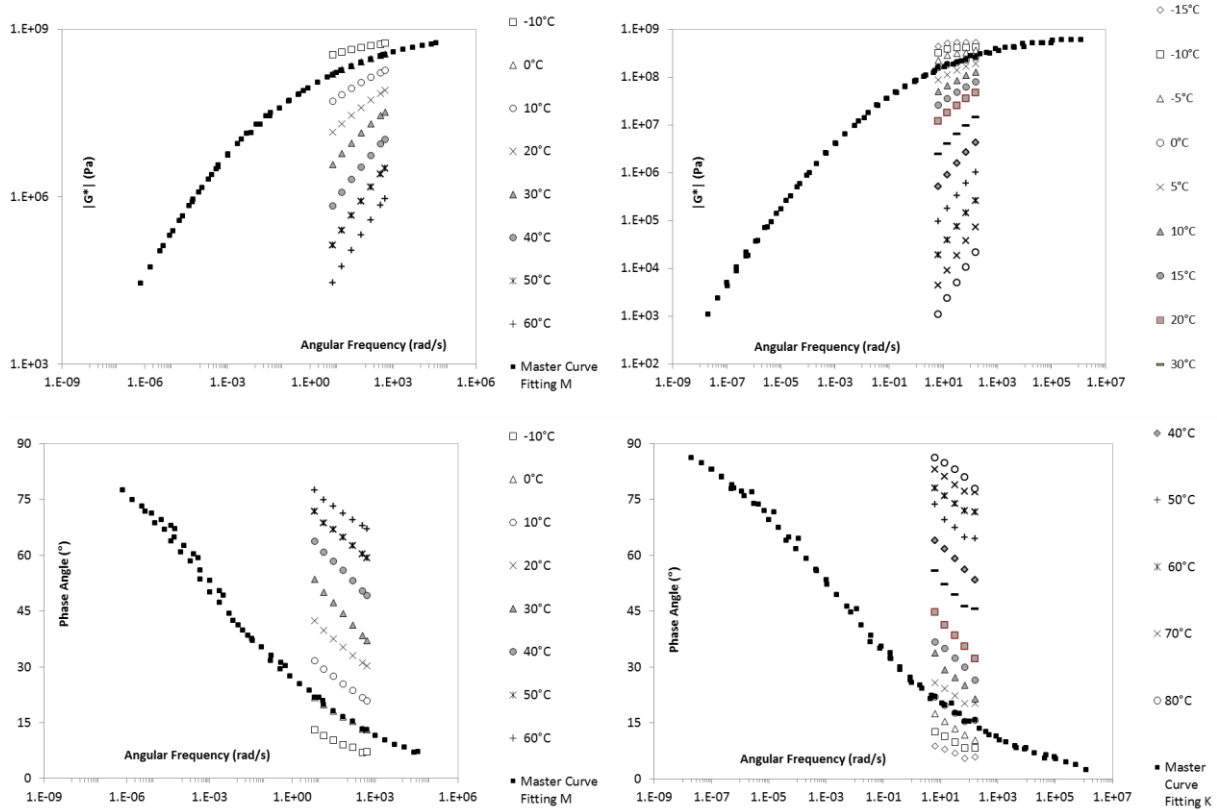


Rheological data measurements from Metravis® (left) and Kinexus® (right)

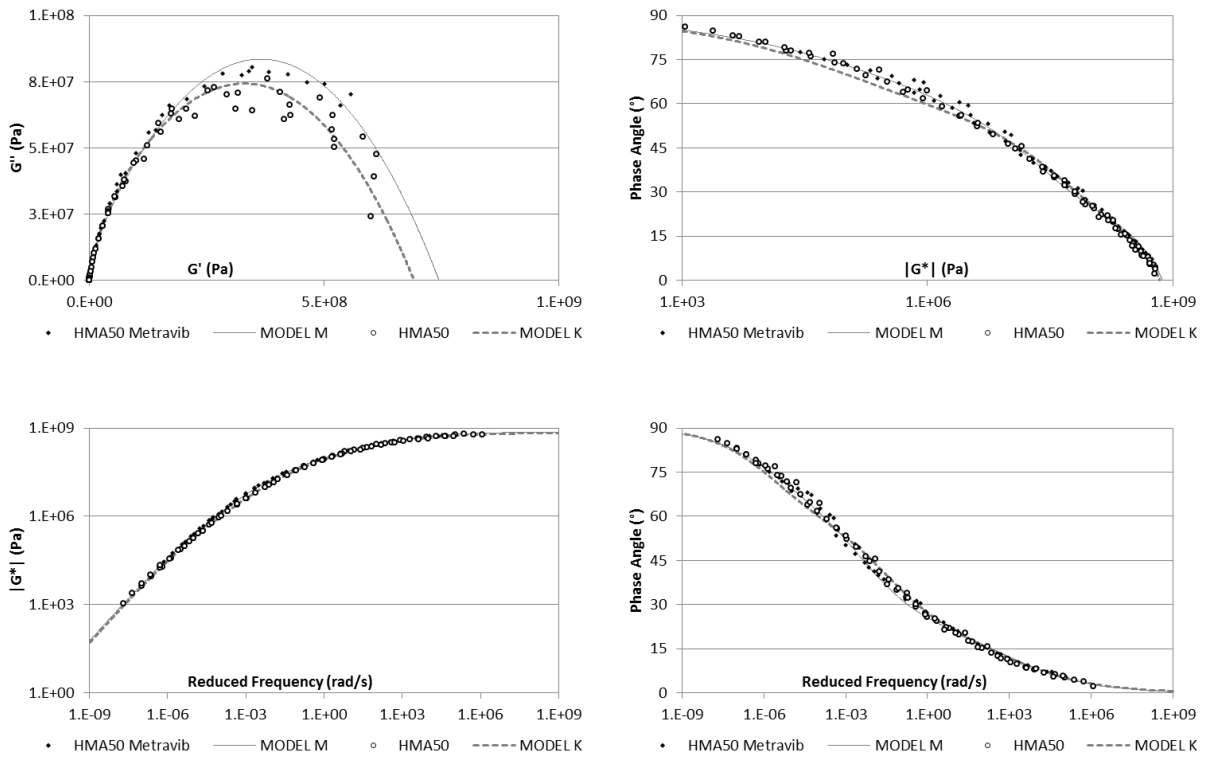


Cole-Cole plan, Black diagram and $|G^*|$ and δ master curves

HMA50

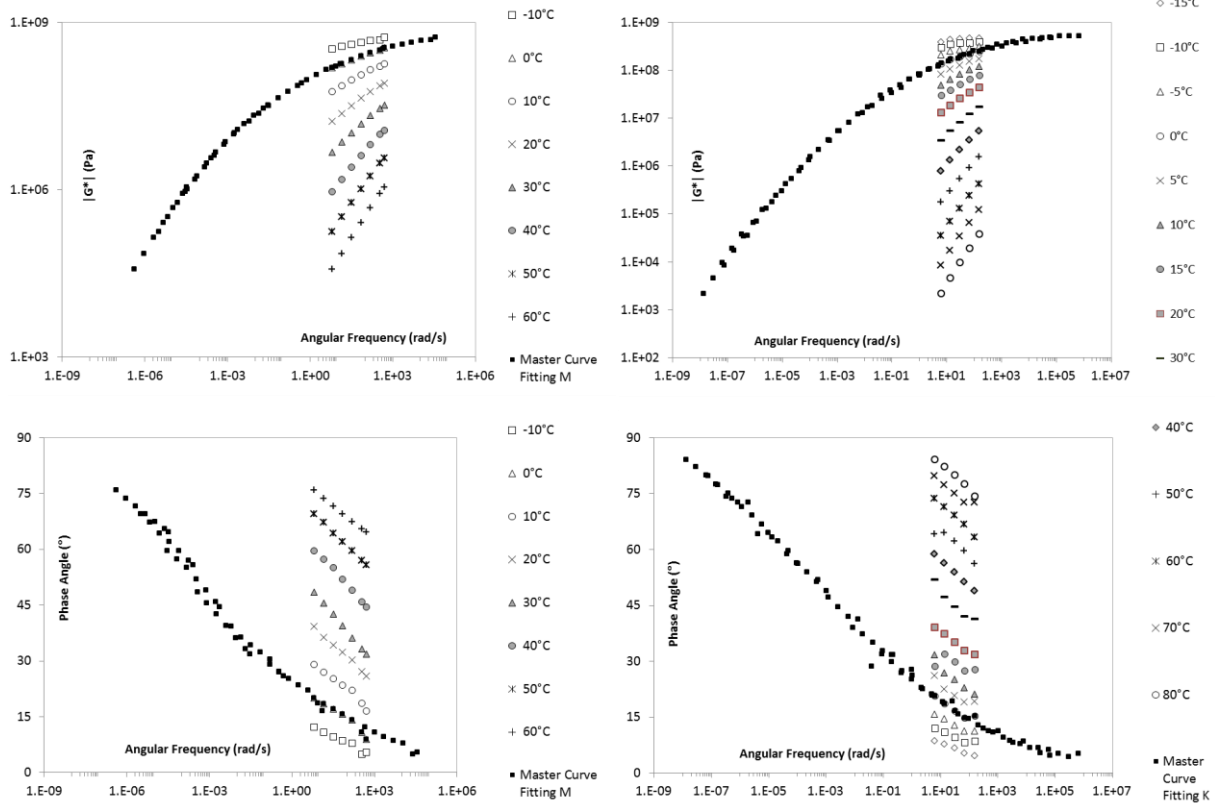


Rheological data measurements from Metravis® (left) and Kinexus® (right)

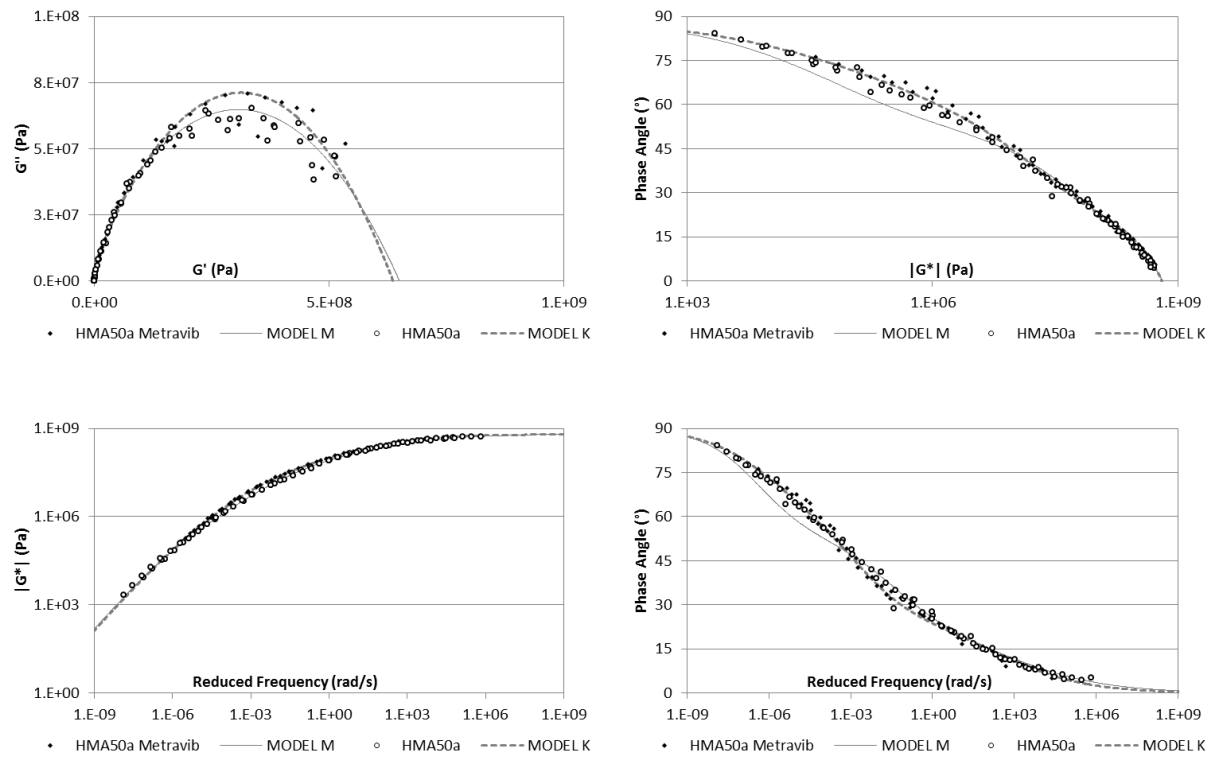


Cole-Cole plan, Black diagram and $|G^*|$ and δ master curves

HMA50a

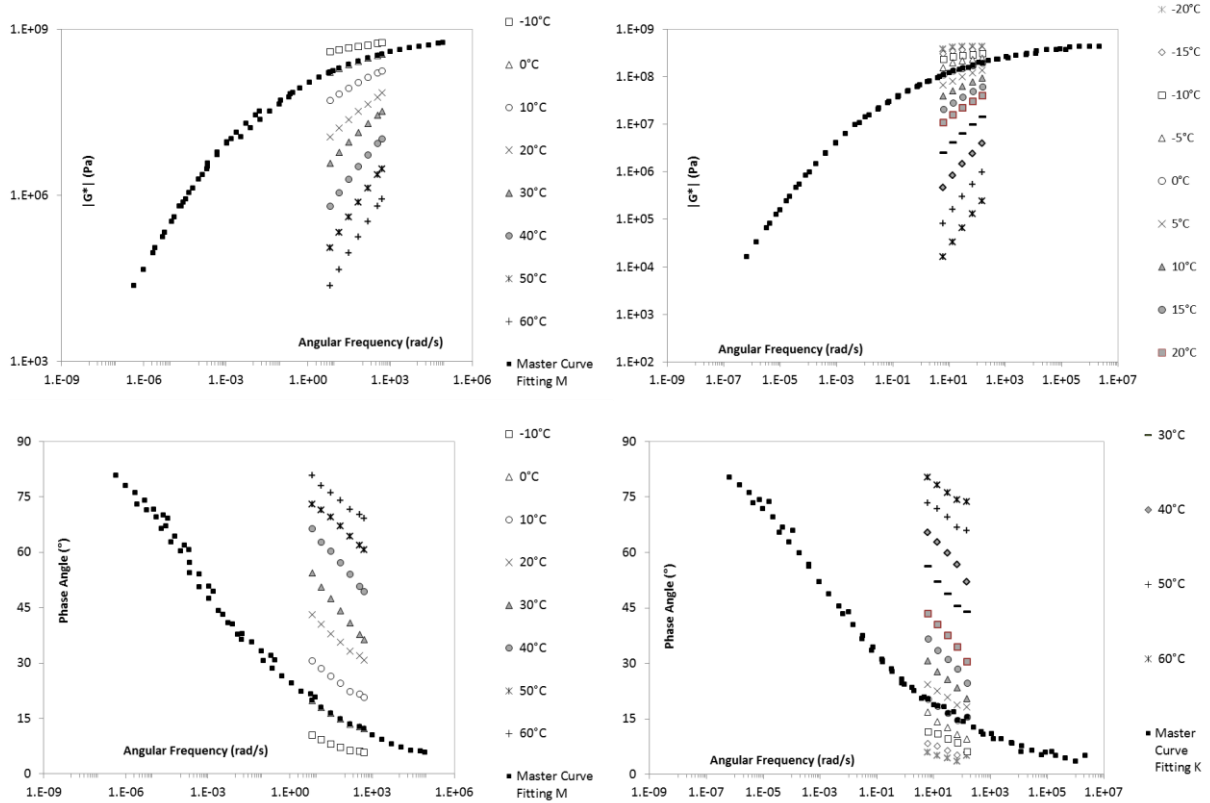


Rheological data measurements from Metravis® (left) and Kinexus® (right)

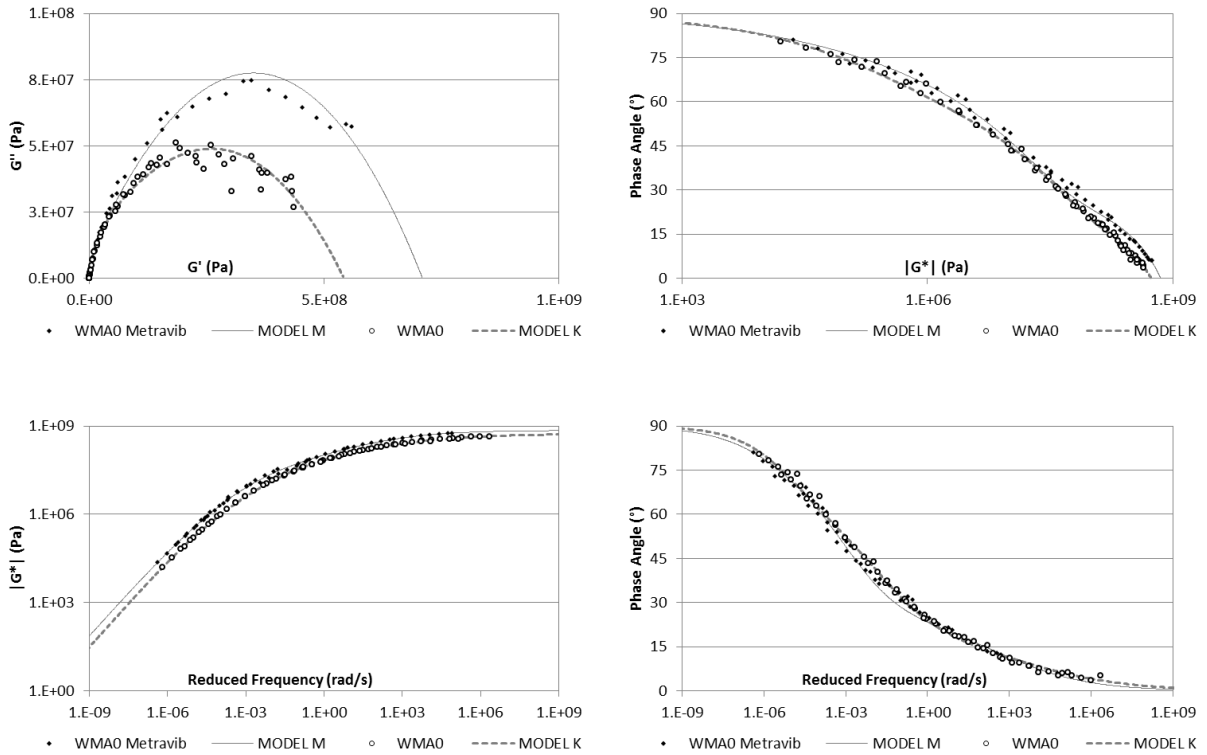


Cole-Cole plan, Black diagram and $|G^*|$ and δ master curves

WMA0

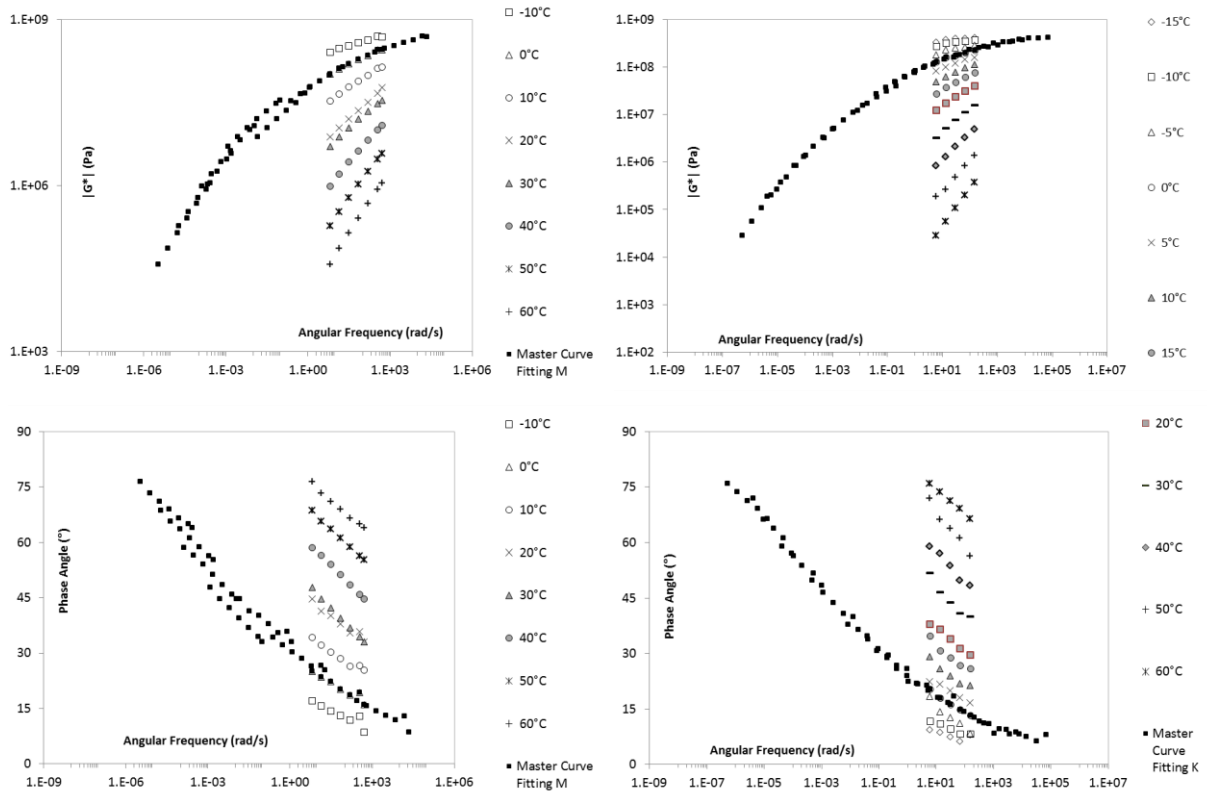


Rheological data measurements from Metravib® (left) and Kinexus® (right)

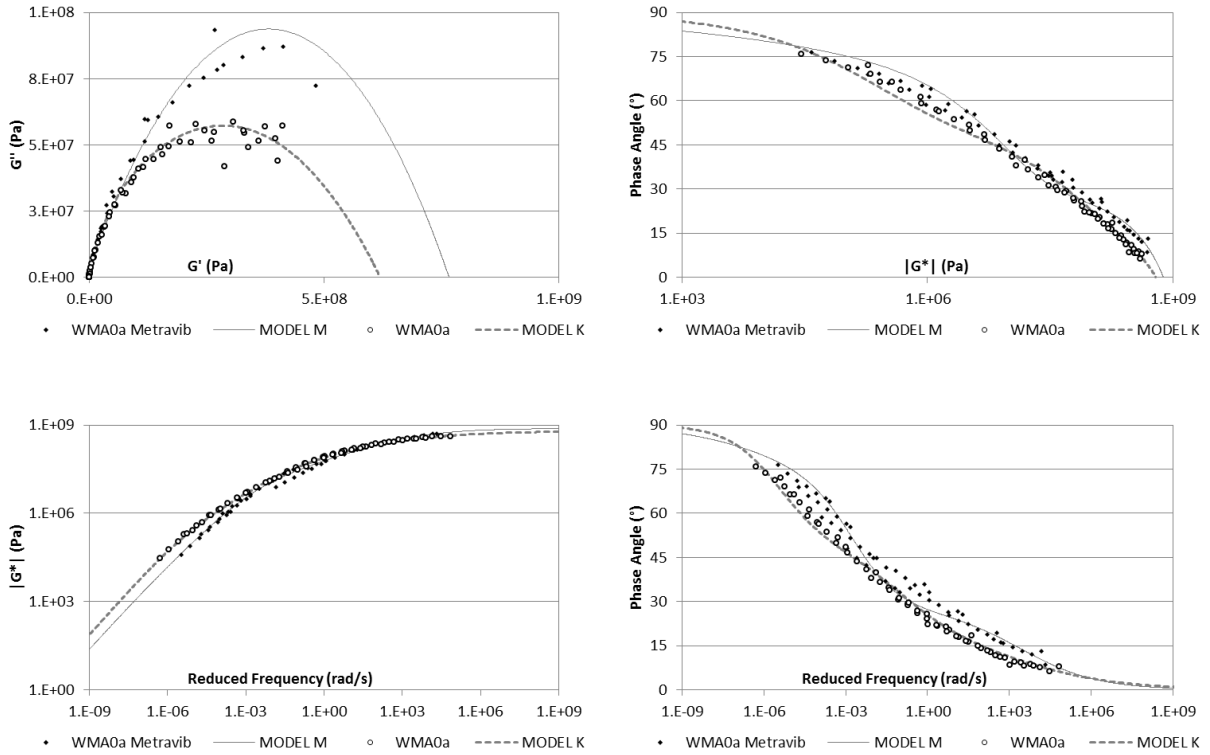


Cole-Cole plan, Black diagram and $|G^*|$ and δ master curves

WMA0a



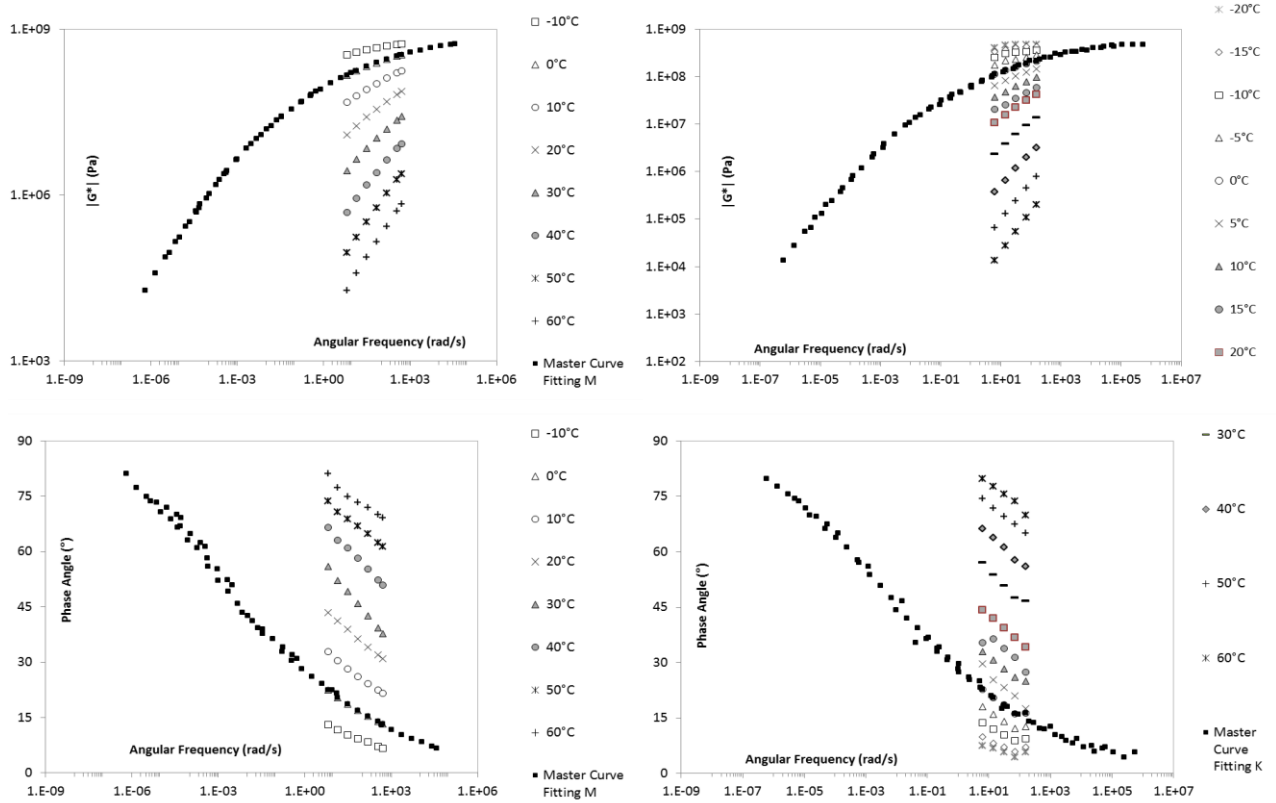
Rheological data measurements from Metravig® (left) and Kinexus® (right)



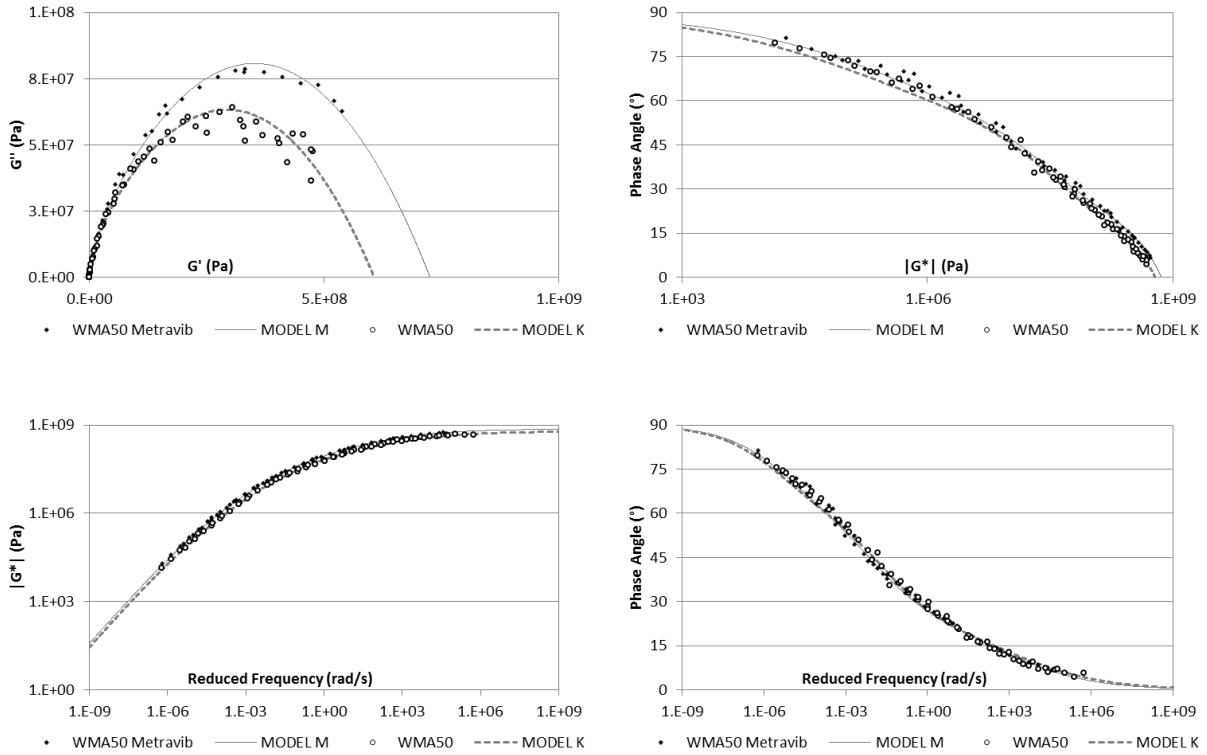
Cole-Cole plan, Black diagram and $|G^*|$ and δ master curves

Annex 4 - Master curves, Black diagrams and Cole-Cole plan of recovered bitumens from asphalt mixtures manufacture

WMA50

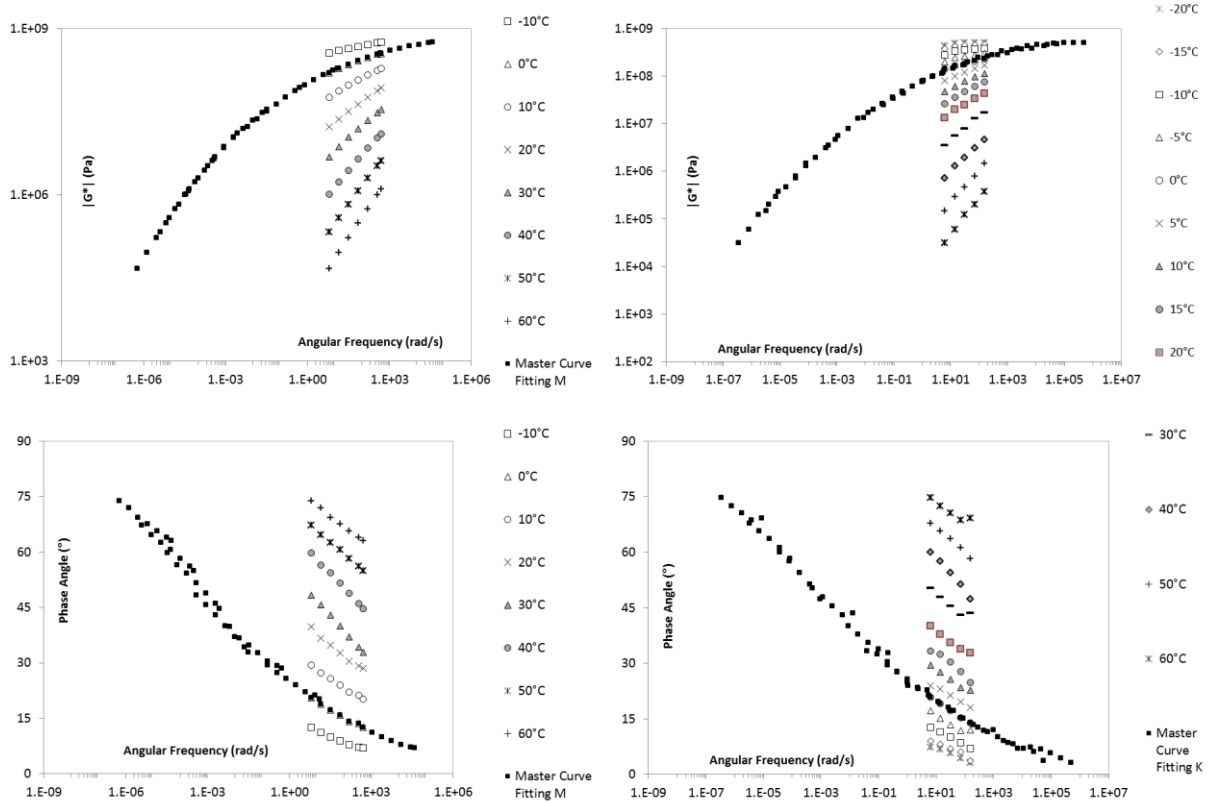


Rheological data measurements from Metravib® (left) and Kinexus® (right)

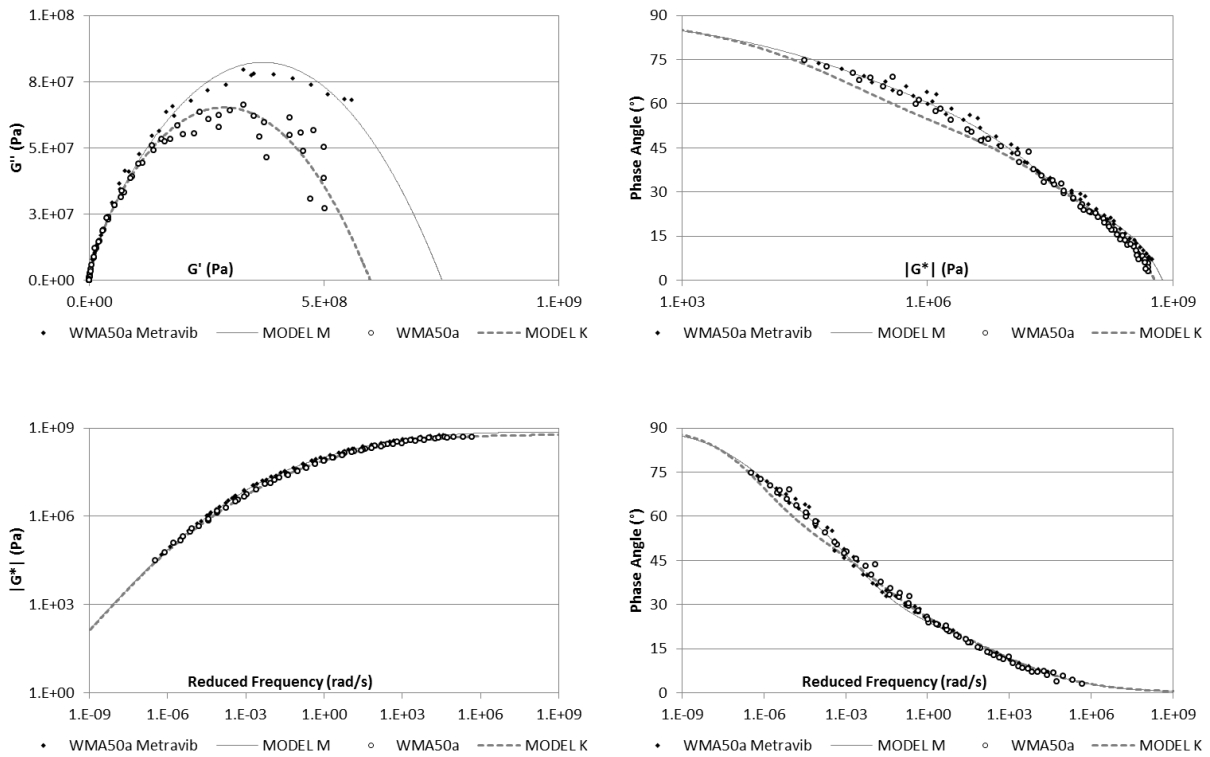


Cole-Cole plan, Black diagram and $|G^*|$ and δ master curves

WMA50a



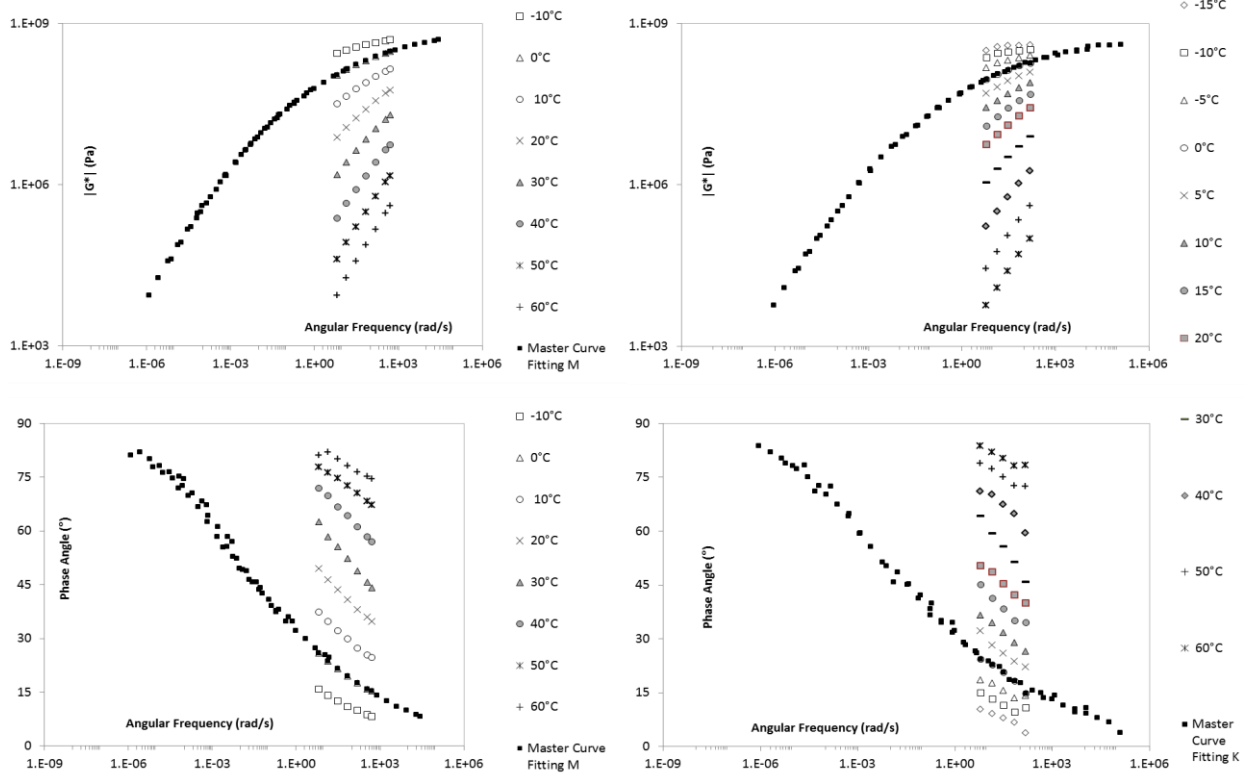
Rheological data measurements from Metravib® (left) and Kinexus® (right)



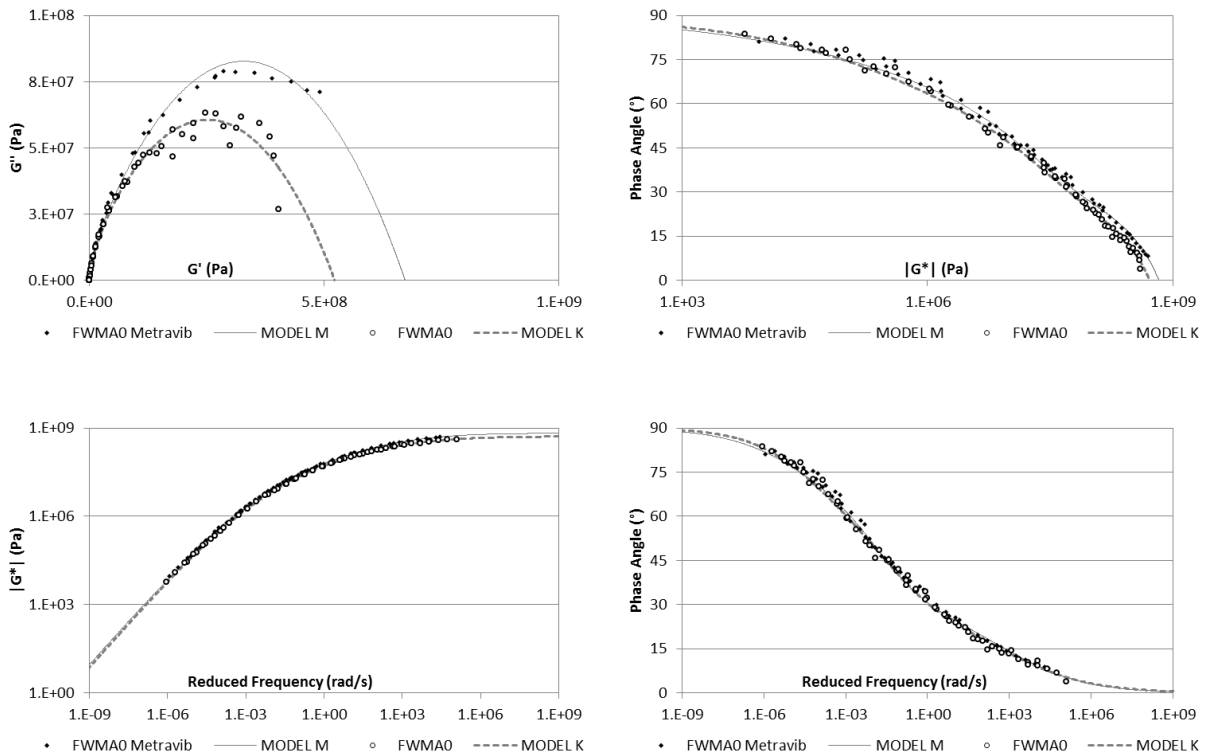
Cole-Cole plan, Black diagram and $|G^*|$ and δ master curves

Annex 4 - Master curves, Black diagrams and Cole-Cole plan of recovered bitumens form asphalt mixtures manufacture

FWMA0

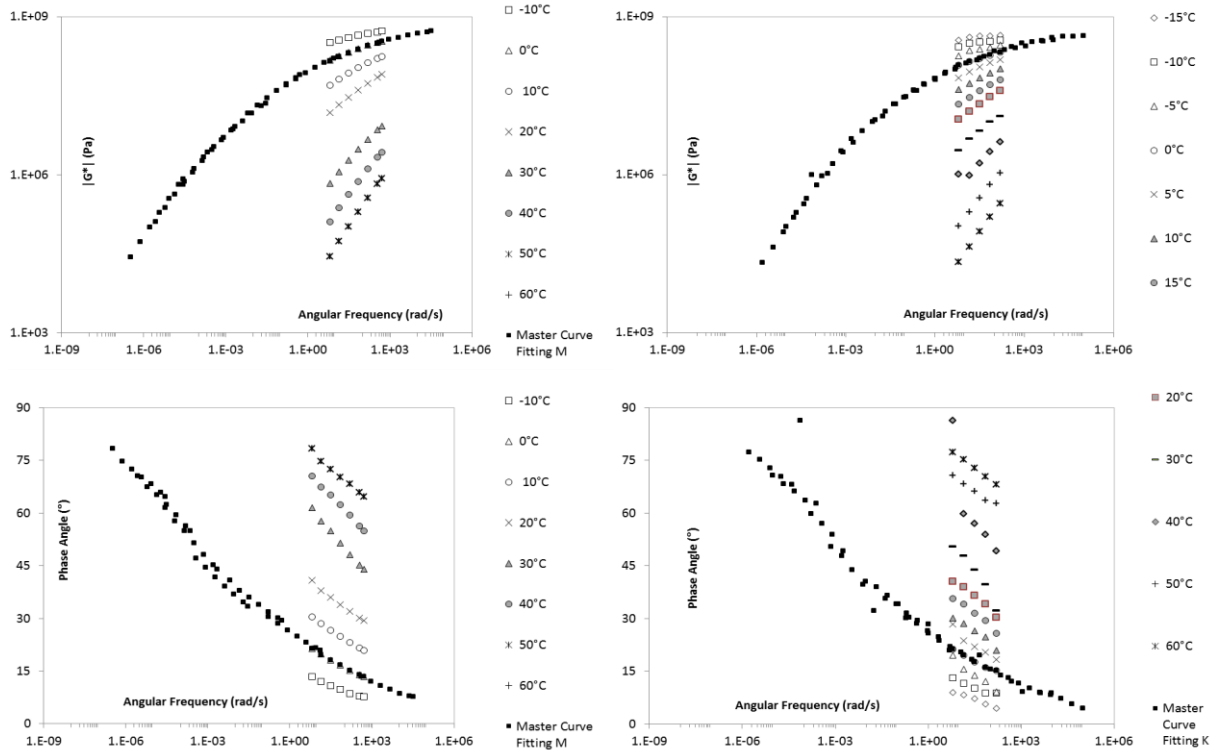


Rheological data measurements from Metravis® (left) and Kinexus® (right)

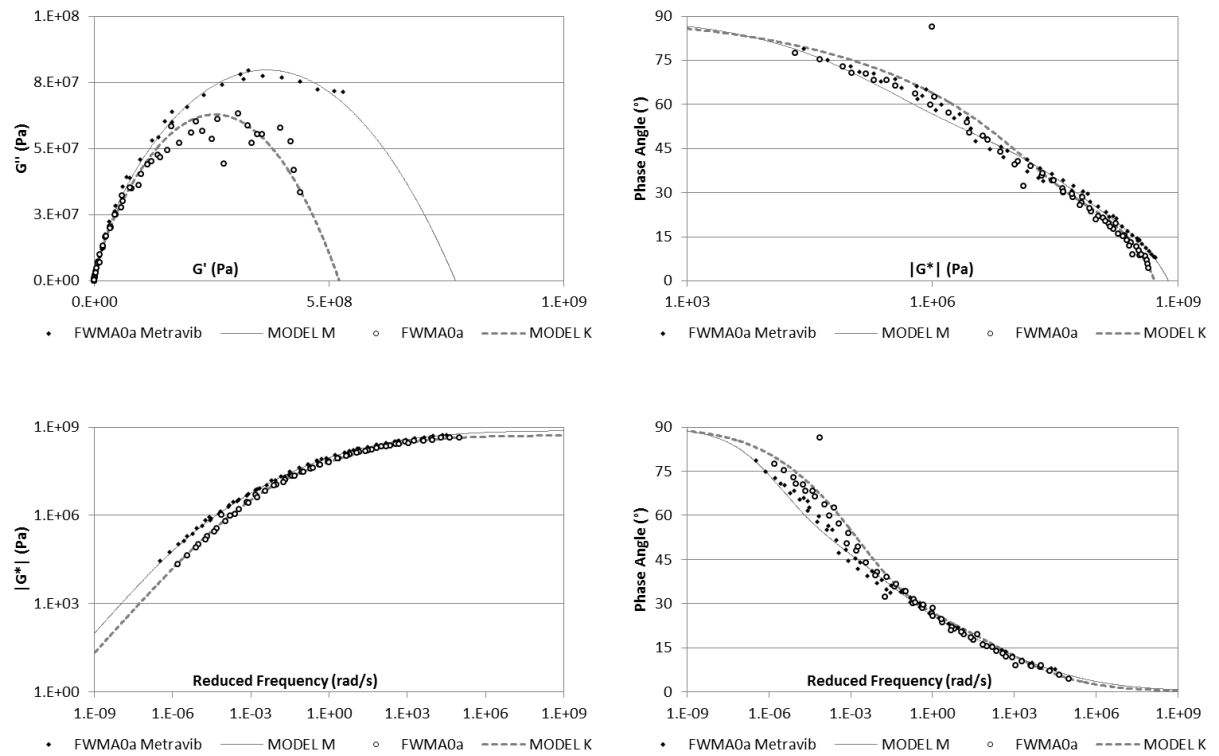


Cole-Cole plan, Black diagram and $|G^*|$ and δ master curves

FWMA0a

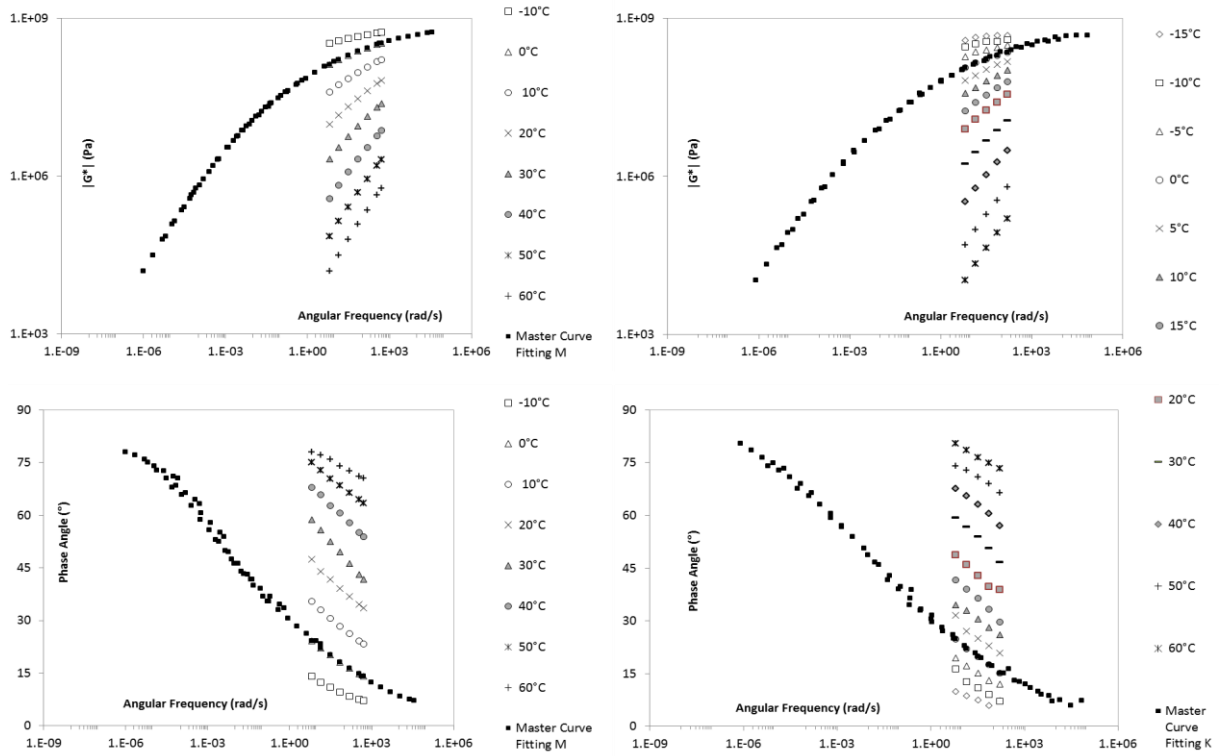


Rheological data measurements from Metravib® (left) and Kinexus® (right)

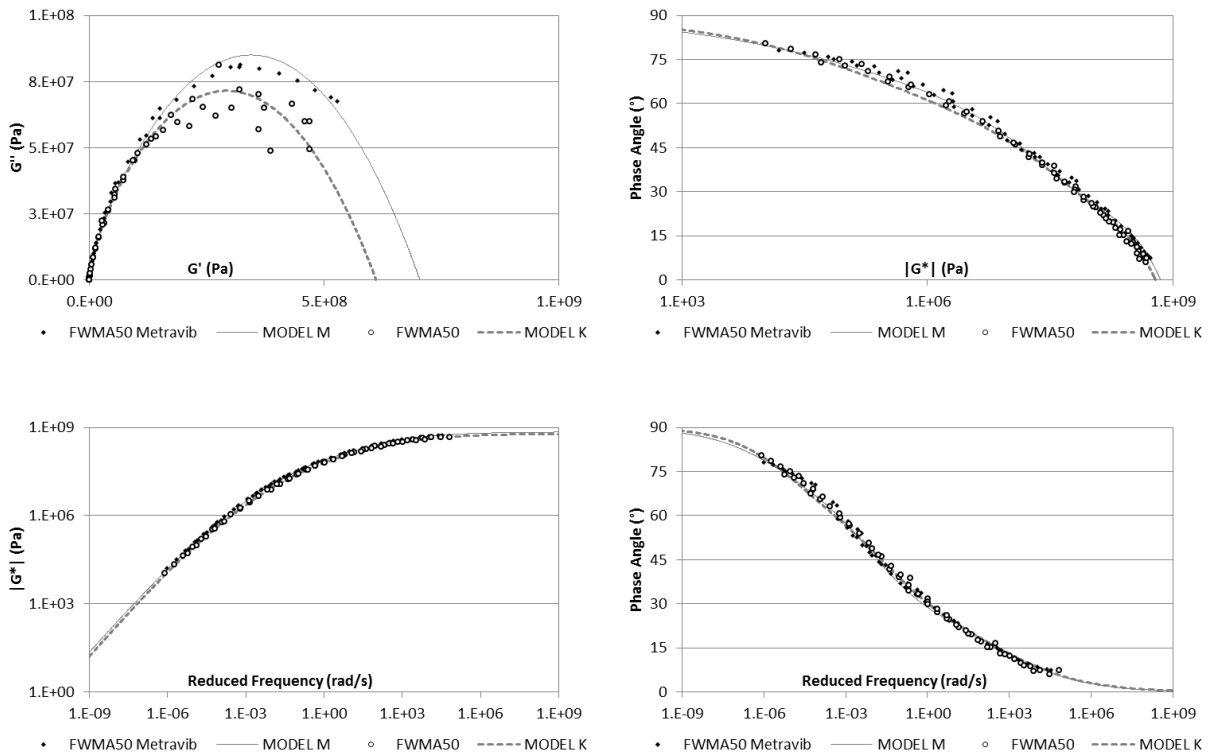


Cole-Cole plan, Black diagram and $|G^*|$ and δ master curves

FWMA50

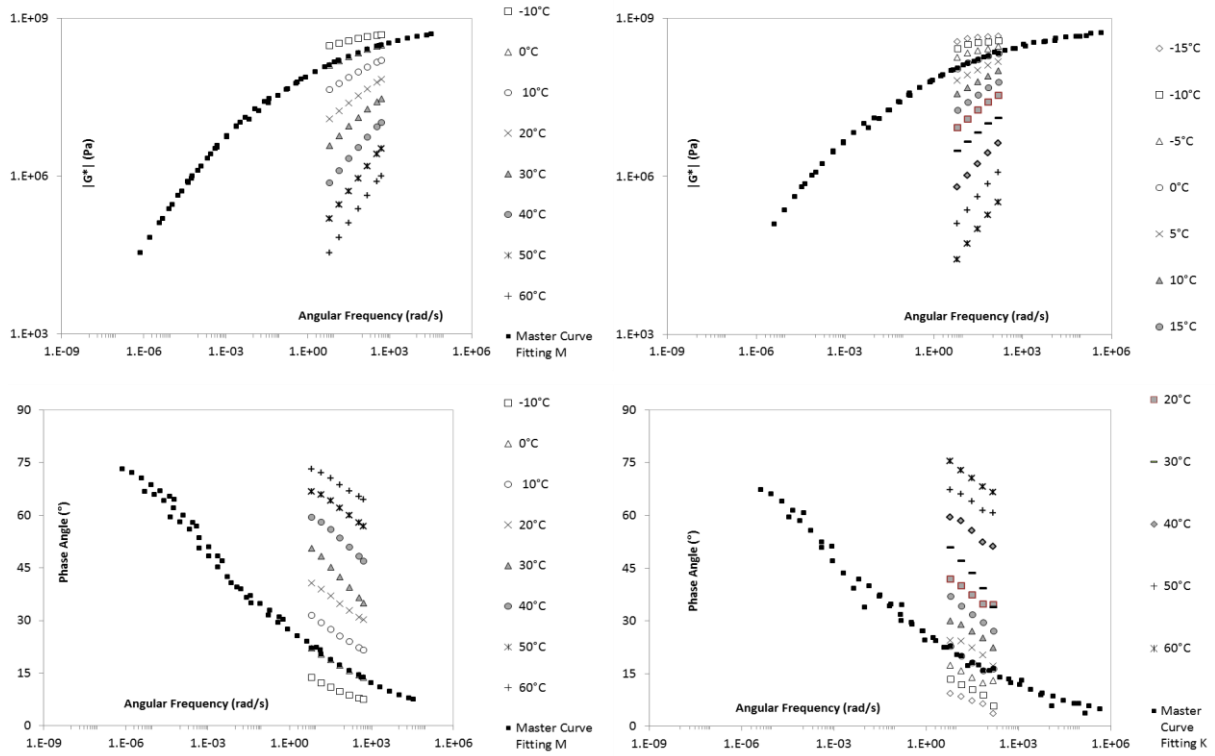


Rheological data measurements from Metravib® (left) and Kinexus® (right)

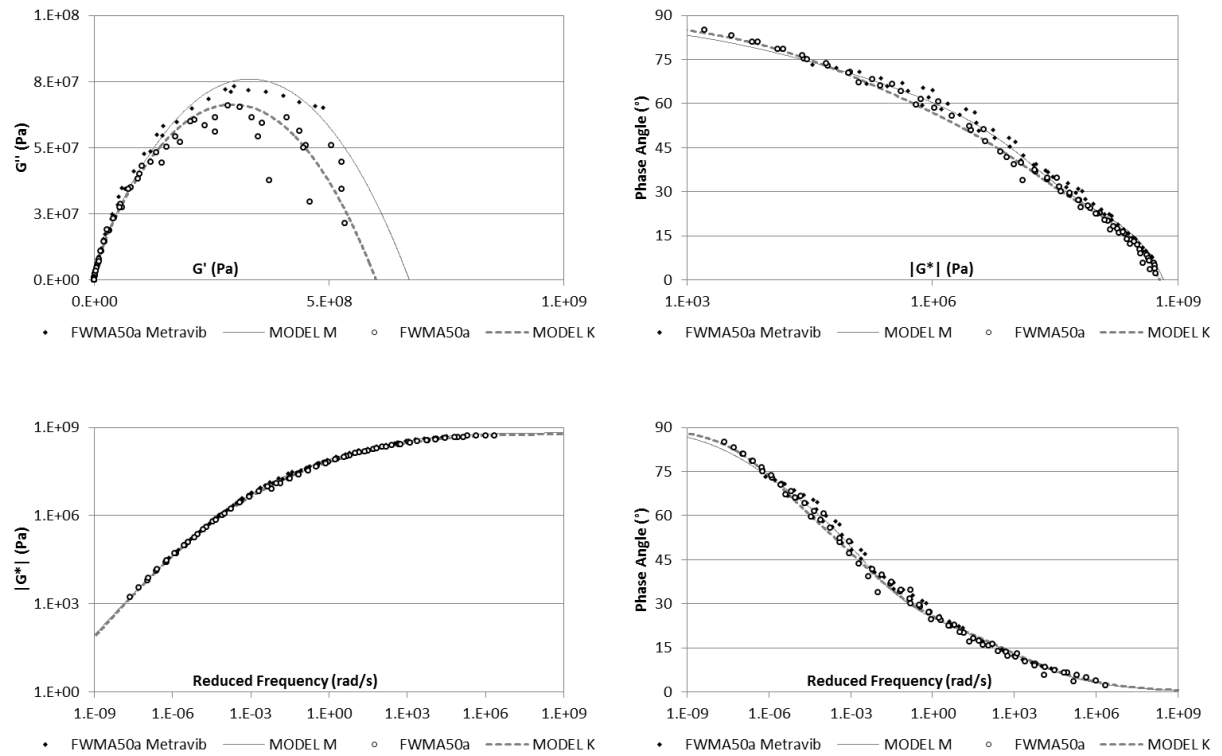


Cole-Cole plan, Black diagram and $|G^*|$ and δ master curves

FWMA50a



Rheological data measurements from Metravis® (left) and Kinexus® (right)



Cole-Cole plan, Black diagram and $|G^*|$ and δ master curves

Annex 5

HUET-SUCH MODELLING PARAMETERS AND δ -METHOD CURVES

FROM KINEXUS® DEVICE

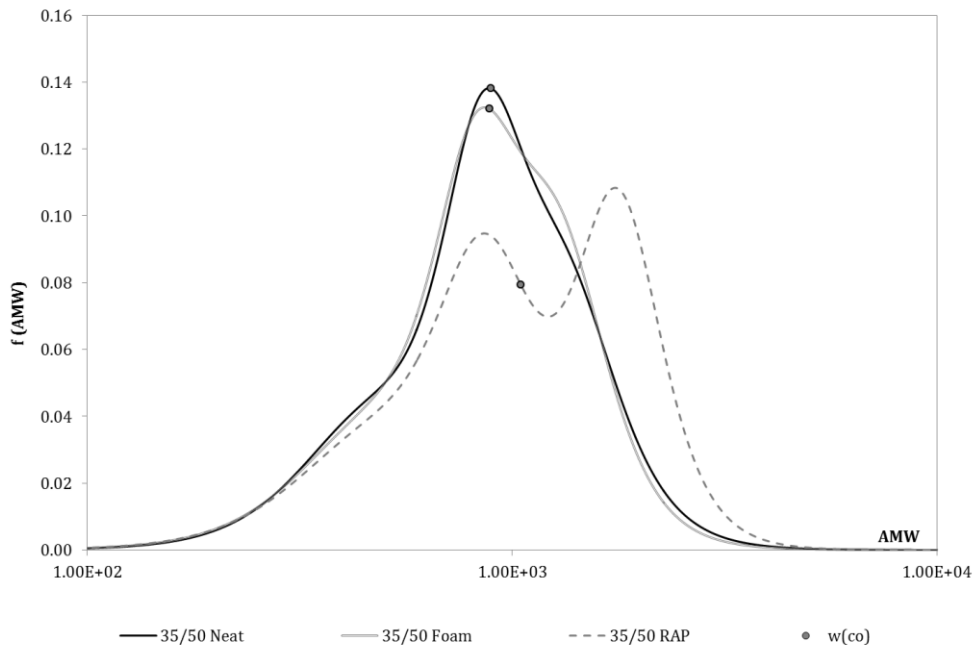
-RECOVERED BITUMENS FROM ASPHALT MIXTURES-

HUET-SUCH MODELLING PARAMETERS

Reference temperature for master curve $T=0^{\circ}\text{C}$

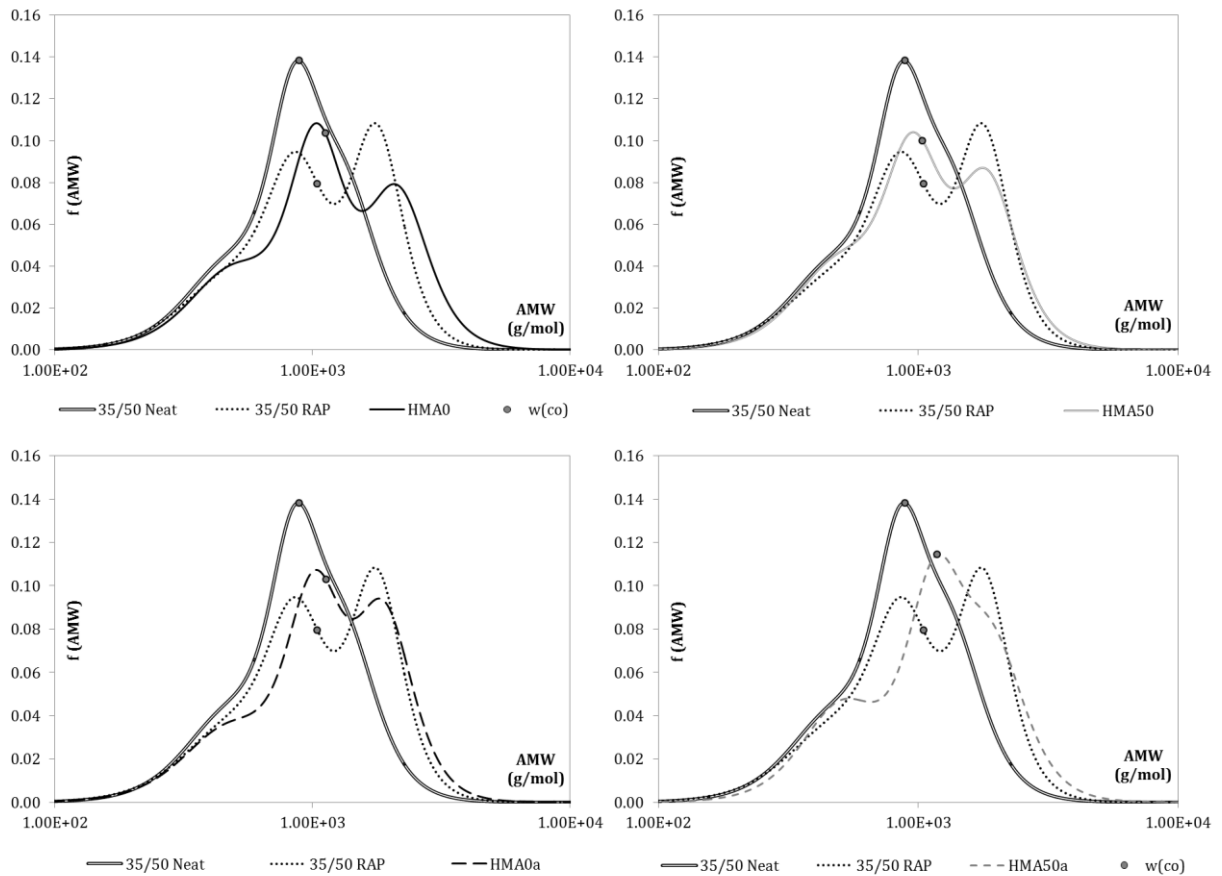
Bitumen	G_{∞} (MPa)	δ	k	h	β	τ (s)	C_1	C_2
35/50 Neat	630.49	4.13	0.26	0.66	37.88	1.54E-01	20.75	124.59
35/50 Foam	568.66	3.63	0.24	0.63	46.18	1.07E-01	20.90	123.74
35/50 RAP	706.85	3.75	0.23	0.59	368.07	1.75E-01	23.37	143.46
HMA0	660.18	5.54	0.25	0.65	212.60	1.25E+00	26.08	151.61
HMA0a	646.73	5.34	0.24	0.62	172.83	9.35E-01	23.68	139.02
HMA50	691.68	4.70	0.26	0.64	162.72	4.59E-01	23.44	140.83
HMA50a	636.38	6.98	0.28	0.66	79.15	2.90E+00	23.59	137.38
WMA0	542.58	4.82	0.22	0.61	112.58	5.13E-01	21.21	122.33
WMA0a	620.03	3.71	0.22	0.56	526.09	2.33E-01	26.74	166.50
WMA50	606.81	5.39	0.26	0.64	119.03	4.08E-01	27.43	174.71
WMA50a	598.39	5.01	0.27	0.60	349.63	6.51E-01	31.55	200.97
FWMA0	523.11	5.11	0.28	0.66	49.68	2.87E-01	20.89	123.09
FWMA0a	522.10	7.08	0.30	0.69	30.43	1.37E+00	20.02	122.39
FWMA50	611.04	4.82	0.28	0.65	92.44	2.99E-01	24.97	157.34
FWMA50a	600.22	6.82	0.27	0.63	158.23	8.15E-01	21.39	122.94

NEAT BITUMENS



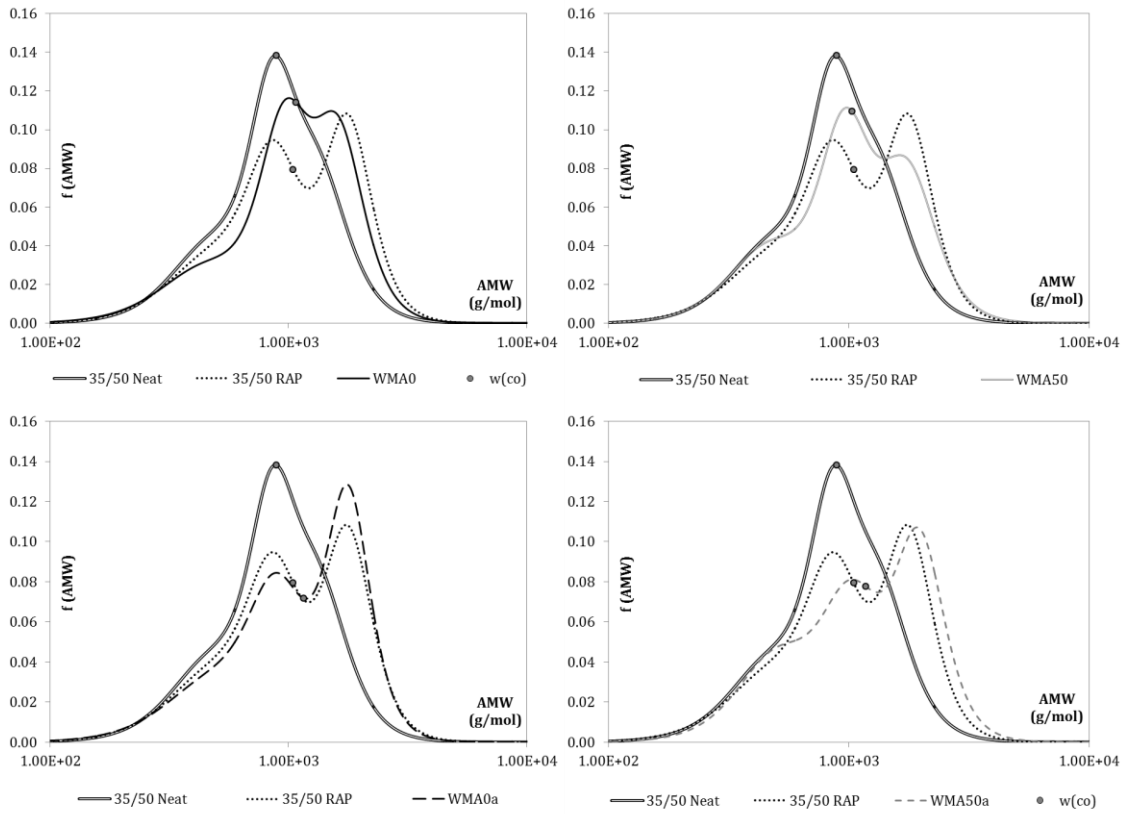
δ -method curves for 35/50 Neat, RAP and Foam bitumens

HMA0 - HMA0a- HMA50 - HMA50a



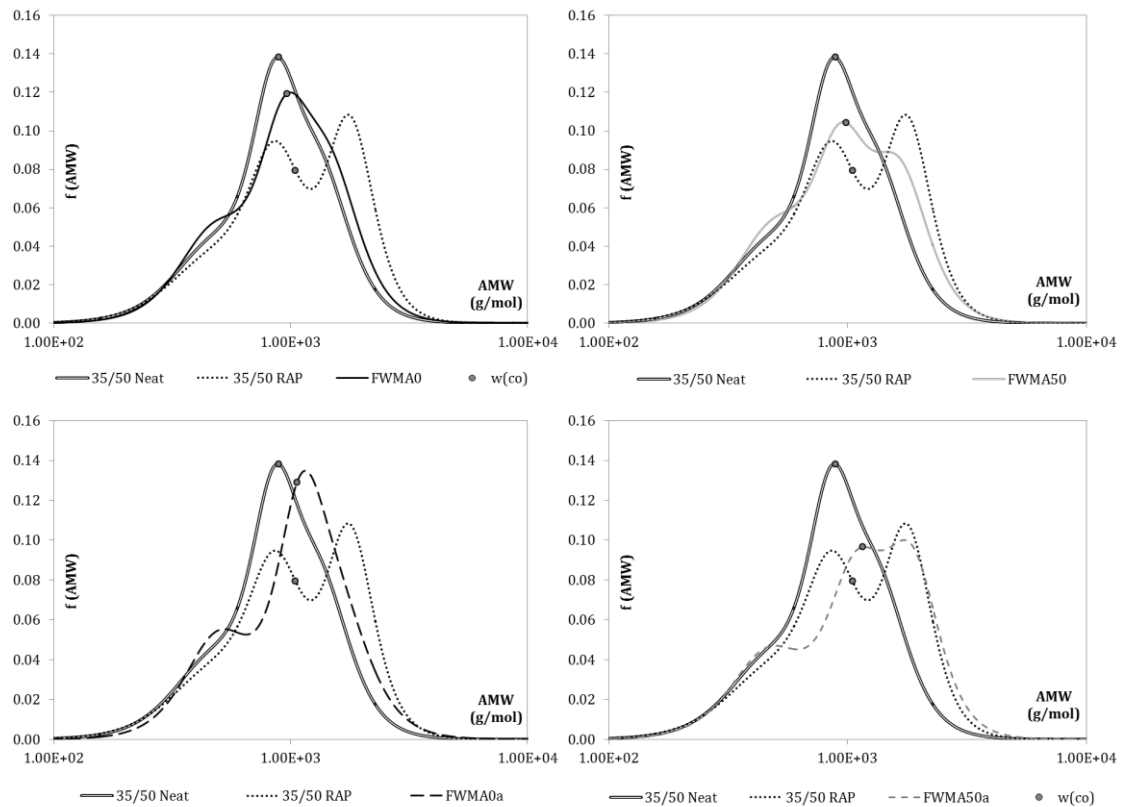
δ -method curves of 35/50 Neat and RAP bitumen compared with recovered asphalt mixture bitumen

WMA0 - WMA0a - WMA50 - WMA50a



δ -method curves of 35/50 Neat and RAP bitumen compared with recovered asphalt mixture bitumen

FWMA0 - FWMA0a - FWMA50 - FWMA50a



δ -method curves of 35/50 Neat and RAP bitumen compared with recovered asphalt mixture bitumen

Annex 6

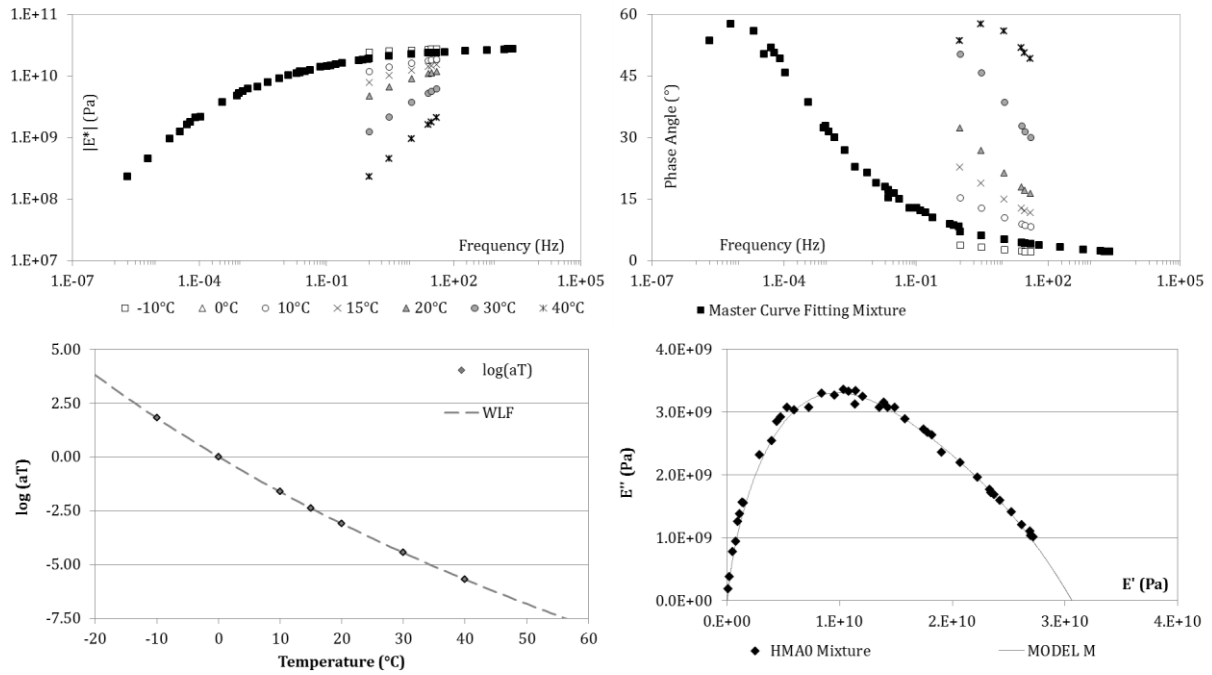
2S2P1D MODELLING PARAMETERS AND MASTER CURVES OF ASPHALT MIXTURES

2S2P1D MODELLING PARAMETERSReference temperature for master curve $T=0^{\circ}\text{C}$

Bitumen	E_0 (MPa)	E_{∞} (MPa)	δ	k	h	β	τ (s)
HMA0	67.73	30,626	1.68	0.19	0.56	26.40	3.01E+01
HMA0a	40.28	31,010	2.02	0.17	0.54	64.08	1.79E+02
HMA50	74.34	32,584	1.79	0.18	0.54	36.23	6.43E+01
HMA50a	77.77	34,874	2.00	0.18	0.54	47.58	1.22E+02
WMA0	67.31	29,653	1.52	0.18	0.55	26.31	2.97E+01
WMA0a	74.72	33,740	1.99	0.17	0.54	47.06	1.84E+02
WMA50	77.59	31,154	1.84	0.18	0.56	26.91	5.51E+01
WMA50a	56.05	34,903	2.03	0.18	0.55	53.52	1.43E+02
FWMA0	43.16	27,155	1.80	0.21	0.61	25.57	2.32E+01
FWMA0a	85.82	33,111	1.86	0.18	0.53	41.07	8.97E+01
FWMA50	60.36	30,823	1.96	0.20	0.59	24.94	4.34E+01
FWMA50a	84.65	34,087	1.98	0.18	0.55	41.77	1.09E+02

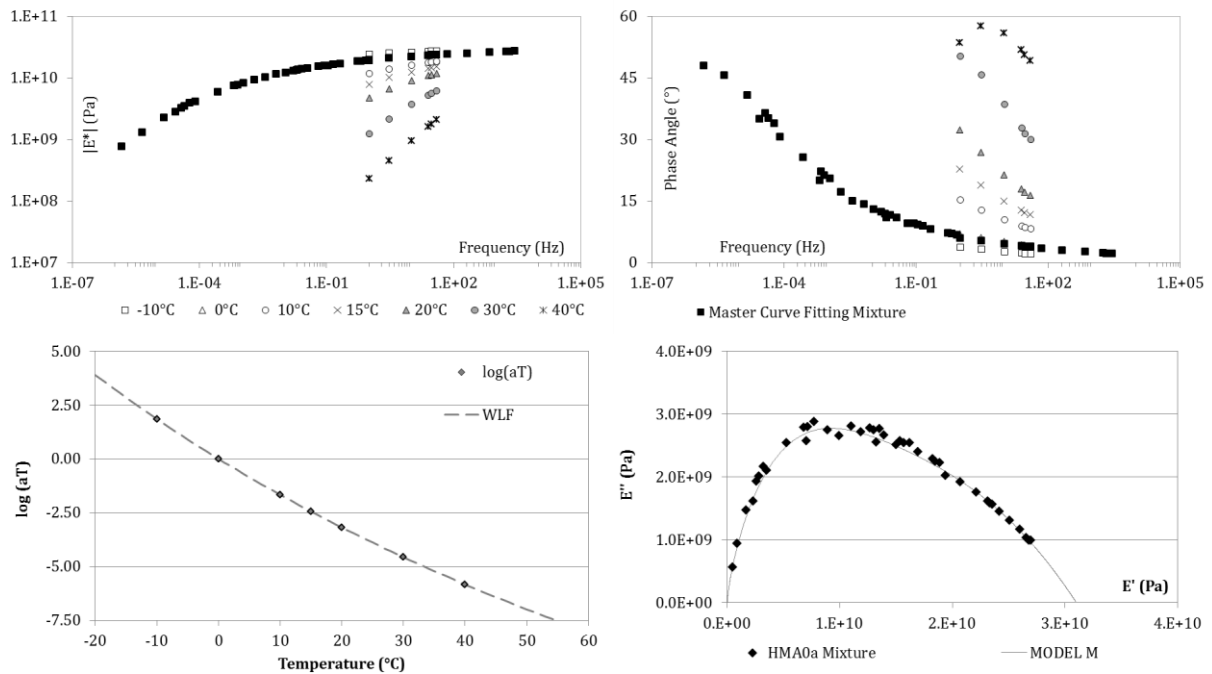
Mixture	C_1	C_2	Mixture	C_1	C_2	Mixture	C_1	C_2
HMA0	34.30	200.90	WMA0	33.25	193.39	FWMA0	35.15	213.36
HMA0a	34.53	196.87	WMA0a	35.26	200.53	FWMA0a	31.61	177.95
HMA50	33.89	202.76	WMA50	33.10	200.60	FWMA50	32.43	196.21
HMA50a	32.56	192.54	WMA50a	30.72	179.00	FWMA50a	30.28	176.96

HMA0



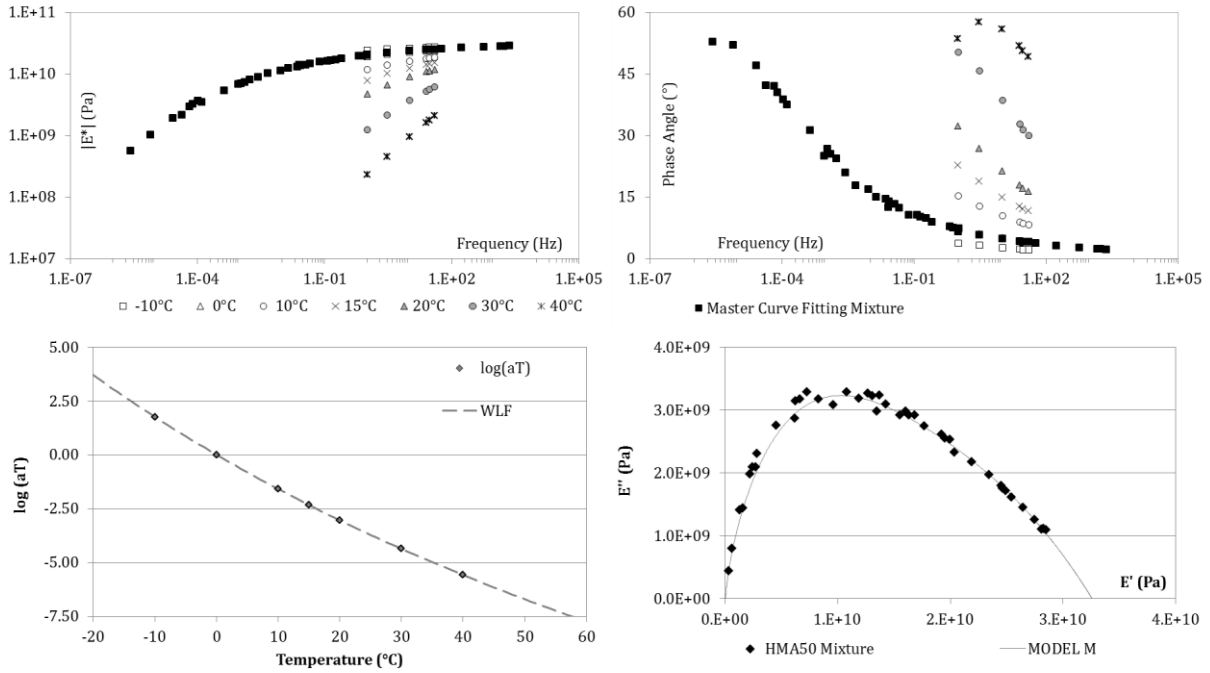
2PB Complex modulus results with, WLF adjustment and Cole-Cole plan (with model)

HMA0a



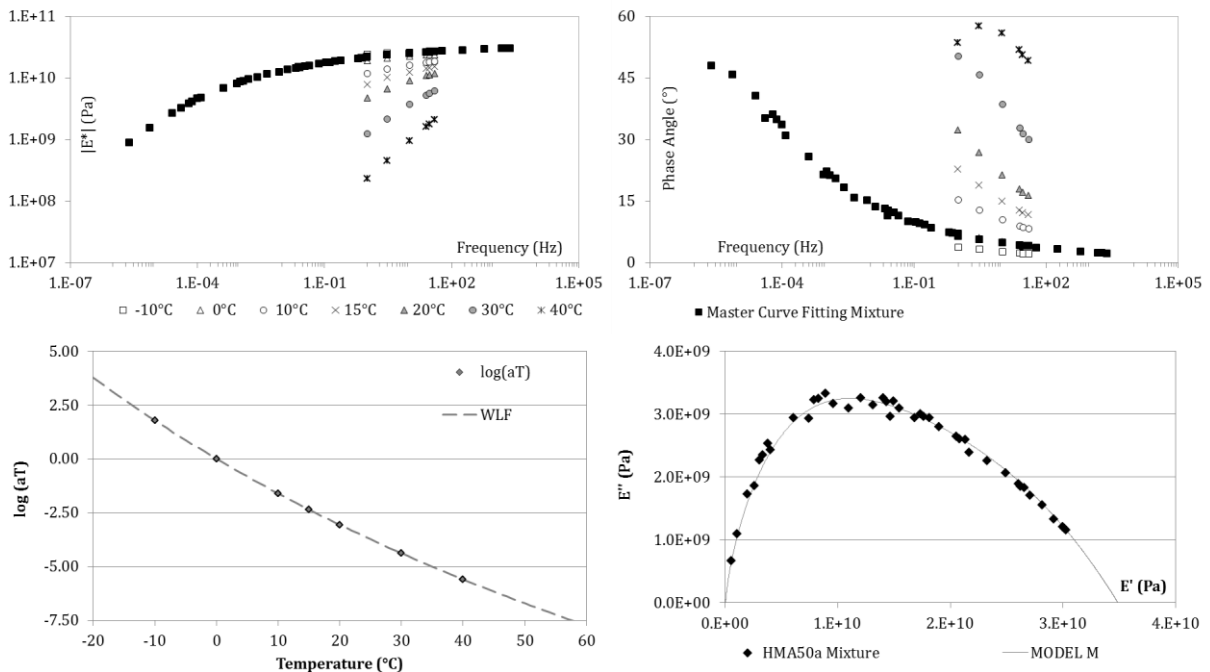
2PB Complex modulus results with, WLF adjustment and Cole-Cole plan (with model)

HMA50



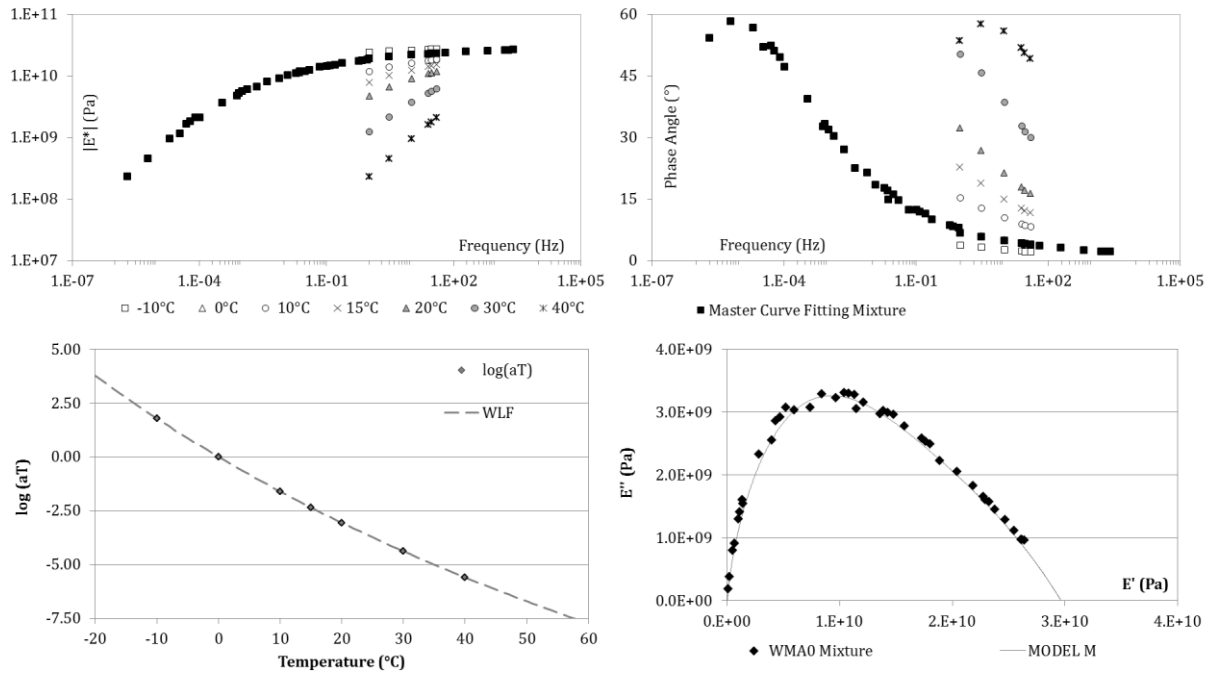
2PB Complex modulus results with, WLF adjustment and Cole-Cole plan (with model)

HMA50a



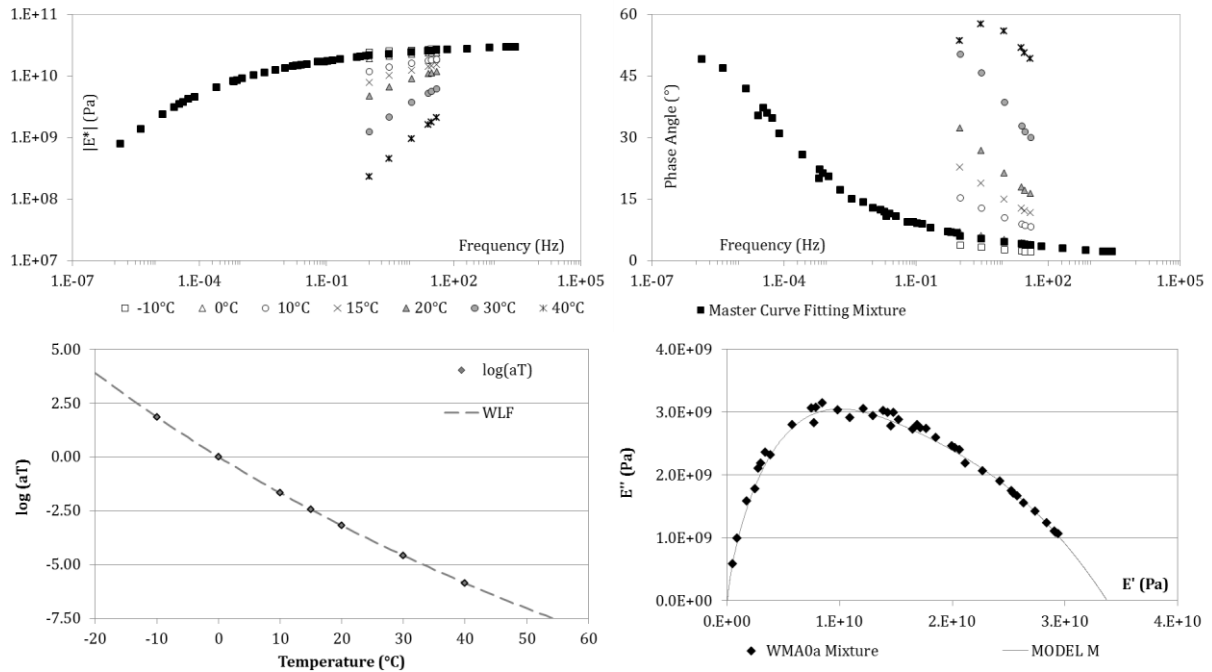
2PB Complex modulus results with, WLF adjustment and Cole-Cole plan (with model)

WMA0



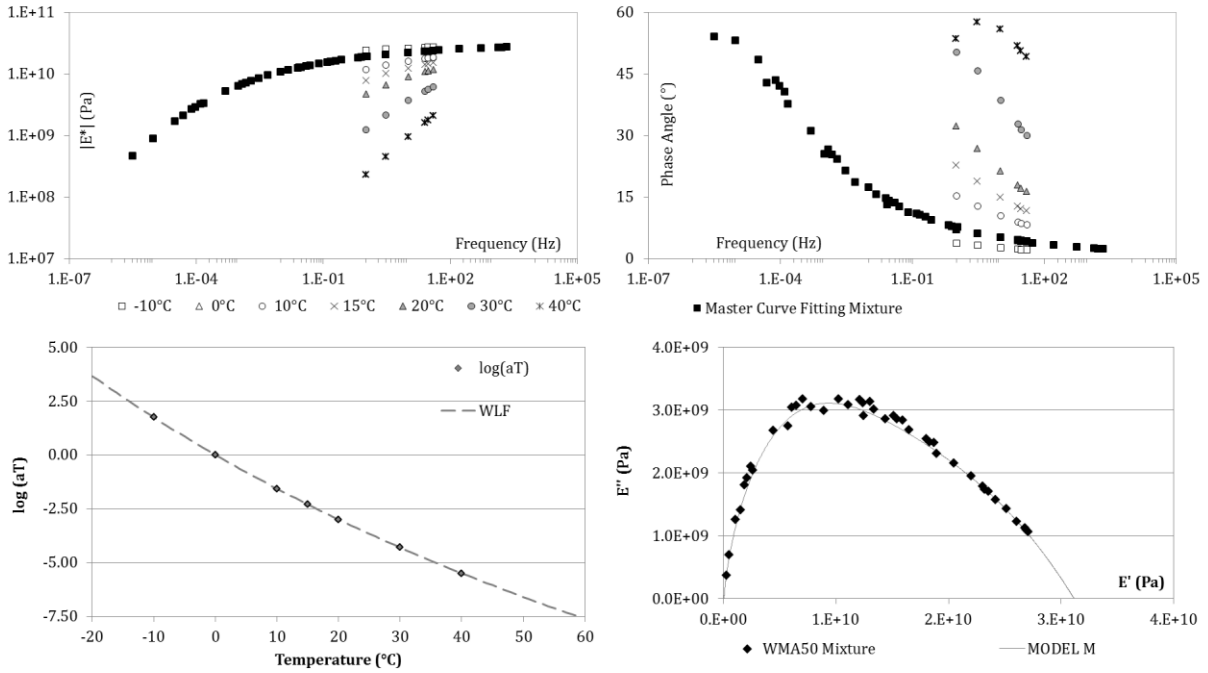
2PB Complex modulus results with, WLF adjustment and Cole-Cole plan (with model)

WMA0a



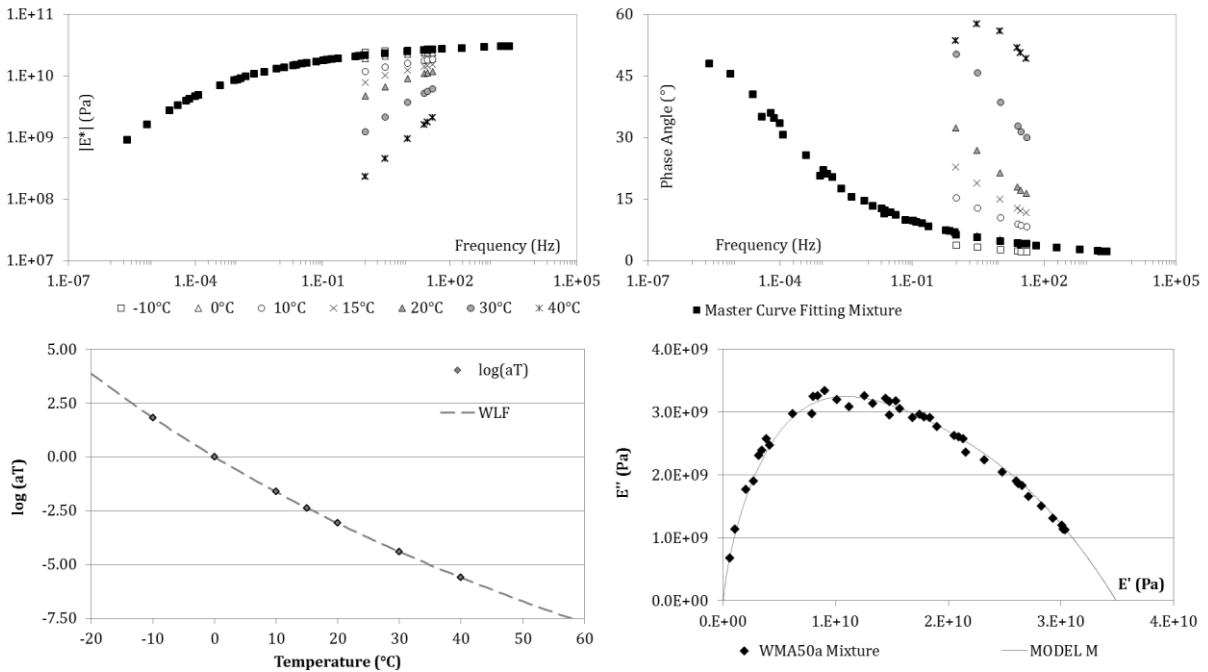
2PB Complex modulus results with, WLF adjustment and Cole-Cole plan (with model)

WMA50



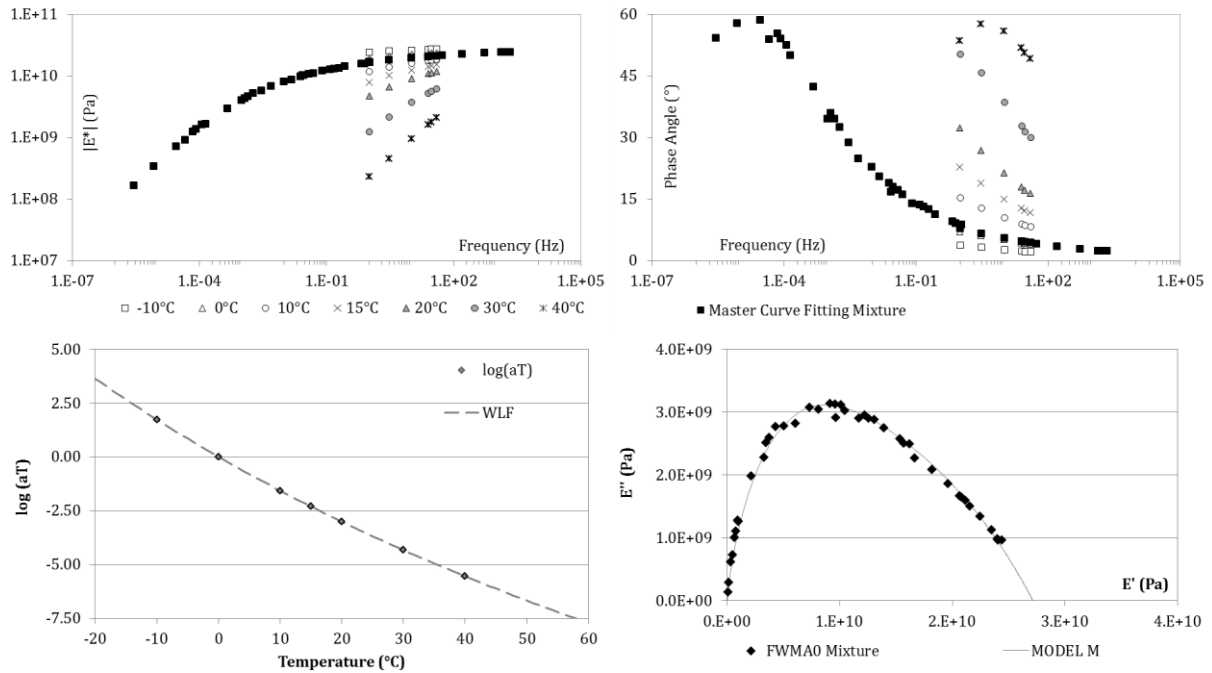
2PB Complex modulus results with, WLF adjustment and Cole-Cole plan (with model)

WMA50a



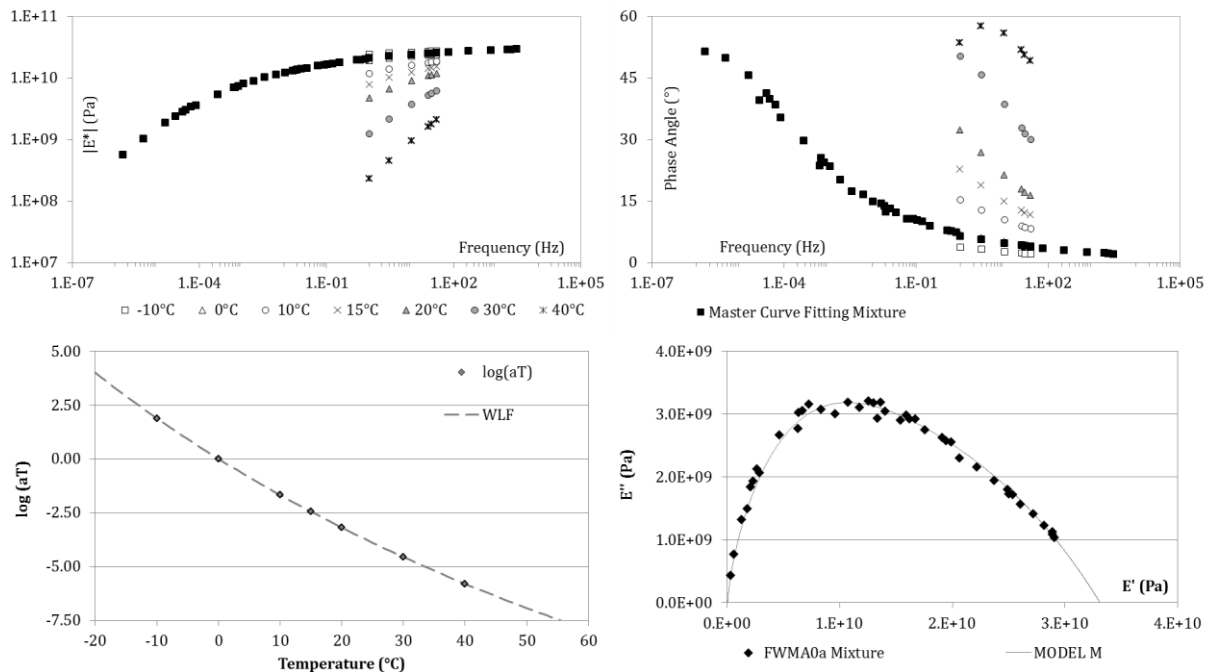
2PB Complex modulus results with, WLF adjustment and Cole-Cole plan (with model)

FWMA0



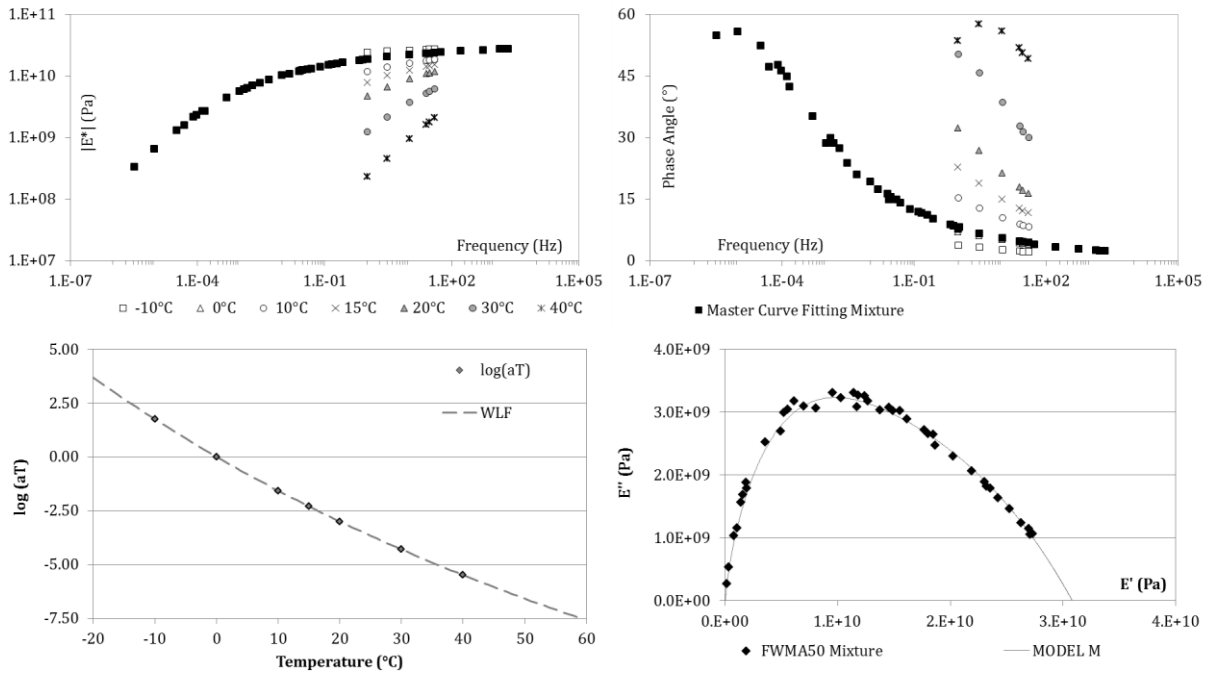
2PB Complex modulus results with, WLF adjustment and Cole-Cole plan (with model)

FWMA0a



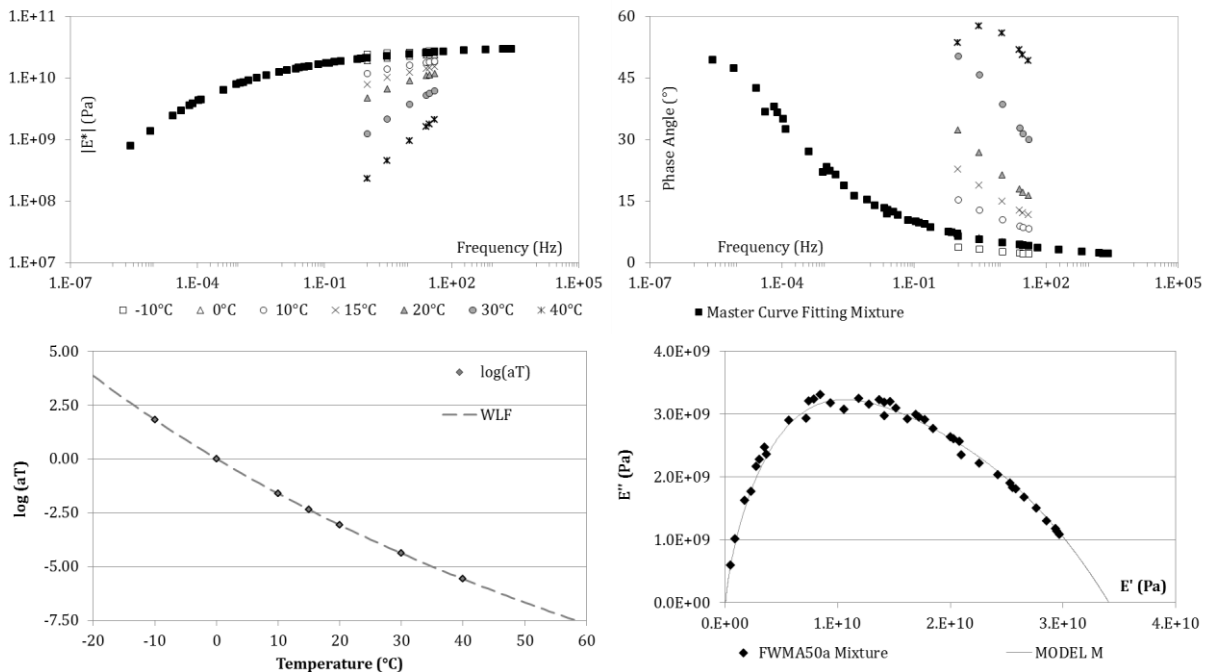
2PB Complex modulus results with, WLF adjustment and Cole-Cole plan (with model)

FWMA50



2PB Complex modulus results with, WLF adjustment and Cole-Cole plan (with model)

FWMA50a

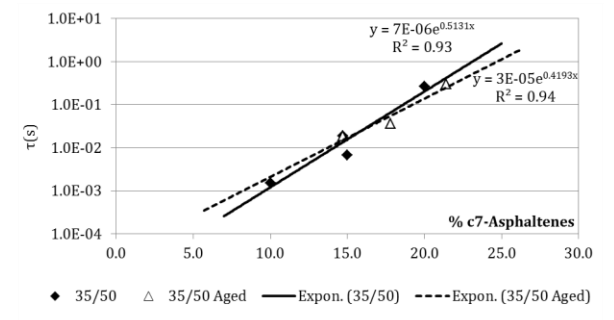
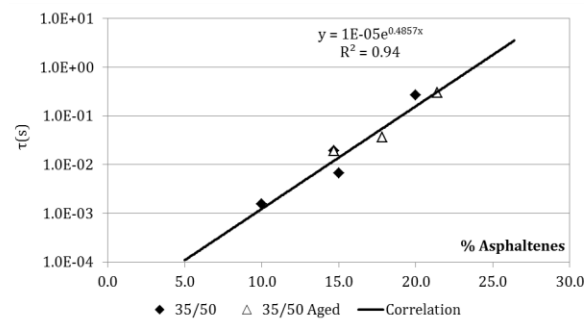
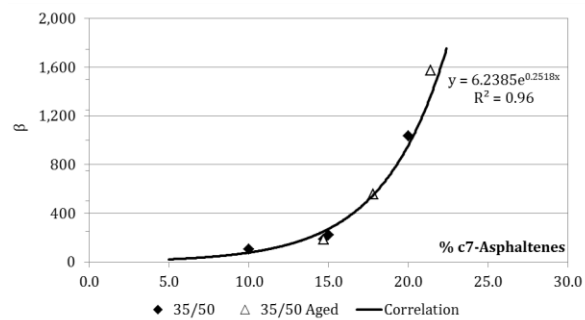
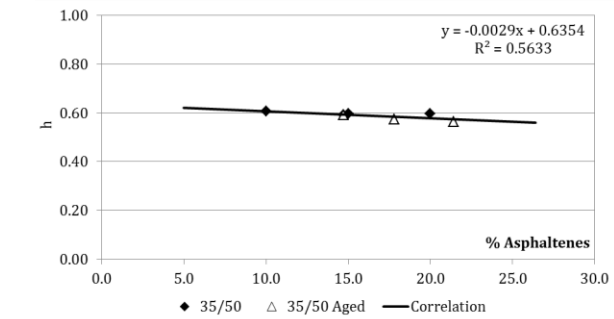
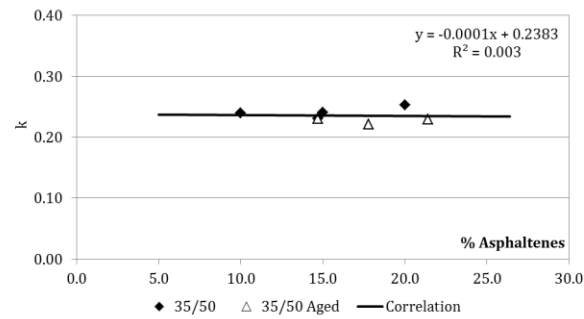
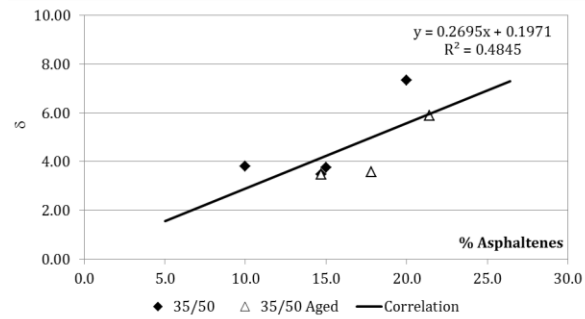
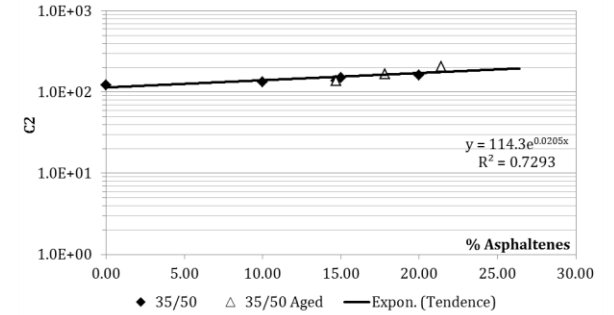
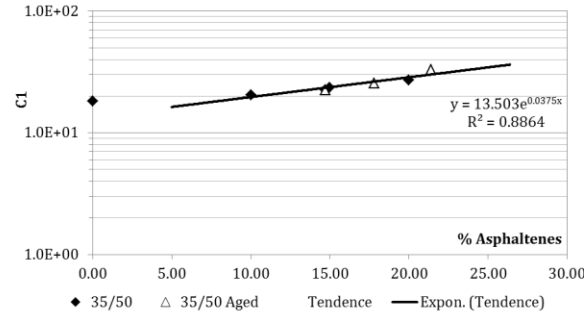
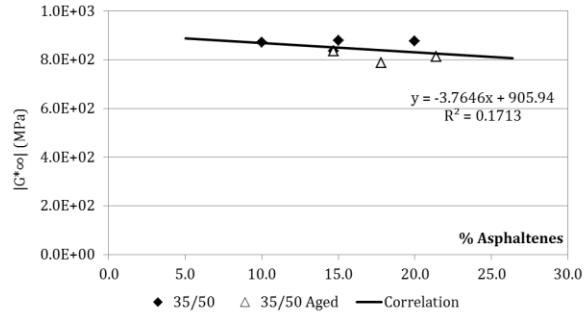


2PB Complex modulus results with, WLF adjustment and Cole-Cole plan (with model)

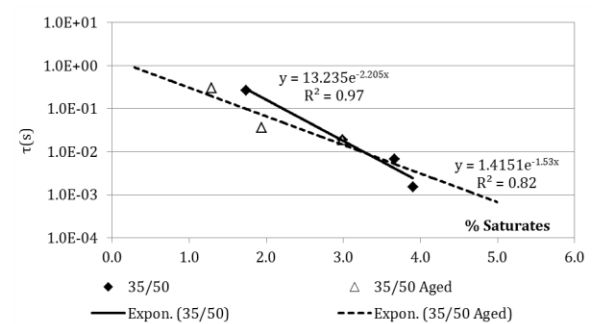
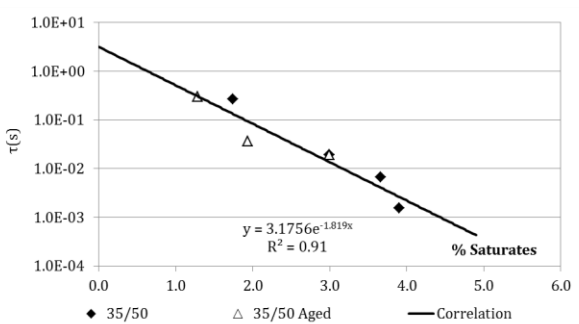
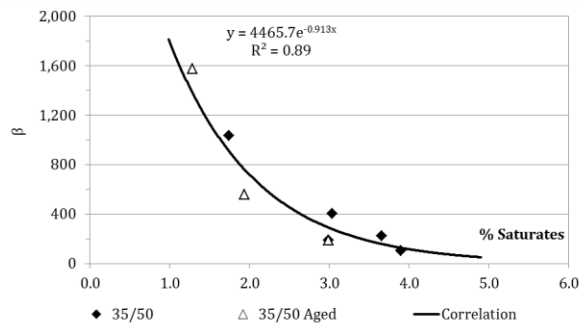
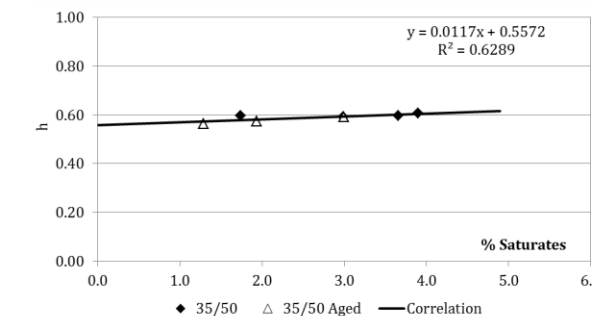
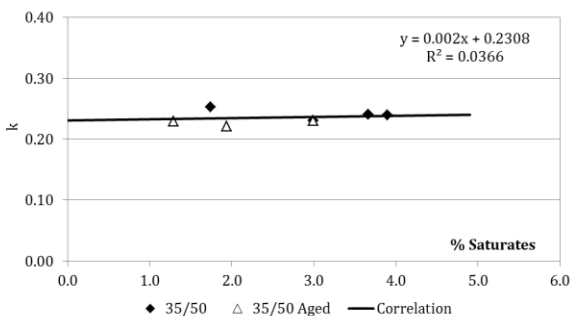
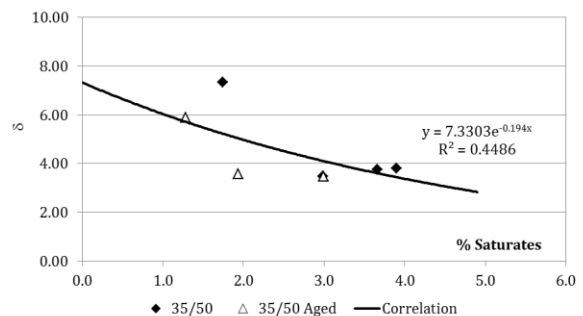
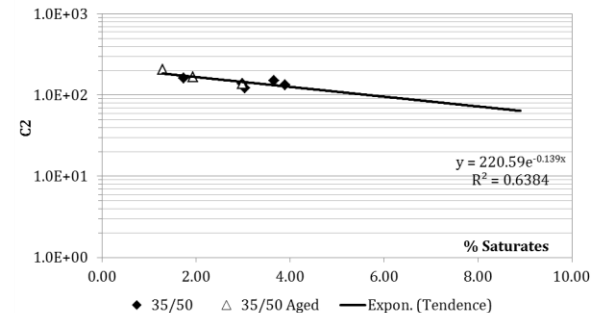
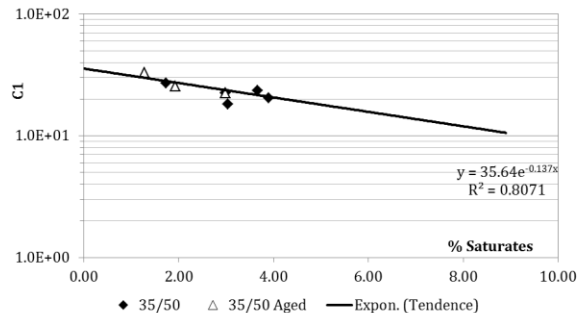
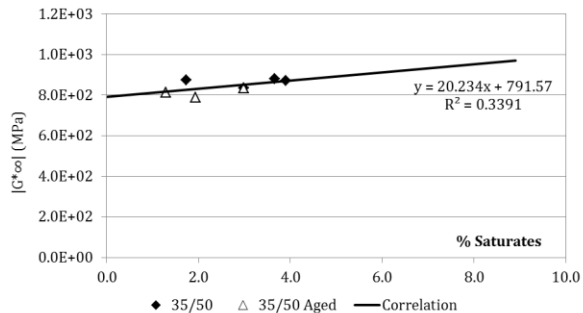
Annex 7

HUET-SUCH MODELLING PARAMETERS BY C7-ASPHALTENES, SARA FRACTIONS, COLLOIDAL INDEX, POLYDISPERSITY, R_{VALUE} AND $W(CO)$

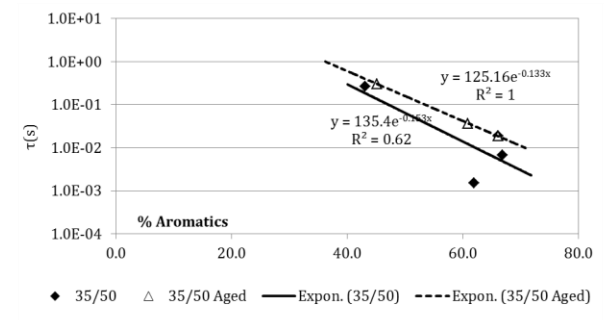
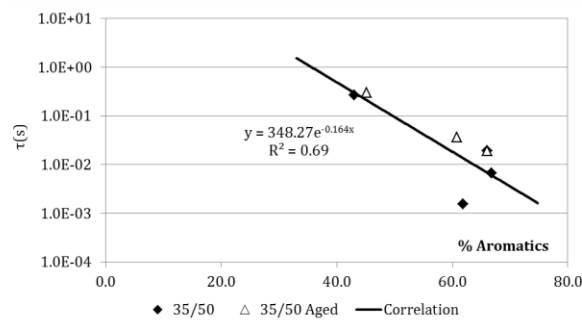
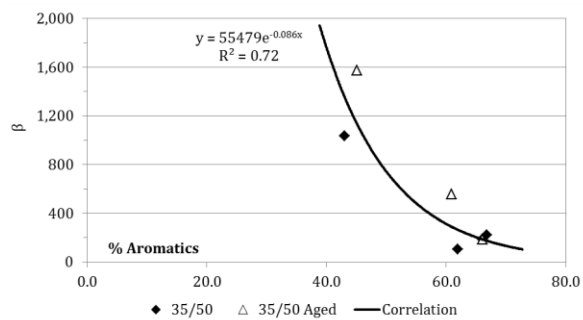
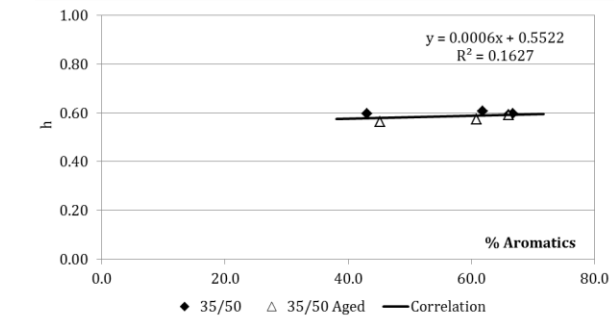
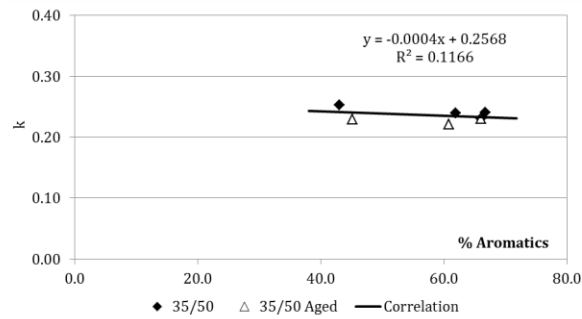
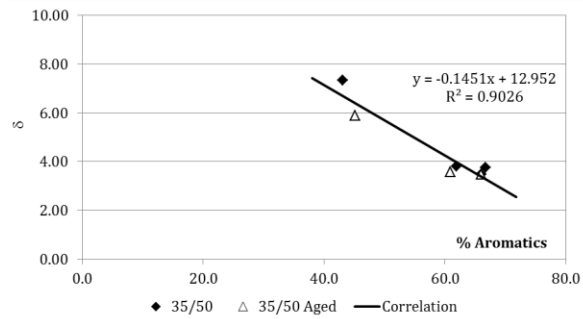
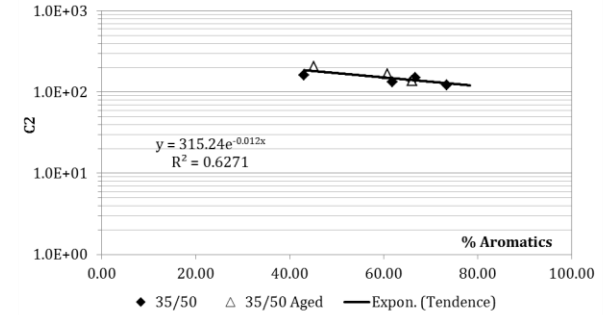
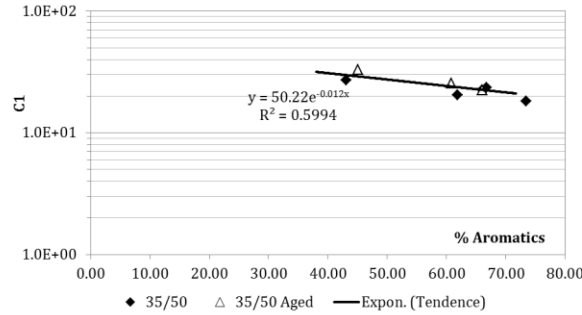
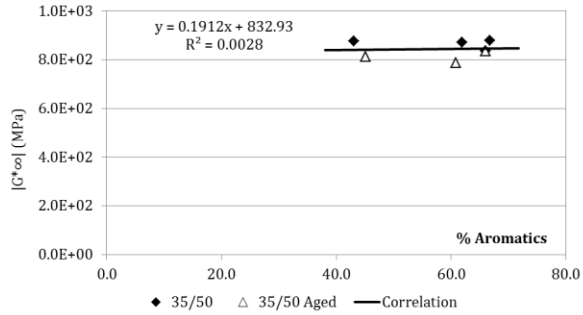
C7-ASPHALTENES



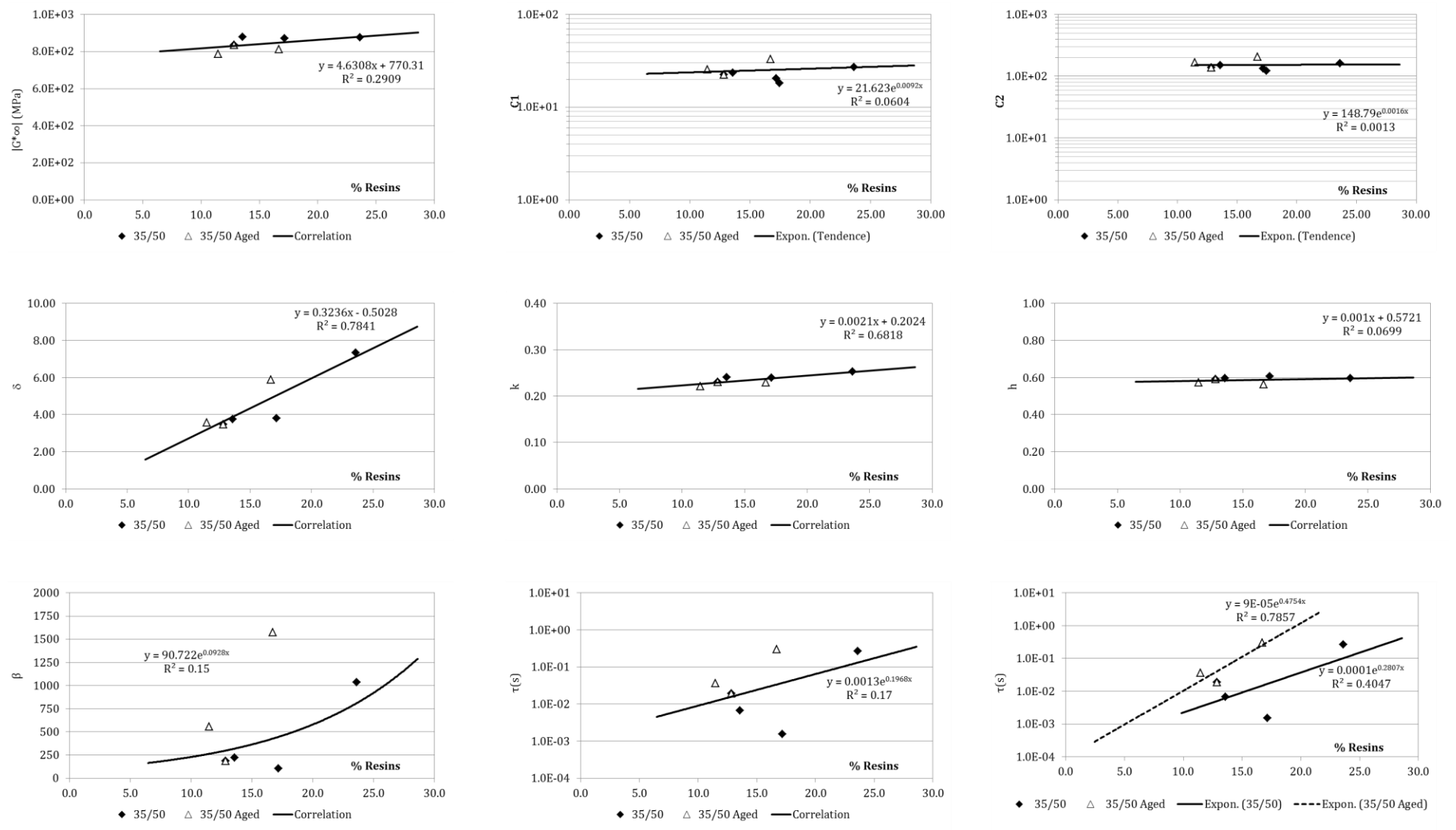
SATURATES



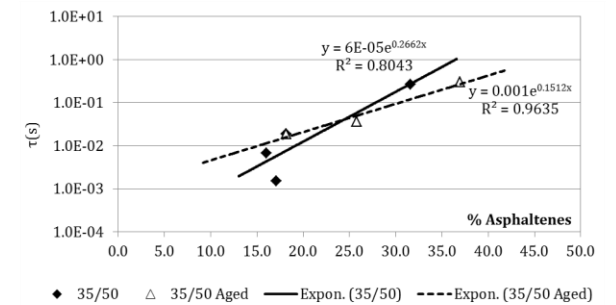
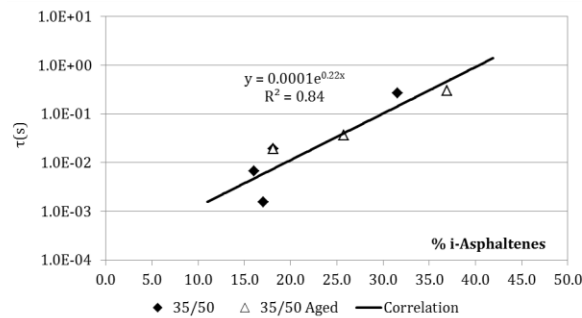
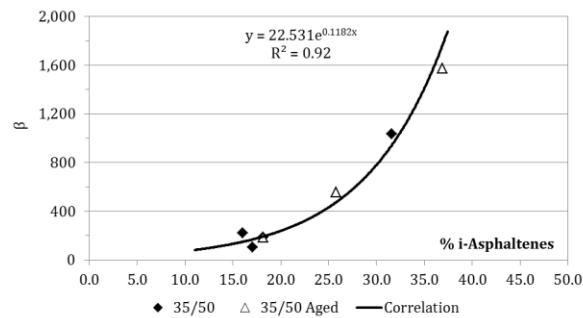
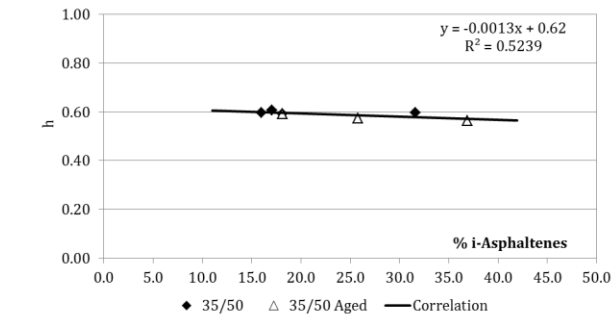
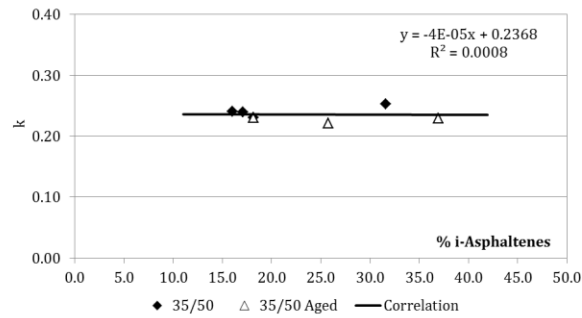
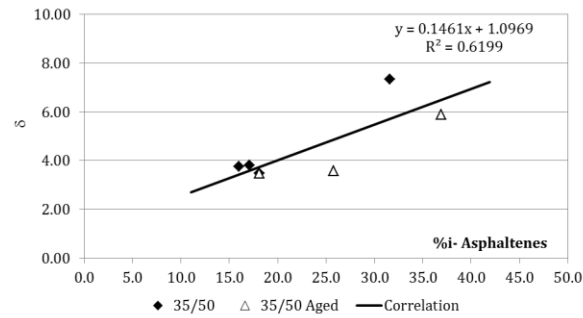
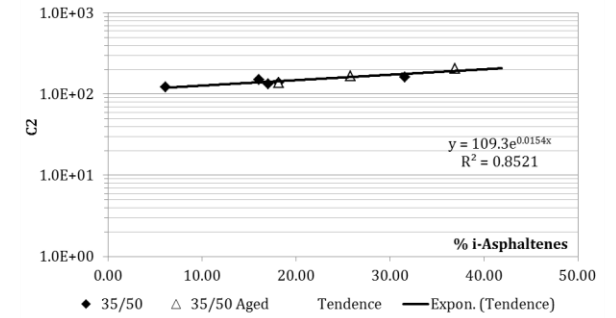
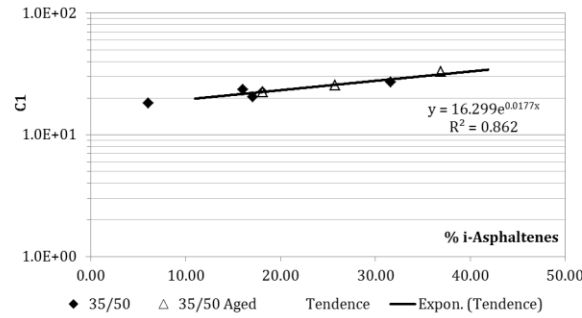
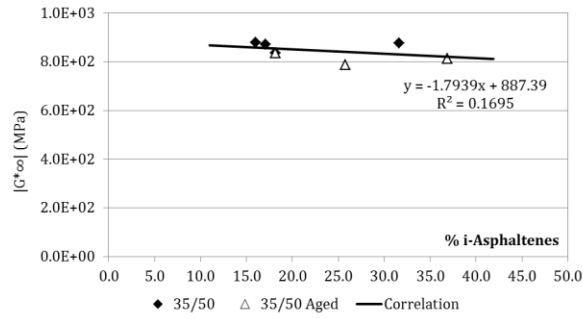
AROMATICS



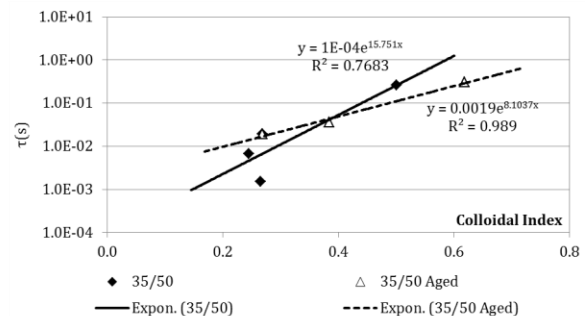
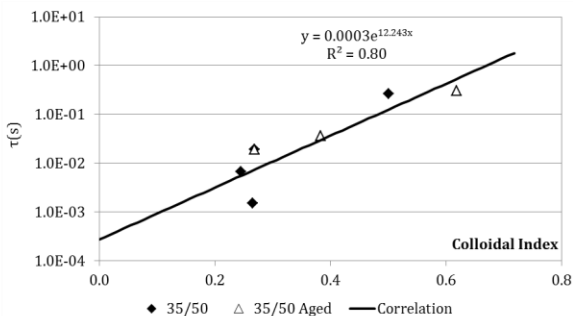
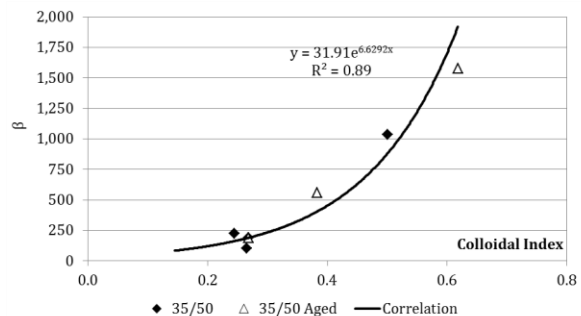
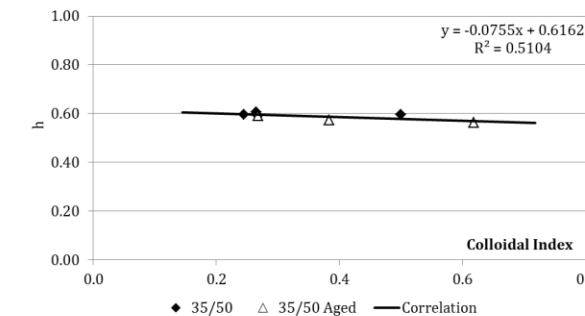
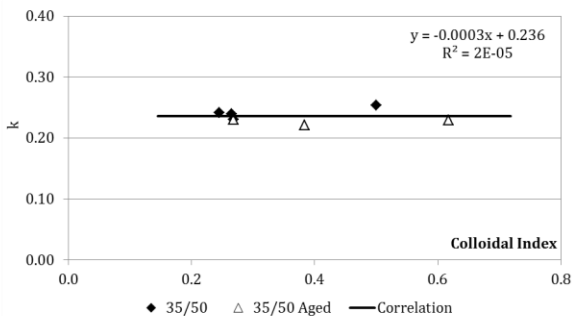
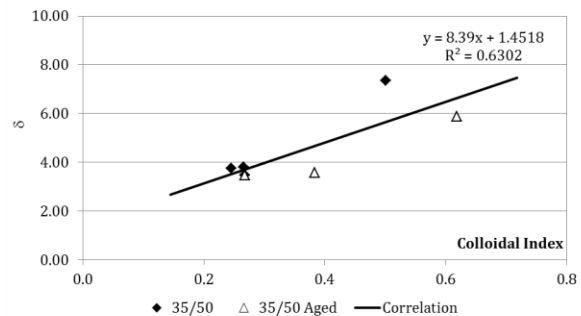
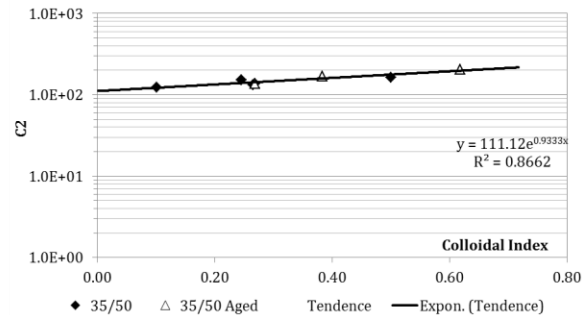
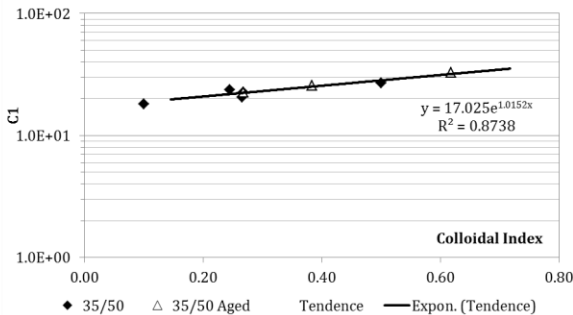
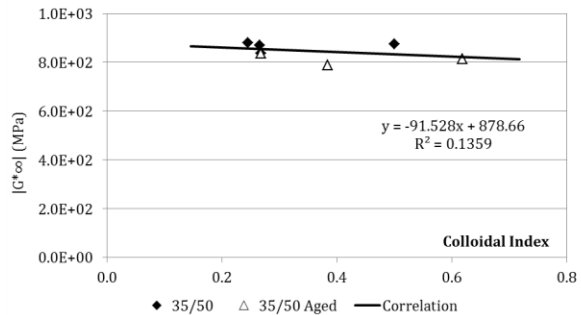
RESINS



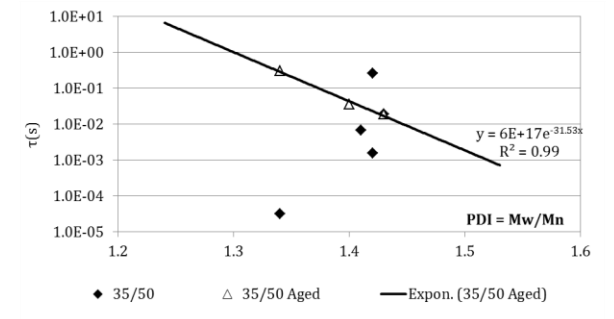
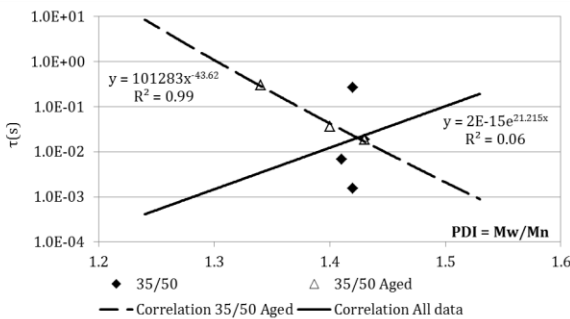
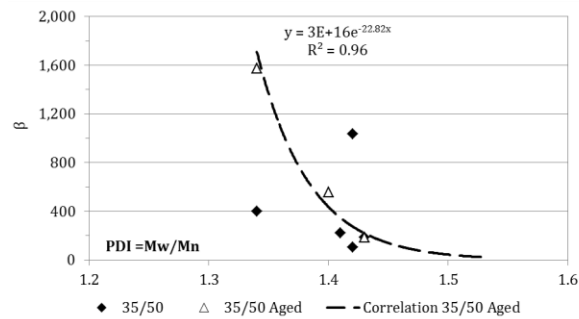
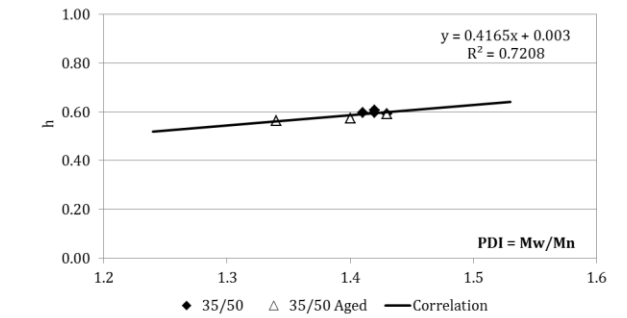
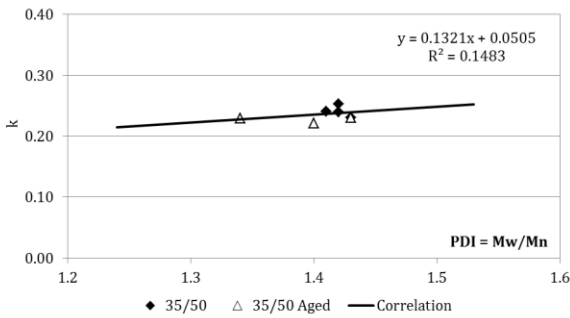
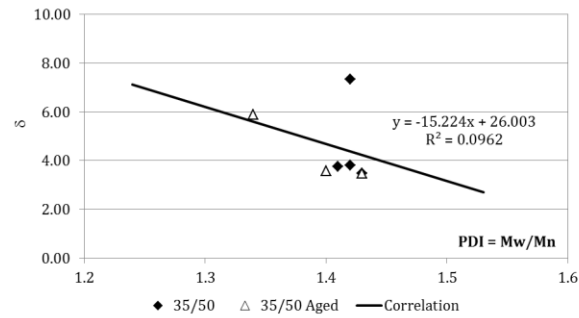
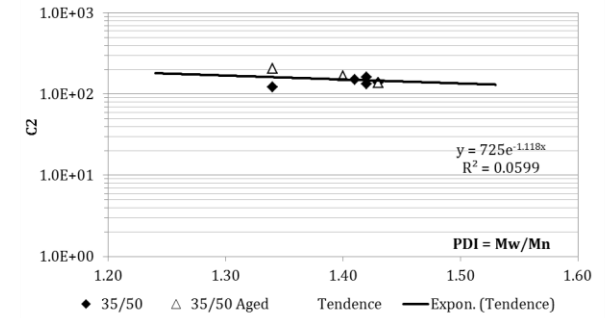
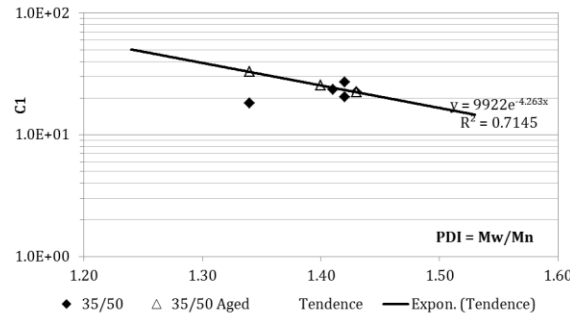
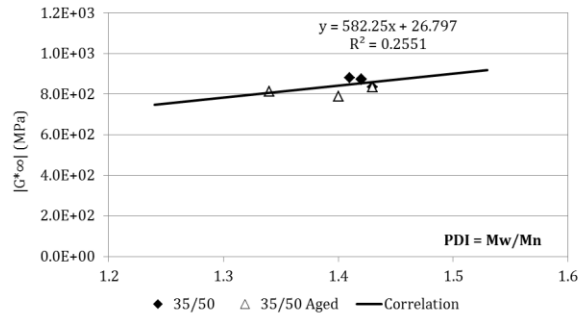
I-ASPHALTENES



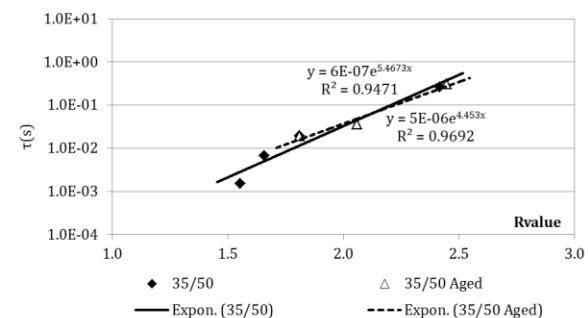
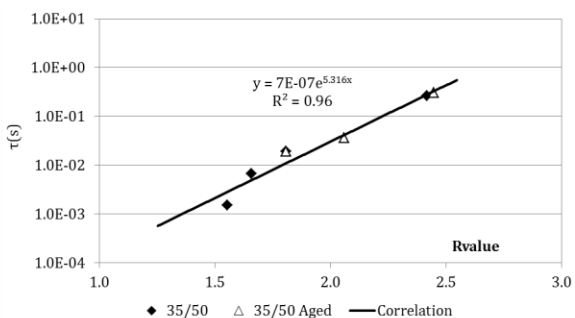
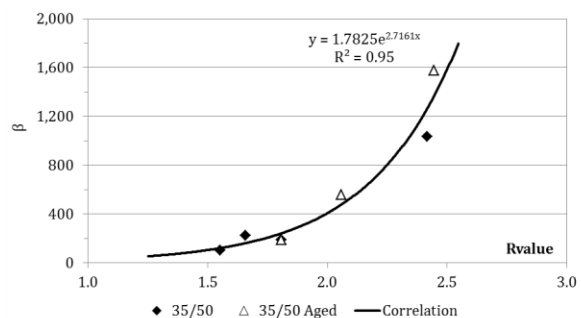
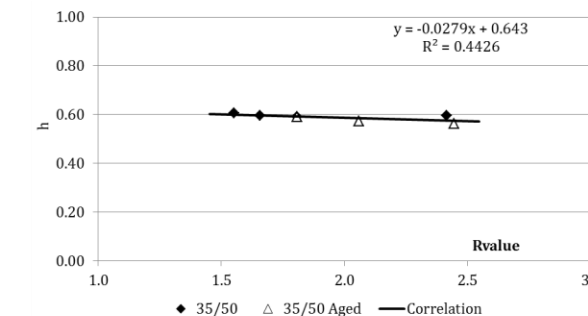
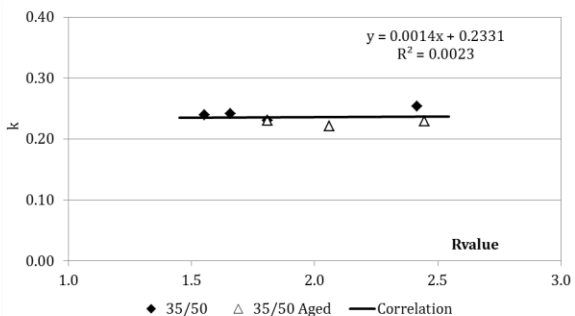
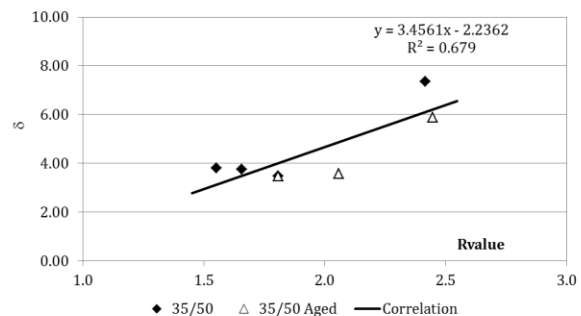
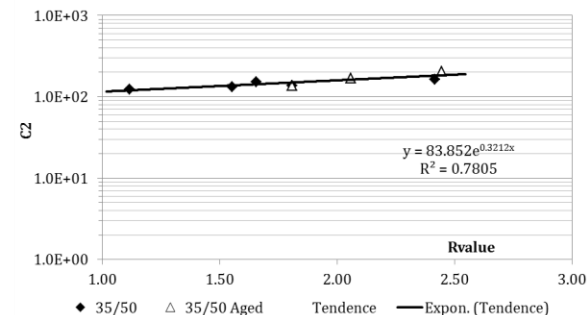
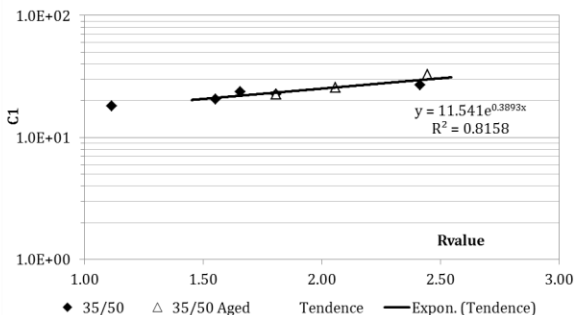
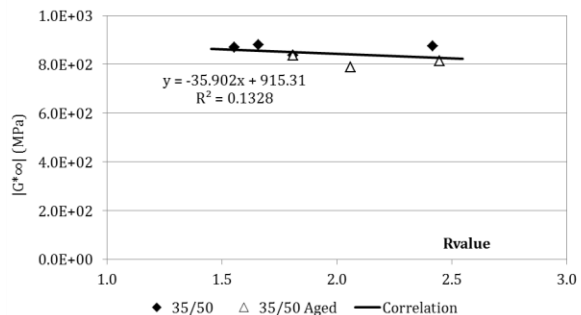
COLLOIDAL INDEX



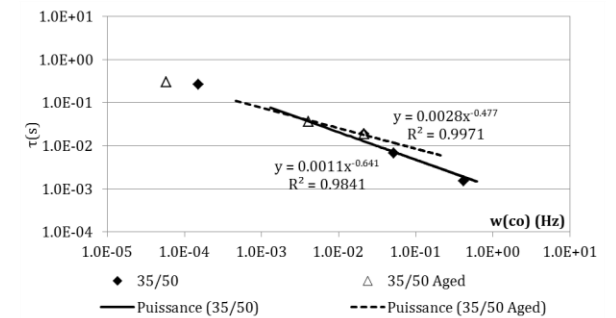
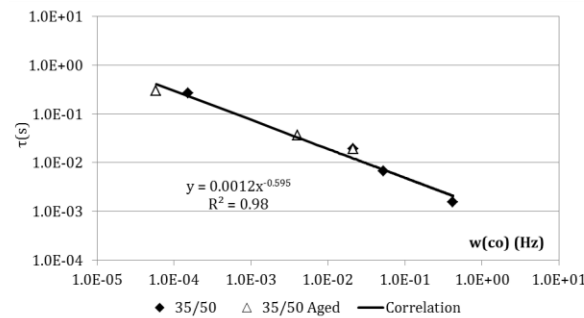
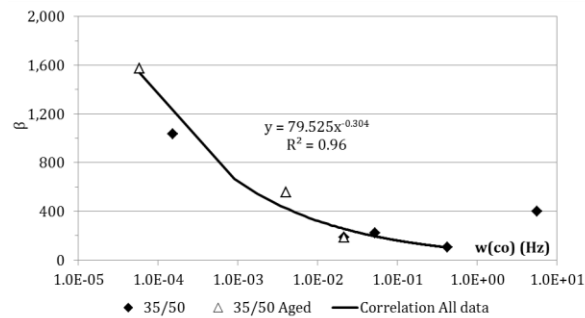
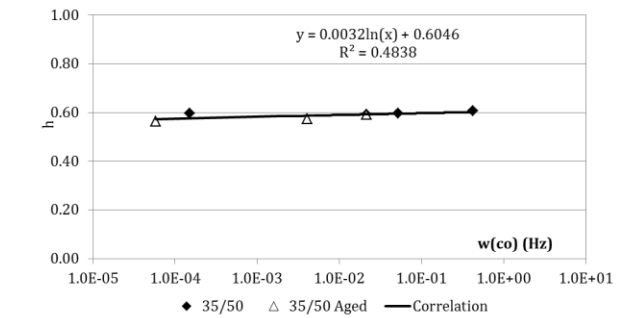
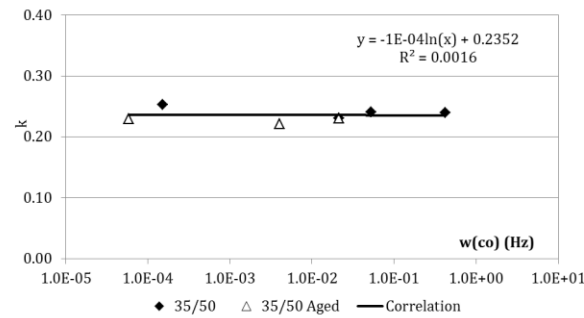
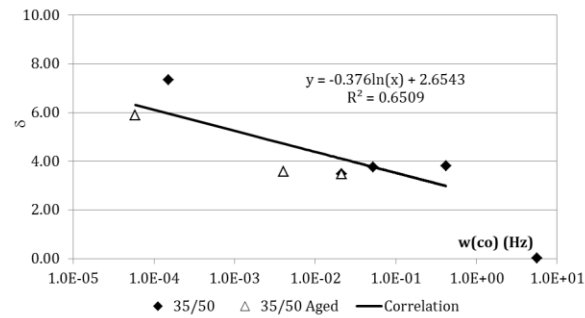
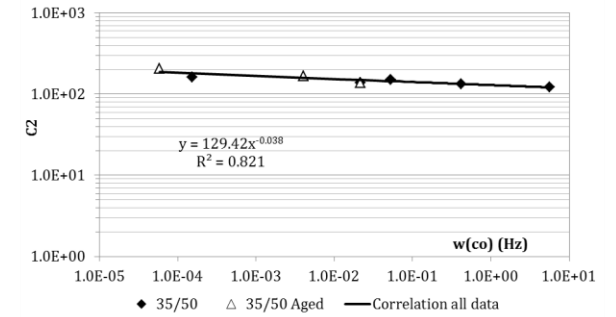
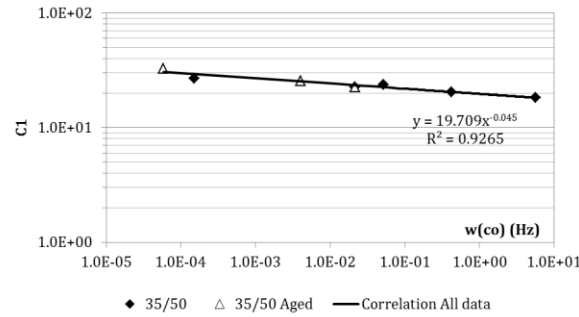
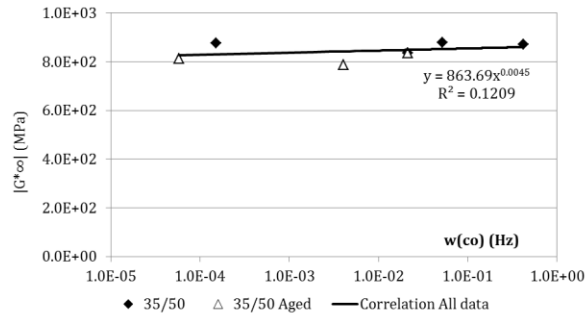
POLYDISPERSITY



RVALUE



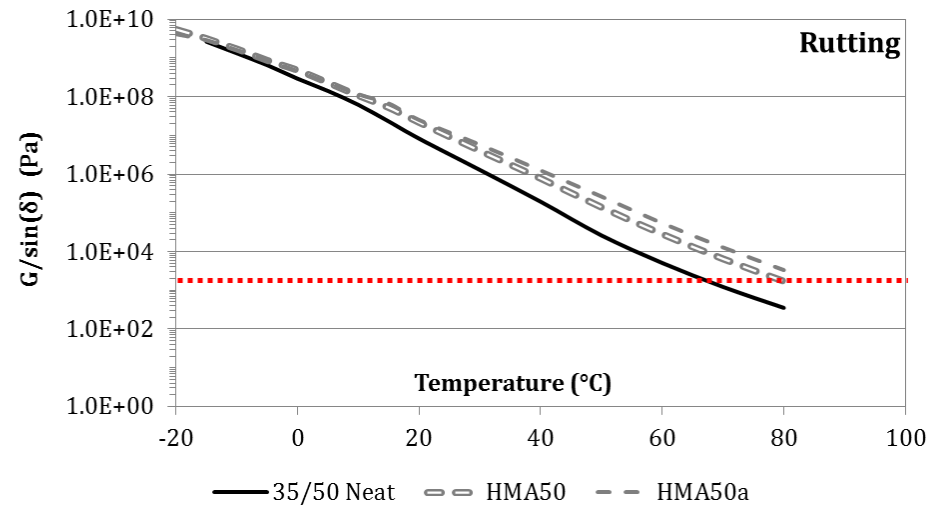
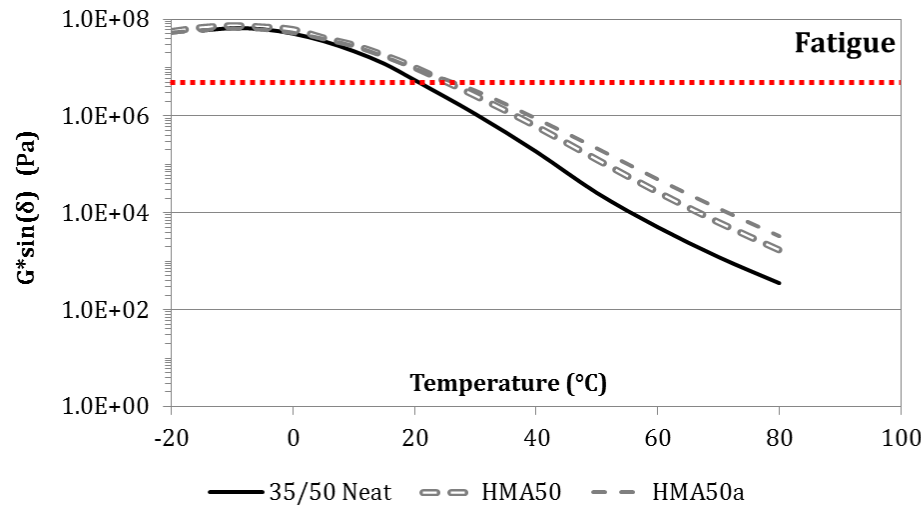
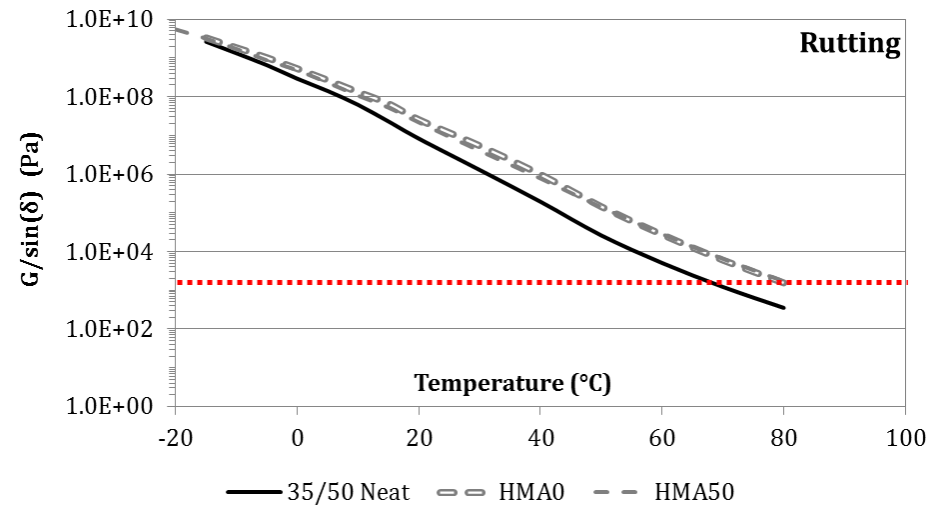
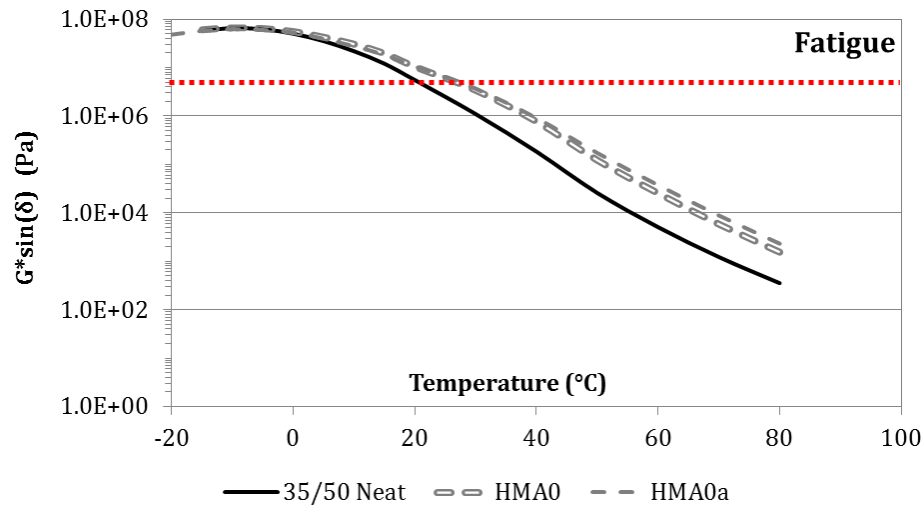
CROSSOVER FREQUENCY



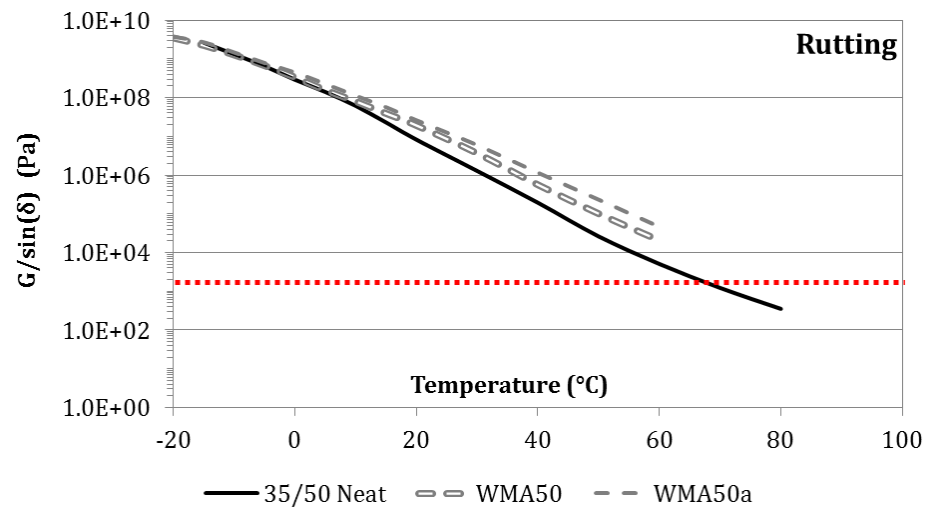
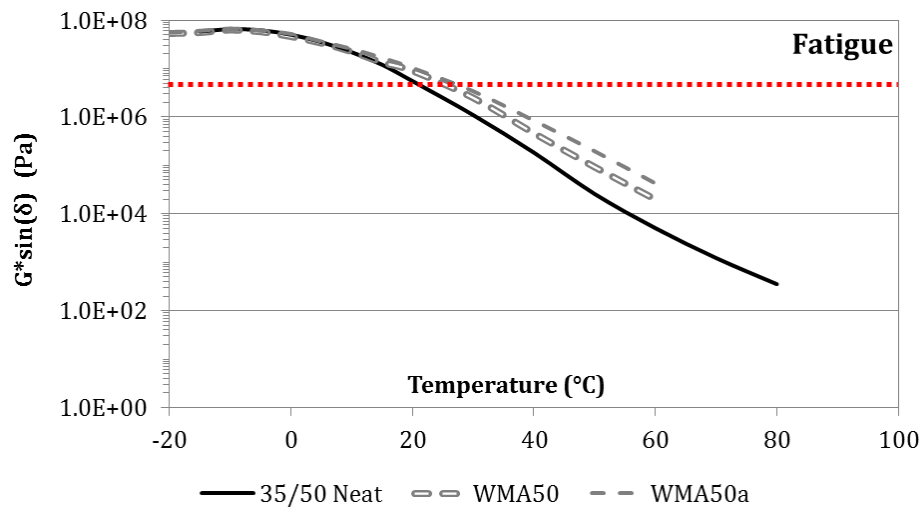
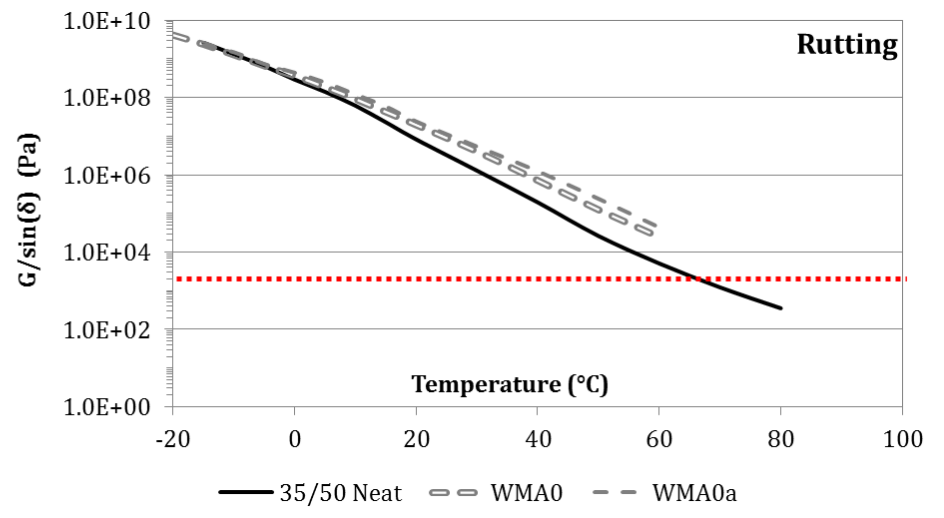
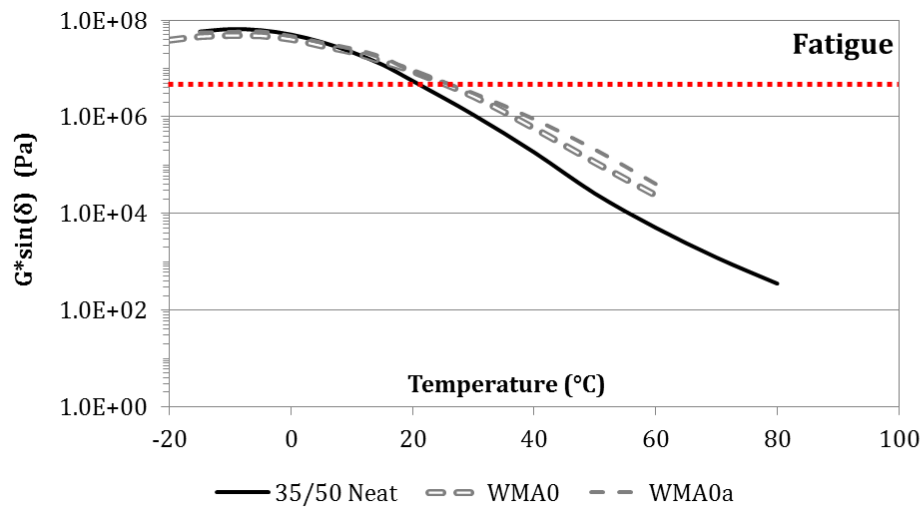
Annex 8

SHRP RUTTING AND FATIGUE PARAMETERS CURVES WITH TEMPERATURE

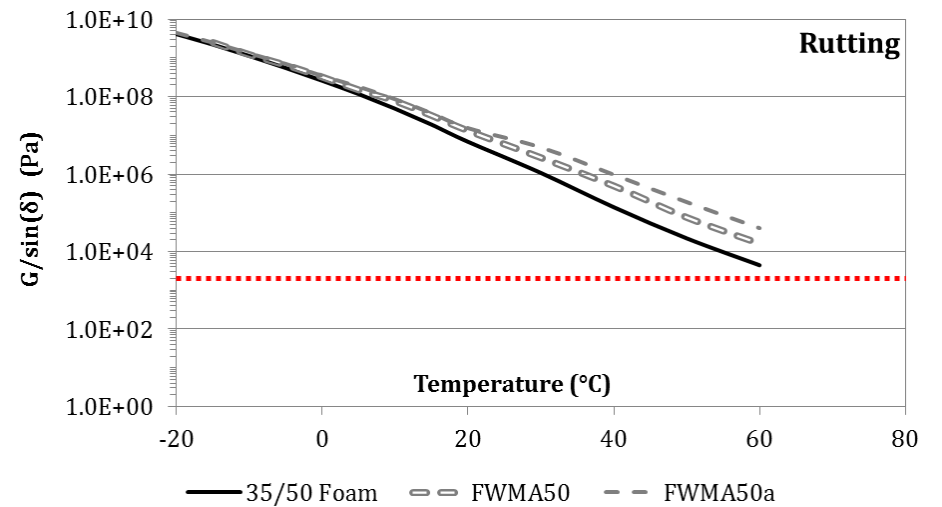
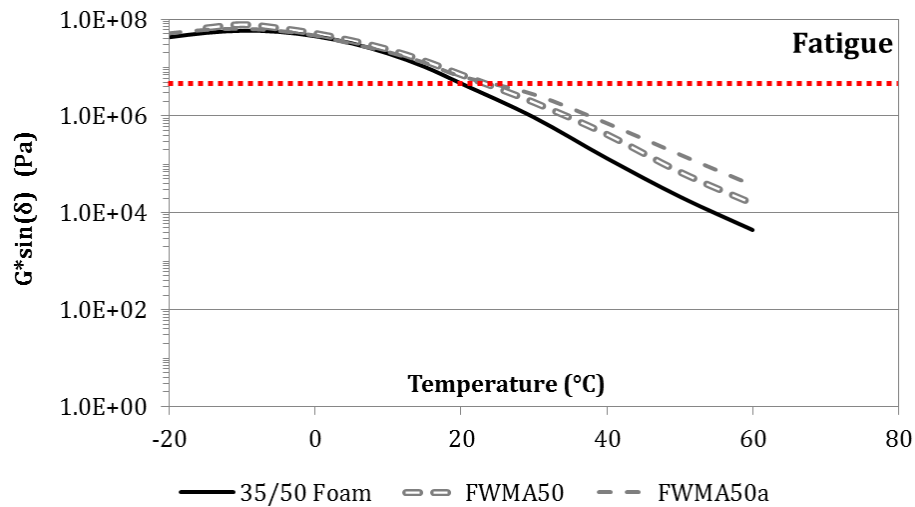
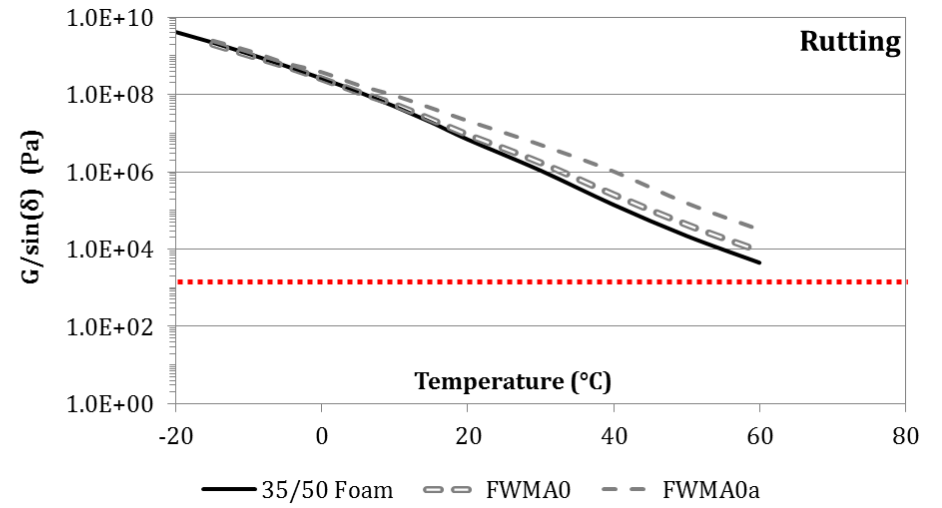
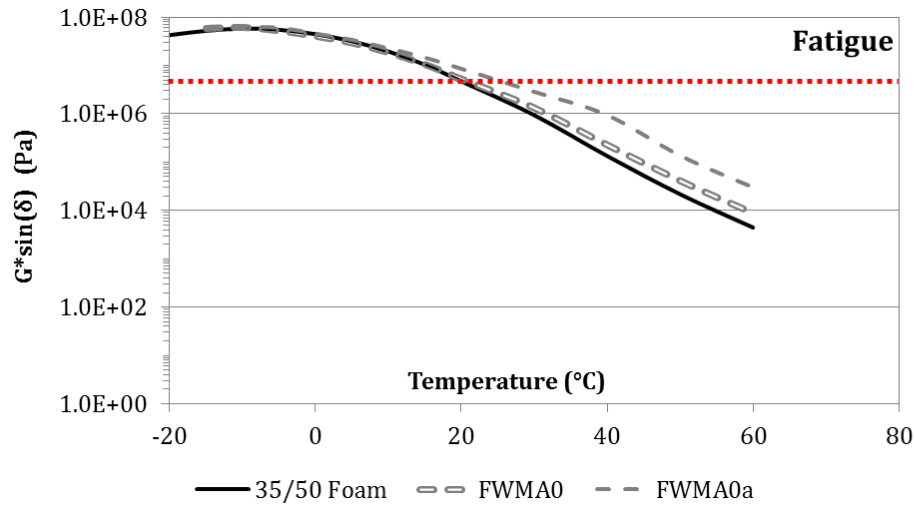
HOT MIX ASPHALT BITUMENS



WARM MIX ASPHALT BITUMENS



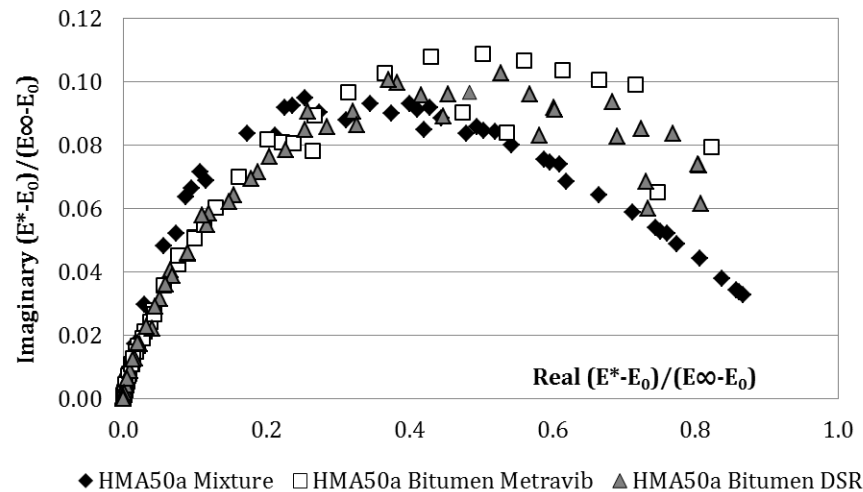
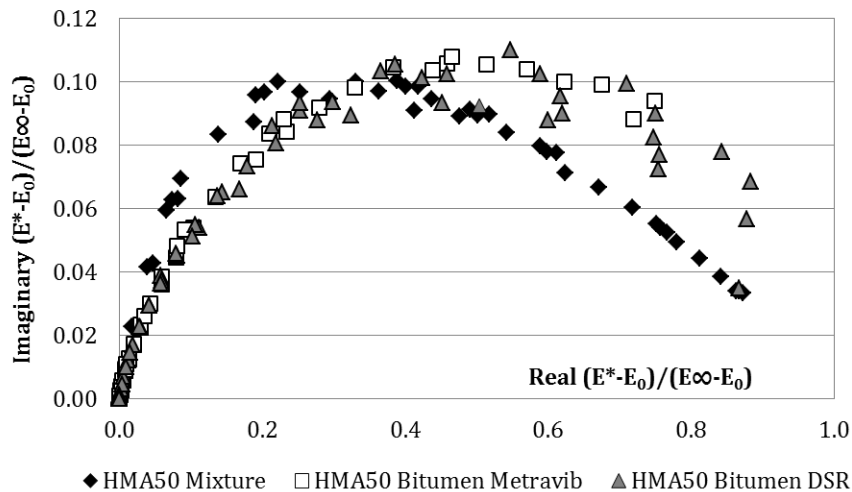
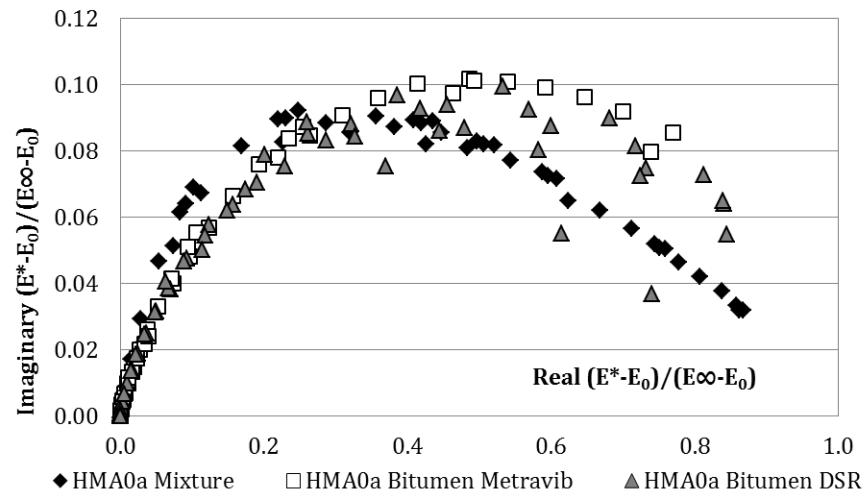
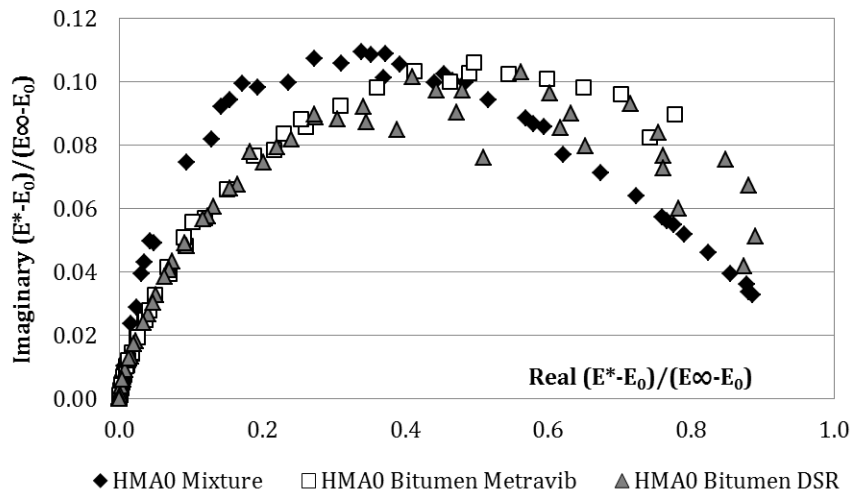
FOAMED WARM MIX ASPHALT BITUMENS



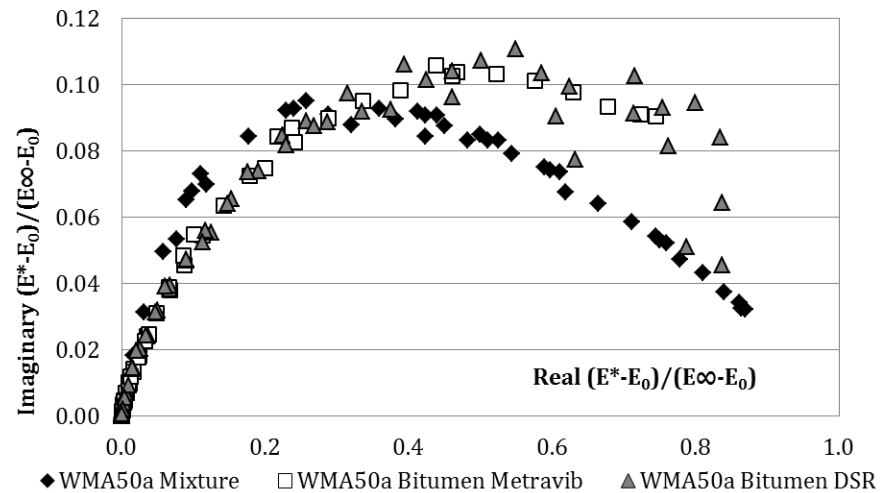
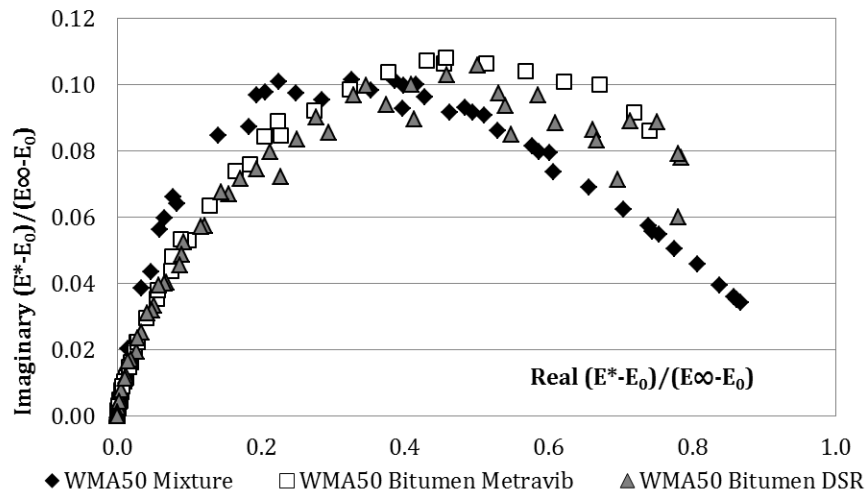
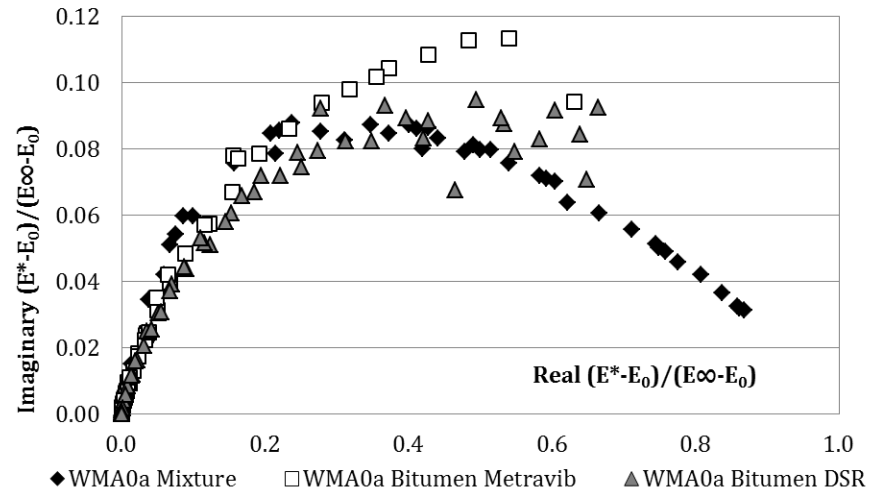
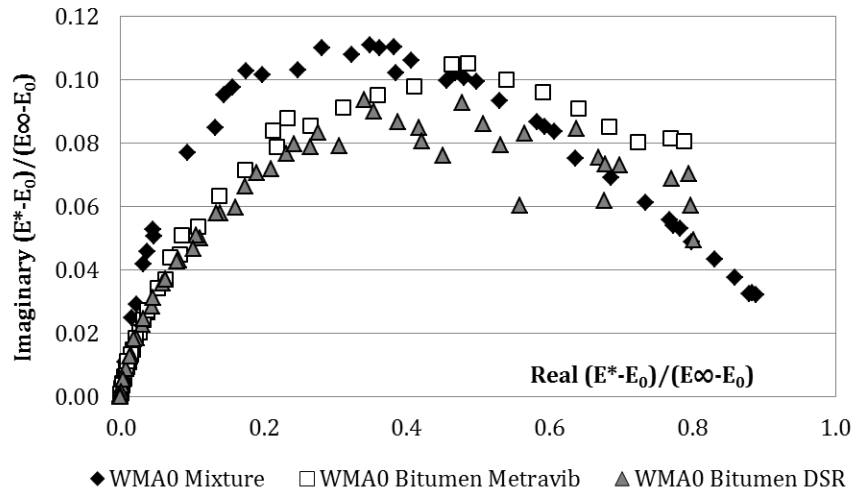
Annex 9

SHStH TRANSFORMATION
BETWEEN ASPHALT MIXTURES RESULTS
AND RECOVERED BITUMEN RESULTS

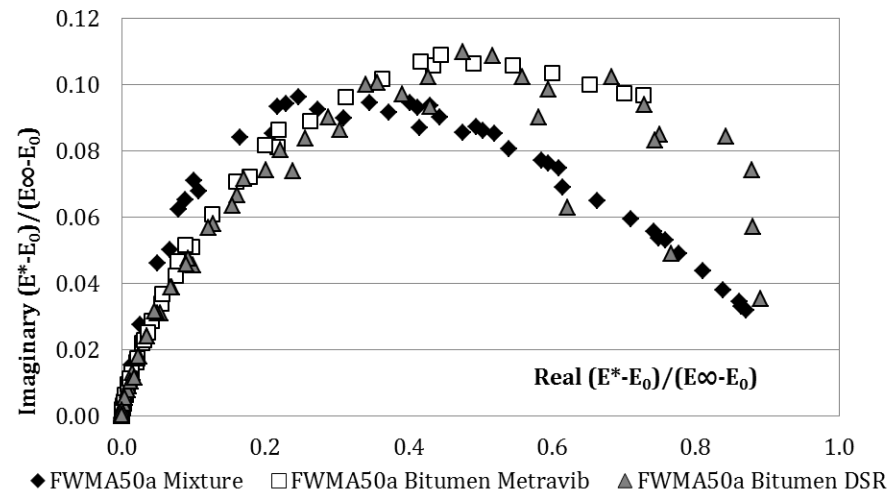
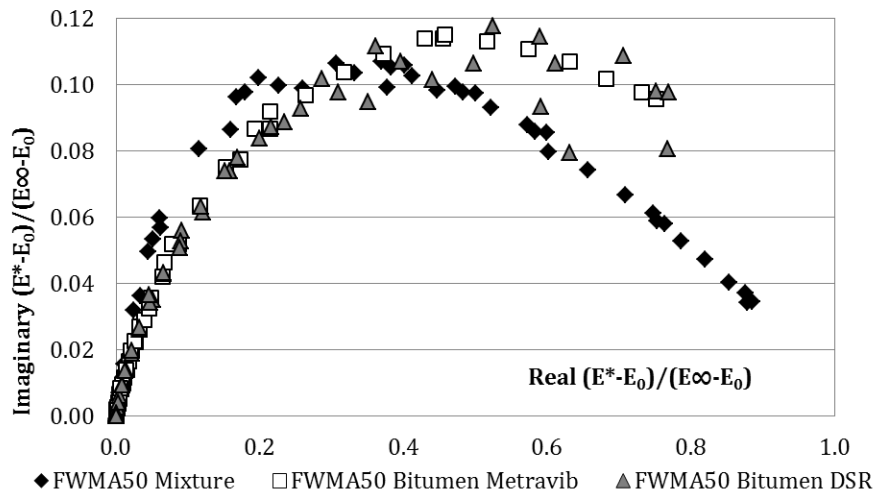
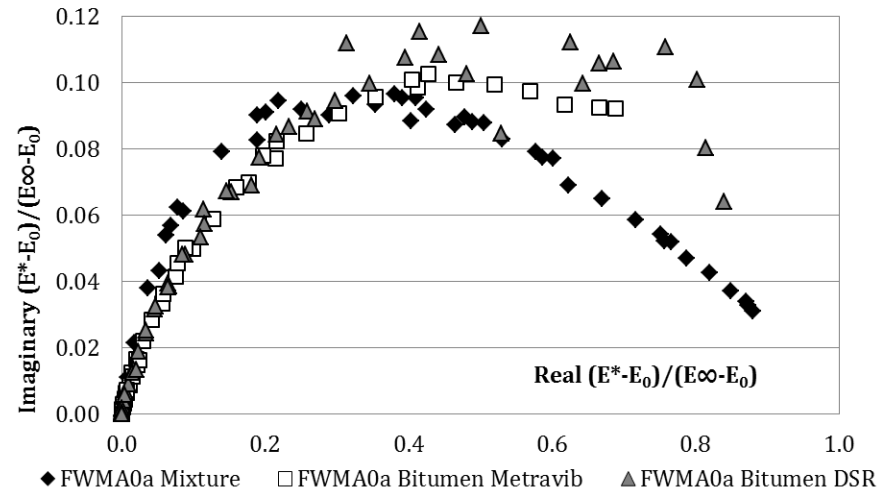
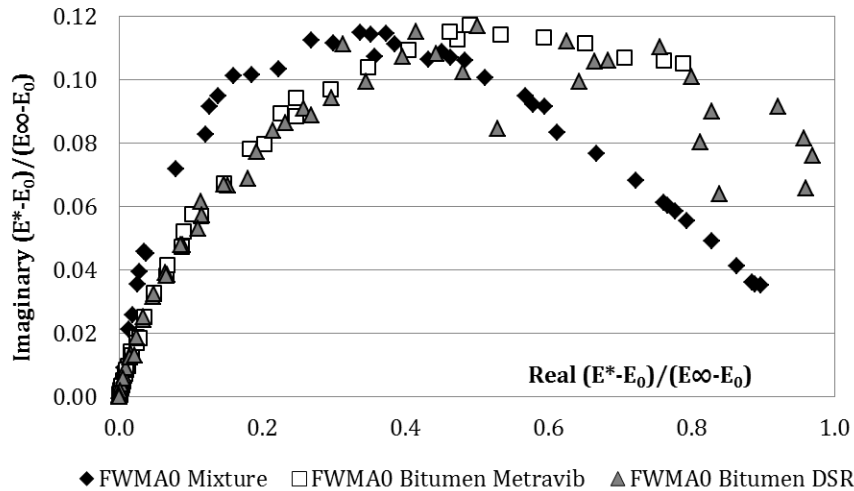
HOT MIX ASPHALT RESULTS



WARM MIX ASPHALT RESULTS



FOAMED WARM MIX ASPHALT RESULTS



Thèse de Doctorat

Miguel Perez Martinez

Titre de la thèse: Durabilité des enrobés tièdes intégrant des recyclés

Title of thesis: Long term performance of low temperature asphalt pavements containing reclaimed asphalt

Résumé

Les routes sont le moyen de transport le plus utilisé dans le monde et le développement d'un pays est souvent mesuré en termes de kilométrage total des routes revêtues. Les chaussées sont essentielles à notre réseau social et l'enrobé bitumineux est le matériau le plus utilisé pour leur fabrication. À l'heure actuelle, le réseau routier européen n'est plus en forte croissance et nécessite surtout un entretien. Dans un contexte de développement durable de plus en plus exigeant, la route pourrait donc représenter sa propre source d'approvisionnement en tirant parti du recyclage. Elle doit aussi limiter les quantités d'énergies et de ressources naturelles nécessaires à sa propre maintenance.

La combinaison des techniques d'enrobés tièdes (WMA) et de taux de recyclage élevés d'agrégats d'enrobés (RAP) apparaît comme une solution permettant d'économiser à la fois l'énergie et les ressources naturelles. Mais sa durabilité doit être éprouvée. Un programme expérimental a donc été mis en place pour montrer l'évolution des performances de ces enrobés bitumineux avec le temps, mettant en évidence la notion de vieillissement essentiellement lié à la fraction bitumineuse. A l'échelle du bitume, l'évaluation à long terme est effectuée notamment en appliquant la

δ -méthode et en comparant avec les mesures de masses moléculaires par GPC à la fois sur des échantillons modèles à teneur en asphaltènes contrôlée et sur des échantillons de laboratoire. A l'échelle de l'enrobé bitumineux, une étude comparative a été réalisée entre un enrobé à chaud traditionnel et des WMAs incluant 0% ou 50% de RAP soumis à une procédure de vieillissement en laboratoire. Les performances à long terme des mélanges sont comparées au moyen d'essais de module complexe et de fatigue.

Les résultats montrent une relation entre l'évolution de la structure des bitumes par vieillissement et les performances mécaniques. Le vieillissement à court terme au moment de la fabrication est beaucoup moins marqué pour les procédés tièdes. Après vieillissement à long terme, les tendances générales sont similaires pour tous les procédés.

Mots-clés

Durabilité, Recyclage, Agrégats d'enrobé, Performance mécanique, moussage du bitume, enrobé tiède, vieillissement

Abstract

Roads are the most widely used mode of transportation in the world, and a country's development is often measured in terms of its total paved roads mileage. Pavements are an essential part of our social network and asphalt concrete is the main material used for manufacturing them. Currently, the European road network is not much growing anymore and mostly needs only maintenance. In a context of increasing demand of performance and durability of asphalt mixtures, a sustainable, durable and economical conception is required. Indeed it could be oriented towards a self-sufficient road providing its own raw materials through recycling while limiting the use of energy and other natural resources for its maintenance.

The combination of warm mix asphalts (WMA) technologies and high rates of reclaimed asphalt pavements (RAP) appears as a solution to achieve both energy and natural resources savings. But it is still ambiguous in terms of durability. Therefore, an experimental program is set up to show the evolution of the performances of such asphalt concretes with time, highlighting the notion of ageing mostly related to the bituminous fraction. At the bitumen scale, the long term assessment is carried out in particular by applying the

δ -method compare with GPC measurements both on model samples with controlled asphaltene content and laboratory aged ones. At the asphalt mixture scale, a comparison study is carried out between a reference HMA and WMAs with 0% - 50% of RAP submitted to a laboratory ageing procedure. The long term performances of the mixtures are compared by means of complex modulus and fatigue testing.

Results show a relation between the evolution of the structure of the bitumen with ageing and the mechanical performances. Short term ageing is less important for warm processes. After ageing, the overall tendencies are similar for all processes.

Key Words

Durability, Recycling, RAP, Mechanical performance, Foaming process, warm mix asphalt, ageing